EFFECT OF MUTUAL INTERFERENCE OF BRIDGE PIERS ON LOCAL SCOUR

ABSTRACT
THESIS
Submitted for the award of the Degree of

Doctor of Philosophy
IN
CIVIL ENGINEERING

BY

MUBEEN BEG

DEPARTMENT OF CIVIL ENGINEERING
ZAKIR HUSAIN COLLEGE OF ENGINEERING & TECHNOLOGY
ALIGARH MUSLIM UNIVERSITY
ALIGARH (INDIA)

June 2008

ABSTRACT

Scour is defined as the erosion of streambed around an obstruction in a flow field. The amount of reduction in the streambed level below the bed level of the river prior to the commencement of scour is referred as the scour depth. A scour hole is defined as depression left behind when sediment is washed away from the riverbed in the vicinity of the structure.

The local scour has the potential to threaten the structural integrity of bridge piers, ultimately causing failure when the foundation of the pier is undermined. Besides the human loss, bridge failures cost millions of dollars in direct expenditure for replacement and restoration in addition to the indirect expenditure related to the disruption of transportation facilities. A series of recent bridge failures due to pier scour, as reported by Wardhana and Hadipriono (2003), S.Dey and Barbhuiya (2004) and Hoffmans and Verheij (1997), rekindled interest in furthering for developing improved ways of estimating the maximum scour depth and protecting bridges against the ravages of scour.

An exhaustive amount of literature which exists on local scour reveals that the problem of local scour around bridge pier received a lot of attention in the past from theoretical and practical point of view in an attempt to quantify the equilibrium depth of scour. However, among the large number of experimental and field studies, (*e.g.*, Laursen and Toch (1956), Chabert and Engeldinger (1956), Chew (1984), Raudkivi (1998), Ettema (1980), Melville and Sutherland (1988), Mostafa (1998) and Johnson (1995) etc.), the problem of scour around a single pier has been mainly focused and more meticulously investigated than the problem of scouring around hydraulically interacting multiple piers. A scanty amount of literature on pier group scour is available [*e.g.*, Hannah (1978), Elliott and Nicollet (1978) and Zarrati *et. al.* (2004, 2006)].

In the case of pier group scour, the presence of several piers can generate a more complex interaction in the hydrodynamic characteristics of the flow field near the piers themselves and therefore, the flow pattern in the channel around the piers gets changed significantly and lead to the occurrence and development of a scour process that is quite different from one which occurs around a single pier. This interaction is particularly evident when the

bridge is not perpendicular to the river flow. Hannah (1978) studied the local scour at piers group and recognized four mechanisms of scour (*e.g.*, reinforcing, sheltering, shed vortices and compressed horseshoe vortices) to occur which make the scour phenomenon more complex and which can modify the depth and shape of the scour hole around the piers.

Therefore, if a bridge pier is merely designed and constructed considering as a single pier, it may lead to the bridge failure because mutual interference of several piers can enhance the scour depth at the piers. In these perspectives, to ensure the stability of the bridge piers, the need of a study on the effect of mutual interference of bridge piers on local scour assumes immense significance which is the subject of present study.

Many situations, which are common in the field where the bridge pier groups are founded in the riverbed in different patterns of arrangements, are worth mentioning.

Due to rapid urbanization and increased traffic volume, it is often required to construct new bridges across the rivers in the proximity of the already existing bridge. There are limitations of spacing between existing and new bridges due to the problem of land acquisition. In that context, the scour depth and bed configuration pattern around the existing and new bridges need to be examined. Furthermore, for geo-technical and economical reasons, pier groups have been more and more popular in bridge design.

A bridge across a river is usually supported on a number of piers placed along its span where piers are located in a direction normal to the flow at some finite spacing. Two or more number of piers are often placed in line with the flow along width of a bridge. Railway tracks and highways are often constructed side by side across the same river such that they are located at some short distance apart. When the river runs through downtown in cities, which are subjected to an increase in population, the existing bridges constructed across the river become inadequate for traffic movement owing to an increase in traffic volume. This results in frequent traffic jams and traffic movement is halted, some times for hours together jeopardizing the whole transport system and causing untold miseries to the people. The stranded transport has to wait for traffic clearance to reach to their destination, which causes delay in achieving their goals. As a result this adversely affects the development of the country and causes enormous economical losses to the

people. In such eventuality, therefore, construction of new bridges for people movement, industrial production etc become imminent and the new bridges are often constructed at very short distances to facilitate the efficient and smooth traffic movement. A number of piers are also provided in the construction of hydraulic structures like an aqueduct to support the trough carrying canal water from one end of the drain to the other. Electricity and telephone lines are often carried across the river wherein electric and telephone polls are founded in the riverbed on a group of piers.

In the background of aforementioned field conditions, different arrangements of piers such as tandem, transverse and staggered, have been identified as study area to accomplish the major objectives of this research using experimental approach.

In order to study the effects of mutual interference of piers on local scour, a series of clear-water scour experiments has been conducted considering different patterns of pier arrangement and relationships have been developed for the estimation of scour depth at group of piers.

In the present investigation, experiments were conducted in a 12.0 m long, 0.756 m wide and 0.55 m deep, glass sided re-circulating rectangular tilting flume under steady uniform flow clear-water scour conditions. Non-ripple forming uniform sediment was used as bed material since, according to Breusers and Raudkivi (1991), ripples do not form at median sediment diameter $d_{50} \geq 0.7$. The bed material used in present experiments is considered uniform as the geometric standard deviation $\sigma_g = \left(\frac{d_{84.1}}{d_{15.9}}\right)^{1/2}$ of the material is less than 1.3~1.5. The experiments were conducted at flow intensity $\frac{u_*}{u_{*_c}} = 0.95$ since according to Raudkivi and Ettema (1977a, b), for non rippling sediments, clear–water scour experiments can run successfully with a flow condition $\frac{u_*}{u_{*_c}} = 0.95$. Average flow depth y_0 of 140 mm was chosen in accordance to the statement of most researchers that the influence of flow depth can be neglected if the ratio of flow depth to pier width $\frac{y_0}{b} > 2$ to 3. Experiments were first conducted on a single pier of diameter (b) 33 mm to form a basis against which the effect of mutual interference of bridge piers configured in different arrangements could

be evaluated. The pier sizes were chosen in accordance to Melville and Sutherland (1988) and Melville (1997) where they showed that the scour depth in uniform sediment is independent of sediment size when sediment coarseness ratio $\frac{b}{d_{50}}$>25. Next, a series of experiments on piers of same diameter as that of single pier, placed in tandem, lateral and staggered arrangement at varied pier spacings, was conducted. Then a series of experiments on a group of piers placed at constant angle of attack (45°) and varied radial pier spacings from 0 to 12 times the pier diameter was considered. Next, a series of experiments with constant radial (R) spacing and varied angles of attack from 0° to 90°, was conducted. A series of experiments was also conducted for two cases of tandem arrangement using two different sizes of piers (33 mm and 66 mm diameter), by placing larger diameter pier at front and smaller diameter pier at rear in first case and smaller diameter pier at front and larger diameter pier at rear in the second case respectively. The selection of the sizes of two piers was made just on a trial basis to get pier size ratios of 2 and 0.5 for the case first and second respectively. The basis of use of two different size piers is the recent technological advancement due to which narrow piers are being preferred and constructed in order to achieve economy. Prior to the experiments on group of piers of different sizes placed in tandem arrangement, a series of experiments was conducted on larger diameter (66 mm) single pier to form a basis against which the effect of mutual interference of piers could be evaluated. In the last phase, experiments were conducted on group of piers with and without collar. A group of piers comprising of cylinders of varied sizes (21.5 mm to 46 mm diameter) with and without collar and aligned to the flow at angles of attack from 0° to 30°, was tested to investigate the use of piers group for scour depth reduction. The selection of different pier sizes for this pier group was made considering the limitation of constriction ratio as suggested by Shen *et. al.* (1966) in order to avoid the blockage effect of pier group on local scour. As Raudkivi (1986) in discussing effects of pier alignment also states that the use of cylindrical columns would produce a shallower scour as compared to a solid pier, a group of two circular piers (41.5 mm diameter) separated at clear spacing of two pier diameter for varied angles of attack to the flow from 0° to 90° with and without collar, was tested to investigate the efficacy of this pier group in reduction of scour depth as compared to the use of a round–nosed rectangular pier of same length to width ratio (4:1) under same flow and sediment conditions.

Extensive data on local scour for different pier arrangements along with the group of piers with and without collar were collected for use in the modeling approach developed herein. The data, like, scour depth, areal extent of scour, scour depth profiles along flow direction and across the flow, were measured and recorded. Further the data on lengths and slopes of scour holes at upstream and downstream face of piers, width of scour holes, length of sediment deposition at downstream face of piers and temporal scour depth variation collected in present experimental programme, were analyzed to evaluate the mutual interference of bridge piers on local scour. Scour and deposition features developed by the flow after completion of the test, were also photographed.

As the analytical prediction of pier group local scour is very difficult due to complex nature of flow patterns occurring around the piers, two different modeling approaches namely, graphical relationships based approach and ANN based approach, have been developed and implemented.

The first approach predicts and analyses the various elements of pier group scour using graphical relationships. This approach considers the graphical presentation of the effect of pier spacing along and across the flow direction and angle of attack of flow, on various elements of pier group scour.

The second approach involves the use of a non-parametric ANN technique based on feed forward back propagation neural network (BPNN) for establishing relationships between pier spacing or angle of attack (the angle between flow direction and the line joining centre of piers) and scour depth. The ANNs could be trained with sufficient accuracy by using only one input variable viz. pier spacing or angle of attack. The results from both experimental based approach as well as ANN based approach were found to be in close agreement with each other (R^2~0.96-0.99).

ANN models are developed using feed forward back propagation learning algorithm in MATLAB neural network toolbox. Application of ANN on author's experimental data produces good estimate of scour depth at pier groups arranged in different patterns and these results are well comparable with existing published data of Hannah (1978), Chabert and Engeldinger (1956) and Richardson *et. al.* (1993). The results reveal that for training and testing sets, all the neural networks trained, produced higher R^2 and lower RMSE

values of the order ~ 0.99. Also, almost all the neural networks trained required relatively equal number of iterations to reach the global minima. The correlation coefficient R^2 between observed and ANN estimated scour depths represents the predictive ability of ANN models. Understanding and analyzing the effect of factors, like pier spacing between the piers or angles of attack of flow, to evaluate their effect on scour depth to accurately and effectively estimate the scour depth and other scour characteristics was the main focus of this research.

Based on the experimental results achieved in present research on pier group scour, significant effect of mutual interference of piers on local scour is found. In the case of tandem arrangement, when a group of two identical circular piers is placed at pier spacing of 1.5 times the pier diameter, the scour depth of front pier gets enhanced by 17 % as compared to the scour depth of an isolated pier whereas placement of it at pier spacing of 12.5 times the pier diameter causes a reduction of 33% in scour depth of rear pier. When a group of three identical circular piers are placed in tandem arrangement, the scour depth of front pier increases by 11% whereas at rear pier gets reduced by about 33.5%, as compared to that of a single pier. The scour depth at middle pier is about 15.5% higher than that of the rear pier. In the case of a group of two different size piers placed in tandem arrangement (such that larger pier is placed at front and smaller one at rear), scour depth at larger pier corresponding to the scour depth of an isolated larger pier, gets enhanced by 8%. However, scour depth at smaller pier corresponding to the scour depth of an isolated smaller pier becomes 0.57 times lower at pier spacing of 35 times the pier diameter The scour depth at smaller pier relative to that of an isolated larger pier becomes 0.33 times of that occurs at 66 mm isolated pier. When a group of two different size piers is placed in tandem arrangement such that smaller pier is placed at front and larger one at rear, scour depth at smaller pier at zero pier spacing increases by 28.5 % as compared to that at an isolated smaller pier, however, the scour depth at larger pier as compared to the scour depth at an isolated larger pier, gets reduced by 23% at the same pier spacing. The scour depth at larger pier as compared to an isolated larger pier gets reduced by 37% at pier spacing of 5 times the diameter of smaller pier.

When a group of two identical circular piers is placed in lateral arrangement (normal to the direction of flow) at zero pier spacing, scour depth is 1.95 times of that occurs at an isolated pier. Though, the scour depth of two piers rapidly decreases at pier spacing of one pier

diameter, nevertheless it remains 21 % higher than that of an isolated pier. At lateral pier spacing of 8 times the pier diameter, although, the scour depth at two piers becomes same as that of an isolated pier, however, the sizes of the scour holes are not identical to that for an isolated pier.

In case of a group of three piers placed in staggered pattern, scour depth at upstream and downstream piers gets increased by 40.5% and 12.5% as compared to that at an isolated pier respectively.

At group of two piers aligned at 45° to the flow at zero radial pier spacing, the scour depth gets enhanced by 12% as compared to that occurs at the group of two piers aligned normal to the flow at zero radial pier spacing. However, when the radial pier spacing between the two piers increases to one pier diameter, the scour depths at front and rear piers gets enhanced by 35% and 38% respectively as compared to that occur at an isolated pier respectively.

When the group of two piers having a clear radial pier spacing of 4 times the pier diameter, are aligned at an angle of 0° to the flow, scour depth at front and rear piers equals to 1.1 and 0.96 times of that occur at an isolated pier. When angle of attack of flow becomes 45°, scour depths at front and rear piers get enhanced by 17.4% and 24.1% as compared to the scour depth of an isolated pier. At 90° angle of attack, the scour depths of two piers become equal but are still 4.5% higher than that at an isolated pier.

These findings acquired in present investigation suggest that the group effect of piers on local scour is highly significant and should be properly incorporated in the pier design.

A major contribution of this study is the experimental description of method of scour depth reduction by applying a collar around group of piers. Enthusiastic results are obtained for pier protection against local scour by the application of collar around group of piers comprising of varying sized cylinders. These experimental results are found in good agreement when compared with the published data of Chabert and Engeldinger (1956). Also, replacement of a rectangular pier with a group of piers is experimentally investigated for economical design of pier by saving the material and reducing the depth of scour and the experimental results so obtained, are well comparable with the published experimental data of Zarrati *et. al.* (2004, 2006).

When a pier group comprising of varied sizes of piers without collar is tested at 0° angle, a reduction of 44% in the scour depth as compared to an isolated pier of diameter equal to the diameter of the largest cylinder used in this pier group, is achieved. The use of this pier group without collar upto an angle of 10° to the flow proves to be very effective as its use reduces the scour depth by 33% as compared to an isolated pier of diameter equal to the diameter of largest pier diameter used in this pier group. It is worthwhile to mention that the use of this pier group without collar produces 43 % reduction in scour depth upto 7.5° angle, 30% at 15° angle and 4.5 % at 30° angle as compared to the round-nosed rectangular pier of same length to width ratio as that of this pier group. Application of collar around this pier group leads to 100% reduction in the scour depth upto 7.5° angle of attack. However, as the angle of attack increases, the percent reduction in scour depth decreases and reaches to 42% at an angle of 30°. These results are in perfect agreement with the findings of Chabert and Engeldinger (1956).

Utilization of a group of two 41.5 mm diameter circular piers with clear spacing of 2 pier diameter between them without collar at 0° angle enhances the scour depth of front pier by 10% as compared to that of an isolated pier while at 45° angle, scour depth of front pier gets increased by 17.7%. At 90° angle, the scour depth at the two piers is found about 16% higher than that of an isolated pier.

Application of a collar to this pier group at angles of attack of flow 0° to 90° yields excellent results at smaller angles of attack. The maximum reduction in scour depth with collar relative to that without collar at 0° angle is found to be78.57%. However, an increase in angle of attack reduces the efficiency of collar in reducing the scour depth. At angle of 90°, the percent reduction remains only 23.07%. These results are well comparable with the findings of Zarrati *et. al.* (2006). Use of this pier group without collar at 0° angle produces a scour depth about 0.89 times of that occur at an isolated round-nosed rectangular pier of the same length to width ratio as that of the pier group.

The results of this study constitute a methodology for realistic estimation of scour depth at group of bridge piers and impact of mutual interference of bridge piers on local scour. The study is expected to provide a valuable record and practical guidance for tackling the problems of pier group local scour.

Synopsis of thesis

Chapter-I presents the introduction of the research carried out in this thesis. In Chapter-II, the background and current state of knowledge of scour, temporal development of scour and literature related to the use of various scour countermeasures including a collar for pier scour mitigation are covered. Chapter-III gives a description of the experimental apparatus, models and procedures. Chapter-IV presents the technique of Artificial Neural Network (ANN) which is used for modeling in this thesis. The graphical representation based analysis of the results generated through experimental program is presented in Chapter V. The analysis of results based on Artificial Neural Network approach is presented in Chapter VI. Finally, the principal conclusions drawn from the results of the study and scope for further studies are presented in Chapter-VII. The summary of flow parameters used in this study and exhaustive experimental data gathered from present investigation is presented in Appendices I-VII.

EFFECT OF MUTUAL INTERFERENCE OF BRIDGE PIERS ON LOCAL SCOUR

THESIS
Submitted for the award of the Degree of

Doctor of Philosophy
IN
CIVIL ENGINEERING

BY

MUBEEN BEG

DEPARTMENT OF CIVIL ENGINEERING
ZAKIR HUSAIN COLLEGE OF ENGINEERING & TECHNOLOGY
ALIGARH MUSLIM UNIVERSITY
ALIGARH (INDIA)

June 2008

DEPARTMENT OF CIVIL ENGINEERING
Z.H. COLLEGE OF ENGINEERING & TECHNOLOGY,
ALIGARH MUSLIM UNIVERSITY, ALIGARH – 202 002, U.P., INDIA

CERTIFICATE

This is to certify that the work embodied in this thesis entitled **"Effect of Mutual Interference of Bridge Piers on Local Scour"** is an original work carried out by **Mr. Mubeen Beg,** Lecturer, Department of Civil Engineering under my supervision and is suitable for submission for the award of **Ph.D. degree** in Civil Engineering of the Aligarh Muslim University, Aligarh, India.

12.7.2008

Professor Mohammad Jamil
(Supervisor & Chairman)

CANDIDATE'S DECLARATION

I hereby declare that the work which is being presented in the thesis entitled **"The Effect of Mutual Interference of Bridge Piers on Local Scour"** in fulfillment of the requirement for the award of the degree of Doctor of Philosophy and submitted in the Department of Civil Engineering of the Z.H. College of Engineering & Technology is an authentic record of my own work carried out under the supervision of Professor Mohammad Jamil, Chairman, Department of Civil Engineering.

The matter presented in this thesis has not been submitted by me for the award of any other degree of this or any other University.

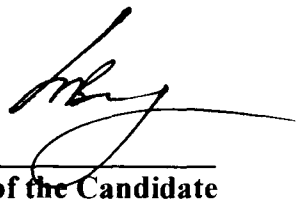

Signature of the Candidate

ABSTRACT

Scour is defined as the erosion of streambed around an obstruction in a flow field. The amount of reduction in the streambed level below the bed level of the river prior to the commencement of scour is referred as the scour depth. A scour hole is defined as depression left behind when sediment is washed away from the riverbed in the vicinity of the structure.

The local scour has the potential to threaten the structural integrity of bridge piers, ultimately causing failure when the foundation of the pier is undermined. Besides the human loss, bridge failures cost millions of dollars in direct expenditure for replacement and restoration in addition to the indirect expenditure related to the disruption of transportation facilities. A series of recent bridge failures due to pier scour, as reported by Wardhana and Hadipriono (2003), S.Dey and Barbhuiya (2004) and Hoffmans and Verheij (1997), rekindled interest in furthering for developing improved ways of estimating the maximum scour depth and protecting bridges against the ravages of scour.

An exhaustive amount of literature which exists on local scour reveals that the problem of local scour around bridge pier received a lot of attention in the past from theoretical and practical point of view in an attempt to quantify the equilibrium depth of scour. However, among the large number of experimental and field studies, (*e.g.*, Laursen and Toch (1956), Chabert and Engeldinger (1956), Chew (1984), Raudkivi (1998), Ettema (1980), Melville and Sutherland (1988), Mostafa (1998) and Johnson (1995) etc.), the problem of scour around a single pier has been mainly focused and more meticulously investigated than the problem of scouring around hydraulically interacting multiple piers. A scanty amount of literature on pier group scour is available [*e.g.*, Hannah (1978), Elliott and Nicollet (1978) and Zarrati *et. al.* (2004, 2006)].

In the case of pier group scour, the presence of several piers can generate a more complex interaction in the hydrodynamic characteristics of the flow field near the piers themselves and therefore, the flow pattern in the channel around the piers gets changed significantly and lead to the occurrence and development of a scour process that is quite different from one which occurs around a single pier. This interaction is particularly evident when the

bridge is not perpendicular to the river flow. Hannah (1978) studied the local scour at piers group and recognized four mechanisms of scour (*e.g.*, reinforcing, sheltering, shed vortices and compressed horseshoe vortices) to occur which make the scour phenomenon more complex and which can modify the depth and shape of the scour hole around the piers.

Therefore, if a bridge pier is merely designed and constructed considering as a single pier, it may lead to the bridge failure because mutual interference of several piers can enhance the scour depth at the piers. In these perspectives, to ensure the stability of the bridge piers, the need of a study on the effect of mutual interference of bridge piers on local scour assumes immense significance which is the subject of present study.

Many situations, which are common in the field where the bridge pier groups are founded in the riverbed in different patterns of arrangements, are worth mentioning.

Due to rapid urbanization and increased traffic volume, it is often required to construct new bridges across the rivers in the proximity of the already existing bridge. There are limitations of spacing between existing and new bridges due to the problem of land acquisition. In that context, the scour depth and bed configuration pattern around the existing and new bridges need to be examined. Furthermore, for geo-technical and economical reasons, pier groups have been more and more popular in bridge design.

A bridge across a river is usually supported on a number of piers placed along its span where piers are located in a direction normal to the flow at some finite spacing. Two or more number of piers are often placed in line with the flow along width of a bridge. Railway tracks and highways are often constructed side by side across the same river such that they are located at some short distance apart. When the river runs through downtown in cities, which are subjected to an increase in population, the existing bridges constructed across the river become inadequate for traffic movement owing to an increase in traffic volume. This results in frequent traffic jams and traffic movement is halted, some times for hours together jeopardizing the whole transport system and causing untold miseries to the people. The stranded transport has to wait for traffic clearance to reach to their destination, which causes delay in achieving their goals. As a result this adversely affects the development of the country and causes enormous economical losses to the

people. In such eventuality, therefore, construction of new bridges for people movement, industrial production etc become imminent and the new bridges are often constructed at very short distances to facilitate the efficient and smooth traffic movement. A number of piers are also provided in the construction of hydraulic structures like an aqueduct to support the trough carrying canal water from one end of the drain to the other. Electricity and telephone lines are often carried across the river wherein electric and telephone polls are founded in the riverbed on a group of piers.

In the background of aforementioned field conditions, different arrangements of piers such as tandem, transverse and staggered, have been identified as study area to accomplish the major objectives of this research using experimental approach.

In order to study the effects of mutual interference of piers on local scour, a series of clear-water scour experiments has been conducted considering different patterns of pier arrangement and relationships have been developed for the estimation of scour depth at group of piers.

In the present investigation, experiments were conducted in a 12.0 m long, 0.756 m wide and 0.55 m deep, glass sided re-circulating rectangular tilting flume under steady uniform flow clear-water scour conditions. Non-ripple forming uniform sediment was used as bed material since, according to Breusers and Raudkivi (1991), ripples do not form at median sediment diameter $d_{50} \geq 0.7$. The bed material used in present experiments is considered uniform as the geometric standard deviation $\sigma_g = \left(\frac{d_{84.1}}{d_{15.9}}\right)^{1/2}$ of the material is less than 1.3~1.5. The experiments were conducted at flow intensity $\frac{u_*}{u_{*c}} = 0.95$ since according to Raudkivi and Ettema (1977a, b), for non rippling sediments, clear–water scour experiments can run successfully with a flow condition $\frac{u_*}{u_{*c}} = 0.95$. Average flow depth y_0 of 140 mm was chosen in accordance to the statement of most researchers that the influence of flow depth can be neglected if the ratio of flow depth to pier width $\frac{y_0}{b} > 2$ to 3. Experiments were first conducted on a single pier of diameter (b) 33 mm to form a basis against which the effect of mutual interference of bridge piers configured in different arrangements could

be evaluated. The pier sizes were chosen in accordance to Melville and Sutherland (1988) and Melville (1997) where they showed that the scour depth in uniform sediment is independent of sediment size when sediment coarseness ratio $\frac{b}{d_{50}}$>25. Next, a series of experiments on piers of same diameter as that of single pier, placed in tandem, lateral and staggered arrangement at varied pier spacings, was conducted. Then a series of experiments on a group of piers placed at constant angle of attack (45°) and varied radial pier spacings from 0 to 12 times the pier diameter was considered. Next, a series of experiments with constant radial (R) spacing and varied angles of attack from 0° to 90°, was conducted. A series of experiments was also conducted for two cases of tandem arrangement using two different sizes of piers (33 mm and 66 mm diameter), by placing larger diameter pier at front and smaller diameter pier at rear in first case and smaller diameter pier at front and larger diameter pier at rear in the second case respectively. The selection of the sizes of two piers was made just on a trial basis to get pier size ratios of 2 and 0.5 for the case first and second respectively. The basis of use of two different size piers is the recent technological advancement due to which narrow piers are being preferred and constructed in order to achieve economy. Prior to the experiments on group of piers of different sizes placed in tandem arrangement, a series of experiments was conducted on larger diameter (66 mm) single pier to form a basis against which the effect of mutual interference of piers could be evaluated. In the last phase, experiments were conducted on group of piers with and without collar. A group of piers comprising of cylinders of varied sizes (21.5 mm to 46 mm diameter) with and without collar and aligned to the flow at angles of attack from 0° to 30°, was tested to investigate the use of piers group for scour depth reduction. The selection of different pier sizes for this pier group was made considering the limitation of constriction ratio as suggested by Shen *et. al.* (1966) in order to avoid the blockage effect of pier group on local scour. As Raudkivi (1986) in discussing effects of pier alignment also states that the use of cylindrical columns would produce a shallower scour as compared to a solid pier, a group of two circular piers (41.5 mm diameter) separated at clear spacing of two pier diameter for varied angles of attack to the flow from 0° to 90° with and without collar, was tested to investigate the efficacy of this pier group in reduction of scour depth as compared to the use of a round–nosed rectangular pier of same length to width ratio (4:1) under same flow and sediment conditions.

Extensive data on local scour for different pier arrangements along with the group of piers with and without collar were collected for use in the modeling approach developed herein. The data, like, scour depth, areal extent of scour, scour depth profiles along flow direction and across the flow, were measured and recorded. Further the data on lengths and slopes of scour holes at upstream and downstream face of piers, width of scour holes, length of sediment deposition at downstream face of piers and temporal scour depth variation collected in present experimental programme, were analyzed to evaluate the mutual interference of bridge piers on local scour. Scour and deposition features developed by the flow after completion of the test, were also photographed.

As the analytical prediction of pier group local scour is very difficult due to complex nature of flow patterns occurring around the piers, two different modeling approaches namely, graphical relationships based approach and ANN based approach, have been developed and implemented.

The first approach predicts and analyses the various elements of pier group scour using graphical relationships. This approach considers the graphical presentation of the effect of pier spacing along and across the flow direction and angle of attack of flow, on various elements of pier group scour.

The second approach involves the use of a non-parametric ANN technique based on feed forward back propagation neural network (BPNN) for establishing relationships between pier spacing or angle of attack (the angle between flow direction and the line joining centre of piers) and scour depth. The ANNs could be trained with sufficient accuracy by using only one input variable viz. pier spacing or angle of attack. The results from both experimental based approach as well as ANN based approach were found to be in close agreement with each other (R^2~0.96-0.99).

ANN models are developed using feed forward back propagation learning algorithm in MATLAB neural network toolbox. Application of ANN on author's experimental data produces good estimate of scour depth at pier groups arranged in different patterns and these results are well comparable with existing published data of Hannah (1978), Chabert and Engeldinger (1956) and Richardson *et. al.* (1993). The results reveal that for training and testing sets, all the neural networks trained, produced higher R^2 and lower RMSE

values of the order ~ 0.99. Also, almost all the neural networks trained required relatively equal number of iterations to reach the global minima. The correlation coefficient R^2 between observed and ANN estimated scour depths represents the predictive ability of ANN models. Understanding and analyzing the effect of factors, like pier spacing between the piers or angles of attack of flow, to evaluate their effect on scour depth to accurately and effectively estimate the scour depth and other scour characteristics was the main focus of this research.

Based on the experimental results achieved in present research on pier group scour, significant effect of mutual interference of piers on local scour is found. In the case of tandem arrangement, when a group of two identical circular piers is placed at pier spacing of 1.5 times the pier diameter, the scour depth of front pier gets enhanced by 17 % as compared to the scour depth of an isolated pier whereas placement of it at pier spacing of 12.5 times the pier diameter causes a reduction of 33% in scour depth of rear pier. When a group of three identical circular piers are placed in tandem arrangement, the scour depth of front pier increases by 11% whereas at rear pier gets reduced by about 33.5%, as compared to that of a single pier. The scour depth at middle pier is about 15.5% higher than that of the rear pier. In the case of a group of two different size piers placed in tandem arrangement (such that larger pier is placed at front and smaller one at rear), scour depth at larger pier corresponding to the scour depth of an isolated larger pier, gets enhanced by 8%. However, scour depth at smaller pier corresponding to the scour depth of an isolated smaller pier becomes 0.57 times lower at pier spacing of 35 times the pier diameter The scour depth at smaller pier relative to that of an isolated larger pier becomes 0.33 times of that occurs at 66 mm isolated pier. When a group of two different size piers is placed in tandem arrangement such that smaller pier is placed at front and larger one at rear, scour depth at smaller pier at zero pier spacing increases by 28.5 % as compared to that at an isolated smaller pier, however, the scour depth at larger pier as compared to the scour depth at an isolated larger pier, gets reduced by 23% at the same pier spacing. The scour depth at larger pier as compared to an isolated larger pier gets reduced by 37% at pier spacing of 5 times the diameter of smaller pier.

When a group of two identical circular piers is placed in lateral arrangement (normal to the direction of flow) at zero pier spacing, scour depth is 1.95 times of that occurs at an isolated pier. Though, the scour depth of two piers rapidly decreases at pier spacing of one pier

diameter, nevertheless it remains 21 % higher than that of an isolated pier. At lateral pier spacing of 8 times the pier diameter, although, the scour depth at two piers becomes same as that of an isolated pier, however, the sizes of the scour holes are not identical to that for an isolated pier.

In case of a group of three piers placed in staggered pattern, scour depth at upstream and downstream piers gets increased by 40.5% and 12.5% as compared to that at an isolated pier respectively.

At group of two piers aligned at 45° to the flow at zero radial pier spacing, the scour depth gets enhanced by 12% as compared to that occurs at the group of two piers aligned normal to the flow at zero radial pier spacing. However, when the radial pier spacing between the two piers increases to one pier diameter, the scour depths at front and rear piers gets enhanced by 35% and 38% respectively as compared to that occur at an isolated pier respectively.

When the group of two piers having a clear radial pier spacing of 4 times the pier diameter, are aligned at an angle of 0° to the flow, scour depth at front and rear piers equals to 1.1 and 0.96 times of that occur at an isolated pier. When angle of attack of flow becomes 45°, scour depths at front and rear piers get enhanced by 17.4% and 24.1% as compared to the scour depth of an isolated pier. At 90° angle of attack, the scour depths of two piers become equal but are still 4.5% higher than that at an isolated pier.

These findings acquired in present investigation suggest that the group effect of piers on local scour is highly significant and should be properly incorporated in the pier design.

A major contribution of this study is the experimental description of method of scour depth reduction by applying a collar around group of piers. Enthusiastic results are obtained for pier protection against local scour by the application of collar around group of piers comprising of varying sized cylinders. These experimental results are found in good agreement when compared with the published data of Chabert and Engeldinger (1956). Also, replacement of a rectangular pier with a group of piers is experimentally investigated for economical design of pier by saving the material and reducing the depth of scour and the experimental results so obtained, are well comparable with the published experimental data of Zarrati *et. al.* (2004, 2006).

When a pier group comprising of varied sizes of piers without collar is tested at 0° angle, a reduction of 44% in the scour depth as compared to an isolated pier of diameter equal to the diameter of the largest cylinder used in this pier group, is achieved. The use of this pier group without collar upto an angle of 10° to the flow proves to be very effective as its use reduces the scour depth by 33% as compared to an isolated pier of diameter equal to the diameter of largest pier diameter used in this pier group. It is worthwhile to mention that the use of this pier group without collar produces 43 % reduction in scour depth upto 7.5° angle, 30% at 15° angle and 4.5 % at 30° angle as compared to the round-nosed rectangular pier of same length to width ratio as that of this pier group. Application of collar around this pier group leads to 100% reduction in the scour depth upto 7.5° angle of attack. However, as the angle of attack increases, the percent reduction in scour depth decreases and reaches to 42% at an angle of 30°. These results are in perfect agreement with the findings of Chabert and Engeldinger (1956).

Utilization of a group of two 41.5 mm diameter circular piers with clear spacing of 2 pier diameter between them without collar at 0° angle enhances the scour depth of front pier by 10% as compared to that of an isolated pier while at 45° angle, scour depth of front pier gets increased by 17.7%. At 90° angle, the scour depth at the two piers is found about 16% higher than that of an isolated pier.

Application of a collar to this pier group at angles of attack of flow 0° to 90° yields excellent results at smaller angles of attack. The maximum reduction in scour depth with collar relative to that without collar at 0° angle is found to be78.57%. However, an increase in angle of attack reduces the efficiency of collar in reducing the scour depth. At angle of 90°, the percent reduction remains only 23.07%. These results are well comparable with the findings of Zarrati *et. al.* (2006). Use of this pier group without collar at 0° angle produces a scour depth about 0.89 times of that occur at an isolated round-nosed rectangular pier of the same length to width ratio as that of the pier group.

The results of this study constitute a methodology for realistic estimation of scour depth at group of bridge piers and impact of mutual interference of bridge piers on local scour. The study is expected to provide a valuable record and practical guidance for tackling the problems of pier group local scour.

Synopsis of thesis

Chapter-I presents the introduction of the research carried out in this thesis. In Chapter-II, the background and current state of knowledge of scour, temporal development of scour and literature related to the use of various scour countermeasures including a collar for pier scour mitigation are covered. Chapter-III gives a description of the experimental apparatus, models and procedures. Chapter-IV presents the technique of Artificial Neural Network (ANN) which is used for modeling in this thesis. The graphical representation based analysis of the results generated through experimental program is presented in Chapter V. The analysis of results based on Artificial Neural Network approach is presented in Chapter VI. Finally, the principal conclusions drawn from the results of the study and scope for further studies are presented in Chapter-VII. The summary of flow parameters used in this study and exhaustive experimental data gathered from present investigation is presented in Appendices I-VII.

ACKNOWLEDGEMENT

I bow in reverence to the Almighty Allah whose benign benediction gave me the required zeal for completion of this work.

I wish to express my deep sense of gratitude to **late Padam Shree Dr. Mohammad. Shafi, Professor Emeritus, Dept. of Geography, AMU, Aligarh** for his encouraging, caring words, inspiration and guidance which have contributed in a significant way towards completion of this thesis. I shall always be indebted to him for checking chapters I and II of my thesis despite his old age. I do not have words to express his all kindness and help. I pray for him, for the best returns from Almighty. May Allah provide him all good things hereafter.

I wish to express my sincere gratitude to my revered and learned supervisor **Prof. Mohammad Jamil, Chairman, Department of Civil Engineering**, Faculty of Engineering and Technology, Aligarh Muslim University, Aligarh for his illuminating, scholarly guidance and creative supervision right from its inception to its culmination in the present work. He has always been inexhaustible source of inspiration and guidance to me. Without his unceasing encouragement and cooperation this work would not have completed. I humbly acknowledge a lifetime's gratitude to him.

I am extremely grateful to **Professor Razaullah Khan, Department of Civil Engineering**, A.M.U., Aligarh for his encouragement, profitable advice, moral support and selfless help extended by him as and when needed.

I express my special thanks to **Gijs Hoffmans**, **Directorate-General** for Public Works and Water Management, Delft, **The Netherlands** and **Dr. Anwar Husain,** Nephrologist, Amsterdam, **The Netherlands**, **Patrick Dare Alabi,** University of Saskatchewan, **Canada**, and **Dr. Monowar Hossain,** professor, Department of Water Resources Engineering, **BUET, Dhaka, Bangladesh** for their wise suggestions and help in the completion of this thesis.

I am extremely grateful to my colleagues Prof. M.M. Ashhar and Prof. **Hussain Abbas**, Mr. F.Ghani, Mr. S.A. Khan, Prof. **V.P.Mital**, Prof **P.A. Saini**, Prof. S.S. Shah, Dr. Mohd. Muzzammil, Dr. S.A. Ansari, Dr, M. Athar, Dr. Talib Mansoor, Mr. Mujib A.

Ansari and Mr. Mahboob Anwar Khan and other teaching staff members of the Department of Civil Engineering, AMU Aligarh for their encouragement and cooperation.

I also extend my sincere thanks to **Dr. Mohd. Shakeel**, Professor, Department of Civil Engineering, Dr. Ahrar Husain, Professor, Institute of Advanced Studies in Education, Jamia Millia Islamia for their encouragement, inspiration and cooperation in completing this work.

My indebtedness towards the kind hospitality and willful support rendered by Prof Dr. **R.D. Gupta** and Mr. Arshad Raza Khan, retired Professors, Department of Civil Engineering, Z.H. College of Engineering & Technology, AMU, Aligarh.

I would like to express my deep gratitude to **Dr. Saif Saeed**, Lecturer, Department of Civil Engineering, J.M.I., New Delhi, for offering his thoughtful insight on Artificial Neural Network at various stages of this research. His companionship all along the vicissitudes of research helped me pull through with my work.

I would like to thank **Mr. Musarrat Ali**, Mr. S. Sarwat Nazir, Dr. Vinod Kumar and other administrative staff of Civil Engineering Dept., **Mr. Mohd. Khalid, Mr. Haseeb Beg** and Mr. Mohd. Jamil, office of the Dean, Faculty of Engineering & Technology, AMU, Aligarh for their administrative help at various stages in my Ph.D. tenure

Thanks are due to my friends, **Dr. Javed Musarrat** and **Dr. Akhtar Haseeb**, Professors, Faculty of Agriculture, **Dr. Saad Tayyab**, professor, University of Malaya, Kuala Lumpur, Malaysia, **Dr. M.H. Beg** and **Dr. Tariq Mansoor**, Professors, Surgery Department, JNMC, **Mr. Nafees Ahamd-II**, Reader, Mechanical Engineering Department, **Dr. Zahid Ali**, Reader, Academic Staff College, **Mr. Mohd. Mohsin**, Lecturer, University Polytechnic, AMU, Aligarh for being at an arms' distance throughout.

I am also very grateful to **Mr. Anis Ahmad,** Warsi Clinic, Medical Road, Aligarh for providing me an immediate medical help whenever needed during the tenure of completion of this thesis.

I am also thankful to all non-teaching staff members, especially **Mr. Mohd. Sajid,** attendant and Mr. Mir Shaukat Ali, J.T.O., Hydraulics Laboratory, Mr. Mohd. Aqeel, attendant, Environmental Engineering Laboratory of Civil Engineering Department,

AMU Aligarh, for their help and cooperation whenever needed in running the laboratory smoothly during the experimentation.

I sincerely acknowledge the help and cooperation, which I received from **Mr. Jameel Ahmad**, in scanning of photographs, composing and typing of my thesis. His sincerity and punctuality will always be remembered.

I extend my thanks to M/S. **Mohd Suhail, Mohd. Aqeel** and Mohd. Jamal for their cooperation in maintaining the computer peripherals in order during the compilation of this thesis.

I would like to thank to M/s Rakhi Studio, Jamalpur, Aligarh for photography during experimentation programme of this thesis.

I owe deep sense of gratitude to All-pervading Spirit whose Devine Light provided me the perseverance, guidance, inspiration, faith and strength to carry on even when the going got tough. My special sincere, heartfelt gratitude and indebtedness are due to my sister Baby, brothers Musharraf Beg, Rais Beg and nephews **Salman Beg** and Osama Beg, for their sincere prayers, constant encouragement and blessings. I am grateful to all of them as they suffered a lot due to my business in the completion of this thesis.

Finally, my heart goes on a spin when I think of the contribution of my **late parents** towards whatever little or much I have been able to achieve. Without their blessings and emotional strength I would have never seen this day. Both of them suffered a lot due to their isolation from me during experimentation. I pray for them, for the best returns from Almighty Allah. May Allah provide them all the good things in the Heaven.

(Mubeen Beg)

TABLE OF CONTENTS

		Page No.
	Candidate's Declaration	*i*
	Abstract	*ii*
	Acknowledgement	*xi*
	Table of Contents	*xiv*
	List of Figures	*xxiii*
	List of Tables	*xxxiv*
	List of Notations	*xxxv*
	List of Photographs	
CHAPTER – I: INTRODUCTION		**1 – 10**
1.1	Local Scour around Single Bridge Pier	2
1.2	Local Scour at Group of Bridge Piers	3
1.3	Mechanism of Scour around Piers Group	5
1.4	Scour Depth Prediction Using Artificial Neural Network (ANN)	6
1.5	Concluding Remark	7
1.6	Aim of the Present Study	7
CHAPTER – II: LITERATURE REVIEW		**11 – 75**
2.0	Introduction	11
2.1	Mechanics of Local Scour around an Isolated Pier	14
	2.1.1 Shape of the scour hole	17
	2.1.2 Length of scour hole	17
	2.1.3 Top width of scour hole	17
	2.1.4 Slopes of scour hole	18
	2.1.5 Bed level variation along flow direction	18
2.2	Classification of Local Scour	19
2.3	Scour Depth Prediction at an Isolated Pier	25
2.4	Parameters Governing Scouring	32
	2.4.1 Influence of approach flow velocity	34
	2.4.2 Influence flow intensity	35
	2.4.3 Influence of flow depth	36
	2.4.4 Influence of sediment size	38
	2.4.5 Sediment coarseness	39
	2.4.6 Influence of pier shape	39
	2.4.7 Influence of pier size	41
	2.4.8 Influence of angle of attack k_θ	42
	2.4.9 Influence of constriction Ratio	46
	2.4.10 Effect of opening ratio	47
	2.4.11 Influence of sediment grading	47
2.5	Equilibrium Scour Depth and Time of Equilibrium	49
	2.5.1 Development of maximum scour depth with time	49
2.6	Interference Effects of Multiple Piers on Flow	50
	2.6.1 Tandem arrangement (*i.e.*, aligned in the flow direction)	50

	2.6.2	Side by side arrangement (*i.e.*, spaced laterally apart)	50
	2.6.3	Staggered arrangement (*i.e.*, spaced both longitudinally and laterally)	50
2.7		Interference Effects of Multiple Piers on Local Scour	51
	(i)	Reinforcing	52
	(ii)	Sheltering	52
	(iii)	Vortex shedding	52
	(iv)	Horseshoe vortex compression	52
	2.7.1	Two Piers in Tandem Arrangement (Angle of attack 0°)	53
	2.7.2	Three Piers in Tandem Arrangement	53
	2.7.3	Two piers in side by side arrangement (Angle of attack 90°)	53
	2.7.4	Piers in staggered arrangement	54
		(a) Phase – I (angle of attack, 45°)	54
		(b) Phase – II (Effect of angle of attack,α)	54
	2.7.5	Tandem arrangement	55
	2.7.6	Side-by-side arrangement	55
	2.7.7	Staggered arrangement	55
2.8		Local Scour Countermeasures	56
	2.8.1	Reduction and protection of scouring around bridge piers	57
	2.8.2	Flow pattern and mechanism of scouring	58
	2.8.3	Armoring devices	58
	2.8.4	Scour protection using rip-rap	59
	2.8.5	Flow altering devices	59
	2.8.6	Scour reduction using slots	59
	2.8.7	Scour reduction using collar	61
	2.8.8	Scour reduction using sacrificial piles	63
	2.8.9	Foundation Caissons	63
	2.8.10	Delta-wings like passive device	63
	2.8.11	Other methods of scour protection	64
	2.8.12	Submerged vanes	64
	2.8.13	Other methods of scour protection	65
	2.8.14	Submerged vanes	65
	2.8.15	Slanting vanes on front face of piers	66
	2.8.16	Stone gabion with geotextile filter	66
	2.8.17	Use of tetrapods as artificial rip-rap	66
	2.8.18	Concrete filled fabric mats	67
	2.8.19	Concluding remarks	67
2.9		Scour Depth Prediction Using Artificial Neural Network (ANN)	67
	2.9.1	Concluding remarks	71
2.10		Conclusion on Review of Literature	71

CHAPTER – III: EXPERIMENTAL PROGRAMME **76 – 101**

3.0	Introduction	76
3.1	Properties of Sediment Used	67
3.2	The Approach Flow and Flow Measurement	78
3.3	Mean Flow Parameters Used in the Experiments	79
3.4	Experimental Set-Up	80
	3.4.1 Duration of experimental runs	83

	3.4.2	Experimental procedure	84
		(i) The temporal development of the scour hole	85
		(ii) The mechanism of local scour	85
		(iii) Water temperature	86
		(iv) Scour hole profiles	86
3.5		Introduction	86
	3.5.1	Phase I: Local scour at single pier	87
	3.5.2	Phase II: Local scour around piers in tandem arrangement	88
	3.5.3	Phase III: Local scour around piers in lateral arrangement	91
	3.5.4	Phase IV: Local scour around piers in staggered arrangement	93
	3.5.5	Phase V: Local scour around piers with constant angle of attack and varying radial pier spacing	94
	3.5.6	Phase VI: Local scour around piers with constant radial pier spacing and varying angles of attack	95
	3.5.7	Phase VII: Local scour protection around piers group	96
		(a) Part one: Local scour around a group of two circular piers with and without collar	96
		(b) Part two: Local scour at a group of varying sized circular piers	99

CHAPTER – IV: MODELING BASED ON ARTIFICIAL NEURAL NETWORKS (ANN) APPROACH **102 –108**

4.0		Artificial Neural Network (*ANN*)	102
4.1		Introduction	102
	4.1.1	Network structure	103
	4.1.2	Learning algorithms	104
	4.1.3	Feed-forward back propagation neural network	105

CHAPTER – V: ANALYSIS OF RESULTS AND DISCUSSION BASED ON GRAPHICAL REPRESENTATION APPROACH **109 – 282**

5.0		Introduction	109
5.1		Single Circular Cylindrical Pier	110
	5.1.1	Flow patterns at a cylindrical pier	110
	5.1.2	Longitudinal profile of scour	112
	5.1.3	Lateral profiles of scour	113
	5.1.4	Areal extent of scour	114
	5.1.5	Temporal variation of scour	116
5.2		Two Circular Piers of Same Size in Tandem Arrangement	117
	5.2.0	Introduction	117
	5.2.1	Variation of scour depth along flume length	117
	5.2.2	Variation of scour depth with pier spacing	119
	5.2.3	Dimensions of scour holes	123
		(a) Length of scour holes	123
		(b) Length of scour hole at upstream face of front pier	124
		(c) Length of scour hole at upstream face of rear pier	124
		(d) Length of scour hole at downstream face of front pier	125
		(e) Length of scour hole at downstream face of rear pier	125
		(f) Slope of scour holes	126

(i) Slope of scour holes at upstream face of front pier 126
(ii) Slope of scour holes at upstream face of rear pier 127
(iii) Slope of scour holes at downstream face of front pier 127
(iv) Slope of scour holes at downstream face of rear pier 128
(g) Width of scour holes 128
(h) Variation of area of scour extents with pier spacing 130
(i) Length of sediment deposition at downstream face of piers 133
5.2.4 Temporal variation of scour depth at front and rear piers 134
5.2.5 Concluding remark 135
5.3 Three Piers of Same Size in Tandem Arrangement 136
5.3.0 Introduction 136
5.3.1 Variation of scour depth along flume length 136
5.3.2 Scour depth at front, middle and rear piers 137
5.3.3 Scour depth at middle and rear piers with respect to front pier 138
5.3.4 Characteristics of scour hole 140
(a) Length of scour hole at upstream face of piers 140
(b) Length of scour hole at downstream face of piers 141
(c) Slope of scour holes 142
(i) Slope of scour hole at upstream face of piers 142
(ii) Slope of scour hole at downstream face of piers 143
(iii) Variation of area of scour extent around front, middle and rear piers with pier spacing 145
(iv) Width of scour holes 146
(v) Length of deposition on downstream of front, middle and rear piers 147
5.3.5 Temporal variation of scour depth at front, middle and rear piers 148
3.5.6 Concluding remarks 149
5.4 Big Pier at Front and Small Pier at Rear (*i.e.*, 66 mm pier at Front and 33 mm Pier at Rear) 149
5.4.0 Introduction 149
5.4.1 Variation of scour depth along flume length 149
(a) Scour depth variation at 66 mm front pier 151
(b) Scour depth variation at 33 mm rear pier 153
(c) Scour depth variation between 66 mm front and 33 mm rear piers 153
(d) Scour depth at 33 mm rear pier with respect to 66 mm front pier 154
5.4.2 Scour hole dimensions 155
(a) Length of scour holes 155
(b) Length of scour holes at upstream face of piers 156
(c) Scour hole length on downstream of piers 158
(d) Scour hole length at downstream face of 66 mm front pier 158
(e) Length of scour hole at downstream face of 33 mm rear pier 159
(f) Variation of area of scour extent with pier spacing 159
(g) Width of scour holes 162
(h) Length of Sediment Deposition 165
5.4.3 Temporal Variation of Scour 166

5.4.4 Concluding remarks 167
5.5 Small Pier at Front and Big Pier at Rear (*i.e.*, 33 mm pier at front and 66 mm pier at rear) 167
5.5.0 Introduction 167
5.5.1 Variation of Scour Depth along Flume Length 168
5.5.2 Variation of Scour Depth at 33 mm Front and 66 mm Rear Piers with Pier Spacing 169
(a) Variation of scour depth at 33 mm front pier 169
(b) Variation of scour depth at 66 mm rear pier 170
(c) Variation of scour depth between 33 mm front and 66 mm rear pier 171
(d) Variation of Scour Depth at 66 mm Rear Pier With Respect to 33 mm Front Pier 171
5.5.3 Scour hole dimensions 172
(a) Shape of scour hole 172
(b) Length of scour holes 172
(c) Deposition of sediment at downstream face of 33 mm front and 66 mm rear pier 176
(i) Length of sediment deposition at downstream face of 33 mm front pier 176
(ii) Length of sediment deposition at downstream face of 66 mm rear pier 177
(d) Width of scour holes 178
(e) Slope of scour holes 178
(f) Variation of areal extent of scour with pier spacing 180
5.5.4 Temporal Variation of Scour 181
5.5.5 Concluding remarks 181
5.6 Lateral Pier Arrangement 182
5.6.0 Introduction 182
5.6.1 Variation of Scour Depth along Flume Length 182
5.6.2 Variation of Scour Depth at Front Face of Piers 182
5.6.3 Scour Holes Characteristics 185
(a) Length of scour holes 185
(b) Length of scour hole at upstream faces of piers 185
(c) Length of scour hole at downstream faces of piers 186
(d) Slope of scour holes 187
(i) Slope of scour holes at upstream faces of piers 187
(ii) Slope of scour holes at downstream faces of piers 187
(e) Variation of area of scour extent with pier spacing 188
(f) Width of scour holes 190
(g) Length of sediment deposition at downstream faces of piers 191
5.6.4 Temporal variation of scour depth 192
5.6.5 Concluding remarks 193
5.7 Staggered Arrangement of Piers 193
5.7.0 Introduction 193
5.7.1 Variation of scour depth along flume length 194
5.7.2 Scour depth variation at upstream and downstream piers 194

5.7.3 Scour depth variation between upstream and downstream piers 195
5.7.4 Scour depth variation at downstream pier with respect to upstream piers scour depth 196
5.7.5 Scour hole dimensions 197
(a) Length of scour holes 197
(b) Width of scour holes 199
(c) Variation of area of scour extent with pier spacing 201
(d) Length of sediment deposition at downstream face of upstream and downstream piers 205
5.7.6 Variation of angle of attack with longitudinal pier spacing 206
5.7.7 Scour depth at downstream pier with respect to an isolated pier at varying angles of attack (i.e., varying longitudinal pier spacing) 206
5.7.8 Temporal variation of scour 207
5.7.9 Concluding remarks 207
5.8 Two Piers at Constant Angle of Attack but Varying Radial Spacing 208
5.8.0 Introduction 208
5.8.1 Variation of scour depth along flume length 209
5.8.2 Scour depth at front and rear piers 209
5.8.3 Scour hole characteristics 210
(a) Scour hole characteristics at front and rear piers 211
(b) Length of scour hole at upstream faces of front and rear pier 211
(c) Length of scour hole at downstream faces of front and rear pier 212
(d) Slope of scour holes 213
(i) Slope of scour holes on upstream of front and rear piers 213
(ii) Slope of scour holes at downstream faces of front and rear piers 214
(e) Deposition of sediment at downstream faces of piers 215
(f) Variation of area of scour extent with radial pier spacings 216
(g) Width of scour holes 218
5.8.4 Temporal variation of scour depth 220
5.8.5 Concluding remark 221
5.9 Two Piers at Constant Radial Spacing but Varying Angles of Attack 'α'. 221
5.9.0 Introduction 221
5.9.1 Variation of scour depth along flume length 222
5.9.2 Scour depth at front and rear piers 222
5.9.3 Variation of bed level between the piers 223
5.9.4 Characteristics of scour holes 225
(a) Length of scour hole at upstream faces of piers 225
(b) Length of scour hole at downstream faces of piers 226
(c) Slope of scour holes at upstream faces of front and rear pier 227
(d) Slope of scour holes at downstream faces of front and rear piers 229
(e) Length of sediment deposition at downstream faces of front and rear piers 230

(f) Area of scour extent around the front and rear piers 230
(g) Width of scour holes at front and rear piers 232
5.9.5 Temporal variation of scour depth 233
5.9.6 Concluding remarks 234
5.10 Local Scour at a Group of Circular Piers of Varying Sizes 234
5.10.0 Experimental depiction of local scour around a group of circular piers of varied sizes aligned at different angles of attack (α) 234
(a) Piers group without collar 234
(b) Piers group with collar 236
5.10.1 Angle of attack (α) = 0° 236
5.10.2 Angle of attack (α) =7.5° 237
5.10.3 Angle of attack (α) =10° 237
5.10.4 Angle of attack (α) =15° 238
5.10.5 Angle of attack (α) = 30° 239
5.10.6 Scour depth at piers group without collar 241
5.10.7 Scour depth at piers group with collar 243
5.10.8 Efficiency of collar in the reduction of scour depth at piers group 244
5.10.9 Location of occurrence of maximum scour depth around piers group with and without collar 245
5.10.10 Characteristics of scour hole 245
(a) Length of scour holes at upstream and downstream of piers group without collar 245
(b) Length of scour hole at downstream end of piers group with collar 246
(c) Length of sediment deposition at downstream end of piers group without collar 247
(d) Length of sediment deposition at downstream end of piers group with collar 248
(e) Height of sediment deposition at downstream end of piers group with and without collar 249
(f) Location of occurrence of maximum deposition of sediment at downstream end of piers group without collar 249
(g) Location of maximum deposition of sediment with collar 250
(h) Areal extents of scour 251
(i) Width of scour holes 252
5.10.11 Temporal development of scour at piers group with and without collar 253
5.11 Local Scour at a Group of Two Piers With and Without Collar 254
5.11.0 Introduction 254
5.11.1 Phase-I: Experiments with single pier 255
5.11.2 Experiments on group of two piers with and without collar 256
5.11.3 Phase II: Experiments without collar 256
5.11.4 Experiments on piers group aligned with the flow (α= 0°) 256
5.11.5 Experiments on piers group aligned with the flow (α= 15°) 258

5.11.6	Experiments with the piers group skewed at ($\alpha = 30°$)	259
5.11.7	Experiments with the piers group skewed at ($\alpha = 45°$)	260
5.11.8	Experiments with the piers group skewed at ($\alpha = 60°$)	261
5.11.9	Experiments with the piers group skewed at ($\alpha = 75°$)	262
5.11.10	Experiments with the piers group skewed at ($\alpha = 90°$)	263
5.11.11	Phase III: Experiments with Collar	264
5.11.12	Experiments with collar at angle of attack at ($\alpha = 0°$)	265
5.11.13	Experiments with collar at angle of attack at ($\alpha = 15°$)	266
5.11.14	Experiments with collar at angle of attack ($\alpha = 30°$)	267
5.11.15	Experiments with collar at angle of attack at ($\alpha = 45°$)	268
5.11.16	Experiments with collar at angle of attack at ($\alpha = 60°$)	269
5.11.17	Experiments with collar at angle of attack ($\alpha = 75°$)	270
5.11.18	Experiments with collar at angle of attack at ($\alpha = 90°$)	271
5.11.19	Variation of scour depth	272
	(a) Maximum scour depth at front and rear piers	272
	(i) Maximum scour depth at front pier	272
	(ii) Maximum scour depth at rear pier	273
	(iii) Maximum scour depth at group of two piers with collar	274
	(iv) Comparison of maximum scour depth at group of two piers and round-nose rectangular pier aligned at varied angles of attack without collar	274
5.11.20	Efficiency of collar in scour depth reduction around a group of two piers	276
5.11.21	Comparison between studies of Zarrati *et. al.* 2006 and present study on scour depth reduction efficiency of collar around two piers aligned in line with flow	276
5.11.22	Comparison of efficiency of collar applied to a group of two piers and a round nose rectangular pier	277
5.11.23	Areal extent of scour	277
5.11.24	Length of scour holes	279
5.11.25	Length of scour hole at downstream face of two piers without collar	279
5.11.26	Length of sediment deposition at the downstream faces of front and rear piers without collar	280
5.11.27	Length of Sediment Deposition at Downstream of 41.5 mm Piers Group with Collar	281
5.11.28	Concluding remarks	282

CHAPTER–VI: ANALYSIS OF RESULTS AND DISCUSSION BASED ON ARTIFICIAL NEURAL NETWORK APPROACH **283 – 306**

5.1	Evaluation of Effect of Mutual Interference of Bridge Piers on Scour Depth around Group of Piers Using (*ANN*) Based Modeling Approach	283
5.2	Parameters Affecting Local Scour around Group of Piers	283
5.3	Equilibrium Scour Depth around a Group of Bridge Piers Founded in Cohesion less sediment	285
5.4	Scour Depth Estimation Using Artificial Neural Network (*ANN*)	288

Based Modeling Approach
(i) Selection of input and output variables 290
(ii) Data normalisation 290
(iii) Design of *ANN* architecture 291
(iv) Training of *ANN* 291
(v) Processing of unseen data 292
5.5 Analysis of Results Obtained from ANN Based Modeling 292

CHAPTER – VII: CONCLUSIONS AND FUTURE SCOPE **307 – 311**

6.0 General 307
6.1 Suggestions for further studies 311

References **312 – 334**

Appendix – I 335 – 365
Appendix – II 366 – 406
Appendix – III 407 – 440
Appendix – IV 441 – 472
Appendix – V 473 – 474
Appendix – VI 475 – 476
Appendix – VII 477 – 478
Appendix – VIII 479 – 479

LIST OF FIGURES

Fig. No.	Title	Page No.
2.1	An organogram showing various types of scour (after Richardson and Davis 1995).	12
2.2	Photograph of local scour at a group of rectangular piers in tandem arrangement (with permission from www.pepe:vasquez. com).	13
2.3	Flow characteristics around a cylindrical pier (after Kothyari *et. al.*, 1989).	14
2.4	Scheme of the horseshoe vertex system (after Yulistianto, 1998).	15
2.5	Illustration of the flow and scour pattern at a circular pier (after Melville & Coleman 2000).	15
2.6	Plan of a scour hole.	17
2.7	Top width of scour hole around a circular pier.	18
2.8	Bed level variation along flow direction.	19
2.9	Diagrammatic illustration of classification of local scour at a bridge pier.	20
2.10	Shields Chart for threshold condition of uniform sediments in water.	21
2.11	Average local scour depth at cylindrical piers in relatively deep water (after Chee 1982).	21
2.12	Laboratory data on average maximum local scour depth at a cylindrical pier (after Chee 1982).	22
2.13	Scour depth for a given pier and sediment size as a function of approach flow velocity (after Chabert and Engeldinger, 1956).	35
2.14	Flow intensity factor (after B.W. Melville, 1997)	35
2.15	Influence of flow depth on scour depth (after Melville & Sutherland, 1988).	36
2.16	Diagrammatic illustration of scour depth at a cylindrical bridge pier in uniform sediment.	38
2.17	Sediments coarseness factor (after Melville & Sutherland, 1988).	39
2.18	Sediment size factor for pier (after B.W. Melville, 1997).	39
2.19	Various shapes of piers.	40
2.20	Diagrammatic scour shapes at round – nosed rectangular pier (a) aligned with the flow (b) at an angle of attack.	42
2.21	Alignment factor Kα for piers not aligned with flow (after Laursen and Toch 1956).	43
2.22	Diagrams which show different stages in the scour process (after Maza and Sánchez, 1964).	44
2.23	Schematic Diagram of Flume with Pier.	47
2.24	Coefficient of k_σ as a function of the geometric standard deviation of the particle size (after Raudkivi and Ettema, 1977a, b).	48
2.25	Scour depth for a given pier and sediment size as a function of time (after Raudkivi and Ettema 1983).	49
2.26	Photo of Schohaire Creek Bridge April 5, 1987. Courtesy of the National Bridge Inventory Web Page.	57

2.27	Diagrammatic flow pattern at a cylindrical pier (after Raudkivi, 1986).	58
2.28	Slot through a pier.	60
2.29	Various Types of Slots.	60
2.30	Schematic illustration of a pier fitted with a collar.	62
2.31	Group of two piers with collar aligned with the flow.	62
2.32	Group of two piers with collar aligned transverse to the flow.	62
2.33	Definition of a delta wing-like passive device (after Gangadhariah and Gupta, 1992).	64
2.34	Flow Modification by Passive Device (after Gangadhariah and Gupta, 1992)	65
2.35	Definition sketch of submerged vanes (after Parker *et. al.*, 1998)	65
2.36	Slanting vanes attached to pier (after Parker *et. al.*, 1998)	66
2.37	Definition sketch of placement of tetrahedron frames (after Parker *et. al.*,1998).	67
3.1	Particle size distribution curve for the sediment used in present study.	77
3.2	Glass sided rectangular re-circulating tilting flume.	80
3.3	Test flume showing its different components.	81
3.4	Pier model arrangement in the flume.	83
3.5	Two piers of same size in tandem arrangement.	88
3.6	Three piers of same size in tandem arrangement.	89
3.7	Two piers of different size in tandem arrangement (larger size (6.6 cm) pier at front).	90
3.8	Two piers of different size in tandem arrangement (smaller size (3.3 cm) pier at front).	91
3.9	Piers of same size in lateral arrangement.	92
3.10	Piers of same size in staggered arrangement.	93
3.11	Piers at constant angle of attack 'α' and varying radial spacing '*R/b*'.	95
3.12	Piers at constant radial spacing '*5b*' and varying angles of attack 'α'.	95
3.13	Plan of a collar plate around two circular piers	96
3.14	Piers with collar at *0°* angle of attack 'α'.	97
3.15	Group of two piers with collar at different angles of attack 'α'	98
3.16	Group of piers of varying sizes without collar.	99
3.17	Piers group having different sizes of piers with and without collar.	100
3.18	A group of piers of varying sizes fitted with a collar.	101
4.1	A neural network processing node (*net* is the sum of weighted input values to the processing neuron).	103
4.2	Architecture of a simple three layer feed-forward neural network	104
4.3	Major neural network learning algorithms.	105
4.4	Typical error surface with local minima (*A* and *C* are the local minima, *B* is the global minimum).	108
5.1	Variation of scour depth along flume length for an isolated pier.	113
5.2	Lateral profile of scour drawn at upstream face of an isolated pier.	113
5.3	Lateral profile of scour drawn at rear face of the an isolated pier.	114
5.4	Lateral profile of scour drawn through the point of maximum sediment deposition.	114
5.5	Areal extent of scour around an isolated pier.	115

5.6	Temporal variation of scour at an isolated pier.	117
5.7	Variation of scour depth at two piers of same size placed in tandem arrangement along flume length at x/b=25.	118
5.8	Variation of scour depth at two piers of same size placed in tandem arrangement along flume length at x/b=30.	118
5.9	Variation of scour depth at two piers of same size placed in tandem arrangement along flume length at x/b=90.	118
5.10	Variation of relative scour depth 'ds/ds_i' at two piers of same size placed in tandem arrangement with pier spacing.	119
5.11	Variation of scour depth at two piers of same size placed in tandem arrangement along flume length at x/b=1.	119
5.12	Variation of scour depth at two piers of same size placed in tandem arrangement along flume length at x/b=10.	120
5.13	Variation of scour depth at two piers of same size placed in tandem arrangement along flume length at x/b=90.	120
5.14	Variation of scour depth 'ds/b' with pier spacing 'x/b' at two piers of same size in tandem arrangement.	121
5.15	Variation of scour depth at rear pier with respect to the scour depth at front pier 'ds_r/ds_f' for two piers of same size placed in tandem arrangement.	122
5.16	Variation of relative length of scour hole at upstream faces of front and rear piers '$L_{shu}/L_{shu(i)}$' with pier spacing 'x/b' for two piers of same size placed in tandem arrangement.	124
5.17	Variation of relative length of scour hole at downstream face of front and rear piers '$L_{shd}/L_{shd(i)}$' with pier spacing 'x/b' for two piers of same size placed in tandem arrangement.	125
5.18	Variation of relative slope of scour hole at upstream faces of front and rear piers '$S_{lu}/\ S_{lu(i)}$' with pier spacing 'x/b' for two piers of same size placed in tandem arrangement.	126
5.19	Variation of relative slope of scour hole at downstream faces of front and rear piers '$S_{ld}\ /S_{ld(i)}$' with pier spacing 'x/b' for two piers of same size in tandem arrangement.	127
5.20	Variation of scour hole width observed at front and rear piers 'w_1/wi' and 'w_2/w_i' with pier spacing 'x/b' for two piers of same size placed in tandem arrangement	129
5.21	Variation of scour hole width with pier spacing 'x/b' for two piers of same size placed in tandem arrangement (computed by the method of Richardson et al., 1993).	130
5.22	Variation of scour hole width observed at rear pier relative to that at front pier 'w_2/w_1' with pier spacing 'x/b' for two piers of same size placed in tandem arrangement.	130
5.23	Areal extent of scour around two piers of same size placed in tandem arrangement at x/b=25.	131
5.24	Areal extents of scour around two piers of same size placed in tandem arrangement at x/b=30.	131
5.25	Areal extents of scour around two piers of same size placed in tandem arrangement at x/b=90.	131
5.26	Variation of area of scour extent around two piers of same size placed in tandem arrangement with pier spacing 'x/b.'	132

5.27	Variation of area of scour extent around two piers of same size placed in tandem arrangement with pier spacing 'x/b'.	132
5.28	Variation of length of sediment deposition at downstream faces of front and rear piers '$L_{dep}/L_{dep(i)}$' with pier spacing 'x/b' for two piers of same size placed in tandem arrangement.	134
5.29	Variation of scour depth at three piers of same size placed in tandem arrangement at x/b=30.	136
5.30	variation of scour depth at three piers of same size placed in tandem arrangement at x/b=60	137
5.31	Variation of scour depth at front, middle and rear piers placed in tandem arrangement relative to the scour depth of an isolated pier 'ds_f/ds_i, ds_m/ds_i and ds_r/ds_i' with pier spacing 'x/b'.	137
5.32	Variation of scour depth at middle and rear pier relative to the scour depth at front pier placed in tandem arrangement 'ds_m/ds_f' and 'ds_r/ds_f' with pier spacing 'x/b'.	138
5.33	Variation of length of scour holes at upstream faces of front, middle and rear piers placed in tandem arrangement '$L_{shu(f)}/L_{shu(i)}$', '$L_{shu(m)}/L_{shu(i)}$' and '$L_{shu(r)}/L_{shu(i)}$' with pier spacing 'x/b'	140
5.34	Variation of relative length of scour hole at downstream faces of front, middle and rear piers placed in tandem arrangement '$L_{shd(f)}/L_{shd(i)}$', '$L_{shd(m)}/L_{shd(i)}$' and '$L_{shd(r)}/L_{shd(i)}$' with pier spacing 'x/b'.	141
5.35	Variation of scour hole slope at upstream faces of front, middle and rear piers placed in tandem arrangement '$S_{lfu(f)}/S_{lu(i)}$, $S_{lfu(m)}/S_{lu(i)}$ and $S_{lu(r)}/S_{lu(i)}$' with pier spacing 'x/b'.	143
5.36	Variation of scour hole slope at downstream faces of front, middle and rear piers placed in tandem arrangement '$s_{ld(f)}/s_{ld(i)}$, $s_{ld(m)}/s_{ld(i)}$ and $s_{ld(r)}/s_{ld(i)}$' with pier spacing 'x/b'.	144
5.37	Variation of scour depth at downstream faces of front, middle and rear piers placed in tandem arrangement with pier spacing 'x/b'(cm).	144
5.38	Areal extant of scour around three piers placed in tandem arrangement at x/b=30.	145
5.39	areal extant of scour around three piers placed in tandem arrangement at x/b=60.	145
5.40	Variation of area of scour extent around three piers placed in tandem arrangement relative to the area of scour extent at an isolated pier 'a_r/a_{ri}' with pier spacing 'x/b'	146
5.41	Spacing versus relative scour hole width 'w_1/w_i', 'w_2/w_i' and 'w_3/w_i' at front, middle and rear piers placed in tandem arrangement.	146
5.42	Variation of relative depth of deposition at downstream faces of front, middle and rear piers placed in tandem arrangement '$l_{dep(f)}/l_{dep(i)}$, $l_{dep(m)}/l_{dep(i)}$ and $l_{dep(r)}/l_{dep(i)}$' with pier spacing 'x/b'.	147
5.43	Variation of scour depth along flume length at 6.6 cm front and 3.3 cm rear piers placed in tandem arrangement at x/b=70.	150
5.44	Variation of scour depth along flume length at 6.6 cm front and 3.3 cm rear piers placed in tandem arrangement at x/b=80.	150
5.45	Variation of relative scour depth at 66 mm front and 33 mm rear piers '$ds_B/ds_{B(i)}$' and '$ds_b/ds_{B(i)}$' placed in tandem arrangement with pier spacing 'x/b'.	151

5.46	Variation of relative scour depth at 6.6 cm front and3.3 cm rear piers 'ds_B/ds_i and '$ds_b/ds_{b(i)}$' placed in tandem arrangement with pier spacing 'x/b'.	152
5.47	Variation of scour depth at 3.3 cm rear pier relative to the scour depth at 6.6 cm front 'ds_b/ds_B' placed in tandem arrangement with pier spacing 'x/b'.	154
5.48	Variation of relative length of scour holes at upstream faces of 6.6 cm front pier and 3.3 cm rear piers '$Lsh_u/Lsh_{u(i)}$'.	155
5.49	Variation of scour depth along flume length at 6.6 cm front and 3.3 cm rear piers placed in tandem arrangement at x/b=2	156
5.50	Variation of scour depth along flume length at 6.6 cm front and 3.3 cm rear piers placed in tandem arrangement at x/b=4.	156
5.51	Variation of relative length of scour hole at downstream faces of 6.6 cm front and 3.3 cm rear piers placed in tandem arrangement '$Lsh_d/Lsh_{d(i)}$' with pier spacing 'x/b'.	158
5.52	Areal extent of scour around 6.6 cm front and 3.3 cm rear piers placed in tandem arrangement at x/b=60	159
5.53	Areal extent of scour around 6.6 cm front and 3.3 cm rear piers placed in tandem arrangement at x/b=70	160
5.54	Areal extent of scour around 6.6 cm front and 3.3 cm rear piers placed in tandem arrangement at x/b=90	160
5.55	Variation of area of extent of scour around 6.6 cm front and 3.3 cm rear pier placed in tandem arrangement with pier spacing 'x/b'	161
5.56	Variation of length of sediment deposition at downstream face of 6.6 cm and 3.3 cm piers placed in tandem arrangement, with pier spacing 'x/b'.	161
5.57	Variation of relative widths of scour hole $w_1/w_{i(b)}$ and $w_2/w_{i(b)}$ at 6.6 cm front and 3.3 cm rear piers placed in tandem arrangement with pier spacing 'x/b'.	163
5.58	Variation of scour depth at 3.3 cm front and 6.6 cm rear piers placed in tandem arrangement at x/b= 40.	168
5.59	Variation of scour depth at 3.3 cm front and 6.6 rear pier placed in tandem arrangement at x/b= 50.	168
5.60	Variation of scour depth at 3.3 cm front and 6.6 rear pier placed in tandem arrangement at x/b= 90.	169
5.61	Variation of relative scour depth at 3.3 cm front and 6.6 cm rear pier and at midway between the two piers placed in tandem arrangement $ds_b/d_{b(i)}$, $ds_B/ds_{b(i)}$ and $ds_{mid}/ds_{b(i)}$ with pier spacing 'x/b'.	170
5.62	Variation of scour depth at 6.6 cm rear pier relative to the scour depth at 3.3 cm front pier placed in tandem arrangement 'ds_B/ds_b' with pier spacing 'x/b'.	171
5.63	Variation of length of scour holes at upstream face of 3.3 cm front and 6.6 cm rear piers placed in tandem arrangement with pier spacing 'x/b'.	173
5.64	Variation of length of scour holes at downstream faces of 3.3 cm front and 6.6 cm rear piers placed in tandem arrangement with pier spacing 'x/b'.	174
5.65	Variation of length of sediment deposition at downstream face of 3.3 cm front and 6.6 cm rear pier placed in tandem arrangement with pier spacing 'x/b'.	176

5.66	Areal extent of scour around 3.3 cm front and 6.6 cm rear piers placed in tandem arrangement at x/b=50.	177
5.67	Variation of relative width of scour holes at 3.3 cm front and 6.6 cm rear piers placed in tandem arrangement '$w_1/w_{b(i)}$ and $w_2/w_{i(b)}$' with pier spacing 'x/b'.	178
5.68	Variation of relative slopes of scour holes at upstream face of 3.3 cm front and 6.6 cm rear piers placed in tandem arrangement '$S_{lu(f)}/S_{lu(bi)}$ $S_{lu(r)}$ /$S_{lu(bi)}$' with pier spacing 'x/b'.	179
5.69	(chart 17) Variation of relative slopes of scour holes at upstream face of 3.3 cm front and 6.6 cm rear piers '$S_{ld(b)}/S_{ld(bi)}$ $S_{ld(B)}$ /$S_{ld(bi)}$' and with pier spacing 'x/b'.	179
5.70	Variations of area of extent of scour around 3.3 cm front and 6.6 cm rear piers placed in tandem arrangement with pier spacing 'x/b'.	180
5.71	Variation of scour depth at piers placed in lateral arrangement at Zc/b= 7	182
5.72	Variation of relative scour depth at piers placed in lateral arrangement 'ds_L/ds_i' with pier spacing 'Z_c/b'.	183
5.73	Variation of scour depth at piers placed in lateral arrangement relative to the pier width 'ds_L/b' with pier spacing 'Zc/b'.	184
5.74	Variation of relative length of scour holes at upstream faces of piers placed in lateral arrangement '$L_{shu(L)}/L_{shu(i)}$' with pier spacing 'Z_c/b'	185
5.75	Variation of relative length of scour holes at downstream faces of piers placed in lateral arrangement '$L_{shd(L)}/L_{shd(i)}$' with pier spacing 'Z_c/b'.	186
5.76	Variation of relative slopes of scour holes at upstream face of piers placed in lateral arrangement '$S_{lu(L)}/S_{lu(i)}$' with pier spacing 'Z_c/b'.	187
5.77	Variation of slope of scour holes at downstream face of piers placed in lateral arrangement '$S_{ld(L)}/S_{lu(i)}$' spacing with pier spacing 'Z_c/b'.	188
5.78	Areal extent of scour around the piers placed in lateral arrangement at Z_c/b=6.	188
5.79	Areal extent of scour around the piers placed in lateral arrangement at Z_c/b=7.	189
5.80	Areal extent of scour around the piers placed in lateral arrangement at Z_c/b=8.	189
5.81	Variation of relative area of scour extent around two piers placed in lateral arrangement '$A_L/2A_i$' with pier spacing Z_c/b	190
5.82	Variation of relative width of scour holes of piers placed in lateral arrangement '$w_L/2w_i$' with pier spacing Z_c/b.	191
5.83	Variation of length of sediment deposition at downstream face of two piers placed in lateral arrangement '$L_{dep(L)}$'with pier spacing 'Z_c/b'	192
5.84	Variation of relative scour depth at upstream and downstream piers placed in staggered arrangement $d_{st(u)}/ds_{(i)}$ and $ds_{st(d)}/ds_{(i)}$ with pier spacing X_c/b.	195
5.85	Variation of relative maximum scour depth at midway between upstream and downstream piers placed in staggered arrangement $d_{st(mid)}/ds_{(i)}$' with pier spacing 'X$_c$/b'	196

5.86	Variation of relative scour depth at downstream pier with respect to that of upstream piers placed in staggered arrangement '$ds_{st(d)}/ds_{st(u)}$' with pier spacing 'X_c/b'.	196
5.87	Variation of length of scour hole at front faces of upstream and downstream piers placed in staggered arrangement with pier spacing 'X_c/b'.	198
5.88	Variation of length of scour hole at rear faces of upstream and downstream piers placed in staggered arrangement with pier spacing 'X_c/b'.	199
5.89	Variation of relative width of scour hole of upstream and downstream piers placed in staggered arrangement $w_{1(st)}/w_i$ and $w_{2(st)}/w_i$ with pier spacing 'X_c/b'	200
5.90	Variation of width of scour hole of downstream pier relative to the scour hole width of upstream piers placed in staggered arrangement '$w_{2(st)}/w_{1(st)}$' with pier spacing X_c/b.	201
5.91	Areal extent of scour around upstream and downstream piers placed in staggered arrangement at X_c/b=40.	202
5.92	Areal extent of scour around upstream and downstream piers placed in staggered arrangement at X_c/b=60.	202
5.93	Variation of relative area of scour extent around upstream and downstream piers placed in staggered arrangement '$a/3a_i$' with pier spacing 'X_c/b'.	203
5.94	Areal extent of scour around upstream and downstream piers placed in staggered arrangement at X_c/b=25.	203
5.95	Areal extent of scour around upstream and downstream piers placed in staggered arrangement at X_c/b=30.	204
5.96	Areal extent of scour around upstream and downstream piers placed in staggered arrangement at X_c/b=50	204
5.97	Areal extent of scour at X_c/b=60.	205
5.98	Variation of length of sediment deposition at rear faces of upstream and downstream piers placed in staggered arrangement with pier spacing X_c/b.	205
5.99	Variation of angle of attack formed by three piers in staggered arrangements with longitudinal pier spacing 'X_c/b'.	206
5.100	Variation of scour depth at downstream pier of piers group placed in staggered arrangement, with respect to that of an isolated pier '$ds_{st(d)}/ds_{(i)}$' at varying angles of attack 'α' formed by three piers in staggered arrangement.	207
5.101	Variation of relative scour depth at front and rear piers placed at constant angle of attack α=45° '$ds_{ca(f)}/ds_{(i)}$' and '$ds_{ca(r)}/ds_{(i)}$' with radial pier spacing 'R/b'.	210
5.102	Variation of length of scour holes at upstream faces of front and rear piers placed at constant angle of attack α=45° '*Lshcau(f)/Lshu(i)*' and '*Lshcau(r)/Lshu(i)*' with radial pier spacing 'R/b'.	211
5.103	Variation of length of scour holes at downstream faces of front and rear piers placed at constant angle of attack α=45° '$Lsh_{cad(f)}/Lsh_{d(i)}$'. and '$Lhs_{cad(r)}/Lsh_{d(i)}$' with radial pier spacing 'R/b'.	212

5.104	Variation of relative slope of scour hole at upstream faces of front and rear piers placed at constant angle of attack α=45° '$S_{lcau(f)}/S_{lu(i)}$' and '$S_{lcau(r)}/S_{lu(i)}$' with radial pier spacing '*R/b.*'	213
5.105	Variation of relative slope of scour holes at downstream faces of front and rear piers placed at constant angle of attack α=45° '$S_{lcad(f)}/S_{ld(i)}$'and '$S_{lcad(r)}/S_{ld(i)}$' with radial pier spacing 'R/b'.	214
5.106	Variation of relative length of sediment deposition at downstream faces of front and rear piers placed at constant angle of attack α=45° '$Ldep_{ca(f)}/Ldep_{(i)}$' and '$Ldep_{ca(r)}/Ldep_{(i)}$' with radial pier spacing '*R/b*'.	215
5.107	Areal extent of scour around front and rear pier placed at constant angle of attack α =45° and *R/b*=11	216
5.108	Areal extent of scour around front and rear piers placed at constant angle of attack α =45° and *R/b*=12	217
5.109	Variation of relative area of scour extent around front and rear piers placed at constant angle of attack α=45° '$A_{cd}/2A_i$' with radial pier spacing '*R/b*'.	217
5.110	Variation of relative width of scour holes of front and rear piers placed at constant angle of attack α=45° '$w_{1(ca)}/w_i$' and '$w_{2(ca)}/w_i$' with radial pier spacing '*R/b*'.	219
5.111	Variation of scour depth at front and rear piers '$ds_{cr(f)}/ds_{(i)}$' and '$ds_{cr(r)}/ds_{(i)}$' with angle of attack 'α'.	223
5.112	Variation of relative scour depth at midway between the front and rear piers $ds_{cr(mid)}/ ds_{(i)}$ with angle of attack 'α'.	224
5.113	Variation of relative length of scour holes at upstream faces of front and rear piers '$Lsh_{cru(f)}/Lsh_{u(i)}$' and '$Lsh_{cru(r)}/Lsh_{u(i)}$' with angle of attack 'α'.	225
5.114	Variation of relative length of scour holes at downstream face of front and rear piers '$Lsh_{crd(f)}/Lsh_{d(i)}$' and '$Lsh_{crd(r)}/Lsh_{d(i)}$' with angle of attack 'α'.	227
5.115	Variation of slope at upstream faces of front and rear piers '$S_{lcr(uf)}/S_{l(ui)}$' and '$S_{lcr(ur)}/S_{l(ui)}$' with angle of attack 'α'.	228
5.116	Variation of slope at downstream faces of front and rear piers '$S_{lcr(df)}/S_{l(di)}$' and '$S_{lcr(dr)}/S_{l(di)}$' with angles of attack 'α'.	229
5.117	Variation of length of sediment deposition at downstream faces of front and rear piers relative to that at an isolated pier '$L_{depcrr(f)}/L_{dep(i)}$' and '$L_{depcr(r)}/L_{dep(i)}$' with angle of attack 'α'.	230
5.118	Areal of extent of scour around front and rear piers placed at constant radial pier spacing R/b and angle of attack=60°.	231
5.119	Variation of relative area of scour extent around front and rear piers 'A_{cr}/A_i' with angle of attack 'α'.	231
5.120	Variation of relative width of scour holes of front and rear piers '$w_{1cr(f)}/w_i$' and '$w_{2cr(r)}/w_i$' with angles of attack 'α'.	223
5.121	Location of maximum scour depth around piers group without collar aligned at different angles of attack 'α'.	235
5.122	Piers group with collar aligned at an angle of attack 'α'.	236
5.123	Piers group with collar at 7.5° angle of attack.	237
5.124	Piers group with collar at 10° angle of attack.	237

5.125	Areal extent of scour at α= 10° (a) without collar (b) with collar.	238
5.126	Piers group with collar at 15° angle of attack.	238
5.127	Areal extent of scour at α = 15° (a) without collar (b) with collar.	239
5.128	Piers group with collar at 30° angle of attack.	240
5.129	Areal extent of scour at α= 30° (a) without collar (b) with collar.	241
5.130	Round-nose rectangular pier and a group of t circular piers of varying diameters, both of same length to width ratio 4:1.	241
5.131	Variation of maximum scour depth at piers group without collar relative to the scour depth at round-nosed rectangular pier '$ds_{pg(woc)}/ds_{(rectp.)}$' with angles of attack 'α'.	242
5.132	Variation of maximum scour depth at piers group with collar relative to the maximum scour depth without collar '$ds_{g(wc)}$ $ds_{g(woc)}$' with angles of attack 'α'.	243
5.133	Variation of percentage reduction in the maximum scour depth at piers group due to the application of collar '$[(ds_{pg(woc)}$-$ds_{pg(wc)})/ds_{gp(woc)}]x100$' with angle of attack.	244
5.134	Length of Scour Holes on Upstream and Downstream of Piers group Without Collar	246
5.135	Variation of Length of scour holes at downstream end of piers group with collar relative to the corresponding length without collar '$L_{sh(wc)}/L_{sh(woc)}$' with angles of attack 'α'.	246
5.136	Variation of length of sediment deposition at downstream end of piers group without collar with angles of attack 'α'.	247
5.137	Variation of length of sediment deposition at downstream end of piers group without collar at an angle of attack relative the corresponding length at zero degree angle of attack $L_{dep(ang.)}/L_{dep(zdeg)}$	248
5.138	Variation of length of sediment deposition at downstream end of piers group with collar versus angles of attack 'α'.	248
5.139	Variation of relative distance of occurrence of maximum sediment deposition '$L_{dep(ang)}$ / $L_{dep(zdeg)}$' at downstream end of piers group with collar at an angle of attack 'α'.	249
5.140	Variation of point of maximum deposition of sediment at downstream end of piers group without collar with angles of attack.	250
5.141	Variation of point of occurrence of maximum sediment deposition at downstream end of piers group with collar corresponding to without collar with angles of attack 'α'.	250
5.142	Variation of maximum height of sediment deposition at downstream end of piers group with collar relative to the corresponding height without collar '$H_{dep(wc)}$'/'$H_{dep(woc)}$' with angles of attack 'α'.	252
5.143	Angle of attack versus percent reduction in areas of extent with collar '$(A_{pg(woc)}$-$A_{pg(wc)})/A_{pg(woc)}$' with angles of attack 'α'.	252
5.144	Angle of attack versus width of scour hole without collar.	252
5.145	Angle of attack versus width of scour hole with collar.	253
5.146	Temporal variation of scour depth at piers group without collar.	253
5.147	Temporal variation of scour hole with collar.	254
5.148	Round-nose rectangular pier and a group of two circular piers, both of same length to width ratio 4:1	254

5.149	Areal extents of scour at α=0° (a) without collar (b) with collar.	257
5.150	Areal extents of scour at α=15° (a) without collar (b) with collar.	258
5.151	Areal extents of scour at α=30° (a) without collar (b) with collar.	259
5.152	Areal extents of scour at α=45° (a) without collar (b) with collar.	260
5.153	Areal extents of scour at α=60° (a) without collar (b) with collar.	261
5.154	Areal extents of scour at α=75° (a) without collar (b) with collar.	262
5.155	Areal extents of scour at α=90° (a) without collar (b) with collar.	263
5.156	Group of two circular piers with collar.	264
5.157	Group of two piers with collar at $\alpha = 0°$.	265
5.158	Group of two piers with collar at $\alpha = 15°$.	266
5.159	Group of two piers with collar at $\alpha = 30°$.	267
5.160	Group of two piers with collar at $\alpha = 45°$.	268
5.161	Group of two piers with collar at $\alpha = 60°$.	270
5.162	Group of two piers with collar at $\alpha = 75°$.	270
5.163	Group of two piers with collar at $\alpha = 90°$.	271
5.164	Angle of attack versus relative scour depth without collar.	273
5.165	Angle of attack versus relative scour depth with collar.	274
5.166	Comparison of scour depths at a group of two piers and a round nose rectangular pier without collar at varying angles of attack 'α'.	275
5.167	Percent reduction in scour depth at group of two piers with respect to that at round-nose rectangular pier without collar.	275
5.168	Percent reduction in scour depth with collar.	276
5.169	Variation of area of scour extent around group of 41.5 mm diameter piers without collar relative to the corresponding area with collar '$A_{woutcol}/A_{withcol}$' with angle of attack 'α'.	278
5.170	Angle of attack versus relative length of scour hole at upstream face of 4.15 piers group without collar.	279
5.171	Variation of length of scour hole at downstream face of piers in 41.5 mm piers group without collar with angles of attack '$L_{sh(d)}/L_{sh(di)}$'	280
5.172	Variation of length of sediment deposition at downstream face of piers group without collar relative to the corresponding length at downstream face of a 4.15 isolated round-nosed rectangular pier '$L_{dep}/L_{depi(rec)}$'	280
5.173	Variation of length of sediment deposition at downstream face of piers group relative to that of without collar 'L_{depwc}/L_{depwoc}' with angles of attack	281
6.1	ANN architectures for two piers in tandem arrangement	293
6.2	ANN architectures for three piers in tandem arrangement	293
6.3	ANN architectures for two piers of different size in tandem arrangement (6.6 cm at front and 3.3 cm at rear)	294
6.4	ANN architectures for two piers of different size in tandem arrangement (3.3 cm at front and 6.6 cm at rear)	294
6.5	ANN architectures for Two piers in lateral arrangement	295
6.6	ANN architectures for three piers in staggered arrangement	295
6.7	ANN architectures for two piers at constant radial distance and varying angles of attack	295
6.8	ANN architectures for two piers at constant angle of attack and varying radial pier spacings *R/b*	296

6.9	ANN architectures for a group of piers comprising of cylinders of different sizes with and without collar	296
6.10	ANN architectures for a group of two piers with and without collar	296
6.11	Scatter plots between neural network estimated and observed scour depth for training and testing data set for two piers in tandem arrangement (a) Front pier (b) Rear pier.	299
6.12	Scatter plots between neural network estimated and observed scour depth for training and testing dataset for three piers tandem arrangement (a) Front pier (b) Middle pier (c) Rear pier (d) Middle pier/Front pier (e) Rear pier/Front pier.	300
6.13	Scatter plots between neural network estimated and observed scour depth for training and testing data set for [6.6 cm pier (Big pier) at front and 3.3 cm pier (small pier) at rear] in tandem arrangement (a) Front pier (b) Midway (c) Rear pier.	301
6.14	Scatter plots between neural network estimated and observed scour depth for training and testing data set for [3.3 cm pier (small pier) at front and 6.6 cm pier (big pier) at rear] in tandem arrangement (a) Front pier (b) Midway (c) Rear pier (d) Rear pier/Front pier.	302
6.15	Scatter plots between neural network estimated and observed scour depth for training and testing dataset for two piers in lateral arrangement.	303
6.16	Scatter plots between neural network estimated and observed scour depth for training and testing dataset for three piers in staggered arrangement (a) Upstream piers (b) Downstream pier (c) Downstream pier/upstream piers.	303
6.17	Scatter plots between neural network estimated and observed scour depth for training and testing dataset for two piers aligned at constant radial spacing *R/b* and varying angles of attack (a) Front piers (b) Rear pier.	304
6.18	Scatter plots between neural network estimated and observed scour depth for training and testing dataset for two piers aligned at constant angle of attack and varying radial spacing R/b (a) Front piers (b) Rear pier.	304
6.19	Scatter plots between neural network estimated and observed scour depth for training and testing dataset for a group of two piers aligned at various angles of attack with and without collar (a) Front piers (without collar) (b) Rear pier (without collar) (c) With collar.	305
6.20	Scatter plots between neural network estimated and observed scour depth for training and testing dataset for a group of varying sized cylinders aligned at various angles of attack (a) Without collar (b) With collar.	306

LIST OF TABLES

Table No.	Title	Page No.
2.1	Classification of local scour processes at bridge pier foundations	38
2.2	Values of shape factor (k_s) for various shapes of pier.	41
2.3	Multiplying factors for flow alignment effects at bridge pier (Melville, 1997).	44
2.4	Values of flow alignment factor (Laursen and Toch, 1956)	45
2.5	Scour depth and factor of angle of attack for round nosed rectangular pier	45
2.6	Scour depth and factor of angle of attack for two circular piers	46
2.7	Scour depth and factor of angle of attack for three circular piers	46
3.1	Properties of sediment used	78
3.2	Computed mean flow parameters	79
3.3	Details of pier sizes and their arrangement used in present study	80
3.4	Duration of experimental runs for clear–water scour	83
5.1	Comparison of observed scour depth at single pier with scour depth computed using existing scour depth predictors	112
5.2	Scour characteristics observed at an isolated pier experiments	112
5.3	Comparison of scour depth observed at piers placed in tandem arrangement in present study with published results of Hannah (1978) for varying pier spacing *'x/b'*	122
5.4	Comparison of scour depths observed at middle pier in three piers tandem arrangement with the scour depths observed at rear pier in two piers tandem arrangement.	139
5.5	Relative Scour Depth, Length of Scour Hole and Slope of Scour Hole at Upstream Face of Piers	228
5.6	Relative Scour Depth, Length of Scour Hole and Slope of Scour Hole at Upstream Face of Piers	264
5.7	Maximum scour depth at group of two piers with collar	272
5.1(I)	Details of ANN Architectures	297
5.2 (I)	Results obtained from ANN based modeling approach	298

LIST OF NOTATIONS

A	Area in m^2
ANN	Artificial Neural Network
ART	Adaptive Resonance Theory Networks
B	Width of the channel
B_c	Channel width
a,b,c	Tri-axial size of sediment
b	Pier width for non circular pier
b_r	Pier size ratio for tandem arrangement of piers
b_{ds}	Width of downstream pier
B_{us}	Width of upstream pier
C	Cohesion of bed material
d	Mean size of sediment
$d_{15.9}$	Sediment size for which 15.9% by weight is finer
d_{50}	Sediment size for which 50% by weight is finer
$d_{84.1}$	Sediment size for which 84.1% by weight is finer
D	Pier diameter
D_v	Mean vortex size
E	Total error of the network
E_p	Error for pattern p
F_d	Densimetric Froude number
Fr	Froude number
F_{rc}	Critical Froude number
f_s	Silt factor
$f(.)$	Activation function
fi	Most common activation function
g	Acceleration due to gravity m/s^2
h	Water depth
h	Thickness of sediment layer
h_s	Scour depth
h_{se}	Equilibrium scour depth
h_{si}	Scour depth for isolated pier
h_{sem}	Maximum equilibrium scour depth
h_{sm}	Maximum scour depth
H_c	Collar elevation
H_s	Scour depth below water surface
i_{Pi}	Value of the i^{th} element of the input pattern
K_d	Sediment size factor
K_i	Flow intensity factor
K_s	Pier shape factor

K_y	Flow depth factor
K_σ	Sediment gradation factor
K_β	Pier alignment factor
K_θ	Factor for angle of attack
K_1	Correction for pier nose shape
K_2	Correction for angle of attack of flow
K_f	Particle shape
k	Constant
k_s	Grain roughness
l	Pier length
MLP	Multilayer Perceptron
m	Constriction ratio
n	Manning's roughness coefficient
o_{Pj}	Output of the node j for pattern p
net_{Pj}	Sum of the inputs
Q	Discharge of water
R	Hydraulic radius m
RBF	Radial Basis Function Network
LVQ	Recurrent Networks, and Learning Vector Quantization
R_b	Hydraulic radius corresponding to bed
R^2	Correlation coefficient
Re	Flow Reynolds number
R_{eb}	Pier Reynolds number
R_{eh}	Flow Reynolds number
R_{eh*}	Critical shear Reynolds number
R_{eD}	Pier Reynolds number
SOM	Self-Organizing Map
s	Specific gravity of submerged sediment particles
$S.F.$	Particle shape factor
S_s	Specific gravity
S_0	Average energy slope
t	Time
T	Water temperature °C
T_1	Dimensionless time scale
t_e	Time to equilibrium scour depth hrs
t_m	Time for maximum scour
t_r	Time scale ratio
t_{Pj}	target input for j^{th} component of the output pattern for pattern p
U	Undisturbed approach flow velocity
U_0	Mean flow velocity
U_a	Mean approach velocity at armour peak = $0.8U_{ca}$
U_c	Critical/Threshold velocity

U_{ca}	Mean approach velocity beyond which armouring is impossible
U_i	Mean approach velocity corresponding to initiation of motion
U_{*c}	Critical shear velocity
U_*	Shear velocity
W	Channel width
W_c	Width of collar
w_0	Fall velocity of sediment particle m/s
w_{ji}	Weight vector
x	Clear longitudinal pier spacing
X_c	Centre to centre longitudinal pier spacing
y_0	Flow depth
y_c	Critical depth of flow
y_s	Depth of scour below the original bed level at a bridge pier
$y_{s\max}$	Maximum equilibrium depth of local scour
y_{se}	Equilibrium scour depth
Z_c	Centre to centre lateral pier spacing
α	Angle of attack of flow
$\alpha_1, \alpha_2, \alpha_3$	Coefficients in Baker (1980a)'s equation
β	Flow angle of attack
γ	Specific weight of water kN/m^3
γ_s	Specific weight of the sediment material kN/m^3
η	Learning rate
η_1, η_2, η_3	Coefficients in Garde (1961)'s equation
η_4	Aspect ratio of the pier to channel width
ν	Kinematic viscosity of fluid m^2/s
ρ	Water density kg/m^3
ρ_s	Sediment density kg/m^3
τ_0	Sediment shear stress
τ_*	Dimensionless shear stress
τ_c	Critical shear stress N/m^2
τ_{*c}	Dimensionless critical bed shear stress
σ	Standard deviation
σ_g	Geometric standard deviation of the sediment size
ϕ	Angle of repose
Ψ	Shape factor

CHAPTER – I

INTRODUCTION

Bridges are the lifelines of a transportation system. They are required wherever waterways are crossed by roads and railways. Piers on which the superstructure of the bridges rest, play an important role in their stability and safety. These piers founded in the stream-bed are subjected to scour as they are obstruction against the flow.

Scour is the process of lowering of river-bed around an obstruction due to removal of the bed material by erosive action of flowing water. Scour takes place in the vicinity of a structure when the flow gets modified due to the presence of the structure in such a way that there is an increase in the bed shear stress. The shear stress around the structure eventually gets reduced by enlargement of the flow cross-section due to scour. The term local scour is used to emphasize the fact that the lowering of the riverbed occurs in the vicinity of the structure. Local scour has been classified in two ways. Shen *et. al.* (1969) differentiated between (i) clear-water scour; when upstream flow does not transport sediment and (ii) live-bed scour; when upstream flow transports sediment.

The threat of local scour around bridge piers has been known for many years. As a result, the estimation of scour depth and areal extent of scour around bridge piers is a major concern of bridge engineers. Underestimation of the scour depth and its areal extent results in design of too shallow a foundation which may consequently cause exposure of foundations endangering the safety of the bridge, overestimation of the scour depth results in uneconomical design of the piers. Great difficulty is experienced sometimes in straightening the pier wells which tend to get tilted while sinking to large depths. Therefore, knowledge of anticipated maximum scour depth for design discharge is essential for a proper design of the foundation of the bridge piers.

In spite of significant amount of research on single pier scour, failure of many bridges has been reported in the literature. Hoffmans and Verheij (1997) have also noted that local scour around bridge piers, as a result of flood flows, is considered to be the major cause of bridge failure. Chiew and Lim (2003) and Chiew (2004) reported the failure of Kaoping Bridge in Southern Taiwan in August 2000. Dey and Barbhuiya (2004) made

reference to the collapse of Bulls Bridge over the Rangikikei River, New Zealand. In this regard, it is interesting to note the statement by Lagasse and Richardson (2001) that, hydraulic factors such as stream instability, long-term streambed aggradation or degradation, general scour, local scour, and lateral migration are responsible for 60% of all U.S. highway bridge failures.

Failure of bridges due to pier scour, as mentioned above and reported in the literature by Wardhana and Hadipriono (2003) and others, has rekindled interest in furthering understanding of the pier scour process and for developing improved ways of protecting bridges against the ravages of scour.

It is well established that mostly, the bridge piers are designed as a single pier. However, a bridge is usually supported on a number of piers (*e.g.*, group of piers). Also, owing to rapid urbanization and increased traffic volume, it is often needed to construct new bridges across the rivers in the proximity of the already existing bridge, where the piers of one bridge may or may not fall exactly in front of the piers of other bridge. Obviously, the occurrence and development of a scour process in such circumstances will be quite different from one which occurs around a single pier. In these perspectives, to ensure the stability of the bridge piers, the need of a study on the effect of mutual interference of bridge piers on local scour assumes immense significance which is the subject of present study. Before proceeding to study on local scour at group of piers, it is imperative to have an insight into the mechanism of local scour at a single pier first.

1.1 Local Scour around Single Bridge Pier

The phenomenon of local scour around a single bridge pier has been extensively studied and also documented by a large number of investigators. Detailed studies on the mechanism of scour around a single bridge pier were made amongst others by Laursen and Toch (1956), Nakagawa and Suzuki (1975), Hjorth (1975), Melville (1975), Ettema (1980), Qadar (1981), Baker (1981), Kothyari (1989), Graf and Yulistiyanto (1998). The system of horseshoe vortices and the down flow at the pier were found to be the main agents responsible for scour.

Till date considerable data have been collected on single pier scour in laboratories and some in the fields with a view to adequately predict the maximum scour depths. As a

result, the number of proposed design relations for maximum scour depths prediction is substantial, but the predicted values are found to be widely scattered and sometimes contradictory. This is probably due to the fact that scour process involves complicated interaction among the flow, the sediment and the bed configuration in time and space.

Many methods for the estimation of maximum scour depth around a bridge pier exist. The practice followed in Indian Railways and other governmental organizations, is to use the Lacey–Inglis method (Lacey, 1929 and Inglis, 1949) for the determination of scour depth. Other methods for estimation of scour depth include those by Laursen and Toch (1956), Shen *et. al.* (1969), Breusers *et. al.* (1977), Melville and Sutherland (1988), Jain (1981), Kothyari *et. al.* (1992a and 1992b), HEC-18 (U.S. Army Corps of Engineers 1991), Dey (1997). These cover both cases of clear water and live-bed scour. Detailed discussion on these methods is provided in Chapter II. In addition, the effects of sediment non-uniformity and/or stratification on scour have also been studied (Ettema, 1980, Kothyari, 1989). The temporal variation of scour depth has also been studied in detail (Chabert and Engeldinger, 1956, Ettema 1980, Yanmaz and Altinbilek, 1991, Kothyari *et. al.* (1992a, 1992b), Dey (1997). But all these studies pertain essentially to a single pier. However, a bridge is not supported on a single pier. Rather, it is supported on more number of piers. The neighboring piers, therefore, can affect each other due to their mutual interaction with the flow. This mutual interaction of piers can adversely affect local scour. In spite of significant amount of research on scour processes, not much attention towards the aspect of pier group scour has been paid by the researchers. Therefore, the aspect of pier group scour is yet to be resolved.

1.2 Local Scour at Group of Bridge Piers

In case of scour around group of piers, the presence of several piers can generate a complex interaction in the hydrodynamic characteristics of the flow field near the piers themselves and therefore, lead to the occurrence and development of a scour process that is quite different from one which occurs around a single pier. This interaction is particularly evident when the bridge is not perpendicular to the river flow. When the local scour occurs in the presence of group of piers, the flow pattern in the channel around the piers is changed significantly. There are many situations in the field where group of piers are founded in the river-bed.

Due to rapid urbanization and increased traffic volume, it is often needed to construct new bridges across the rivers in the proximity of the already existing bridge. There are limitations of spacing between existing and new bridges due to the problem of land acquisition. In that context, the scour depth and bed configuration pattern around the existing and new bridges need to be examined. Furthermore, for geo-technical and economical reasons, pier groups have been more and more popular in bridge design, however, the scour mechanisms around piers group are much more complex and design local scour depths more difficult to predict.

The safe and economical design of bridge piers requires accurate prediction of maximum scour depth around them; however, the accurate estimation of scour depth and extent of scour around bridge piers is difficult. The difficulty is further compounded at group of piers due to the effect of their mutual interference on local scour.

Local scour around a single bridge pier is affected by a large number of inter-dependant variables. The flow, sediment and pier characteristics are the main variables affecting this phenomenon. For given conditions of these variables, the scour depth also varies with time. As a consequence of extensive research by several investigators on the phenomenon of local scour around a single bridge pier, a large number of design relationships have been bequeathed to the bridge designer. Not withstanding this, many bridges still suffer damage by local scour. This is not surprising as the local scour at bridge piers involves the complexities of the three-dimensional turbulent flow field around a pier together with the mechanics of sediment transport. The complexities are further intensified in the presence of group of piers due to their mutual interaction. In addition to the variables affecting local scour around a single pier, spacing of piers and arrangement of their placement in the riverbed also affect the scour depth around group of piers.

Study on the problem of local scour around the group of piers placed in the riverbed in various arrangements, is still in its initial stages. Only a few investigators have studied the phenomenon of scouring around piers group. Hannah (1978), Nicollet *et. al.* (1978), Breusers and Raudkivi (1991), Vittal *et. al.* (1994), Babaeyan-Koopaei and Valentine (1999), Choi *et. al.* (2001) and Sadek & Ismail (2002) have made some studies on scour around group of piers. However, these studies have provided limited data. Furthermore,

no study is available on temporal variation of scour depth around group of piers founded in the river-bed at short spacing in different arrangements.

1.3 Mechanism of Scour around Piers Group

In addition to parameters affecting scouring around a single pier, for a pier that is part of a group of piers, group effects are also important. The presence of group of piers in the river-bed can generate a complex interaction in the hydrodynamic characteristics of the flow field near the piers themselves and therefore, lead to the occurrence and development of a scour process that is quite different from one which occurs around a single pier.

(Hannah, 1978) has recognized four mechanisms of scour to occur at piers group; 1) reinforcing; that leads to increased scour depth at the upstream pier and overlapping of scour hole of front pier with that of the rear pier; 2) sheltering; by the upstream pier can reduce the effective approach velocity for the downstream pier and reduce the scour depth at the rear pier; 3) vortices shed; from the upstream pier are convected downstream (if the downstream pier is close to the path of vortices, this will assist scouring by lifting material from the downstream scour hole); and 4) compressed horseshoe vortex; when piers are placed transversely to the flow, each will have its own horseshoe vortex. The interaction between piers in a group intensifies the reinforcing and compressed horseshoe vortex effects, which make the scour phenomenon more complex and which can modify the depth and shape of the scour hole around the piers group?

Based on the extensive research carried out over the years, various equations have been developed for the estimation of equilibrium scour depth at bridge piers; however, almost all the equations have been derived for the case of a single pier. If a bridge pier is merely designed and constructed on the basis of such equations, it may lead to the bridge failure.

In addition, it is also evident that even most of the experimental studies have focused only on a single bridge pier. At present there is virtually no practicable method available to confidently predict the scour depths at group of bridge piers founded in riverbed. A conclusion to be drawn is that the effect of mutual interference of bridge piers on local scour is not adequately investigated. Therefore, scouring around pier groups is still a field

of active research. This study deals with the investigation of the effect of mutual interference of bridge piers on local scour in a steady clear water approach flow.

The changing nature of river in alluvial plains poses many difficulties for the design of bridges in a river. Therefore, the change in the bed configuration in the vicinity of bridges must be forestalled or accommodated in the design of bridges to avoid the risk of eventual failure (Smith, 1976).

1.4 Scour Depth Prediction Using Artificial Neural Network (ANN)

It is extremely difficult to formulate mathematical models that accurately represent the scour process and the geometry of the scour hole which develops under the influence of three dimensional flow field around a pier. Thus, it is a common practice to apply empirical relationships based on the regression methods performed on laboratory data for estimation of the scour around a pier. However, due to complexity of the scour problem empirical relationship based on laboratory data are not strong enough to deal with the problem of estimating the scour depth around a pier. Moreover, since there are numerous effective parameters and the interaction of these parameters is highly complicated, therefore, the accuracy of the empirical relationship is very subjective and highly depends on the users' ability and knowledge. In the light of above numerous approaches for the estimation of scour depth around piers have been carried out in the past (Laursen and Toch, 1956; Shen, 1971; Hancu, 1971; Breusers *et. al.*, 1977; Melville and Sutherland, 1988; and DOT U.S., 1993). In addition, some relevant studies on the mechanism of flow around pier type structures have been conducted recently (Sumer and Fredose, 1994, 1997). However, there is a lack of reliable formulas for predicting the scour depth to cover all possible ranges from the aforementioned methods. The results from the existing method show up to 100% variation resulting in an increase in the cost of the protection methods against scour and the foundation of the piers. Recognizing these difficulties and the importance of improving prediction capabilities a great number of researchers have been engaged in exploring and refining methods for improving traditional physical based analysis.

Recently Artificial Neural Networks (ANNs) are being widely applied in various areas of hydrology and water resources engineering to overcome the problem of exclusive and the

non-linear relationships. A few investigators have addressed the uncertain issue of scour around pier type structures with the help of the ANN. Examples of latter studies include (Azmatullah *et. al.*, 2007; Bateni and Jeng, 2006; Bateni *et. al.*, 2006; Choi and Cheong, 2006; Jeng *et.. al.*, 2005; Azinfar *et. al.*, 2004; Khosronejat *et. al.*, 2004; Kambekar and Deo, 2003; Liriano and Day, 2001; and Trent *et. al.*, 1993). Kambekar and Deo (2003) carried out scour data analysis using neural networks. Khosronejad *et. al.* (2004) carried out estimation of scour hole properties around vertical piles using ANNs. Jeng *et. al.* (2005) made neural network assessment for scour depth around bridge piers. The equilibrium scour depth was modeled as a function of five variables; flow depth, mean velocity, critical flow velocity, mean grain diameter and pier diameter. Bateni *et. al.* (2006) applied Bayesian neural networks for prediction of equilibrium and time dependent scour depth around bridge piers. Choi and Cheong (2006) investigated prediction of local scour around bridge pier using ANNs. Sixty four data sets from four different experiments were used to train the model. The prediction results by ANN were better than the results produced by empirical relationships. Bateni and Jeng (2006) carried out estimation of pile group scour using adaptive neuro-fuzzy approach. Lee *et. al.* (2007) applied neural network modeling for estimation of scour depth around bridge piers. The Back-propagation neural network (BPN) was used to predict the scour depth in order to overcome the problem of exclusive and the non-linear relationships. It was found that the scour depth around bridge piers can be efficiently predicted using the BPN.

1.5 Concluding Remark

From review of literature on application of ANNs in hydrology and water resources engineering, it can be concluded that ANN provides a higher level of accuracy in solving the particular problem when compared to empirical relationships. ANN may therefore be a viable alternative in the evaluation of mutual interference effect of bridge piers on local scour provided a reliable database is available.

1.6 Aim of the Present Study

The present investigation was taken up keeping in view the foregoing gaps in the knowledge. The principal objective of this study was to investigate the development of local scour around group of piers founded in the riverbed in different configurations, by

conducting a carefully controlled set of experiments for studying the effect of mutual interference of bridge piers on local scour. Larger scour depths need deep pier foundations, which is a costly proportion. As a result, various devices (i.e., armoring devices and flow altering devices) for scour depth reduction were investigated by many researchers. The armoring devices such as placing the rip-rap and gabion around the pier were investigated by several investigators (Brice *et., al.*; 1978; Croad, 1993; Parola, 1993; Yoon *et. al..*, 1995; Maynord, S.T. (1995), Worman 1989, (Lim and Chiew, 1996 and 1997); Lim, 1998; Chiew and Lim, 2000; Lim and Chiew, 2001). Likewise, the flow altering devices were investigated by many researchers such as providing an array of piles in front of the pier(Chabert and Engeldinger, 1956 and Melville and Hadfield,1999), a collar around the pier (Schneible, 1951; Thomas 1967; Tanaka and Yano 1967; Ettema 1980; Chiew, 1992; Kumar *et. al.*, 1999, Zarrati *et. al.*, 2004), submerged vanes(Odgard and Wang 1987), a delta-wing-like fin in front of the pier (Gupta and Gangadharaiah, 1992), a slot through the pier(Chiew, 1992, Kumar *et. al.*, 1999) and partial pier-groups (Vittal *et. al.*, 1994).

The flow altering devices can be more economical, especially when the rip-rap material in required amount is not available near the bridge site or is expensive. The effect of collar in reducing scour depth was previously studied on single circular piers by Tanaka and Yano (1967), Ettema (1980), Chiew (1992) and Kumar (1999) and on rectangular pier by Zarrati *et. al.* (2004). However, scanty work has been carried out on the application of collar around a group of piers. Therefore, the scope of the study was broadened so as to be an investigation of the reduction of the depth of local scour by applying a collar around group of piers.

The present investigation is oriented to study the following aspects of pier group scour.

(I) To study the effect of mutual interference of bridge pier scour on local scour for the following cases of pier arrangements.

  (a) To study the local scour around single pier to form a basis for evaluating the effect of mutual interference of bridge pier groups.

  (b) Two identical circular cylindrical piers placed in tandem arrangement at varied pier spacing.

(c) One pier of larger size on upstream and one pier of smaller size at the downstream placed in tandem arrangement at varied pier spacing.

(d) One pier of smaller size on upstream and one pier of larger size on downstream placed in tandem arrangement at varied pier spacing.

(e) Three circular cylindrical piers of same size placed in tandem arrangement at varied pier spacing.

(f) Two circular cylindrical piers of same size placed at constant angle of attack but varying radial distances.

(g) Two circular cylindrical piers of same size placed at constant radial distance but varying angles of attack.

(h) Two identical circular cylindrical piers of same size placed in transverse arrangement at varied transverse spacing.

(i) Three identical circular cylindrical piers placed in staggered arrangement such that two of them located in transverse direction on upstream at fixed transverse pier spacing and one pier on downstream placed along the bisector of the two upstream piers at varied longitudinal pier spacing.

(II) To study the reduction of scour depth by applying a collar around group of piers.

(III) To study the temporal variation of scour depth for the above cases.

(IV) Modeling for the evaluation of the effect of mutual interference of bridge piers on local scour.

(VI) Modeling for the evaluation of scour reduction efficiency of collar around group of piers as scour countermeasure.

To achieve these objectives an almost totally experimental approach was adopted, that is, it was felt that most effective way to bring to light the better understanding of effective means to deal with scour around bridge piers group founded at short spacing, was through observations of the scour process in an extensive experimental programme.

Whereas, Hannah (1978) was primarily interested in mechanism of scour around the bridge piers group, this study investigates the effects of mutual interference of bridge piers on the depth of local scour. The experimental programme has produced results, which provide the bridge designer with a means of predicting the maximum depth of local scour that may occur at group of bridge piers founded in different configurations in the riverbed at short spacing.

Chapter-I presents the introduction of the research carried out in this thesis The current state of knowledge of the local scour around a single pier, around group of piers and scour reduction at single pier, is presented in Chapter II. Chapter III deals with the experimental programme undertaken to investigate the local scour around the group of piers. Chapter IV presents the background of artificial neural (ANN) technique which is to be used in present research for modeling the scour depth at pier group. The graphical representation based analysis of the results generated through experimental program is presented in Chapter V. The analysis of results based on Artificial Neural Network approach is presented in Chapter VI. Principal conclusions drawn from the results of the study and scope for further studies are presented in Chapter VII. The summary of flow parameters used in this study and exhaustive experimental data gathered from present investigation is presented in Appendices I-VII.

CHAPTER – II

LITERATURE REVIEW

2.0 Introduction

A vast amount of literature exists on the topic of local scour around bridge piers. Different aspects of scour processes at bridge piers have been studied from time to time but mainly for the case of an isolated bridge pier. Since the objective of the present study is to evaluate the effect of mutual interference of bridge piers on local scour, literature review is focused on the scour around group of piers. The literature, reviewed in this chapter is under the following categories:

(i) Mechanics of local scour around an isolated pier.

(ii) Scour depth prediction at an isolated pier.

(iii) Parameters governing scouring.

(iv) Mechanism of local scour at group of piers.

(v) Interference effects of multiple piers on flow.

(vi) Interference effects of multiple piers on local scour.

(vii) Reduction and protection of scouring around bridge piers

(viii) Scour depth prediction using artificial neural network (ANN)

(ix) Conclusion on literature review

Scour is defined as the erosion of streambed around an obstruction in a flow field (Chang, 1988). The amount of reduction in the streambed level below the bed level of the river prior to the commencement of scour is referred as the scour depth. A scour hole is defined as depression left behind when sediment is washed away from the riverbed in the vicinity of the structure.

The total scour at a river crossing consists of three components that, in general, can be added together (Richardson and Davis, 1995). They include general scour, contraction scour and local scour. Fig. 2.1 shows sub-divisions of scour.

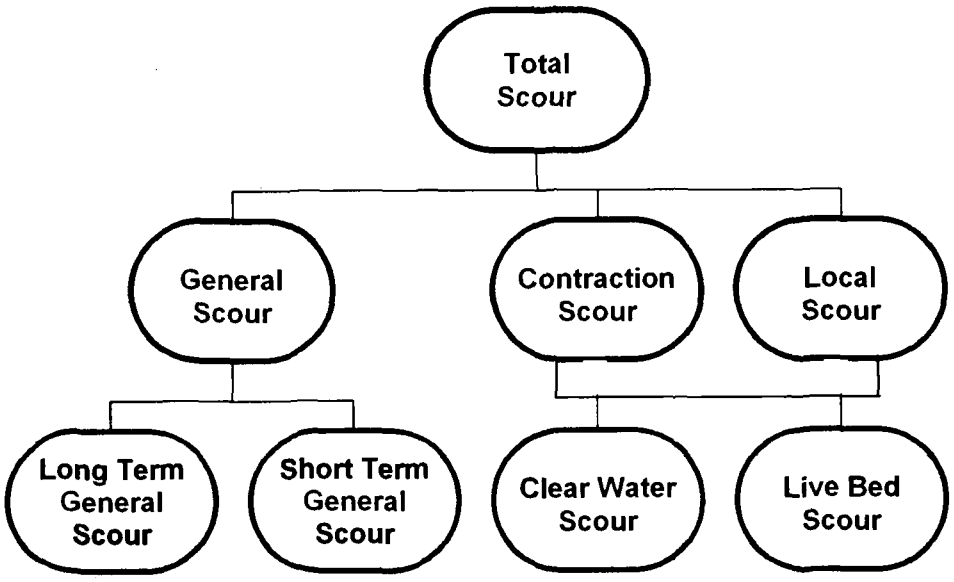

Fig. 2.1 An organogram showing various types of scour (after Richardson and Davis 1995)

General scour refers to the changes in river bed elevation due to natural/human-induced causes with the effect of causing an overall lowering of the longitudinal profile of river channel. It occurs through a change in the river regime resulting in general degradation of the bed level. General scour develops irrespective of the existence of a bridge. General scour can further be divided into long-term and short-term scour, with the two types being differentiated by the temporal development of the scour (Cheremisinoff *et. al.*, 1987). Short term general scour occurs in response to a single or several closely spaced floods whereas long term general scour develops over a significantly longer time period, usually of the order of several years, and includes progressive degradation and lateral bank erosion.

In contrast to general scour, localized scour is directly attributable to the existence of a bridge or other riverine structures. Localized scour can further be divided into contraction and local scour.

Contraction scour occurs as a result of the contraction of a channel either due to a natural means or human alteration of the floodplain. The effect of contraction is an increase in the average flow velocity, which consequently causes an increase in the erosive forces exerted on the channel bed. It results in the lowering of the channel bed.

Local scour refers to the removal of sediment from the immediate vicinity of bridge piers or abutments. It occurs due to the interference of pier or abutment with the flow, which results in an acceleration of flow, creating vortices that remove the sediment material in

the immediate surrounding of the bridge pier or abutment. Figure 2.2 shows the typical appearance of the local scour around bridge piers. As it is related to the main thrust of this study, local scour is discussed in much more detail in the following sections.

Fig. 2.2 Photograph of local scour at a group of rectangular piers in tandem arrangement (with permission from www.pepe:vasquez.com)

The problem of scour around an isolated pier has been extensively studied and also documented by several investigators like, Chabert and Engeldinger (1956), Laursen and Toch (1956), Liu *et. al.* (1961), Shen *et. al.* (1969), Melville (1975), Hjorth (1975), Melville and Raudkivi (1977), Ettema (1980), Baker (1981), Jain (1981), Raudkivi and Ettema (1983), Melville and Sutherland (1988), Kothyari (1989), Dargahi (1990), Yanmaz and Altimbilek (1991), HEC-18 (1991), Kothyari *et. al.* (1992 a and b), Garde *et. al.* (1995), Kumar (1996), Dey (1997), Ahmed and Rajaratnam (1998), Graf and Istiarto (2002) and Sheppard (2004).

The process of scour is affected by a large number of variables. The flow, fluid, pier and sediment characteristics are the main variables affecting the pier scour. For given conditions, the scour also varies with time and spacing between the piers. Depending upon whether the flow approaching the pier is transporting sediment or not, the pier scour is classified as (i) clear-water scour; when approaching flow does not carry any sediment (ii) live-bed scour; when approaching flow carries sediment. In general, the equilibrium scour depths in live-bed conditions are slightly smaller than those in clear-water condition Shen *et. al.* (1969). Main objective of the present investigation is to study the influence of mutual interference of bridge piers on local scour; therefore, a brief review of existing literature on pier scour around an isolated pier is presented below.

2.1 Mechanics of Local Scour around an Isolated Pier

Flow mechanism of scouring around a bridge pier is very complex and has been investigated by various investigators (Chabert and Engeldinger, 1956; Hjorth, 1975; Melville, 1975; Melville and Raudkivi, 1977; Dargahi, 1990; Melville, 1997; Graf and Yulistiyanto, 1998; Graf and Istiarto, 2002; Ahmed F. and Rajaratnam N., 1998). It has long been established that the basic mechanism causing local scour at piers is the downflow at the upstream face of the pier and formation of vortices at the base of the pier Heidarpour *et. al.* (2003).

When a pier is placed in a current, the flow is accelerated around the pier; however, the flow decelerates as it approaches the pier coming to rest at the upstream face of the pier. The approach flow velocity, therefore, at the stagnation point on the upstream side of the pier is reduced to zero, which results in pressure increase at the pier face. The associated stagnation pressures are highest near the surface, where the deceleration is greatest, and decreases downwards (Melville and Raudkivi 1977). As the velocity is decreasing from the surface to the bed, a downward velocity gradient develops on the upstream side of the pier. The vertical velocity gradient of the flow is transformed into a pressure gradient on the leading edge of the pier. It is recognized that this adverse pressure gradient in the longitudinal direction and the favorable pressure gradient in the vertically downward direction near the pier causes the formation of horseshoe vortex system and down-flow in front and around the pier and wake vortices behind it as shown in Figs. 2.3 a, b and Fig. 2.4.

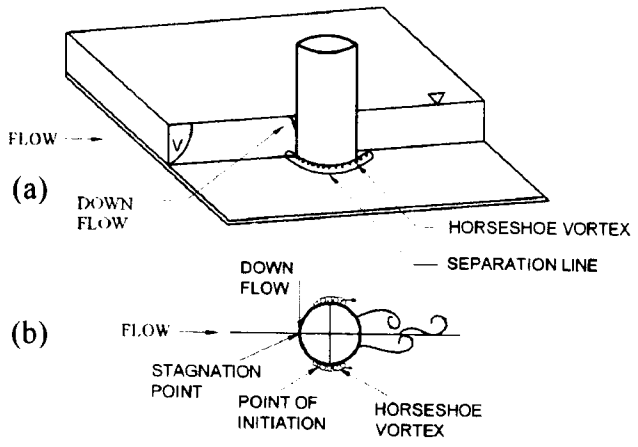

Fig. 2.3 Flow characteristics around a cylindrical pier (after Kothyari *et. al.*, 1989)

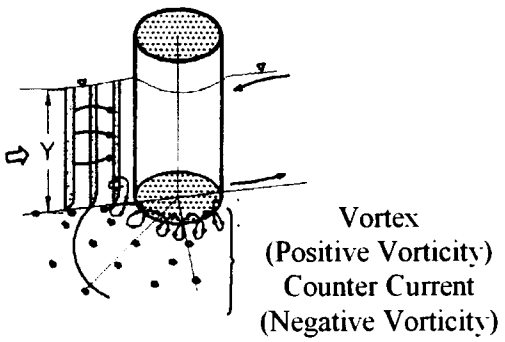

Fig. 2.4 Scheme of the horseshoe vertex system (after Yulistianto, 1998)

At the water's surface, the flow and pier interaction forms a bow wave known as the surface roller. Beyond the points of flow separation on the pier, wake vortices occur as shown in Fig. 2.4 Scour is a consequence of such three-dimensional pattern of flow. Locally, shear stress increases at the bed within the vicinity of the pier. If the bed is erodible (and the shear stresses are of sufficient magnitude), a scour hole forms around the pier. This phenomenon is known as local or pier- induced sediment scour.

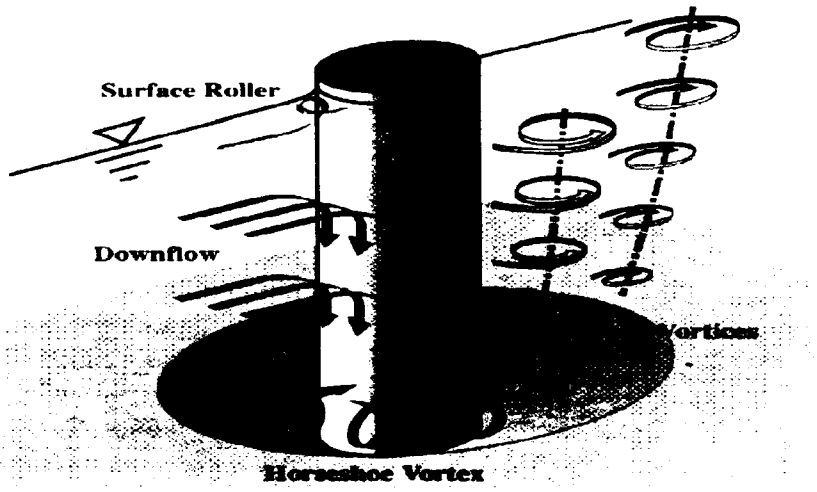

Fig.2.5 Illustration of the flow and scour pattern at a circular pier (after Melville & Coleman 2000)

As illustrated in the Fig. 2.5 the strong vortex motion caused by the existence of the pier, entrains bed sediments within the vicinity of the pier base (Lauchlan and Melville 2001). The downflow rolls up as it continue to create a hole and, through interaction with the oncoming flow, develops into a complex vortex system. The vortex then extends downstream along the sides of the pier. This vortex is often referred to as horseshoe vortex because of its similarity to a horseshoe (Breusers *et. al.*, 1977). The horseshoe vortex is very effective in transporting the dislodged particles away past the pier.

As shown in Fig. 2.5 besides the horseshoe vortex in the vicinity of the pier base, there are also vertical vortices downstream of the pier referred to as wake vortices (Dargahi 1990). The separation of flow at the sides of the pier produces the so called wake vortices. The wake vortices are not stable and shed alternately from one side of the pier and then the other. It should be noted, however, that both the horseshoe and wake vortices erode material from the base region of the pier. The intensity of the wake vortices drastically reduces with distance downstream, such that sediment deposition is common immediately downstream of the pier (Richardson and Davis 1995).

The so-called horseshoe vortex develops as a result of separation of flow at the upstream rim of the scour hole formed around the pier due to the removal of sediment by water current. The flow separates at the sides of the pier and the separation surfaces enclose the wake downstream of the pier. The horseshoe vortex extends downstream, past of the sides of the pier for a few pier diameters, before losing its identity and becoming part of general turbulence.

Scour hole development commences at the sides of the cylinder with the holes rapidly propagating upstream around the perimeter of the cylinder to meet on the centerline. The eroded material is transported downstream by the flow. Soon after the commencement of scouring, a shallow hole, concentric with the cylinder, is formed around most of the perimeter of the cylinder (about 120°) but not in the wake region. The down flow acts like a vertical jet eroding a groove in front of the pier. The eroded material is carried around the pier by the combined action of accelerating flow and the spiral motion of the horseshoe vortex. The down flow is turned 180° in the groove and the upward flow is deflected by the horseshoe vortex in the upstream direction, up the slope of the scour hole. At this turning point, the lip of the groove is often very sharp and the face is almost vertical. The groove becomes shallow or disappears altogether when scour approaches its equilibrium depth. The rim collapses irregularly in local avalanches of bed material. The deflection of the down flow ejects this material up to where the horseshoe vortex tends to push some of it up the slope. The rest is picked up by the flow, which carries it into and behind the wake region where a bar develops. The upstream part of the scour hole develops rapidly and has the shape of frustum of an inverted cone with slope equal to the angle of repose of the bed material under erosion conditions. The salient features of scour

hole around an isolated circular cylindrical pier reported in literature (Richardson *et. al.*, 1993) are as under:

2.1.1 Shape of the scour hole

In plan, the shape of scour hole around a circular pier resembles to the frustum of an inverted cone. The shape of the scour hole at upstream face of the pier is semicircular in plan (Fig. 2.6).

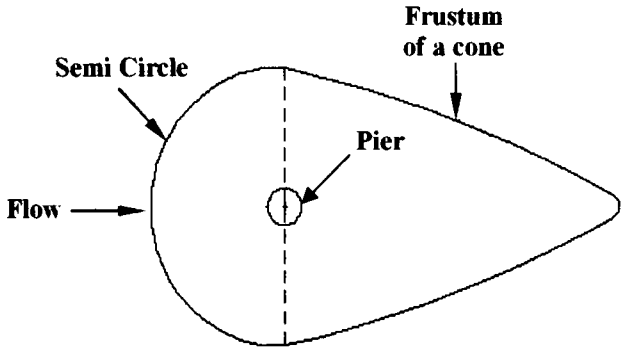

Fig.2.6 Plan of a scour hole

2.1.2 Length of scour hole

Scour hole length is the distance from the upstream face of a pier to the upstream edge of scour hole (upstream length) or to the downstream edge of the scour hole (downstream length). The total length of the scour hole is the sum of the upstream and down stream lengths of scour hole. The downstream length of the scour hole is greater than the upstream length of scour hole.

2.1.3 Top width of scour hole

The top width of scour hole has been found to be a function of scour depth and the angle of repose of bed material. The angle of repose, 'ϕ' is the maximum slope angle upon which non-cohesive material rests without moving and is a measure of the inter-granular friction of the bed material. The upstream slope of the scour hole is nearly the same as the angle of repose of the bed material.

As shown in Fig. 2.7, Richardson *et. al.* (1993) calculated the top width of scour hole by summing up of the scour hole width at the left, right, and upstream side of a pier.

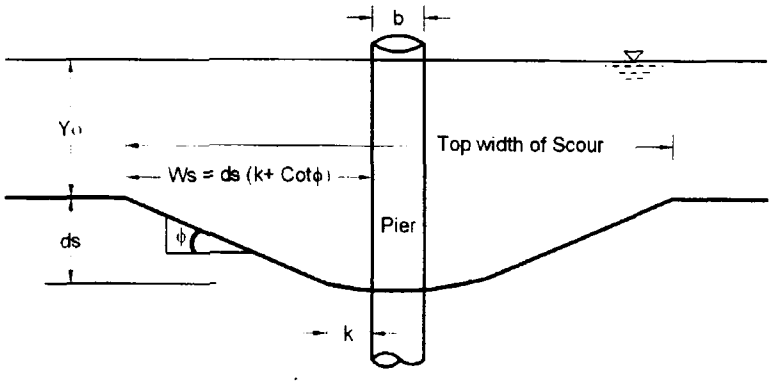

Fig.2.7 Top width of scour hole around a circular pier

Top width of scour hole = $2Ws+b$ (2.1)

Where, $Ws = ds\ (K+cot\phi)$ (2.1.1)

In which,

Ws = the distance measured perpendicularly from the upstream side of the pier to the far edge of the scour hole.

ds = scour depth

K = bottom width of scour hole as a fraction of scour depth $(0-1.0)ds$

ϕ = angle of repose of the bed material

2.1.4 Slopes of scour hole

Along the length of flume, the slope of scour hole is more at upstream face of the pier than at the downstream face of the pier. In equilibrium condition, the slope of the scour hole at upstream face of pier is nearly same as the angle of repose of the bed material.

2.1.5 Bed level variation along flow direction

The bed level at upstream edge of scour hole is equal to the general level of sediment bed; however, it decreases towards downstream with minimum at the upstream face of the pier. Moving further downstream, the bed level increase and approaches to the general bed level at a distance of few pier diameters from the downstream face of the pier. Henceforth the bed level rises above general bed level reaching to a maximum at a distance of few diameters from downstream face of the pier. Thereafter bed level

decreases and reaches to general bed level at a distance of few diameters from the downstream face of the pier (Fig. 2.8).

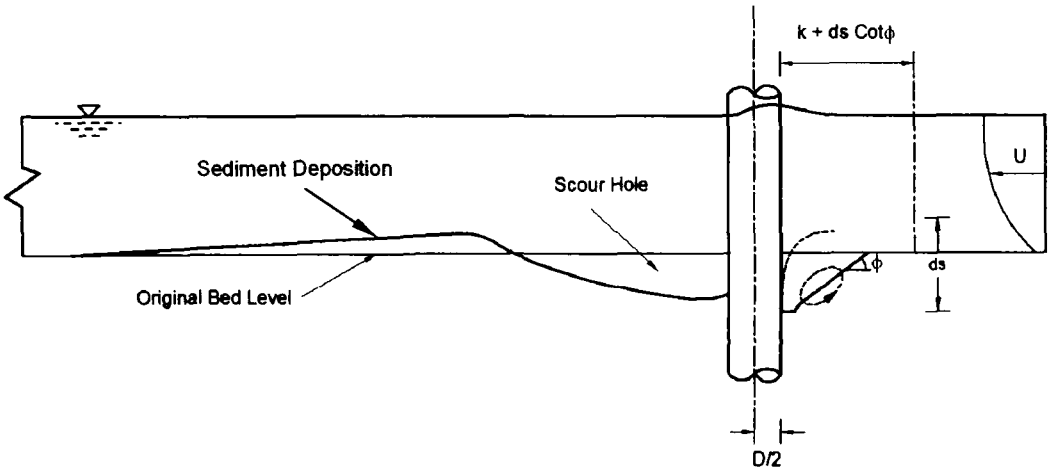

Fig.2.8 Bed level variation along flow direction

2.2 Classification of Local Scour

Based on mode of transport of sediment by the approaching flow, the local scour is classified as either clear-water or live-bed scour (Chabert and Engeldinger 1956). These classifications depend on the ability of the flow approaching the pier to transport bed material (Chiew and Melville 1987). When there is no movement of sediment on the bed away from the pier (*i.e.*, where the influence of the pier on the flow is negligible) the phenomenon is known as clear-water scour. Raudkivi and Ettema (1983) defined clear-water scour as occurring when the bed material at the upstream side of the pier is not in motion. Under clear-water conditions, the bed shear stresses away from the pier are less than critical shear stress required for sediment movement. At the pier, an initial period of rapid erosion is followed by an equilibrium, which is reached when the flow alteration by the scour hole reduces the magnitude of the shear stress such that sediment can no longer be mobilized and removed from the scour hole (Breusers *et. al.*, 1977).

When sediment is in motion on the bed away from the pier, the process is known as live-bed scour. In this case, the bed shear stresses away from the pier are greater than the critical value required to mobilize and transport the sediment. Generally, initial scour rates tend to be greater in live-bed scour than in clear-water scour and equilibrium scour depth is attained more quickly. Under live-bed scour conditions; sediment from upstream

of the pier is continuously transported into the scour hole (Dey 1999). In this case, the equilibrium condition is reached when the amount of sediment entering the scour hole is equal to the amount being removed (Melville 1984). Under live-bed scour conditions, bed forms occur and propagate through the scour hole. Thus the scour hole depth will fluctuate in time even after the "equilibrium" condition has been reached. Fig. 2.9 compares typical clear-water and lives bed scour time series.

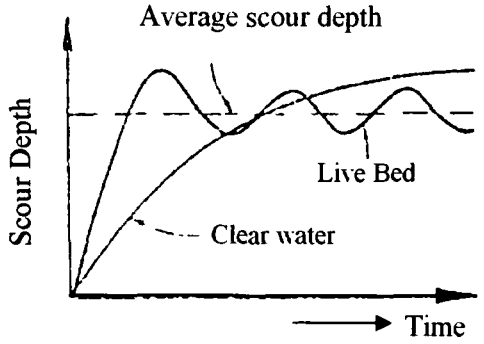

Fig.2.9 Diagrammatic illustration of classification of local scour at a bridge pier

In coarse-grained material (sands and gravels) an equilibrium local scour condition is rapidly attained with time in live-bed condition (and then oscillates in response to the passage of bed forms). On the other hand, an equilibrium condition is achieved slowly and asymptotically in clear-water condition (Raudkivi and Ettema, 1983).

The parameter used to determine the scour regime (*i.e.*, clear-water scour or live-bed scour) is the ratio of the upstream velocity to the threshold or sediment critical velocity to cause sediment movement in the bed. This ratio, known as the flow intensity, may take one of the two forms, depending on the velocity used. If the shear stress or bed friction velocity U_* is used, the ratio becomes U_*/U_{*_c}. The shear velocity U_* is defined as $U_* = \sqrt{\tau/\rho}$, where τ is the bed shear stress. The threshold or critical shear velocity U_{*_c}, corresponds to the critical shear stress τ. In this form, the flow intensity can be thought of as a shear stress ratio where $\tau/\tau_c = (U_*/U_{*_c})^2$. Therefore, this form has a direct correlation to the sediment transport, since most transport equations are in terms of bed shear stress. The critical shear velocity can be determined for given uniform sediment using Fig. 2.10 and equation (2.2), however the value of U_* is usually not readily

available for prototype flow situations and must be derived using velocity profile assumptions (Melville & Sutherland, 1988).

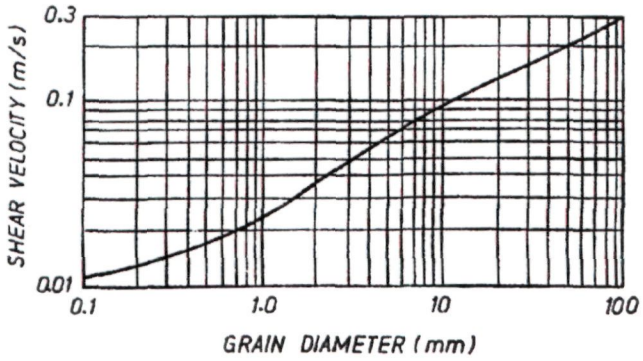

Fig. 2.10 Shields chart for threshold condition of uniform sediments in water

$$\frac{U_c}{U_{*c}} = 5.75 \log\left(5.53 \frac{y}{d_{50}}\right) \tag{2.2}$$

The second more common form of the flow intensity uses the depth average approach velocity V and the critical depth averaged approach velocity V_c. The critical depth averaged approach velocity is the minimum depth averaged velocity of the approach flow for which sediment motion will occur for given sediment. This form of the flow intensity (V/V_c) requires that a vertical profile be known or assumed (usually logarithmic) to calculate the critical depth averaged velocity V_c from Shields' diagram for given sediment.

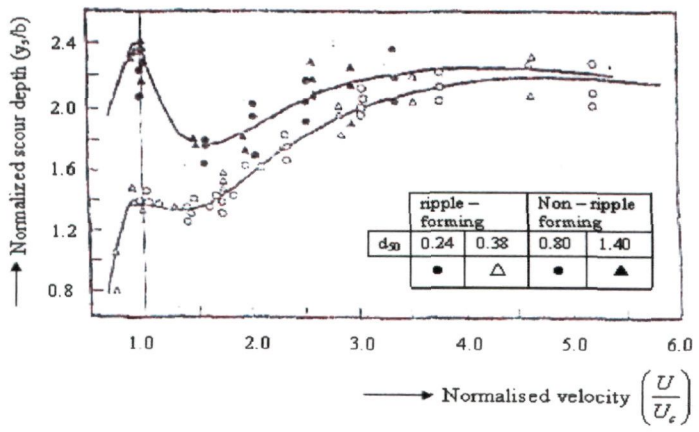

Fig.2.11 Average local scour depth at cylindrical piers in relatively deep water (after Chee 1982).

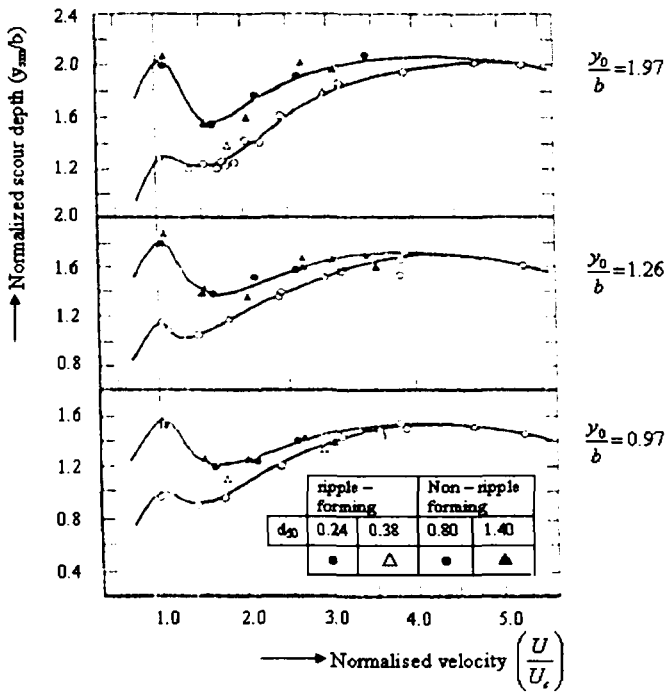

Fig.2.12 Laboratory data on average maximum local scour depth at a cylindrical pier (after Chee 1982)

Generally, by definition clear-water scour occurs when $0.5 \leq V/V_c < 1$ and live-bed scour occurs when $V/V_c \geq 1$ (Melville and Chiew 1999). Most researchers place the lower limit for clear-water scour between $V/V_c = 0.4$ and 0.5. The maximum scour depth occurs at $V = V_c$ (Fig. 2.11 and 2.12). According to Richardson and Davis (1995), the maximum clear-water scour depth is about 10 percent greater than the equilibrium depth of scour for live-bed pier scour. The time taken for equilibrium scour depth to develop increases rapidly with flow velocity in clear-water conditions but decreases rapidly for live-bed scour (Melville and Chiew 1999). Richardson and Davis (2001) mentioned that typical clear-water scour situations can be found in (a) coarse-bed material stream, (b) flat gradient streams during low flow, (c) local deposits of larger bed materials that are larger than the biggest fraction being transported by the flow, (d) armoured streambeds where the only location that tractive forces are adequate to penetrate the armour layer are at piers and/or abutments, and (e) vegetated channels or over bank areas.

Melville (1975) described the stages of scour in terms of the mechanisms of scour at each phase:

(i) Accelerated flow due to distortion of the streamlines by the cylinder:

(ii) Flow separation and horseshoe vortex development and intensification as the hole develops, and

(iii) Avalanching (or sliding) of material down the sides of the scour hole once the hole is large enough to contain the horseshoe vortex.

Melville found that the angle of the sloped sides of the scour hole was the angle of repose of the sediment. This angle did not change as the scour hole grew

Most researchers agree on the general process of scour hole development, while differing on some of the details. Generally, for a single cylindrical pier, there is an initial stage during which sediment is removed from the sides of the pier where the flow has been accelerated as predicted by potential flow theory. At this point, the scour resembles sediment transport on a flat bed. Ettema (1980) and Hjorth (1975) found that the points of initiation of scour occur at roughly ± 45° from the leading edge of the pier. Melville (1975) found the maximum shear stress at the unscoured bed at ± 100 degrees.

As the scour hole grows, it spreads toward the leading edge of the pier, where the down flow has been established and the horseshoe vortex originates. The down flow and horseshoe vortex loosen and mobilize the sediment; and the mobilized sediment is carried downstream of the pier by the horseshoe vortex and the main channel flow.

Melville (1975) observed that the horseshoe vortex is initially small in cross-section and relatively weak as is the associated down flow occurring in the plan of stagnation. As the hole deepens, the down flow strengthens, and the horseshoe vortex grows in size and strength and descends into the developing scour hole. As the scour hole enlarges, the circulation associated with the horseshoe vortex continues to increase, but at a decreasing rate, as the cross- sectional area of the hole increases and equilibrium is approached.

Avalanching of material down the sides of the scour hole occurs once the hole is large enough to contain the horseshoe vortex, causing the hole to widen. Many researchers (Nakagawa and Suzuki 1975, Hjorth 1977, and Ettema 1980) observed that the actual mobilization and removal of sediment is limited to an area immediately adjacent to the pier at the base of the scour hole. As the material slides down the sides of the hole, it is mobilized in this erosion or entrainment zone. Once a sediment particle is put into suspension, it is swept downstream. If the particle is carried high enough, it may interact

with the wake vortices, be carried higher into the water column, and be transported and deposited well downstream. Otherwise, the sediment particle may be swept directly behind the pier and enter the relatively calm wake region between the shedding vortices. Here it will settle out and form the characteristic mound behind the pier.

Eventually, the hole becomes deep enough that the strength of the horseshoe vortex and the down flow are weakened and can no longer mobilize and remove sediment from the scour hole. In the live-bed case, the amount of sediment removed is exactly equal to the deposited in the hole from upstream. At this point an equilibrium is established and the hole has reached its maximum size for the given flow condition.

There are varying hypothesis concerning the main agent responsible for pier scour. For example, Laursen and Toch (1956) and Shen *et. al.* (1966) identified the horseshoe vortex to be the main agent responsible for local scour around bridge pier. Based on the concept of horseshoe vortex, Roper *et. al.* (1967), Baker (1981), Kothyari *et. al.* (1992a and b) and many others have presented models for scour prediction. Extending the experimental study of flow around a cylinder on a horizontal non-mobile bed carried out recently by Graf and yulistiyanto (1998), an experimental investigation of flow pattern in the scour hole around a cylinder has also been carried out recently by Graf and Istiarto (2002). More recently Muzzammil and Gangadhariah (2003) have studied experimentally the chracteristics of horseshoe vortex and have presented a model for scour prediction.

On the other hand, Raudkivi (1986) noted that the horseshoe vortex is a consequence of scour, not the cause of it and Melville (1975), Hjorth, (1975), Ettema (1980), Raudkivi (1998), Chiew and Melville (1987), and Johnson and Ayyub (1992) observed the down flow in front of the pier as a main agent responsible for pier scour. Chiew (1984) identified the down flow as the main cause of local scour and describe the scour hole as inverted right circular cone with the pier as its axis. The angle that the slope of the hole makes with the vertical is approximately equal to the angle of repose of the sediment. It is worthwhile to note one common assertion of many studies is that the secondary circulation generated by the presence of pier is responsible for the local scour at bridge piers. However, some investigators emphasized that the down flow resulting from the vertical pressure gradient on the stagnation plane is the main cause of local scour and secondary circulation is the result of scour, this idea has been contradicted by the other

studies. Tanaka *et. al.* (1967) showed that the down flow is generated secondarily by the vortex motion and does not affect directly the local scour.

Dargahi (1990) contradicted the view of Melville and Raudkivi (1977) that vertical down flow was the main scouring agent. He argued that the vertical down flow was the cause of formation of corner vortex, which could not be the scouring agent. He concluded that the wake scouring was due to the primary wake vortices and the accelerated side flow, and suggested that periodicity of sediment transport was controlled by the shedding frequency of wake vortices.

2.3 Scour Depth Prediction at an Isolated Pier

Many formulae have been proposed for the prediction of local scour depth at bridge piers based on the different approaches. Breusers *et. al.* (1977) has presented a comprehensive survey on this topic. A brief summary of the better-known formulae is presented here.

Inglis *et. al.* (1939) carried out model studies on piers in connection with the Hardinge Bridge Works over the River Ganges in India. They found that the scour depth could be expressed as

$$\frac{Hs}{b}=2.32(q_1^{2/3})^{0.78} \tag{2.3}$$

Where q_1 is the discharge in m^3/s per m. A major disadvantage of this formula is considered to be the combination of undisturbed water depth and scour depth. The formula was later modified using regime depth relation by Blench (1962).

Inglis (1949), based on the analysis of scour data from various Indian bridge sites, proposed a formula for the scour depth

$$H_s=2H_1 \tag{2.4}$$

Where $$H_1=0.473\left(\frac{q}{f}\right)^{1/3}$$ = the Lacey regime depth (2.4.1)

$H_s=h_s+h$ = scour depth measured below the water surface (2.4.2)

H_s = scour depth measured below the original bed level

h = depth of flow

q = discharge

f = silt factor = $1.76\ (d)^{1/2}$ (2.4.3)

d = mean size of sediment in mm.

This formula was adopted for designing railway bridge pier foundation in India. Being based on regime approach, which tends to concentrate on overall dimensions without accounting for the internal mechanism of the scouring process, it is not necessarily accurate.

Laursen and Toch (1956) proposed a design curve from model studies for live-bed scour at square nosed pier aligned with the flow, which was expressed by Neill (1964), as

$$\frac{H_s}{D}=1.5\left(\frac{h}{D}\right)^{0.3} \tag{2.5}$$

The formula is based on Laursen's observation that only in the case of clear-water scour the flow velocity and sediment size have any significant effect on scour depth.

A comprehensive and systematic investigation on the influence of various parameters on local scour around bridge piers, spurs and abutments was carried out at the University of Roorkee, India. As a result of this study, a generalized relation for scour depth prediction was proposed by Garde (1961) as

$$\frac{H_s}{h}=\left(\frac{4n_1n_2n_3}{\alpha}\right)F_r^{n'} \tag{2.6}$$

In which F_r= Froude number = $\frac{U}{(gh)^{1/2}}$, $n_1, n_2, and\ n_3$ are functions of particle drag coefficient (CD), F_r and foundation shape and n' is function of CD. The ratio $\alpha=(B-D)/B$ is the opening ratio, where B is the channel width.

Larras (1963) analyzed exhausting laboratory data and some field data in an attempt to work out a formula for maximum scour depth at the initiation condition of sediment motion. He gave the following relation

$$H_{sm}=1.05k_\theta k_s D^{3/4} \tag{2.7}$$

Where k_θ and k_s are factors accounting for angle of attack and pier shape respectively. He also proposed empirical value of k_θ and k_s for different conditions.

Shen *et. al.* (1969) proposed a clear-water scour formula in terms of R_{ed}, on the basis of the vortex strength model known as the Shen I formula

$$H_s = 0.000223\, R_{ed}^{0.619} \tag{2.8}$$

Alternatively the authors proposed the Shen II formula for clear-water scour

$$\frac{H_s}{h} = 2\, F_r^{0.43} \left(\frac{D}{h}\right)^{0.645} \tag{2.9}$$

And the Shen III formula for live-bed scour

$$\frac{H_s}{h} = 3.4\, F_r^{2/3} \left(\frac{D}{h}\right)^{2/3} \tag{2.10}$$

It may be added here that Shen et al's relations are on the conservative side and their plots show much scatter of data. Moreover, the Shen I formula is not dimensionally homogeneous.

Hancu (1971) proposed equation for local scour at piers

(i) the Hancu I formula for clear-water conditions,

$$\frac{h_s}{D} = 2.42 \left(\frac{2U}{U_i} - 1\right) \left(\frac{U^2}{gD}\right)^{1/3} \tag{2.11}$$

$$\frac{h_s}{D} = 2.42 \left(\frac{U_i^2}{gD}\right)^{1/3} \tag{2.11.1}$$

in which, U_i is the mean flow velocity at the initiation condition of sediment motion.

Coleman (1971) analyzed the data of Shen *et. al.* (1969) and the results of his own experiments on circular piers under condition of continuous sediment transport and proposed the relation

$$\frac{h_{sm}}{D} = 1.49 \left(\frac{U_i^2}{gh}\right)^{1/10} \tag{2.13}$$

Breusers (1972) proposed a design relation for circular piers, based on the notion that for live-bed scour and for water depths greater than $2D$, h_{sm} is a function of pier shape and size only as

$$h_{sm} = 1.4D \tag{2.14}$$

This relation was obtained from laboratory and field data.

Breusers et al (1977) made a critical and extensive review of literature on model and field scour data and design relations, and suggested a design relation,

$$\frac{h_s}{b} = f\left(\frac{U}{U_i}\right) 2.0 \tan\left(\frac{h}{D}\right) k_\theta \, k_s \tag{2.15}$$

in which $f\left(\frac{U}{U_i}\right) = 0$ for $\frac{U}{U_i} < 0.5$ (2.15.1)

$= \frac{2U}{U_i} - 1$ for $0.5, <= \frac{U}{U_i} <= 1.0$ (2.15.2)

$= 1.0$ for $\frac{U}{U_i} > 1.0$ (2.15.3)

They recommended $k_s = 1.0$ for circular and rounded piers $k_s = 0.75$ for streamlined shape and $k_s = 1.3$ for rectangular piers and proposed the use of the Laursen chart for angle of attack.

Baker (1980 a), based on vortex strength approach, proposed a scour depth relation for the clear-water case as

$$\frac{h_s}{D} = (\alpha_1 F_{rd} - \alpha_2) \tan h\left(a_3 \frac{h}{d}\right) \tag{2.16}$$

in which, $F_{rd} = \frac{U}{(sgd)^{1/2}}$ (2.61.1)

$$\alpha_1, \alpha_2, \alpha_3 = fn\left(d \frac{(sgd)^{1/2}}{V}\right) \tag{2.16.2}$$

s = Specific gravity of submerged particles.

fn = Functional relation

Jain (1981) analyzed available scour data and proposed the enveloping equation for maximum clear-water scour as

$$\frac{h_{sm}}{D}=1.84\left(\frac{h}{D}\right)^{0.3}(F_{ri})^{0.25} \tag{2.17}$$

in which $F_{ri}=\frac{U_i}{(gh)^{1/2}}$ = Froude number at the sediment initiation condition. This relation is similar to Laursen and Toch's equation but includes sediment size effect.

Qadar (1981) proposed a relation of scour depth, on the basis of the vortex strength approach as

$$h_s=5.68(co)^{1.28} \tag{2.18}$$

in which $co=u_0 r_0; u_0=0.092 D^{-0.5} U^{0.83}$ *and* $r_0=0.1D$ (2.18.1)

This relation is valid for fine sediment only and for clear-water condition. It is not dimensionally homogeneous.

Melville *et. al.* (1988) proposed design relation of scour depth for both uniform and non-uniform sediments as

$$\frac{h_s}{D}=K_i K_h K_d K_s K_\theta \tag{2.19}$$

in which, $K_i=2.4\left|U-\left(\frac{U-U_i}{U_i}\right)\right|$ if $U-\left(\frac{U_a-U_i}{U_i}\right)<1$ (2.19.1)

$=2.4$ if $U-\left(\frac{U_a-U_i}{U_i}\right)\geq 1$ (2.19.2)

$K_h=1$ if $\frac{h}{D}>2.6$ (2.19.3)

$=0.78\left(\frac{h}{D}\right)^{0.255}$ if $\frac{h}{D}<2.6$ (2.19.4)

$K_d=1$ if $\frac{D}{d}>25$ (2.19.5)

$=0.57\log\left(2.24\frac{D}{d}\right)$ if $\frac{D}{d}<25$ (2.19.6)

K_s = Shape factor as proposed by Breusers et al (1977),

K_θ = angle of attack effect (Laursen chart)

U_a = mean approach velocity at the armor peak $=0.8\,U_{ca}$ and

U_{ca} = mean approach velocity beyond which armoring of the cannel bed is incompressible.

Garde et al (1989) proposed the following relations for clear-water and live-bed scour depths respectively.

Clear-water Scour: $$\frac{h_s}{D}=0.66\left(\frac{D}{d}\right)^{0.75}\left(\frac{h}{D}\right)^{0.16}\left(\frac{U^2-U_c^2}{(sgd)}\right)^{0.4}\alpha^{-0.3} \quad (2.20)$$

Live Bed Scour: $$\frac{h_s}{D}=0.88\left(\frac{D}{d}\right)^{0.67}\left(\frac{h}{D}\right)^{0.4}\alpha^{-0.3} \quad (2.21)$$

In which U_c is the approach flow velocity at the initiation of scour and α is the opening ratio as defined earlier.

Kamil *et. al.* (2002) presented the following relation for the estimation of equilibrium scour depth for clear-water scour condition:

$$\frac{Z_{max}}{h} = 0.8\left[1-Exp\left\{-a_1\left(\frac{U_0 T}{v}\right)\right\}\right] \quad (2.22)$$

Where Z_{max} = elevation of the bed above a datum

h = flow depth

a_1 = 5.32×10^{-4}

U_0 = average flow velocity

T = Time from beginning of the scour process

v = Kinematic Viscosity of water

Muzzammil and Gangadhariah (2003) presented the following scour depth equation for clear-water scour condition.

$$\frac{h_{sm}}{D} = \left[10.93\left(\frac{U_c}{U_i}\right)^2 d^{*0.02}\left(\frac{U_c}{V_{\theta c}}\right)^{1/4}\right]\left(\frac{h}{D}\right)^{1/3} \quad (2.23)$$

Where h_{sm} = Maximum equilibrium scour depth

D = Diameter of pier model

U = mean approach velocity corresponding to initiation of scour

U_i = Mean approach velocity corresponding to initiation of sediment motion.

$V_{\theta r}$ = Maximum tangential velocity of vortex at equilibrium.

H = Depth of flow.

$d*$ = Dimensionless sediment number. U_c was estimated by the following equation of Garde *et. al.* (1989)

$$\frac{U_c^2}{sgd} = 1.2\left(\frac{D}{d}\right)^{-0.11}\left(\frac{h}{d}\right)^{0.16} \tag{2.24}$$

Wherein s = specific gravity of sediment

g = acceleration due to gravity

d = Mean size of sediment

Sheppard *et. al.* (2004) proposed the following equations for predicting local scour depth

For Clear water Scour

$$\frac{d_{se}}{b} = 2.5 f_1\left(\frac{y_0}{b}\right) f_2\left(\frac{U}{U_c}\right) f_3\left(\frac{b}{d_{50}}\right) \tag{2.25}$$

Where,

$$f_1\left(\frac{y_0}{b}\right) = \tan h\left[\left(\frac{y_0}{b}\right)^{0.4}\right] \tag{2.25.1}$$

$$f_2\left(\frac{U}{U_C}\right) = 1 - 1.75\left[\log\left(\frac{U}{U_C}\right)^2\right] \tag{2.25.2}$$

$$f_3\left(\frac{b}{d_{50}}\right) = \frac{\left(\frac{b}{d_{50}}\right)}{\left[0.4\left(\frac{b}{d_{50}}\right)^{1.2} + 10.6\left(\frac{b}{d_{50}}\right)^{-0.13}\right]} \tag{2.25.3}$$

The scour depth prediction formulae as reported above, and others that are not included here, give widely divergent results when employed at particular bridge site. This underlines the need for rigorous assessment of the influence of flow and bed conditions on local scour.

2.4 Parameters Governing Scouring

The wide range of predicted and measured values of scour depths at bridge piers, for what appears to be identical conditions, can be explained by the effects of a variety of specific parameters.

Factors which affect the magnitude of the local scour depth at piers as given by Richardson and Davis (1995), Raudkivi and Ettema (1983) and Lagasse *et. al.* (2001) are (1) approach flow velocity, (2) flow depth, (3) pier width, (4) gravitational acceleration, (5) pier length if skewed to main flow direction, (6) size and gradation of the bed material, (7) angle of attack of the approach flow to the pier, (8) pier shape, (9) bed configuration, (10) pier spacing in case of multiple piers, (11) orientation of piers with respect to the main flow direction and (12) ice or debris jams.

The depth of local scour is a function of a number of parameters, many of which are interrelated. For a single circular cylinder in an erodible bed, the factors influencing local scour can be divided into those describing the fluid, those describing the sediment, those describing the flow and those describing the pier (Breusers *et. al.*, 1977).

The parameters describing the fluid are fluid mass density (ρ) and dynamic fluid viscosity (μ) or kinematic fluid viscosity $(\nu = \mu / \rho)$, both of which are dependent on fluid temperature and salinity.

The parameters describing the sediment are:

(i) Characteristic grain diameter $(d \text{ or } d_g)$, which may be the median diameter (d_{50}).

(ii) Particle shape

(iii) Standard deviation of the grain size distribution $\left(\sigma_g = \sqrt{\frac{d_{84}}{d_{60}}} \right)$.

(iv) Density of sediment (ρ_s).

(v) Fall velocity (w_0) and

(vi) Angle of repose of the sediment (ϕ)

The parameters describing the flow are:

(vii) Flow intensity

(viii) Depth of the approach flow (y_0).

(ix) Depth averaged velocity of the approach flow (V)

(x) Shear velocity (V_*)

(xi) Velocity distribution.

(xii) Roughness of the approach flow (k_s).

(xiii) Energy slope of the flow (S_0).

(xiv) Bed slope (S_b).

(xv) Bed shear stress (τ).

The parameters describing the pier are:

(xvi) Pier size (b).

(xvii) Pier shape.

(xviii) Spacing, number and orientation of piers with respect to the main flow direction (i.e. angle of attack α).

In addition, there are derived parameters. Combining two or more of the above parameters, for example the critical shear velocity $(V_{*_c})$and the critical depth averaged velocity of the approach flow (V_c) to form the ratio (V/V_c), which is referred as flow intensity.

Dey (1997) also indicated the time of scouring as an additional parameter. Also, Oliveto and Oliveto and Hager (2002) and Oliveto and Oliveto and Hager (2005) found that the principal parameter influencing the scour process is the densimetric particle Froude number. The definition of densimetric Froude number as given by Oliveto and Hager (2002) is

$$F_d = V/(g' d_{50})^{1/2} \tag{2.26}$$

$$g' = [(\rho_s - \rho)/\rho]g \tag{2.26.1}$$

where, 'g' is the relative gravitational acceleration, ρ_s, is the sediment density, ρ is the fluid density, V is the approach flow velocity, d_{50} is the median sediment size and F_d is densimetric Froude number.

The parameters affecting the local scour around smooth cylindrical pier in cohesionless spherical sediment under uniform flow conditions can be assembled into the following dimensionless groups;

$$\frac{d_s}{D}=f\left[\frac{V}{V_c},\frac{Y_0}{D},\frac{D}{d_{50}},S_s,\frac{\rho_s}{\rho},\sigma_g,\frac{t}{t_0},\frac{V}{\sqrt{gy_0}},\frac{V}{\sqrt{gd_{50}}},\frac{V^2}{[(S_s-1)gd_{50}]},\left(\frac{Vd_{50}}{\nu}\right),\left(\frac{VD}{\nu}\right)\right] \quad (2.27)$$

The large number of interacting parameters makes the analysis of the local scour of the bed sediment around a bridge pier very difficult.

The influence of various hydraulic and sedimentological factors on scour depth around bridge piers has been studied by many investigators. Hjorth (1975), Breusers *et. al.* (1977) and Melville (1988) have reviewed much of the literature on this aspect. Some of its salient points are described here.

2.4.1 Influence of approach flow velocity

As the approach velocity (U) increases to certain fraction (0.5 for cylindrical piers) of the critical velocity U_c, scour will commence close to the pier (Hancu 1967, Nicollet 1971). The scour depth then increases almost linearly with velocity until the approach velocity is equal to U_c (Fig. 2.13, Chabert and Engeldinger 1956). When the approach velocity exceeds U_c, bed load movement is introduced and the problem is transformed into the live-bed scour problem. Once bed movement is fully established, the depth of scour is reduced somewhat below the scour depth at U_c. There is no longer any equilibrium scour depth but the depth of scour oscillates around a mean value. Recent studies have shown that as velocity exceeds the threshold velocity, the local scour depth first decreases and then increase again (Melville 1988).

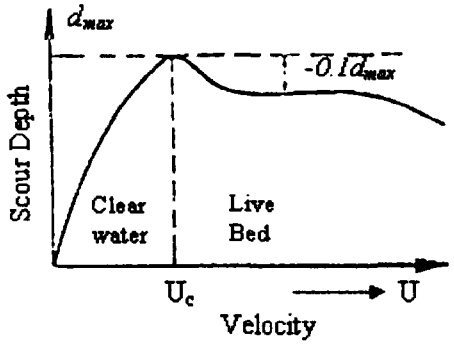

Fig.2.13 Scour depth for a given pier and sediment size as a function of approach flow velocity (after Chabert and Engeldinger, 1956)

2.4.2 Influence flow intensity

The ratio V/V_c is a measure of flow intensity and determines whether grain motion occurs on the channel bed (Melville and Chiew 1999). For $V/V_c<1$, clear–water scour conditions exist for both uniform and non–uniform sediments. Under clear-water conditions, the local scour depth in uniformly graded sediment increases almost linearly with velocity to a maximum at the threshold velocity (Melville and Coleman 2000). If the geometric standard deviation of the particle size distribution $\sigma_g < 1.5$, the sediment can be considered uniform. Live-bed scour occurs for $V/V_c > 1.0$. Under live-bed conditions, the local scour depth in uniform sediment first decreases and then increases again to a second peak, but the threshold peak is not exceeded provided the sediment is uniform. The same trend was observed by Chabert and Engeldinger (1956), Ettema (1980), Raudkivi and Ettema (1983), Laursen and Toch (1956), Breusers *et. al.* (1977) and Chiew (1984). For non-uniform sediments ($\sigma_g > 1.5$) armoring occurs on the channel bed and in the scour hole. Melville (1997) gave the flow intensity factor as shown in Fig. 2.14

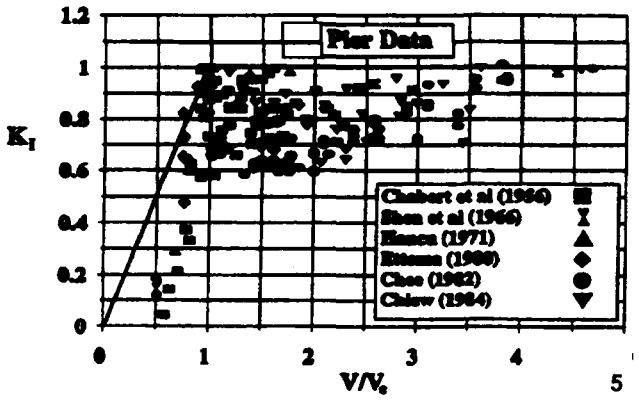

Fig.2.14 Flow intensity factor (after B.W. Melville, 1997)

Armor layer formation within the scour hole is known to reduce scour depths, as discussed by (Raudkivi and Ettema, 1977). The scour depth decreases from the threshold or clear-water peak value at $V/V_c=1$ to a minimum at about $V/V_c=1.5\ to\ 2$, at which stage the bed features are developed.

2.4.3 Influence of flow depth

The influence of flow depth on the scour depth has been discussed by many authors (*e.g.*, Chabert and Engeldinger 1956; Laursen and Toch 1956; Dey 1997; Breusers *et. al.*, 1977; Breusers and Raudkivi, 1991; Hoffmans and Verheij, 1977; Ettema, 1980; Melville and Sutherland, 1988; and Melville and Coleman, 2000).

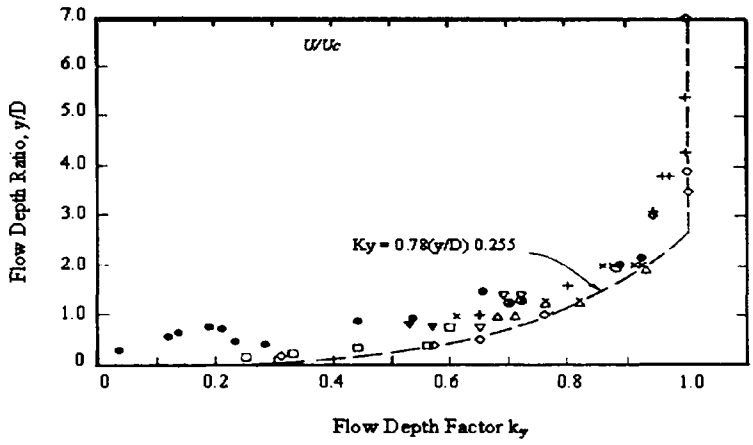

Fig.2.15 Influence of flow depth on scour depth (after Melville & Southerland, 1988)

This factor gives the most conflicting statements. For the case of live–bed scour most of authors claim that below some limiting water depth, scour depth decreases with decreasing water depth, but for water depth greater than the limiting depth, the depth of scour becomes independent of water depth. The limiting depth is believed to be equal to one or two times the pier width, on the other hand Laursen (1958) and most researchers influenced by the regime theory insist that for constant velocity, the depth of scour increases with increasing water depth.

For clear-water case an increase of water depth will increase (U_i). Thus the depth of scour decreases as the depth of flow increases. Even for this case there is a limiting water depth, under which the depth of scour will decrease with decreasing water depth.

The influence of flow depth is assumed to depend predominantly on the ratio of U_* / U_{*c} and y_0 / b. Breusers *et. al.* (1977) discuss the influence of y_0 / b but do not distinguish between clear-water and live-bed scour. Most researchers state that for a constant U_* / U_{*c}, the influence of flow depth can be neglected for $y_0 / b > 2$ to 3.

Neill (1964) used the data by Laursen and Toch (1956) to show that the depth of local scour is a function of depth of flow, for constant discharge is generally steepest, it increases again with further increase in V / V_c to a new peak value at the transition flat bed condition.

$$\frac{y_s}{y_0} = 1.5 \left(\frac{b}{y_0} \right)^{0.7} \tag{2.28}$$

Melville (1988) interpreted the water depth influence in terms of the interaction between the surface roller and the horseshoe vortex. He argued that the presence of the pier causes a surface roller around the pier and the horseshoe vortex at the base of the pier. The two rollers have opposite senses of rotation. In principle, so long as they do not interfere with each other, the local scour depth is insensitive to depth of flow. With increasing flow depth, the interference reduces until there is no significant effect of $y_0 / b \sim 3$. As the flow depth decreases, the surface roller becomes relatively more dominant and causes the horseshoe vortex to be less capable of entraining sediment from the scour hole. Therefore, for shallower flows, the scour depth is reduced.

Based on his envelope curves, Melville (1997) reported that the scour depth is independent of flow depth when $y_0 / b > 1.43$, however, this value is different from usually accepted value of $y_0 / b > 3 - 4$ (Breusers *et. al.* 1977; Ettema 1980; and Raudkivi 1986).

The flow shallowness b / y_0 (where b and y_0 are the pier diameter and flow depth, respectively) can be used to classify the influence of flow depth in relation to the width of the pier (Melville and Coleman 2000). Table 2.1, as adapted from Melville and Coleman (2000), shows a classification of local scour processes at bridge pier foundation.

Table 2.1. Classification of local scour processes at bridge pier foundations

Class	b/y_0	Local scour dependence
Narrow	$b/y_0 < 0.7$	$y_s \propto b$
Intermediate width	$0.7 < b/y_0 < 5$	$y_s \propto (by)^{0.5}$
Wide	$b/y_0 > 5$	$y_s \propto y_0$

2.4.4 Influence of sediment size

Early laboratory studies of local scour showed the effect of sediment size to be relatively minor. However, recent studies have shown that sediment size has definite bearing on the mechanism of scour (Nicollet 1971, Ettema 1980). Breusers *et. al.* (1977) argue that the influence of grain size (d) is limited for single particle size sediment.

Breusers and Raudkivi (1991) reported on the work of Raudkivi and Ettema (1977a, b). It was observed that a sediment size of $d_{50} \leq 0.7mm$ leads to a formation of ripples, whereas sediment size of $d_{50} \geq 0.7mm$ do not cause ripples (Fig. 2.16). Acoording to Raudkivi and Ettema, for non-ripple- forming sediments $(d_{50} \geq 0.7mm)$, experiments can run successfully with a flow condition, $V_* / V_{*c} \approx 0.95$, without the upstream bed being disturbed by the approach flow, whereas with finer sands $(d_{50} \geq 0.7mm)$ a flat bed cannot be maintained for the same flow condition. Breusers and Raudkivi (1991) concluded that ripples usually develop at shear velocity V_* above $0.6V_{*c}$, for sediment of size, $d_{50} \geq 0.7mm$.

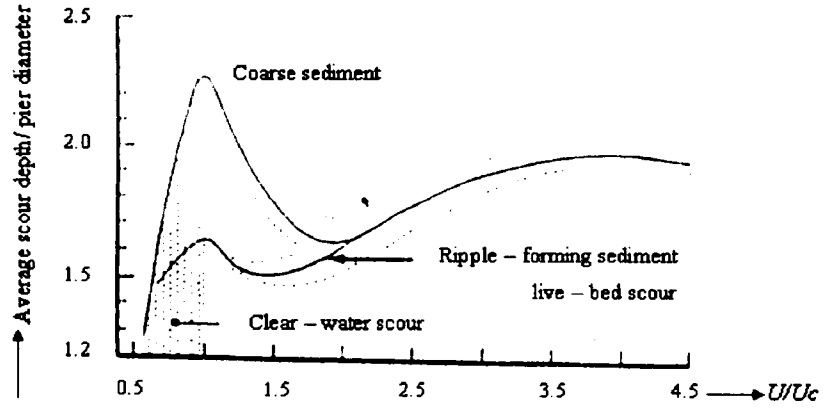

Fig.2.16 Diagrammatic illustration of scour depth at a cylindrical bridge pier in uniform sediment.

2.4.5 Sediment coarseness

The development and equilibrium depth of local scour are modified by the relative size b/d_{50} of the pier and sediment. According to Melville and Coleman (2000), b/d_{50} is referred as the sediment coarseness. Ettema (1980) for clear-water flows and Chiew (1984) for live-bed scour defined the influence of sediment size on scour depth at circular piers for uniform sediments. According to Ettema (1980), the local scour is independent of the sediment size if $b/d_{50} > 50$. For $b/d_{50} < 50$, he explained that the reduction in scour for relatively large sediments were due to the large particles impeding the erosion process at the base of the scour hole and dissipating some of the flow energy in the erosion zone. Melville & Sutherland (1988) and Melville (1997) have shown that for design purpose, the scour depth in uniform sediments is independent of sediment size when $b/d_{50} > 25$ as shown in Figs. 2.17 and 2.18.

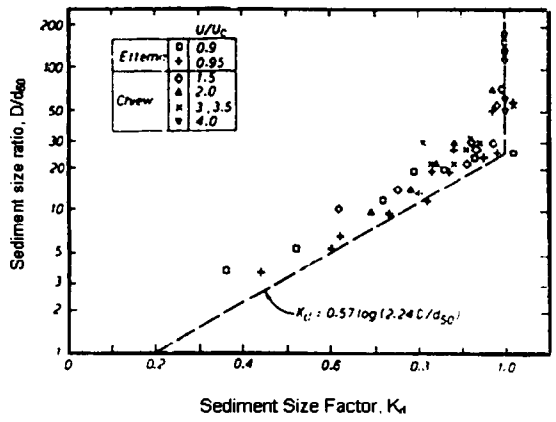

Fig.2.17 Sediments coarseness factor (after Melville & Sutherland, 1988)

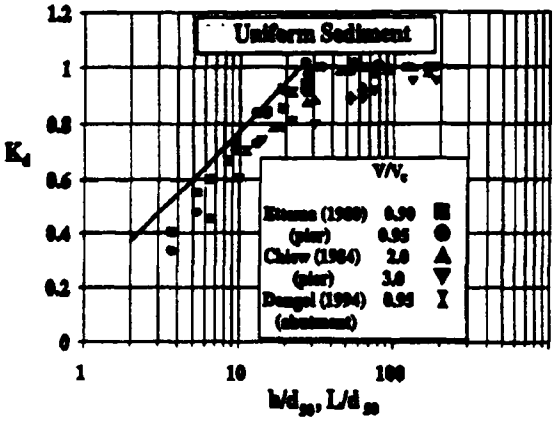

Fig.2.18 Sediment size factor for pier (after B.W. Melville, 1997)

2.4.6 Influence of pier shape

The most common shapes of piers used are circular, rectangular, square, rectangular with chamfered end, oblong, lenticular and Joukowski. Fig. 2.19 shows a schematic illustration of some pier shapes. The effect of pier shape has been reported by many researchers (*e.g.* Laursen and Toch 1956, Dey (1997), Breusers et al. 1977, Breusers and Raudkivi 1991, Melville and Coleman 2000).

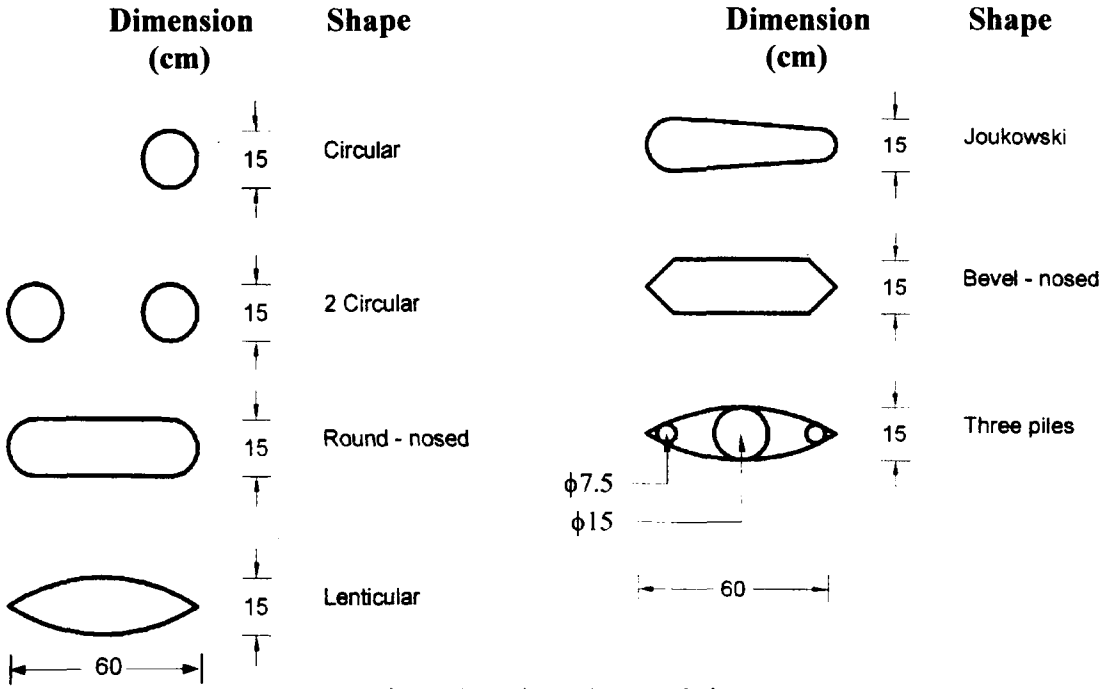

Fig.2.19 Various shapes of piers

Most investigators expressed similar opinions on the pier shape. The general conclusion is: the blunter the pier the deeper the scour (Keutner 1932, Laursen and Toch 1956, Shen *et. al.*, 1969). Richardson *et. al.* (1993) contended that the shape effect for circular cylindrical piers and square shape, round-nosed piers the shape factor K_s is reasonably constant, indicating that shape effects are insignificant. The shape of the downstream end of the pier is concluded to be of little significance on the maximum scour depth. The pier shape is often accounted for by using a shape factor. Melville and Chiew (2000) cited the work of Mostafa (1994) in which shape factor for uniform piers, was proposed. In practice, shape factors are only significant for zero degree angle of attack to the flow because even a small angle of attack will eliminate any benefit from a streamlined shape (Melville and Chiew 2000).

For piers aligned with the flow, values of shape factor, k_s are summarized in Table 2.1 in terms of width to over all length ratio, b/l, and pier shape, Dietz (1972).

The cylinder is used for comparative purposes. In practice, shape factors are important only if axial flow can be assured. Even a small angle of attack of the approach flow will eliminate any benefit from pier shape.

Table-2.2: Values of shape factor (k_s) for various shapes of pier.

S. No.	Pier Shape	b/l	b'/l'	k_s
1.	Cylindrical			1.0
2.	Rectangular	1:1		1.22
3.	--do--	1:3		1.08
4.	--do--	1:5		0.99
5.	Rectangular with semi-circular nose	1:3		0.9
6.	Semicircular nose with wedge-shaped tail	1:5		0.86
7.	Rectangular with semi-chamfered corners	1:4		1.01
8.	Rectangular with semi- wedge-shaped nose	1:3	1:2	0.76
9.	--do--		1:4	0.65
10.	Elliptic	1:2		0.83
11.	--do--	1:3		0.8
12.	--do--	1:5		0.61
13.	Ventricular	1:2		0.8
14.	--do--	1:3		0.7
15.	Aerofoil	1:3.5		0.8

2.4.7 Influence of pier size

It is a fact that the horseshoe vortex system whose dimension is a function of the pier diameter (see, Kothyari *et. al.*, 1992). Shen *et. al.* (1969) observed that the size of the horseshoe vortex is proportional to the pier Reynolds number R, which in turn is a function of the pier diameter. Under clear-water conditions, pier size influence the time taken to reach the ultimate scour depth but not its relative magnitude y_s/b, if the effect of relative depth, y/b, and coarseness b/d_{50} on the local scour depth are excluded (Breusers and Raudkivi 1991). They also concluded that the volume of the local scour hole formed around the upstream half of the perimeter of the pier is proportional to the cube of the pier diameter.

The effect of pier size on the depth of scour local is of major interest when laboratory data are interpreted for field use. The opinions presented on the relationship between pier size and equilibrium scour depth are quite diverging. Roughly these opinions can be summarized as: all other factors being kept constant, the scour depth varies as D^{β} where D is the pier width and $0.5 <= \beta \leq 1$. For instance Breusers (1972) proposes $\beta = 1$, Laursen (1958) design curve corresponds to $\beta = 0.7$, Larras (1963) suggests $\beta = 0.75$ and Shen *et. al.* (1969) found $\beta = 0.619$. Melville (1997) indicated that d_s is independent of b when $b/y_0 > 5$.

2.4.8 Influence of angle of attack k_θ

The angle of attack of flow for piers is the angle between the flow direction and the major axis of the pier alignment. The depth of local scour for all shapes of pier, except cylindrical, depends strongly on the alignment to flow. The depth of scour is a function of the projected width of the pier (Fig. 2.20 a, b), i.e. the width normal to the flow (Breusers and Raudkivi 1991), where the projected width of the pier is the width normal to the flow direction. As the angle of attack increases, the scour depth increases due to the increase in effective frontal width of the pier (Melville and Coleman, 2000) and the point of maximum scour depth moves along the exposed side of the pier towards the rear, and the scour depth at the rear becomes greater than that at the front face of the pier as shown in Fig 2.13. The angle of attack, for which the scour becomes deeper at the rear, depends on the ratio of the length of the pier to its width. Values of alignment factor K_θ for piers given by Richardson *et. al.* (2001) are reasonably consistent with the widely used Laursen and Toch. (1956) curve. In practice, the angle of attack at bridge crossings may change significantly during floods for braided channels, and it may change progressively over a period of time for meandering channels (Melville and Coleman 2000).

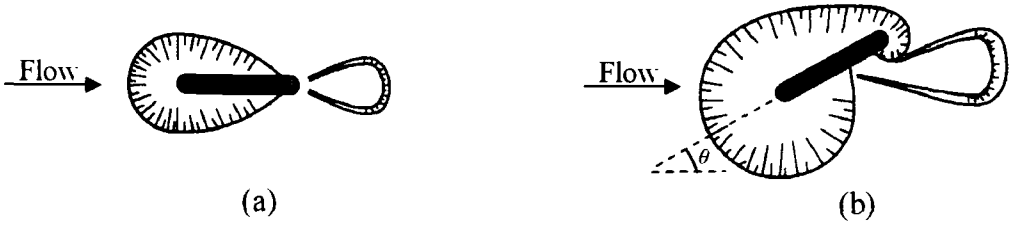

Fig.2.20 Diagramatic scour shapes at round – nosed rectangular pier (a) aligned with the flow (b) at an angle of attack

The value of alignment factor K_θ can be computed using the following equation of Richardson and Davis (2001).

$$K_\theta = (\text{Cos } \theta + l/b \text{ Sin } \theta)^{0.65} \qquad (2.29)$$

In which, θ is the angle of attack of flow, l is the length of pier, b is the pier width.

Laursen and Toch. (1956, 1953) investigated the influence of pier shape and angle of attack on scour depth. They defined the coefficient for angle of attack 'k_θ' as the ratio of scour depth at an angle of attack 'θ' to that at zero degree angle of attack and found that

length of round nosed pier has no influence for zero angle of attack and length/width ratios of 1 to 20. The authors presented also a graphic design relation for rectangular pier under zero angle of attack, which was expressed by Neill (1964 b) as:

$$\frac{ds}{b}=1.5(y_0/b)^{0.3} \tag{2.30}$$

The Laursen and Toch (1956) curve (Fig. 21) for flow alignment effects at bridge piers are widely used. For piers consisting of circular piers with spacing of more than '3b' (Dietz, 1973) and of course for a single circular pier, no influence of angle of attack has to be considered.

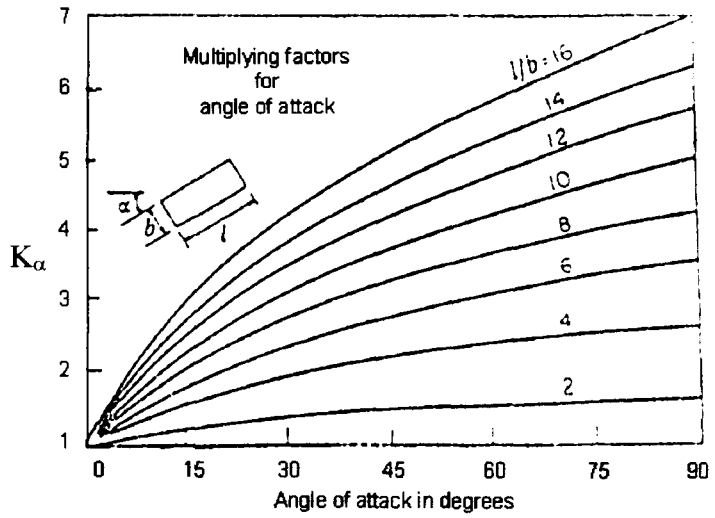

Fig.2.21 Alignment factor K_α for piers not aligned with flow (Laursen and Toch 1956)

A pier consisting of two or more circular pier seems to be an attraction over where there is influence of appreciable angle of attack (Chabert and Engeldinger 1956). They performed an extensive programme of measurement on the various aspects of local scour around piers. Also many devices to reduce the scour were tested (see, Fig 10, Breusers *et. al.*, 1977). Influence of pier shape and angle of attack can be seen in Fig. 10 of Breusers *et. al.*, (1977) wherein it is shown that at an angle of attack the scour depth may be minimized by streamlining the pier.

Melville (1997) gave multiplying factors shown in Table 2.2 for flow alignment effects at bridge pier.

Table 2.3 Multiplying factors for flow alignment effects at bridge pier (Melville, 1997).

Type	x/b	$k_s k_\theta$		
		$\theta<5°$	$\theta=5°-45°$	$\theta=90°$
Single row	2	1.12	1.4	1.2
	4	1.12	1.2	1.1
	6	1.07	1.16	1.08
	8	1.04	1.12	1.02
	10	1.0	1.0	1.0
Double row	2	1.5	1.8	-
	4	1.35	1.5	-

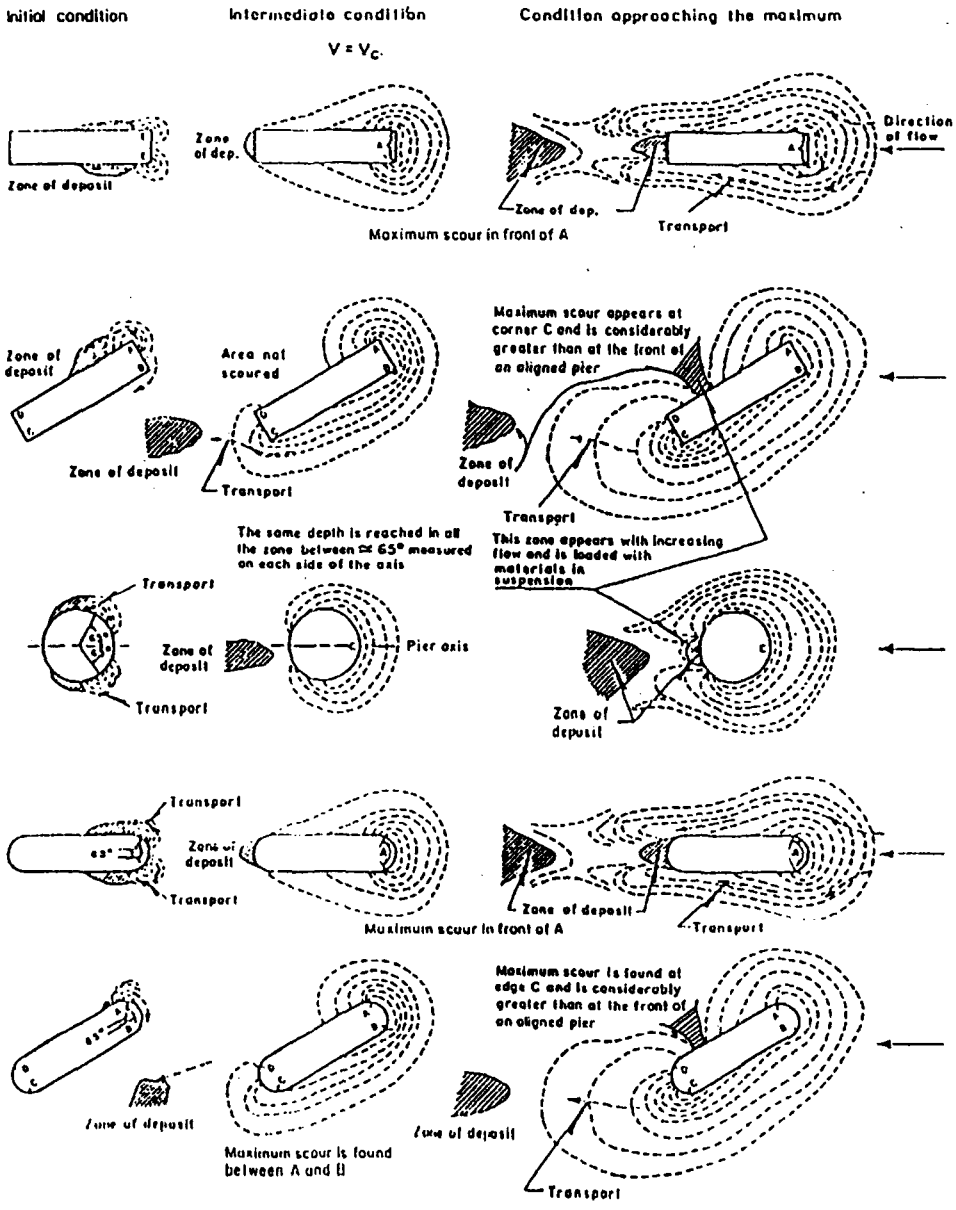

Fig.2.22 Diagrams that show different stages in the scour process (after Maza and Sánchez, 1964)

Richardson *et. al.* (1993) also investigated the effect of flow alignment on scour depth. The values of the alignment factor for piers given in Richardson et al. (1993) are reasonably consistent with Laursen and Toch (1956) curve. The angle of attack of alignment for piers is defined as the angle between the flow direction and the major axis of the non - circular pier. Flow alignment effect can be very important at bridge piers with value $k_\theta = 5$, which is possible for large θ.

The significance of flow alignment effects at pier means single circular cylindrical pier ($k_\theta = 1$ irrespective of θ) or piers comprising of a single row of circular columns ($k_s k_\theta < 1.2$ for all θ and $x/b > 4$) are to be preferred to other types when significant flow angles can occur. Flow alignment factors for rectangular pier are given in Table-2.3.

Table 2.4-values of flow alignment factor (Laursen and Toch, 1956)

Pier $l/b=4$	$\theta=0°$	15°	30°	45°	60°	90°	120°	150°
k_θ	1	1.5	2	2.3	-	2.5	-	-

Chabert and Engeldinger (1956) investigated the effect of angle of attack on scour depth for various shapes of piers. For round nosed rectangular having length to width ratio equal to 4, the scour depths and factor of angle of attack k_α are tabulated under given hydraulic conditions as shown in Table 2.4.

Table 2.5 Scour depth and factor of angle of attack for round nosed rectangular pier

Hydraulic conditions	**Angle of attack** α	**Maximum scour depth** d_s **(cm)**	k_α **= scour depth at angle** α **/scour depth at zero angle**
$V=0.65\ m/s$	0	20	1
$d_{50}=3\ mm$	7.5	25	1.25
$y=15cm$	15	30	1.5
$b=15cm$	30	39	2

Similarly, for two circular piers the scour depths and factor of angle of attack are tabulated in table 2.5.

Table 2.6 Scour depth and factor of angle of attack for two circular piers

Hydraulic conditions	Angle of attack α	Maximum scour depth ds (cm)	k_α =scour depth at angle α/scour depth at zero angle
V=0.65 m/s	0	22.5	1.125
d_{50}=3 mm	7.5	22.25	1.125
y=15 cm	15	22	1.1
b=15 cm	30	21	1.05

For three piles as shown in Fig. 2.14, the scour depths and factor of angle of attack k_α are tabulated in table 2.6.

Table 2.7 Scour depth and factor of angle of attack for three circular piers

Hydraulic conditions	Angle of attack α	Maximum scour depth d_s (cm)	k_α = scour depth at angle α/scour depth at zero angle
V=0.65 m/s	0	15	0.75
d_{50}=3 mm	7.5	17.5	0.875
y=15 cm	15	20	1.0
b=15 cm	30	26.5	1.25

2.4.9 Influence of constriction Ratio

The constriction ratio influences the equilibrium scour depth at piers. Shen *et. al.* (1966) suggest that for the purpose of experimental investigation, the flume width should be at least 8 times the pier size for clear- water scour conditions so that blockage effects are minimized. This value is generally accepted for clear-water experiments. However, for live- bed scour it has been found that the flume width should be at least 10 times the pier size otherwise scour depths are reduced due to bed features being modified as they propagate through the constriction.

2.4.10 Effect of opening ratio

The opening ratio α is defined as $\alpha = \frac{(B-b)}{B}$ where B is the center-to-center spacing of the piers and b is the pier width (Fig. 2.23). When b is small compared to B, α is close to unity and flow around one pier does not affect that around the other. However, as α decreases, the interference effects become more pronounced and scour depth increases, in such a case $\frac{y_{se}}{b}$ or $\frac{y_{sc}}{y_0} \propto \alpha^{-n}$. Here y_{se} and y_{sc} are scour depths below the water surface for sediment transporting and clear-water flows respectively. The analysis of extensive data collected by Garde *et. al.* (1987) indicates that $n=30$.

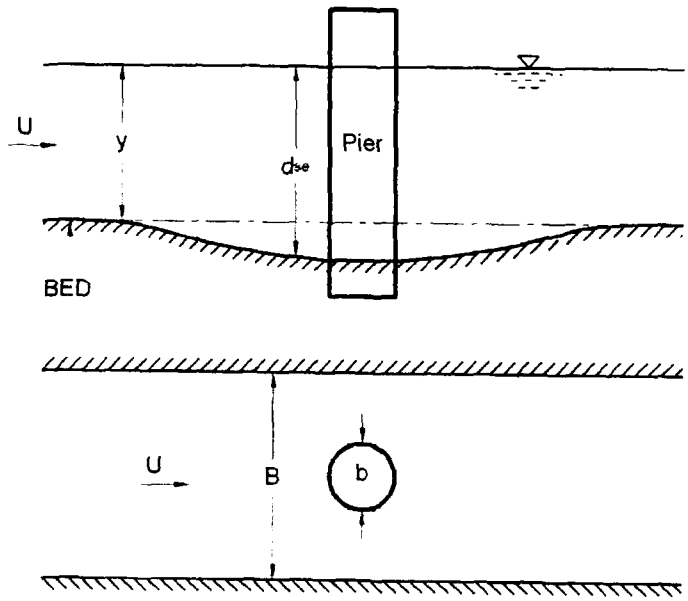

Fig.2.23 Schematic Diagram of Flume with Pier

2.4.11 Influence of sediment grading

The effect of grain size distribution on the local depth of scour at a pier was studied by Raudkivi and Ettema (1977a, b). Sediment gradation is usually characterized using the geometric standard deviation of the grain size,

$$\sigma_g = \left(\frac{d_{84}}{d_{15.9}} \right)^{1/2} \tag{2.31}$$

Ettema (1980) and Garde *et. al.* (1989) showed that both the rate of scour and the equilibrium scour depth decreases as the standard deviation of the particle size distribution increases due to the formation of armor layer at the base of the scour hole.

Raudkivi *et. al.* (1977) showed that the depth of clear-water scour is a function of standard deviation σ of the grain size distribution of the bed material and independent of the grain size in coarse grained, non-ripple-forming sediment (d > 0.7 mm) where $d_s/b=2.1-2.3$ for $\sigma=0$ and decreases with increasing σ/d_{50}.

In practice the possible maximum value of the equilibrium depth of clear-water scour, $y_{se}(\sigma)/b$ can be estimated from

$$y_{se}(\sigma)/b= \quad k_{se}\frac{y_{se}}{b}\ k_{se}\ y_{se}/b \tag{2.32}$$

Where y_{se} the equilibrium is scour depth in uniform sediment, $\sigma_g \cong 1.0$. The k_σ value as a function of σ_g, depends on whether the sediment is ripple forming or not as shown in Fig.2.24.

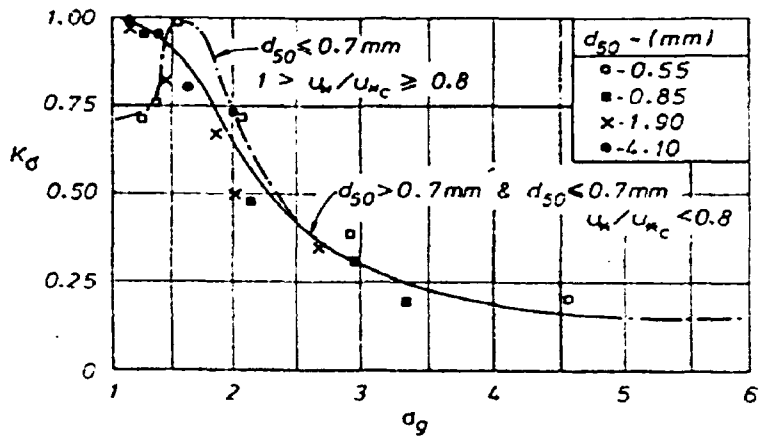

Fig.2.24 Coefficient of k_σ as a function of the geometric standard deviation of the particle size (after Raudkivi and Ettema, 1977a, b)

Under live-bed conditions the major effects of sediment grading are the following:

(i) The grain size and grain size distribution affect the type and height of bed features and hence, the range of variation of scour depth from its mean value under given conditions;

(ii) The grain size distribution affects the armoring process of the bed and hence, the mean scour depth at given conditions of flow;

(iii) If the larger grains of the distribution are near the threshold condition, they tend to accumulate in the local scour hole. This increases the porosity of the bed and more of the downflow disperse there, *i.e.*, its ability to scour is reduced:

(iv) If the large grains become large relative to the pier size, the local scour depth decreases.

2.5 Equilibrium Scour Depth and Time of Equilibrium

Equilibrium scour is said to occur when the scour depth does not change appreciably with time. The concept of an equilibrium scour condition is widely reported in literature Franzetti *et. al.* (1982). They refer to equilibrium as the state of scour development where no further change occurs with time. Several investigators have come up with different definitions of time to equilibrium scour depth (*e.g.* Heidarpour et al., 2003; Zarrati *et. al.*, 2004; Mia and Nago 2003; and Sheppard *et. al.*, 2004). Ettema (1980) defined the time to equilibrium scour as the time at which no more than 1 mm of incremental scour was realized within a timeframe of four hours. Sheppard *et. al.* (2004) and Melville and Chiew (1999) stopped their experiments when the change in the scour depth did not exceed 5% of the pier diameter during a 24 -hour period. The variation of scour depth with time is shown by Raudkivi and Ettema (1983) in Fig. (2.25).

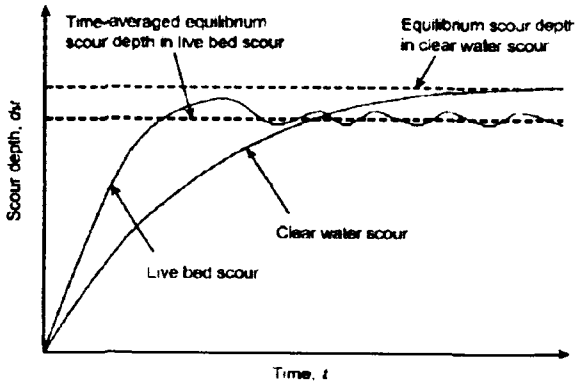

Fig.2.25 Scour depth for a given pier and sediment size as a function of time (Raudkivi and Ettema 1983)

2.5.1 Development of Maximum Scour Depth with Time

The behavioral pattern of scour at a cylindrical pier with respect to the variation of scour depth with time was discussed by Chabert and Engeldinger (1956). In clear-water scour,

equilibrium scour depth is approached asymptotically with time, while in live-bed scour, the scour develops rapidly and then fluctuates in response to the passage of bed-forms. The equilibrium scour depth in live-bed scour is 10% less than that in clear-water scour 10% condition (Shen *et. al.*, 1969).

2.6 Interference Effects of Multiple Piers on Flow

Many investigators have extensively studied the interference effects of two proximate circular cylinders placed in a free stream flow over rigid flat bed. The main findings of the investigation are well documented in Zdrakovich (1977 a, b, and 1987). A brief outline of the distinct features of the flow may be noted as follows:

2.6.1 Tandem arrangement (*i.e.*, aligned in the flow direction)

When the longitudinal spacing (X_c) is less than a certain critical spacing X_{cr} =1.9*b to* 3.5*b*, the downstream cylinder shields the wake of the upstream cylinder producing stagnant fluid in the intermediate space and suppressing the vortex shedding from the upstream cylinder completely. The actual value of X_{cr} depends on R_eD and free stream turbulence.

2.6.2 Side by side arrangement (*i.e.*, spaced laterally apart)

There exists a bistable characteristic of the flow in the gap between cylinders for $1.4 \leq Z_c / b \geq 2.0$ where Z_c is the lateral spacing of the cylinders. In this case, the flow in the gap biases towards one cylinder and then switches to the other intermittently. Consequently frequencies of vortex shedding exist with the higher value corresponding to the narrow wake and the lower value of the wide wake.

2.6.3 Staggered arrangement (*i.e.*, spaced both longitudinally and laterally)

The flow is characterized by biased flow towards the upstream cylinder so that the near wake of the upstream cylinder is always narrower than that of the downstream cylinder. As a result the frequency of the vortex shedding for the former body is always higher than for the later.

The flow around two cylinders in simple shear flow was investigated by El-Taher (1982, 1984, and 1985). It was found that influence effects in a linearly sheared flow normal to

the cylinder axis were larger than the corresponding effects in potential flow. Also, the free stream shear had a stabilizing effect on the intermittent change over flow pattern at the critical arrangements.

It must be noted that the flow characteristics at the junction of multiple piers with bed, which are related to the scour process, have not been studied so far.

2.7 Interference Effects of Multiple Piers on Local Scour

Local scour at a bridge pier is considerably influenced by nearby piers. Studies on this aspect of local scour reported in literature are reviewed here.

Timonoff (1929) performed a model study to investigate the importance of stream wise spacing of bridge piers in the case of parallel bridges. Based on the observed sheltering effect of upstream pier on the downstream pier he recommended that new bridge piers should be located in the immediate vicinity of old piers and axially aligned.

Tison (1940) carried out a model study to investigate the lateral spacing of piers, placed in side-by-side arrangement, on scour depths. He found a mutual interference on maximum scour depth for $Z_c / b \geq 4.3$, where Z_c / b is the lateral spacing of piers measured from center to center.

Dietz (1973) made a study of the angle of attack (θ) on maximum scour depth around laterally separated circular piers. He concluded that scour depth is not influenced by (θ) for $Z_c / b \geq 3$.

Basak *et. al.* (1975) showed that for a row of square piers aligned with the flow, maximum scour always occurred at the upstream face of the first pier where no influence of spacing and number of piers on scour depth was found. For other piers minimum scour was observed for $X_c / b = 4$ for rows perpendicular to the flow (that is, side by side arrangement), scour depth was found to decrease with increase in spacing upto $X_c / b = 5$.

Hannah (1978) carried out detailed investigation on local scour at groups of cylindrical piles with steady and uniform flow and clear-water condition. Four of the mechanisms involved in the scouring process at pile group were identical as:

(i) Reinforcing

It causes increased scour depths at the front pile. Bed material is continuously lifted from the base of the hole by the flow, which is not, however, capable of removing this material from the scour hole. When the downstream pile is so placed that the scour holes overlap, the bed level is lowered at the rear of the upstream scour hole. It is, thus, easier for the flow to remove material from this hole and it deepens. As the pile separation increases, the reinforcing effect decreases gradually and disappears when the maximum bed level between the piles returns to the undisturbed bed level.

(ii) Sheltering

The presence of an upstream pile can cause a reduction in effective approach velocity for downstream pile. This reduction weakens the effect of horseshoe vortex and thereby reduces scour at the downstream pile. A second form of sheltering occurs if the material scoured from the upstream pile is deposited on the bed in front of the downstream pile. Flow is then deflected up from the bed near the downstream pile, which reduces the horseshoe vortex strength. As pile separation increases, the velocity deficit in the wake of the upstream pile disappears and the sheltering effect decreases. All the studies of scour around pier groups substantiate the existence of sheltering mechanism for small angles of attack.

(iii) Vortex shedding

Vortices shed from an upstream pile are convected downstream. When a second pile is so placed close to one of the vortex shedding paths, the vortices assist in lifting the material from the scour hole. The scouring potential of the shed vortex is a function of its convection speed and of the distance between the path and the affected pile. This effect, therefore, decreases more rapidly for piles in line with the flow than for those at angles of attack which place downstream piles on the paths traced by vortices shed by upstream pile.

(iv) Horseshoe vortex compression

When piles are placed transverse to the flow, each will have, except at very close spacing, its own horseshoe vortex. As pile spacing is decreased, the inner arms of the horseshoe vortices will be compressed. This causes velocities within the arms to increase with a consequent increase in scour depths. This compression also exists for piles in staggered arrangement.

The interference effects on scour depth at places in various arrangements as reported by Hannah (1978) can be summarized as under.

2.7.1 Two Piers in tandem arrangement (Angle of attack 0°)

The scour depth at the front pier is the same as for a single pier at $X_c / b=1$. As separation between the piers increases, the front pile experiences the reinforcing effect which reaches a maximum at $X_c / b=2.5$ and is evident up-to $X_c / b=11$. For larger spacings, the scour depth is the same as for a single pier.

The scour depth at the rear pier is reduced due to sheltering effect. At $X_c / b=1$, the sheltering is complete with the two piers acting as one entity. The maximum scour depth in the resulting scour hole occurs at the front pier with the scour depth at the rear pier being only 87% of the maximum. As separation between the piers increases, the sheltering effect reduces and at $X_c / b=2$, a horseshoe vortex forms around the rear pier and increases in strength with separation. Therefore, vortices shed from front pier close enough to the rear pier, enhances the scouring. Scour depths at the rear pier thus increases with separation and reach maximum at $X_c / b=6$. At larger separations, scour depths reduce as a result of decrease in the vortex shedding effect and attain a maximum at $X_c / b=1.7$. With further separation, only the wake sheltering effect remains and this too progressively weakens.

2.7.2 Three piers in tandem arrangement

With three piers in line at equal spacings up to x/b=6, (x is the centre to centre pier spacing between the piers and b is the pile diameter) the scour at the middle pile was deeper and at the third pile, shallower than at the downstream pile of the two-pile group.

2.7.3 Two piers in side by side arrangement (Angle of attack 90°)

At $Z_c / b=1$, the piers act as a twin pier and its scour depth has been found to be 1.93 h_{si} (h_{si} = scour depth for isolated pier) in accordance with the notion of scour depth being proportional to the front width of the pier. It has been found that the scour depth decreases rapidly with separation to $1.3\,h_{si}$ at $Z_c / b=1.5$. Separate horseshoe vortices form

only at $Z_c/b=2$, but their arms are compressed due to the close spacing, thereby increasing their scouring potential. The horseshoe vortices get progressively de-compressed as Z_c/b increases and at $Z_c/b>8$ the scour depth is essentially that of a single pier. The scour holes become separate entities at $Z_c/b>11$.

2.7.4 Piers in staggered arrangement

This case was investigated in two phases. In the first phase the angle of attack was fixed at 45° and the separation between the piers was varied. The effect of angle of attack at constant radial spacing $R=5b$, was investigated in the second phase of investigation.

(a) Phase – I (angle of attack, 45°)

The scour depth of twin pier was found to be $1.77h_{si}$. The scour depth at the rear pier exceeded that at a front pier for all values of R/b between 1 and 11. At greater separation, the piers were found to be acting independently having scour depths equal to that of a single pier. Increased scour depths at the rear pier were attributed to the action of vortex shedding from the front pier and compression of the horseshoe vortices between the two piers, which together overcome any sheltering effect. The maximum difference between front and rear scour depths was observed at $R/b=4$.

(b) Phase – II (Effect of angle of attack,α)

The scour depth at the front pier is found to be relatively insensitive to angle of attack, varying by less than 5% of its value at $\theta=0°$. Scour depths at the rear pier are much more sensitive to changes in angle of attack. At small angles, ($\theta<15°$), the dominant effect at the rear pier is sheltering by the front pier. As (θ) increases, sheltering is reduced and the pier is affected by vortex shedding. Consequently, scour depth increases reaching a maximum for $R/b=5$ at approximately $\theta=45°$. Scour depths reduce when the pier moves clear of the shed vortices and approach that of a single pier as (θ) approach $90°$.

Elliott and Baker (1985) investigated the effect of lateral spacing on scour depth for clear-water conditions. They too demonstrated the enhanced scouring affect of close

lateral spacing $(Z_c/b)<7$, and explained increased scour effect by compression of horseshoe vortices and the accelerated flow in the contracted zone between piers.

Shah (1988) investigated mutual interference effects of neighboring bridge piers on scour depths using fine sand for two bed configurations namely, threshold condition and ripple bed condition. Significantly among his results, for staggered pattern (two upstream piers laterally separated and downstream pier on the normal bisector of the former), he reported that the downstream pier scour depth exceeds the isolated pier scour depth, but the former asymptotically approaches the latter for large X_c/b. He also found that an increase in the lateral spacing of upstream piers diminishes the mutual interference effect on their scour depth. Salient points emerging from the above account on interference effects are summarized below.

Babaeyan-Koopaei and Valentine (1999), Choi et al. (2001) Sidek and Ismail (2002) have made some studies on scour around group of piers. However, these studies have provided limited data.

2.7.5 Tandem arrangement

All investigators have reported that rear pier scour depth is less than that of isolated pier, but there is some difference in opinion regarding the front pier scour depth. Timonoff (1929), Basak *et. al.* (1975) and Shah (1988) have reported that the front pier scour depth is not affected by the presence of the rear piers, whereas Hannah (1978) reported an increase in the front pier scour depth due to the reinforcing effect.

2.7.6 Side-by-side arrangement

Interference effects resulting in increased scour depths have been always observed for lateral spacing less than some limiting spacing between $3b$ and $8b$. Beyond the limiting spacing, no effect of one pier on its neighboring pier scour depth was observed.

2.7.7 Staggered arrangement

Hannah (1978) showed that the front pier scour depth is far less sensitive to the angle of attack compared to the rear pier scour depth. The latter increases from $h_s/h_{si}=0.95$ at

$\theta=0°$ to around $h_s / h_{si}=1.2$ at $\theta=45°$, and then starts decreasing, where h_{si} is the depth of scour for an isolated pier.

It is evident from the literature cited above that there is paucity of information on the effects of mutual interference on local scour at bridge piers. The following deficiencies, in particular, may be noted.

(1) Most studies of local scour around bridge piers are confined to an isolated pier. The studies of local scour at multiple piers are limited and also confined to limited extent.

(2) All of the available scour depth models are developed for an isolated pier. Almost no scour depth model, except Elliott et al. model for transverse piers, is cited in the literature which takes into account the effect of mutual interference of bridge piers on local scour.

(3) The flow characteristics at the junction of multiple piers with bed, which are related to the scour process, have not been studied so far.

(4) The interference effects on local scour due to multiple piers have been observed and recognized but information on this aspect is limited, and rigorous physically sound modeling does not seem to within reach yet.

(5) Most studies of scour protection are confined to an isolated pier and the studies concerning scour protection at multiple piers are scarce.

2.8.0 Local scour countermeasures

The local scour has the potential to threaten the structural integrity of bridge piers, ultimately causing failure when the foundation of the pier is undermined. Besides the human loss, bridge failures cost millions of dollars in direct expenditure for replacement and restoration in addition to the indirect expenditure related to the disruption of transportation facilities. A series of recent bridge failures due to pier scour, as reported by Wardhana and Hadipriono, (2003), S. Dey and Barbhuiya (2004) and Hoffmans and Verheij (1997), rekindled interest in furthering for developing improved ways of estimating the maximum scour depth and protecting bridges against the ravages of scour (Fig. 2.26).

Fig. 2.26 Photo of Schohaire Creek Bridge April 5, 1987. Courtesy of the National Bridge Inventory Web Page.

2.8.1 Reduction and protection of scouring around bridge piers

Scour around bridge piers as a result of flooding is the most common cause of bridge failure (Richardson and Davis, 1995; Johnson and Dock, 1996; Lagasse *et. al.*, 1995; Melville and Hadfield, 1999). The bridge failures result in excessive repairs, loss of accessibility, or even death (Chiew, 1995).The potential cost including human toll and monetary cost of bridge failure due to scour damage has highlighted the need for better scour prediction and protection methods. A large depth of foundation is required for bridge piers to overcome the effect of scour which is a costly proportion. Therefore, for safe and economical design, scour around the bridge piers is required to be controlled.

The problem of local scour of sediment around bridge piers has been studied extensively for several decades. The design guides, like- HEC-18 (Richardson and Davis, 1995) and the Indian Road Congress Code IRC-78 ("standard" 1983) - require deep and expensive pier embedment in rivers. To reduce this depth of embedment, efforts have been made to reduce the depth of scour by placing the riprap around the pier (Brice *et. al.*, 1978; Croad, 1993; Parola,1993; Yoon *et. al.*, 1995; Worman 1989, (Lim and Chiew, 1996 and 1997); Lim, 1998; Chiew and Lim, 2000; Lim and Chiew, 2001), providing an array of piles in front of the pier (Chabert and Engeldinger, 1956 and Melville and Hadfield,1999), a collar around the pier (Schneible, 1951; Thomas 1967; Tanaka and Yano 1967; Ettema 1980; Chiew, 1992; kumar *et. al.*, 1999, Zarrati *et. al.*, 2004, Zarrati *et. al.*, 2006), submerged vanes (Odgard and Wang 1987), a delta-wing-like fin in front of the pier (Gupta and Gangadharaiah, 1992), a slot through the pier (Chiew, 1992; Kumar *et. al.*, 1999) and partial pier-groups (Vittal *et. al.*, 1994) and tetrahedron frames placed around the pier.

2.8.2 Flow pattern and mechanism of scouring

The performance of any scour protection device around bridge piers depends on how the device counters the scouring process. Flow mechanism of scouring around a bridge pier is very complex and has been investigated by various researchers (Chabert and Engeldinger, 1956; Hjorth, 1975; Melville, 1975; Melville and Raudkivi, 1977; Dargahi, 1990; Ahmed and Rajaratnam, 1998 and Graf and Istiarto, 2002).

The vortex system and down-flow are the principal causes of local scour. At the upstream face of the pier, the approach flow velocity goes to zero. This causes an increase in pressure. Due to this phenomenon the water surface level in front of pier increases. As the flow velocity decreases from the surface to the bed, the dynamic pressure on the pier face also decreases downwards. The downflow digs a hole in front of the base of the pier, rolls up and by interaction with the coming flow forms a complex vortex system (Fig.2.27).

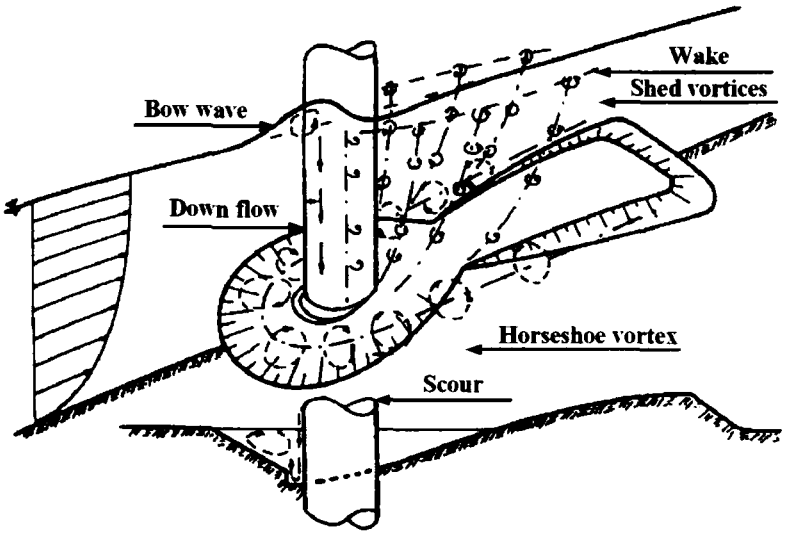

Fig. 2.27 Diagrammatic flow pattern at a cylindrical pier (after Raudkivi, 1986)

Based on mechanism of scour, countermeasures to control the local scour at bridge piers can be grouped in two categories.

2.8.3 Armoring devices

Using this device, the streambed resistance is increased by placing the riprap and gabions around the piers. Several researchers (Brice *et al.*, 1978; Croad, 1993; Parola, 1993; Yoon *et. al.*, 1995; Chiew, 1995; Worman 1989, (Lim and Chiew, 1996 and 1997); Lim

et. al., 1998; Chiew and Lim, 2000; Lim and Chiew, 2001) have attempted to determine the size and extent of the riprap layer.

2.8.4 Scour protection using rip-rap

One of the methods to stop the scouring action of horse-shoe vortex is to provide materials, which cannot be detached from its position. The use of riprap stones to deal with pier scour problems is very common in civil engineering practice. However, riprap layers often fail to protect bridges during floods despite placement of riprap stones around its foundation. One of the main reasons of such failure is the general movement of sediment during severe flood conditions. During floods, a live-bed condition with the presence of bed features, *e.g.* ripples and dunes, is very likely to occur. The movement of bed sediment along the channel and the propagation of bed features cause the immobile riprap stones to lose their stability, eventually embedding into the bed. This type of failure, earlier reported by Lim *et al.*, (1998) and Chiew and Lim (2000), has also been reported by Brice *et. al.* (1978), Croad (1993) and Lim and Chiew (1996 and 1997) in field and laboratory studies, respectively. Various design criteria have been suggested (Bonasoundas, 1973; Neill, 1973; Richardson *et. al.*, 1993; Posey, 1974; Breusers *et. al.*, 1977 and Chiew, 1995). The parametric studies on the embedment process of riprap stones have also been conducted (Chiew, 1995; Chiew and Lim 2000; Hager, 2006).

2.8.5 Flow altering devices

Using flow altering devices, the shear stresses on the riverbed, in the vicinity of pier, are reduced by altering the flow pattern around a pier which in turn reduces the scour depth at the pier.

Attempts have been made by several investigators to reduce the depth of scour around a pier using flow altering devices (Schneible, 1951; Chabert and Engeldinger, 1956; Thomas, 1967; Tanaka and Yano, 1967; Ettema, 1980; Odgard and Wang, 1987; Chiew, 1992; Gupta and Gangadharaiah, 1992; Chiew, 1992, Vittal *et. al.*, 1994; Melville and Hadfield, 1999; Kumar *et. al.*, 1999; and Zarrati *et. al.*, 2004, 2006).

2.8.6 Scour reduction using slots

Reduction of scouring by indirect method can be achieved by using a slot through the pier, which helps to pass most of the flow through it because of a favorable pressure gradient and balance would be left to cause much reduced scour damage (Chiew,

1992;Vittal *et. al.*, 1994; Kumar *et. al.*, 1999). The basic principle of using a slot is either to divert the downflow away from the bed, or to reduce the downflow impinging on the bed. The width, length and location of the slot are significant parameters. When the slot is placed near the bed, the oncoming flow at the bottom boundary layer accelerates through the slot as a horizontal jet.

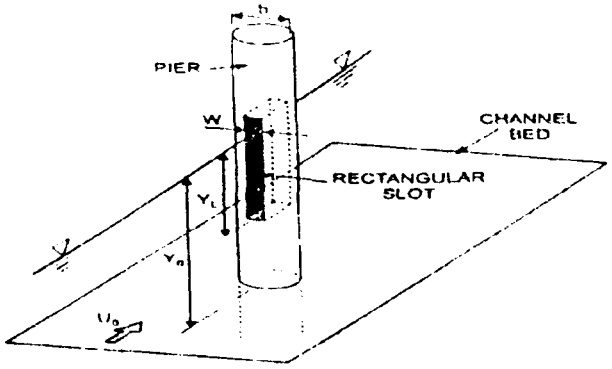

Fig.2.28 Slot through a pier

Since the downflow at the pier is perpendicular to the jet, the latter deflects the downflow away from the bed, reducing its scouring potential. There are limitations on the use of a slot through pier. The danger of choking of the slot space due to debris and floating materials is very high. They also reduce the strength of pier structure. Hence, they cannot be considered as good scour protection device. Chiew (1992) proposed a vertical slot in a cylindrical pier of scour reduction. Kumar *et. al.* (1999) also used piers slot for scour reduction (Fig. 2.28). Various types of slots as shown in Fig. 2.29 have been used by several investigators

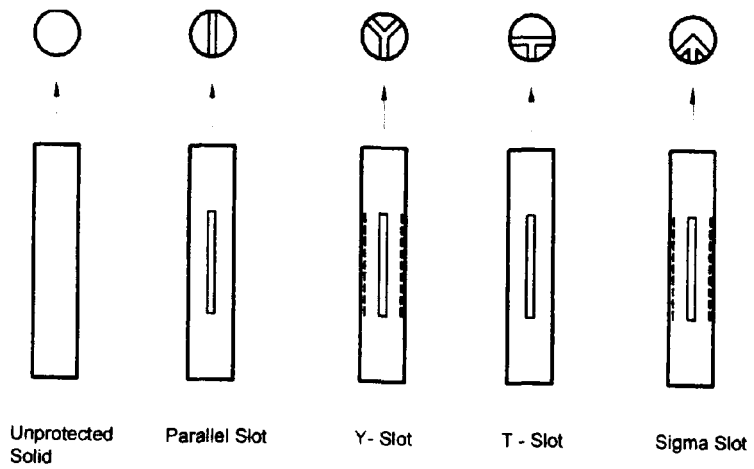

Fig.2.29 Various Types of Slots

2.8.7 Scour reduction using collar

When a collar is installed around the pier, the direct impact of the down flow on the streambed is prevented, which not only causes reduction in the maximum scour depth but also the rate of scouring is also reduced considerably. Reduction in the rate of scouring reduces the risk of pier failure when the duration of flood is low.

The scour reduction efficiency of collars has already been established in earlier studies (Zarrati *et. al.*, 2006; Zarrati *et. al.*, 2004; Kumar *et. al.*, 1999; Chiew, 1992; Ettema, 1980; Tanaka and Yano, 1967; Thomas 1967; Schneible, 1951). Chiew (1992) also tested a collar with an effective width of three times the pier diameter installed at 0.2b above the sediment bed together with a slot 0.25 D wide with a length of $2b$ near the bed and reported zero scour depth at the pier. Kumar *et. al.* (1999) performed a series of experiments on effectiveness of collar for control of scouring around circular bridge piers. They concluded that with a collar at the bed when W is 4 times pier width, there will be no scour in front and sides of the pier, but a deep scour hole forms at the pier's rear. For the use of collars around piers Kumar *et. al.* (1999) derived the following design relationship

$$\left(\frac{ds_p - ds_c}{ds_p}\right) = 0.057\left(\frac{B}{b}\right)^{1.612}\left(\frac{H}{Y_0}\right)^{0.837} \qquad (2.33)$$

Where:

ds_p = depth of scour on pier without a collar
ds_c = depth of scour on pier with a collar
B = diameter of collar
b = diameter of circular pier
H = elevation difference between water surface and collar surface
Y_0 = depth of water above bed elevation

Zarrati *et. al.* (2004) conducted a series of experiments using a collar for control of scouring around rectangular pier having a collar with the same width all around the pier. They used two sizes of collars ($W = 2b$ and $W = 2b$). As the rectangular piers are sensitive to the angle of attack of flow and scour depth around them increases rapidly with an increase in angle of attack (Laursen and Toch, 1956; Ettema *et. al.*, 1998), Zarrati *et. al.* (2004) also performed some experiments with varying angles of attack.

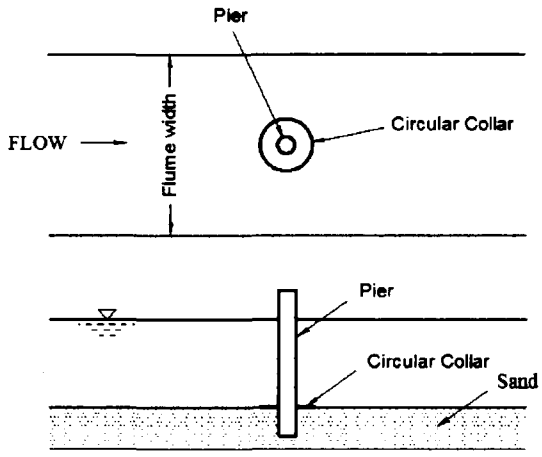

Fig.2.30 Schematic illustration of a pier fitted with a collar

Zarrati *et. al.* (2006) examined experimentally the scour depth reduction efficiency of collar around a group of two circular piers aligned with the flow (Fig.2.31) and transverse to the flow (Fig.. 2.32).

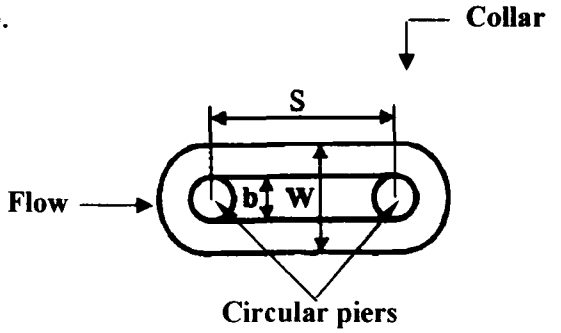

Fig. 2.31 Group of two piers with collar aligned with the flow

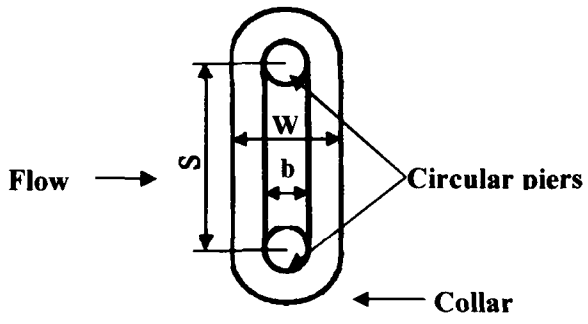

Fig. 2.32 Group of two piers with collar aligned transverse to the flow

The space between two piers was covered with rip-rap. The data showed that in the case of two piers in line, combination of continuous collars and riprap results in the most significant scour reduction. Experiments however, indicated that collars were not so effective in reduction of scouring around two transverse piers.

2.8.8 Scour reduction using sacrificial piles

A group of piles located upstream of the pier generates as many turbulent wakes as the number of piles and creates relatively low velocity wake region with interacting individual pile wakes. The net result is reducing the horse-shoe vortex strength and consequent reduction in scour depth significantly. Vittal *et. al.* (1994) studied a group of three circular smaller size cylinders as a replacement of an equivalent pier having a diameter circumscribing the three smaller size cylinders to reduce the scour depth.

Chabert and Engeldinger (1956), conducted experiments to investigate the scour reduction using sacrificial piles. A recent laboratory study of use of sacrificial piles to protect pier against scour is reported by Melville and Hadfield (1999). They concluded that effectiveness of sacrificial piles as a scour counter-measure is dependent on the velocity flow angle and flow intensity. For sacrificial piles are ineffective as scour counter-measure under live-bed condition. For sacrificial piles produces moderate reduction in scour depth. Submerged piles were found slightly more effective than full depths. Finally they concluded that sacrificial piles may not be recommended as effective scour counter-measure, unless the flow remains aligned and the flow intensity is small.

2.8.9 Foundation caissons

Chabert and Engeldinger (1956) investigated a circular pier founded on a circular caisson and concluded that the best system appeared to be a caisson having diameter three times the diameter of pier and the top elevation above half the diameter of the pier below the natural bed. They reduced the scour depth one-third that reached with the pier alone.

Shen and Schneider (1969) investigated a variant of the caisson system in which the caisson surrounded by vertical lip (cut off sheet pile) was used. The main idea was to contain the horse-shoe vortex in side an enclosure allowing it escape downstream. The lip certainly allows a reduction in dimensions of the caisson.

2.8.10 Delta-wings like passive device

The geometrical feature of delta-wing like passive device shown in Fig. 2.33. The passive device was developed using aerodynamic principal flow past delta-wing like plate with negative angle of attack. This position of delta-wing reverses the sense of rotation of trailing vortices.

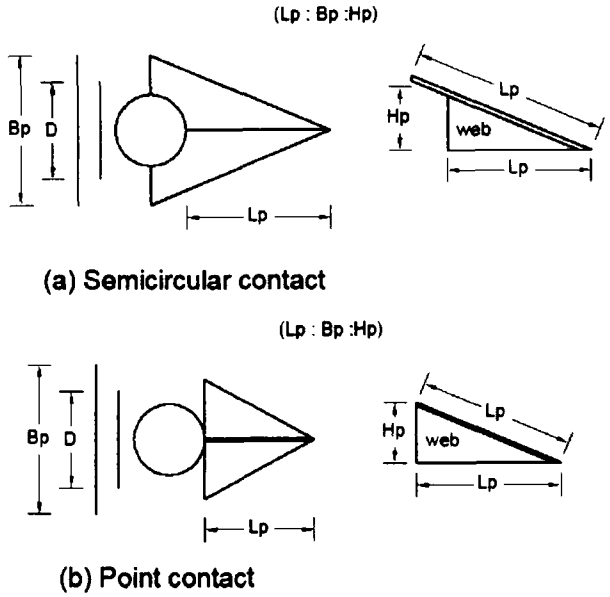

Fig.2.33 Definition of a delta wing-like passive device (after Gangadhariah and Gupta, 1992)

When this device attached to the leading edge of the pier junction, it modifies rotational direction of the horseshoe vortex as shown in Fig.2.33. Reversal in the direction of rotation of horseshoe vortex causes the scouring away from the pier and depositing the sediment near the pier. This action strengths the stability. Gangadhariah and Gupta (1992) proposed the use of a delta wing like device infront of the pier for scour reduction.

2.8.11 Other methods of scour protection

Among other methods available in literature a few are discussed here. They are submerged vanes (Iowa vanes), slanting vanes on the front face of the piers and armoring using different types of artificial material (Parker *et. al.*, 1998).

2.8.12 Submerged vanes

Various vanes rectangular plates were held at an angle in the horizontal direction of flow. They diverted the flow to one side and also caused tip vortices generation at their rear edge. These tip vortices were able to disrupt the horse-shoe vortex which might result in reduction in scour depth. The array of vanes provided upstream of the pier directed the eroded sediment into the scour hole and thus retarded the scouring process. Sketch showing dimensions and plan layout in front of bridge piers is shown in Fig.2.34.

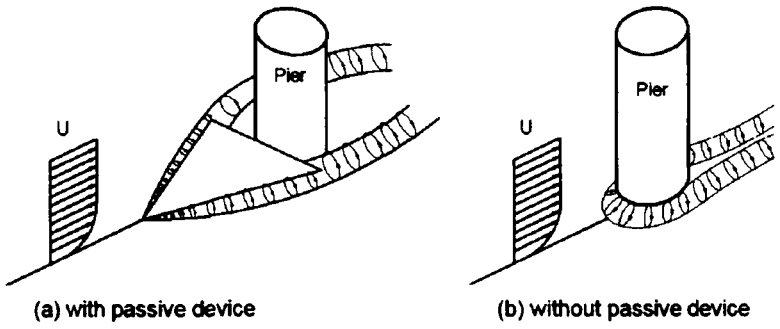

Fig.2.34 Flow Modification by Passive Device (after Gangadhariah and Gupta, 1992)

2.8.13 Other methods of scour protection

Among other methods available in literature a few are discussed here. They are submerged vanes (Iowa vanes), slanting vanes on the front face of the piers and armoring using different types of artificial material (Parker *et. al.*, 1998).

2.8.14 Submerged vanes

Various vanes rectangular plates were held at an angle in the horizontal direction of flow. They diverted the flow to one side and also caused tip vortices generation at their rear edge. These tip vortices were able to disrupt the horse-shoe vortex which might result in reduction in scour depth. The array of vanes provided upstream of the pier directed the eroded sediment into the scour hole and thus retarded the scouring process. Sketch showing dimensions and plan layout in front of bridge piers is shown in Fig.2.35.

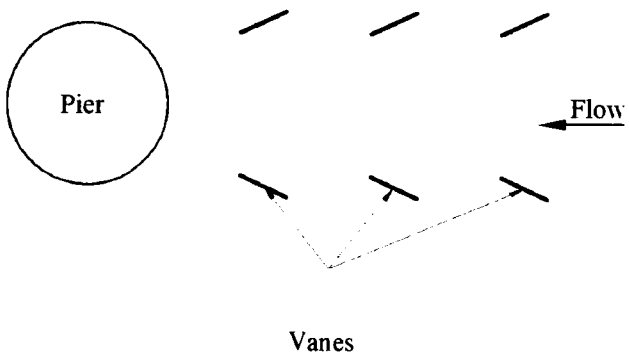

Fig.2.35 Definition sketch of submerged vanes (after Parker *et. al.*, 1998)

2.8.15 Slanting vanes on front face of piers

Slanting vanes with downward orientation were attached on either side of splitter plate locating on the line of symmetry of the pier front face. The details of the vane are shown in Fig.2.36. The design principal of this is to suppress down swelling zone of horse-shoe vortex. This device needs further testing for its use.

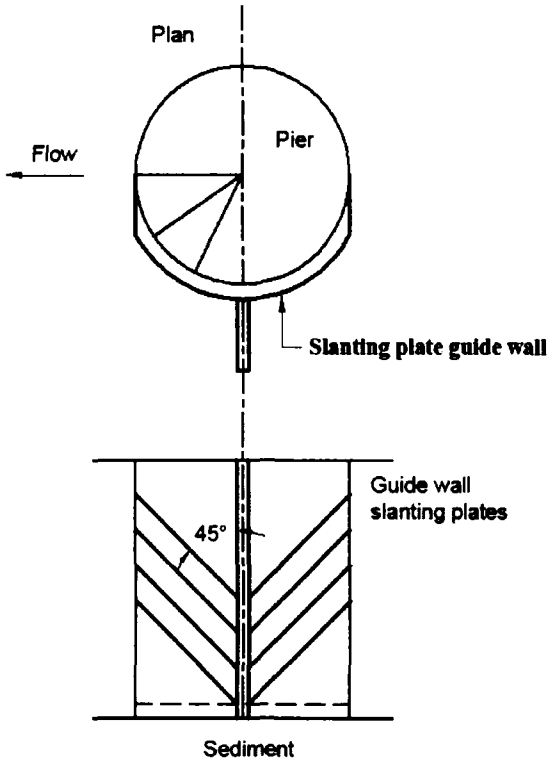

Fig.2.36 Slanting vanes attached to pier (after Parker *et. al.*, 1998)

2.8.16 Stone gabion with geotextile filter

Stone gabions consist of bundles of stones laid in wired net box and each gabion is interconnected with the neighboring stone box. Geotextile filter is used below the stone gabion. This is needed to stop the suction of sediment from the bed through the gabion due to resulting reactions of scouring mechanisms. Geotextile filter is of non-woven type.

2.7.17 Use of tetrapods as artificial rip-rap

Artificial materials like tetrapods (Fig. 2.37) may be stacked around bridge pier. They interlock themselves by creating good bond in between. Their performance as scour protection device is good. (Parker *et. al.*, 1998).

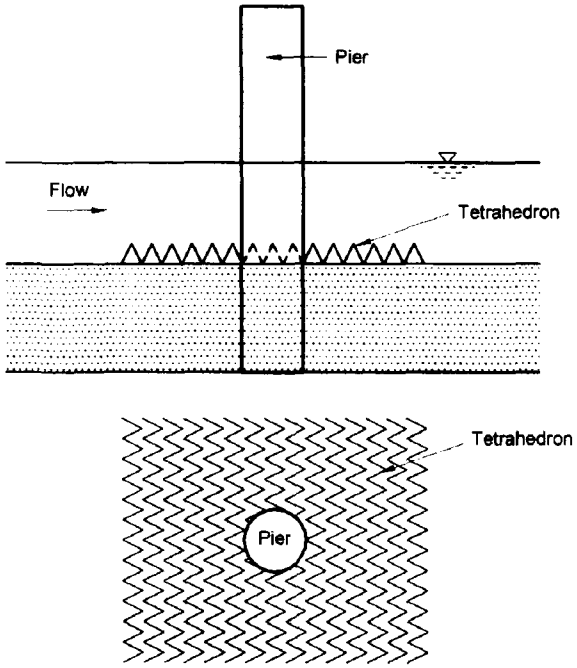

Fig. 2.37 Definition sketch of placement of tetrahedron frames (after Parker *et. al.*, 1998)

2.7.18 Concrete filled fabric mats

These are similar to riprap. Concrete filled fabric mats are laid around the bridge piers. They form rigid surface, which prevents scouring action. (Parker *et. al.*, 1998).

2.8.19 Concluding remarks

Flow altering devices can be more economical, especially when the riprap material in required amount is not available near the bridge site or is expensive. However, there are certain limitations on the use of these flow altering devices to reduce the scour depth at piers. A slot may be blocked by floating debris. In addition to this, its construction is difficult. Sacrificial piles may become ineffective when the flow approaching the piers changes its direction. A thin collar plate skirting around bridge piers at or below the bed level which diverts the down flow and shields the streambed from its direct impact is therefore, a very effective mean of protection against scour. The application of collar around a single cylindrical and rectangular pier has been tested; however, scanty information is available in literature about the application of collar on group of piers.

2.9 Scour Depth Prediction Using Artificial Neural Network (ANN)

It is extremely difficult to formulate mathematical models that accurately represent the scour process and the geometry of the scour hole which develops under the influence of

three dimensional flow field around a pier. Thus, it is a common practice to apply empirical relationships based on the regression methods performed on laboratory data for estimation of the scour around a pier. However, due to complexity of the scour problem empirical relationship based on laboratory data are not strong enough to deal with the problem of estimating the scour depth around a pier. Moreover, since there are numerous effective parameters and the interaction of these parameters is highly complicated, therefore, the accuracy of the empirical relationship is very subjective and highly depends on the users ability and knowledge. In the light of above numerous approaches for the estimation of scour depth around piers have been carried out in the past (Laursen and Toch, 1956; Shen, 1971; Hancu, 1971; Breusers *et. al.*, 1977; Melville and Southerland, 1988; and DOT U.S., 1993). In addition, some relevant studies on the mechanism of flow around pier type structures have been conducted recently (Sumer and Fredsoe, 1994, 1997). However, there is a lack of reliable formulas for predicting the scour depth to cover all possible ranges from the aforementioned methods. The results from the existing method show up to 100% variation resulting in an increase in the cost of the protection methods against scour and the foundation of the piers. Recognizing these difficulties and the importance of improving prediction capabilities a great number of researchers have been engaged in exploring and refining methods for improving traditional physical based analysis.

Recently Artificial Neural Networks (ANNs) are being widely applied in various areas of hydrology and water resources engineering to overcome the problem of exclusive and the non-linear relationships. Some of the examples of ANNs application are the prediction of rainfall intensity (French *et. al.*, 1992), assessment of the stability of an armor unit and rubble mound breakwater and estimation of wave forces acting on structures (Mash, 1992), river flood forecasting (Campolo *et. al.*, 1997; Tide forecasting (Tsai and Lee, 1999; Lee and Jeng, 2002 and Lee, T.L., 2004), earthquake induced liquefaction (Lee *et. al.*, 2002), simulation of wave parameters, end depth computation in inverted semicircular channels Dey *et. al.* (2004), (Makarynskyy *et. al.*, 2004 and Makarynskyy, 2005), storm surge prediction (Lee T.L., 2006). Sediment transport in open channels (Trent *et. al.*, 1993) prediction of estuarine instabilities (Grubert J.P., 1995) sediment load prediction in rivers (Nagy, H.M., 2002).

Birikundavyi *et. al.* (2002) investigated the performance of neural networks as potential models capable of forecasting daily stream flows. An appropriate model was identified and the results were compared with the results produced by conceptual model presently in

use. It was found that the neural networks perform better than the deterministic model for upto 5-day ahead forecasts. It was also found that the results obtained with the neural network approach were far superior to the once obtained with the classic model.

Nagy *et. al.* (2002) used an ANN model to estimate the natural sediment discharge in river in terms of sediment concentration. Several trials were made to design a suitable architecture of the network. The model was trained with measured field data of variables selected on the basis of fluid and sediments dynamics. Model validation was done with a large number of data from several rivers. The results indicated that a neural network approach estimates sediment concentration well compared to conventional methods.

Coppola *et. al.* (2003) demonstrated the feasibility of training an ANN for accurately predicting transient water levels in a complex multilayered ground water system under variable state, pumping and climate conditions. The ANN was trained to predict transient water levels in response to changing pumping and climate conditions. The trained ANN was verified with ten sequential seven day periods and the results compared against both measured and numerically simulated ground water levels. The results indicate that the ANN technology has the potential to serve as a powerful prediction and management tool for many types of ground-water problems.

A few investigators have addressed the uncertain issue of scour around pier type structures with the help of the ANN. Examples of latter studies include (Azmatullah *et. al.*, 2007; Bateni and Jeng, 2007; Bateni *et. al.*, 2006; Choi and Cheong, 2006; Jeng et. al, 2005; Azinfar *et. al.*, 2004; Khosronejat *et. al.*, 2004; Kambekar and Deo, 2003; Liriano and Day, 2001; and Trent *et. al.*, 1993).

Kambekar and Deo (2003) carried out scour data analysis using neural networks. Different networks were develop to predict the scour depth based on the input parameters of wave height, wave period, water depth, pile diameter, maximum wave particle velocity, maximum shear velocity, Shields parameters and Keulegan carpenter number. The design neural network was able to provide a better alternative to the statistical curve fittings with weight matrix developed to predict non-dimensional scour depth from the input of the wave height, wave period and water depth.

Khosronejad *et. al.* (2004) carried out estimation of scour hole properties around vertical piles using ANNs. Two different ANNs including multilayer perception and radial basis functions neural networks were used for this purpose. It was demonstrated that the designed ANNs could satisfactorily modeled non-linear relationships between input parameters (wave height), water depth, wave period, maximum velocity, maximum shear velocity and Shields parameters) and output parameters (scour hole depth and width of scour hole).

Jeng *et. al.* (2005) made neural network assessment for scour depth around bridge piers. The equilibrium scour depth was modeled as a function of five variables; flow depth, mean velocity, critical flow velocity, mean grain diameter and pier diameter.

Bateni *et. al.* (2007) applied Bayesian neural networks for prediction of equilibrium and time dependent scour depth around bridge piers. The equilibrium scour depth was modeled as a function of five variables; flow depth and mean velocity, critical flow velocity, median grain diameter and pier diameter. The time variation of scour depth was also modeled in terms of equilibrium scour depth, equilibrium scour time, scour time, mean flow velocity and critical flow velocity. The Bayesian network predicted equilibrium and time dependents scour depth much better when it was trained with the original scour data, rather than using a non-dimensional scour data.

Choi and Cheong (2006) investigated prediction of local scour around bridge pier using ANNs. Sixty four data sets from four different experiments were used to train the model. The prediction results by ANN were better than the results produced by empirical relationships.

Bateni *et. al.* (2007) made neural networks and neuro-fuzzy assessment for scour depth around bridge piers. Two alternative approaches, ANNs and adaptive neuro-fuzzy reference system (ANFIS) were used to estimate the equilibrium and time dependent scour depth with numerous reliable data sets. The ANN models, multilayer perception using back propagation algorithm (MLP/B) and radial basis using orthogonal least square algorithm (RBF/OLS) were used.

Bateni and Jeng (2007) carried out estimation of pile group scour using adaptive neuro-fuzzy approach. Two combinations of input data were used to predict the scour depth; the first input combination involved dimensional parameters such as wave height, wave period and water depth, while the second combination contained dimension less numbers

including Reynolds number, the Keulegan-carpenter number, the Shields parameters and the sediment number. The validation results showed that ANFIS performed better than the existing empirical formulas.

Azmatullah *et. al.* (2007) used alternative neural networks to estimate the scour between spillways. The network inputs were characteristic head and discharge intensity over the spill ways while the output was the predicted scour depth at downstream of the bucket. The study showed that the traditional equation based methods predicting design scour downstream of a ski-jump bucket could better be replaced by ANN.

Lee *et. al.* (2007) applied neural network modeling for estimation of scour depth around bridge piers. The Back-propagation neural networks (BPN) were used to predict the scour depth in order to overcome the problem of exclusive and the non-linear relationships. It was found that the scour depth around bridge piers can be efficiently predicted using the BPN.

2.9.1 Concluding remarks

From review of literature on application of ANNs in hydrology and water resources engineering, it can be concluded that ANN provides a higher level of accuracy in solving the particular problem when compared to empirical relationships. ANN may therefore be a viable alternative in the evaluation of mutual interference effect of bridge piers on local scour provided a reliable database is available.

2.10 Conclusion on Literature Review

There are varying hypotheses concerning the main agent responsible for pier scour. Laursen and Toch (1956) and Shen *et. al.* (1966) identified the horseshoe vortex to be the main agent responsible for local scour around bridge pier. On the other hand Raudkivi (1986) argued that horseshoe vortex is a consequence of scour, not the cause of it. Melville (1975), Hjorth (1975), Ettema (1980), Raudkivi (1986), Chiew and Melville (1987) and Jhonson and Ayyub (1992) observed the downflow infront of the pier as a main agent responsible for pier scour. Chiew (1984) identified the downflow as the main cause of local scour and describe the scour hole as inverted right circular cone with the pier as its axis. Dargahi (1990) contradicts the view of Melville and Raudkivi (1977) that downflow was the main scouring agent. Tanaka et al. (1967) showed that the down flow is generated secondarily by the vortex motion and does not affect directly the local scour.

Richardson and Devies (1995), Raudkivi and Ettema (1983) and Lagasse *et. al.* (2001) identified the various factors governing local scour such as the parameters describing the sediment, flow and pier. However, Dey. S. (1997) indicates the time as an additional parameter and Oliveto and Hager (2002, 2003) found particle Froude number as the principal parameter of local scour.

Flow depth parameter gives the most conflicting statements. For the case of live bed scour most of the investigator claim that below some limiting water depth scour depth decreases with decreasing water depth, but for water depth greater than the limiting depth, depth of scour becomes independent of water depth. On the other hand Laursen (1958) insists that for constant velocity the depth of scour increases with increasing water depth. Breusers *et. al.* (1977) discusses the influence of y_0 / b but does not distinguish between clear water and live bed scour. Most researcher state that for a condition u_* / u_{*_c}, the influence of flow depth can be neglected for $y_0 / b > 2$ to 3. Based on his envelop curves Melville (1997) report that the scour depth is independent of flow depth when $y_0 / b > 1.43$. Early laboratory studies on local scour show the effect of sediment side to be relatively minor. However, recent studies of Nicollet (1971) and Ettema (1980) have shown that the sediment side has definite bearing on the mechanism of scour.

According to Ettema, the local scour is independent of the sediment size if $\frac{b}{d_{50}} > 50$.

Melville and Sutherland (1988) and Melville (1997) have shown that for design purpose the scour depth in uniform sediments is independents of sediment size when $\frac{b}{d_{50}} > 25$.

Most researchers expressed similar opinion on the pier shape. The general conclusion is the blunter the pier the deeper the scour. According to Chabert and Engeldinger (1956) a pier comprising of two or more circular piers seems to be an attraction over where there is influence of appreciable angle of attack.

The concept of an equilibrium scour condition is widely reported in literature. Several investigators namely, Ettema (1980) Melville and Chiew (1999) Heidarpour *et. al.* (2003), Zarrati *et. al.* (2004), Mia and Nago (2003) and Sheppard et al. (2004) have come up with diverged definitions of time to equilibrium scour depth. Ettema (1980) defined the time to equilibrium scour as the time at which no more than 1 mm of incremental scour was

realized within a timeframe of four hours. Melville (1984) defined equilibrium scour as that in which sediment entering the scour hole is equal to the amount being removed. Melville and Chiew (1999) and Sheppard *et. al.* (2004) stopped their experiments when the change in the scour depth did not exceed 5% of the pier diameter during a 24-hour period.

The scour depth prediction formulae as reported above and others that are not included here, give widely divergent results when employed at particular bridge site. This underlines the need for rigorous assessment of the influence of flow piers and bed condition on local scour.

Till date, extensive research on local scour has been carried out; nevertheless failure of many bridges due to local scour has been reported in the literature. Indeed, local scour around bridge pier received a lot of attention in the past from theoretical and practical point of view in an attempt to quantify the equilibrium depth of scour. However, among the large number of experimental and field studies, (*e.g.*, Laursen and Toch (1956), Chabert and Engeldinger (1956), Chew (1984), Raudkivi (1998), Ettema (1980), Melville and Sutherland (1988), Ettema *et. al.* (1998) and Johnson (1995) etc.), the problem of scour around a single pier has been mainly focused and more meticulously investigated than the problem of scouring around group of piers. A scanty amount of literature on pier group scour is available [*e.g.*, Hannah (1978), Elliott and Nicollet (1978) and Zarrati *et. al.* (2004, 2006)].

Bridge failures due to local scour have highlighted the need for better scour protection methods. For the reduction of pier scour depth, use of several devices has been reported in the literature. As compared to armoring devices, flow altering devices are reported to be more economical, especially when the rip-rap material in required amount is not available near the bridge site or is expensive. However, certain limitations on the use of these flow altering devices to reduce the scour depth at piers are highlighted in the literature. A slot may be blocked by floating debris and its construction is difficult. Sacrificial piles may become ineffective when the flow approaching the piers changes its direction. Use of a thin collar plate skirting around bridge pier at or below the bed level is reported to be a very effective mean of protection against scour. The application of collar around a single cylindrical and rectangular pier has been tested by (Schneible, 1951; Chabert and Engeldinger, 1956; Thomas, 1967; Tanaka and Yano, 1967; Ettema, 1980;

Odgard and Wang, 1987; Chiew, 1992; Gupta and Gangadharaiah, 1992; Chiew, 1992, Vittal *et. al.*, 1994; Melville and Hadfield, 1999; Kumar *et. al.*, 1999; and Zarrati *et. al.*, 2004), however, scanty information is available in literature about the application of collar on group of piers. Perhaps, only Zarrati *et. al.* (2006) have attempted the reduction of local scour by using collar at pier group.

Literature on modeling of scour depth indicate that It has been a common practice to apply empirical relationships based on the regression methods performed on laboratory data for estimation of the scour around a pier. However, due to complexity of the scour problem empirical relationship based on laboratory data are not strong enough to deal with the problem of estimating the scour depth around a pier. In the light of above, Laursen and Toch, 1956; Shen, 1971; Hancu, 1971; Breusers *et. al.*, 1977; Melville and Southerland, 1988; and DOT U.S., 1993, have attempted to model the scour depth at an isolated pier.

Recognizing these difficulties and the importance of improving prediction capabilities several researchers have been engaged in exploring and refining methods for improving traditional physical based analysis. A few investigators have addressed the uncertain issue of scour around pier type structures with the help of the artificial neural network (ANN). Studies carried out by Azmatullah *et. al.*, 2007; Bateni and Jeng, 2006; Bateni *et. al.*, 2006; Choi and Cheong, 2006; Jeng *et. al.*, 2005; Azinfar *et. al.*, 2004; Khosronejat *et. al.*, 2004; Kambekar and Deo, 2003; Liriano and Day, 2001; and Trent *et. al.*, 1993, showed that ANN performed better than the existing empirical formulas. It is worth mentioning that all of these investigators have attempted application of ANN for the estimation of scour depth around an isolated pier only.

It is evident from the literature cited above that there is paucity of information on the effects of mutual interference on local scour at bridge piers. The following deficiencies, in particular, may be noted.

(3) Most studies of local scour around bridge piers are confined to an isolated pier. The studies of local scour at multiple piers are limited and also confined to limited extent.

(4) All of the available scour depth models are developed for an isolated pier. Almost no scour depth model, except Elliott et al. model for transverse piers, is cited in the

literature which takes into account the effect of mutual interference of bridge piers on local scour.

(3) The flow characteristics at the junction of multiple piers with bed, which are related to the scour process, have not been studied so far.

(4) The interference effects on local scour due to multiple piers have been observed and recognized but on this aspect, rigorous physically sound modeling does not seem to within reach yet.

(5) Scanty amount of research work on protection of group pier scour using collar is available in the literatue.

(6) ANN may be a viable alternative in the evaluation of mutual interference effect of bridge piers on local scour provided a reliable database is available.

CHAPTER – III

EXPERIMENTAL PROGRAMME

3.0 Introduction

It is well known that experimental methods are helpful in understanding and analyzing the behavior of complex flow situations which otherwise cannot be subjected to purely theoretical analysis. The experimental set-up, measurement techniques and the experimental procedure adopted are presented in this chapter. In view of the objectives set out for the present study, there is a need for collection of data, therefore, it was planned to conduct laboratory experiments to study the effect of mutual interference of bridge piers on local scour by systematically varying the size, shape, pier alignment and location of piers in different configurations with varying spacing between the piers. It was hoped that each set of experiments would lead to recommendations for the design of bridge pier.

In all the experiments, smooth circular cylindrical piers were used because of their symmetry and the data available for comparison purposes. The approach flow was steady uniform for all experiments. The stage of particle motion expressed in terms of the shear velocity parameter U_* / U_{*_c}, was set so that all the experiments were performed at the clear-water local scour condition $U_* / U_{*_c} < 1.0$.

3.1 Properties of Sediment Used

The sediment used in present investigation was cohesionless coarse sand falling in the range 16mm to 1/16mm. Therefore, sediment properties were determined by standard sieve analysis. The sediment for the grain size analysis was sampled from the deepest portion of the scour holes around the piers. Using the data obtained from sieve analysis, the particle-size distribution curve has been plotted as shown in Fig. 3.1.

The median size, d_{50} of the sediment sample was taken as the representative particle size of the sediment. The sediment properties computed from the data obtained from sieve analysis are listed in Table 3.1.

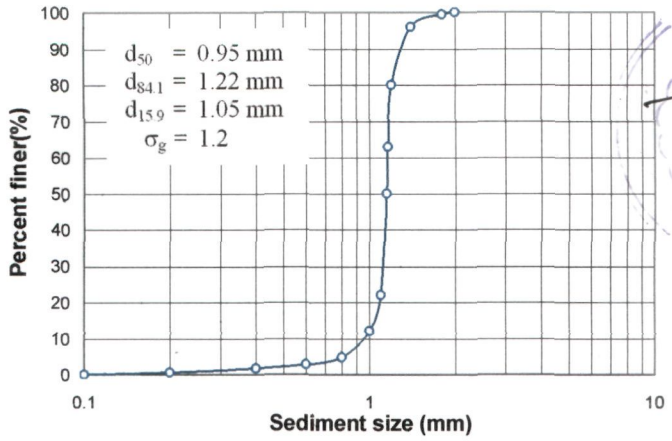

Fig. 3.1 Particle size distribution curve for the sediment used in present study

The mean particle size of the sediment sample, d_{50} is more conveniently referred as 'd' in subsequent chapters of the thesis. The geometric standard of particles size distribution of bed sediment used in present experiments is determined by substituting the values of $d_{15.9}, d_{84.}$ and d_{50} in Equation 3.1.

The degree of uniformity of the particle size distribution of sediments is defined by the value of its standard deviation, σ. The most common and convenient measure of standard deviation used in studies of the distribution of particle sizes is the geometric standard deviation,

$$\sigma_g = \left(\frac{d_{84.1}}{d_{15.9}}\right)^{1/2} = \frac{d_{84.1}}{d_{50}} = \frac{d_{50}}{d_{15.9}} \tag{3.1}$$

The published experimental data related to the erosion of non-uniform bed sediments indicates that bed sediment with a value of σ_g less than about 1.5 may be considered as being virtually of a uniform particle size. The value of σ_g of sediment used in the experiments is within the 1.5 limit and it can thus be considered as being uniform sediment. The specific gravity of sediments was verified by a volumetric analysis with specific gravity flask. The influence of the particle shape is defined by the shape factor ψ and angle of reposeϕ.

The Shield function was used to calculate the critical shear velocity U_{*_c} for the d_{50} particle size of sediment. It was assumed that the mean particle shape factor,

$S.F = \frac{c}{\sqrt{ab}}$, had a negligible influence on the value of U_{*_c} for the sediment size, where a, b *and* c are the lengths of the mutually perpendicular axes of a particle, of which 'c' is the shortest.

The fall velocity of the mean particle size w_{50} was determined from the relationship by Rouse (1937) as presented in the A.S.C.E. (1975), 'Sedimentation Engineering' manual. The angles of static particle repose ϕ were determined from the slopes of small heaps of dry particles.

Table 3.1 Properties of sediment used

$d_{84.1}$ (mm)	$d_{15.9}$ (mm)	Median Size d_{50} (mm)	Geometric mean size d_g(mm)	Geometric standard σ_g(mm)	Specific gravity S_s	Fall velocity of sediment w_0 (m/s)	Shape factor ψ	Angle of Repose ϕ
1.03	0.73	0.95	0.867	1.187	2.65	0.1	1.0	32°

The flume to pier width ratios in the present experiments are greater than the minimum value of 8 suggested by Shen *et. al.* (1966).

All the pier sizes used in the flume, except 66.0 mm diameter pier size, were smooth galvanized mild steel circular tubes. 66.0 mm diameter pier was made from P.V.C. tube.

The scour depth at the piers was measured with a 3 mm diameter point gauge mounted on the mobile carriage that traversed the flume. The scour depths could be measured to within 0.1 mm using point gauge..

3.2 The Approach Flow and Flow Measurement

The approach flow for each experiment was initially set so that the experiments were run for similar values of the shear velocity ratio u_* / u_{*_c}, for all the experiments. The channel slope S_0, was adjusted so that the flow had a uniform flow depth over the working section in the flume. Required value of the slope S_0 was estimated from $S_0 = \frac{u_*^2}{gy_0}$.

A honeycomb grill ensured that the flow was straight and two-dimensional before approaching the working section. The flow entered the flume via an inlet reservoir at the

upstream end of the flume. A uniform two-dimensional flow was produced by passing the flow through a wooden transition and a wire grill installed in the reservoir.

3.3 Mean Flow Parameters Used in the Experiments

Since the maximum depth of scour is reported by Raudkivi, 1990 to occur at the threshold of bed material motion, all tests in present experimental programme were conducted just close to this condition. The threshold of bed material motion was found by experiment when the pier was not installed. Threshold of bed material motion was defined as condition such that although finer bed materials move, the overall average elevation of the bed is not lowered more than 2-3 mm during the period of the experiment. These tests showed that with an average flow depth of 140 mm and a flow rate of0.04141 m^3/s, the bed material would be at incipient motion. The ratio of shear velocity in these experiments to the critical shear velocity calculated from Shield's diagram was about 0.95.

The computed mean flow parameters used in this investigation are listed in Table 3.2. Details are given in Appendix V – VII.

Table 3.2 Computed mean flow parameters

Discharge Q (m^3/s)	Depth of flow y_0 (mm)	Mean velocity U_0(m/s)	Threshold velocity U_c (m/s)	Bed hydraulic radius R_b
0.04141	140.0	0.391	0.4127	0.0858

Critical shear velocity U_{*c}(m/s)	$\frac{U_0}{U_c}$	Froude Number F_r	Critical Froude number F_{rc}	Particle Reynolds number R_{ed}
0.029	0.95	0.3328	0.35028	370.5

Flow Reynolds number R_{eh}	Critical shear Reynolds number R_{eh*}	Critical shear stress τ_c	Dimensionless critical bed shear stress τ_{*c}	Average energy slope S_0
54600	21.85	0.0858	0.06	0.001

Details of pier sizes and patterns of pier arrangements used in present study are given in Table-3.3.

Table 3.3 Details of pier sizes and their arrangement used in present study

Pier type used in present study Circular piers	Pier diameters used in present study b (mm)
(1) Single pier	21.5, 33 , 41.5, 46 , 66
(2) Piers group (tandem-arrangement)	33
(i) two circular piers of same size	33
(ii) two circular piers of different sizes	33 - 66
(iii) three circular piers of same size	33
(3) Piers group (transverse/lateral - arrangement)	33
(4) Piers group (staggered- arrangement)	33
(i) Constant radial distance and variable angle of attack	33
(ii) Constant angle of attack and variable radial distances.	33
(iii) Three circular piers in staggered pattern such that two piers on upstream at fixed lateral spacing and one pier on downstream along the bisector of upstream piers at varied pier spacings.	33
(5) Piers group using collar	
(i) Two circular piers with and without collar and aligned at different angles of attack	41.5
(ii) Group of piers of varied sizes with and without collar and aligned at different angles of attack.	21.5, 33, 46

3.4 Experimental Set-Up

Experiments were conducted in a glass sided rectangular recirculating tilting flume, 11.0 m long, 0.756 m wide and 0.55 m deep. The general view of the experimental set-up is shown in Fig. 3.2.

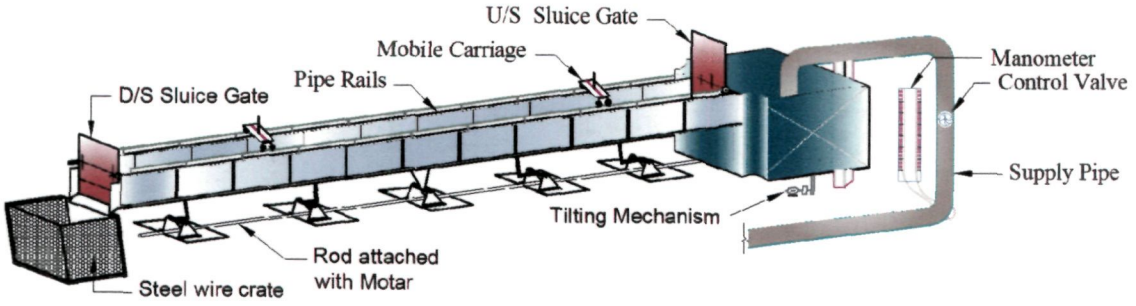

Fig. 3.2 Glass sided rectangular re-circulating tilting flume

Flume bed was composed of fairly uniform alluvial sand ($d_{50} = 0.95\,mm$ and $\sigma_g = 1.187$), collected from the river Chambal near Etawah in Uttar Predesh, India. Water was supplied to the flume from a constant head overhead tank, which got its supply from the laboratory water supply system. Flow straightners were provided at the upstream end of the flume to ensure uniformly distributed flow across the width of the flume and minimum turbulence in the flow. Water supply into the flume was regulated by operating a valve in the water supply pipeline. The flume discharge was measured by a calibrated bend meter and the mean velocity of flow was computed from the discharge. The computed velocity was further checked by the Pitot tube readings. Water surface level and bed level in flume were measured using a point gauge with a sharp bottom mounted on a mobile carriage which could be traversed over adjustable rails mounted on the two walls of the flume. The rails were kept parallel to the flume bed. A tailgate was provided at the downstream end of the flume, which was operated to adjust the depth of flow in the flume. A transition of wooden block was fitted tightly at the entrance of the flume to ensure smooth flow without disturbing the sediment bed in the flume. A sediment trap was provided at the downstream end to collect sediment coming from the upstream bed. The test section for all the experiments was located at 3.5 m from the flume inlet. The plan and elevation of the test flume showing its different components are shown in Figs. 3.3.

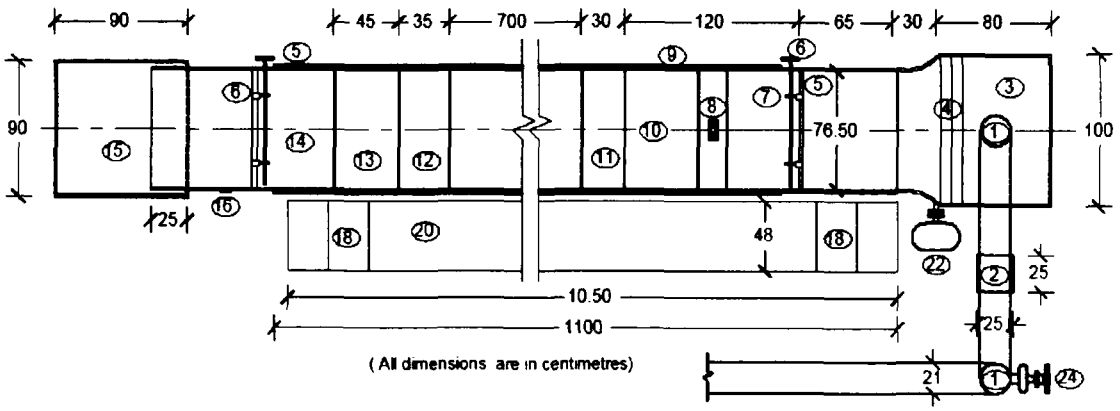

PLAN

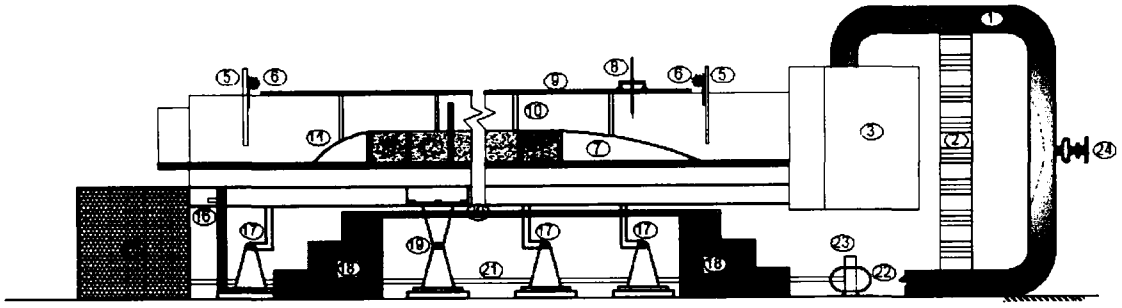

Fig.3.3 Test flume showing its different components

Legends:

① Inlet supply pipe	② Supply pipe support	③ Reservoir
④ Steel gratings	⑤ Tail gate	⑥ Tail gate lifting mechanism
⑦ Upstream wooden transition	⑧ Mobile Carriage	⑨ Pipe rails
⑩ Inlet channel	⑪ Upstream sediment trap	⑫ Test section
⑬ Downstream sediment trap	⑭ Downstream wooden transition	⑮ Steel wire crate
⑯ slope measuring scale	⑰ Pivot	⑱ Steps
⑲ Central pivot	⑳ Walk way	㉑ Pipe attached with gearbox
㉒ Motor	㉓ Gearbox	㉔ Supply control valve

Circular piers of galvanized iron having diameters 21.5 mm, 33 mm, 41.5 mm, 46 mm, and P.V.C. pipe of diameter of 66 mm were chosen as the pier models. Pier sizes were so selected that blockage effect in the flume was negligible and according to Melville and Sutherland (1988) and Melville (1997) where they showed that the scour depth in uniform sediment is independent of sediment size when sediment coarseness ratio $\frac{b}{d_{50}} > 25$. The mean depth of flow was kept constant at 140 mm in all sets of experiments. The selection of sediment coarseness for present experiments is made on the basis of conclusions drawn by Ettema (1980) by plotting his laboratory data for six pier sizes and sediment sizes from d_{50} = 0.24 mm to 7.8 mm in which he showed that the maximum value of clear water scour $(ds/b)_{max}$ is unaffected by the particle size as long as the value of $\frac{b}{d_{50}}$ is larger than 25.

Sand was filled in the flume to a constant thickness of 25 cm over working section in the flume. At the entrance of the flume, graded layers of glass beads, followed by a wooden transition block, were placed to obtain a smooth flow without disturbing sand bed in the flume. A sediment trap was provided at the outlet of the sand bed. As such, water flowing

out of the flume was clear and virtually sediment free. The pier model arrangement in the flume is shown in Fig. 3.4.

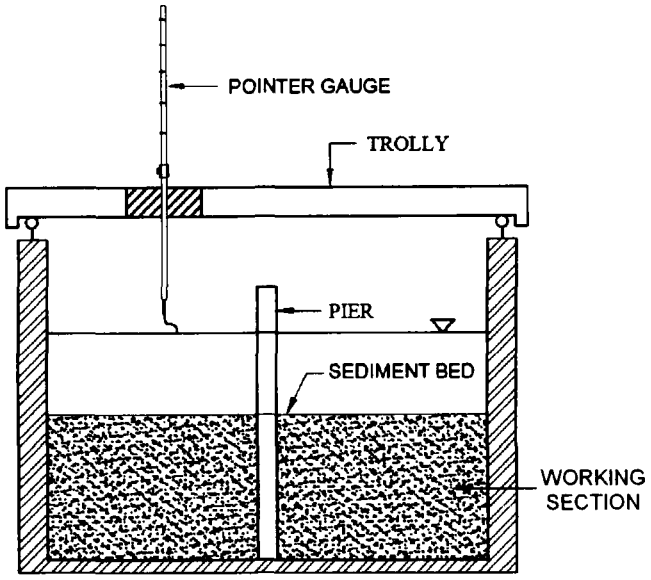

Fig. 3.4 Pier model arrangement in the flume (side view)

3.4.1 Duration of experimental runs

Theoretically scour depth develops asymptotically with time. However, it is practically not possible to run the experiment for such a long duration. It has been observed that the rate of scour development is high initially and becomes low after a few hours. Further it is well known that coarser sediments take less time to reach equilibrium condition than finer sediments. To serve as guide to decide the duration of each run in the present investigation, the following investigation for clear- water scour are quoted below in Table 3.4.

Table 3.4 Duration of experimental runs for clear–water scour

Investigator	Sediment size	Duration
Chiew and Melville (1987)	1.45 mm	100 minutes
Yee Meng Chiew (1922)	0.33 mm	72 hours
Gupta and Gangadhariah (1992)	0.16 mm	4 hours
Jones and Kilgore (1992)	0.38 mm	4 hours
Hannah (1978)	0.75 mm	7 hours

In each set of experiments, one long- term experiment was carried out until the rate of scouring was negligible. This was defined as the time when the scour depth did not

change by more than 5% of the pier diameter over a period of 24 hours, as suggested by Melville and Chiew (1999). The next tests in each set of experiments were then carried out to the time when about 90% of maximum scouring was expected based on the results of long-term experiment.

Clear water experiments have to run continuously for several days before equilibrium conditions are approached. An exception occurs if the geometric standard deviation of the sediments $\sigma_g \cong 1.3 - 1.5$. In this range the coarse grains armor the surface but are not large enough to armor the scour hole where the agitation is higher. Then, clear-water scour depth of the same order as observed with non-ripple forming sediments can be reached in the laboratory. It was found that 50-60 hours was necessary for long-term experiments. With performing a long-term test in 24 hours with a single pier, Hannah (1978) showed that 80% of scour depth occurred in first 7 hours and all tests with pier groups were carried out for 7 hours duration. Results were then extrapolated to find the maximum depth of scour. Since in present study clear-water experiments were conducted using coarse sediment of 0.95 mm median diameter, duration of 10 hours was considered adequate. In the case of experiments on piers group with collar, test duration was more.

3.4.2 Experimental procedure

Prior to each experiment, the sediment bed in the flume was leveled by hand using 0.75 m long timber board and a sprit level. The ends of the board aligned to lines marking the bed surface position on the outside of the glass walls of the flume. Once the sediment bed surface was leveled, the model piers were inserted in the test section vertically in desired configuration and at desired spacing between them projecting well above the water surface. Water was allowed to enter the flume slowly such that the predetermined flow depth and discharge could be adjusted. The flow was adjusted using the inlet valve and the tailgate to achieve steady and uniform flow condition. For all sets of experiments, the depth of flow in the flume could be adjusted by operating the tail-gate located at the downstream end of the flume and inlet valve in the supply line. Uniform flow conditions were established by setting the discharge, and then adjusting the slope of the flume until the bed and water surface slopes were nearly parallel to each other. Each experiment commenced from a condition of still water at the predetermined flow depth over a leveled bed surface.

Shen *et. al.* (1966) suggest that, for the purpose of experimental investigation, flume width should be at least 8 times the diameter of the pier whereas, Chiew and Melville (1987) suggest this ratio to be 10 in order to make the blockage effect negligible. At lower values of blockage ratio, Shen *et. al.* (1969) and Chiew and Melville (1987) felt that there will be side wall confinement and scour depth will be affected. Therefore, dimensions of the pier groups were so chosen that there was negligible blockage effect of the piers group on scour depth. The tests were performed for sufficient time to obtain equilibrium scour depth. The scour depths were measured with the help of point gauge with 0.1 mm accuracy which could be moved over adjustable rails mounted on the walls of the flume. To overcome the difficulty of observing the development of the scour hole, strong light source was used which permitted the ease in taking precise temporal scour depth measurements. Pier groups in different configurations and with varying spacing were investigated for flow condition close to incipient motion (Table 3.2). The time of start of initial movement, and of water surface establishment were recorded.

At the end of experiment the water supply to the flume was gradually stopped and the water was drained off the flume with extreme care so that the scour hole and scour and scour patterns developed by the flow around the model piers, were not disturbed. Since the bed profiles before and after stopping the flow were same, profiles of the sediment bed were measured after the runs were stopped. Detailed measurements of the scoured area around the model piers were then made with the help of point gauge and finally photographs were taken.

The following observations were made from each experiment.

(i) The temporal development of the scour hole

The depth of scour was recorded at regular intervals as the scour hole formed. The frequency of the scour depth measurements decreased as the rate of scouring decreased. The experiment was stopped when no change occurred to the maximum depth of the scour hole over a minimum period of four hours.

(ii) The mechanism of local scour

The visual record of the important features distinguishing the development of local scour around a cylinder pier was kept with the aid of photographs and sketches. These were accompanied by notes.

(iii) Water temperature

These were recorded at intervals throughout each run.

(iv) Scour hole profiles

At the completion of each experiment, the profile of the scour hole in the plane of symmetry of the pier and parallel to the flow direction was recorded with the 3 mm diameter point gauge supported by the mobile carriage of the flume used. The upstream cone angle, and exit slope cone angle of the scour holes, were determined from the scour hole profile. Experimental program is performed in the following phases

3.5 Introduction

A bridge is commonly supported on a group of piers. The group of piers in a single bridge or in two consecutive bridges existing at proximate spacing between them across a river, may possess different configurations in the river bed and mutually interact with the river flow in an entirely different manner as compared to a single bridge pier. These configurations may be tandem, lateral and staggered arrangement of piers.

The arrangement of bridge piers in which the piers are located in the river bed in line with the flow is called tandem arrangement of piers. The number of piers in tandem arrangement may be two or more. The piers in tandem arrangement often exist in a single bridge however, sometimes the two consecutive bridges existing at short distance between them across a river, may have the pier positions in the river bed in line with the flow. In some cases, the two consecutive bridges existing at proximate distance between them across a river have piers of different sizes which may hold their positions in the river bed in tandem arrangement.

The arrangement of several bridge piers in the river bed in a direction transverse to the flow is called lateral arrangement of bridge piers.

In staggered arrangement three piers may interfere with each other such that two piers lie on upstream normal to the flow direction and third pier on downstream along bisector of the distance between the upstream piers. Also, some times piers of new and existing bridges may face each other such that the flow makes an angle with the line joining their centres. This angle and the radial distance between the piers can vary.

Keeping in mind the various cases of bridge pier arrangements in the field, the experiments in present study have been performed to evaluate the effect of mutual interference of bridge piers on local scour. Since the effect of mutual interference is evaluated by comparing the scour depths at piers group located in a particular arrangement with the scour depth at single pier, experiments on single pier have also been conducted under the same hydraulic conditions.

3.5.1 Phase I: Local scour at single pier

A series of experiments was first performed on single pier models of different diameters to provide a basis against which the pier group scour could be evaluated.

Circular smooth galvanized iron pipes having diameters 33 mm, 41.5 mm, and 66 mm were used as isolated model piers. These pier sizes were so selected that their blockage effect in the flume was insignificant.

Before the start of the experimental run, the single pier model of a given diameter was set centrally and vertically into the sediment bed in the flume. The pier was installed at a distance of 3.50 metres downstream of the flume inlet projecting well above the water surface. The flume was flooded with water slowly with the help of the inlet valve in the supply line and steady and uniform flow of desired depth and velocity was achieved by adjusting the inlet valve and the tail gate.

It is well known that at circular piers the maximum scour depth occurs at the nose of the pier. Therefore, during the experimental runs, the scour depth was measured at the nose of the pier at regular time intervals of 15, 30, 45, 60, 90, 120, 150, 180, 210, 240, 270, 300, 360, 420, 480, 540 and 600 minutes with the help of the point gauge. The mean approach flow depth was kept constant at 140 mm throughout the experiments. At the end of the experimental run, the water supply was gradually stopped and the water was drained off from the flume with extreme care that there was no disturbance in the scour hole and the scour patterns developed around the pier. Since there was no difference in the dynamic and static scour depths, detailed measurements of scoured area around the pier were made in static condition. Finally, the photographs of the scoured area around the pier were taken.

3.5.2 Phase II: Local scour around piers in tandem arrangement

An exhaustive series of experiments was performed to investigate the effect of mutual interference of bridge piers on local scour by placing a group of piers in line with the flow at varying clear pier spacing x/b= 0,1, 2, 4, 6, 8, 10, 12.5, 15, 20, 25, 30, 35, 40, 50, 60, 70, 80 and 90. Circular galvanized iron pipes of diameter 33 mm, and P.V.C. pipe of 66mm diameter were used as bridge pier models in this series of experiments. This experimental study was conducted in four parts

The first part investigated the effect of mutual interference of bridge piers on local scour when the piers in tandem arrangement were of the same size and shape. In this series of experiments 33 mm diameter circular galvanized iron pier models were used. The experiments in this series were conducted using a group of two pier models, located centrally and vertically in the flume sediment bed in tandem arrangement at varying clear pier spacing of x/b = 0, 1, 2, 4, 6, 8, 10, 12.5, 15, 20, 25, 30, 40, 50, 60, 70, 80 and 90, where x is the clear spacing between the piers and b is the diameter of the pier. The piers arrangement used in this series of experiments is shown in Fig.3.5.

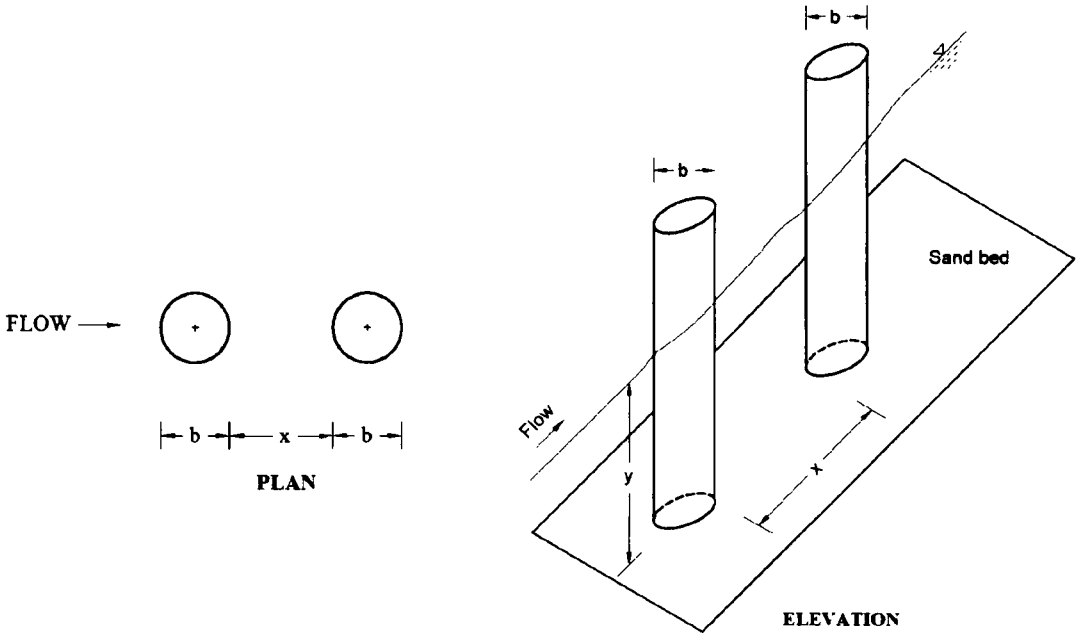

Fig. 3.5 Two piers of same size in tandem arrangement

In second part, a subsidiary series of experiments was conducted using three pier models of 33 mm diameter arranged in line with the flow at equal spacing between them. The arrangement of piers used in this series is shown in Fig. 3.6.

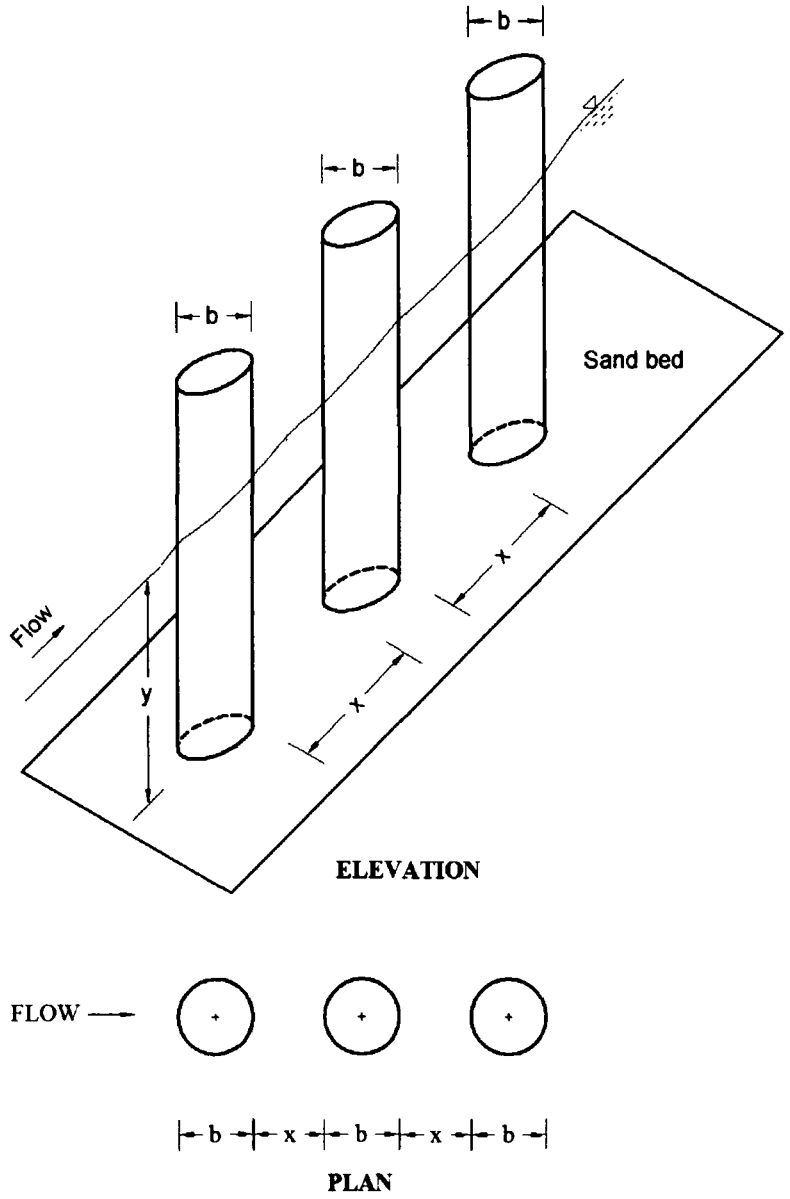

Fig. 3.6 Three piers of same size in tandem arrangement

The third part investigated the effect of mutual interference of bridge piers on local scour using a group of two piers of different size located in tandem arrangement such that the larger size pier was on upstream of the smaller size pier. In this series of experiments 6.6cm and 3.3cm diameter circular pier models were used. As shown in Fig. 3.7, 66 mm diameter pier was located on upstream of 33 mm diameter pier in tandem arrangement in the flume sediment bed at varying clear pier spacing x/b= 0, 1, 2, 4, 6, 8, 10, 12.5, 15, 20, 25, 30, 35, 40, 50, 60, 70, 80 and 90, where x is clear the distance between the piers and b is the width of smaller pier.

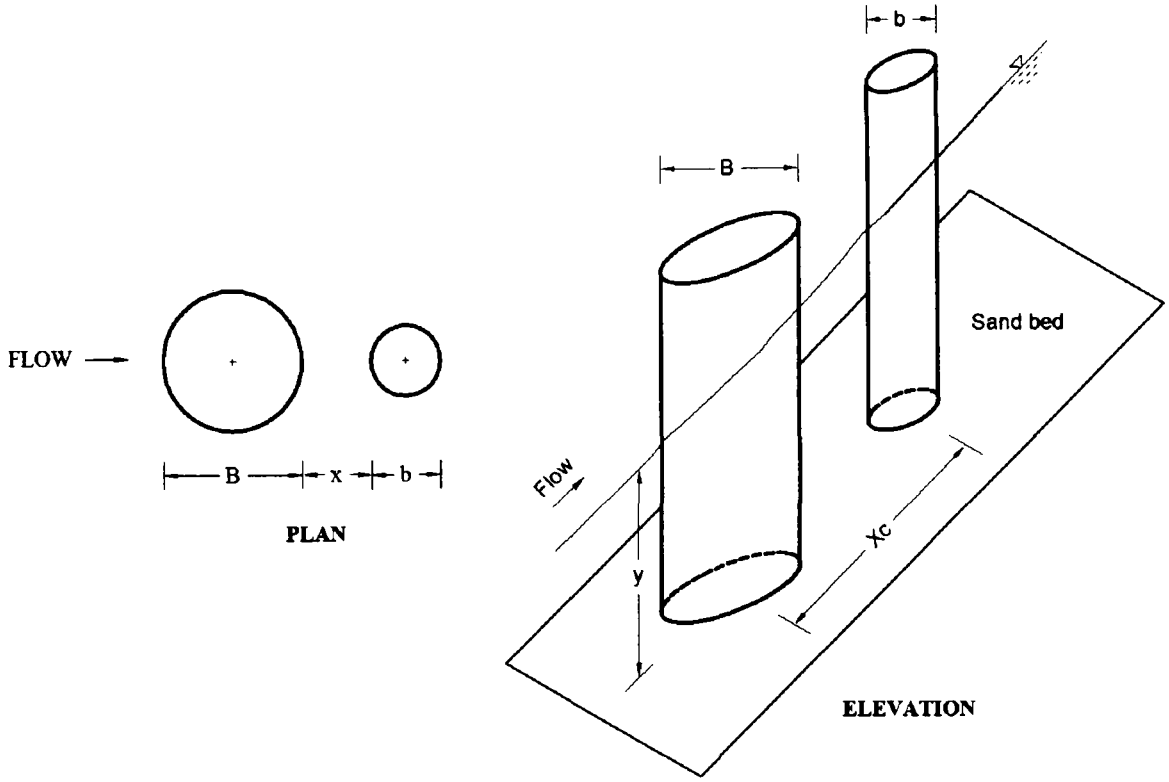

Fig. 3.7 Two piers of different size in tandem arrangement (Larger size (6.6 cm) pier at front)

The fourth part investigated the effect of mutual interference of two bridge pier models of different sizes located in tandem arrangement such that the smaller pier model was on upstream of the larger pier. In this series of experiments 33 mm diameter pier was located on upstream of 66 mm diameter pier in tandem arrangement at varying clear pier spacing x/b = 0,1,2,4,6,8,10,12.5,15,20,25,30,35,40,50,60,70,80 and 90, where x is center to center the distance between the piers and b is the pier width of smaller pier. Fig.3.8 shows the arrangement of piers used in this series.

The hydraulic and sediment conditions were kept same in the experimental series conducted in these four parts.

Before the start of each experiment conducted in four parts of the above mentioned series of experiments conducted, the model piers were set centrally and vertically in the sediment bed in the flume at desired pier spacing, the sediment bed around the piers was fairly leveled.

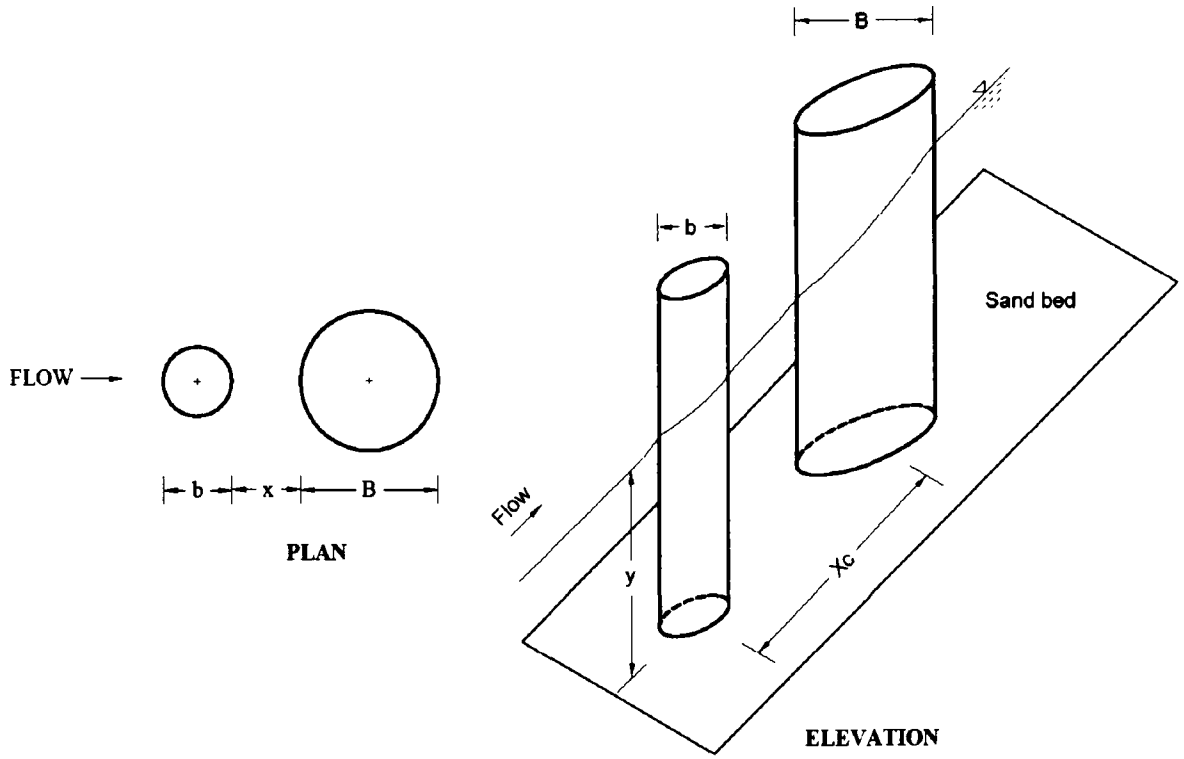

Fig. 3.8 Two piers of different size in tandem arrangement (small size pier at front)

The flume was flooded with water slowly with the help of the inlet valve provided in the supply line and steady and uniform flow of desired depth and velocity was achieved by adjusting the inlet valve and the tail gate. Each experiment commenced from a condition of still water at the predetermined flow depth over a leveled sediment bed surface in the flume.

During the experimental runs, the scour depths were measured at the nose of the piers at regular interval of time of 15, 30, 45, 60, 90, 120, 15, 180, 210, 240, 270, 300, 360, 420, 480, 540 and 600 minutes with the help of the point gauge. On the completion of experimental run, the supply of water to the flume was gradually stopped and water was drained off from the flume carefully so that the scour holes and the scour patterns developed around the piers were not disturbed. Detailed measurements of the scoured area around the piers were made. Finally the scour holes and scour patterns developed around the piers were photographed.

3.5.3 Phase III: Local scour around piers in lateral arrangement

A series of experiments was conducted to investigate the effect of mutual interference of bridge piers on local scour for the piers located in a direction transverse to the flow at varying lateral pier spacing. In this series of experiments, two circular pier models of 33

mm diameter were used. The two pier models were set vertically in the sediment bed in the flume at varying lateral spacing, $\frac{Z_c}{b}$ = 1, 2, 3, 4, 5, 6, 7, 8 and 9 where Z_c is the center to center lateral spacing between the piers and b is the pier diameter. As shown in Fig. 3.9 the two piers were so set in the flume sediment bed that the axis joining the centers of the two piers was at right angles to the flow direction and the centers of the two piers were located at equidistance from the center of the flume.

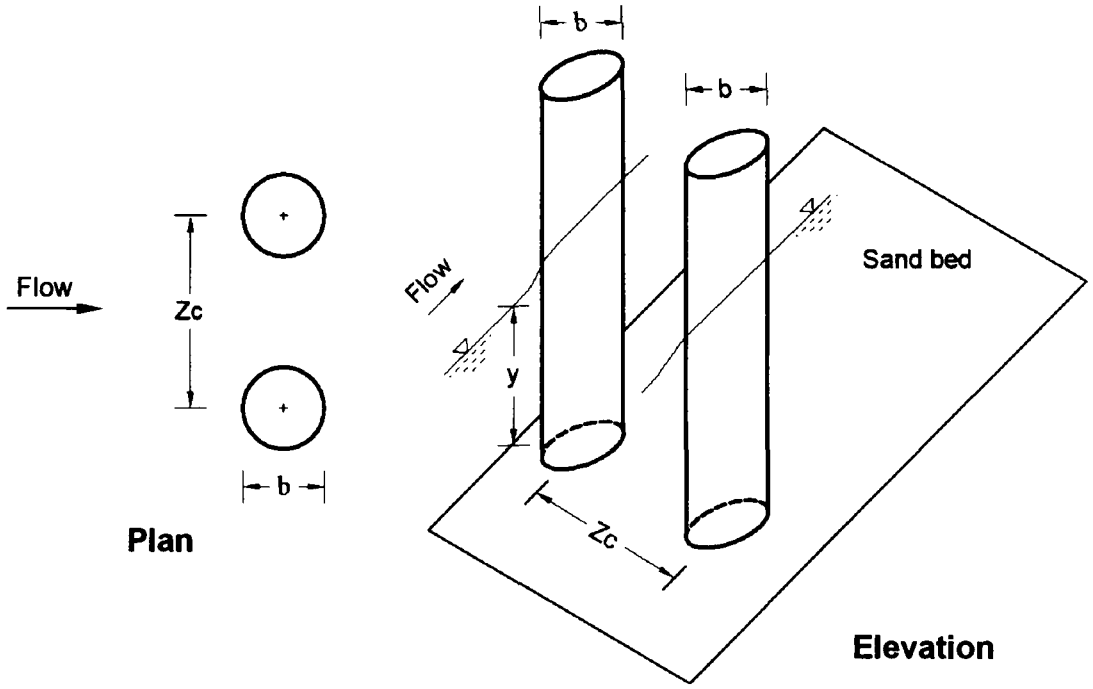

Fig. 3.9 Piers of same size in lateral arrangement

After the piers were set in the sediment bed, the sediment bed around the piers was fairly leveled and the experiments were run with the same procedure as that in the series of experiments conducted on a single pier.

During the experimental runs, the scour depths were measured at the nose of the two piers at regular interval of time of 15, 30, 45, 60, 90, 120, 150, 180, 210, 240, 270, 300, 360, 420, 480, 540 and 600 minutes with the help of the point gauge. On the completion of the experimental run, the water supply to the flume was gradually stopped and the water from the flume was drained off carefully so that the scour holes and the scour patterns around the piers developed by the flow were not disturbed. The detailed measurements of the scoured area around the piers were made and thereafter the photographs of the scour patterns were taken.

3.5.4 Phase IV: Local Scour around piers in staggered arrangement

This series of experiments investigated the effect of mutual interference of bridge piers on local scour when the piers were located in staggered arrangement. Three circular pier models of 33 mm diameter were used in these experiments. The arrangement of piers is shown in Fig. 3.10. Two of the three pier models were set on upstream across the flume at right angles to the flow direction at fixed centre to centre lateral spacing between the piers, $\frac{Z_c}{b}=9$ where Z_c is the center to center lateral spacing between the upstream piers and b is the diameter of the pier model. The third pier model was located on downstream along the bisector of the upstream pier models at varied clear longitudinal pier spacing $X_c/b = 5, 10, 15, 20, 25, 30, 35, 40, 50, 60, 70, 80$ and 90, where x is the center to center distance between the upstream and downstream pier models along the length of the flume and b is the diameter of the pier model. The lateral centre to centre pier spacing $\frac{Z_c}{b}$ was set at 9 because at this lateral pier spacing, the scour depths at piers are said to be free from the effect of lateral mutual interference and only the interference of the downstream pier remains to affect the scour depth at piers.

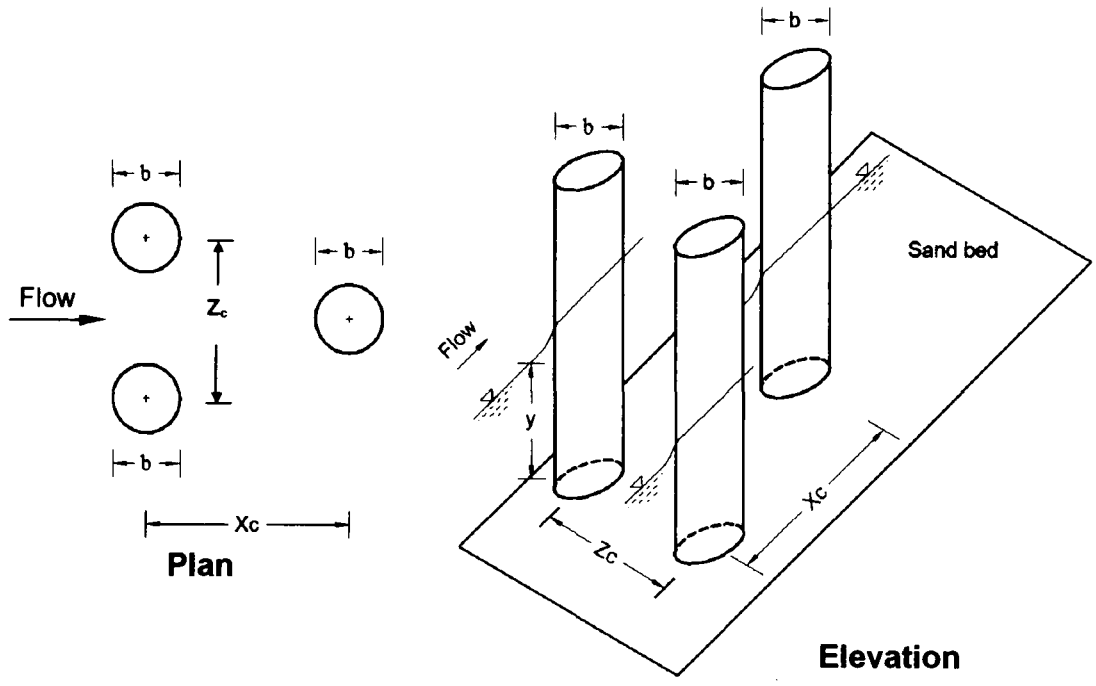

Fig. 3.10 Piers of same size in staggered arrangement

Prior to each experimental run, the piers were set vertically in the sediment bed in the flume at desired locations, the sediment bed around the piers was fairly leveled and then the experiment was run with the same procedure as that at single pier. Temporal measurements of scour depth during the experimental runs were made at the nose of the piers at regular interval of time of 15, 30, 45, 60, 90, 120, 150, 180, 210, 240, 270, 300, 360, 420, 480, 540 and 600 minutes with the help of the point gauge. On the completion of experimental run, the supply of water to the flume was gradually stopped and water from the flume was drained off carefully so that the scour holes and the scour patterns around the piers developed by the flow were not disturbed. Photographs of the scour holes and scour patterns were then taken and detailed measurements of the scoured area around the piers were made and recorded.

3.5.5 Phase V: Local scour around piers with constant angle of attack and varying radial pier spacing

The objective of this series of experiments was to investigate the effect of mutual interference of bridge piers on local scour in the condition when the piers were interacting with one another at an angle of attack of flow.

In this series of experiments, two circular pier models of 33 mm diameter were set vertically in the sediment bed of the flume at constant angle of attack of 45° and varying clear radial spacing between the piers of 0,1,2,3,4,5,6,7,8,9,10,11,12. As shown in Fig. 3.11, the two piers were so located in the flume sediment bed at a particular radial spacing and 45° angle of attack that the perpendicular distances of their centers from the center of the flume were equal. The sediment bed around the piers was fairly leveled and the experiments were performed with the same procedure as that at the single pier. The temporal scour depth measurements during the experimental runs and detailed measurements of scoured area around the piers after stopping the experiments, were also be made in the same manner as that at single pier. The angle of attack of 45° degrees was selected because, the effect of mutual interference is said to be maximum at this angle of attack as reported by Hannah (1978).

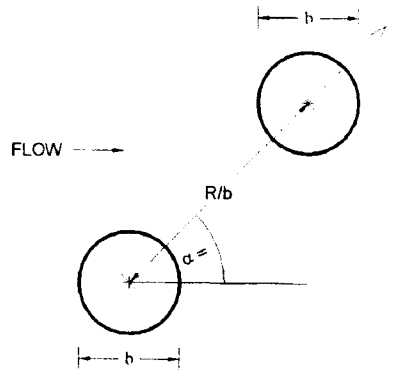

Fig. 3.11 Piers at constant angle of attack 'α' and varying radial spacing 'R/b'

3.5.6 Phase VI: Local scour around piers with constant radial pier spacing and varying angles of attack

The objective of this series of experiments was to investigate the effect of mutual interference of bridge piers on local scour for the case when the piers were interacting with one another at constant angle of attack but varying radial spacing between them.

In this series of experiments, two circular pier models of 33 mm diameter were set vertically in the sediment bed of the flume at constant centre to centre radial pier spacing $R/b=5$ and varying angles of attack 0°, 15°, 30°, 45°, 60°, 75° and 90°. As shown in Fig. 3.12, the two piers were so located in the sediment bed at a particular radial spacing and at 45° angle of attack that the perpendicular distances of their centers from the center of the flume were equal. The sediment bed around the piers was fairly leveled and the experiments were performed with the same procedure as that on single pier. The temporal scour depth measurements during the experimental runs and detailed measurements of scoured area around the piers after stopping the experiments, were also be made in the same manner as that at single pier.

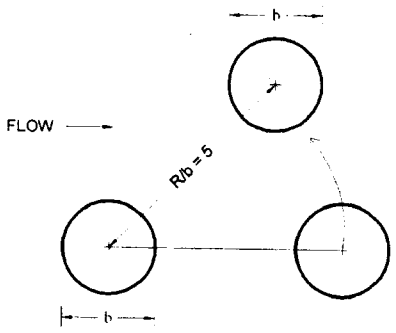

Fig. 3.12 Piers at constant radial spacing '$5b$' and varying angle of attack 'α'

3.5.7 Phase VII: Local Scour protection around piers group

Larger scour depths need deep pier foundations, which is a costly proportion. Therefore, for safe and economical design, scour around the bridge piers is required to be controlled. As a result, various devices (i.e., armoring devices and flow altering devices) for scour depth reduction have been investigated by many researchers.

As the flow altering devices can be more economical, especially when the riprap material in required amount is not available near the bridge site or is expensive, several researchers in earlier studies have conducted experiments on the application of collar as a flow altering device, but only around a single pier. A collar around the pier diverts the down flow and shields the streambed from its direct impact. Since a scanty information is available in literature about the application of collars on group of piers, an experimental study on application of collar around groups of pier has been carried out in present study. This study has been carried out in two parts.

(a) Part one: Local scour around a group of two circular piers with and without collar

A series of experiments was conducted to investigate the scour depth reduction efficiency of a collar plate skirted around a group of two circular piers aligned at varying angles of attack to the flow. A group of two pier models of 41.5 mm diameter was used in this series of experiments. In all experiments of this series, the center to center spacing between the pier models was kept constant at $3b$, where b is the diameter of the pier used in the group of piers. A thin collar plate having width equal to 2.5 times the pier diameter was used around the group of the two piers. The collar plate with its dimensions in centimeters is shown in Fig. 3.13.

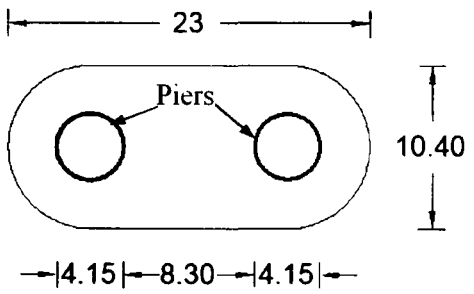

Fig.3.13 Plan of a collar plate around two circular piers

The piers group with collar plate skirted around it is shown in Fig. 3.14. The experiments were conducted on the piers group with and without collar plate skirted around it at varying angles of attack of 0°, 15°, 30°, 45°, 60°, 75° and 90° to the flow.

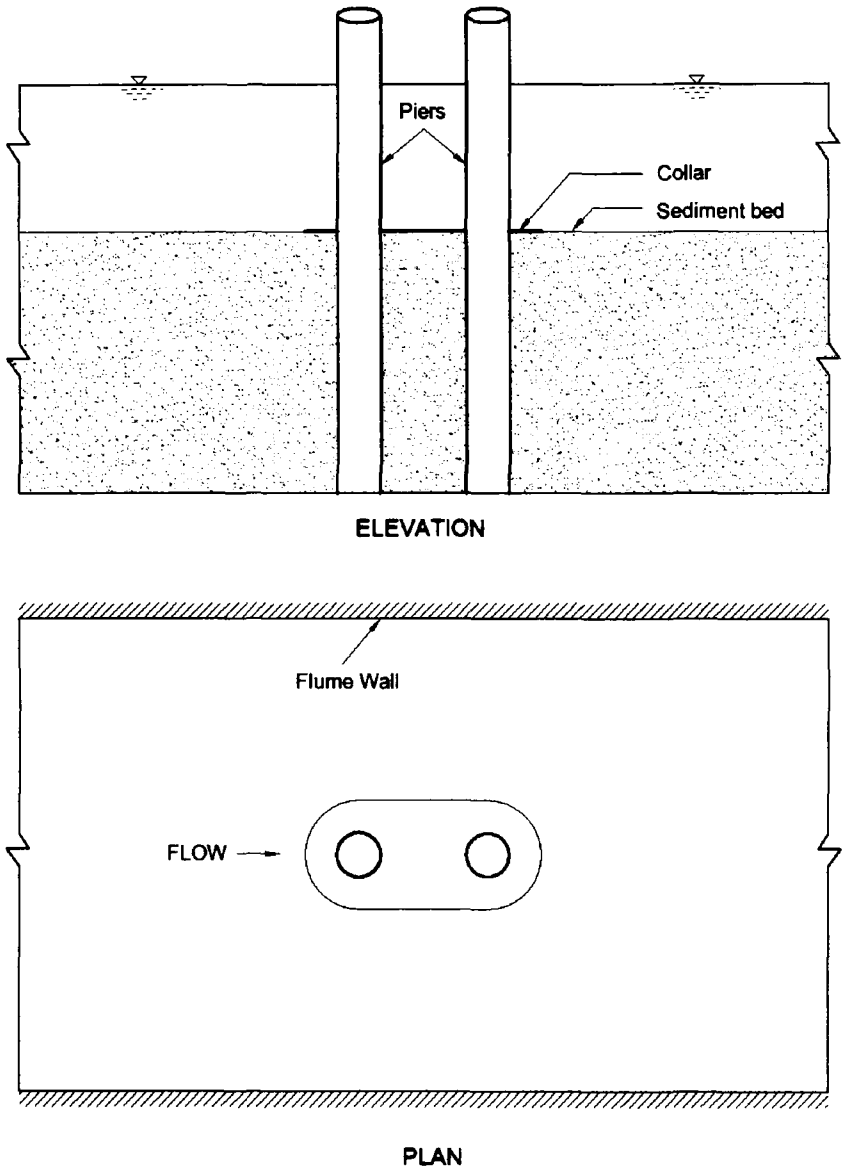

Fig.3.14 Piers with collar at 0° angle of attack

In experiments with collar around the piers group, the collar plate was installed at the initial bed level of the sediment in the flume. The collar width and elevation were chosen based on previous studies discussed in Chapter II. Wider collars are more effective, but construction of collars wider than 3 times the pier diameter is considered impracticable. Also, the efficiency of a collar increases at lower elevations since less flow can penetrate below it (Tanaka and Yano 1967). When a collar is installed below the bed level, penetration of flow below the collar is reduced however; the depth above the collar

becomes a part of the scour hole. Zarrati *et. al.* (2004) in their study with rectangular piers showed that lowering of the elevation of collar below the streambed level increases the extension of the scour hole around the pier, and depth of the scour hole downstream of the collar. It was therefore decided to install the collar at the initial bed level in all the experiments in present study. In all, 14 experiments were conducted in this series, seven with collar and seven without collar. The collar plate with piers aligned at various angles of attack are shown in Fig.3.15

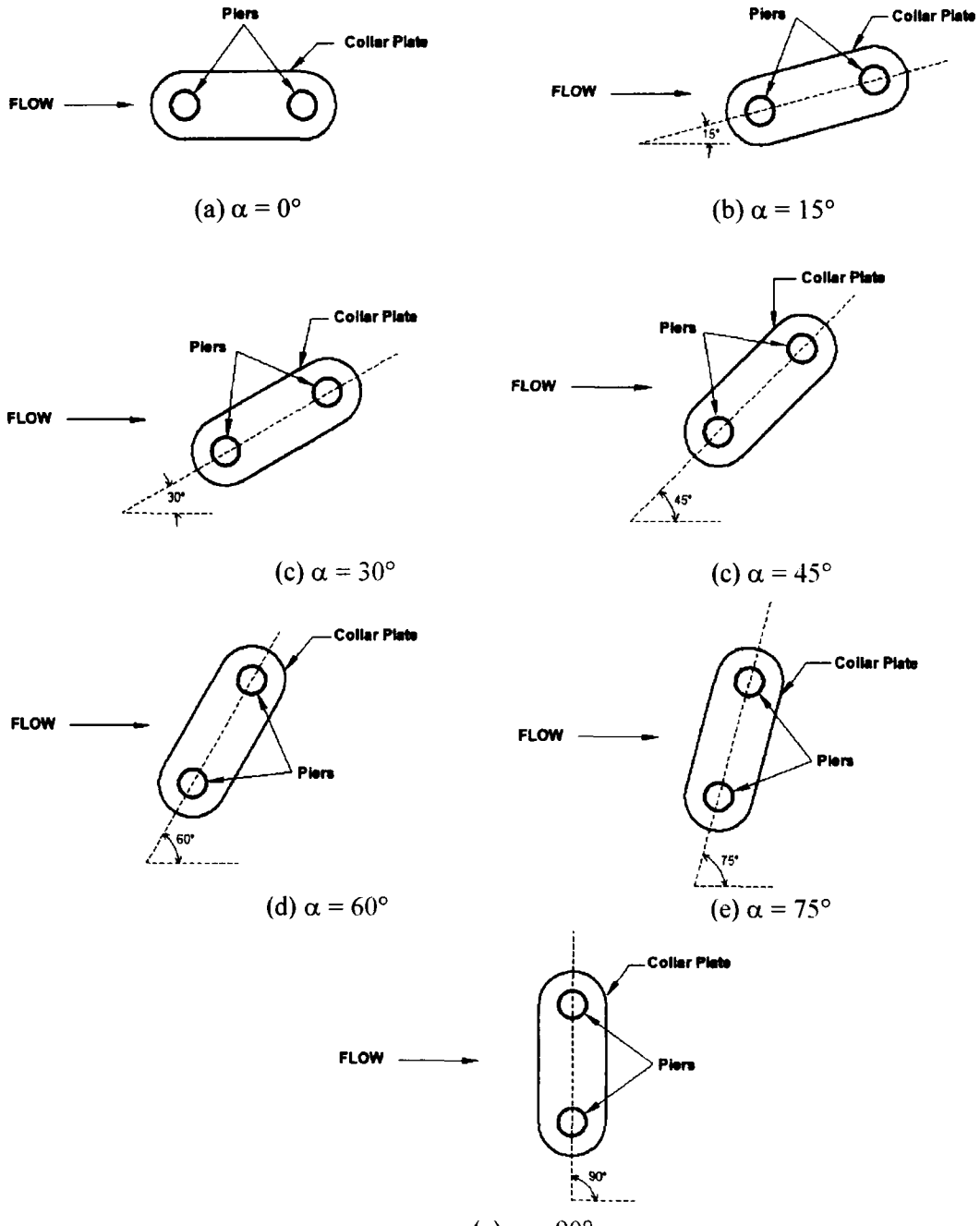

Fig. 3.15 Group of two piers with collar at different angles of attack 'α'

Experiments were first conducted on 41.5 mm diameter single pier which was used in the piers group, to form a basis against which the piers group scour could be evaluated.

Prior to each experiment, the two piers in the group were set vertically in the sediment bed of the flume at center to center spacing equal to $3b$ and at desired angle of attack without collar, where b is the diameter of the model pier. The two piers in the sediment bed were so set symmetrically that the perpendicular distances of their centers from the center of the flume were equal. The sediment bed around the piers was fairly leveled and the experiments were performed under the same experimental procedure as that used in the experiments conducted at a single pier of 4.15 cm diameter. During the experimental runs, the scour depths were measured at the nose of the piers at regular intervals of time. On the completion of experimental run, the supply of water to the flume was gradually stopped and water from the flume was drained off with extreme care so that the scour holes and the scour patterns around the piers were not disturbed. Photographs of the scour patterns developed around the piers were then taken and detailed measurements of the scoured area around the piers were made and recorded. The experiment was then repeated with collar plate skirted around the piers group.

(b) Part two: Local scour at a group of varying sized circular piers

This part investigated the effect of the shape of piers group and a thin collar plate skirted around it on depth of local scour. Using circular cylinders of different diameters, the groups of piers were formed in lenticular type configuration. Initial tests were performed on a pier group which was formed using 25.5 mm, 46 mm and 58.5 mm circular cylinders as shown in Fig. 3.16.

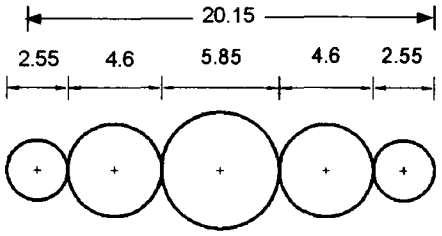

(b) Without collar

Fig.3.16 Group of piers of varying sizes without collar

The aspect ratio of the piers group (length of piers group/width of the piers group) was equal to 3.513. Shen *et. al.* (1966) suggest that, for the purpose of experimental investigation, the flume width should be at least 8 times the diameter or the projected width of the pier to be used in the study. At lower values of blockage ratio, Shen et al. felt that there will be side wall confinement and scour depth will be affected. When the test at 30° angle of attack was conducted using this pier group, the effect of flume walls was observed as the flume walls restricted the development of the areal extent on downstream of the piers group. To obviate this difficulty associated with conducting the study using this group of piers at 30° angle of attack, only two tests were conducted using this piers group, one at 0° and other at 15° angles of attack with and without collar.

To avoid flume wall effect on scour at higher degrees of angle of attack, another piers group was formed using 21.5 mm, 33 mm and 41.5 mm diameter circular cylinders as shown in Fig. 3.14.

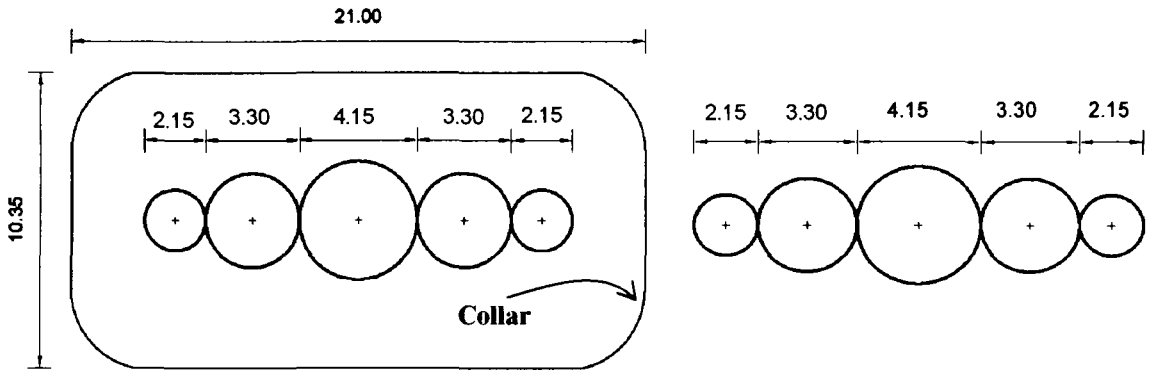

(a) With collar (b) Without collar

Fig.3.17 Piers group having different sizes of piers with and without collar

The ratio of the flume width to the projected width of this piers group at 30° angle of attack was less than 8. The aspect ratio of this piers group was 3.63. The arrangement of piers group in the flume with collar is shown in Fig.3.15.

Experiments were conducted using this piers group with and without collar skirted around it at 0°, 7.5°, 15° and 30° angles of attack. The group of piers was set in the flume sediment bed centrally and vertically aligned at a particular angle of attack and the experiments were conducted with and without collar around the group of piers with the same procedure as that at single pier experiments.

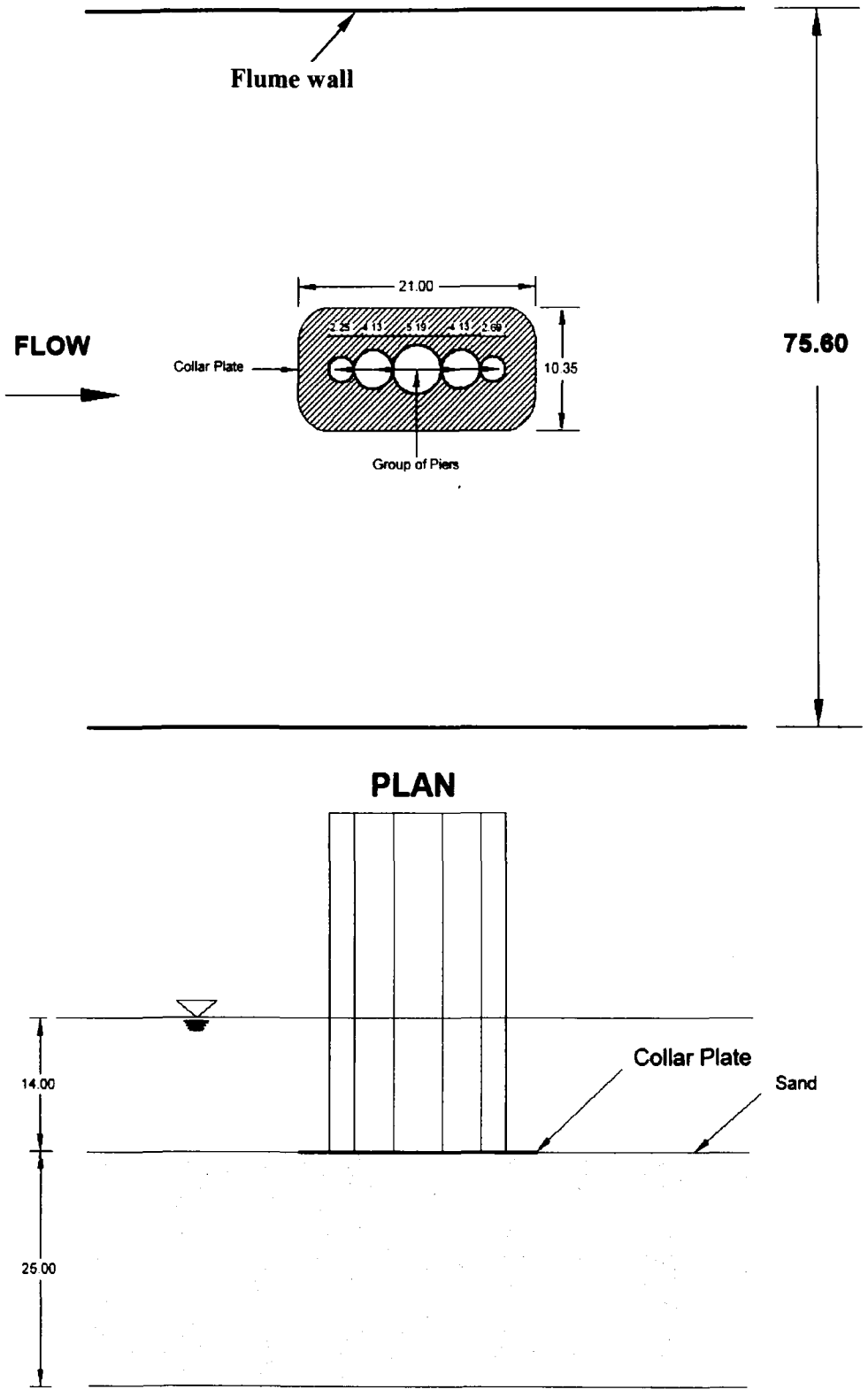

Fig. 3.18 A group of piers of varying sizes fitted with a collar

CHAPTER – IV

MODELLING BASED ON ARTIFICIAL NEURAL NETWORKS (ANN) APPROACH

4.0 Artificial Neural Network (*ANN*)

4.1 Introduction

A new mathematical model that has emerged recently, and has made a great impact in the scientific community is the artificial neural networks (ANNs). ANN has attracted increasing attention from researchers in various fields aiming to solve a wide range of complex non-linear problems. Artificial neural networks are heuristic algorithms, in that they can learn from experience *via* samples and can subsequently be applied to recognize unprocessed data. Learning is defined as self adjustment of the network weights in response to changes in data. These systems are intended, in an extremely simple way, to imitate the behavior of the network of neurons in the human brain. Based on the biological theory of the human brain, artificial neural networks are models that attempt to parallel and simulate the functionality and decision making processes of the human brain.

The primary aim of the ANNs is to improve the performance of computer recognition processes by simulating the superior characteristics of the human brain. The power of artificial neural network techniques rests in their unique advantages that may be listed as follows:

- they are non-parametric
- they have arbitrary decision boundary capabilities
- it is easy to incorporate different types of data and input structures
- they can generalise better towards unprocessed data

Of the advantages of ANN techniques, the most important one may be their nonparametric nature *i.e.* there is no underlying assumption about the frequency distribution of the data. They learn the characteristics of the training dataset (or the internal structure of these data), typically in an iterative way, so they may be called data-dependent techniques. It is also worth noting that artificial neural networks can give considerably better results for small training datasets compared to conventional

theoretical, empirical or semi-empirical models (Hepner *et al.*, 1990; Blamire, 1994; Paola, 1994 and Foody, 1995).

4.1.1 Network structure

The basic element of an artificial neural network is the processing node (Fig. 4.1) that corresponds conceptually to the neuron of the human brain. Each processing node receives and sums a set of input values, and passes this sum through an activation function providing the output value of the node, which in turn forms one of the inputs to a processing node in the next layer of the ANN.

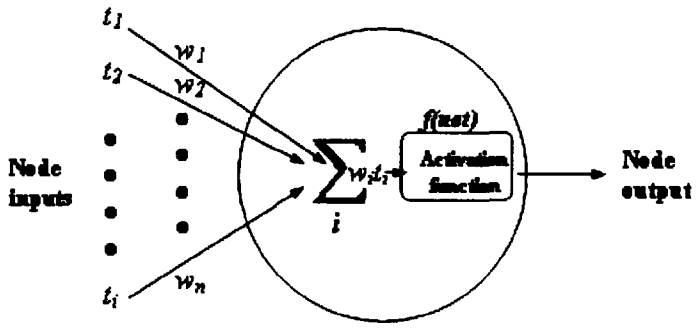

Fig. 4.1 A neural network processing node (*net* is the sum of weighted input values to the processing neuron)

Processing nodes make up a set of fully interconnected layers, except that there are no interconnections between nodes within the same layer in the standard feed forward back propagation neural networks (discussed later in section 4.1.4). The structure of a feed-forward artificial neural network includes three types of layers: input layer, output layer and hidden layer (Fig. 4.2). The input layer introduces the distribution of the data to the network. The output layer is the final processing layer that has a set of values (or codes) to represent the desired output to be recognised. The layers between the input and output layer are called hidden layers. These hidden layers, of which there may be only one, perform the basic calculations. It is through these layers that the internal representations of the input patterns can be produced. A typical neural network consists of one input layer, one or two hidden layers and one output layer.

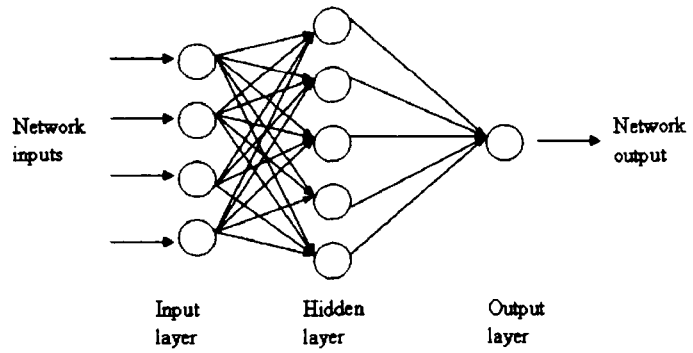

Fig. 4.2 Architecture of a simple three layer feed-forward neural network

4.1.2 Learning algorithms

A learning algorithm is the core of an ANN application as it is necessary to make the network neurons and weights capable of performing a useful task by understanding the internal structure of the data. There are many learning strategies developed for different neural network models and the major ones are given in Fig. 4.3.

It is possible to categorise neural network models in terms of two criteria. The first one is based on whether the model employs a supervised or an unsupervised learning strategy. While in supervised models input and output information is provided to adjust the weights in such a way that the network can produce the given outputs from the inputs, only input information is provided in unsupervised models to find out possible classes in the dataset. Major unsupervised neural network models are Kohonen Self-Organising Map (SOM), Adaptive Resonance Theory Networks (ART), Hopfield networks, and Grossberg networks, whilst most common supervised models are the Perceptron, Multilayer Perceptron (MLP), Radial Basis Function Network (RBF), Recurrent Networks, and Learning Vector Quantization (LVQ).

However, for training feed-forward neural networks the most popular technique is the backpropagation algorithm introduced by Rumelhart *et. al.* (1986). If the information advances from input layer to output layer, the learning method is called "feed-forward". Conversely, if the information proceeds from output layer to input layer, the network is termed "feed-back". There are a number of learning algorithms developed for different neural network models.

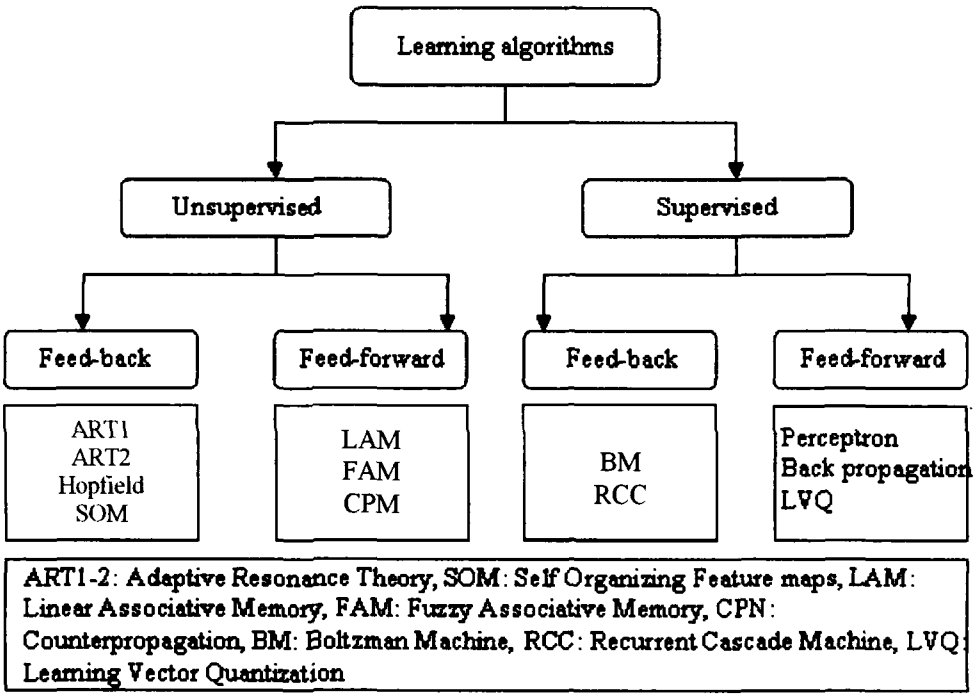

Fig. 4.3 Major neural network learning algorithms

According to Werbos (1995), it has been used in about 70% of ANN applications and defined backpropagation as a procedure for efficiently calculating the derivatives of some output quantity of a nonlinear system, with respect to all inputs and parameters of that system, through calculations proceeding backwards from outputs to inputs.

4.1.3 Feed-forward back propagation neural network

The backpropagation neural network algorithm, also called the generalised delta rule, is an iterative gradient descent training procedure. It is carried out in two stages. In the first stage, after all the network weights have been randomly initialised, the input data are presented to the network and propagated forward to estimate the output value for each pattern set. In the second stage, the difference (error) between known and estimated output is fed backward through the network and the weights are changed in such a way that the difference is minimised. The whole process is repeated with weights being recalculated at every iteration until the error is minimal, or else lower than a given threshold value. A processing node sums the inputs multiplied by the weights of interconnections and then estimates the output of the node using the activation function:

$$net_{Pj} = \sum w_{ji} i_{Pi} \tag{4.1}$$

$$o_{Pj} = f(net_{Pj}) \tag{4.2}$$

where net_{Pj} is the sum of the inputs, w_{ji} is the weight vector, i_{Pi} is the value of the i^{th} element of the input pattern, o_{Pj} is the output of the node j for pattern p, and $f(.)$ is the activation function, which is usually a nonlinear function. The most common activation function used is the sigmoid function and is written as;

$$f_j = \frac{1}{1+e^{-\sum w_{ji} i_{Pi}}} \tag{4.3}$$

The sigmoid function is a bounded and monotonically increasing function that provides a graded nonlinear response enabling the neural network to map any nonlinear process.

The algorithm minimises the error that is the sum of the differences between the actual and calculated output values. The error for pattern p is estimated from:

$$E_P = \frac{1}{2}\sum_j (t_{Pj} - o_{Pj})^2 \tag{4.4}$$

Where t_{Pj} is the target input for j^{th} component of the output pattern for pattern p, o_{Pj} is the j^{th} element of the actual (calculated) pattern produced by the presentation of input pattern p. The total error of the network can then be estimated from;

$$E = \sum E_P \tag{4.5}$$

New weights are estimated by updating the weights with Δw_{ji}

$$w_{ji} = w_{ji} + \Delta w_{ji} \tag{4.6}$$

$$\Delta w_{ji} = -\eta \frac{\partial E}{\partial w_{ji}} \tag{4.7}$$

where η is a term called the learning rate that must be initially set by the user. It is used to control the degree of the change in the weights in response to errors in the output during each cycle.

The mathematical theory underlying the backpropagation algorithm is presented only briefly above, as the details are beyond the scope of this study, but can be found in

numerous sources, such as Rumelhart *et. al.* (1986), Pao (1989), Paola (1994), Bishop (1995) and Ripley (1996).

Training a feed-forward neural network using the backpropagation algorithm involves setting several initial parameters including network structure, learning rate, momentum term and activation function. Of these parameters, two (network structure and activation function) are discussed in later sections. The value of the learning rate has a great impact on the success of ANN applications. If the learning rate is set too high, the learning algorithm may not reach the global minimum, and an increase in error can be observed. If the learning rate is too small, then the process of searching the minimum error will be slow, resulting in long computation times.

Another important issue is to define a stopping criterion for the learning process, as it is unusual for real-world problems to train a network until the training error is zero. A convergence criterion must be defined to prevent overtraining. This can be considered as a threshold value. When the network reaches this value, training is stopped and the trained network is tested for its performance. There are two methods that have been suggested to find out the best time to terminate the learning process in terms of best generalisation performance. The first method involves employing a validation set for testing the performance of the trained networks during the learning process. Learning is stopped when the error on the validation set starts to rise. According to Ripley (1996), 'this is dangerous as it is often encountered examples in which, after an initial drop, the error on the validation set rises slowly for a large number of iterations, then falls dramatically to a small fraction of its previous minimum'. Another problem of using a validation set occurs in cases that there are a limited number of data available that are only enough to form the training and test sets.

The second solution is early stopping, to which, Wang *et al.* (1994) states that a network has better generalisation performance when learning is stopped at a certain time before the global minimum of the empirical error is reached. In addition, for a fixed number of learning examples, the larger the ratio $d\,n$, where d is the number of weights (or nodes) and n is the number of samples, the larger is the improvement in generalisation error if the algorithm is stopped before the global minimum is reached. It is assumed that when the learning reaches the global minimum, the network loses its generalization capabilities

as it becomes too specific and is likely to become trapped into a local minimum, as illustrated in Fig. 4.4.

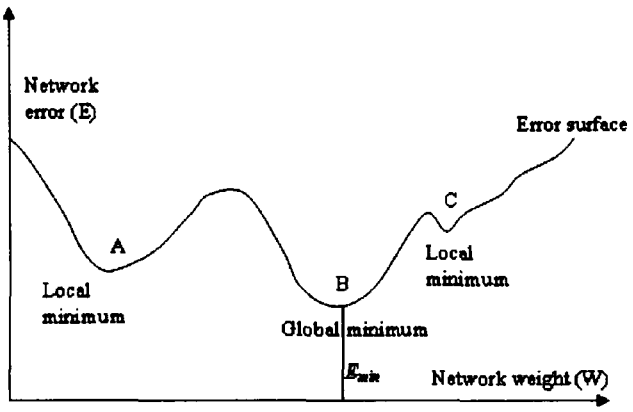

Fig. 4.4 Typical error surface with local minima (A and C are the local minima, B is the global minimum).

Despite its simplicity, it has been reported by researchers that the backpropagation algorithm gives reasonably good results for many problems related to sediment transport. It is also easy to implement computationally, compared to others. The main drawback of the backpropagation learning algorithm is that there is no guarantee of convergence to minimum error.

CHAPTER – V

ANALYSIS OF RESULTS AND DISCUSSION BASED ON GRAPHICAL REPRESENTATION APPROACH

5.0 Introduction

The aim of this chapter is to describe and analyze the data collected during present extensive experimental study on the effect of mutual interference of bridge piers on local scour and to implement the neural network based approach for estimating the scour depth around group of cylindrical bridge piers. The data acquired on various characteristics of local scour around a single pier are interpreted to form a basis against which the data collected on piers group local scour could be analyzed. Also the experimental observations made in the present study are compared with those reported by Laursen and Toch (1956), Chabert Engeldinger (1956), Breusers *et. al.* (1977), Hannah (1978), Jain, S.C. (1981), Richardson *et. al.* (1993, 2001), Melville (1997), Kothyari *et. al.* (1992 a) and HEC-18 (CSU).

The analysis of mutual interference of bridge piers on local scour is being carried for the following patterns of pier arrangements:

(i) Single pier of 33 mm diameter.
(ii) Two piers of 33 mm diameter in tandem arrangement.
(iii) Three piers of 33 mm diameter in tandem arrangement.
(iv) 66 mm diameter pier on upstream and 33 mm diameter pier on downstream in tandem arrangement.
(v) 33 mm diameter pier on upstream and 66 mm diameter pier on downstream in tandem arrangement.
(vi) Two piers of 33 mm diameter at constant angle of attack but varying radial distances.
(vii) Two piers of 33 mm diameter at constant radial distance but varying angles of attack.
(viii) Two piers of 33 mm diameter in transverse arrangement.
(ix) Three piers of 33 mm diameter in staggered arrangement.
(x) A group of piers of varying sizes with and without collar at varying angles of attack.

(xi) A group of two piers of 41.5 mm diameter at fixed pier spacing with and without collar at varying angles of attack.

The experiments for the above mentioned pier arrangements were carried out until the equilibrium scour depth was attained that is, when the scour depth did not change appreciably with time. The equilibrium scour depths were noted. The data on temporal variation for these runs are given in Appendix I. Appendices V to VII give the sediment and hydraulic details for the same data.

Prior to start the experiments on group of piers placed in arrangements (ii) to (ix) mentioned above, a series of experiments on a single pier was performed first so as to have a basis for the evaluation of the effect of mutual interference of piers on local scour.

5.1 Single Circular Cylindrical Pier

A series of experiments was performed on a 33 mm single circular cylindrical pier to have a basis against which the effect of mutual interference of piers on scour depth can be analyzed. In these experiments, the flow, sediment and pier conditions were kept same as that of piers group experiments as to directly compare the pier group results.

As the single pier scour results have to be used to form a basis for analyzing results on group of piers placed in different arrangement, it is imperative to have clear understanding of flow mechanisms around a single pier.

5.1.1 Flow patterns at a cylindrical pier

It is established fact that flow patterns past a single pier protruding from a plane boundary in uniform open channel flow is complex. This complexity further increases with the development of scour hole. The flow pattern past a single pier is separated into its components:

(i) Down flow in front of the pier
(ii) Horseshoe vortex
(iii) Cast off vortices and wake
(iv) Bow wave

In present case of single pier experiments, the flow was observed to separate at the sides of the pier and the separation surface enclosed the wake, downstream of the pier. The separation resulted in the development of the concentrated "Cast off" vortices in the interface between the flow and the wake. Near the bed, these vortices were observed to interact with horseshoe vortex causing the trailing part to oscillate laterally at the frequency of vortex shading. Cast off vortices with their low pressure centres were observed lifting sediments from the bed like tiny tornados.

The commencement of scour hole development was observed at the sides of the pier with the holes quickly propagating upstream around the perimeter of the cylinder to meet on the centre line. The eroded material was observed being transported downstream by the flow. Soon after the commencement of scouring, a shallow hole, concentric with the cylinder, was formed around most of the perimeter of the cylinder but not in the wake region. The downflow was acting like a vertical jet eroding a groove in front of the pier. The eroded material was carried around the pier by a combined action of accelerating flow and spiral motion of the horseshow vortex.

The downflow was turning 180° in the groove and the upward flow was deflected by the horseshoe vortex in the upstream direction, up the slope of the scour hole, the groove almost disappeared altogether when scour approached to its equilibrium depth. The rim was observed to collapse irregularly in local avalanches of the bed material. The deflection of the downflow ejected this material upto where the horseshow vortex was observed to push some of it up the slope. The rest was picked up and carried by the flow into and behind the wake region where a bar developed. The upstream part of the scour hole developed more quickly. The scour hole assumed the shape of a frustum of an inverted cone with slope equal to the angle of repose of the bed material under erosion conditions.

To verify the maximum scour depth obtained in present experimental conditions for a single pier, a comparison has been made with the scour depths computed from the existing relationships reported by Laursen and Toch (1956), Breusers *et. al.* (1977), Jain (1981), Melville (1997) and HEC- 18 (CSU) design scour equation (see, Table 5.1). The scour depth observed in present study is very close to the scour depth predicted by the equations of Laursen and Toch (1956), SC Jain (1981) and HEC-18.

Table 5.1 Comparison of observed scour depth at single pier with scour depth computed using existing scour depth predictors

Investigators	Scour depth (*ds/b*)
Present study	2.1
Laursen & and Toch.,1956	2.082
Breusers *et al.*, 1977	3.54
Jain, 1981	2.152
Melville, 1997	2.28
HEC-18 (CSU)	2.08

Some of the salient scour characteristics observed around an isolated pier are given in Table 5.2.

Table 5.2 Scour characteristics observed at an isolated pier experiments

Scour Characteristics	Observed values of scour characteristics
Maximum scour depth at nose of the pier 'ds_i' or '$ds_{n(i)}$'	6.9 cm
Normalized equilibrium scour depth '$ds_{n(i)}/b$'	2.1
Maximum scour depth at rear face of the pier '$ds_{rf(i)}$'	5.2 cm
Top width of scour hole along upstream and downstream faces of the pier '$w_{n(i)}$' and '$w_{rf(i)}$'respectively.	25 cm
Length of scour-hole from upstream face of the pier '$L_{shu\ (i)}$'	11.2 cm
Length of scour-hole from downstream face of the pier '$L_{shd\ (i)}$'	29.5 cm
Upstream slope of scour hole 'ϕ'	32.2°
Downstream slope of scour hole 'θ'	10°
Length of sediment deposition on downstream of the pier '$L_{dep(i)}$'	82 cm
Area of scour hole '$A_{sh(i)}$'	875.06 cm^2
Area of extent of scour 'A_i'	2687.94 cm^2

In view of providing protection to pier against local scour, the study of scour and deposition pattern and location of the deepest scour is considered to be of utmost importance (Vittal *et al.*, 1994). In the light of its relevance, longitudinal scour profile, lateral scour profiles and areal extent of scour are measured at the end of present experiments and plotted as shown in Figs. 5.1 to 5.5 respectively and the same are also depicted in Fig. P1.

5.1.2 Longitudinal profile of scour

Fig. 5.1 illustrates the longitudinal scour profile, which shows the deepest scour occurrence at the nose of the pier. From Fig. 5.1, it is inferred that from downstream face of pier the scour depth below original bed level decreases along the flow direction and approaches to zero at the original bed level at a distance of 29.5 cm from the downstream face of the pier. Deposition of sediment occurs beyond 29.5 cm from downstream face of the pier.

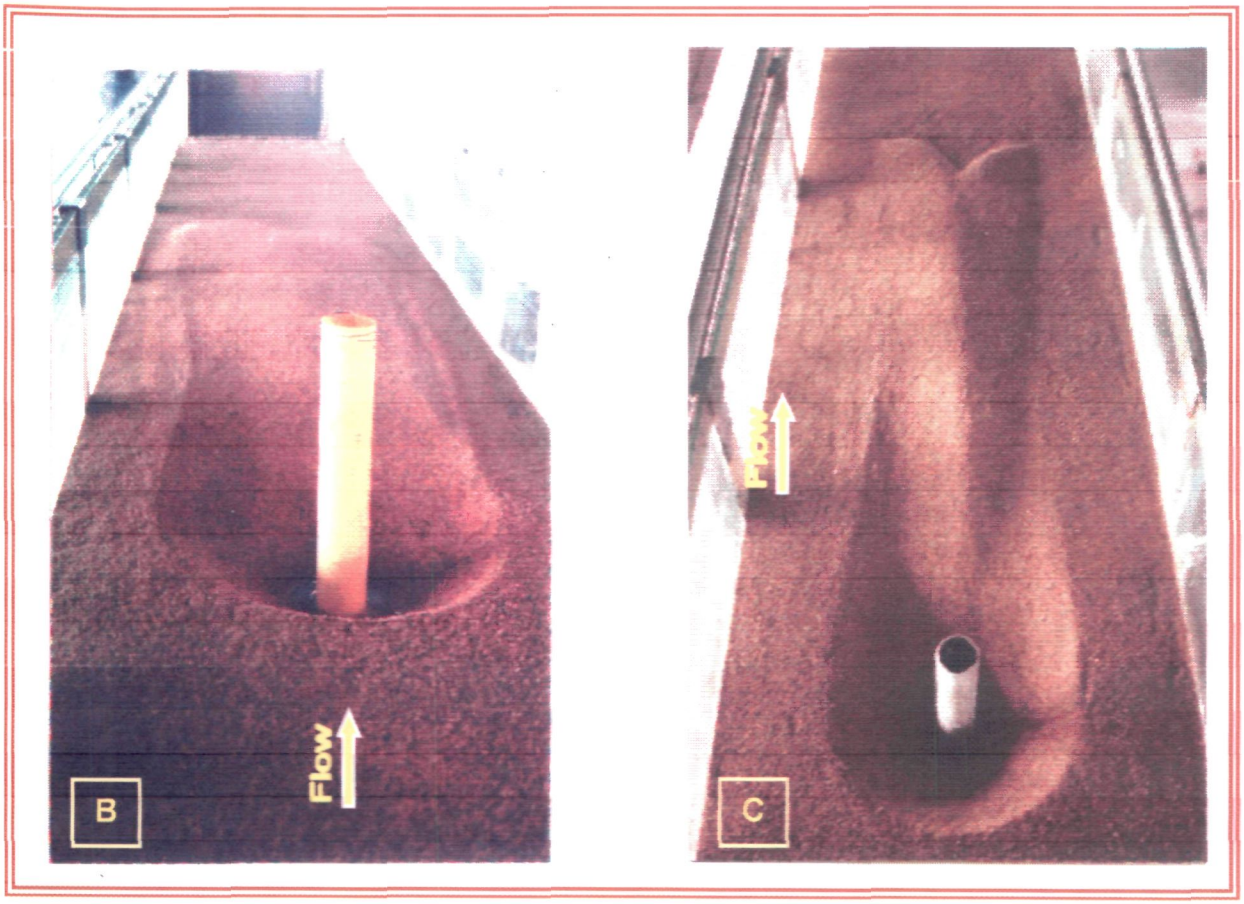

Fig. P1: Scour and deposition patterns around single circular cylindrical piers of diameter (A) 3.3 cm (B) 6.6 cm (C) 4.15 cm

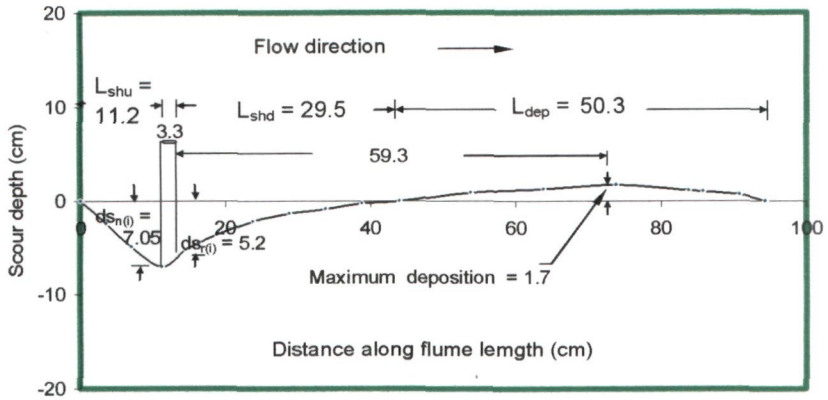

Fig. 5.1 Variation of scour depth along flume length for an isolated pier $ds_{n(i)}$ and $ds_{rf(i)}$ (where $ds_{n(i)}$ = scour depth at nose of pier, $ds_{rf(i)}$ = scour depth at rear face of pier).

5.1.3 Lateral profiles of scour

Figs. 5.2, 5.3 and 5.4 show the lateral scour profiles plotted along the width of the flume at the upstream and the downstream faces of the pier and at the section of maximum deposit respectively. It can be seen in Figs.5.2 and 5.3 that the maximum scour depth occurs at the centre of the upstream face of the pier (i.e., at the nose) while at the downstream face, maximum scour occurs at 0.8 cm away on either sides of the centre (Fig.5.3). The maximum sediment deposition is observed along the centre line of the scour extent as is clearly illustrated in Fig.5.4, at a distance of 59.3 cm from the downstream face of the pier.

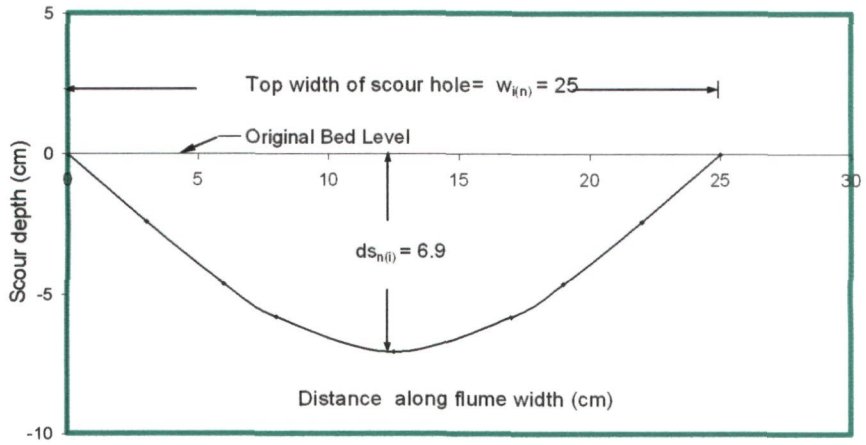

Fig. 5.2 Lateral profile of scour drawn at upstream face of an isolated pier (where $ds_{n(i)}$ = scour depth at nose of pier, $w_{n(i)}$ = top width of scour hole at upstream face of the pier).

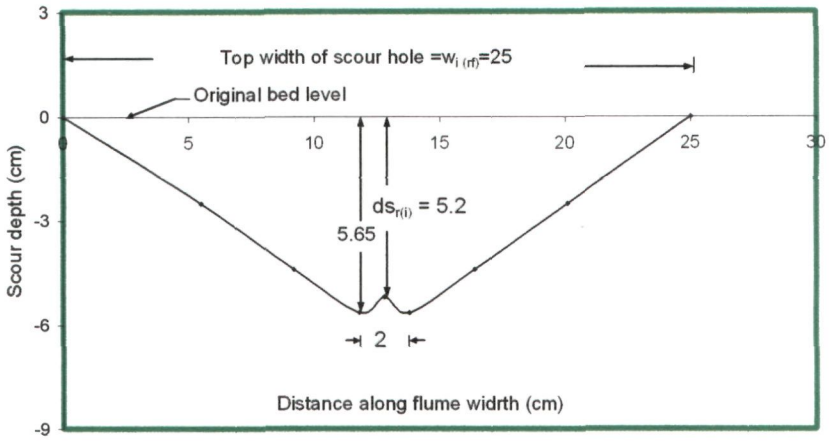

Fig. 5.3 Lateral profile of scour drawn at rear face of the an isolated pier (where $ds_{rf(i)}$ = scour depth at rear face of pier, $w_{rf(i)}$ = top width of scour hole).

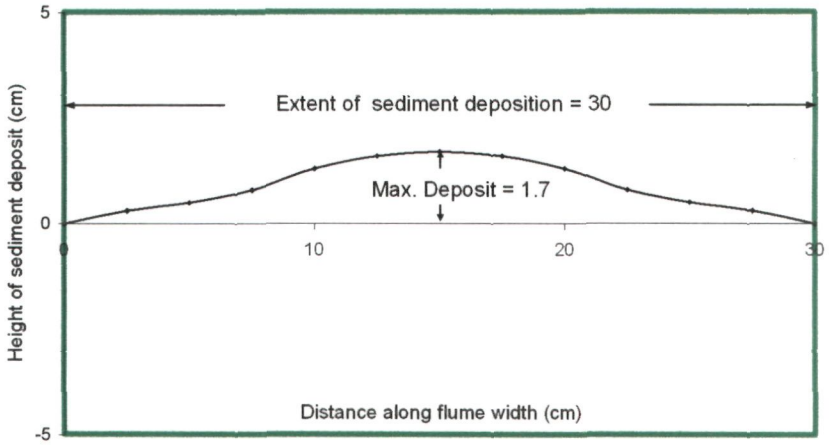

Fig. 5.4 Lateral profile of scour drawn through the point of maximum sediment deposition.

5.1.4 Areal extent of scour

Fig. 5.5 depicts the areal extent of scour around an isolated pier with zones of scour and deposition distinctly marked. As seen in Fig. 5.5, the shape of the scour hole at upstream face of the pier is semicircular in plan while moving downstream, width of scour extent decreases followed by a sudden increase at a distance of 29.5 cm from the pier. Lengthwise deposition of sediment in the direction of flow is observed to be more along the centre line of the scour extent and less while moving away from the centre line on either side. The reason for this can be attributed to the scouring mechanism as reported in earlier studies of Nakagawa and Suzuki (1975), Hjorth (1977), Ettema (1980) and Dey and Raikar (2007).

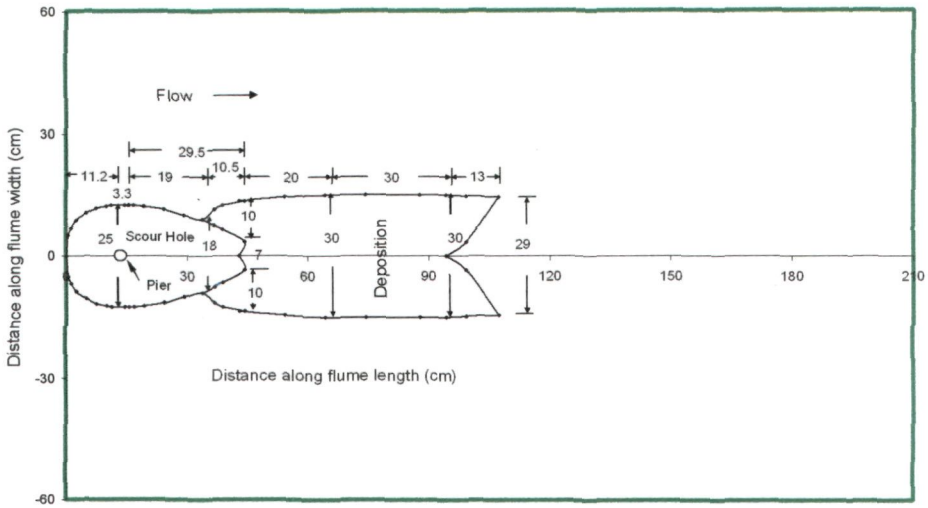

Fig. 5.5 Areal extent of scour around an isolated pier

The actual mobilization and removal of sediment is observed in an area immediately adjacent to the pier base in the scour hole. The particles lifted not high enough into the flow are swept directly behind the pier and enters the relatively calm wake region between the shedding vortices forming the mound behind the pier. The particles carried high enough into the flow interact with the wake vortices and are transported and deposited well downstream.

At the last stage of experiment, the sediment was observed resting permanently on the sloping surface of the scour hole without moving further down the slope of scour hole. When the experiment was over, the top width of scour hole normal to the flow direction was measured through the nose of pier. The angle of slope of scour hole was also measured. The upstream slope of the scour hole is observed to be same as the angle of repose of the bed material 'ϕ'.

To study the scour hole dimensions, it is necessary to examine the scour process on upstream and downstream of a pier. The scour on upstream is governed by the horseshoe vortex while on downstream is mainly a result of wake vortices which are formed by the rolling up of the unstable shear layers generated at the surface of the pier and detached from it at the separation points. The wake vortex system with a low pressure zone in the centre acts somewhat like a vacuum cleaner and picks up the bed material. The transport of the picked up material, however, depends on the strength of the eddies shedding from the pier and being convected by the main flow.

Since the knowledge of scour hole dimensions is important in determining the extent of countermeasures needed to prevent scour at piers, some of the important features of scour hole are analyzed as under.

The top width of scour hole observed at the upstream face of single pier (see, Table 5.2) tallies well with that computed from relationship of Richardson *et al.* (1993). The median ratio of scour hole width to scour depth '$w_{n(i)}/ds_i$' is obtained as 3.623 and the median ratio of scour hole width to the pier width '$w_{n(i)}/b$' is obtained as 7.576 and the maximum ratio of scour depth to pier width 'ds_i/b' is 2.1.

Scour hole Length is the distance from upstream face of pier to the upstream edge of the scour-hole (upstream length) or to the downstream edge of the scour hole (downstream length). The total length of scour hole is equal to the sum of the upstream and downstream lengths plus the diameter of the pier. The downstream scour hole length is affected by the flow pattern and pier misalignment to flow and is generally greater than the upstream scour hole length.

It is evident from the observations given in Table 5.2, that the median ratio of upstream scour hole length to pier width '$L_{shu(i)}/b$' is 3.394 and the median ratio of downstream scour hole length to pier width '$L_{shd(i)}/b$' is 8.94. The downstream slope is observed to be less than the upstream slope since the flow pattern around a bridge pier might have caused the downstream length of scour hole to exceed the upstream length. The lowest elevation of bed in a scour-hole is observed at the upstream at a distance less than half of the pier width from the upstream face of the pier.

5.1.5 Temporal variation of scour

The data on temporal variation of scour depth around the single pier collected in present study are plotted and compared with the predictor of Kothyari *et. al.* (1992 a) as shown in Fig.5.6.

These single pier local scour results are utilized in the following sections to form the basis for the analysis of results obtained from the data collected in present study on local scour at group of piers placed in different arrangements. The data on temporal variation of scour around a single pier are given in Appendix-I.

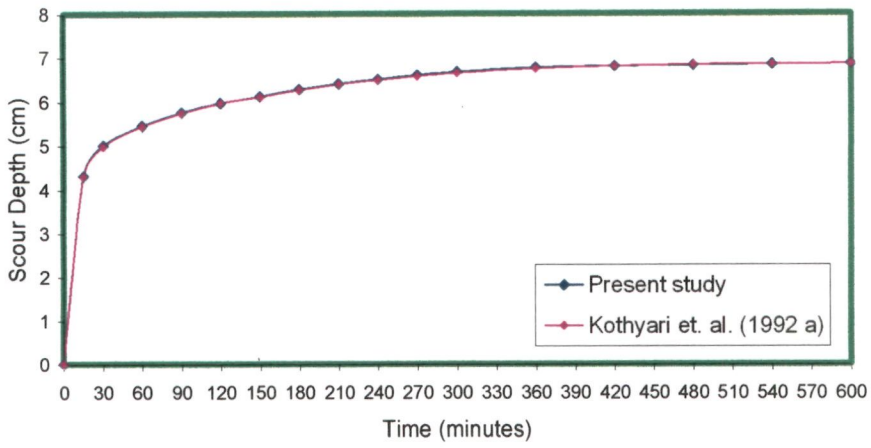

Fig. 5.6 Temporal variation of scour at an isolated pier

5.2 Two Circular Piers of Same Size in Tandem Arrangement

5.2.0 Introduction

When two piers were testified in tandem arrangement in present experiments, it was observed that the vortex system including horseshoe and wake vortices excavated the scour holes around the front and rear piers in a similar manner as an isolated pier. Down-flow at the upstream face of the piers impinged the streambed and dug a hole in front of the piers and the flow separation downstream of the piers produced the wake vortices. The scour holes around the piers were observed to be independent of one other except for the cases with pier spacings x/b=0 and 1.

In present study, effect of mutual interference between front and rear piers is investigated by plotting longitudinal profiles of scour, lateral profiles of scour and areal extents of scour for varied pier spacings *'x/b'* as shown in Appendix-II, Appendix-III and Appendix-IV respectively. Out of the total cases of longitudinal scour profiles and areal extent of scour, some typical cases are chosen for analysis and discussion in this part of present study. The photographs showing scour and deposition patterns developed on the bed around the piers were taken at the end of each experiment. Photographs of some distinctive cases are shown in Fig. P2. The analysis of results achieved from present experimental data is made under the following heads.

5.2.1 Variation of scour depth along flume length

Using the data collected in present experiments on two piers placed in tandem arrangement, the longitudinal profiles of scour along the central line of flume in flow direction are plotted as shown in Appendix-II. The overlapping of longitudinal profiles developed around front and rear piers shown in Fig.5.7, demonstrates existence of the effect of mutual interference of two piers on local scour upto pier spacing x/b<30.

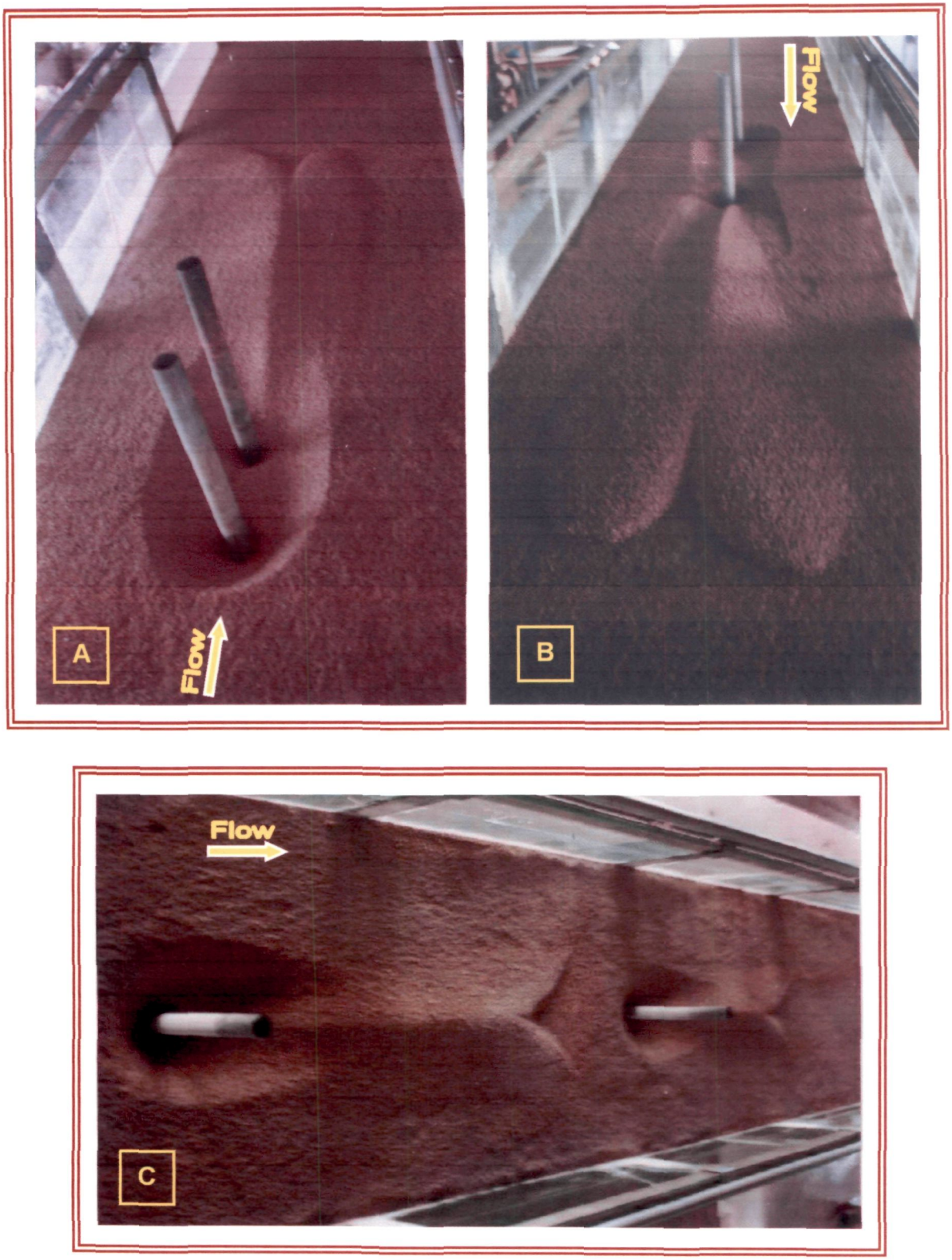

Fig. P2: Scour and deposition patterns around two piers placed in tandem arrangement at varied pier spacings *x/b* (A) *x/b*=4 (B) *x/b*=16 (C) *x/b*=40

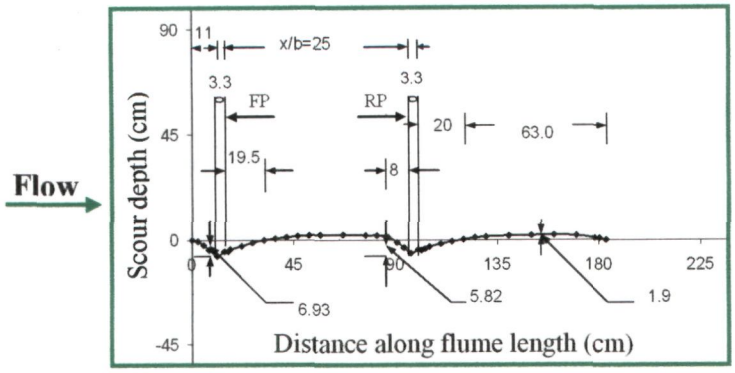

Fig. 5.7 Variation of scour depth at two piers of same size placed in tandem arrangement along flume length at x/b=25

However, as depicted in Fig.5.8, the longitudinal profiles of scour get separated from one another at pier spacing x/b=30, although, the length of the rear pier profile remains smaller than that of the front one.

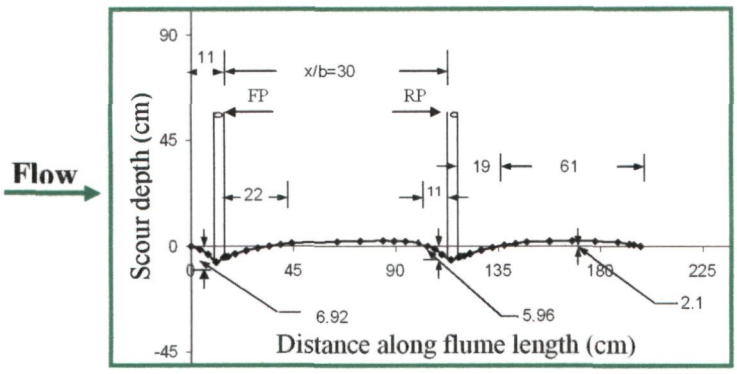

Fig. 5.8 Variation of scour depth at two piers of same size placed in tandem arrangement along flume length at x/b=30

Fig.5.9 reveals that when the pier spacing x/b approaches to 90, the lengths of longitudinal profiles of front and rear piers become similar to that of an isolated pier signifying that the two piers are freed from the effects of mutual interference.

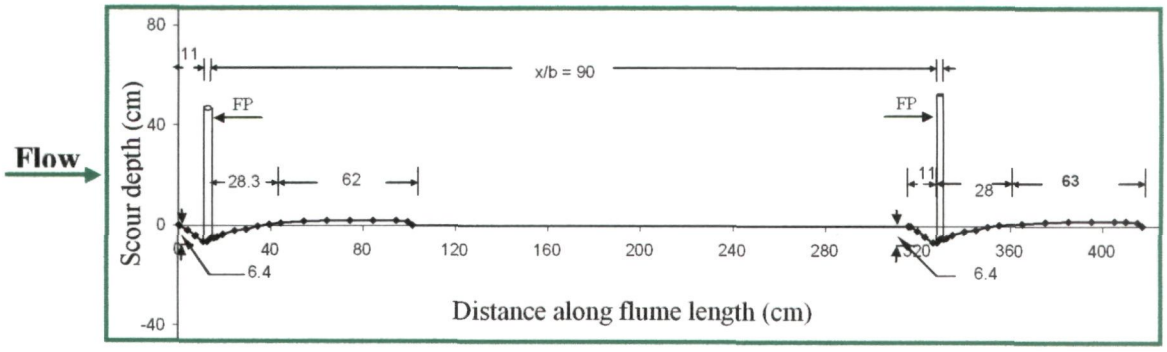

Fig. 5.9 Variation of scour depth at two piers of same size placed in tandem arrangement along flume length at x/b=90

5.2.2 Variation of scour depth with pier spacing

Fig. 5.10 shows the variation of relative scour depths *'ds_f/ds_i'* and *'ds_r/ds_i'* observed at front and rear piers respectively with relative pier spacing *'x/b'*.

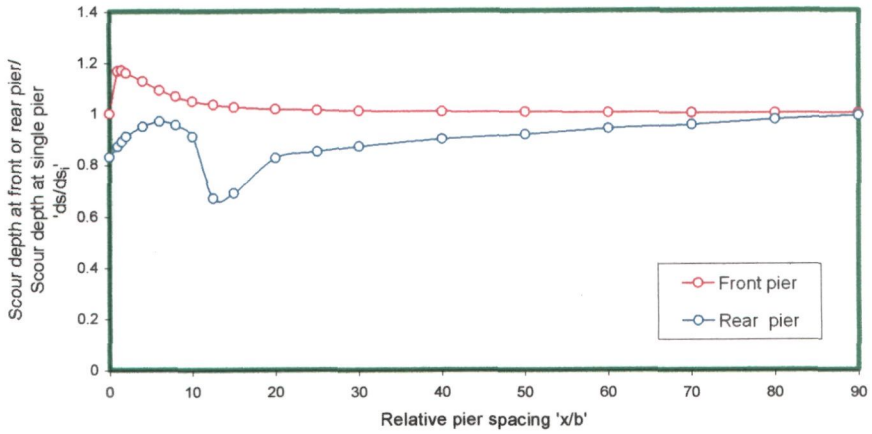

Fig. 5.10 Variation of relative scour depth *'ds_f/ds_i'* and *'ds_r/ds_i'* at two piers of same size placed in tandem arrangement with pier spacing *'x/b'* (where ds_f = scour depth at front pier, ds_r = scour depth at rear pier and ds_i = scour depth at an isolated pier).

At pier spacing *x/b*=0, the scour depth at front pier is same as that at an isolated pier. With an increase in pier spacing, the scour depth at front pier increases due to the reinforcing effect induced by the rear pier. At *x/b*=1.5, the reinforcing effect on front pier is maximum as a result of which the scour depth at the front pier is maximum at this pier spacing. Thereafter, the reinforcing effect decreases upto *x/b*=10. At larger pier spacing, (*i.e.*, *x/b*>10), the reinforcing effect weakens and the scour depth at front pier approaches to that at an isolated pier at *x/b*=90. For pier spacings up to *x/b*=5, the rear pier scour hole partially overlaps and reduces the height of the exit slope of the scour hole around the front pier. This causes the scour around the front pier to be reinforced or to become deeper than a scour hole around an isolated pier. As shown in Fig (5.11), the difference between the original bed level and the base of the rear pier scour hole is maximum at *x b*=1.

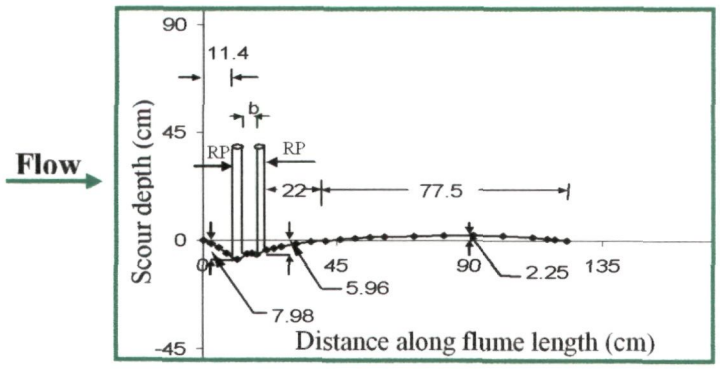

Fig. 5.11 Variation of scour depth at two piers of same size placed in tandem arrangement along flume length at *x b*=1

Taking into consideration the variation of bed level between the two piers it can be noticed in Fig. 5.12 that as the pier spacing *x/b* increases and reaches to 10, the bed level between the two piers increases and reaches to the original bed level due to deposition of the bed material which is scoured and transported from the front pier scour hole.

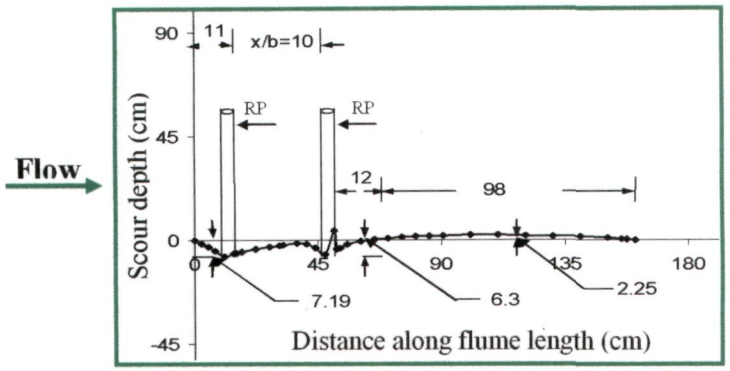

Fig. 5.12 Variation of scour depth at two piers of same size placed in tandem arrangement along flume length at *x b*=10

As demonstrated in Fig.5.13, the bed level between the two piers increases above the original bed level at *x/b*>10 due to dominant deposition of the bed material transported from the front pier scour hole.

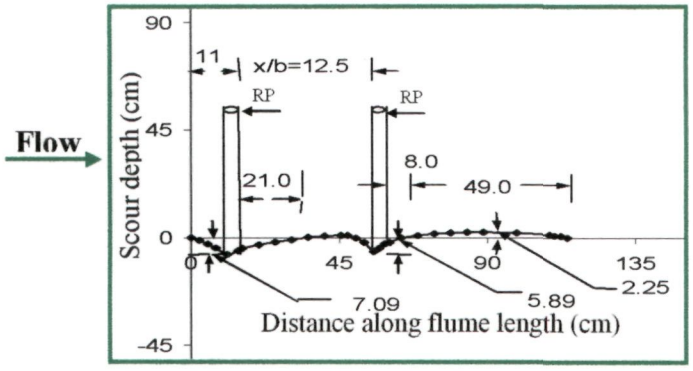

Fig. 5.13 Variation of scour depth at two piers of same size placed in tandem arrangement along flume length at *x b*=12.5

As regards to the rear pier scour depth variation, it is evident from Fig. 5.10 that the scour depth at the rear pier is significantly influenced due to the sheltering effect of the front pier. This sheltering effect produced by front pier reduces the effective approach flow velocity for the rear pier and provides sediment transport into scour hole formed around it, results in the formation of weak vortex system and thus results in reduced scour depth at the rear pier. At x/*b* = 0, the sheltering of the rear pier is complete and the scour depth at the rear pier is about 86 % of the scour depth at the front pier (*i.e.*, maximum scour depth at single pier).

With an increase in the pier spacing, the sheltering effect reduces and separate scour holes at the front and rear piers are formed at pier spacing x/b=1. From x/b = 1 to 6, there is an increase in the scour depth at rear pier. The reason for this increase in scour depth is attributed to the striking action of wake vortices shed from the front pier which pass very close to the rear pier thereby causing an increase in the scouring strength of the horseshoe vortex in the rear pier scour hole. As noticed in Fig. 5.10, the scour depth at rear pier approaches to maximum and close to that of an isolated pier at x/b= 6. However, at x/b>6, the shed vortices become less effective in removing bed-material from the rear pier scour hole as they pass far away from the rear pier. At larger pier spacing the level of bed between the two piers builds up due to dominant deposition of the bed material transported by the flow from the front pier scour hole. The built up bed between front and rear piers interferes with the horseshoe vortex in the rear pier scour hole. With diminishing effect of shed vortices effect and building up of the bed between the two piers, the scour depth at rear pier starts decreasing and reaches to a minimum at x/b = 12.5. With further increase in pier spacing, the rear pier becomes free from effect of shed vortices and the scour depth reaches to the scour depth of an isolated pier at x/b=90.

The ratio of maximum scour depth at the upstream face of front and rear pier to the pier diameter 'ds_f/b' and 'ds_r/b' are plotted against pier spacing 'x/b' as shown in Fig 5.14. The value of this ratio 'ds_f/b' for front pier is observed as 2.43, at pier spacing x/b = 1.5. Also, for the case of rear pier, the value of ration 'ds/b' is observed to be 2.06 at pier spacing x/b=90.

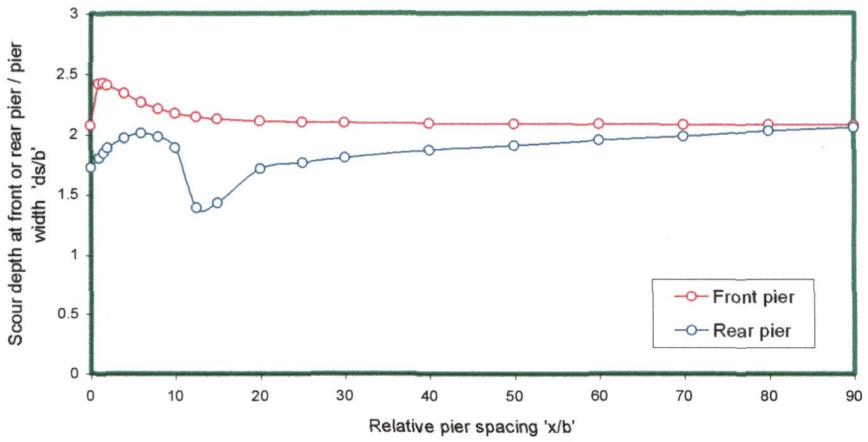

Fig 5.14 Variation of scour depth 'ds_f/b' and 'ds_r/b' with pier spacing 'x/b' at two piers of same size in tandem arrangement (where ds_f=scour depth at front pier, 'ds_r/b' = scour depth at rear pier and b= pier diameter).

The scour depths at rear pier with respect to the scour depth at front pier 'ds_r/ds_f' are plotted against the relative pier spacing 'x/b' as shown in Fig. 5.15. The value of 'ds_r/ds_f' at pier spacing x/b=0, is 0.83. Between pier spacing x/b= 0 and 1 the value of 'ds_r/ds_f' decreases and increases thereafter, upto pier spacing x/b=10. Between pier spacing x/b=10 and 12.5, there is a decrement in the value of 'ds_r/ds_f'. Beyond pier spacing x/b=12.5, the value of 'ds_r/ds_f' increases. The reason for this variation in the values of 'ds_r/ds_f' with pier spacing is same as that for the variation of scour depth as discussed in section 5.2.2 of this chapter.

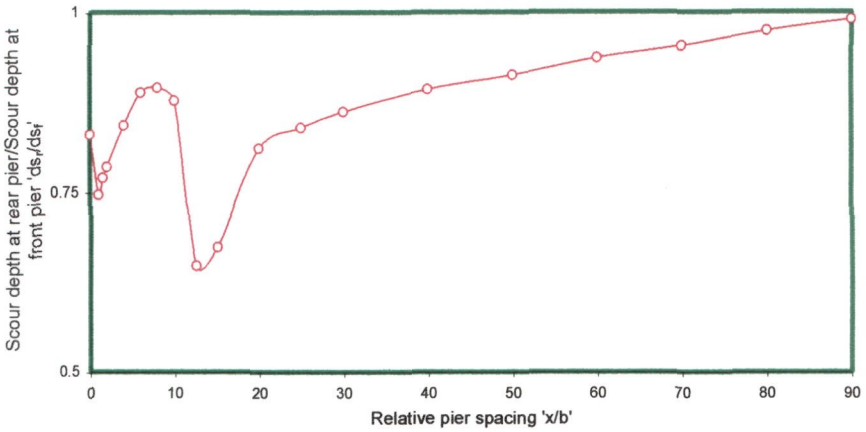

Fig 5.15 Variation of scour depth at rear pier with respect to the scour depth at front pier 'ds_r/ds_f' for two piers of same size placed in tandem arrangement (where ds_r = scour depth at rear pier, ds_f = scour depth at front pier)

The scour depths observed at front and rear piers at varying pier spacing are compared with published results of Hannah (1978) as shown in Table 5.3.

Table 5.3 Comparison of scour depth observed at piers placed in tandem arrangement in present study with published results of Hannah (1978) for varying pier spacing 'x/b'

Pier Spacing x/b	Maximum scour depth with respect to pier diameter observed at two piers in tandem arrangement			
	Present study		Hannah (1978)	
	Front Pier	Rear Pier	Front Pier	Rear Pier
0	2.075758	1.722879	1.909091	1.660909
1	2.420333	1.805909	2.226000	1.718182
1.5	2.428636	1.847424	2.233636	1.737273
2	2.407879	1.888939	2.214545	1.756364
4	2.341455	1.97197	2.153455	1.832727
6	2.266727	2.013485	2.084727	1.851818
8	2.214833	1.982348	2.037000	1.718182
10	2.177470	1.888939	2.002636	1.613182
12.5	2.148409	1.390758	1.975909	1.546364
15	2.127652	1.432273	1.956818	1.527273
20	2.113121	1.7125	1.943455	1.546364
25	2.102742	1.764394	1.933909	1.594091
30	2.096515	1.805909	1.928182	1.641818

The scour depths observed at front and rear piers by Hannah (1978) are comparably less than the scour depths measured in the present study under similar flow conditions (Table 5.3). In the present study, minimum scour depth at front face of rear pier is observed at pier spacing x/b = 12.5 instead of at pier spacing x/b=16 as reported by Hannah (1978). The reason for this disparity in results can be attributed to the longer duration of experimental runs and imposition of higher stresses (*i.e.*, higher value of U/U_*) used in present study. The re-approchement of equilibrium scour depth at front pier earlier than the rear one is due to the fact that rear pier being in shelter of the front pier.

The task of modelling for the estimation of scour depth at front and rear piers for varied pier spacings 'x/b' is accomplished by using ANN models the details of which are presented in Tables 6.1 and 6.2 (Chapter VI) and ANN architectures Fig 6.10 (Chapter VI). The estimated scour depths are plotted against observed scour depths as shown in scatter grams (Fig. 6.11, Chapter VI). The average values of correlation coefficient R^2 between observed and ANN estimated scour depths as given in Table 6.2 (Chapter VI) are 0.9976 for front pier and 0.9846 for rear pier respectively. The closeness of the data points to the line of best agreement shown in Fig. 6.11 (Chapter VI) also indicates the excellent agreement between observed and ANN estimated values of scour depths. As given in Table 6.2 (Chapter VI), the values of *rmse* for training data sets for front and rear piers are 7.69×10-4 and 5.7×10-4 while the corresponding values for testing data sets are 1.39×10-3 and 2.87×10-3 respectively. The higher values of R^2 and lower values of *rmse* are indicative of the accuracy in the scour depths produced by ANN models.

5.2.3 Dimensions of scour holes

Since the knowledge of scour hole dimensions is important in determining the extent of countermeasures needed to reduce scour at piers, various parameters explained as under using present experimental data are determined.

(a) Length of scour holes

To study the characteristics of scour holes developed around front and rear piers, the length of scour holes at upstream and downstream face of front and rear piers and the slope of scour holes in the direction of flow are obtained from longitudinal profiles of scour as shown in Appendix-II. The top widths of scour holes at upstream face of front and rear piers are obtained from lateral profiles of scour as shown in Appendix-III.

(b) Length of scour hole at upstream face of front pier

Fig. 5.16 shows the variation of relative length of scour holes '$L_{shu(f)}/L_{shu\ (i)}$' and '$L_{shu\ (r)}/L_{shu\ (i)}$' at the upstream faces of front and rear piers with pier spacing x/b. At pier spacing x/b=0, the length of scour hole at upstream face of the front pier is observed to be same as that of an isolated pier. Between pier spacing x/b=0 to 2 the scour hole length at upstream face of front pier increases due to an increase in reinforcing effect on front pier and decreases thereafter, upto pier spacing x/b=10 due to the decrease in reinforcing effect. The reinforcing effect disappears completely beyond pier spacing x/b=10 and the length of scour hole on upstream face of front pier remains constant.

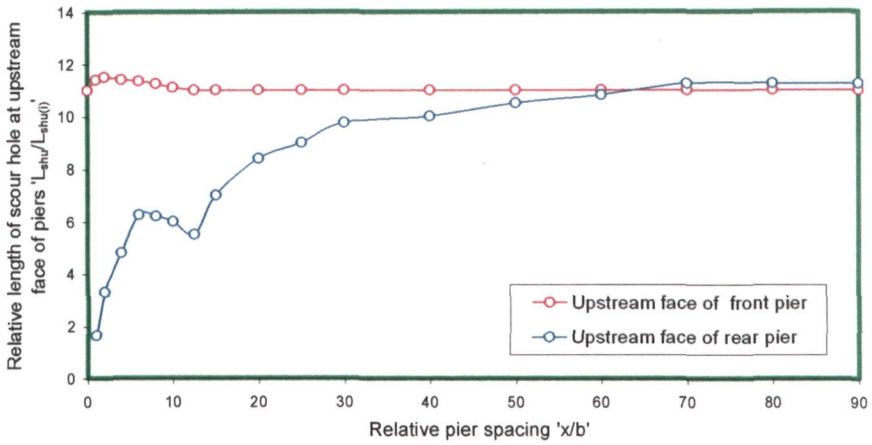

Fig 5.16 Variation of relative length of scour hole at upstream faces of front and rear piers '$L_{shu(f)}/L_{shu(i)}$' and '$L_{shu\ (r)}/L_{shu(i)}$' with pier spacing 'x/b' for two piers of same size placed in tandem arrangement (where $L_{shu(f)}$ = Length of scour hole at upstream face of front pier, $L_{shu\ (r)}$ = Length of scour hole at upstream face of rear pier and $L_{shu(i)}$ = length of scour hole at upstream face of isolated pier).

(c) Length of scour hole at upstream face of rear pier

The variation in the length of scour hole at upstream face of rear pier is shown in Fig. 5.16. It is observed that upto pier spacing x/b=6 the length of scour hole increases. This increase in the rear pier scour hole length is attributed to the enhancement in the scouring strength caused by the striking impact of shed vortices originating from front pier. For pier spacings ranging from x/b=6 to 12.5 the length of scour hole decreases due to the diminution in the scouring strength as a result of sheltering of rear pier caused by the bed material deposited at upstream face of rear pier and due to the diminishing state of shed vortices effect on rear pier. Beyond pier spacing x/b=12.5, as the rear pier being freed from all effects, the length of scour hole on upstream face of rear pier increases and reaches to that of an isolated pier at pier spacing x/b=90.

(d) Length of scour hole at downstream face of front pier

The variation of scour hole length at downstream faces of front and rear piers '$L_{shd(f)}/L_{shd(i)}$' with pier spacing 'x/b' is shown in Fig. 5.17. It is observed that the length of scour hole increases upto x/b=10. The reason for this increment is the complex flow pattern on downstream of front pier caused by the interaction of horseshoe vortex with the shed vortices originating from the front pier.

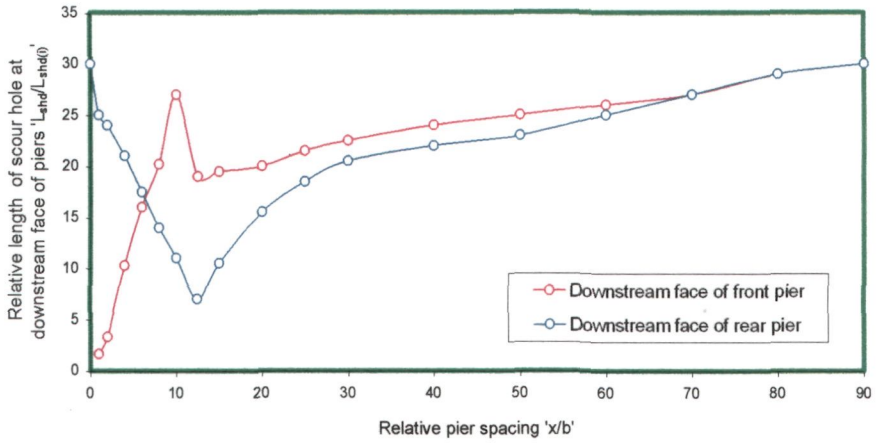

Fig 5.17 Variation of relative length of scour hole at downstream faces of front and rear piers '$L_{shd(f)}/L_{shd(i)}$' and '$L_{shd(r)}/L_{shd(i)}$' respectively with pier spacing 'x/b' for two piers of same size placed in tandem arrangement (where $L_{shd(f)}$ = Length of scour hole at downstream face of front pier, $L_{shd(r)}$ = Length of scour hole at downstream face of rear pier, and $L_{shd(i)}$ = Length of scour hole at downstream face of an isolated pier).

The front pier experiences the reinforcing effect upto pier spacing x/b=10, which dominates on the flow pattern upto this pier spacing and results in an increase in scour hole length. Steep reduction in rear pier scour hole length at pier spacing $10<x/b<12.5$ indicates a rapid decrease in horseshoe vortex strength causing a drastic change in flow pattern. Beyond pier spacing x/b=12.5, the scour hole length increases and reaches to that of an isolated pier at pier spacing x/b=90. This increase in scour hole length indicates the diminishing state of the effect of mutual interaction of flow with horseshoe vortex and wake vortices originating at the front pier. The length of scour hole at pier spacing x/b=90 being equal to that of an isolated pier suggests that the two piers apparently become free from mutual interference.

(e) Length of scour hole at downstream face of rear pier

Fig.5.17 shows the effect of pier spacing on the length of scour hole at downstream face of rear pier '$L_{shd(r)}/L_{shd(i)}$'. It is examined that the scour hole length decreases upto pier

spacing x/b=12.5. The effect on the flow pattern caused by the sheltering of rear pier by front pier and the sediment deposit on the bed at the upstream face of rear pier are the reasons for this decrement. Beyond pier spacing x/b= 12.5, the increase in the length of scour hole indicates the weakening of this sheltering effect. The equal lengths of scour hole around two piers at pier spacing x/b=90 indicate the complete disappearance of the sheltering effect on rear pier.

(f) Slope of scour holes

The slopes of scour holes on the upstream and downstream faces of front and rear piers are plotted against pier spacing *'x/b'* as shown in Figs. 5.18 and 5.19. As is evident from Appendix-II, distinction between the scour holes at upstream face of rear pier and downstream face of front pier is difficult at pier spacing x/b=0, therefore, the slope at downstream face of front pier is plotted for pier spacings greater than zero.

(i) Slope of scour holes at upstream face of front pier

It is observed in Fig. 5.18 that the slope of the scour hole on upstream face of front pier '$S_{lu(f)}$ / $S_{lu(i)}$' increases between pier spacing x/b=0 and 1, which is primarily due to an increase in the reinforcing effect on front pier. Between pier spacing x/b= 1 and 30, the substantial decrement in the reinforcing effect on front pier occurs which causes reduction in the scour depth and hence in the slope of scour hole. At pier spacing x/b>30 the reinforcing effect almost disappears and the corresponding slope of scour hole remains fairly constant.

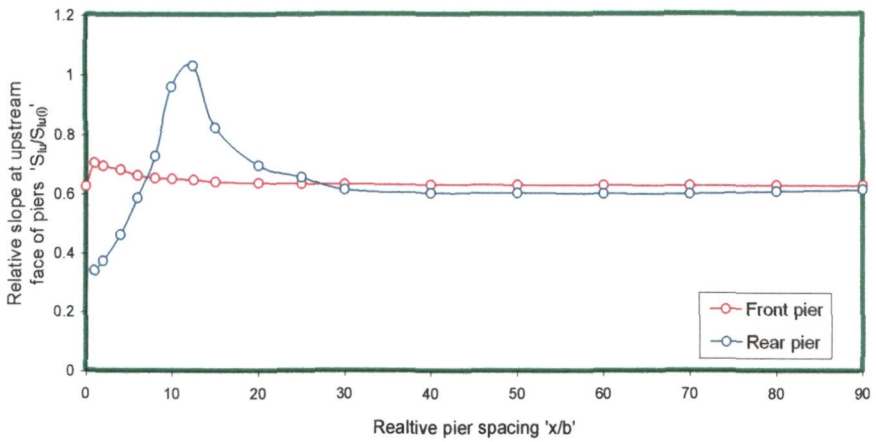

Fig 5.18 Variation of relative slope of scour hole at upstream faces of front and rear piers '$S_{lu(f)}$ / $S_{lu(i)}$' and '$S_{lu(r)}$ / $S_{lu(i)}$' respectively with pier spacing *'x/b'* for two piers of same size placed in tandem arrangement (where $S_{lu(f)}$ = slope of scour hole at upstream face of front pier, $S_{lu(r)}$ = slope of scour hole at upstream face of rear pier and $S_{lu(i)}$=slope of scour hole at upstream face of isolated pier).

(ii) Slope of scour holes at upstream face of rear pier

As illustrated in the above Fig. 5.18, the length of scour hole at the upstream face of the rear pier increases upto pier spacing x/b= 12.5. At x/b<10, the bed level between the two piers remains below the original bed level and the downstream part of front pier scour hole and the upstream part of rear pier scour hole are separated by a narrow thin brim. With an increase in pier spacing the height of this brim reaches to the original bed level at pier spacing *'x/b'* greater than 10 which in turn results in an increase in the scour hole slope upto pier spacing x/b=12.5. Further, it is observed that the sediment deposition starts at the bed upstream of rear pier at pier spacing x/b>10. When pier spacing *'x/b'* increases beyond 12.5, the sediment deposited on the bed upstream of rear pier slips down into the scour hole causing reduction in the scour depth and slope upto pier spacing x/b=30. Thereafter, the approachment of bed material scoured from front pier scour hole to the rear pier scour hole stops substantially. As a result, the scour depth at rear pier is not much affected and the slope of the scour hole '$S_{lu(r)}/S_{lu(i)}$' remains fairly invariable upto pier spacing x/b=90.

(iii) Slope of scour holes at downstream face of front pier

Fig. 5.19 shows the effect of pier spacing *'x/b'* on the slope of scour hole at the downstream faces of front and rear piers. An increase in slope is observed upto pier spacing x/b=10, which is attributed to the dominance of reinforcing effect over the interaction of flow with the horseshoe vortex and wake vortices originating from front pier.

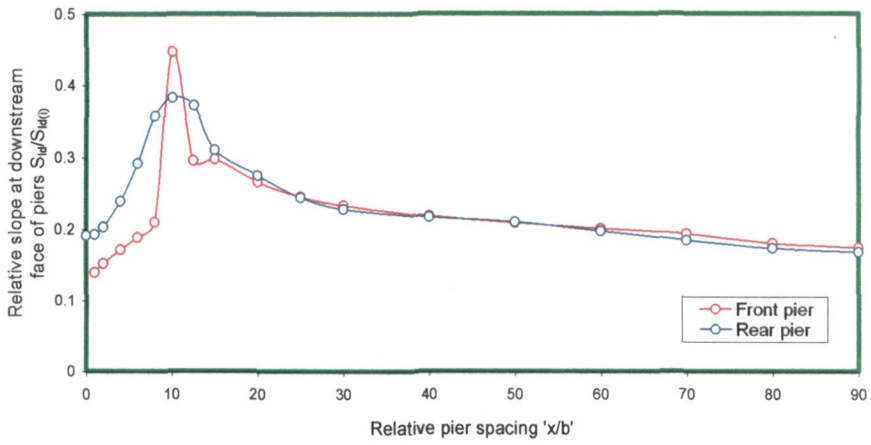

Fig 5.19 Variation of relative slope of scour hole at downstream faces of front and rear piers '$S_{ld(f)}/S_{ld(i)}$' and '$S_{ld(r)}/S_{ld(i)}$' respectively with pier spacing *'x/b'* for two piers of same size in tandem arrangement (where $S_{ld(f)}$ = slope of scour hole at downstream face of front pier, $S_{ld(r)}$ = slope of scour hole at downstream face of rear pier and $S_{ld(i)}$ = slope of scour hole at downstream face of isolated pier).

Beyond x/b=10, the slope decreases, which is indicative of the initiation of decrement in the mutual interaction of flow with horseshoe vortices and wake vortices originating from front pier. At pier spacing x/b=90, the slope becomes the same as that of an isolated pier signifying the two piers to become virtually free from mutual interference.

(iv) Slope of scour holes at downstream face of rear pier

Fig. 5.19 shows the effect of pier spacing 'x/b' on the slope of scour hole at the downstream face of rear pier. It is observed that the slope of scour hole increases upto pier spacing x/b=10. It is also observed in Appendix-II that deposition of sediment does not occur in between the two piers upto pier spacing x/b=10 and thus the entire bed material scoured from front pier scour hole gets transported and deposited at downstream face of the rear pier. The reason for this is the dominance of sheltering effect on rear pier upto pier spacing x/b=10, due to which wake vortices originating from front pier become weak in strength and causes the bed material to deposit at close proximity of the downstream face of rear pier. This deposition of sediment causes an increase in the bed level at the downstream face, which in turn increases the slope of the scour hole. However, at pier spacing x/b>10, the sheltering effect on rear pier reduces, and the velocity of flow approaching the rear pier increases as a result of which the strength of wake vortices enhances. This change in flow mechanism results in an increase in the scouring intensity and deposition of bed material farther away at downstream face with flattened peak, and ultimately leads to an increase in the scour hole length and decrease in the scour hole slope.

(g) Width of scour holes

The lateral profiles of scour at upstream face of front and rear piers Appendix-III are used for the computation of relative top width of scour holes. Fig.5.20 illustrates as to how the pier spacing 'x/b' affects the relative width of scour holes 'w_1/w_i' and 'w_2/w_i' of front and rear piers respectively, where, w_1 is the top width of scour hole at upstream face of front pier, w_2 is the top width of scour hole at upstream face of rear pier and 'w_i' is the top width of scour hole at upstream face of an isolated pier. It is noticed that the relative width of scour hole 'w_1/w_i' at pier spacing x/b=0, is equal to that of an isolated pier. Whereas, at pier spacing x/b= 1, a 20% increase in the scour hole width is observed as

compared to that of an isolated pier. This increase is due to the enhancement in scour depth caused by reinforcing effect on front pier. At pier spacing $x/b>1$, there is a weakening in the reinforcing effect at front pier due to which the scour depth decreases and the relative width of scour hole 'w_1/w_i', decreases and reaches to that of an isolated pier at pier spacing $x/b=15$. Due to the complete disappearance of reinforcing effect, the width of scour hole 'w_1/w_i' remains fairly constant upto $x/b=90$.

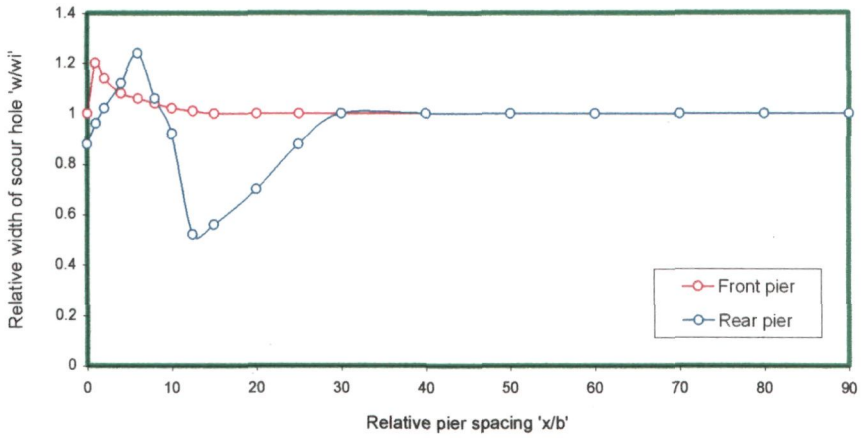

Fig 5.20 Variation of scour hole width observed at front and rear piers 'w_1/wi' and 'w_2/w_i' with pier spacing 'x/b' for two piers of same size placed in tandem arrangement (where w_1 = width of scour hole of front pier, w_2= width of scour hole of rear pier and w_i= width of scour hole of an isolated pier).

Fig. 5.20 reveals the variation in the relative width of scour hole w_2/wi at upstream face of rear pier with pier spacing x/b. Upto pier spacing $x/b=6$, an increase in w_2/wi is noticed. The reason for this increase in w_2/w_i is attributed to the effect of shed vortices which originate from front pier and pass very close to the rear pier, dominates on scouring at rear pier causing an increase in scour depth and the width of scour hole w_2/wi.

At $6<x/b<12.5$, a decrement in the values of w_2/w_i is observed which is due to the dominance of sheltering of front pier. For pier spacings $12.5<x/b>30$, the sheltering effect on rear pier gets reduced considerably due to which the width of scour hole 'w_2/w_i' increases. At pier spacing $30<x/b<90$, 'w_2/w_i' remains constant which implies that the two piers become free from mutual interference effects. A comparison of Figs. 5.20 and 5.21 reveal the observed widths of scour holes at front and rear piers to be in good agreement with the results of Richardson *et. al.* (1993).

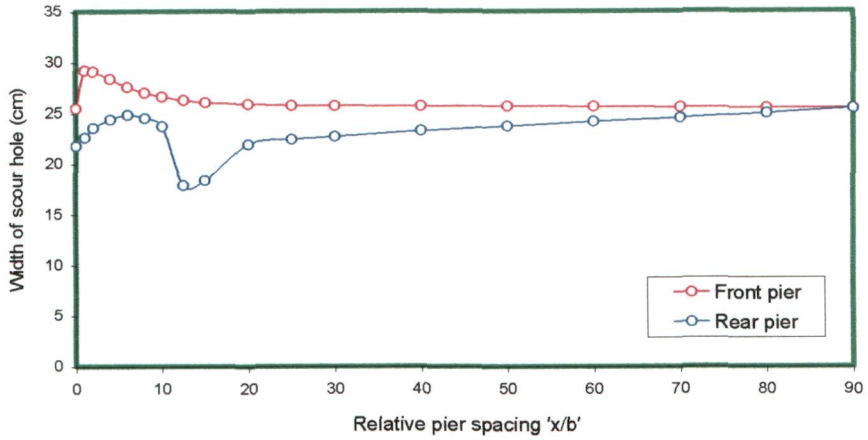

Fig 5.21 Variation of scour hole width with pier spacing '*x/b*' for two piers of same size placed in tandem arrangement (computed by the method of Richardson *et al.*, 1993).

The widths of scour hole at rear pier with respect to the widths of scour hole at front pier w_2/w_1 are plotted against pier spacing *x/b* as shown in Fig.5.22. It is observed that the value of w_2/w_1 increases upto pier spacing x/b=6. This increase indicates the dominance of the effect of shed vortices on rear pier. At pier spacing x/b>6, the value of 'w_2/w_1' decreases and reaches to a minimum at pier spacing x/b=12.5. This decrease indicates the dominance of the sheltering effect on rear pier. For spacings x/b >12.5, 'w_2/w_1' increases and reaches to that of an isolated pier at x/b=30.

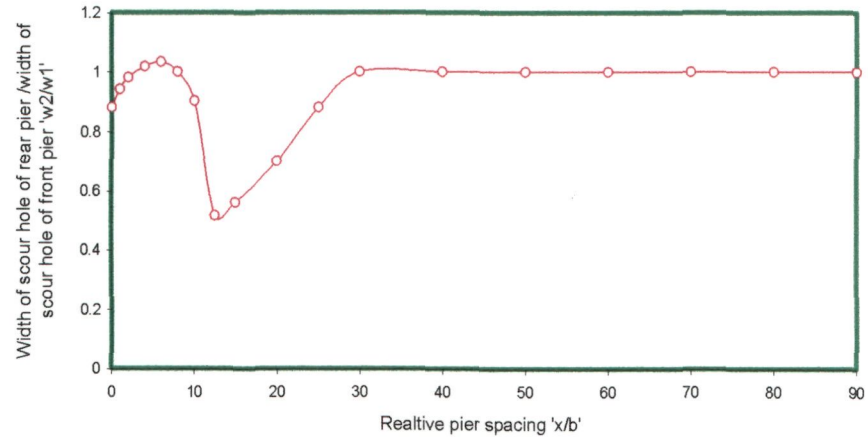

Fig 5.22 Variation of scour hole width observed at rear pier relative to that at front pier 'w_2/w_1' with pier spacing '*x/b*' for two piers of same size placed in tandem arrangement.

(h) Variation of area of scour extents with pier spacing

The plots of areal extents of scour around the front and rear piers for varying pier spacings '*x/b*' are shown in Appendix-IV. It can be seen in Fig. (5.23) that the extents of scour around the front and rear piers overlap each other upto pier spacing x/b<30.

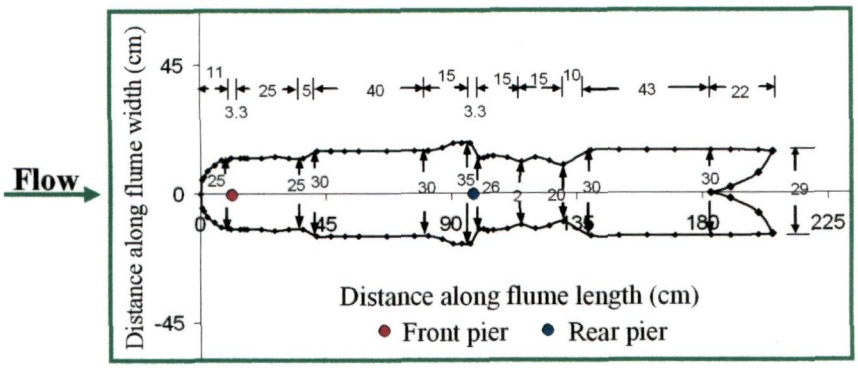

Fig. 5.23 Areal extent of scour around two piers of same size placed in tandem arrangement at x/b=25

Though the extents of scour around front and rear piers as shown in Fig. (5.24) are separated from each other at x/b=30, the size of extent around rear pier still remains smaller than that around the front pier.

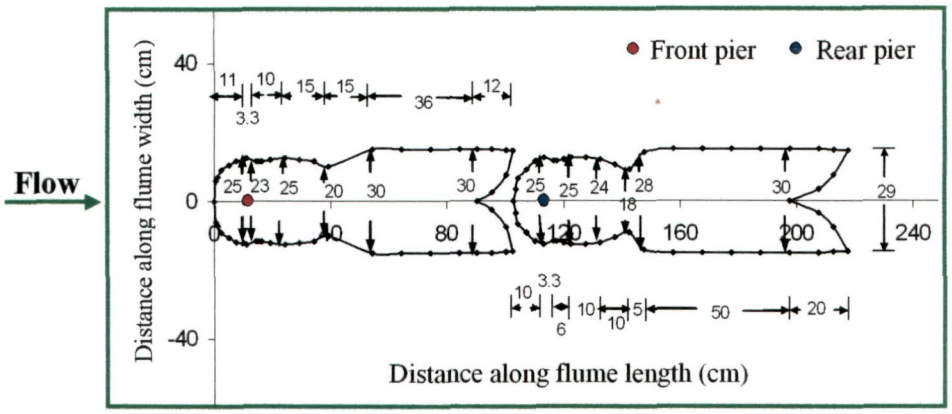

Fig. 5.24 Areal extents of scour around two piers of same size placed in tandem arrangement at x/b=30

However, as the pier spacing 'x/b' approaches to 90, Fig. 5.25 reveals that the extents of scour around front and rear piers become identical in shape and size and similar to that around a single pier signifying that the two piers have become free from effects of mutual interference.

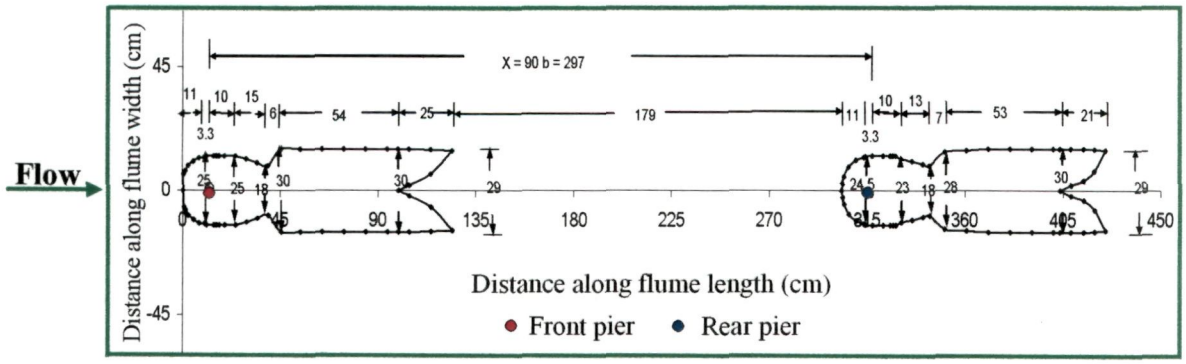

Fig. 5.25 Areal extents of scour around two piers of same size placed in tandem arrangement at x/b=90

The variation of area of scour extent around the front and rear piers with pier spacing is shown in Fig. 5.26.

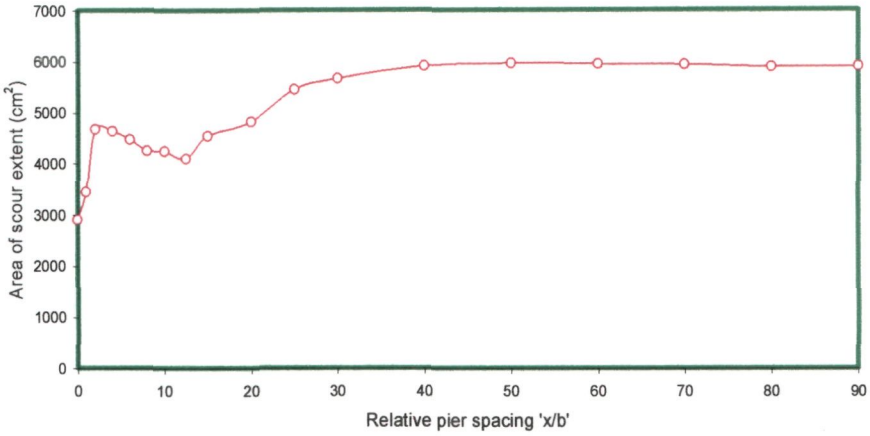

Fig 5.26 Variation of area of scour extent around two piers of same size placed in tandem arrangement with pier spacing '*x/b*'

The ratios of area of scour extent at varying pier spacing *x/b* to that of an isolated pier (*i.e.*, relative area of scour extent) are computed using experimental data gathered in present study and the same are plotted against pier spacing *x/b* as shown in Fig.5.27. The relative area of scour extent observed at pier spacing *x/b*=0 is nearly same as that around an isolated pier. Between *x/b*=0 to 2, the relative area of scour extent increases This increase is attributed to the reinforcing effect of rear pier on front pier which has its dominance over the flow pattern and facilitates in lifting and spreading scoured bed material over larger area around the two piers in this range of pier spacing.

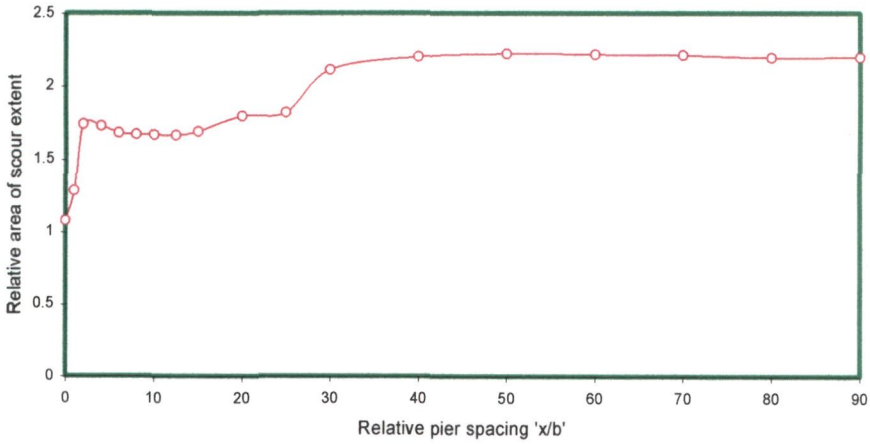

Fig 5.27 Variation of area of scour extent around two piers of same size placed in tandem arrangement with pier spacing '*x/b*'.

At pier spacing ranging from x/b= 2 to 12.5, Fig. 5.27 shows a decreasing trend in the relative area of scour extent which suggests the dominance of the sheltering effect of front pier and of the bed material deposited on the bed upstream of the rear pier, over the flow pattern. This sheltering effect results in low scouring strength around the rear pier and weakens the lifting and transporting potential of the vortex system around the rear pier. At pier spacing x/b>12.5, the relative area of scour extent again increases. This increase is credited to the weakening of the effects of reinforcing, sheltering and vortex shedding at two piers. The relative areas of scour extents around front and rear piers are same and nearly equal to the areal extent around an isolated pier at pier spacing x/b=90 which indicates that the two piers become virtually free from the effect of mutual interference.

(i) Length of sediment deposition at downstream face of piers

The length of sediment deposition on downstream face of front and rear piers relative to that downstream of an isolated pier are plotted against pier spacing as shown in Fig. 5.28. No deposition of sediment is observed on downstream of front pier upto pier spacing x/b=10. The entire bed between two piers is in scouring upto pier spacing x/b=10. The reason for this is the high strength of the wake vortices downstream of front pier induced by intensive interaction of flow with the piers and sediment bed. Due to this increase in strength of wake vortices the sediments scoured from front pier scour hole do not deposit on the bed downstream of front pier and gets transported to downstream of the rear pier. In the range of pier spacings x/b= 10 to 30, Fig.5.28 shows an increase in the length of sediment deposition on downstream of front pier. This happens because of a decrease in the strength of wake vortices originating from front pier, which causes some of the sediment particles to deposit on downstream of the front pier and some of it gets transported to downstream of rear pier. At pier spacing $x/b \geq 30$, the strength of wake vortices weakens further and causes major amount of sediment scoured from front pier scour hole to deposit on the bed downstream of front pier and very little of it transported to downstream of rear pier, as a result of which the length of deposition is maximum at pier spacing x/b =30. Thereafter, the wake vortices of front pier weakens further and they do not remain able to transport the sediment particles further downstream as a result of which the length of deposition remains nearly invariable at pier spacing x/b=30 to 90.

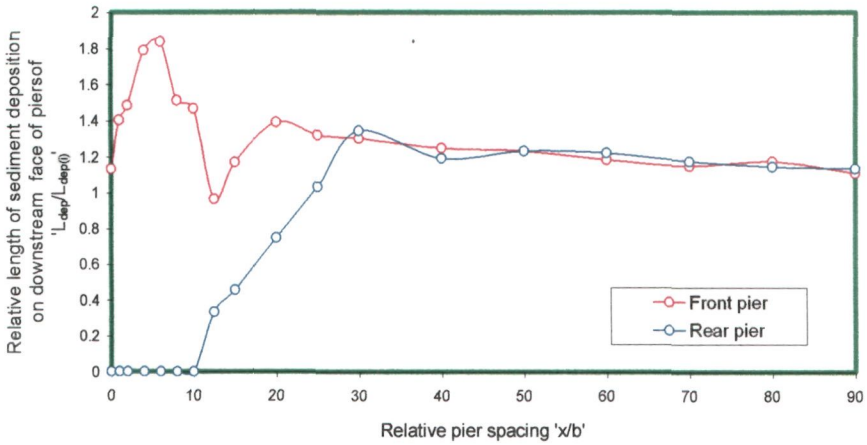

Fig.5.28 Variation of length of sediment deposition at downstream faces of front and rear piers '$L_{dep}/L_{dep(i)}$' with pier spacing 'x/b' for two piers of same size placed in tandem arrangement (where L_{dep} = length of sediment deposition at downstream face of front or rear piers, $L_{dep(i)}$ = length of sediment deposition at downstream face of isolated pier).

Fig. 5.28 shows an increase in the length of sediment deposition on downstream face of rear pier upto pier spacing x/b=6. This increase is attributed to the increase in the strength of wake vortices originating from rear pier. This increase in strength of wake vortices of rear pier is caused by the striking action of shed vortices approaching from front pier, which pass close enough to the rear pier. At x/b>6, the shed vortices approaching from front pier become less effective in removing bed-material from the rear pier scour hole as they pass farther away from the rear pier. At larger pier spacing the bed built up between the two piers due to dominant deposition of the bed material transported by the flow from the front pier scour hole, interferes with the vortex system in the rear pier scour hole. With diminishing shed vortices effect from front pier and building up of the bed between the two piers, the length of sediment deposition at the rear pier starts decreasing reaching minimum apparently at x/b = 12.5. With further increase in pier spacing, the rear pier starts becoming free from all mutual interference effects and the length of sediment deposition tends to reach to that of a single pier.

The photographs shown in Fig.P2 clearly demonstrate the scour and deposition patterns developed on the bed around the piers and explain well the scour characteristics discussed above.

5.2.4 Temporal variation of scour depth at front and rear piers

The data collected on temporal variation of scour around front and rear piers placed in tandem arrangement are given in Appendix-I. From the plots of these data (not shown

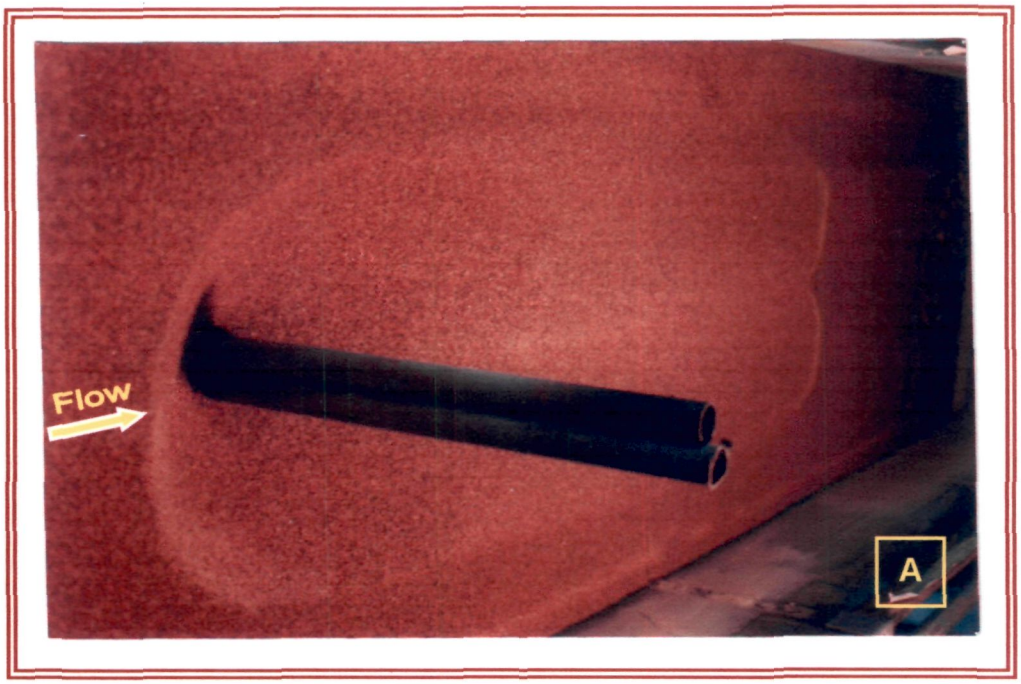

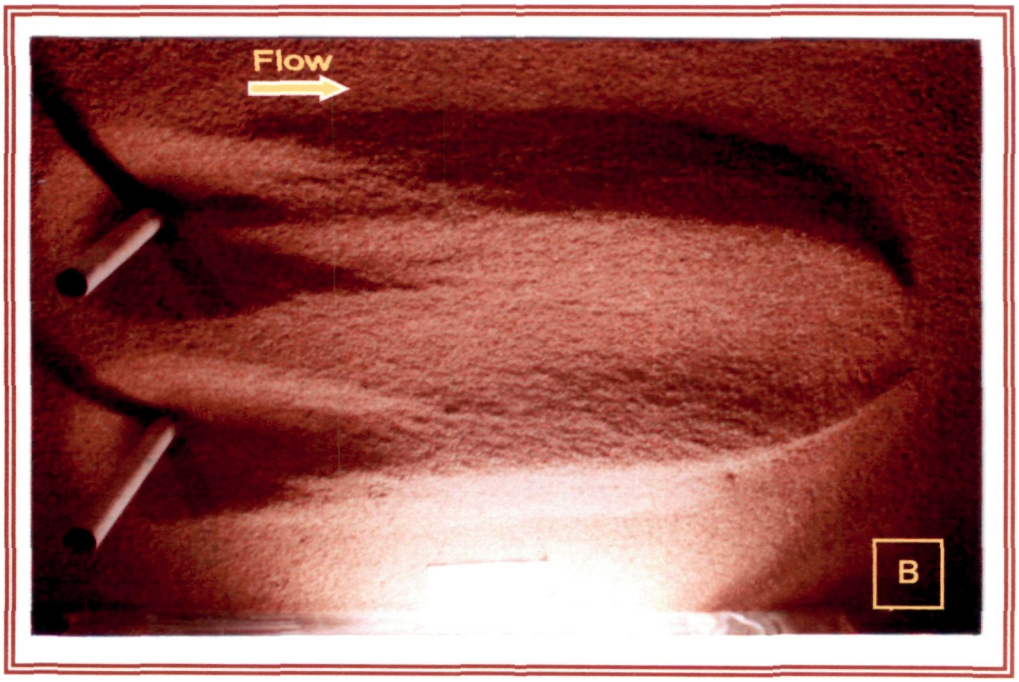

Fig. P8: **Scour and deposition patterns around two piers of same size placed in lateral arrangement at varied lateral pier spacing Z_c/b (A) Z_c/b=0 (B) Z_c/b=7**

here), it is noticed that the rate of scouring at rear pier lacks behind the front pier up-to pier spacing x/b= 30. To ascribe a reason to this happening, it is worth to mention that at short pier spacings, the bed material scoured from the front pier scour hole moves into the scour hole of the rear pier. As a result, flow takes more time to remove the bed material from the rear pier scour hole and the scour depth at the front pier approaches to equilibrium earlier than at the rear pier. Due to sheltering effect of the front pier on the rear pier, the scour depth at the rear pier remains smaller than the scour depth at the front pier. However, at larger pier spacing the bed material from the front pier scour hole does not reach the scour hole of the rear pier and sheltering effect of the front pier also vanishes, the scour depths at the front and the rear piers approaches to equilibrium simultaneously. The scour depth attained for varied pier spacings at a particular time at two piers in tandem arrangement can be obtained by plotting the data on temporal variation of scour depth given in Appendix-I.

5.2.5 Concluding remarks

Comparison of results achieved from present experimental data on two piers in tandem arrangement with those of an isolated pier reveals that the reinforcing and sheltering effects are dominant factors in the local scouring process at two piers in tandem arrangement. The reinforcing effect causes a maximum increase in the local scour depth at the front pier by 17% at x/b=1.5, however at x/b>1.5 it decreases and approaches to the scour depth of an isolated pier at relative pier spacing x/b=90. The sheltering effect of front pier causes a reduction in local scour depth at rear pier up to an extent of 17% at relative pier spacing x/b=0. At pier spacing x/b=12.5, a maximum reduction of 33 % in scour depth at rear pier occurs due to the diminishing state of vortex circulation caused by sheltering effect of front pier. Beyond x/b=12.5, the scour depth at rear pier increases and approaches to the scour of an isolated pier at pier spacing x/b=90. From these findings it can be concluded that the rear pier in tandem arrangement should be placed at x/b=12.5 to achieve economy and safety. Comparison of the scour depths obtained in the present study with those reported by Hannah (1978) reveals that minimum scour depth at front face of rear pier occurs at pier spacing x/b = 12.5 instead of at pier spacing x/b=16. For two piers tandem arrangement, ANN models designed in present study for scour depth prediction produce scour depths very close to the observed values of scour depths.

5.3 Three Piers of Same Size in Tandem Arrangement

5.3.0 Introduction

In order to analyze the results collected from present experimental data on local scour at three piers in tandem arrangement, the longitudinal scour profiles, lateral profile of scour and areal extents of scour are plotted against relative pier spacing *'x/b'*. Longitudinal scour profiles illustrating the scour depths and length of scour holes are shown in Appendix-II. The lateral cross-sections of scour holes at upstream face of front, middle and rear piers are shown in Appendix-III and the areal extents of scour showing scour hole widths around the piers are shown in Appendix-IV. The data on temporal variation of scour depth are given in Appendix-I. Some distinctive cases of longitudinal and areal extents of scour are used for the analysis and discussion in this section. In order to analyze the results, photographs showing the scour and deposition patterns on the bed around the piers were taken at the end of each experiment. Photographs for some typical cases are shown in Fig. P3.

5.3.1 Variation of scour depth along flume length

In order to evaluate the effect of mutual interference among front, middle and rear piers on local scour, present experimental data collected on scour depth around front, middle and rear piers along the center line of flume in flow direction area plotted in longitudinal profiles for varied pier spacing *'x/b'* as shown in Appendix-II. It can be seen in Fig. 5.29 that the longitudinal profiles of scour around front, middle and rear piers are just on the verge of separation from each other as the pier spacing *x/b* approaches to 30, however, the length of longitudinal profile around rear pier remains smaller than those at middle and front ones.

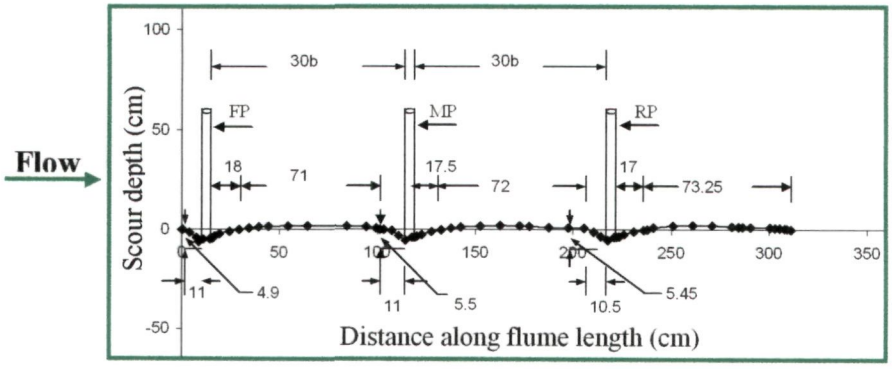

Fig. 5.29 Variation of scour depth at three piers of same size placed in tandem arrangement at *x/b*=30.

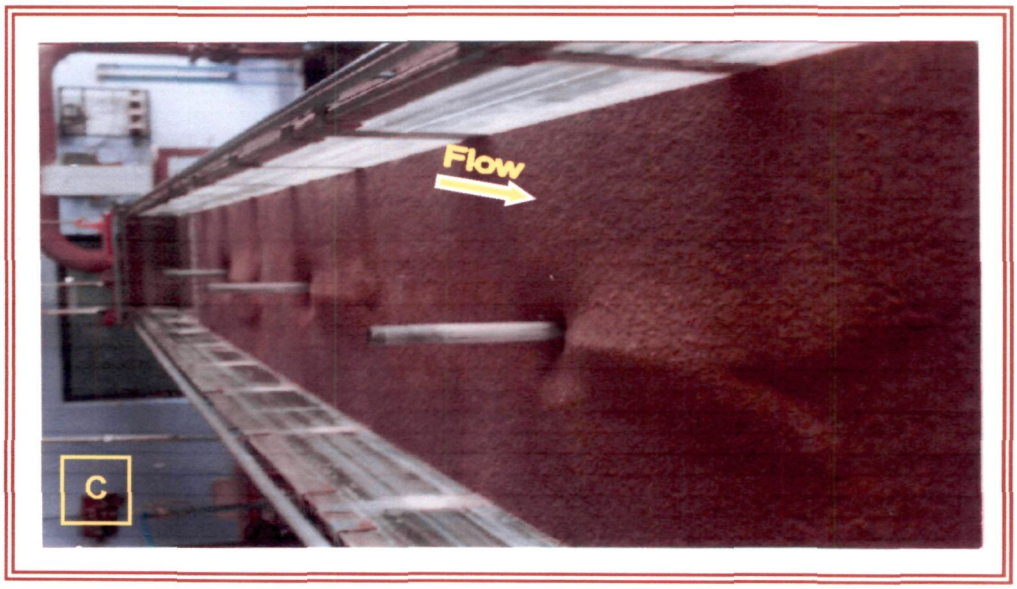

Fig. P3: Scour and deposition patterns around three piers placed in tandem arrangement at varied pier spacings *x/b* (A) *x/b*=10 (B) *x/b*=30 (C) *x/b*=60

Fig.5.30 shows that at larger pier spacing the lengths of the longitudinal profiles around front, middle and rear piers approach to that around an isolated pier which clearly indicates that the three piers start getting freed from the effect of mutual interference.

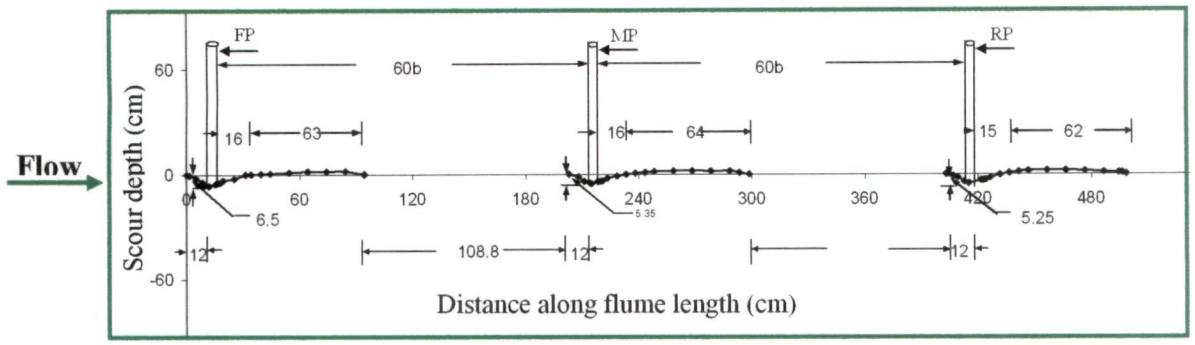

Fig.5.30 Variation of scour depth at three piers of same size placed in tandem arrangement at x/b=60

5.3.2 Scour depth at front, middle and rear piers

The relative scour depths at front, middle and rear piers aligned in tandem arrangement 'ds_f/ds_i, ds_m/ds_i and ds_r/ds_i' are plotted against relative pier spacing 'x/b' as shown in Fig.5.31.

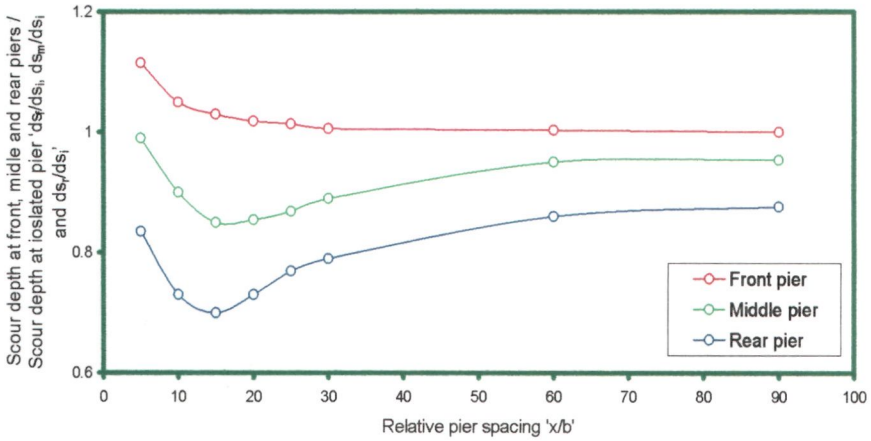

Fig.5.31 Variation of scour depth at front, middle and rear piers placed in tandem arrangement relative to the scour depth of an isolated pier 'ds_f/ds_i, ds_m/ds_i and ds_r/ds_i' with pier spacing 'x/b'(where ds_f=scour depth at front pier, ds_m=scour depth at middle pier, ds_r=scour depth at rear pier and ds_i = scour depth at an isolated pier).

As can be seen, scour depth 'ds_f/ds_i' at front pier increases upto pier spacing x/b=30 due to the reinforcing effect of middle pier. Beyond x/b=30, the reinforcing effect on front pier deceases due to which the scour depth ds_f/ds_i approaches to that of an isolated pier at pier spacing x/b=90. At middle pier, the scour depth 'ds_m/ds_i' remains less than that at an

isolated pier, except at pier spacing x/b=5, where it is less close to the value observed at an isolated pier. The reason for the scour depth being less at middle pier is the sheltering effect of front pier and the sheltering effect of sediment deposited on the bed upstream of middle pier. Maximum sheltering effect at middle pier is reflected from the lowest value of scour depth at pier spacing x/b=15 beyond which the sheltering of middle pier reduces which causes an increase in the scour depth which gradually approaches to that of an isolated pier at pier spacing x/b=90. Fig.5.31 depicts the trend in the variation of scour depth 'ds_r/ds_i' at rear pier with pier spacing 'x/b', which is similar to middle pier with the difference that the magnitudes of the scour depth over the entire range of pier spacing 'x/b' remain smaller than that is observed at middle pier. The occurrence of lower scour depths 'ds_r/ds_i' at rear pier is a result of sheltering of the rear pier caused by the front and middle piers.

5.3.3 Scour depth at middle and rear piers with respect to front pier

The scour depth at middle and rear piers with respect to that at front pier 'ds_m/ds_f' and 'ds_r/ds_f' are plotted against pier spacing 'x/b' as shown in Fig. 5.32.

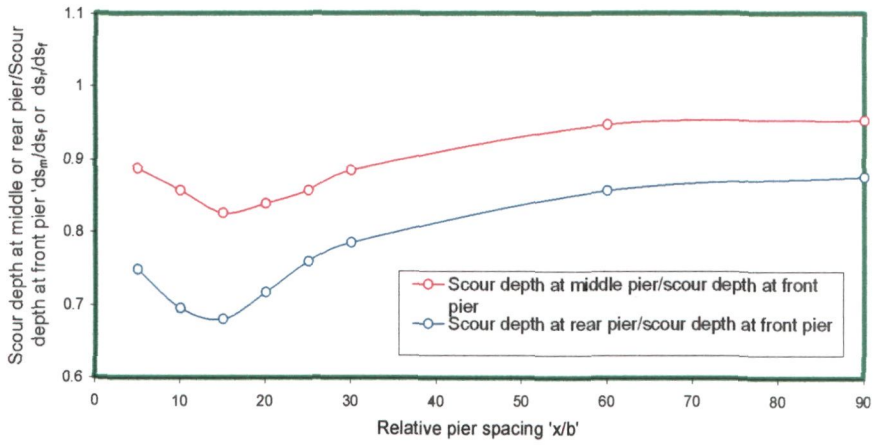

Fig. 5.32 Variation of scour depth at middle and rear pier relative to the scour depth at front pier placed in tandem arrangement 'ds_m/ds_f' and 'ds_r/ds_f' with pier spacing 'x/b' (where ds_f = scour depth at front pier, ds_m = scour depth at middle pier, ds_r = scour depth at rear pier).

The trend in the variation of 'ds_m/ds_f' and 'ds_r/ds_f' with pier spacing 'x/b' as observed in Fig. 5.32 is first decreasing upto pier spacing x/b=15 and then increasing upto pier spacing x/b=90 such that the values of both the ratio remain below unity upto pier spacing x/b=90. The reason for this variation in the ratios 'ds_m/ds_f' and '$ds_r/_{dsf}$' is obviously the same as that for the scour depth variation at three piers discussed in section 5.3.2 of this Chapter.

Comparing the observed scour depth at front pier, it is noticed that the maximum scour depth at front pier is about 11.53% more than that of an isolated pier while the maximum scour depth at middle pier is about 15.47% higher than that at rear pier and about 1.02 % smaller than that of an isolated pier. Similarly the maximum scour depth at rear pier is about 16.5 % smaller than that of an isolated pier and 33.56% smaller than at front pier and less than the middle pier.

Comparison of scour depths observed at middle pier in case of three piers tandem arrangement with the scour depth observed at rear pier in two piers tandem arrangement as given in Table 5.4, illuminates that the scour depth at middle pier is deeper than the scour depth at rear pier for the case of two piers in tandem arrangement. However, the scour depth at rear pier in three piers tandem arrangement is lower than those at rear pier in two piers tandem arrangement. These results are found in good agreement when compared with the results reported by Hannah, 1978 (ref. Chapter II).

Table 5.4 Comparison of scour depths observed at middle pier in three piers tandem arrangement with the scour depths observed at rear pier in two piers tandem arrangement.

Pier spacing *'x/b'*	Scour depth at middle pier of three piers group in tandem arrangement	Scour depth at rear pier of two piers group in tandem arrangement
	ds_{mp}/ds_i	ds_r/ds_i
5	0.99	0.96
10	0.90	0.91
15	0.85	0.69
30	0.89	0.87
60	0.95	0.94

For the estimation of scour depth at front, middle and rear piers placed in tandem arrangement placed at varied pier spacings *x/b*, ANN models the details of which are given in Tables 6.1 and 6.2 (Chapter VI) and ANN architectures Fig.6.24 (Chapter VI), are applied to the present experimental data. The estimated values of scour depth at front, middle and rear piers are plotted against the observed values of scour depth as shown in scatter gram Fig. 6.23 (Chapter VI). Table 6.2 (Chapter VI) gives the values of average correlation coefficient R^2 between observed and ANN estimated scour depths as 0.9906, 0.9930 and 0.9963 for front, middle and rear piers respectively. As given in Table 6.2 (Chapter VI), for the training and testing data sets, average *rmse* values for front, middle

and rear piers are 0.50935×10^{-4}, 0.5885×10^{-4} and 0.5625×10^{-4} respectively. The closeness of the data points to the line of best agreement in scatter grams shown in Fig. 6.23 (Chapter VI), low values of *rmse* and higher values of R^2 given in Table 6.2 (Chapter VI), all, indicate the accuracy of ANN models in predicting the scour depth.

5.3.4 Characteristics of Scour Hole

Since the knowledge of scour hole dimensions is important in determining the extent of countermeasures needed to reduce scour at piers, various parameters explained as under using present experimental data are determined.

(a) Length of scour hole at upstream faces of piers

The length of scour holes at the upstream face of front, middle and rear piers with respect to the length of scour hole observed at upstream face of an isolated pier '$L_{shu(f)}/L_{shu(i)}$', '$L_{shu(m)}/L_{shu(i)}$' *and* '$L_{shu(r)}/L_{shu(i)}$', are plotted against pier spacing '*x/b*' as shown in Fig. 5.33.

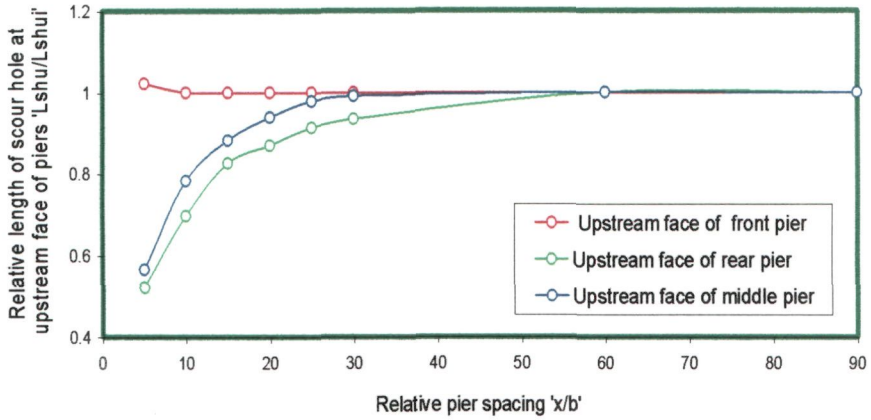

Fig. 5.33 Variation of length of scour holes at upstream faces of front, middle and rear piers placed in tandem arrangement '$L_{shu(f)}/L_{shu(i)}$', '$L_{shu(m)}/L_{shu(i)}$' *and* '$L_{shu(r)}/L_{shu(i)}$' with pier spacing '*x/b*' (where $L_{shu(f)}$ = length of scour hole at upstream face of front pier, $L_{shu(m)}$ = length of scour hole at upstream face of middle pier, $L_{shu(r)}$ = length of scour hole at upstream face of rear pier and $L_{shu(i)}$ = length of scour hole at upstream face of isolated pier).

It is noticed in Fig. 5.33, that the length of scour hole at upstream face of front pier '$L_{shu(f)}/L_{shu(i)}$' is fairly constant over the entire range of pier spacing '*x/b*' which indicates that there is no significant increase in length of scour hole due to reinforcing effect on front pier. The increase in length of scour hole on upstream face of middle pier '$L_{shu(m)}/L_{shu(i)}$' with an increase in pier spacing upto x/b=60, indicates reduction in the

sheltering effect caused by the front pier on middle pier. The increasing trend in the scour hole length at upstream face of rear pier '$L_{shu(r)}/L_{shu(i)}$' upto pier spacing x/b=60, infers to the reduction in the effect of sheltering offered by the middle and front piers on rear pier. However, between pier spacing x/b=60 to 90, the unvarying length of scour hole indicates the disappearance of the sheltering effect on middle and rear piers.

(b) Length of scour hole at downstream face of piers

The ratio of the lengths of scour hole at downstream face of front, middle and rear piers with respect to the length of scour hole observed at downstream face of an isolated pier '$L_{shd(f)}/L_{shd(i)}$', '$L_{shd(m)}/L_{shd(i)}$' *and* '$L_{shd(r)}/L_{shd(i)}$' are plotted against pier spacing 'x/b' as shown in Fig.5.34.

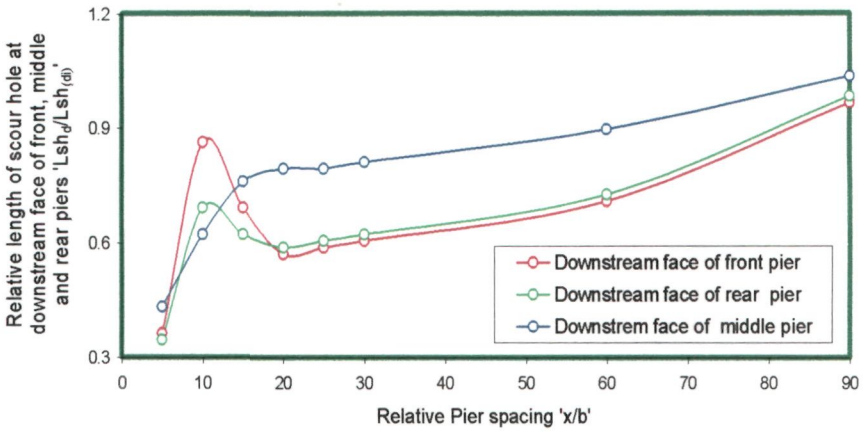

Fig. 5.34 Variation of relative length of scour hole at downstream faces of front, middle and rear piers placed in tandem arrangement '$L_{shd(f)}/L_{shd(i)}$', '$L_{shd(m)}/L_{shd(i)}$' *and* '$L_{shd(r)}/L_{shd(i)}$' with pier spacing 'x/b'(where $L_{shf\,(d)}$ = length of scour hole at downstream face of front pier, $L_{shm(d)}$= length of scour hole at downstream face of middle pier, $L_{shr(d)}$= length of scour hole at downstream face of rear pier and $L_{sh(di)}$ = length of scour hole downstream at face of isolated pier).

An increasing trend in the length of scour holes at downstream face of front and middle piers '$L_{shd(f)}/L_{shd(i)}$', '$L_{shd(m)}/L_{shd(i)}$' is noticed upto pier spacing x/b=10. The reason for this trend is ascribed to high turbulence between front and middle, and middle and rear piers generated due to strong interaction of the piers with the flow approaching to the middle and rear piers and with the sediment bed, due to which deposition of sediment does not occur on the bed at upstream face of middle and rear piers and one brim is observed to form between front and middle piers and the other between middle and rear piers such that the level of this brim remains below the original sediment bed level upto pier spacing

x/b=10. In addition to this, the wake vortices originating from front pier enhance the strength of horseshoe vortex of middle and rear piers. As a result, the strength of wake vortices originating from middle and rear piers increases which in turn causes the length of scour hole at downstream face of front and middle piers to increase upto pier spacing x/b=10. As the pier spacing 'x/b' exceeds from 10, the level of turbulence in the flow approaching to the middle and rear piers decreases as a result of which the deposition of sediment on the bed on upstream of middle pier begins due to which the level of the above mentioned brim between front and rear piers increases. Consequently, slope of the scour hole increases. As a result, the length of scour hole on downstream of front pier decreases and reaches to a minimum at x/b=20. With further increase in pier spacing 'x/b', the bed material deposited on the bed upstream of middle pier gets transported by the approaching flow and slips down into the middle pier scour hole causing a decrease in the level of the brim at upstream of middle pier scour hole and hence a decrease in the slope of the corresponding scour hole. As a result, the length of scour hole at downstream face of front pier increases and reaches to that what is observed at an isolated pier at x/b=90.

Furthermore, Fig. 5.34 reveals that the curves for front and middle piers are very close to each other. This closeness in the values of length of scour holes at downstream face of front and middle piers indicates intense interaction of flow with the wake vortices between front and middle pier and between middle and rear piers as compared to the rear pier which is free from any obstruction interacting with the flow on its downstream.

It is also observed that the length of scour hole at downstream face of rear pier '$L_{shd(r)}/L_{shd(i)}$' increases with an increase in pier spacing 'x/b'. This increase is ascribed to the flow pattern around the rear pier. As compared to front and rear piers, where the interaction of flow with piers causes back flow, which offers a resistance to flow, no back flow occurs at downstream face of rear pier

(c) Slope of scour holes

(i) Slope of scour hole at upstream face of piers

The slope of scour holes along the flow direction at the upstream face of front, middle and rear piers '$S_{lfu(f)}/S_{lu(i)}$, $S_{lfu(m)}/S_{lu(i)}$' and '$S_{lu(r)}/S_{lu(i)}$' are plotted against pier spacing 'x/b' as shown in Fig. 5.35. As evident from Fig. 5.35, a decrease in front pier scour hole slope

'$S_{lfu(f)}/S_{lu(i)}$', is observed upto pier spacing x/b=30. The reason for this decrease in slope is the decrease in the scour depth caused due to the reduction in the reinforcing effect on front pier. At pier spacing 0>x/b>30, the slope remains fairly constant and is nearly equal to that of an isolated pier at pier spacing x/b=90. The upstream slope observed for front pier scour hole is nearly equal to the angle of repose of the bed material (*i.e.*, 32°).

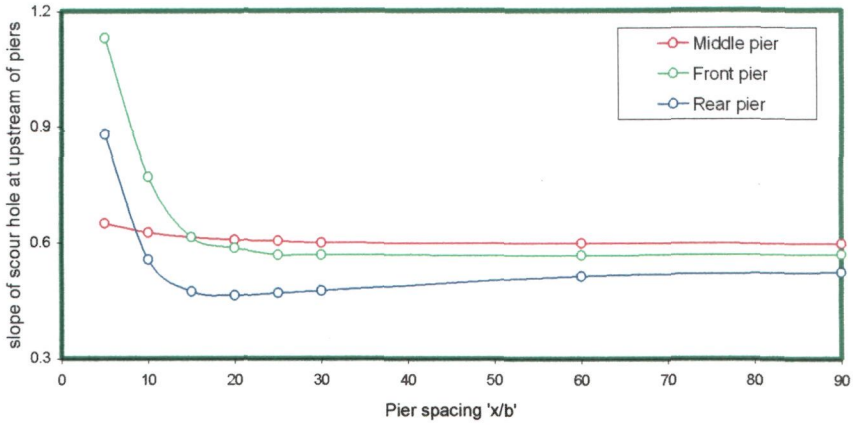

Fig. 5.35 Variation of scour hole slope at upstream faces of front, middle and rear piers placed in tandem arrangement '$s_{ld(f)}/s_{ld(i)}$, $s_{ld(m)}/s_{ld(i)}$ and $s_{ld(r)}/s_{ld(i)}$' with pier spacing 'x/b'(where $S_{lfu(f)}/S_{lu(i)}$= slope of scour hole at upstream face of front pier, $S_{lfu(f)}/S_{lu(i)}$ = slope of scour hole at upstream face of middle pier, $S_{lu(r)}/S_{lu(i)}$ = slope of scour hole at upstream face of rear pier and $S_{lu(i)}$ = slope of scour hole at upstream face of an isolated pier).

The slope of scour hole at upstream face of middle pier $S_{lfu(m)}/S_{lu(i)}$ decreases upto pier spacing x/b= 25 and then remains invariable beyond this pier spacing. The flow pattern between middle and rear piers generated by the interaction of piers and sediment bed with the flow approaching to the piers are responsible for this decrease in scour hole slope. Beyond pier spacing x/b=25, the flow pattern is insignificantly affected by the mutual interaction of piers and thus the slope remains fairly constant upto pier spacing x/b=90.

The slope of scour hole at upstream face of rear pier $S_{lu(r)}/S_{lu(i)}$ decreases upto pier spacing x/b=20. The decrease in scour depth and an increase in scour hole length on upstream face of rear pier resulted from interaction of approaching flow with the middle and the rear piers, is the reason for this decrease in upstream slope of rear pier scour hole. As the scour depth and scour hole length variation remains fairly constant beyond pier spacing 20, the associated upstream slope of rear pier scour hole remains constant upto pier spacing x/b=90.

(ii) Slope of scour hole at downstream face of piers

The slope of scour holes at downstream face of front, middle and rear piers '$S_{ld(f)}/S_{ld(i)}$, $S_{ld(m)}/S_{ld(i)}$ and $S_{ld(r)}/S_{ld(i)}$' are plotted against pier spacing as shown in Fig. 5.36.

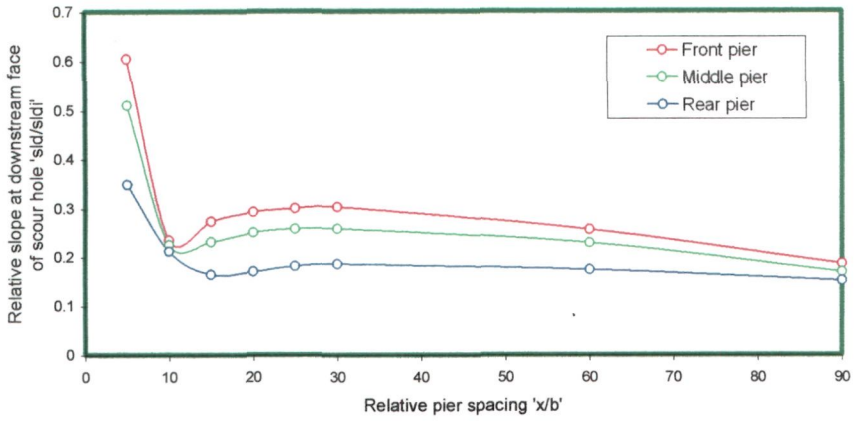

Fig. 5.36 Variation of scour hole slope at downstream faces of front, middle and rear piers placed in tandem arrangement '$S_{ld(f)}/S_{ld(i)}$,, $S_{ld(m)}/S_{ld(i)}$ and $S_{ld(r)}/S_{ld(i)}$' with pier spacing '*x/b*'(where $S_{lf(u)}$ = slope of scour hole at downstream face of front pier, $S_{lm(u)}$ = slope of scour hole at downstream face of middle pier, $S_{lr(u)}$ = slope of scour hole at downstream face of rear pier and $S_{l(ui)}$ = slope of scour hole at downstream face of an isolated pier).

Similar trend is observed in the variation of scour hole slope at downstream faces front, middle and rear piers. The slope at downstream face of the three piers decreases upto pier spacing *x/b*=10 and then increases upto pier spacing *x/b*=30 and again decreases and reaches to a minimum at pier spacing *x/b*=90. To identify with this variation, refer Fig. 5.34 where a steep increase in the length of scour hole at downstream face of three piers is observed. Fig. 5.34 depicts a decrease in the length of scour hole beyond pier spacing *x/b*=10 while the slope of scour hole at downstream face of three piers marginally varies upto pier spacing *x/b*=30. As a result, an increase in the slope of the scour holes is observed in Fig.5.36. For pier spacings *x/b* > 30, an increase in the length of scour holes as observed in Fig. 5.34 and marginal increase in scour depth at downstream face of three piers as observed in Fig 5.37 causes a decrease in slope of scour holes at downstream face of front, middle and rear piers.

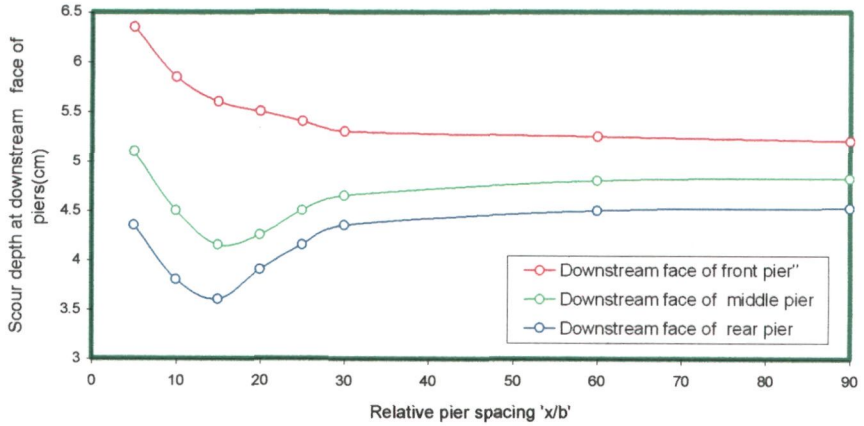

Fig. 5.37 Variation of scour depth at downstream faces of front, middle and rear piers placed in tandem arrangement with pier spacing '*x/b*'(cm).

(iii) Variation of area of scour extent around front, middle and rear piers with pier spacing

The areal extents of scour around front, middle and rear piers are plotted for varied pier spacing '*x*/*b*' as shown in Appendix-IV. The areal extents of scour shown around three piers in Fig. 5.38 overlap each other at pier spacings *x*/*b*<30 and are just on the verge of separation from each other as the pier spacing *x*/*b* approaches to 30.

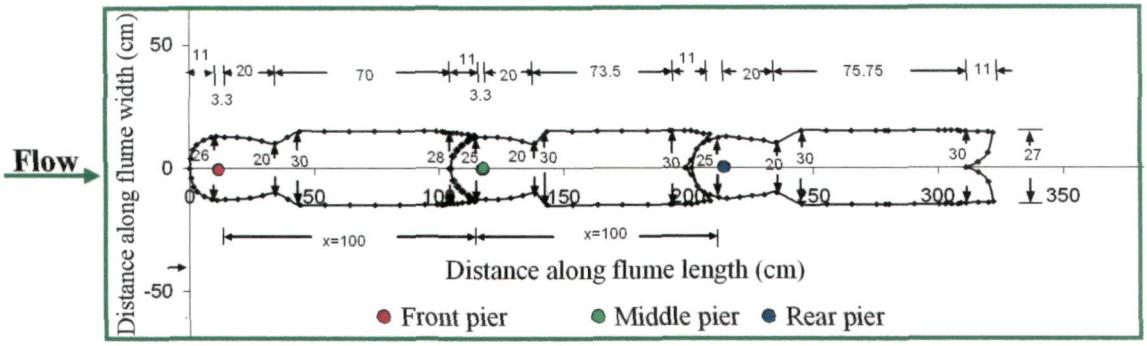

Fig.5.38 Areal extant of scour around three piers placed in tandem arrangement at *x*/*b*=30

At pier spacing *x*/*b*=60, Fig. 5.39 shows that the shape and size of the areal extents of scour around front, middle and rear piers become considerably similar to that around a single pier which indicates that the three piers become free from the effects of mutual interference.

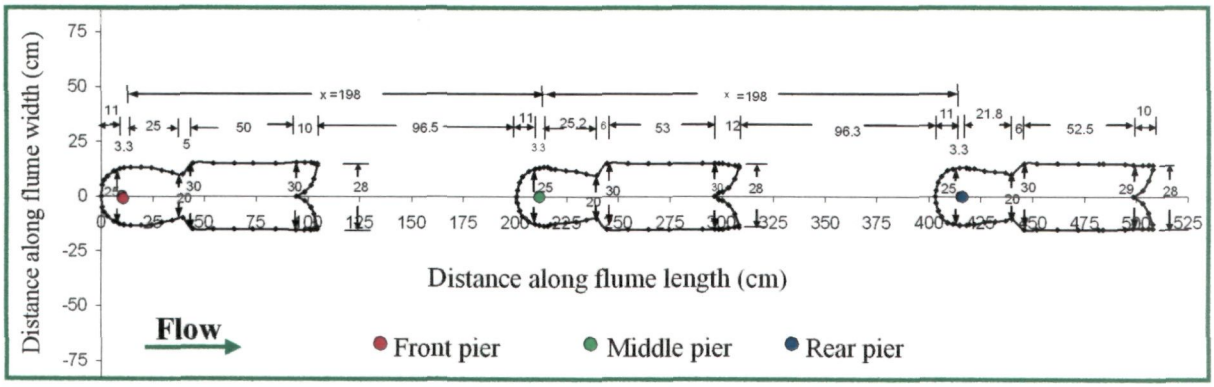

Fig. 5.39 Areal extant of scour around three piers placed in tandem arrangement at *x*/*b*=60

The areas of scour extent for various pier spacings relative to that of an isolated pier are computed and plotted against pier spacing '*x*/*b*' as shown in Fig.5.40. The relative area of scour extent decreases with pier spacing and reaches to a minimum at pier spacing *x*/*b*=15. The reason for this decrease is the generation of flow pattern by the strong interaction of flow with piers and the sediment bed between the piers.

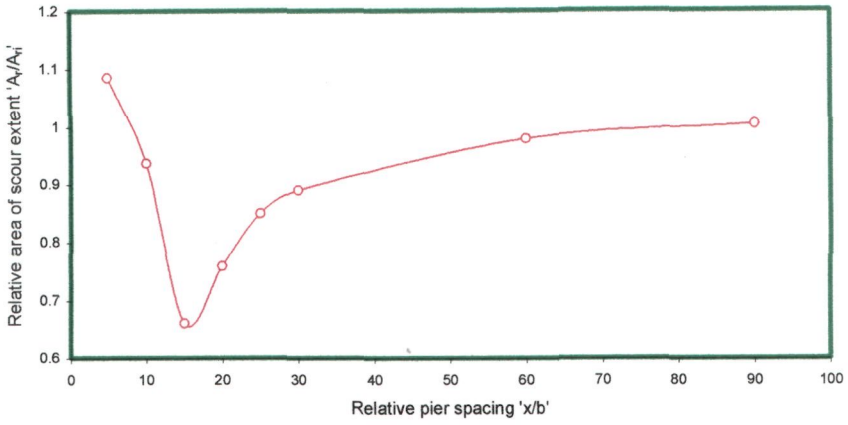

Fig. 5.40 Variation of area of scour extent around three piers placed in tandem arrangement relative to the area of scour extent at an isolated pier 'A_r/A_{ri}' with pier spacing 'x/b'(where A_r = area of extent of scour around three piers, A_{ri} = area of extent of scour around isolated pier)

However, as the pier spacing 'x/b' increases beyond 15, the flow pattern changes around the piers and the area of scour extent increases. At pier spacing x/b=90, the area of scour extent around front, middle and rear piers approaches nearly to that of an isolated pier. Fig. P3 shows the scour and deposition features developed on the bed around the front, middle and rear piers.

(iv) Width of scour holes

In order to analyze the width of scour holes, the lateral profiles of scour are drawn at upstream face of front, middle and rear piers across the flume for varying pier spacings x/b and are shown in Appendix-III. The widths of scour holes at upstream face of front, middle and rear piers relative to scour hole width of an isolated pier; 'w_1/w_i', 'w_2/w_i', and 'w_3/w_i' respectively, are plotted against pier spacing 'x/b' and are shown in Fig 5.41.

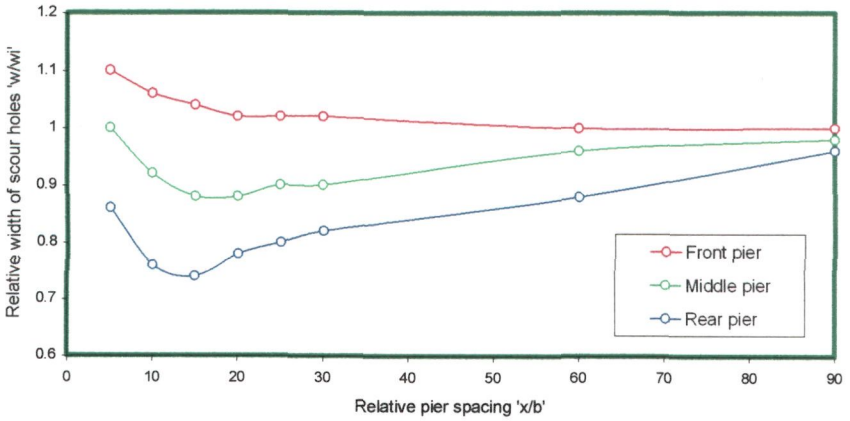

Fig. 5.41 Spacing versus relative scour hole width 'w_1/w_i', 'w_2/w_i' and 'w_3/w_i' at front, middle and rear piers placed in tandem arrangement (where w_1, w_2 and w_3 = width of scour hole of front, middle and rear piers, w_i = width of isolated pier).

A similarity in Fig.5.31 and Fig. 5.41 is indicative of dependence of scour hole width on the scour depth at three piers.

The width of front pier scour hole w_1/w_i decreases upto pier spacing x/b=30. This decrement is caused due to decrement in the scour depth owing to reduction in the reinforcing effect on front pier. At pier spacing x/b>30, the reinforcing effect diminishes, consequent upon which scour depth becomes constant and the width of scour hole becomes invariable.

For middle and rear piers, Fig.5.41 shows a decrease in the widths of scour hole upto pier spacing x/b=15 due to a decrement in scour depth caused by sheltering effect of front pier on middle pier and of middle pier on rear pier. Beyond this pier spacing, Fig. 5.41 shows an increase in the widths of scour hole 'w_2/w_i' and 'w_3/w_i' which corresponds to an increase in scour depth due to diminishing state of all effects.

(v) Length of deposition on downstream of front, middle and rear piers

The lengths of sediment deposition occurring at downstream face of front, middle and rear piers are labeled on longitudinal profiles of scour Appendix-II. The length of sediment deposition at downstream of three piers relative to that observed at downstream face of an isolated pier, '$L_{dep}/L_{dep\ (i)}$' are plotted against pier spacing 'x/b' as shown in Fig. 5.42.

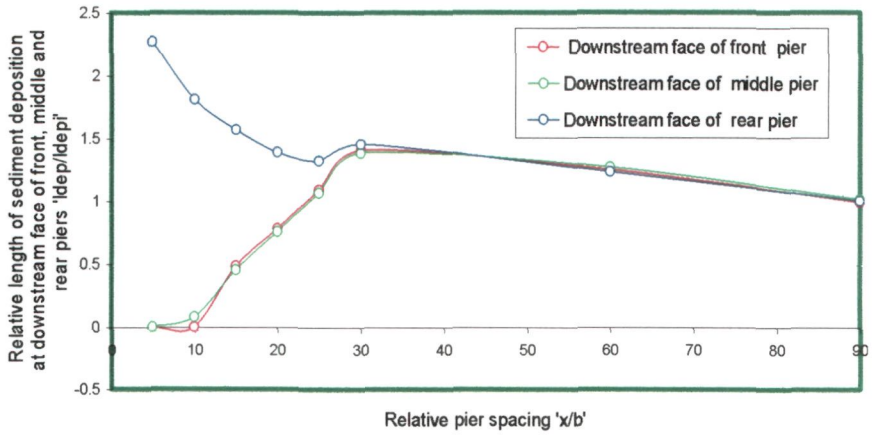

Fig.5.42 Variation of relative depth of deposition at downstream faces of front, middle and rear piers placed in tandem arrangement '$L_{dep(f)}/L_{dep(i)}$,, $L_{dep(m)}/L_{dep(i)}$ and $L_{dep(r)}/L_{dep(i)}$' with pier spacing 'x/b'(where $L_{dep(f)}$= length of sediment deposition at downstream face of front pier, $L_{dep(m)}$ = length of sediment deposition at downstream face of middle pie $L_{dep(r)}$ = length of sediment deposition at downstream face of rear pier and $L_{dep(i)}$ = length of sediment deposition at downstream face of isolated pier).

It is noteworthy that the variation in the length of sediment deposition occurring at downstream faces of front and middle piers '$L_{dep(f)}/ L_{dep(i)}$', and '$L_{dep(m)}/ L_{dep(i)}$' is identical. This is due to the sediment deposition affected between front and middle and middle and rear piers caused by the interaction of approaching flow with the vortices generated around the front and middle piers. However, as no pier exists on downstream of rear pier, it is free from such interaction. Fig. 5.42 shows an increase in length of deposition on downstream of front and middle piers '$L_{dep(f)}/L_{dep(i)}$' and '$L_{dep(m)}/L_{dep(i)}$' upto pier spacing x/b=30. Thereafter, it decreases and approaches to that of an isolated pier. Moreover, the length of deposition at the downstream face of rear pier '$L_{dep(r)}/L_{dep(i)}$' decreases up-to pier spacing x/b=25. This is because of the fact that at shorter pier spacing (*i.e.*, $x/b \leq 10$), the entire bed material scoured from the scour holes of three piers and transported by the wake vortices gets deposited on downstream of rear pier and no deposition of sediment occurs on downstream of front pier which is evident from Fig. 5.42. However, at pier spacing $10 < x/b \leq 25$, some of the bed material scoured from the scour holes of front and middle piers deposits on their downstream side while rest of the bed material deposits on downstream of rear pier. At pier spacing $x/b > 25$, the length of sediment deposition occurring on downstream of rear pier follows the same variation as observed for front and middle piers which indicates that the flow pattern at three piers becomes identical beyond pier spacing $x/b > 25$. At pier spacing $x/b = 90$, the length of sediment deposition occurring on downstream of rear pier is nearly equal to that of an isolated pier.

The photographs shown in Fig.P3 visibly reveal the scour characteristics which are analyzed and discussed above.

5.3.5 Temporal variation of scour depth at front, middle and rear piers

Appendix-I gives the data collected in present study on temporal variation of scour depth at front, middle and rear piers placed in tandem arrangement. The plots of these data (not shown here) reveal that middle and rear piers slowest follow the rate of scouring at rear pier respectively. The sheltering effect of front and middle piers and transport of bed material scoured from front and middle pier scour holes into the rear pier scour hole causes this slowest rate of scouring at rear pier. At larger pier spacings, the piers get relieved from the sheltering effect and the bed material scoured from front and middle piers does not reach to the rear pier scour hole as a result of which the scour depth approaches to equilibrium simultaneously at front, middle and rear piers. The scour depth attained for varied pier

spacings at a particular time at three piers in tandem arrangement can be obtained by plotting the data on temporal variation of scour depth given in Appendix-I.

5.3.6 Concluding remarks

The maximum scour depth observed at front pier, is about 11.53% deeper than that of an isolated pier while the maximum scour depth at middle pier is about 1.02 % shallower than that of an isolated pier and about 15.47% deeper than that at rear pier. Similarly, the maximum scour depth at rear pier is less than at middle pier, about 16.5 % shallower than that of an isolated pier and 33.56% shallower than at front pier. As the scour depths at middle and rear piers are lowest at pier spacing x/b=15 and also the scour depth at front pier is very close to that of an isolated pier, it can be suggested that in the case of three piers tandem arrangement the middle pier be placed at clear pier spacing x/b=15 from front and rear piers.

5.4 Big Pier at Front and Small Pier at Rear (*i.e.*, 66 mm pier at Front and 33 mm Pier at Rear)

5.4.0 Introduction

In order to analyze the results obtained from present experiments for local scour at two piers [66 mm diameter pier (*i.e.*, big pier) at front and 33 mm diameter (*i.e.*,, small pier)] at rear in tandem arrangement, the longitudinal profiles of scour, lateral profile of scour and areal extents of scour, are plotted against relative pier spacing *'x/b'*. Longitudinal scour profiles illustrating the scour depths and length of scour holes are shown in Appendix-II. The lateral cross-sections of scour holes are shown in Appendix-III and the areal extents of scour showing scour hole widths at the piers are shown in Appendix-IV. Some typical cases of longitudinal and areal extent of scour are used for analysis and discussion in this section. The temporal variation of scour depth is given in Appendix-I. In order to enlighten the scour characteristics around 66 mm front and 33 mm rear piers for varied pier spacings, the photographs showing the scour and deposition patterns around 66 mm front and 33 mm rear piers were taken at the end of each experiment and shown in Fig. P4 & P5. The analysis of results achieved from present experiments is presented as under:

5.4.1 Variation of scour depth along flume length

To explore the effect of mutual interference of two piers of unequal sizes, *e.g.*, 66 mm pier (big pier) at front and 33 mm pier (small pier) at rear in tandem arrangement on local scour,

longitudinal profiles of scour are plotted through 66 mm front and 33 mm rear piers along center line of flume in flow direction using the data on scour depth collected in present study as shown in Appendix-II. It is noticeable in Fig. 5.43 that the longitudinal profiles of scour around 66 mm front and 33 mm rear piers overlie each other upto x/b=70. However, due to non approachment of bed material scoured from 66 mm front pier scour hole to the 33 mm rear pier scour hole, longitudinal profiles around 66 mm front and 33 mm rear piers start separating from each other at pier spacing x/b=70 which indicates that the two piers start getting freed from the effect of mutual interference.

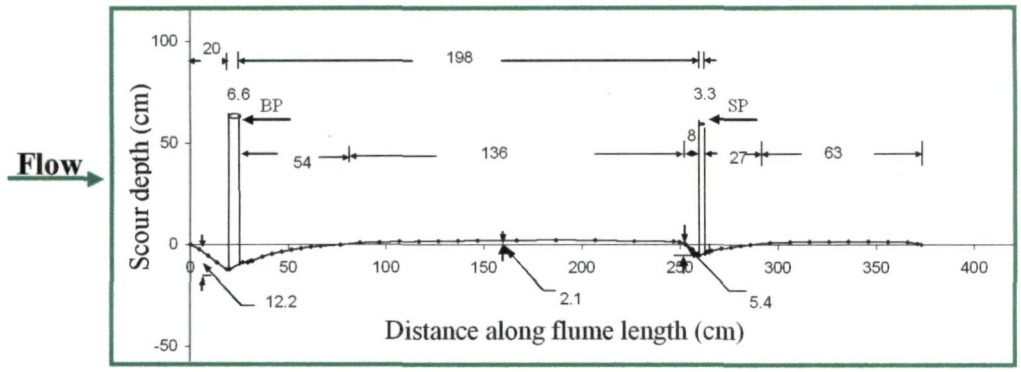

Fig.5.43 Variation of scour depth along flume length at 66 mm front and 33 mm rear piers placed in tandem arrangement at x/b=70

However, at pier spacing x/b>70, Fig. 5.44 the longitudinal profiles of 66 mm front and 33 mm rear piers become identical to that around 66 mm and 33 mm isolated piers respectively indicating that the two piers being freed completely from mutual interference.

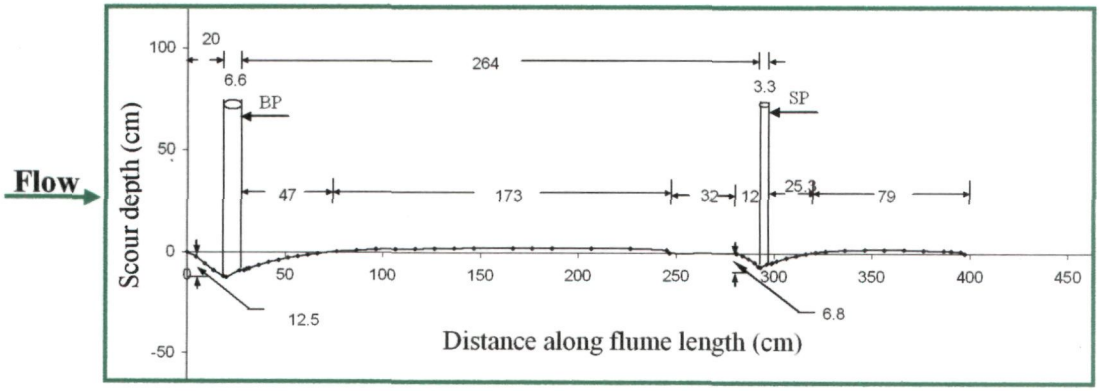

Fig. 5.44 Variation of scour depth along flume length at 66 mm front and 33 mm rear piers placed in tandem arrangement at x/b=80

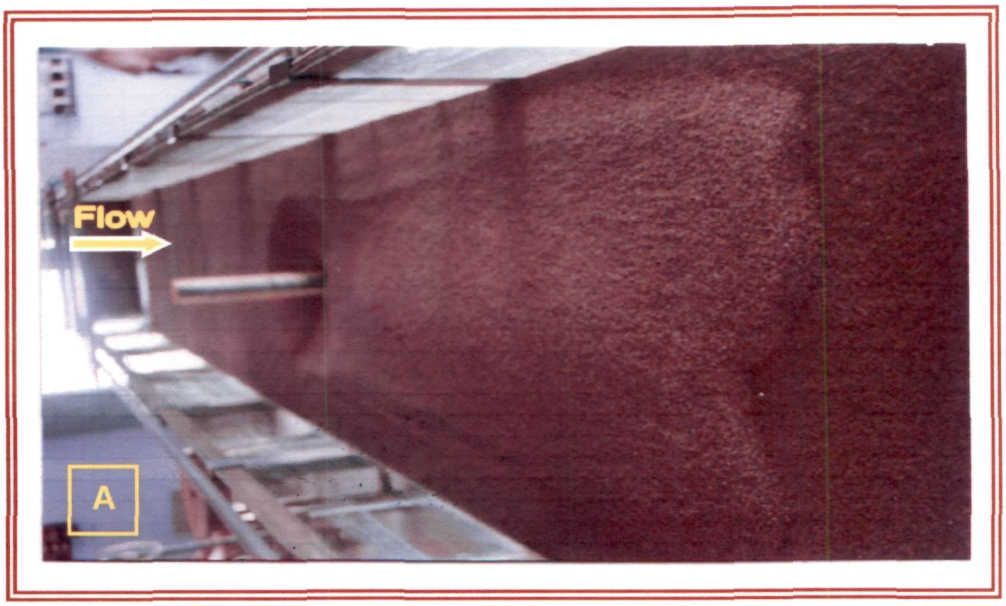

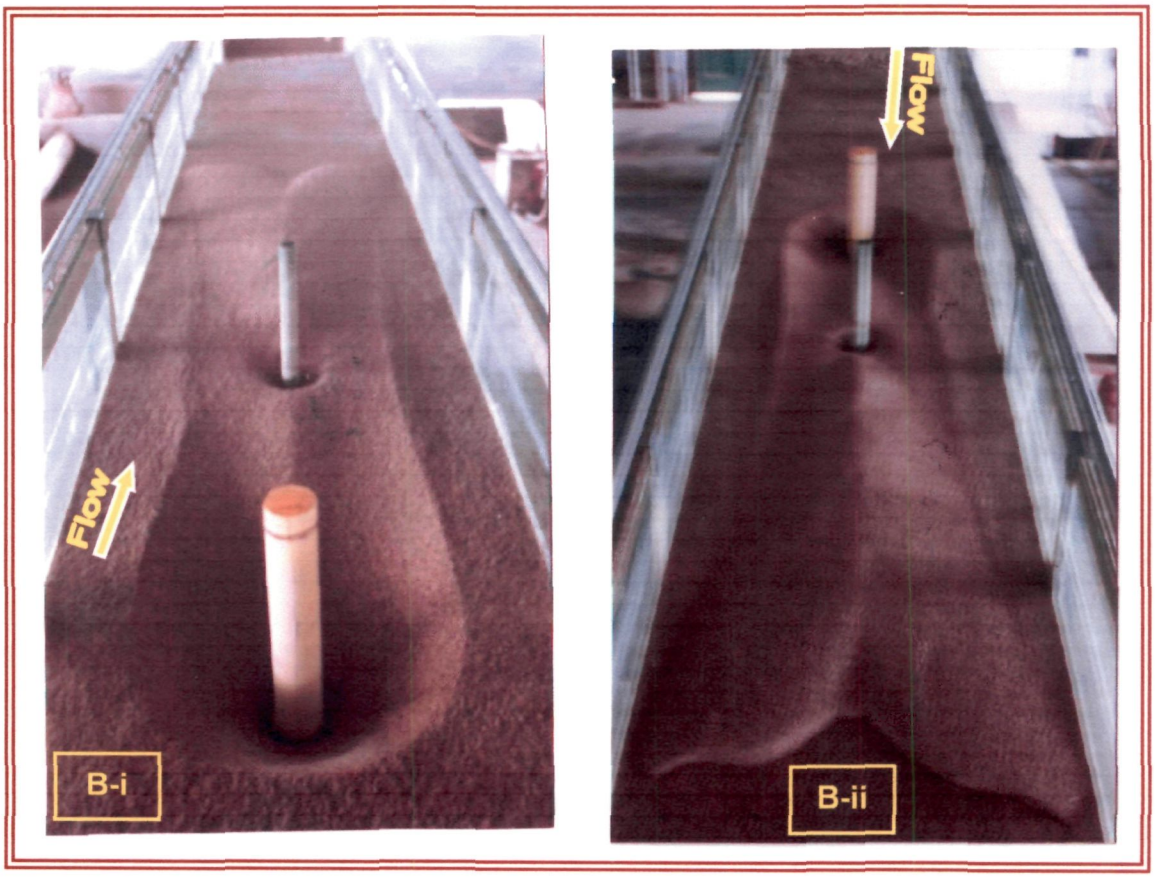

Fig. P4: Scour and deposition patterns around two piers (big pier at front and small pier at rear) placed in tandem arrangement at varied pier spacings *x/b* (A) *x/b*=0 (B) [i & ii] *x/b*=22

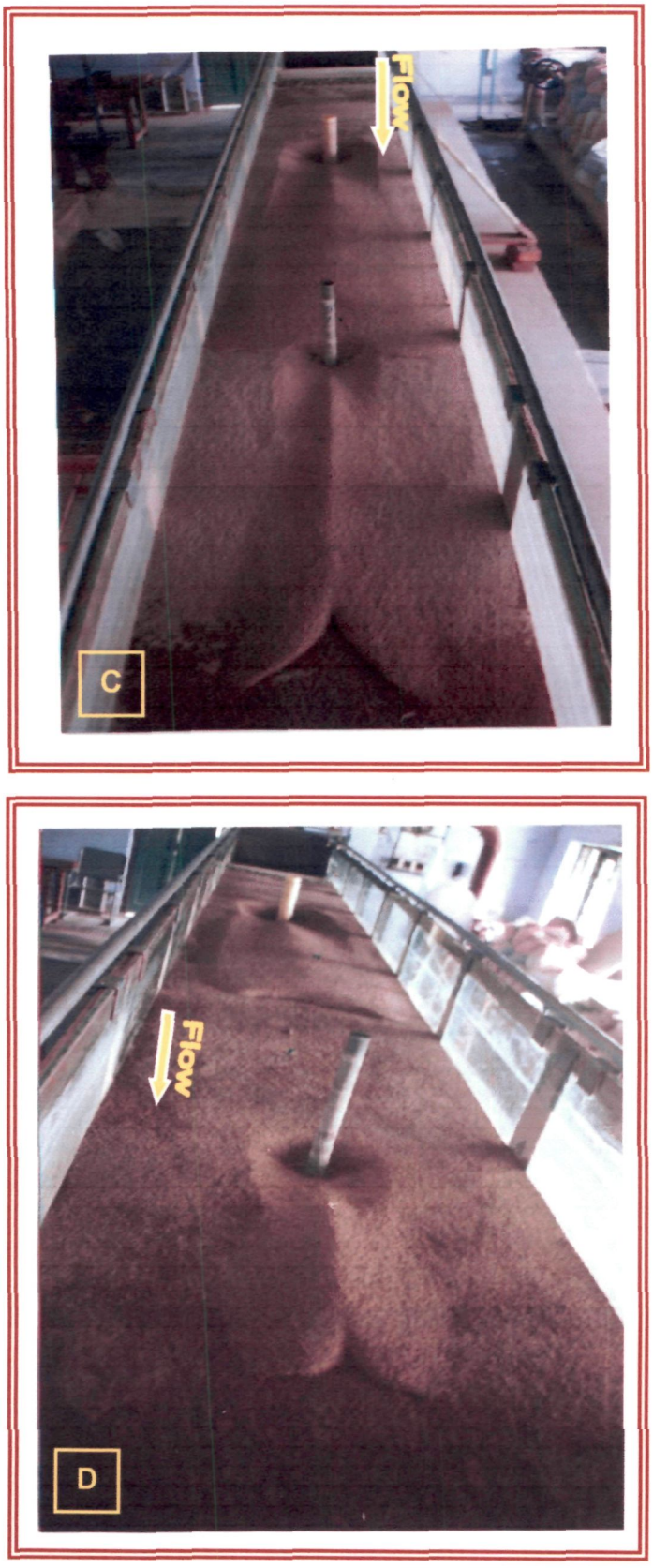

Fig. P5: Scour and deposition patterns around two piers (big pier at front and small pier at rear) placed in tandem arrangement at varied pier spacings *x/b* (C) *x/b*=70 (D) *x/b*=90

(a) Scour depth variation at 66 mm front pier

The variation of relative scour depths at 66 mm front and 33 mm rear piers as compared to that at 66 mm isolated pier *i.e.*, *'dsB/dsB(i)'* and *'dsb/dsB(i)'* with pier spacing *x/b* is shown in Fig. 5.45. It is noteworthy that the scour depths at 66 mm front and 33 mm rear piers at pier spacing *x/b*=0, are about 97 % and 78.5% of the scour depth at 66 mm isolated pier respectively. With an increase in pier spacing, the scour depth at 66 mm pier also increases and reaches to a maximum value (1.08 times the scour depth at an isolated pier) at *x/b*= 10. Further, at *x/b*>10, the scour depth decreases and approaches to that of 66 mm isolated pier at *x/b* = 90. The scour and deposition patterns around 66 mm diameter isolated pier are shown in Fig. PI.

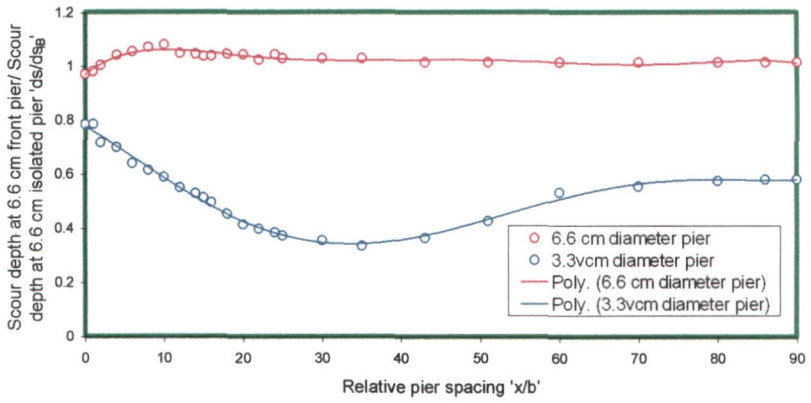

Fig. 5.45 Variation of relative scour depth at 66 mm front and 33 mm rear piers *'$ds_B/ds_{B(i)}$'* and *'$ds_b/ds_{B(i)}$'* placed in tandem arrangement with pier spacing *'x/b'* (where ds_B = scour depth at 66 mm front pier, ds_b = scour depth at 33 mm rear pier, $ds_{B(i)}$ = scour depth at 66 mm diameter isolated pier).

The scour depths at nose of 66 mm front pier *'ds_B'* and 33 mm rear pier *'ds_b'* relative to the corresponding quantity for an isolated pier *'$ds_{b(i)}$'* have been plotted against relative pier spacing *'x/b'* as shown in Fig 5.46, where, *'x'* is the clear spacing between 66 mm front and 33 mm rear piers along the flume length and *'b'* is the diameter of rear pier.

Fig. 5.46 illustrates that the scour depth at 66 mm front pier at pier spacing *x/b*=0, is 1.67 times of scour depth at 33 mm isolated pier *'$ds_{b(i)}$'*. With an increase in pier spacing, the scour depth at 66 mm pier also increases and reaches to a maximum value (1.86 times the scour depth at 33 mm isolated pier) at *x/b*= 10. Further, at *x/b*>10, the scour depth decreases and approaches to that of 66 mm isolated pier at *x/b* = 90.

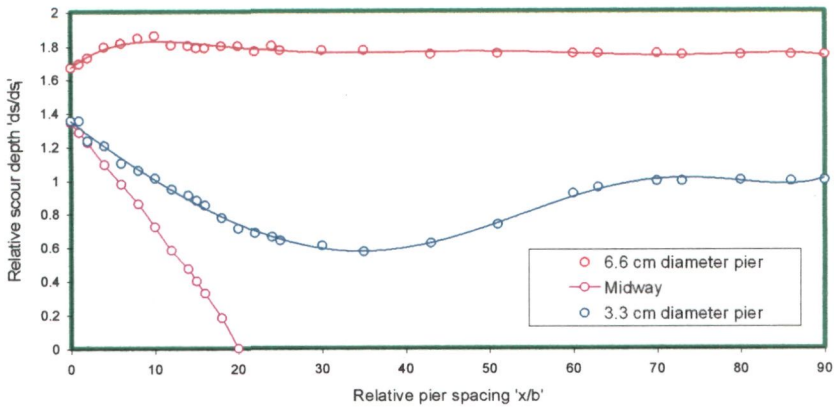

Fig. 5.46 Variation of relative scour depth at 66 mm front and 33 mm rear piers '$ds_B/ds_{b(i)}$' and '$ds_b/ds_{b(i)}$' placed in tandem arrangement with pier spacing 'x/b' (where ds_B = scour depth at 66 mm front pier, ds_b = scour depth at 33 mm rear pier, $ds_{b(i)}$ = scour depth at 33 mm diameter isolated pier).

In experiments on 66 mm isolated pier, the bed material was observed to be continuously lifting from the base of the scour hole by the flow, but the flow was not capable of removing this material from the scour hole. However, when 33 mm diameter pier was placed at the downstream of 66 mm diameter pier at short spacing, 66 mm front pier experienced reinforcing effect due to the presence of 33 mm rear pier and the scour holes around both piers overlapped each other and caused the lowering of the bed level at the rear side of 66 mm front pier. This lowering of bed resulted in an ease for flow to remove the continuously lifting sediment particles from 66 mm front pier scour hole and the scour hole around 66 mm front pier increased in depth as compared to the scour depth around 66 mm isolated pier.

At pier spacing $0<x/b\leq10$, the increase in scour depth at 66 mm front pier is attributed to the reinforcing effect at 66 mm front pier due to the presence of the 33 mm rear pier. As shown in Fig. 5.46, the scour depth at 66 mm front pier is maximum at x/b=10 which indicates that the reinforcing effect is maximum at x/b=10 beyond which, the gradual reduction in scour depth points towards the reduction in the reinforcing effect. At pier spacing x/b=90, the reinforcing effect at 66 mm front pier almost disappeared and the scour depth approached to that of 66 mm isolated pier.

The maxima at x/b=10, can be explained by the fact that at short pier spacing x/b, 33 mm rear pier overlaps and reduces the height of the exit slope of the scour hole around the 66

mm front pier consequently, 33 mm rear pier increases the vortex rotation around 66 mm front pier in the form of forward interference.

(b) Scour depth variation at 33 mm rear pier

Fig 5.46 illustrates the dependence of scour depth at 33 mm rear pier with varying pier spacing *x/b*. At *x/b* = 0, the scour depth is 1.353 times the scour depth at 33 mm isolated pier. As *x/b* increases, scour depth decreases and reaches to a minimum (*i.e.*, 0.57 times the scour depth at 33 mm isolated pier at *x/b*=35. This reduction in scour depth is attributed first, to the shielding of 33 mm rear pier by 66 mm front due to which a reduction in the approach flow velocity for 33 mm rear pier is caused, as a result of which the strength of horseshoe vortex and scour depth at 33 mm rear pier gets reduced and second, to the deflection of flow caused by the bed material, which gets scoured from around 66 mm front pier and deposits at the upstream face of 33 mm rear pier. The vortices shedding from 66 mm front pier strike at the 33 mm rear pier reinforces the strength of the horseshoe vortex at the base of 33 mm rear pier and results in an increase in the scour depth.

At pier spacing *x/b*>35, the scour depth at 33 mm rear increases and reaches to that of an isolated 33 mm pier at *x/b*=90. This increment in scour depth is ascribed to the effect of shed vortices approaching from 66 mm front pier, which strike the 33 mm rear pier. The striking action of these vortices reinforces the strength of horseshoe vortex at 33 mm rear pier and results in increased scour depths.

At pier spacing *x/b*>35, the sheltering and vortex shedding effects from 66 mm front pier almost disappear and the scour depth reaches to that of an isolated 33 mm rear pier at *x/b*=90.

(c) Scour depth variation between 66 mm front and 33 mm rear piers

Fig. 5.46 shows the bed level variation between the 66 mm front and 33 mm rear piers. At pier spacing, *x/b*=0, level of the bed between the piers is minimum (ds_m is maximum) and equal to the level of bed at the base of the 33 mm rear pier scour hole. However, as pier spacing increases (upto *x/b* = 20), bed level also increases as the bed material scoured from 66 mm front pier scour hole gets deposited between the piers. At x/*b*=20, the scour

at the upstream face of the 33 mm rear pier is balanced by the sediment deposition from the66 mm front pier scour hole and thus, the bed between the piers remains at its original level (ds_m=0). For spacing $x/b \geq 20$, (ds_m<0), the sediment deposition from 66 mm front pier scour hole becomes dominant. For these spacings, the reinforcing effect at 66 mm front pier becomes weak and disappears completely leading to the development of a longitudinal bed profile similar to that of 33 mm isolated pier.

(d) Scour depth at 33 mm rear pier with respect to 66 mm front pier

Fig. 5.47 shows the variation of relative scour depth 'ds_b/ds_B', where 'ds_B' is the scour depth at 66 mm front pier and 'ds_b' is the scour depth at 33 mm rear pier. It can be seen that the 'ds_b/ds_B' decreases as the pier spacing 'x/b' increases and reaches to a minimum at x/b=35. 'ds_b/ds_B', then increases and reaches to a value equal to '$ds_b/ds_{b(i)}$' (*i.e.*, relative scour depth at 33 mm isolated pier) at x/b= 90.

The decrease in 'ds_b/ds_B' upto x/b=35 can be attributed to the sheltering effect of 66 mm front pier on 33 mm rear pier while the increase in 'ds_b/ds_B' at pier spacings x/b=35 to x/b=90 can be ascribed to the diminishing state of sheltering effect of 66 mm front pier and dominance of vortex shedding effect on 33 mm rear pier caused by the presence of 66 mm front pier.

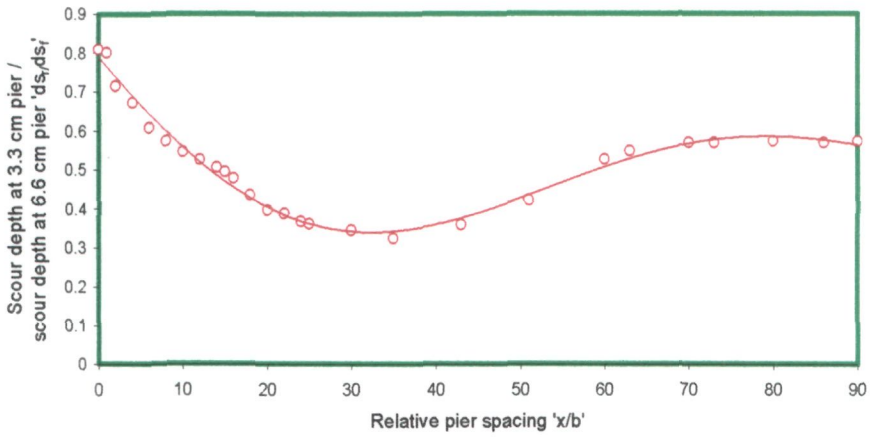

Fig. 5.47 Variation of scour depth at 33 mm rear pier relative to the scour depth at 66 mm front 'ds_b/ds_B' placed in tandem arrangement with pier spacing 'x/b'(where ds_b = scour depth at 33 mm pier, ds_B= scour depth at 66 mm pier).

In order to estimate the scour depth, ANN models with details given in Tables 6.1 and 6.2 (Chapter VI) and ANN architectures shown in Fig.6.13 (Chapter VI), are applied to the

authors experimental data on 66 mm front and 33 mm rear piers placed at varied pier spacings *x/b*. The ANN estimated scour depths are plotted against the observed scour depths in scatter grams as shown in Fig. 6.33 (Chapter VI). Table 6.2 (Chapter VI) gives average values of correlation coefficient R^2 between observed and ANN estimated scour depths for 66 mm front and 33 mm rear piers as 0.9685 and 0.9869 and the average *rmse* values for 66 mm front and 3.3 rear piers as 0.863×10^{-4} and 0.4812×10^{-3} respectively. Closeness of the data points to the line of best agreement as shown in scatter grams Fig. 6.13 (Chapter VI), higher R^2 values and lower *rmse* values indicate the accuracy of ANN models in predicting the scour depth at 66 mm front and 33 mm rear piers.

5.4.2 Scour hole dimensions

Keeping in mind the importance of scour hole dimensions in determining the extent of countermeasures needed to prevent/control scour at piers, various parameters explained as under using present experimental data are determined.

(a) Length of scour holes

The lengths of scour holes at upstream face of 66 mm front and 33 mm rear piers are plotted against pier spacing *'x/b'* as shown in Fig.5.48.

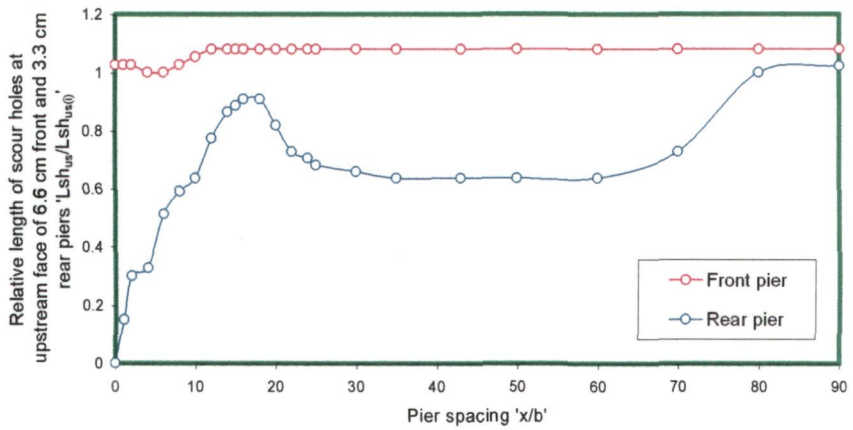

Fig. 5.48 Variation of relative length of scour holes at upstream faces of 66 mm front pier and 33 mm rear piers *'$Lsh_u/Lsh_{u(i)}$'* (where Lsh_u=length of scour holes at upstream face of 66 mm front and 33 mm rear piers, $Lsh_{u(i)}$=length of scour hole at up stream face of an isolated pier).

As shown in Fig 5.49, it is observed that upto $x/b = 2$, no distinction can be made between the downstream part of 66 mm front pier scour hole and upstream part of 33 mm rear pier scour hole.

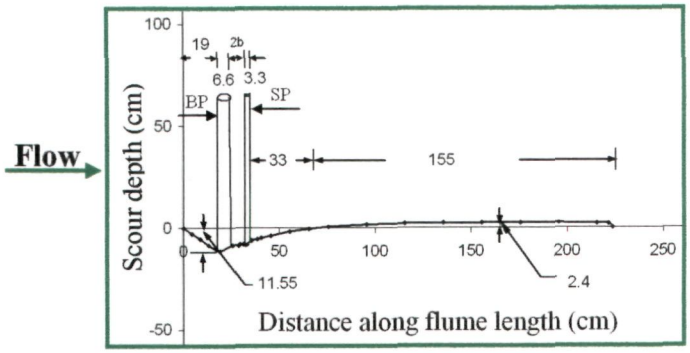

Fig. 5.49 Variation of scour depth along flume length at 66 mm front and 33 mm rear piers placed in tandem arrangement at x/b=2

However, at pier spacing x/b=4 and onward, separate scour holes form around the two piers which can be seen in the Fig. 5.50.

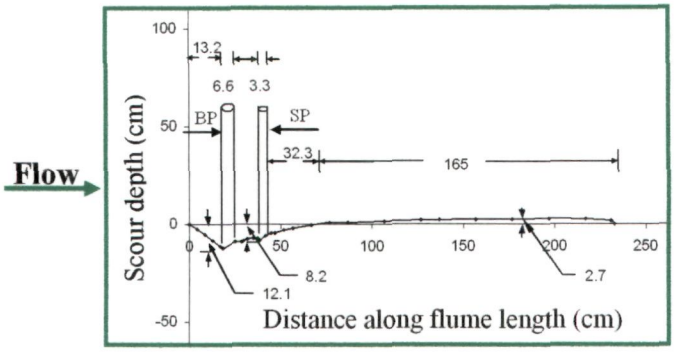

Fig. 5.50 Variation of scour depth along flume length at 66 mm front and 33 mm rear piers placed in tandem arrangement at x/b=4

(b) Length of scour holes at upstream face of piers

As shown in Fig. 5.48, the lengths of scour hole on upstream face of the 66 mm front pier are fairly constant except with a little variation upto x/b =10 which is attributed to the reinforcing effect of 33 mm rear pier.

Referring to Fig.5.56 of section 5.4.2(f) of this chapter for the analysis of variation in the length of scour holes, it is evident that the sediment deposition between the piers begins at x/b>18, therefore, level of the bed between 66 mm front pier and 33 mm rear pier remains below the original bed level. The level of the brim separating the scour holes of two piers remains below the level of the original bed upto x/b=18. The level difference worked out between the level of the brim and the sediment bed at downstream face of the 66 mm

front pier or upstream face of the 33 mm rear pier determines the scour depth for pier spacing $x/b \leq 18$. The length of the scour hole downstream of 66 mm front pier is the horizontal distance between the downstream face of the 66 mm front pier and the brim of the scour holes between two piers. The length of the scour hole upstream of 33 mm rear pier is the horizontal distance between the brim between two scour holes between the two piers and the upstream face of the 33 mm rear pier.

The length of scour hole at upstream face of 33 mm rear pier increases upto $x/b=18$, thereafter it decreases up-to $x/b=35$ and from $x/b=35$ to 60, it remains fairly constant. From $x/b= 60$, the length of scour hole again increases and reaches to that at single pier at $x/b=90$.

At shorter pier spacings 33 mm rear pier lies in the wake of 66 mm front pier and the scour holes of two piers overlap one another such that a common brim is formed between downstream face of 66 mm front pier and upstream face of 33 mm rear pier. When the pier spacing increases, 33 mm rear pier lies out of 66 mm front pier wake and the brim between the two scour holes migrates towards 66 mm front pier, the size of 33 mm rear pier scour hole increases and thus the length of scour hole at upstream face of 33 mm rear pier increases. This trend continues upto pier spacing $x/b=18$.

At pier spacing $x/b>18$, bed material scoured from 66 mm front pier scour hole starts depositing on the bed in front of 33 mm rear pier due to which length of the scour hole at upstream face of 33 mm rear pier starts decreasing. This decreasing trend in the length of scour hole at upstream face of 33 mm rear pier continues upto $x/b=35$ and in the process some of the bed material deposited on the bed in front of 33 mm rear pier moves along with the flow towards downstream, slides down into 33 mm rear pier scour hole and then gets flushed out of it towards the downstream of 33 mm rear pier. Between pier spacings $60<x/b>35$, the input of scoured bed material into 33 mm rear pier scour hole remains nearly equal to output of the bed material from 33 mm rear pier scour hole as a result of which length of scour hole at upstream face of 33 mm rear pier remains nearly constant. At $x/b>60$, the movement of bed material deposited in front of 33 mm rear pier towards downstream of 66 mm front stops short of reaching to 33 mm rear pier scour hole due to which the length of the scour hole at upstream face of 33 mm rear pier increases and reaches to that of 33 mm isolated pier at pier spacing $x/b = 90$.

(c) Scour hole length on downstream of piers

The lengths of scour holes at downstream face of 66 mm front and 33 mm rear piers are shown in longitudinal profiles in Appendix-II. It is noticed that the parts of scour holes at downstream face of 66 mm front pier and upstream face of 33 mm rear pier are not identifiable at *x/b* pier spacing $x/b \leq 2$, however, at larger spacings scour holes are easily identifiable with a brim formed between them and the variation is shown in Fig. 5.51.

(d) Scour hole length at downstream face of 66 mm front pier

At $x/b = 0$, the length of the scour hole at downstream face of 66 mm front pier is nearly same as the scour hole length of 66 mm isolated pier, however, as *x/b* increases upto 18, the scour hole length at downstream face of 66 mm front pier increases and then decreases at $18 < x/b < 90$, and reaches to that of 66 mm isolated pier.

This variation in the length of scour hole at shorter pier spacing *'x/b'* can be analyzed as; 33 mm rear pier shields the wake of 66 mm front pier and results in the overlapping of the scour holes. However, as pier spacing increases, shielding of 66 mm front pier wake by the 33 mm rear pier is reduced, the overlapping of scour holes gets reduced and thus the length of scour hole at downstream face of 66 mm front pier increases upto pier spacing $x/b=18$. At pier spacing $x/b>18$, bed material scoured from 66 mm front pier scour hole starts depositing on the bed downstream of big pier due to which the bed level at the downstream end of 66 mm front pier scour hole increases, the slope of scour hole increases and thus the length of scour hole decreases and reaches to that of 66 mm isolated pier at $x/b=90$.

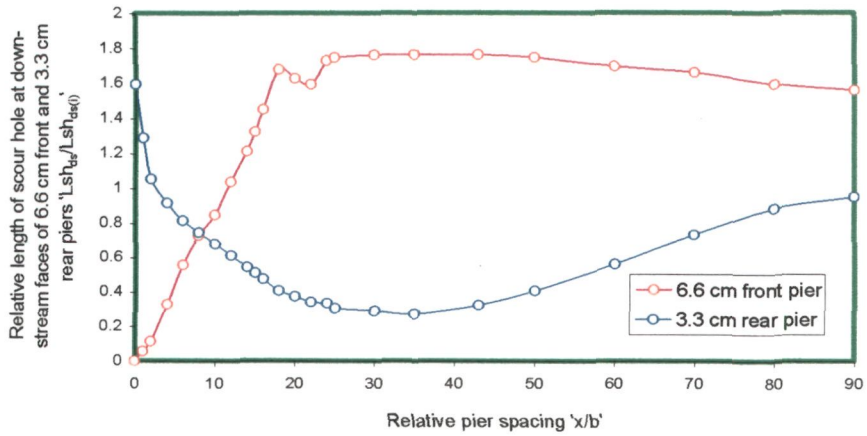

Fig. 5.51 (chart 5) Variation of relative length of scour hole at downstream faces of 66 mm front and 33 mm rear piers placed in tandem arrangement *'$Lsh_d/Lsh_{d(i)}$'* with pier spacing *'x/b'* (where, Lsh_d = Length of scour hole at downstream faces of 66 mm front and 33 mm rear piers, $Lsh_{d(i)}$ = Length of scour hole at downstream face of an isolated pier.

(e) Length of scour hole at downstream face of 33 mm rear pier

Fig. 5.51 shows the lengths of scour hole at downstream face of 33 mm rear pier. At x/b=0, the two piers act like a single entity and the scour pattern around two piers at this spacing is similar to that of 66 mm isolated pier.

Between pier spacings $0<x/b<35$, the scour hole length at the downstream face of 33 mm rear pier decreases. This decrease is attributed to the reduction in scour depth at 33 mm rear pier due to the sheltering effect of 66 mm front pier and also due to the sheltering of 33 mm rear pier by the bed material deposited on the bed upstream of 33 mm rear pier. As the pier spacing increases upto x/b=90, the sheltering effect on 33 mm rear pier decreases and the effect of shed vortices from 66 mm pier on 33 mm rear pier increases. The net effect results in an increased scour depth at 33 mm rear pier and thus larger scour hole length. At x/b=90 the length of scour hole at downstream face of 33 mm rear pier becomes same as that of 33 mm single pier.

(f) Variation of area of scour extent with pier spacing

The areal extents of scour around the 66 mm front and 33 mm rear piers are plotted for varied pier spacings 'x/b' as shown in Appendix-IV. It can be noticed in Fig. 5.52 that upto pier spacing $x\ b<70$, the extent of scour of 66 mm front pier overlaps the scour extent of 33 mm rear pier.

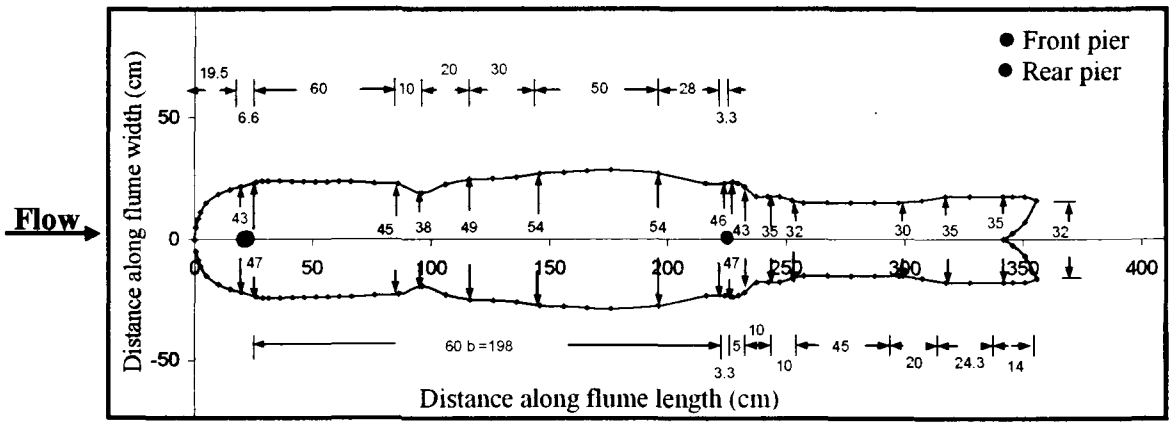

Fig. 5.52 Areal extent of scour around 66 mm front and 33 mm rear piers placed in tandem arrangement at $x\ b$=60

However, areal extents of scour of 66 mm front and 33 mm rear piers tend to gets separate from each other at $x/b\geq70$, as the Fig. 5.53 illustrates.

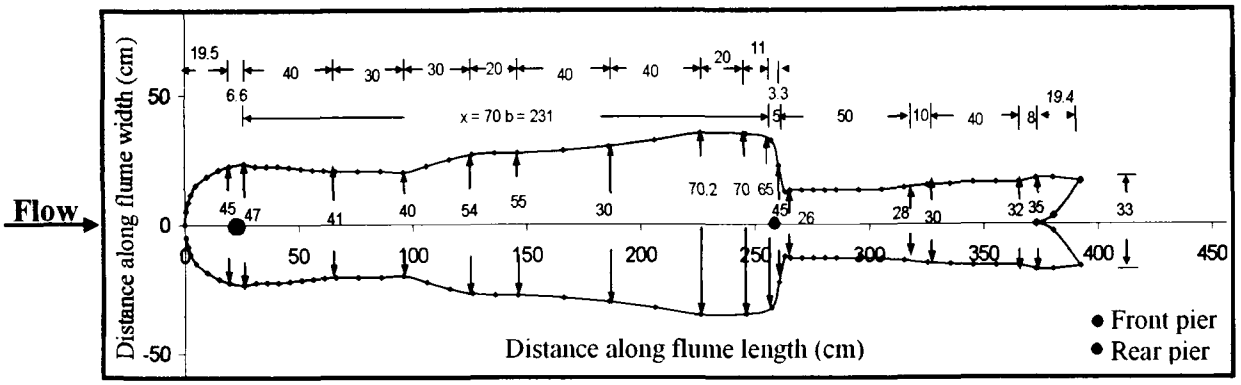

Fig. 5.53 Areal extent of scour around 66 mm front and 33 mm rear piers placed in tandem arrangement at x/b=70

The areal extents of scour around 66 mm front and 33 mm rear piers become almost similar to that of 66 mm and 33 mm isolated piers respectively at x/b=90 as revealed in Fig 5.54.

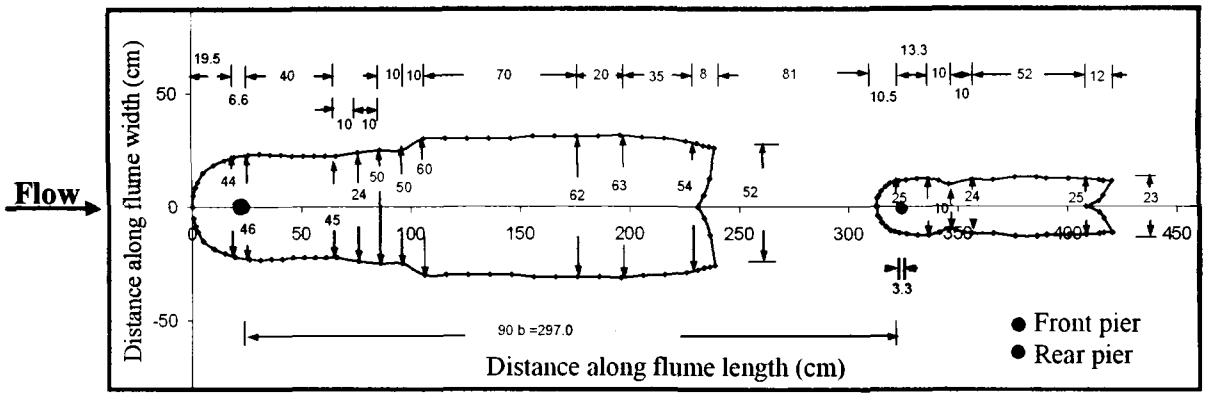

Fig. 5.54 Areal extent of scour around 66 mm front and 33 mm rear piers placed in tandem arrangement at x/b=90

In order to study the effect of pier spacing on the extent of scour, the areas of scour extent are plotted against pier spacing 'x/b' as shown in Fig. 5.55. It can be seen that the area of scour extent is minimum at x/b=0, then increases upto pier spacing $x/b \leq 18$ and rapidly decreases beyond this pier spacing upto $x/b \leq 22$. Henceforth, the area of scour extent around the piers increases rapidly reaching to a maximum at pier spacing x/b= 25. Beyond x/b=25, the area of scour extent gradually decreases and as the pier spacing 'x/b' reaches to 90, the area of extent of scour around 66 mm front and 33 mm rear piers become identical to that of 66 mm and 33 mm isolated piers. The abovementioned variation in the area of scour extent is the result of severe interaction of horseshoe vortices generating around the piers with the wake vortices of big and small piers.

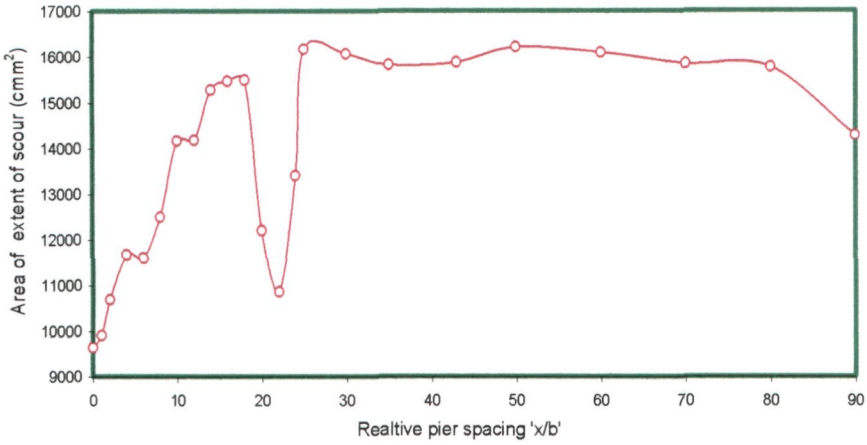

Fig. 5.55 Variation of area of extent of scour around 66 mm front and 33 mm rear pier placed in tandem arrangement with pier spacing *'x/b'*

Further observation of Fig. 5.55 reveals that the area of scour extent at pier spacing x/b=0 is more or less equal to the area of scour extent around 66 mm isolated pier. This clearly indicates the presence of 33 mm rear pier at downstream face of 66 mm front pier at x/b=0 has insignificant effect on area of scour extent. Fig 5.56 shows that upto x/b=18, no deposition of bed material takes place between the two piers and the total scoured bed material is transported and deposited on downstream of 33 mm rear pier and along the sides of scour hole due to which length of sediment deposition on downstream of 33 mm rear pier remains longer and results in an increase in the area of scour extent. As shown in Fig. 5.55, the pier spacing x/b = 22 appears to be critical at which there is steep reduction in area of scour extent. It can thus be concluded that the mutual interference effect between the two piers is predominant in the zone $25>x/b>0$.

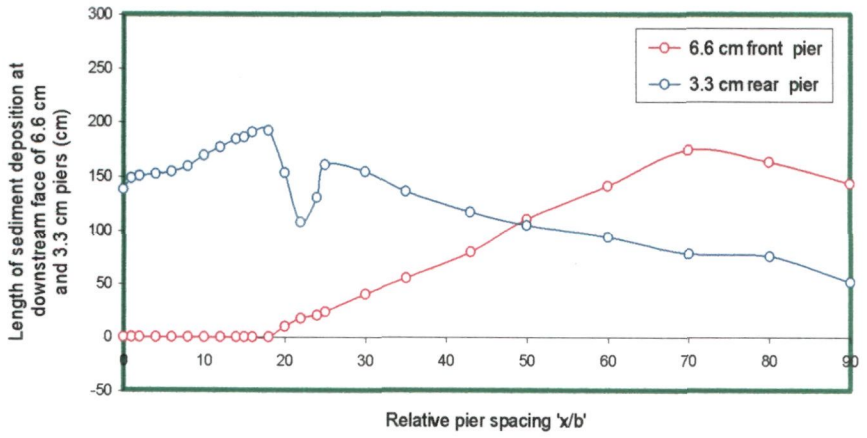

Fig. 5.56 Variation of length of sediment deposition at downstream face of 66 mm and 33 mm piers placed in tandem arrangement, with pier spacing x/b.

The decrease in the area of scour extent between $18 \leq x/b < 22$ can be attributed to the weakening of strength of horseshoe vortex at 33 mm rear pier owing to its interaction with the wake vortices of 66 mm front pier thereby making the wake vortices at 33 mm rear pier unable to lift and transport the bed material upto longer distance along flume length and width.

Areal extents of scour shown in Appendix-IV show a notable difference in the shape and area the scour extents at $x/b=18$ and $x/b=22$. At pier spacing $25>x/b>22$, it appears that the strength of horseshoe vortex and wake vortices at 33 mm rear pier decreases rapidly which consequently results in a steep rise in the area of scour extent. At pier spacing $x/b>25$, 33 mm rear pier is presumed to be relatively free from the interference effects of 66 mm front pier as the area of scour extent after gradually decreasing, approaches nearly to that what is observed around 66 mm and 33 mm isolated piers at $x/b=90$. This clearly suggests that the two piers become considerably free from mutual interference.

(g) Width of scour holes

In earlier studies (Richardson *et al.*, 1993), the top width of scour hole at a single pier has been found to be a function of scour depth and the angle of repose of the bed material. However, present in present study on pier group scour the scour hole width has been found to be affected by the presence of another pier placed in the vicinity of existing pier also.

In Fig.5.56 and Appendix-III, it is noticed that at $0<x/b<20$, major amount of bed material scoured from around 66 mm front pier gets transported to downstream of 33 mm rear pier and small amount of it gets deposited along sides of scoured bed between two piers. At pier spacing $20<x/b<70$ some of the bed material scoured from 66 mm front pier deposits on the bed on upstream of 33 mm rear pier scour hole while some of it deposits on the bed along exterior sides of 33 mm pier scour hole The rest amount of scoured bed material moves along with the flow through the 33 mm rear pier scour hole towards downstream of the 33 mm rear pier. At pier spacing $x/b>70$, the bed material scoured from 66 mm front pier scour hole stops moving further downstream and does not reach the 33 mm rear pier scour hole. As a result, 66 mm front pier scour hole gets separated from 33 mm rear pier scour hole. As the pier

spacing *'x/b'* approaches to 90, the scour holes around 66 mm front and 33 mm rear piers become identical to that what are developed around 66 mm and 33 mm isolated piers indicating the two piers being freed from mutual interference.

To study the effect of pier spacing on width of the scour holes, the scour depth profiles at upstream face of piers along flume width of are plotted against pier spacing *'x/b'* as shown in Appendix-III. The width of scour holes at upstream face of 66 mm front pier 'w_1'and at upstream face of 33 mm rear pier 'w_2' are made dimensionless with the corresponding quantities $w_{i(B)}$ and $w_{i(b)}$ for 66 mm and 33 mm isolated piers respectively.

As shown in Appendix-III, the lateral profiles of scour at front face of 66 mm front pier resemble a V- shaped section. The average equilibrium slope of scour hole at upstream face of 66 mm front pier measures to be 32°, which is same as the angle of repose of the bed material.

The variation of relative widths of scour hole '$w_1/w_{i(B)}$' and '$w_2/w_{i(b)}$'at 66 mm front and 33 mm rear pier against pier spacing *'x/b'* is shown in Fig. 5.57. It is noticed that, the values of '$w_2/w_{i(b)}$' and '$w_1/w_{i(B)}$', at x/b=0, are nearly same which essentially indicates the existence of 33 mm rear pier in the wake of 66 mm front pier has no effect on scouring.

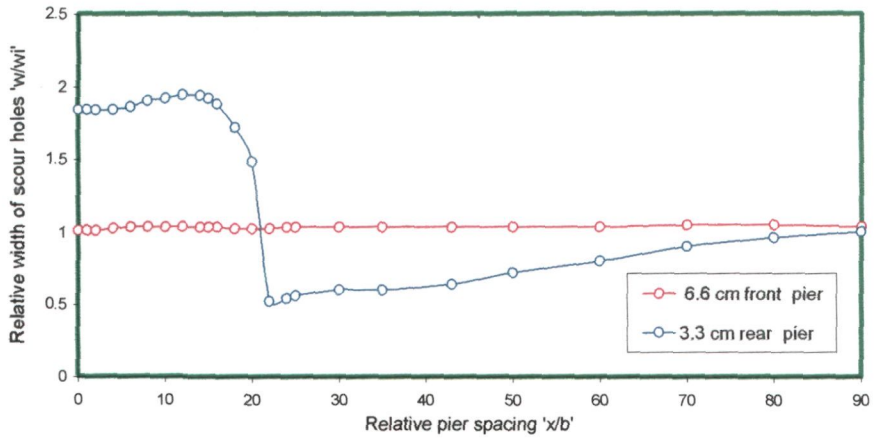

Fig. 5.57 Variation of relative widths of scour hole '$w_1/w_{i(b)}$' and '$w_2/w_{i(b)}$' at 66 mm front and 33 mm rear piers placed in tandem arrangement with pier spacing *'x/b'* (where w_1 = width of scour hole at upstream face of 66 mm front pier, w_2 = scour hole width at upstream face of 33 mm rear pier, $w_{i(b)}$ = scour hole width of 33 mm isolated pier).

Fig.5.57 illustrates the variation of relative scour hole width at 66 mm front pier '$w_1/wi_{(B)}$' with pier spacing *x/b*. A little variation in the width of scour hole of 66 mm front pier

'$w_1/w_{i(B)}$'is observed upto pier spacing $x/b<20$. This marginal increase in '$w_1/wi_{(B)}$' at pier spacing $18>x/b>0$, is attributed to the reinforcing effect induced by the presence of 33 mm pier on downstream of 66 mm pier due to which the scour depth at 66 mm front pier increases and causes an increase in the width of scour hole at 66 mm front pier. It can be noticed that '$w_1/w_{i(B)}$' is fairly constant at pier spacings $x/b>22$, the reason of which is ascribed to the interplay between reinforcing and sheltering effects. However, the relative scour hole width '$w_2/wi_{(b)}$' at 33 mm rear pier initially increases upto $x/b=14$, decreases afterwards from $x/b=14$ to 22 and finally increases at $22<x/b<90$. At $x/b=90$, '$w_1/w_{i(B)}$' and '$w_2/w_{i(b)}$' reach approximately to the corresponding quantities for 66 mm and 33 mm isolated piers.

Comparing Fig. 5.57 and Fig. 5.46 it is clear that the trend of the variation of scour hole width and the scour depth at 66 mm front pier is almost alike. This indicates that the parameter governing the width of scour hole at upstream face of 66 mm front pier is the scour depth, which is in the line as the findings of Richardson *et. al.*, 1993.

The lateral profiles of scour at the upstream face of 33 mm rear pier are shown in Appendix-III. It is observed that the lateral profiles of scour at upstream face of 33 mm rear pier resemble to a symmetrical compound channel section. Appendix-III shows as to how the size and shape of the scour hole at small pier changes with increasing pier spacing x/b. The increase in scour hole width at the upstream face of 33 mm rear pier at pier spacing $0<x/b<14$, can be attributed to the complex flow pattern generated by the mutual interaction of horseshoe vortex at 33 mm rear pier with wake vortices of 66 mm front pier.

During experiments it was observed that at pier spacing $x/b<14$, the major amount of bed material scoured from 66 mm front pier scour hole was deposited at the downstream face of 33 mm pier and very little of it along the sides of 66 mm front pier scour hole., due to which the scour hole width at $0<x/b\leq14$ increases gradually as shown in Fig 5.57 Beyond $x/b=14$, larger amount of bed material deposits on the bed along the sides of the hole at upstream face of 33 mm rear pier which leads to an increase in the bed level of the sides of scour hole and hence causes a decrease in the top width of scour hole 'w_2'. As revealed in Appendix-II, at pier spacing $14<x/b<20$, the deposition of bed material at the sides of scour hole becomes dominant due to which the elevation of the sides scour hole further increases and tries to approach to the original bed level causing a reduction in the width of the scour hole. It is evident in Appendix-III that, upto pier spacing $x/b\leq20$, the entire

bed between the two piers lies below the original bed level. Furthermore, at $x/b \geq 20$, the bed level at the sides rises above the original bed level causing further decrease in the width of scour hole. At this stage the cross section of scour hole assumes the shape as that of 66 mm isolated pier scour hole.

Fig 5.57 shows that at $x/b>20$ the bed material deposited at upstream face of 33 mm rear pier shelters the 33 mm rear pier against the incoming flow which causes reduction in effective velocity of flow for 33 mm rear pier. This provides ease in deposition for the sediment particles around the 33 mm pier, thereby causing reduction in the scour depth and the width of scour hole. Further, the vortices shedding from the 66 mm front pier pass away from 33 mm rear pier and do not assist in the scouring process at 33 mm rear pier. This diminishing state of vortex shedding effect of 66 mm front pier on 33 mm rear pier causes a decrease in the scour depth and width at 33 mm rear pier.

Appendix-II shows that at $x/b>20$, the deposition of more and more bed material along the edges of middle cross-section of scour hole while maintaining the same side slope, causes an increase in the width of 33 mm rear pier scour hole. At these spacings, the 33 mm rear pier is relieved from the interference of 66 mm front pier. As a result of which 33 mm rear pier attains the same shape and size of scour hole as that what are observed at 33 mm isolated pier.

(h) Length of Sediment Deposition

Fig 5.56 shows as to how the length of sediment deposition on downstream of 33 mm rear pier varies with pier spacing x/b. It is observed that at $0<x/b<18$, the length of sediment deposition increases. Between $x/b=18$ to 22, it decreases and again increases between at $x/b=22$ to 25. Thereafter, it decreases and approaches to that at 33 mm isolated pier at $x/b=90$.

The reason for this increase in length of sediment deposition on downstream of 33 mm rear pier upto $x/b=18$ can be attributed to the enhancement in the strength of wake vortices emerging from 33 mm rear pier which is caused by the striking action of wake vortices of 66 mm front pier. This leads to the transportation and deposition of the entire bed material scoured from around 66 mm front pier on the bed downstream of 33 mm rear pier upto farther distance.

At x/b>18, the bed material scoured from 66 mm front pier begins to deposit on the bed upstream of 33 mm rear pier. This deposited bed material interacts with the flow approaching to 33 mm rear pier and causes considerable decrease in the approach flow velocity, which provides a relatively still pocket of water upstream of 33 mm rear pier and facilitates deposition of sediment. Owing to this, wake vortices at 33 mm rear pier become unable to lift and transport the bed material upto longer distance downstream of 33 mm rear pier and causes a decrease in the length of sediment deposition. As shown in Fig 5.56, this effect of sediment deposition dominates upto pier spacing x/b=22. Thereafter, the shielding and vortex shedding effects of 66 mm front pier, the shielding effect of bed material deposited on the bed upstream of 33 mm rear pier and the effect of mutual interaction of wake vortices of 66 mm front pier with horseshoe vortex of 33 mm rear pier appear to have such a combined influence that the length of sediment deposition increases upto x/b=25. Thereafter, the flow characteristics approach gradually to that for 33 mm isolated pier and the length of sediment deposition at downstream face of 33 mm rear pier tends to reach to that of 33 mm isolated pier at x/b=90.

Photographs shown in Figs. P4 & P5 evidently reveal the scour characteristics discussed above and thus authenticate the analysis of results.

5.4.3 Temporal variation of scour

The data collected in this study on temporal variation of scour around 66 mm front and 33 mm rear piers placed in tandem arrangement are given in Appendix-I. From the plots of these data (not shown here), it is noticed that the rate of scouring at 33 mm rear pier lacks behind the 66 mm front pier upto pier spacing x/b=70. To ascribe a reason to this happening, it is worth to mention that at short pier spacings, the bed material scoured from the 66 mm front pier scour hole moves into the scour hole of 33 mm rear pier. As a result, the scour depth at the 66 mm front pier approaches to equilibrium earlier than at the 33 mm rear pier because flow takes more time to remove the bed material transported from the 66 mm front scour hole. Due to sheltering effect of the 66 mm front pier on 33 mm rear pier, the rate of scour at 33 mm rear pier remains slower than the rate of scour at 66 mm front pier. However, at larger pier spacing the bed material from 66 mm front pier scour hole does not arrive at the scour hole of 33 mm rear pier and as the sheltering effect of 66 mm front pier also vanishes, the scour depths at 33 mm rear piers approaches to

equilibrium. The scour depth attained for varied pier spacings at a particular time at 66 mm front and 33 mm rear piers in tandem arrangement can be obtained by plotting the data on temporal variation of scour depth given in Appendix-I.

5.4.4 Concluding remarks

The maximum scour depth at 66 mm front pier at pier spacing x/b=0, is observed to be 95 % of the scour depth at 66 mm isolated pier. At x/b= 10, scour depth increases to a maximum value (1.077 times the scour depth at an isolated pier). At x/b>10, the scour depth decreases and approaches to that of 66 mm isolated pier at x/b = 90. The maximum scour depth at 33 mm rear pier is observed to be 1.35 times to that of 33 mm isolated pier. It is notable that at x/b >0, scour depth decreases and reaches to a minimum (*i.e.*, 0.57 times the scour depth at 33 mm isolated pier) at x/b=35. At pier spacing x/b>35, the scour depth at 33 mm rear increases and reaches to that of an isolated 33 mm pier at x/b=90.

Based on present results obtained on 66 mm front and 33 mm rear piers placed in tandem arrangement, it can be suggested that 33 mm rear pier be placed at x/b=35 as the scour depth at this pier spacing at 33 mm rear pier is a minimum and also the scour depth at 66 mm front pier is very close to that of an 66 mm isolated pier.

5.5 Small Pier at Front and Big Pier at Rear (i.e., 33 mm pier at front and 66 mm pier at rear)

5.5.0 Introduction

In order to analyze the results obtained in this case of present study on local scour at two piers [33 mm pier (small pier) at front and 66 mm pier (big pier) at rear] in tandem arrangement, the longitudinal scour profiles, lateral profile of scour hole and areal extents of scour are plotted against relative pier spacing 'x/b'. Longitudinal scour profiles illustrating the scour depth and length of scour holes are shown in Appendix-II. The lateral cross-sections of scour holes are shown in Appendix-III. The temporal variation of scour depth is given in Appendix-I.

The areal extents of scour showing scour hole widths at the piers are shown in Appendix-IV. Some typical cases of these areal extents are considered for the analysis and discussion in this section. The photographs showing the scour and deposition patterns

around the 33 mm front and 66 mm rear piers were taken at the end of each experiment. Photographs for some distinctive cases are shown in Fig. P6 & P7. The analysis is carried out under the following heads:

5.5.1 Variation of scour depth along flume length

The data on scour depth collected in present study around two unequal sized piers *i.e.*, small pier (33 mm pier) at front and big pier (66 mm pier) at rear along center line of flume in the direction of flow are plotted for varied pier spacings x/*b* and are shown in Appendix-II. As illustrated in Fig. 5.58, the longitudinal scour profile through 33 mm front pier overlaps with the longitudinal profile through 66 mm rear pier upto pier spacing *x/b* = 40.

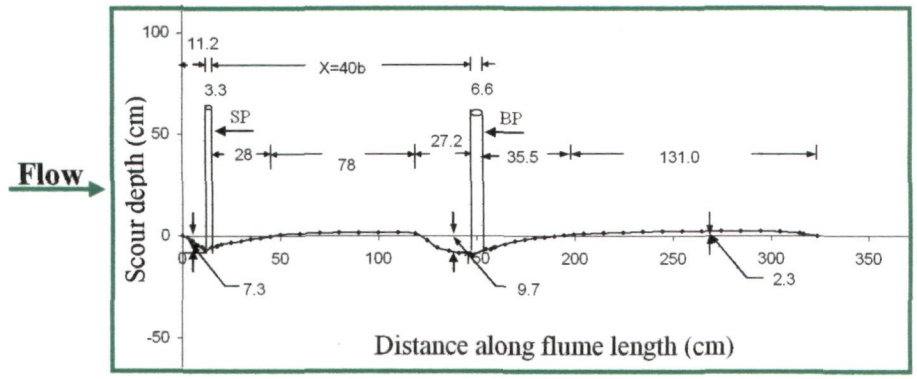

Fig. 5.58 Variation of scour depth at 33 mm front and 66 mm rear piers placed in tandem arrangement at *x b*= 40

However, as illustrated in Fig 5.59, these profiles become entirely independent at pier spacing *x/b*>40.

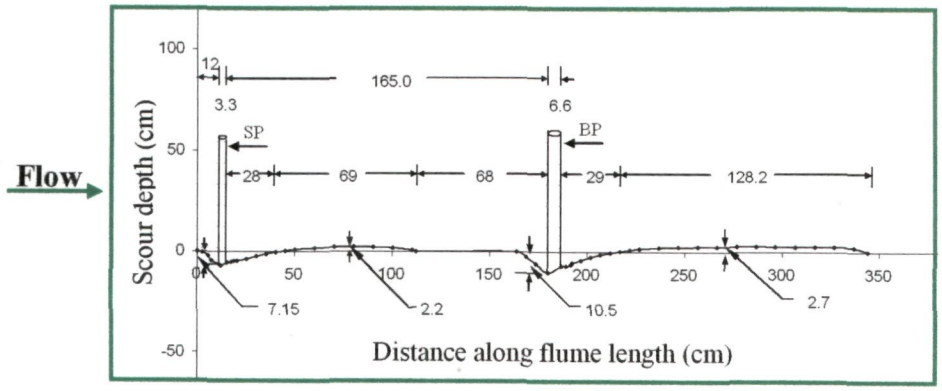

Fig. 5.59 Variation of scour depth at 33 mm front and 6.6 rear pier placed in tandem arrangement at *x b*= 50

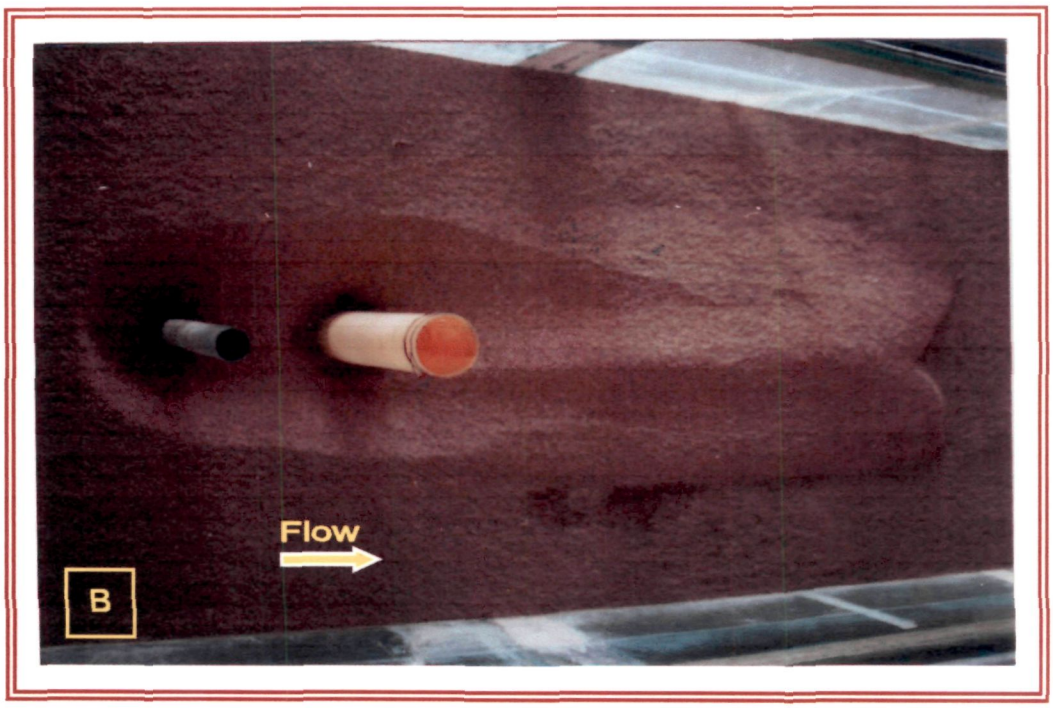

Fig. P6: Scour and deposition patterns around two piers (small pier at front and big pier at rear) placed in tandem arrangement at varied pier spacings x/b (A) x/b=0 (B) x/b=5

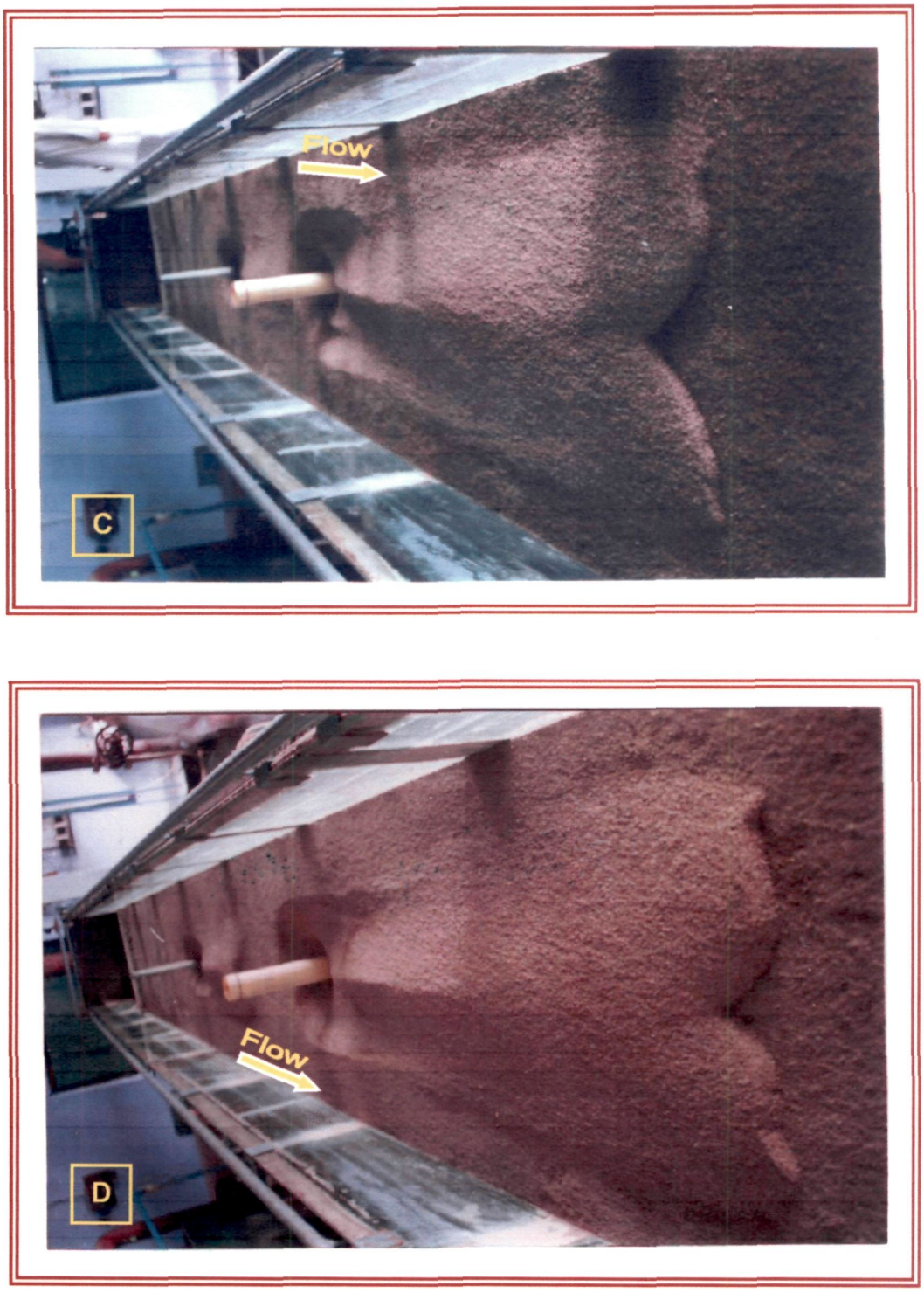

Fig. P7: Scour and deposition patterns around two piers (small pier at front and big pier at rear) placed in tandem arrangement at varied pier spacings *x/b* (C) *x/b*=40 (D) *x/b*=50

As demonstrated in Fig 5.60, the longitudinal profiles through 33 mm front and 66 mm rear piers assume the shape and dimensions as that of isolated 33 mm and 66 mm piers respectively when pier spacing *'x b'* approaches to 90.

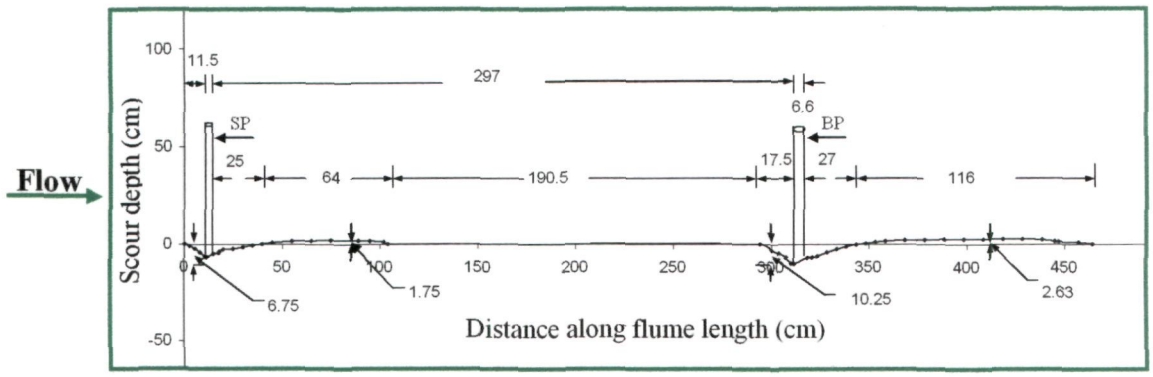

Fig. 5.60 Variation of scour depth at 33 mm front and 6.6 rear pier placed in tandem arrangement at $x\ b$= 90

5.5.2 Variation of scour depth at 33 mm front and 66 mm rear piers with pier spacing

(a) Variation of scour depth at 33 mm front pier

The scour depth measured at 33 mm front and 66 mm rear piers are made dimensionless by dividing it with the scour depth measured at 33 mm isolated pier and the same are plotted against longitudinal pier spacing *'x/b'* as shown in Fig 5.61, where, x is the clear spacing between 33 mm front and 66 mm rear piers and b is the diameter of 33 mm front pier.

Fig.5.61 reveals that at x/b =0, the relative scour depth *'$ds_b/ds_{b(i)}$'* at 33 mm front pier is maximum, which is about 28.5 % more than at 33 mm isolated pier. At x/b ranging between 0 and 3, decrement of about 19 % in the scour depth is observed. Beyond x/b=3, the value of *'$ds_b/ds_{b(i)}$'* gradually decreases and approaches to that of 33 mm isolated pier at pier spacing x/b=90. It is also observed in Fig. 5.61 that, at x/b=0, the relative scour depth *'$ds_B/ds_{B(i)}$'* at 66 mm rear pier, is nearly equal to that of 66 mm isolated pier. The scour and deposition patterns around 66 mm isolated pier are shown in Fig. PI.

The maxima in scour depth at x/b=0 indicates the existence of maximum reinforcing effect of 66 mm rear pier on 33 mm front pier. Substantial decrease in reinforcing effect occurs between x/b= 0 to 3, which causes steep reduction in relative scour depth at 33 mm front small pier.

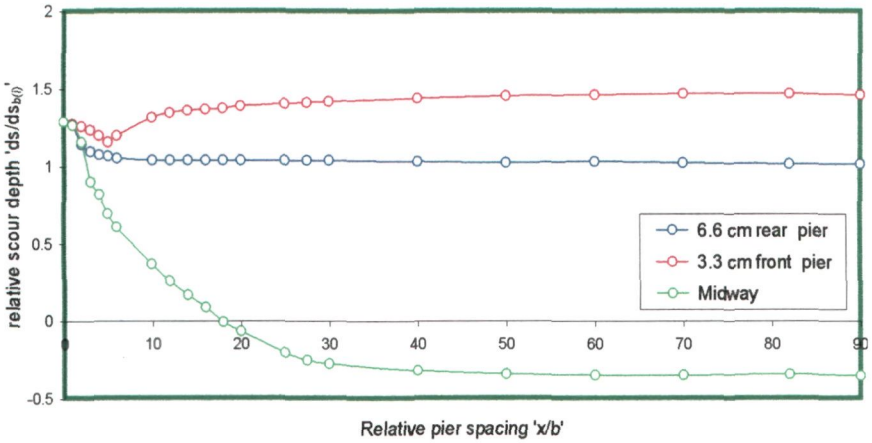

Fig. 5.61 Variation of relative scour depth at 33 mm front and 66 mm rear pier and at midway between the two piers '$ds_b/d_{b(i)}$, $ds_B/ds_{b(i)}$ and $ds_{mid}/ds_{b(i)}$' placed in tandem arrangement with pier spacing 'x/b'(where ds_b=scour depth at 33 mm front pier, ds_B = scour depth at 66 mm rear pier $ds_{b(i)}$ = scour depth at 33 mm isolated pier).

Thereafter, the reinforcing effect decreases gradually, which causes a gradual decrease in this relative scour depth. At x/b=90 the scour depth at 33 mm front pier becomes identical that what is observed at 33 mm isolated pier.

(b) Variation of scour depth at 66 mm rear pier

Fig. 5.61 depicts the variation of relative scour depth at 66 mm rear pier. It is observed that at x/b=0, the relative scour depth at 66 mm rear and 33 mm front piers is almost same, however, as compared to the scour depth at 66 mm isolated pier, the scour depth is about 23% less at of 66 mm rear pier. Beyond x/b=0, the value of '$ds_B/ds_{b(i)}$' decreases and reaches to a minimum at x/b=5. Thereafter, the value of '$ds_B/ds_{b(i)}$' increases and reaches to that of 66 mm isolated pier at x/b=90.

The measured data plotted in Fig. 5.61, outlines that, 33 mm front pier when placed in front of 66 mm rear pier at x/b=0, acts like a sacrificial pile due to which the flow gets deflected and the velocity of flow approaching to 66 mm rear pier gets retarded thereby causes a decrease in the strength of horseshoe vortex around 66 mm rear pier It is noticed that, the scour depth around 66 mm rear pier decreases by 23 % at pier spacing x/b=0. The maximum reduction in '$ds_B/ds_{b(i)}$' occurs at pier spacing x/b=5 which clearly indicates the existence of maximum sacrificial effect of 33 mm front pier for 66 mm rear pier. At x/b=5, the reduction in relative scour depth is about 37%. As the pier spacing 'x/b' increases beyond 5, 66 mm rear pier leaves the wake of 33 mm front pier, deflection of flow starts reducing and the flow starts approaching to the 66 mm rear due to which 66 mm rear pier

starts experiencing lesser sacrificial effect from 33 mm front pier thereby increasing scour depth at 66 mm rear pier which reaches to that at 66 mm isolated pier at x/b=90.

(c) Variation of scour depth between 33 mm front and 66 mm rear pier

Fig 5.61 shows the bed level variation between the 33 mm front and 66 mm rear piers. At x/b=0, the bed level between 33 mm front and 66 mm rear piers is minimum (*i.e.*, scour depth, ds_m, is maximum) and equals to the bed level of the base of 66 mm rear pier scour hole. Upto pier spacing x/b=18, bed level between the piers lies below the original bed level. At pier spacing x/b >18, the bed level increases as some of the bed material scoured from the 33 mm front pier scour hole gets deposited on the bed between the two piers. At this pier spacing, the scouring in front of the 66 mm rear pier is balanced by the sediment deposition from the 33 mm front pier scour hole and thus, the bed between the piers remains at its original level (ds_m=0). For spacing $x/b \geq 18$, ($ds_m < 0$), the deposition of sediment on the bed in front of 66 mm rear pier becomes dominant as the strength of wake vortices weakens due to reduction in the reinforcing effect at 33 mm front pier and due to relatively calm pocket of water prevailing between the piers. At x/b = 90, 33 mm front and 66 mm rear piers assume the same longitudinal profiles as those of 33 mm and 66 mm isolated piers.

(d) Variation of Scour Depth at 66 mm Rear Pier With Respect to 33 mm Front Pier

Fig. 5.62 shows the variation in scour depth 'ds_B' at 66 mm rear pier with respect to the scour depth 'ds_b' at 33 mm front pier with pier spacing 'x/b'.

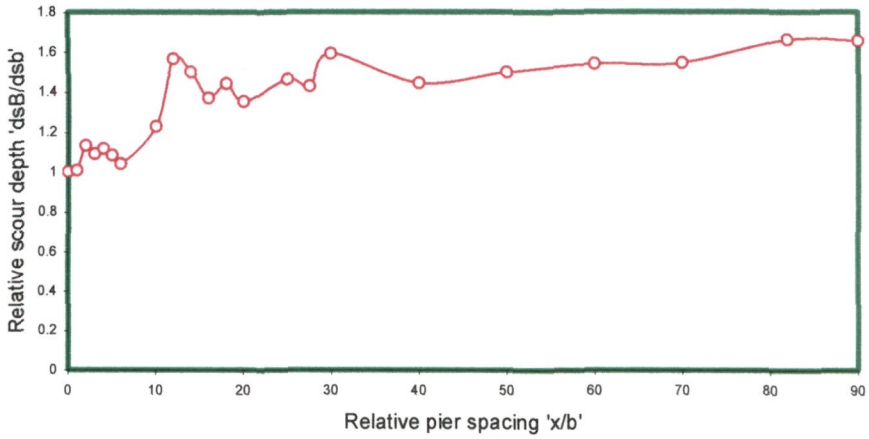

Fig.5.62 Variation of scour depth at 66 mm rear pier relative to the scour depth at 33 mm front pier placed in tandem arrangement 'ds_B/ds_b' with pier spacing 'x/b' (where ds_B= scour depth at 66 mm rear pier, ds_b= scour depth at 33 mm front pier).

From Fig. 5.62 it is observed that the relative scour depth 'ds_B/ds_b' increases as the pier spacing 'x/b' increases from 0 to 3, and decreases in the range of pier spacing 'x/b' from 3 to 5 and thereafter increases and reaches to a maximum value at x/b=90.

The increase in 'ds_B/ds_b' at $0<x/b<2$ can be attributed to the reinforcing effect of 66 mm rear pier on small pier. The decrease in 'ds_B/ds_b' from x/b=2 to 6 is due to the dominance of sacrificial effect of 33 mm front pier on 66 mm rear pier. The sacrificial effect of 33 mm front pier starts decreasing beyond x/b=6 as a result of which the value of 'ds_B/ds_b' starts increasing, reaching to a maximum at x/b=90.

For the purpose of scour depth estimation, ANN models with details given in Tables 5.1 and 6.2 (Chapter VI) and architectures shown in Fig. 6.4 (Chapter VI), are applied to the authors experimental data on 33 mm front and 66 mm rear pier in tandem arrangement at varied pier spacings. The ANN estimated scour depths are plotted against observed scour depths in scatter grams Fig. 6.14 of (Chapter VI.) Closeness of the data points to the line of best agreement in these scatter grams, higher values of correlation coefficient R^2 and lower *rmse* values indicate the accuracy of ANN models in predicting the scour depth.

5.5.3 Scour hole dimensions

Since the knowledge of scour whole dimensions is vital in determining the extent of countermeasures needed to prevent/control scour at piers, various parameters explained as under using present experimental data are determined.

(a) Shape of scour hole

As can be seen shown in Appendix-IV, the shape of scour holes (in plan) developed around 33 mm front and 66 mm rear piers resemble to the frustum of an inverted cone and the shape of upstream part of scour holes is semi-circular in plan. It is also observed that for all pier spacings the lengths of upstream part of scour holes are shorter along the flume length as compared to the downstream part.

(b) Length of scour holes

The lengths of scour hole at the upstream and downstream faces of 33 mm front and 66 mm rear piers placed in tandem arrangement are shown in Appendix-IV. It can be observed in Appendix-II that for pier spacings 'x/b' ranging from 0 to 2, no clear

distinction can be made between the boundaries of downstream part of 33 mm front pier and the upstream part of 66 mm rear pier scour holes.

However, as shown in Appendix-II, at x/*b* = 3 and beyond, the boundaries get separated which is distinctly identified by the common brim formed between the two piers.

Fig. 5.63 shows the variation of scour hole length at the upstream face of 33 mm front pier with varied pier spacing *x/b*. It is observed that the length of scour hole at upstream face of small pier is maximum at pier spacing *x/b*=0.

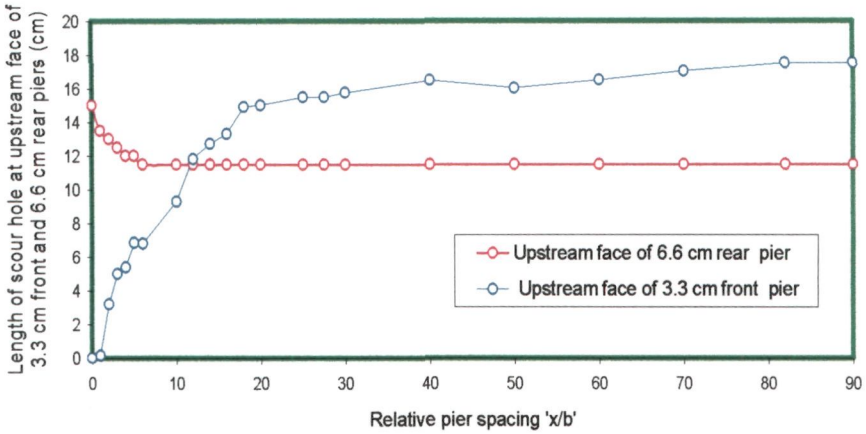

Fig. 5.63 Variation of length of scour holes at upstream face of 33 mm front and 66 mm rear piers placed in tandem arrangement with pier spacing *'x/b'*.

This maxima indicates the existence of large reinforcing effect due to 66 mm rear pier at this pier spacing. The length of scour hole at the upstream face decreases upto pier spacing *x/b*= 5. This decreasing trend indicates the weakening of reinforcing effect as pier spacing reaches to 5. Beyond *x/b*=5, the length of scour hole at upstream face of 33 mm front pier remains fairly constant which clearly indicates the disappearance of the reinforcing effect of 66 mm rear pier. The above justification gains strength by comparing Figs. 5.63 and.5.61, which suggest that the scour depth is influenced by the reinforcing effect of 66 mm rear pier, in the same way the length of scour hole at the upstream of 66 mm rear pier is influenced by its reinforcing effect at pier spacings $0<x/b<5$.

Fig. 5.64 depicts the variation in the length of scour hole at the downstream face of 33 mm front pier with pier spacing *x/b*. It is observed that the length of scour hole on downstream of small pier increases with an increase in pier spacing and reaches to a maximum at *x/b*=40. Thereafter, it gradually decreases and approaches to that of an 33 mm isolated pier at *x/b*=90.

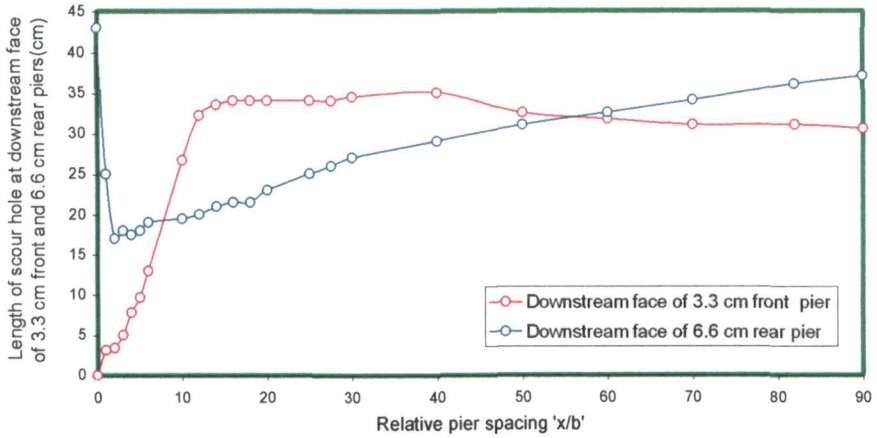

Fig. 5.64 Variation of length of scour holes at downstream faces of 33 mm front and 66 mm rear piers placed in tandem arrangement with pier spacing *'x/b'*.

It is evident from Fig. 5.61 and Appendix-II that the sediment deposition on the bed between the two piers begins at $x/b>40$, and therefore, bed level lies below the original bed level ($ds_m>0$) upto $x/b=40$. The downstream part of scour hole of 33 mm front pier and the upstream part of scour hole of 66 mm rear pier are demarcated by a brim which lies below the original bed level upto $x/b=40$. To estimate the scour hole length, level difference between the brim and sediment bed at downstream face of the 33 mm front pier or upstream face of the 66 mm rear pier determines the scour depth for pier spacing $x/b\leq40$. The length of the scour hole at downstream face of 33 mm front pier is the horizontal distance between the downstream face of the 33 mm front pier and the brim formed between the two scour holes.

For pier spacing $x/b\leq2$, independent horseshoe vortices around two piers are not developed, as a result of which the scour holes between the piers are not distinguishable. However, at pier spacing $x/b>2$, independent horseshoe vortices around piers are formed which results in the formation of a brim between the piers which makes it possible to distinguish the downstream part of 33 mm front pier and upstream part of 66 mm rear pier scour holes.

Since the wake of 33 mm front pier gets interrupted due to the presence of 66 mm rear pier, the length of scour hole downstream of 33 mm front pier remains shorter at shorter pier spacings. However, as the pier spacing increases, interference of wake of 33 mm front pier by 66 mm rear pier gets reduced as a result of which the brim migrates towards 66 mm rear pier and length of scour hole at downstream face of 33 mm front pier

increases. At x/b=40, the wake of the 33 mm front pier gets completely freed from 66 mm rear pier interference and a fully developed downstream part of 33 mm front pier scour hole is formed. The scour hole length at the downstream face of small pier is maximum at x/b=40, after which a marginal decrease in scour hole length occurs which can be attributed to the flow pattern developed between the piers.

As shown in Appendix-II, the length of the scour hole at the upstream face of 66 mm rear pier is the horizontal distance between the brim and the upstream face of the 66 mm rear pier. Fig. 5.63 depicts the variation in the scour holes length at upstream face of 66 mm rear pier with pier spacing 'x/b'. Fig.5.63 reveals that as the pier spacing increases, the length of scour hole increases and reaches to a maximum at x/b=40. Thereafter, it decreases and reaches close to that of an isolated 66 mm rear pier at x/b=90.

As shown in Appendix-II, upto $x/b \leq 2$, no distinction can be made between downstream part of scour hole of 33 mm front and upstream part of scour hole of 66 mm rear pier. However, at pier spacing $x/b \geq 3$, these can be clearly identified. At short pier spacing x/b, upstream part of 66 mm rear pier scour hole is influenced by the wake of the 33 mm front pier. As the pier spacing 'x/b' increases (*i.e.*, x/b>40), the influences of 33 mm front pier wake on the 66 mm rear pier decreases. As shown in Appendix-II, the influence of 33 mm front pier disappears completely at pier spacing x/b=40. As a result of this, the length of scour hole at upstream face of 66 mm rear pier increases upto pier spacing x/b=40. As evident from Fig 5.65, the deposition of bed material which is scoured from 33 mm front pier scour hole, begins on upstream of 66 mm rear pier at pier spacing x/b>40. The deposition of this bed material on the bed upstream of 66 mm rear pier increases the slope of upstream part of 66 mm rear pier scour hole hence results in decrease of the length of scour hole at upstream face of 66 mm rear pier.

The length of scour hole at downstream face of 66 mm rear pier decreases and reaches to a minimum at x/b=2, and then, it increases and reaches to of an isolated 66 mm that at single pier at x/b=90. The comparison of Fig. 5.61 and Fig. 5.64 shows similar trend of variation in the scour depth and scour holes length at downstream face of 66 mm rear pier with pier spacing x/b. This similarity in trends indicates the scour holes length at downstream face of 66 mm rear pier to be a function of scour depth. The flow approaching to 66 mm rear pier carries some of the bed material deposited at upstream

end of 66 mm rear pier into the 66 mm rear pier scour hole and then to the downstream of 66 mm rear pier where it gets deposited. As a result, the bed level on downstream of 66 mm rear pier increases and the length of scour at downstream face of hole of 66 mm rear pier decreases.

(c) Deposition of sediment at downstream face of 33 mm front and 66 mm rear pier

(i) Length of sediment deposition at downstream face of 33 mm front pier

Fig.5.65 depicts the variation in the length of sediment deposition at the downstream face of piers with pier spacing '*x/b*'. It is observed that at pier spacings $x/b \leq 16$, intensive interaction of flow with the sediment bed and the piers is generated. As the pier spacing *x/b* increases beyond 16, the turbulence in the flow between the piers dampens due to which the bed material scoured from 33 mm front pier scour hole begins to deposit on the bed downstream of 33 mm front pier. As a result of this the length of sediment deposition at the downstream face of 33 mm front pier increases and reaches to a maximum at pier spacing $x/b=40$.

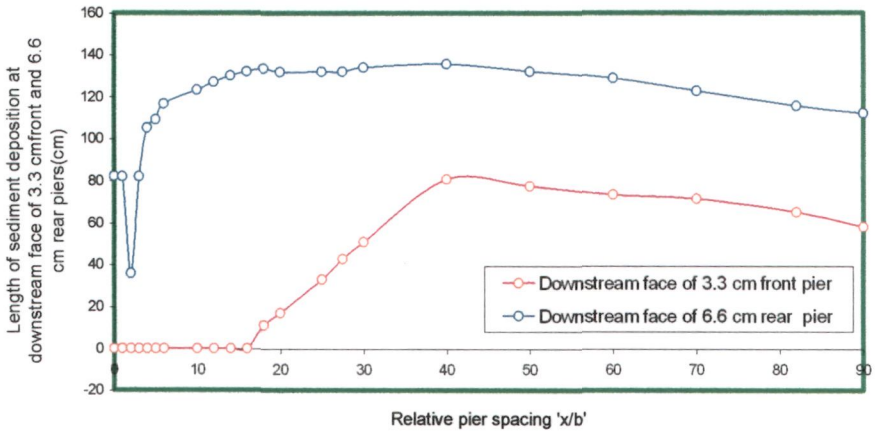

Fig. 5.65 Variation of length of sediment deposition at downstream face of 33 mm front and 66 mm rear pier placed in tandem arrangement with pier spacing '*x/b*'.

At pier spacing $x/b>40$, the length of sediment deposition decreases and approaches to that of 33 mm isolated pier at pier spacing $x/b=90$. The maxima in length of sediment deposition at pier spacing $x/b=40$ indicates the critical spacing beyond which the wake of 33 mm front pier begins to be relieved freed from the interference of 66 mm rear pier. At pier spacing $x/b>40$, the bed material deposited on the bed on upstream of 66 mm rear pier scour hole, slides down into the 66 mm rear pier scour hole and, then moves out of it

and gets transported by the incoming flow towards downstream of 66 mm rear pier and thus results in a reduction in the length of sediment deposition.

At $x/b \geq 50$, as illustrated in Fig. 5.66, the longitudinal scour profiles through 33 mm front and 66 mm rear pier get alienated from one another.

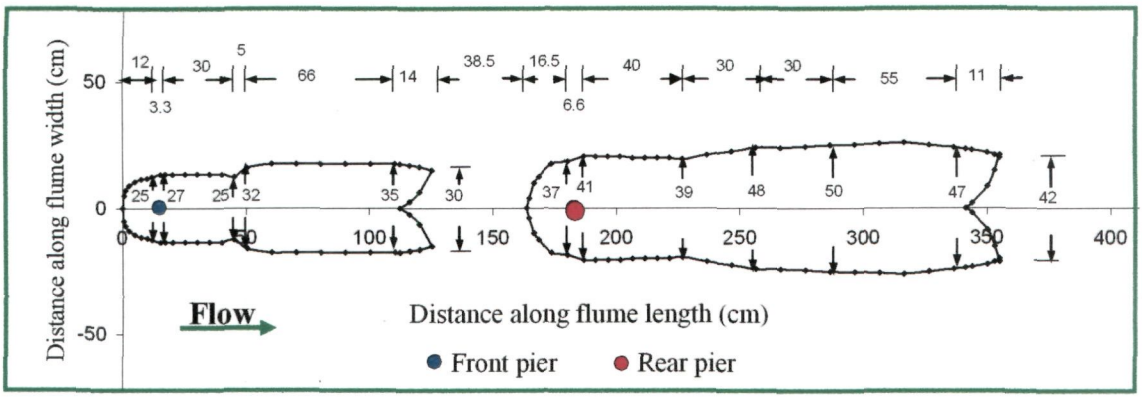

Fig. 5.66 Areal extent of scour around 33 mm front and 66 mm rear piers placed in tandem arrangement at x/b=50

(ii) Length of sediment deposition at downstream face of 66 mm rear pier

The variation in the length of sediment deposition at downstream face of 66 mm rear pier with pier spacing '*x/b*' is shown in Fig. 5.65 It is observed that at $x/b \leq 1$, the length of sediment deposition is less than the length of deposition on downstream of 66 mm isolated pier. To ascribe a reason for the length of sediment deposition being less, it is understood that the presence of 33 mm pier at front results in the deflection of flow which causes flow interaction with the sediment bed to become weak, incapable of carrying the sediment further downstream. In addition to this, the presence of 33 mm pier at front of 66 mm rear pier causes reduction in the strength of horseshoe vortex around 66 mm rear pier. As shown in Fig. 5.65, at pier spacing x/b=2, the length of sediment deposition is observed to be minimum. This minima reflects the effect of deflection of flow by 33 mm front pier being maximum at x/b=2. At pier spacing x/b>2, the length of sediment deposition after abruptly rising reaches to a maximum at pier spacing x/b=40. This increase in the length of sediment deposition indicates the initiation of reduction in the effect of deflection of flow. At pier spacing x/b>40, the length of sediment deposition gradually decreases until the wake of 66 mm rear pier gets fully developed at pier spacing x/b=90.

(d) Width of scour holes

For interpreting the effect of pier spacing on the width of scour holes, the scour hole width of 33 mm front and 66 mm rear piers with respect to the corresponding widths of isolated pier scour holes *'$w_1/w_{b(i)}$'* and *'$w_2/w_{b(i)}$'* are plotted in Fig. 5.67.

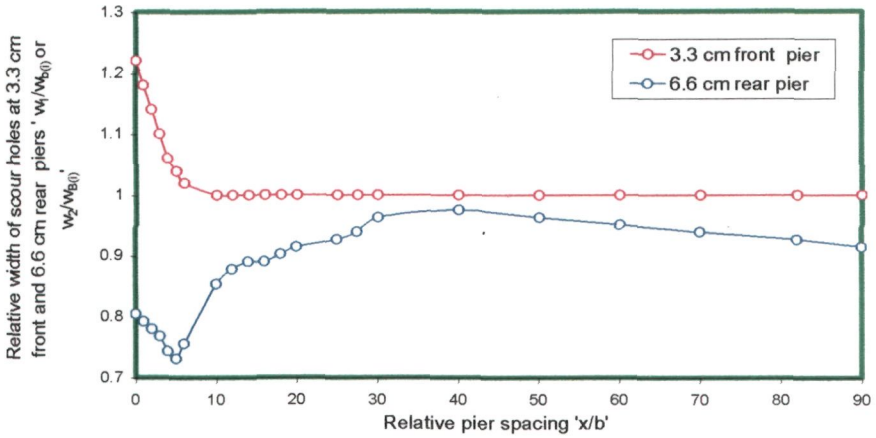

Fig. 5.67 Variation of relative width of scour holes at 33 mm front and 66 mm rear piers placed in tandem arrangement *'$w_1/w_{b(i)}$ and $w_2/w_{i(b)}$'* with pier spacing *'x/b'* (where w_1 = width of scour hole of 33 mm front pier, $w_{b(i)}$ = width of scour hole of 33 mm isolated pier, w_2 = width of scour hole 6.6 rear cm pier and $w_{B(i)}$ = width of 66 mm isolated pier).

The similarity in the variation of relative width of scour holes (Fig. 5.67) and the scour depth around the two piers (Fig. 5.61) suggest the width of scour holes being the function of scour depth which is also reported by Richardson *et. al.* (1993).

(e) Slope of scour holes

Appendix-II shows that that at pier spacings *'x/b'* upto 2, the demarcation between downstream part of scour hole of 33 mm front and upstream part of scour hole of 66 mm rear is not identifiable. The variation in longitudinal slope of scour holes at upstream face of 33 mm front and 66 mm rear piers with pier spacing *'x/b'* is shown in Fig. 5.68. It can be noticed that for 33 mm front pier this variation is fairly constant except at pier spacing x/b=10, which is attributed to reinforcing effect of 66 mm rear pier. Fig. 5.68 shows a steep rise in the slope for 66 mm rear pier, at pier spacing $3<x/b\leq4$. On further increasing the pier spacing, the slope decreases and approaches to a value, which is nearly equal to the angle of repose of bed the material (*i.e.*, 32°). This variation is ascribed to the complex variation in the flow pattern occurring between the piers due to the interaction of 33 mm front pier wake and shed vortices with the horseshoe vortex at the 66 mm rear pier.

Fig.5.69 shows steep reduction in slope for downstream part of 33 mm front pier scour hole at pier spacing $3<x/b\leq12$ and this variation remains fairly constant upto pier spacing x/b=90, which is attributed to the complex flow pattern generated in between the piers.

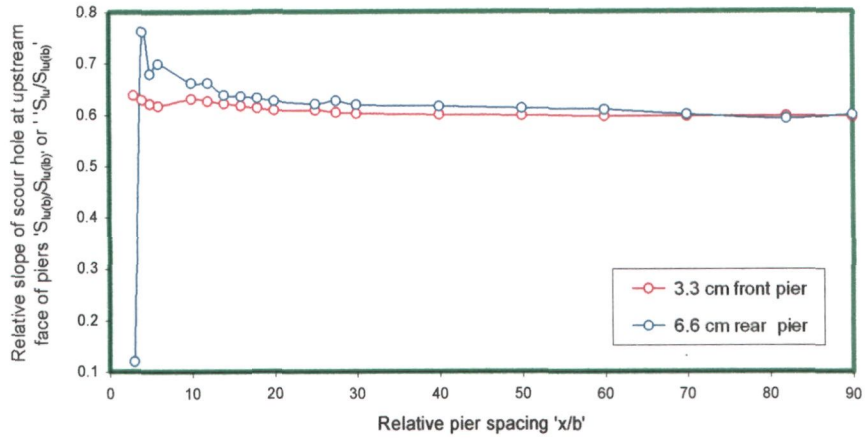

Fig. 5.68 Variation of relative slopes of scour holes at upstream face of 33 mm front and 66 mm rear piers placed in tandem arrangement '$S_{lu(f)}/S_{lu(bi)}$ and $S_{lu(r)}/S_{lu(bi)}$' with pier spacing 'x/b' (where $S_{lu(f)}$ = slope of scour hole at upstream face of 33 mm front pier, $S_{lu(r)}$ = slope of scour hole at upstream face of 66 mm rear pier, $S_{lu(bi)}$ = slope of scour hole at upstream face of 33 mm isolated pier, $S_{lu(Bi)}$ = slope of scour hole at upstream face of 66 mm isolated pier).

An increasing trend in the values of the upstream slope of 66 mm rear pier scour hole in the range of pier spacings $0<x/b\leq3$ can be seen in Fig. 5.68, after which the slope remains invariable upto pier spacing x/b=90.

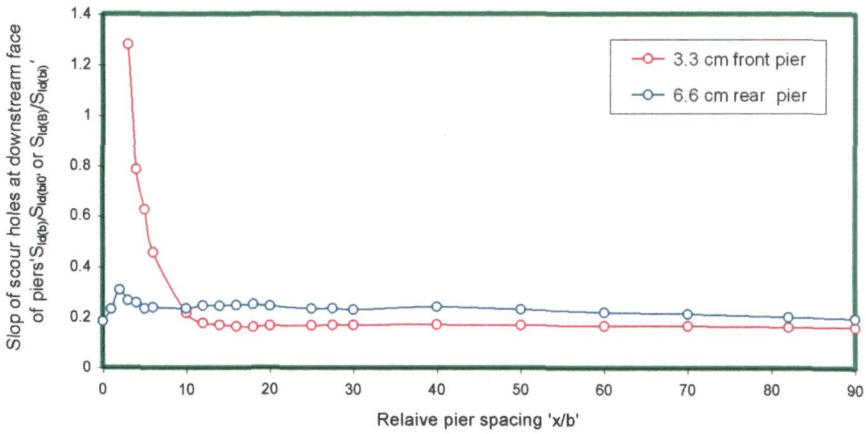

Fig. 5.69 Variation of relative slopes of scour holes at upstream face of 33 mm front and 66 mm rear piers '$S_{ld(f)}/S_{ld(bi)}$ and $S_{ld(r)}/S_{ld(bi)}$' with pier spacing 'x/b' (where $S_{ld(f)}$ = slope of scour hole at upstream face of 33 mm front pier, $S_{ld(r)}$= slope of scour hole at upstream face of 66 mm rear pier, $S_{ld(bi)}$ = slope of scour hole at upstream face of 33 mm isolated pier, $S_{ld(Bi)}$ = slope of scour hole at upstream face of 66 mm isolated pier).

(f) Variation of area of scour extent with pier spacing

Appendix-IV shows the areal extents of scour around 33 mm front and 66 mm rear piers in tandem arrangement for varied pier spacings *'x/b'*. A scrutiny of the Appendix-IV reveals that the areal extents of scour around the piers overlap one another upto *x/b*=40. Beyond this pier spacing areal extents of scour around piers become independent. As the pier spacing *'x/b'* approaches to 90, the shape and size of areal extents of scour around 33 mm front and 66 mm rear piers become similar to that around isolated 33 mm and 66 mm piers respectively. The areas of scour extents around 33 mm front and 66 mm rear piers are plotted against pier spacing *'x/b'* as shown in Fig. 5.70 The area of scour extent is observed to be in a decreasing trend between the pier spacing *x/b*=0 to 1. This effect is demonstrated experimentally such that 33 mm front pier deflects the flow laterally due to which the bed material scoured from the scour hole moves on the bed across the flow and does not get deposited over the larger length. At pier spacing *x/b*>1, the area of the extent of scour increases and reaches to a maximum at pier spacing *x/b*=40. This increase indicates the gradual decrease in sacrificial effect of 33 mm front pier due to which the bed material scoured from scour holes begins to deposit on the bed along the channel length.

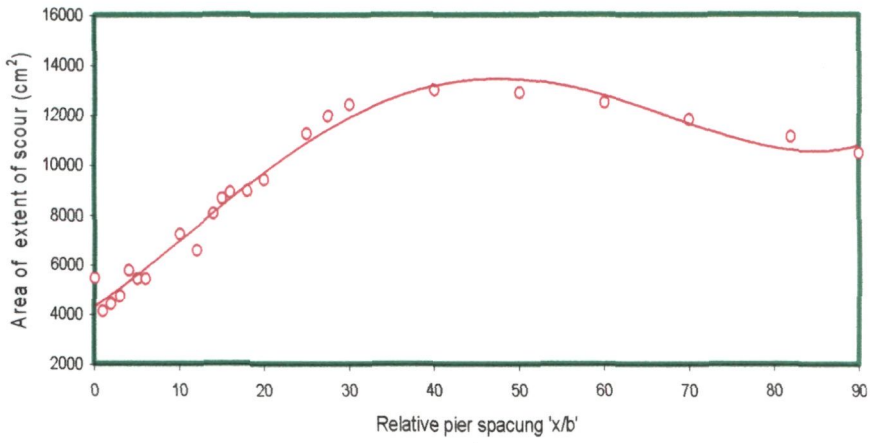

Fig. 5.70 Variation of area of extent of scour around 33 mm front and 66 mm rear piers placed in tandem arrangement with pier spacing *'x/b'*.

The decrease in the area of scour extent at pier spacings $x/b>40$, is due to the fact that the bed material between the piers deposits due to the presence of relatively calm and quite pocket of water in the wake of 33 mm front pier.

Photographs shown in Fig. P6 & P7 substantiate the interpretation of results on scour characteristics discussed above.

5.5.4 Temporal variation of scour

The data collected in this study on temporal variation of scour around 33 mm front and 66 mm rear piers placed in tandem arrangement are given in Appendix-I. From the plots of these data (not shown here), it is noticed that the rate of scouring at 66 mm rear pier lacks behind the 33 mm front pier up-to pier spacing $x/b= 70$. To ascribe a reason to this happening, it is worth mentioning that at short pier spacings, the bed material scoured from the 33 mm front pier scour hole moves into the scour hole of 6.6cm rear pier. As a result, the scour depth at the 33 mm front pier approaches to equilibrium earlier than at the 66 mm rear pier because flow takes more time to remove the bed material transported from the 33 mm front scour hole. Due to sheltering effect of the 33 mm front pier on 66 mm rear pier, the scour depth at 6.6cm rear pier remains smaller than the scour depth at 33 mm front pier. However, at larger pier spacing the bed material from 33 mm front pier scour hole does not reach to the scour hole of 66 mm rear pier and sheltering effect of 33 mm front pier also vanishes, the scour depths at 33 mm front and 66 mm rear piers approaches to equilibrium simultaneously. The scour depth attained for varied pier spacings at a particular time at 33 mm front and 66 mm rear piers in tandem arrangement can be obtained by plotting the data on temporal variation of scour depth given in Appendix-I.

5.5.5 Concluding remarks

At $0<x/b<5$, the scour depth considerably reduces at 66 mm rear pier. It can thus be argued that 33 mm front pier acts like a sacrificial pile for 66 mm rear pier. The scour depth at 33 mm front pier at pier spacing $x/b=0$ is observed to be maximum, however at $x/b=5$, the scour depth considerably reduces. Therefore, it is suggested that 66 mm rear pier be placed at $x/b=5$ from 33 mm front pier to achieve better economy.

5.6 Lateral Pier Arrangement

5.6.0 Introduction

To analyze the results obtained from present experiments on two piers of same size placed at right angles to the flow with varying lateral pier spacing Z_c/b, the longitudinal profiles of scour, areal extents of scour, lateral profiles of scour and temporal profile of scour are plotted as shown in Appendix-II, Appendix-III and Appendix-IV respectively.

Some distinctive cases of longitudinal profiles and areal extent of scour are used in this section for analysis and discussion. In order to have an insight into the characteristics of scour around laterally placed piers, the photographs showing the scour and deposition patterns around the piers are taken at the end of the tests and shown in Fig. P8.

5.6.1 Variation of scour depth along flume length

The data on scour depth collected in present study along the length of flume are plotted for varied lateral pier spacings 'Z_c/b' as shown in Appendix-II. It can be seen in Fig. 5.71 that the longitudinal profiles around two piers become considerably similar in size and shape signifying that the two piers start getting freed from the effect of mutual interference when the pier spacing 'Z_c/b' approaches to 7.

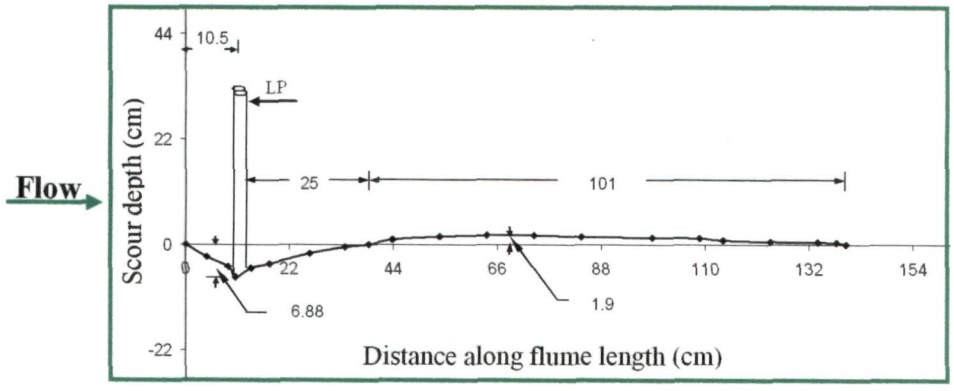

Fig.5.71 Variation of scour depth at piers placed in lateral arrangement at Z_c/b= 7

5.6.2 Variation of scour depth at front faces of piers

During experiments it was observed that both piers scoured to the same depth (± 3mm). Therefore, the maximum scour depths observed at two piers are averaged and plotted against lateral pier spacing 'Z_c/b' as shown in Fig. 5.72.

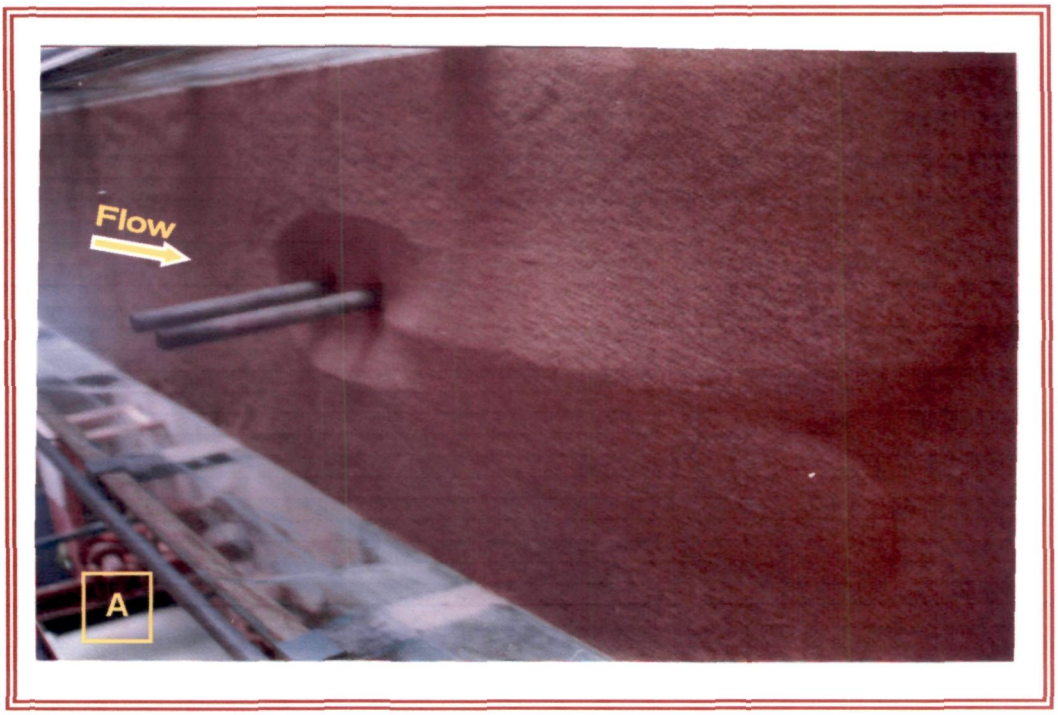

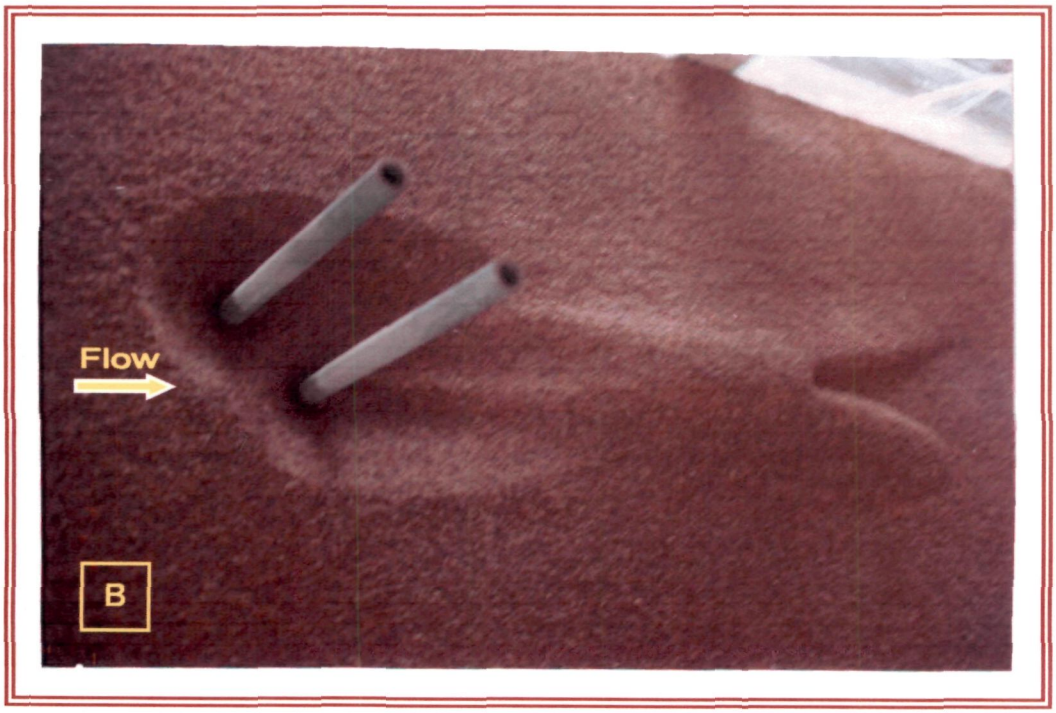

Fig. P13: Scour and deposition patterns around two piers aligned at constant radial spacing and varying angles of attack α (A) α=0° (B) α=45°

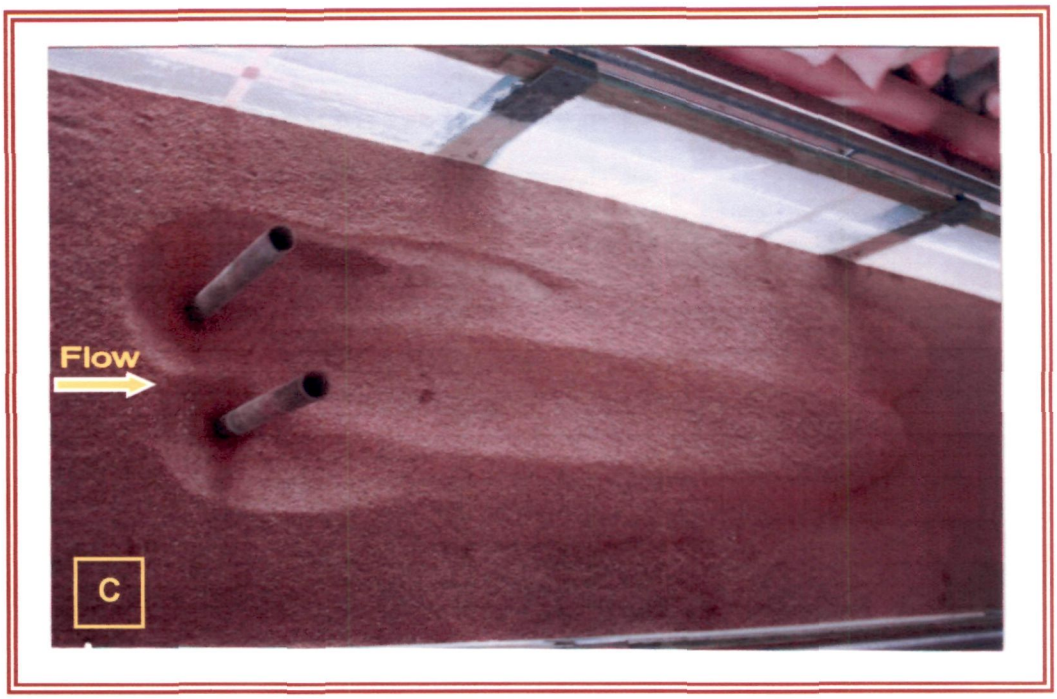

Fig. P14: Scour and deposition patterns around two piers aligned at constant radial spacing and varying angles of attack α (C) α=75° (D) α=90°

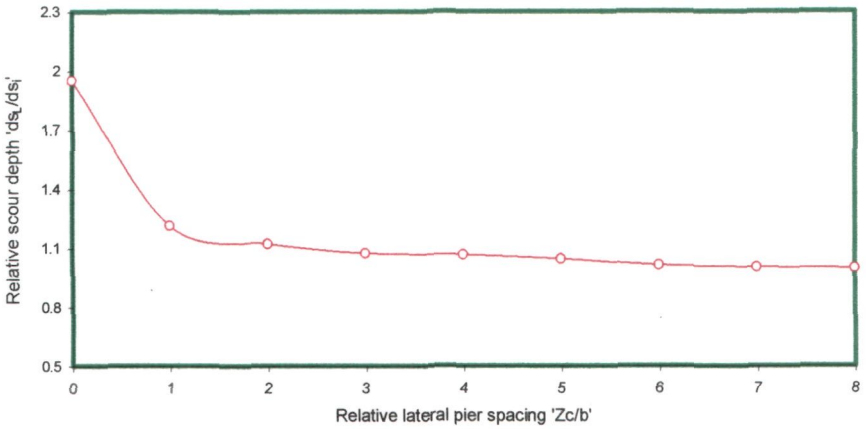

Fig.5.72 Variation of relative scour depth at piers placed in lateral arrangement 'ds_L/ds_i' with pier spacing Z_c/b (where ds_L = scour depth at lateral piers, ds_i = scour depth at an isolated pier).

The maximum scour depth at two piers having their line of centres at 90° to the approach flow is sensitive to the lateral spacing 'Z_c/b' between them. At small lateral pier spacing 'Z_c/b', the inner arms of horseshoe vortices between two piers are compressed due to which the flow between the two piers gets accelerated and the strength of horseshoe vortices at two piers increases. This increase in the strength of horseshoe vortex causes an increase in the scour depth. When the pier spacing increases, the compression of horseshoe vortices between the two piers reduces and leads to a decrease in scour depth.

Appendix-II depicts the longitudinal scour profiles showing the maximum scour depth, length of scour holes and length of deposition.

The relative scour depth 'ds_L/ds_i' observed at the upstream face of two piers are plotted against relative lateral pier spacing 'Z_c/b' as shown in. Fig.5.72.

It is worth mentioning that when the two piers are placed at lateral pier spacing Z_c/b=0, the scour depth ds_L is about 1.95 time's ds_i. This is in accordance with the concept of scour depth being proportional to the frontal width of the pier. The scour depth reduces rapidly with piers separation and reaches to about 1.21 (*i.e.*, 'ds_L' about 21% more than 'ds_i') at lateral pier spacing Z_c/b=1. The reason for this scour depth being more at Z_c/b=1 is the increase in the strength of horseshoe vortex caused by the compression of inner limbs of horseshoe vortices between the two piers. As the pier spacing Z_c/b increases, the effect of compression of horseshoe vortices reduces. Thereafter, the scour depth reduces gradually and reaches to that of an isolated pier at lateral pier spacing Z_c/b=8.

The scour depths observed at the nose of piers relative to the front width of piers '*ds/2b*' are plotted against lateral pier spacing 'Z_c/b' as shown in Fig. 5.73.

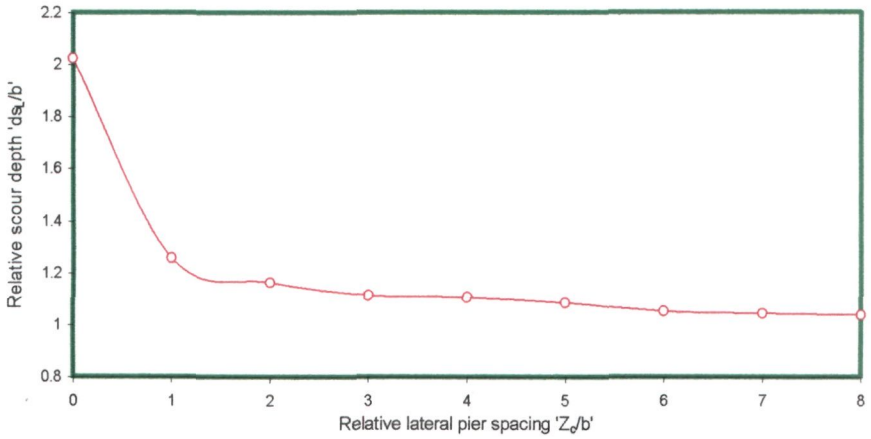

Fig. 5.73 Variation of scour depth at piers placed in lateral arrangement relative to the pier width 'ds_I/b' with pier spacing '*Zc/b*' (where ds_L = scour depth at lateral piers, b= pier diameter).

It can be noticed that the value of '*ds/2b*' at pier spacing Z_c/b=0 is about 2.03 times of that observed at an isolated pier. It is noteworthy that the value of '*ds/2b*' rapidly reduces to 1.26 as lateral pier spacing Z_c/b approaches to 1. This decrease in the value of 'ds_I/ds_i' occurs due to decrease in frontal width. Beyond $Z_c/b=1$, the value of 'ds_I/ds_i' gradually decreases and reaches very near to unity. This decrease in the values of 'ds_I/ds_i' with pier spacing 'Z_c/b' is due to reduction in the effect of compression of horseshoe vortices between the piers.

To accomplish the task of modeling, ANN models the details of which are given in Tables 6.1 and 6.2 (Chapter VI) and ANN architectures Fig.6.5 (Chapter VI), are applied to authors experimental data collected on two piers placed in lateral arrangement at varied lateral pier spacings *Zc/b* to estimate the scour depth at two piers. Scatter grams plotted between ANN estimated and observed scour depths are shown in Fig. 6.15 (Chapter VI). The values of correlation coefficient R^2 and *rmse* between observed and ANN estimated scour depth are given in Table 6.2 (Chapter VI). The closeness of the data points to the line of best agreement shown in scatter grams indicates that ANN models produce excellent estimates of scour depth. The lower *rmse* values also signify the predictive ability of ANN models.

5.6.3 Scour hole characteristics

It was experimentally observed that the flow accelerated between the piers placed at right angles to flow at shorter pier spacings *'Zc/b'* which resulted in an increase in the strength of horseshoe vortices at two piers. As a result of this the scour depth increased for same flow, sediment and pier conditions. The characteristics of scour hole vary with the variation in lateral pier spacing *'Z_c/b'*. The analysis of important characteristics of scour holes like, length and slope of scour holes at the upstream and downstream face of piers, length of sediment deposition at downstream face of piers, width of scour holes and areal extent of scour are discussed in the successive sections.

Since the knowledge of scour holes dimensions is imperative in determining the extent of countermeasures needed to prevent/control scour at piers, various parameters explained as under using present experimental data are determined.

(a) Length of scour holes

The length of scour holes measured at the upstream and downstream face of two piers relative to that of an isolated pier are plotted against lateral pier spacing *'Z_c/b'*, as shown in Figs. 5.74 and Fig. 5.75.

(b) Length of scour hole at upstream faces of piers

The relative lengths of scour hole at upstream face of piers *'$L_{shu(L)}/L_{shu(i)}$'* are plotted against lateral pier spacing *'Z_c/b'* as shown in Fig. 5.74.

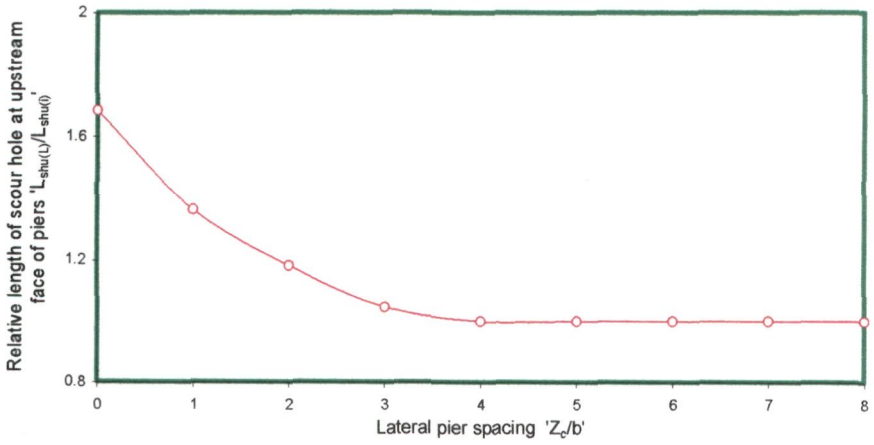

Fig.5.74 Variation of relative length of scour holes at upstream faces of piers placed in lateral arrangement *'$L_{shu(L)}/L_{shu(i)}$'* with pier spacing *'Z_c/b'*(where $L_{shu(L)}$ = length of scour hole at upstream face of lateral piers , $L_{shu(i)}$ = length of scour hole at upstream face of an isolated pier).

It is observed that the length of scour hole at upstream face of piers '$L_{shu(L)}$' at lateral pier spacing Z_c/b=0, is about 1.68 times more, than at an isolated pier. This increment occurs due to more frontal width of piers at Z_c/b=0. As the pier spacing Z_c/b increases, frontal width decreases due to gap created between two piers as a result of which '$L_{sh\ u(L)}/L_{shu(i)}$' decreases and a decrement of about 63.6 % is noticed at lateral pier spacing Z_c/b=3. Thereafter, a gradual decrease in the length of scour hole '$L_{shu(L)}/L_{shu(i)}$' is observed. This decrease is caused due to the reduction in the effect of compression of horseshoe vortices at piers with increasing pier spacing Z_c/b. The values of '$L_{shu(L)}/L_{shu(i)}$' gradually reaches close to unity at lateral pier spacing Z_c/b=8, which indicates the disappearance of effect of mutual interference between the piers.

(c) Length of scour hole at downstream faces of piers

The relative length of scour holes at the upstream face of piers are plotted against lateral pier spacing 'Z_c/b' as shown in Fig. 5.75.

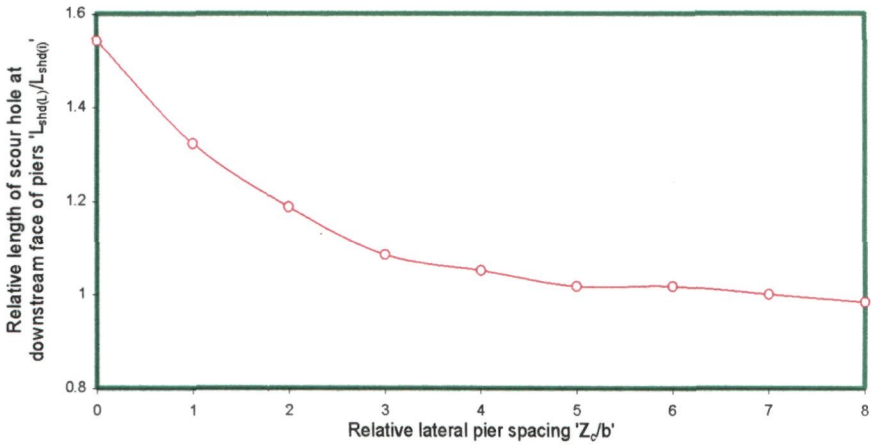

Fig. 5.75 Variation of relative length of scour holes at downstream faces of piers placed in lateral arrangement '$L_{shd(L)}/L_{shd(i)}$' with pier spacing 'Z_c/b' (where $L_{shd(L)}$ = Length of scour hole at downstream face of lateral piers, $L_{shd(i)}$ = length of scour hole at downstream face of an isolated pier).

Fig. 5.75 reveals that the length of scour hole '$L_{shd(L)}$' at lateral pier spacing Z_c/b=0, is about 1.51 times more than what is observed at an isolated pier. This increment in the value of '$L_{shd(L)}/L_{shd(i)}$' occurs due to more frontal width of piers at Zc/b=0. As the pier spacing Z_c/b increases, separation of piers causes a decrease in the value of '$L_{shd(L)}/L_{sh\ d(i)}$' and a decrement of about 42.6% in the value of '$L_{shd(L)}/L_{shd(i)}$' is noticed at lateral pier spacing Z_c/b=3. As pier spacing Z_c/b further increase, the increment in the pier spacing

Z_c/b causes a reduction in the effect of compression of horseshoe vortices between the two piers which consequently causes a decrease in the value of '$L_{shd(L)}/L_{sh\ d(i)}$'. At lateral pier spacing Z_c/b=8, the value of '$L_{shd(L)}/L_{shd(i)}$' approaches to unity which suggests the disappearance of the effect of compression of horseshoe vortices between the two piers.

(d) Slope of scour holes

(i) Slope of scour holes at upstream faces of piers

The slope of scour holes observed at the upstream face of two piers relative to the slope observed at upstream face of an isolated pier '$S_{lu(L)}/S_{lu(i)}$' are plotted against lateral pier spacing 'Z_c/b' as shown in Fig. 5.76. At Z_c/b=0, frontal width of piers is more, therefore, the size of scour hole is more, however, increase in length of scour hole is not proportional to the increase in the scour depth. As a result, higher value of '$S_{lu(L)}/\ S_{lu(i)}$' can be seen in Fig. 5.76 at Z_c/b =0. As the pier spacing Z_c/b increases, frontal width decreases due to separation of piers.

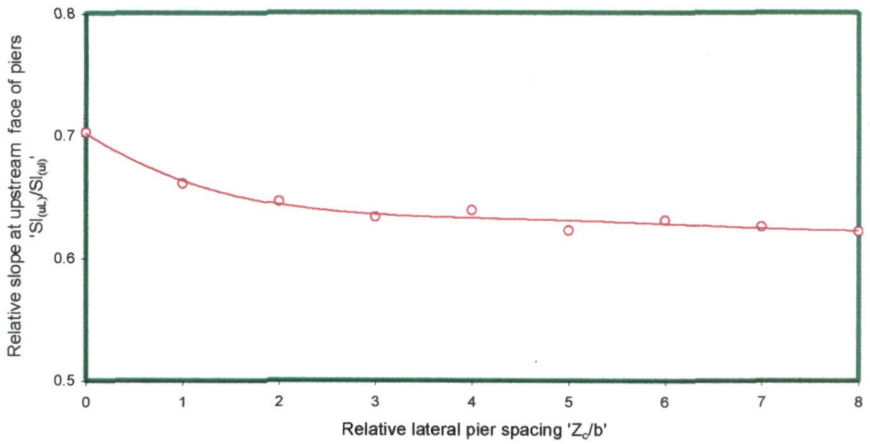

Fig. 5.76 Variation of relative slopes of scour holes at upstream face of piers placed in lateral arrangement '$S_{lu(L)}/S_{lu(i)}$' with pier spacing 'Z_c/b' (where $S_{lu(L)}$ = slope of scour hole at upstream face of lateral piers, $S_{lu(i)}$ = slope of scour hole at upstream face of an isolated pier).

With further increase in pier spacing Z_c/b, the slope '$S_{lu(L)}/S_{lu(i)}$' approaches to unity which is a pointer towards the state of two piers being free from mutual interference.

(ii) Slope of scour holes at downstream faces of piers

Fig. 5.77 shows the relative slope of scour holes at the downstream face of two piers '$S_{ld(L)}/S_{ld(i)}$' with respect to the lateral pier spacing 'Z_c/b'.

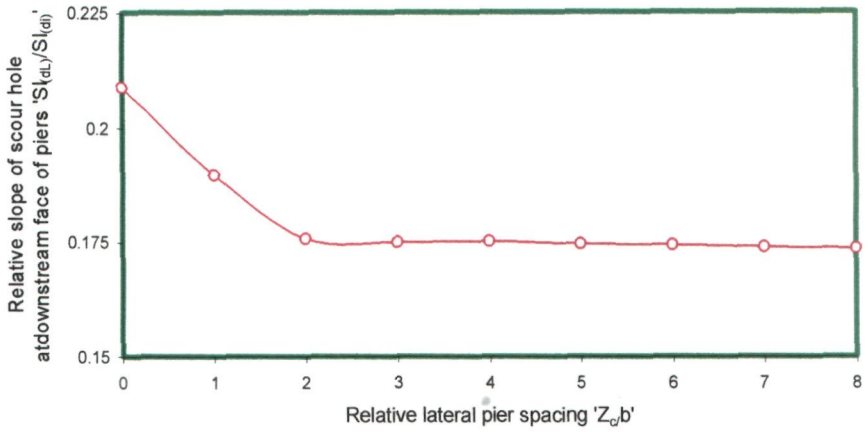

Fig. 5.77 Variation of slope of scour holes at downstream face of piers placed in lateral arrangement '$S_{ld(L)}/S_{lu(i)}$' spacing with pier spacing Z_c/b (where $S_{ld(L)}$ = slope of scour hole at downstream face of lateral piers, $S_{ld(i)}$ = slope of scour hole at downstream face of an isolated pier).

At shorter values of Z_c/b, inner arms of horseshoe vortices at downstream faces of two piers are compressed as a result of which the flow is accelerated between the piers and causes increased scour depths to occur, however, as shown in Figs.5.72 and 5.75, this increment in scour depth is not in proportion to the increase in the length of scour hole. Consequently, increased values of '$S_{ld(L)}/S_{ld(i)}$' at pier spacing $Z_c/b=2$ are resulted. However, as noticed in Fig. 5.77, at pier spacings $Z_c/b\geq2$, the of slope of scour holes at the downstream face of piers is close to that observed at an isolated pier which indicates the diminishing state of mutual interference effect of piers.

(e) Variation of area of scour extents with pier spacing

The areal extents of scour around the two laterally placed piers are plotted for varied pier spacings 'Z_c/b' and shown in Appendix-I. It can be seen in Fig. 5.78 that the areal extents of scour around the two piers overlap each other upto pier spacing $Z_c/b=6$.

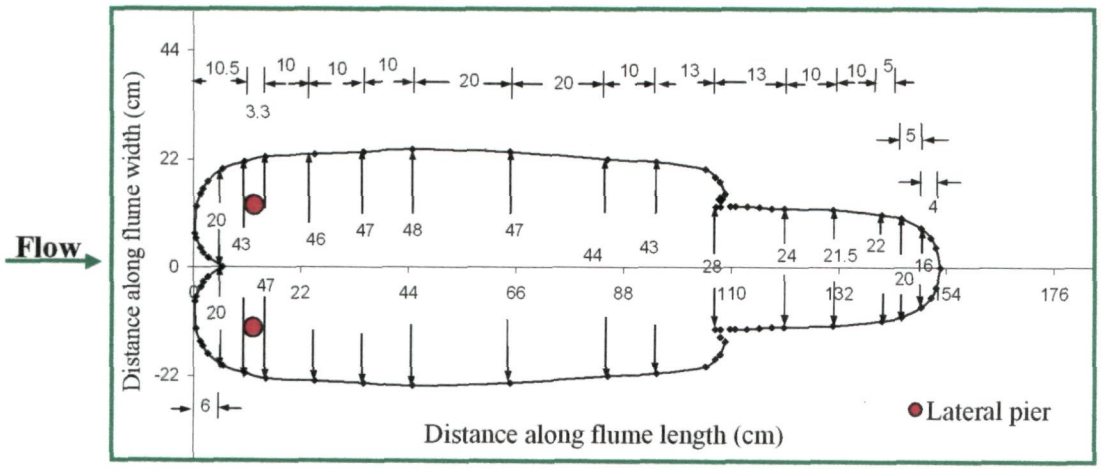

Fig. 5.78 Areal extent of scour around the piers placed in lateral arrangement at $Z_c/b=6$

It is clear from Fig. 5.79 that the extents of scour get partially separated from one another at Z_c/b=7.

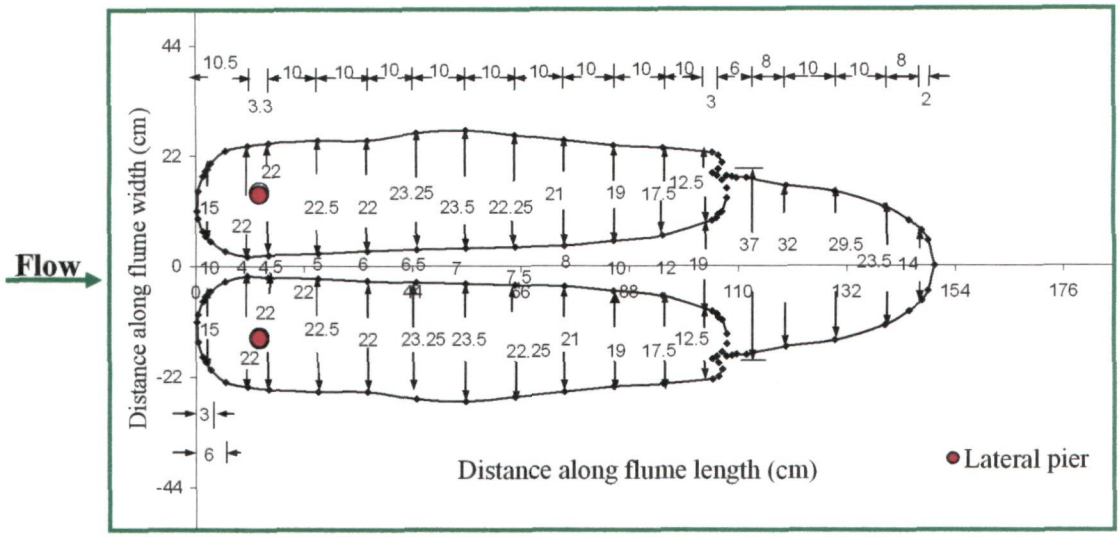

Fig. 5.79 Areal extent of scour around the piers placed in lateral arrangement at Z_c b=7

However, at pier spacing Z_c/b=8, as illustrated in Fig. 5.80, the areal extents of scour get completely separated from each other and become similar in shape and size to that around an isolated pier, demonstrating that the two piers become free of effects of mutual interference.

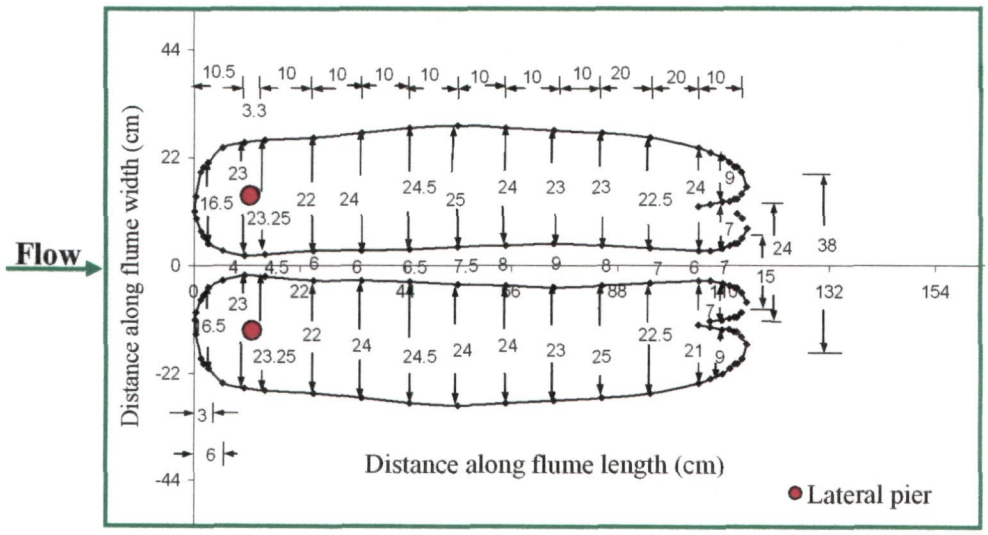

Fig.5.80 Areal extent of scour around the piers placed in lateral arrangement at Z_c b=8

The areas of scour extents around the lateral piers estimated from the plots of areal extent of scour Appendix-IV are divided by twice the area of scour extent estimated for an

isolated pier to obtain the relative areas of the scour extent '$A/2A_i$' and the same are plotted against lateral pier spacing 'Z_c/b' as shown in Fig.5.81.

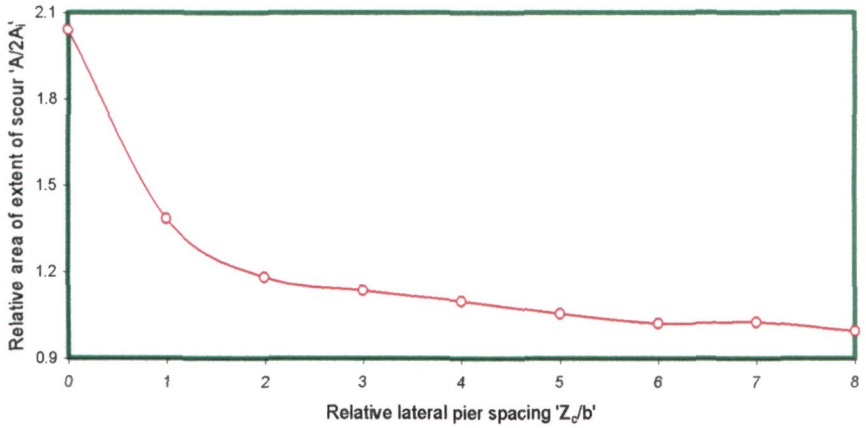

Fig. 5.81 Variation of relative area of scour extent around two piers placed in lateral arrangement '$A_L/2A_i$' with pier spacing Z_c/b (where A_L = area of scour extent around the lateral piers, A_i= area of scour extent around an isolated pier).

It is noticed that the value of '$A_L/2A_i$' is maximum at pier spacing Z_c/b=0. This maxima occurs, since, as the frontal width of piers at this pier spacing is twice that of an isolated pier. At Z_c/b=1, a rapid decrease of 65.55 % in the value of '$A_L/2A_i$' is observed. Appendix-IV shows a remarkable difference between the areal extents of scour at pier spacing Z_c/b=0 and Zc/b>0; which is because of entirely different flow mechanism at these pier spacings.

At lateral pier spacing Z_c/b=1,2,3,4 and 5, the values of areas of scour extent '$A_L/2A_i$' are about 38.5%, 18%, 13.45,10% and 5.4% times more than that at an isolated pier. The values of areas of scour extent '$A_L/2A_i$' gradually decrease and reach close to that at an isolated pier at lateral pier spacing Z_c/b=8. When the pier spacing between two piers Z_c/b increases beyond 1, the flow pattern around two piers become similar to around an isolated pier due to which area of scour extent '$A_L/2A_i$' decreases and approaches to that of an isolated pier.

(f) Width of scour holes

The top width of scour hole 'w_L' at two lateral piers is the horizontal distance between the outer edges of the scour hole measured along flume width across the noses of two piers. The top width of scour hole of a single pier can be estimated from the relationship of Richardson *et al.* 1993, (refer Chapter II) therefore, top widths 'w_L' are divided by twice

the top width of an isolated pier to obtain the relative width $w_L/2wi$, which are plotted against relative pier spacing Z_c/b as shown in Fig. 5.82.

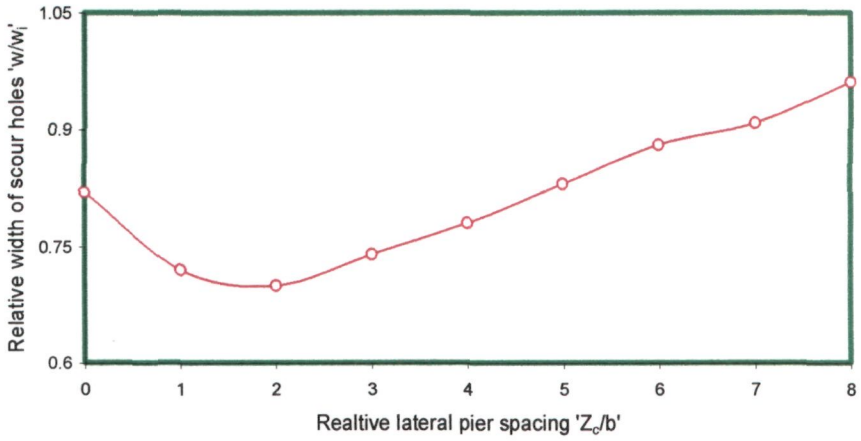

Fig.5.82 5.52 Variation of relative width of scour holes of piers placed in lateral arrangement '$w_L/2w_i$' with pier spacing Z_c/b. (where w_L = width of scour hole of two lateral pier, w_i= width of isolated pier).

The top width 'w_L' measured at Z_c/b=0 is 1.64 times of top width of a single 'w_i' pier. This increase in width of scour hole is attributed to more frontal width of piers at this pier spacing as the depth of scour and hence the top width of scour hole are directly proportional to the frontal width of pier. When the two piers are separated from one another, the frontal width decreases as a result of which the scour depth decreases and consequently the top width of scour hole decreases. Fig.5.82 shows that the value of '$w/2w_i$' reduces to 0.72 at pier spacing Z_c/b=1. However, the value of '$w/2w_i$' increases between pier spacings Z_c/b=1 and 8. This increase in the values of '$w/2w_i$' is caused due to an increase in pier spacing 'Z_c/b' since the lateral distance between the outer edges of scour extent increases with pier spacing Z_c/b. The value of '$w/2w_i$' approaches nearly equal to 0.92 at pier spacing Z_c/b=8, which indicates the diminishing state of mutual interference of piers.

(g) Length of sediment deposition at downstream faces of piers

The length of sediment deposition '$L_{dep(L)}$' occurring at the downstream face of piers at varied pier spacing 'Z_c/b' are shown in Appendix-III. These lengths '$L_{dep(L)}$' are divided by the length of sediment deposition '$L_{dep\ (i)}$' occurring at the downstream face of an

isolated pier and the values of relative length of sediment deposition '$L_{dep(L)}/L_{dep(i)}$' are plotted with respect to the pier spacing 'Z_c/b' as shown in Fig. 5.83.

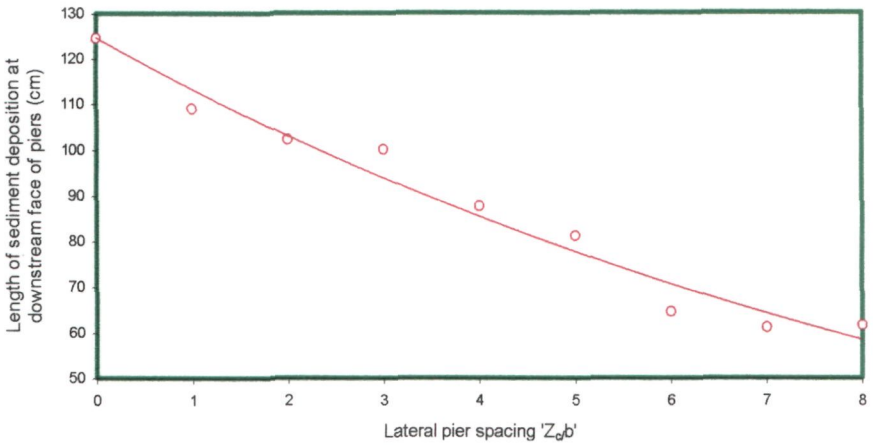

Fig. 5.83 Variation of length of sediment deposition at downstream face of two piers placed in lateral arrangement '$L_{dep(L)}$' with pier spacing 'Z_c/b'

It can be seen that at pier spacing Z_c/b=0, the value of '$L_{dep}/L_{dep(i)}$' is maximum. This maxima is due to the fact that at Z_c/b=0, frontal width of piers is equal to twice the width of an isolated pier. It is also evident that '$L_{dep}/L_{dep(i)}$' decreases with an increase in pier spacing Z_c/b, since, the increment in pier spacing Z_c/b causes decrease in frontal width and thereby a decrease in the length of sediment deposition. At pier spacing Z_c/b=8, the length of sediment deposition approaches to that measured at an isolated pier.

Photographs shown in Fig. P8 authenticate the interpretation of results on scour characteristics analyzed and discussed above.

5.6.4 Temporal variation of scour depth

The data collected in this study on temporal variation of scour depth at two piers placed in transverse arrangement are given in Appendix-I. The plots of these data (not shown here), reveal that the rate of scour depth decreases as the lateral pier spacing '*Zc/b*' increases. At '*Zc/b*' = 8, the rate of scouring at two piers tends to become identical to that at an isolated pier. To understand the rationale behind this decrement is the fact that at large lateral pier spacing *Zc/b*, the inner arms of the horseshoe vortices around the two piers cease to interfere with each other which causes a decrease in the effect of compression of horseshoe vortices around the two piers. As a result the scouring strength and rate of scouring at two piers decreases.

5.6.5 Concluding remarks

Compression of horseshoe effect is the dominant effect on the scour depth at two piers of same size placed at right angles to the flow. At Zc/b=0, the maximum scour depth is observed as 1.95 times of that at an isolated pier. At Zc/b=1, the scour depth, though rapidly decreases but remains 21 % deeper than that an isolated pier. At Zc/b=6, the scour depth nearly approaches to that at an isolated pier. At Zc/b=8, the scour depth virtually becomes free from mutual interference and the scour holes developed around two piers assume the same shape and size as that of an isolated pier. Based on the findings of this research it can be suggested that the two piers should be placed at $Zc/b \geq 8$ to achieve economy in design and construction of piers.

5.7 Staggered Arrangement of Piers

5.7.0 Introduction

In order to analyze the results obtained from present experiments for the case of local scour at three piers placed in staggered arrangement, the longitudinal scour profiles, lateral profile of scour hole and areal extents of scour are plotted against relative pier spacing *'x/b'*. Longitudinal scour profiles illustrating the scour depths and length of scour holes are shown in Appendix-II. The lateral cross-sections of scour holes are shown in Appendix-III and the areal extents of scour showing scour hole widths at the piers are shown in Appendix-IV. The temporal variation of scour depth is presented in Appendix-I. Some distinctive cases of areal extent of scour and longitudinal profile of scour are considered herein for analysis and discussion. In order to analyze the results on scour around staggered piers, photographs showing scour and deposition patterns developed around the piers were taken at the end of each experiment. Photographs for some typical pier cases are shown in Figs. P9 & P10.

As the objective of this part of present study is to investigate the effect of longitudinal spacing between upstream and downstream piers placed in staggered arrangement on bridge pier local scour, the transverse pier spacing between the upstream piers is kept same at Z_c/b=9 since at this transverse pier spacing the effect of compression of horseshoe vortices between the two transverse piers is negligible as found in present study (Section 5.6 of this chapter) and also reported by Hannah (1978). The analysis of results achieved from experiments in this part of present study is carried out under the following heads:

5.7.1 Variation of scour depth along flume length

In order to analyze the results obtained from present experiments on staggered piers arrangement, the scour depths at upstream and downstream piers along flume length in flow direction are plotted for varied longitudinal pier spacing 'X_c/b' and shown in Appendix-II. The depth of local scour, length of the scour holes at the upstream and downstream faces of piers and length of sediment deposition at the downstream face of piers, are illustrated in these longitudinal scour profiles. It can be seen that at short pier spacing 'X_c/b', the rate of scouring at downstream pier remains higher than the upstream ones owing to the increased scour intensity caused by the approachment of flow from two upstream piers at an angle of attack 'α' up-to 45°. However, as the pier spacing 'X_c/b' increases to 90, the total angle of attack of two upstream piers falls below 7.5° at which the effect of angle of attach at downstream pier becomes insignificant. As a result, the rate of scouring at upstream and downstream piers becomes identical to that at an isolated pier.

5.7.2 Scour depth variation at upstream and downstream piers

The relative scour depths measured at upstream piers '$d_{s(u)}/ds_{(i)}$' and downstream pier '$d_{s(d)}/ds_{(i)}$' are plotted against the relative pier spacing 'X_c/b' as shown in Fig.5.84. It is observed that the scour depth at upstream and downstream piers initially increases with pier spacing and reaches to a maximum at pier spacing X_c/b=10. The reason for this maxima in scour depth at the downstream pier at X_c/b=10, can be attributed to the approaching flow, which after interacting with the two upstream piers, approaches to the downstream pier at such an angle of attack at which the strength of horseshoe vortex at downstream pier is highly enhanced. The arrangement of two upstream piers at lateral pier spacing Z_c/b = 9 and downstream pier at longitudinal pier spacing X_c/b = 10 produces an angle of attack of 22.25° each with the two upstream piers. As a result, the total effective angle of attack equals to 45° which has been found to be the most critical angle of attack producing severe effect on scour depth (Hannah, 1978). At pier spacing X_c/b>10, the scour depth at the downstream pier decreases with increasing pier spacing and reaches to a minimum at X_c/b=40. Thereafter, it increases upto pier spacing X_c/b=65 and then remains invariable upto X_c/b=90. The decrease in scour depth at the downstream pier at $10<X_c/b\leq40$, is attributed to the sheltering of downstream pier by the wakes of upstream piers due to which the velocity of flow approaching towards downstream pier decreases.

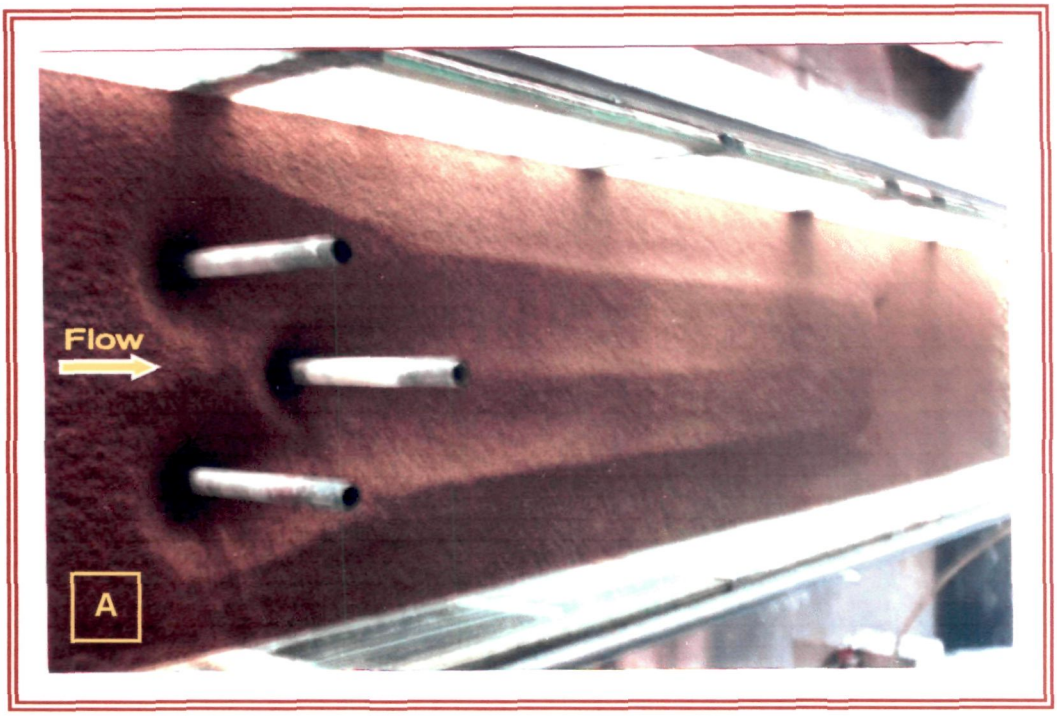

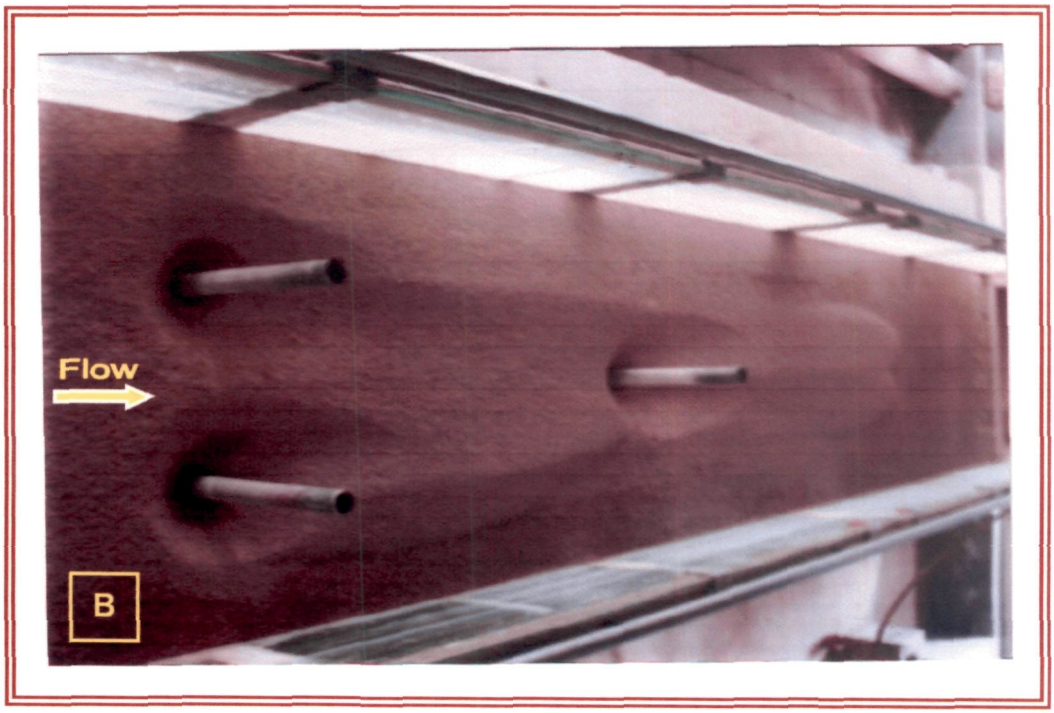

Fig. P9: Scour and deposition patterns around three piers of same size placed in staggered arrangement at varied pier spacing *Xc/b* (A) *Xc/b*=5 (B) *Xc/b*=20

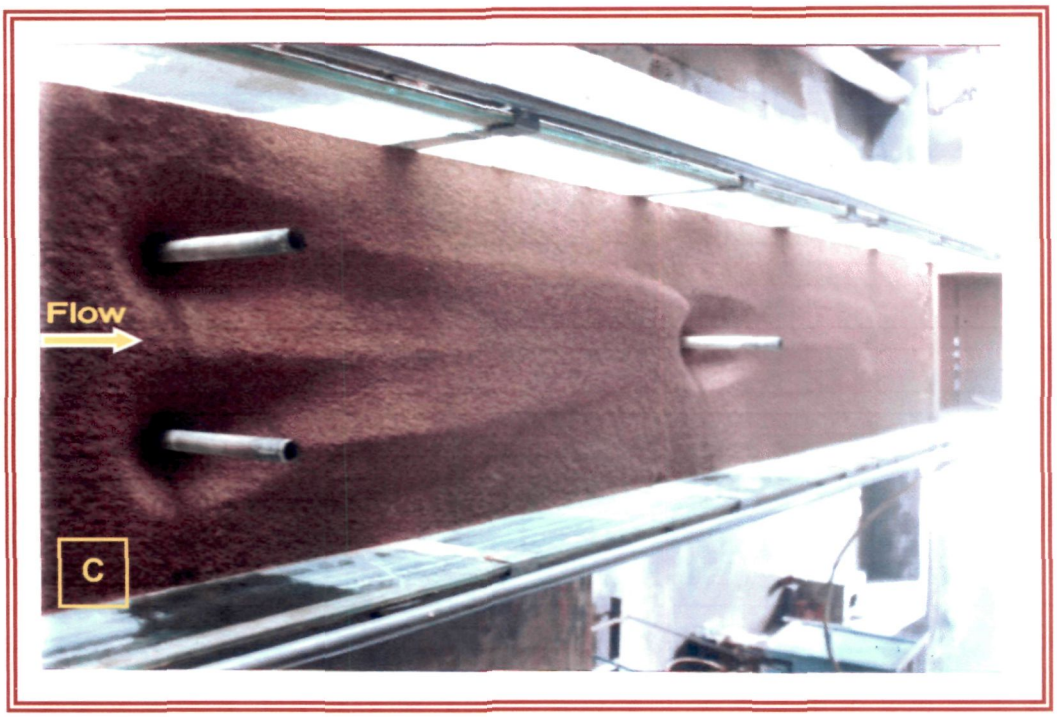

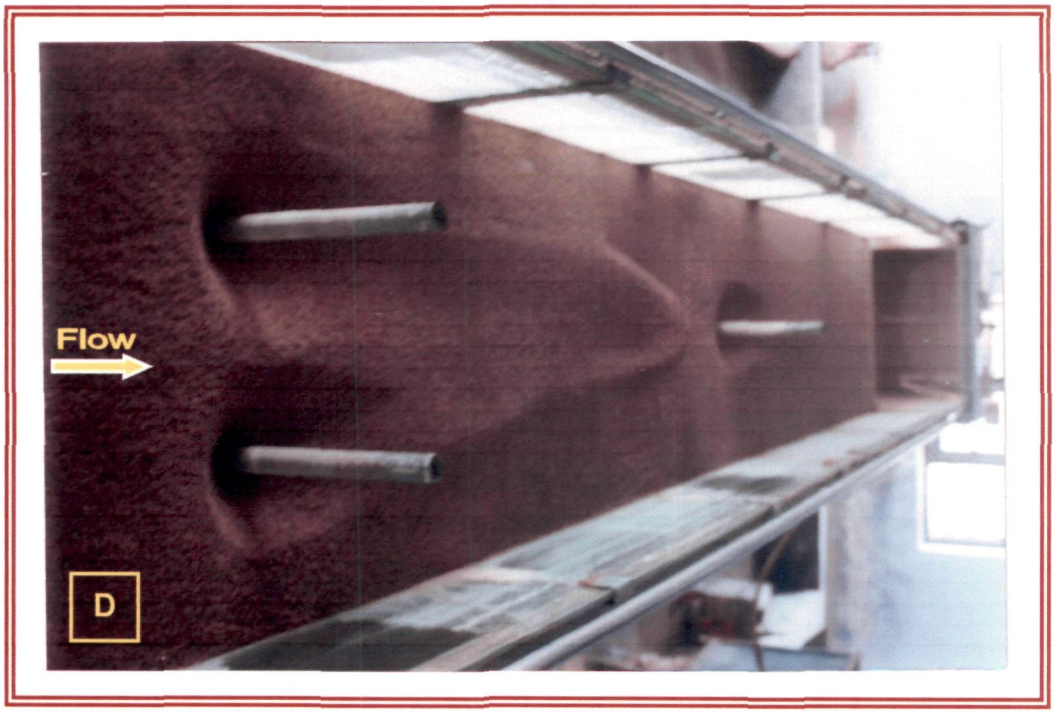

Fig. P10: Scour and deposition patterns around three piers of same size placed in staggered arrangement at varied pier spacing *Xc/b* (C) *Xc/b*=50 (D) *Xc/b*=60

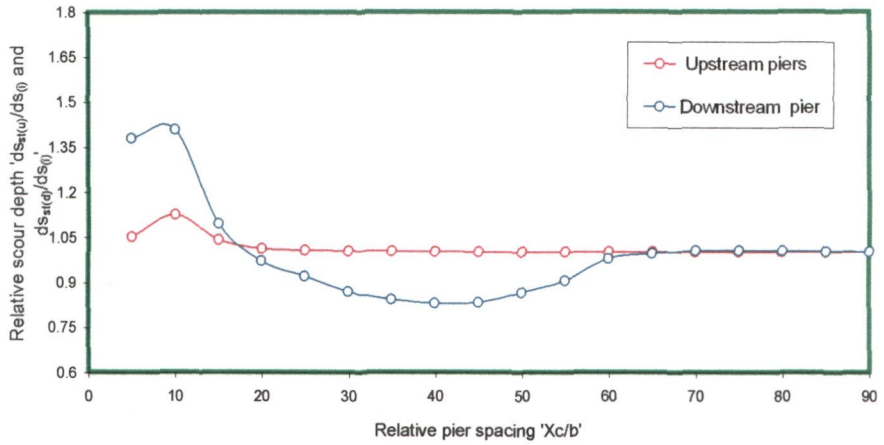

Fig. 5.84 Variation of relative scour depth at upstream and downstream piers placed in staggered arrangement '$d_{st(u)}/ds_{(i)}$' and '$ds_{st(d)}/ds_{(i)}$' with pier spacing X_c/b (where $ds_{st(u)}$ = scour depth at upstream piers, $ds_{st(d)}/ds_i$ =scour depth at downstream pier and $ds_{(i)}$ = scour depth at isolated pier).

Also, at these pier spacings, the total effective angle of attack produced by the upstream piers remains $\leq 30°$ which causes less effect on the scour depth as investigated by Hanna (1978). The increasing trend in scour depth at downstream pier at $40<X_c/b\leq65$ indicates an increase in the velocity of flow approaching towards downstream pier due to the reduction in the sheltering effect of wakes of upstream piers. At $X_c/b\geq65$, the downstream pier goes out of the wake region of upstream piers as a result of which the velocity of flow approaching to the downstream pier regains its original value and the scour depth remains fairly constant and is same as that of an isolated pier upto pier spacing $X_c/b=90$. Another reason for the scour depth being constant can be attributed to the total effective angle of attack produced by the upstream and downstream piers at longitudinal pier spacing $65<X_c/b\leq90$ being less than 7.5° which has an insignificant effect on the scour depth as established by Hannah (1978).

The increase in scour depth at the upstream piers in the range $5<X_c/b\leq10$, is attributed to the reinforcing effect caused by the downstream pier, which remains dominant as evident from Fig. 5.84 upto $X_c/b=20$. Beyond this spacing, the reinforcing effect at upstream piers disappears almost completely and the scour depth becomes constant for pier spacing $20<X_c/b<90$.

5.7.3 Scour depth variation between upstream and downstream piers

Fig. 5.85 shows variation of bed level (*i.e.*, maximum scour depth) between upstream and downstream piers. It is observed that the bed level between the upstream and downstream piers decreases upto $X_c/b=30$, remains constant between pier spacing $X_c/b= 30$ to 60 and increases thereafter upto $X_c/b=90$.

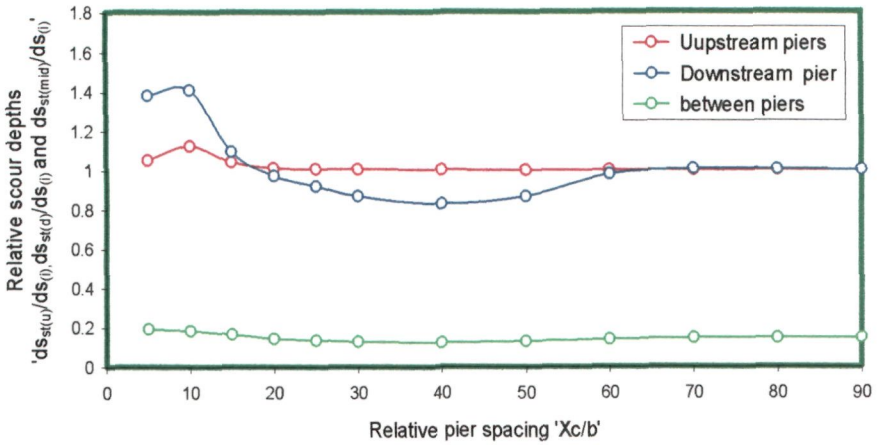

Fig.5.85 Variation of relative maximum scour depth at midway between upstream and downstream piers placed in staggered arrangement '$d_{st(mid)}/ds_{(i)}$' with pier spacing 'X_c/b' (where $d_{st(mid)}$= scour depth at midway between the piers, $ds_{(i)}$ = scour depth at isolated pier).

The decrease in bed level up-to X_c/b=30, is attributed to the shielding effect of wakes developed at the downstream end of the piers placed at the upstream. Bed level remains constant between X_c/b=30 to 60 due to the balance maintained between effects of shed vortices of upstream piers and shielding of wakes of upstream piers by downstream pier.. The increase in bed level between X_c/b= 60 and 90 is ascribed to a decrease in the shielding effect of wakes of upstream piers.

5.7.4 Scour depth variation at downstream pier with respect to upstream piers scour depth

The scour depth at downstream pier with respect to that at upstream piers '$ds_{st(d)}/ds_{(u)}$' are plotted against pier spacing 'X_c/b' as shown in Fig.5.86. It is observed that the relative scour depth at downstream pier '$ds_{st(d)}/ds_{(u)}$' decreases as the pier spacing 'X_c/b' increases and reaches to a minimum at pier spacing X_c/b=40.

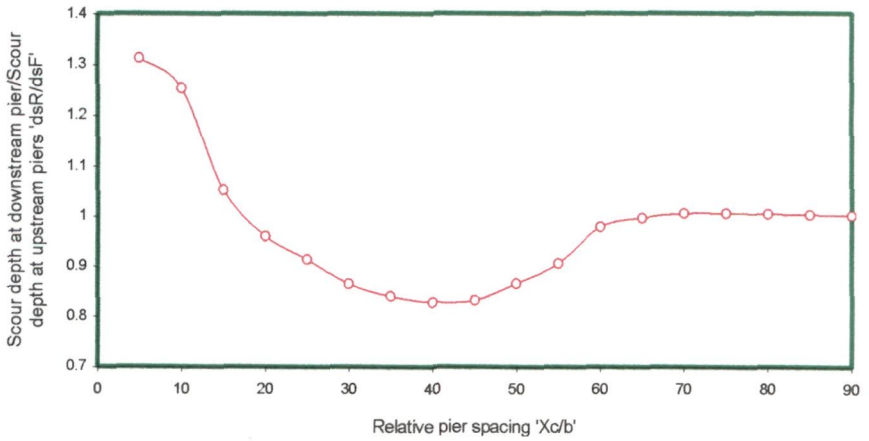

Fig. 5.86 Variation of relative scour depth at downstream pier with respect to that of upstream piers placed in staggered arrangement '$ds_{st(d)}/ds_{st(u)}$' with pier spacing 'X_c/b' (where, $ds_{st(u)}$ = scour depth at upstream piers, $ds_{st(d)}$ = scour depth at downstream pier).

This decrease in '$ds_{st(d)}/ds_{st(u)}$' is due to a decrease in the velocity of flow approaching towards downstream pier. This decrease in approach flow velocity is caused by the shielding of downstream pier by the wakes of upstream piers. At $40< X_c/b\leq65$, the shielding of the downstream pier by the wakes of upstream piers starts diminishing due to which, the velocity of flow approaching towards the downstream pier increases resulting in an increase the relative scour depth. '$ds_{st(d)}/ds_{st(u)}$' The value of '$ds_{st(d)}/ds_{st(u)}$' reaches to a maximum at pier spacing $X_c/b=65$. The constant value of '$ds_{st(d)}/ds_{st(u)}$' at $65<X_c/b<90$ indicates the complete disappearance of the shielding effect of wakes of upstream piers and the effect of angle of attack of flow as the total angle of attack produced at pier spacings $Z_c/b=9$ and $X_c/b=90$ is less than 7.5°.

ANN models with details given in Tables 6.1 and 6.2 (Chapter VI), have been applied to authors experimental data for the estimation of scour depth at upstream and downstream piers placed at varied longitudinal pier spacings *Xc/b*. The scatter grams between observed and ANN estimated scour depths are shown in Fig.6.16 (Chapter VI) The average values of correlation coefficient R^2 between observed and ANN estimated scour depths for upstream and downstream piers are evaluated from Table 6.2 (Chapter VI) as 0.8758 and 0.9912 respectively. Likewise, the average values of *rmse* for upstream and downstream piers from Table 6.2 (Chapter VI) are evaluated as $1.99\text{x}10^{-3}$ and $2.171\text{x}10^{-3}$ respectively. The lower values of *rmse* and higher values of R^2 signify the accuracy of scour depths estimated by ANN models.

5.7.5 Scour hole dimensions

Since the knowledge of scour hole dimensions is vital in determining the extent of countermeasures needed to prevent/control scour at piers, various parameters explained as under using present experimental data are determined.

(a) Length of scour holes

The variation of length of scour holes at the front and rear face of upstream and downstream piers against pier spacing 'X_c/b' is shown in Fig. 5.87 and Fig. 5.88 respectively. As evident from Fig. 5.86, the length of scour hole at front face of upstream piers increases upto $X_c/b\leq10$ due to reinforcing effect of downstream pier but, this effect diminishes thereafter, and as a result, scour hole length remains constant upto $X_c/b=90$.

As shown in Fig. 5.87, the length of scour hole at front face of downstream pier increases as X_c/b increases and reaches to a maximum value at X_c/b=10. The occurrence of maxima in the length of scour hole at this pier spacing can be attributed to the maximum enhancement in the strength of horseshoe vortex caused by the flow approaching towards downstream pier at 45° (*i.e.*, 22.5°+22.5°) angle of attack. At X_c/b>10 the length of scour hole at the front face of downstream pier decreases and reaches to a minimum value at Xc/b=60. The reason for this decrease is the shielding effect of wakes developed at the downstream end of upstream piers and also to the diminishing effect of the angle of attack being less than 30° (*i.e.*, total angle produced at pier spacings Z_c/b=9 and X_c/b=60).

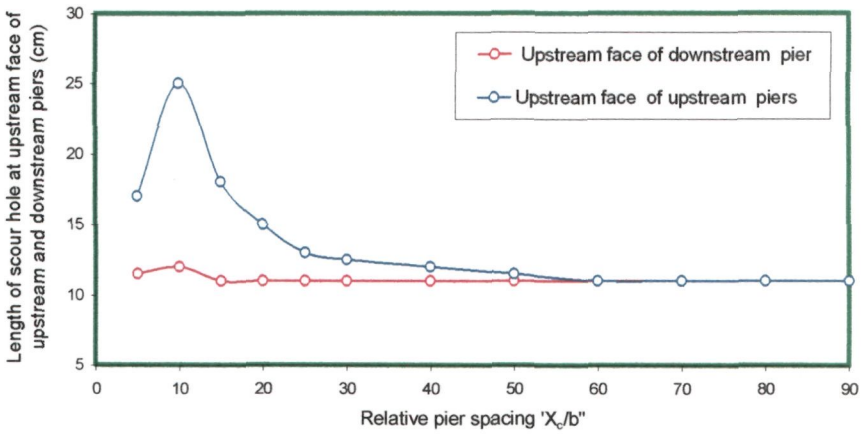

Fig.5.87 Variation of length of scour hole at front faces of upstream and downstream piers placed in staggered arrangement with pier spacing 'X_c/b'.

At 60<X_c/b≤90, the length of scour hole at the upstream face of downstream pier remains constant which indicates the diminishing state of the shielding effect of upstream piers wakes and the disappearance of effect of angle of attack because of it being less than 7.5°.

The variation in the length of scour holes at downstream face of piers is shown in Fig. 5.88. It is noticed that the length of scour hole at the downstream face of upstream piers increases as pier spacing 'X_c/b' increases and reaches to a maximum value at X_c/b= 10. This maxima in length of scour hole is caused by the reinforcing effect induced by the downstream pier. Between 10<X_c/b≤40, there is a steep reduction in the length of scour hole at downstream face of upstream piers which is due to sudden decrease in the reinforcing effect of the downstream pier and the development of complex flow pattern between upstream and downstream piers as a result of interaction of wake vortices of upstream piers and the horseshoe vortex around downstream pier.

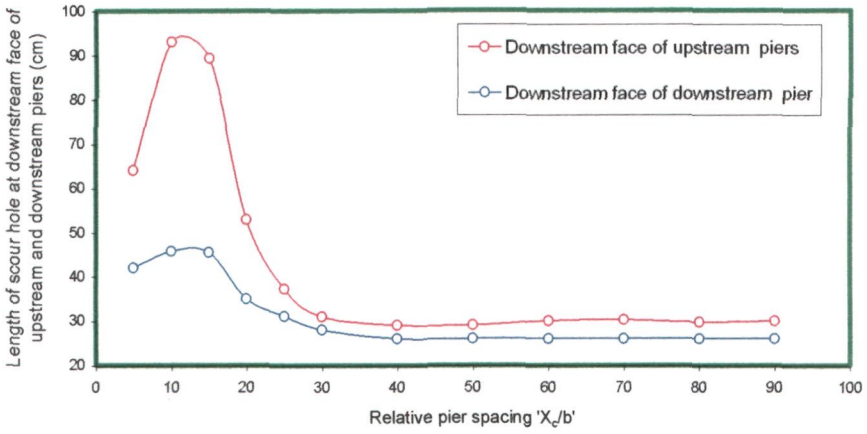

Fig. 5.88 (Chart 6) Variation of length of scour hole at rear faces of upstream and downstream piers placed in staggered arrangement with pier spacing *'X_c/b'*.

Fig.5.88 illustrates an increase in the length of scour hole at the rear face of downstream pier upto X_c/b=15. This increase is due to an enhanced scouring potential developed around downstream pier due to the approaching flow towards downstream pier at an angle of attack. The effect of angle of attack decreases beyond pier spacing x/b=15 and the length of scour hole reaches to minimum at X_c/b=40. The downstream pier remains free of these effects and the length of scour hole remains constant at pier spacings $40 \leq X_c/b \leq 90$.

(b) Width of scour holes

To study the effect of longitudinal pier spacing *'X_c/b'* on the scour hole width, the lateral profiles of scour holes at front face of upstream and downstream piers are plotted against varying pier spacings X_c/b and are shown in Appendix-III.

The scour hole widths at the upstream face of piers relative to the scour hole width at an isolated pier are plotted against pier spacing *'X_c/b'* as shown in Fig.5.89. This variation shows that the scour hole width at upstream piers *'w_1/b'* (where *'w_1'* is the horizontal distance normal to the flow direction along the noses of the upstream piers and measured between the outer edges of upstream piers scour holes) remains constant over the entire range of pier spacing except at *'X_c/b'* upto 10 which indicates that the reinforcing effect of downstream pier beyond pier spacing, X_c/b=10, does not significantly affect the relative width of scour holes.

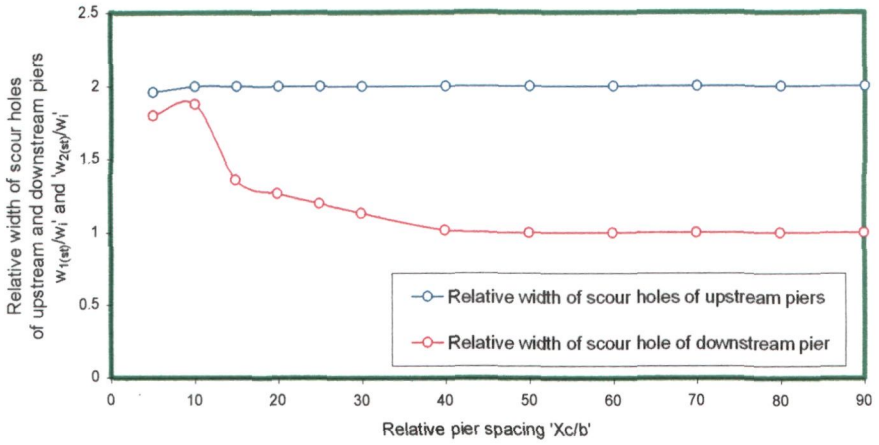

Fig. 5.89 Variation of relative width of scour hole of upstream and downstream piers placed in staggered arrangement $w_{1(st)}/w_i$ and $w_{2(st)}/w_i$ with pier spacing 'X_c/b' (where $w_{1(st)}$= width of upstream piers scour hole, $w_{2(st)}$ = width of downstream pier scour hole and w_i= width of an isolated pier scour hole).

However, the scour hole width of downstream pier relative to the upstream piers '$w_{2(st)}/w_{1(st)}$' (where, '$w_{2(st)}$' and '$w_{1(st)}$' are the horizontal distances measured normal to the direction of flow and through the noses of the downstream and upstream piers respectively and between the outer edges of scour holes of upstream and downstream piers) at front face of downstream pier, increases as the pier spacing increases and approaches to a maximum at pier spacing X_c/b=10. This increase in scour hole width indicates the dominance of the effect of angle of attack of flow approaching from upstream piers towards the downstream pier. As the pier spacing 'X_c/b' exceeds 10, there occurs a steep reduction in the scour hole width at front face of downstream pier and this trend continues upto pier spacing X_c/b=15. This decrease in the width of scour hole 'w_2/b' is due to a sudden decrease in the magnitude of angle of attack. At $15<X_c/b\leq50$, the downstream scour hole width '$w_{2(st)}/b$' further decreases due to further reduction in the magnitude of angle of attack at these pier spacings. Beyond X_c/b =50, the effective angle of attack of flow falls below 7.5° at which it has no effect on the scour hole width '$w_{2(st)}/b$'. As a result the downstream pier becomes free from all the effects and its scour hole width 'w_2/b' remains constant at $50<X_c/b<90$.

The downstream scour hole widths with respect to upstream scour hole widths '$w_{2(st)}/w_{1(st)}$' are plotted against pier spacing 'X_c/b' and are shown in Fig.5.90. The value of '$w_{2(st)}/w_{1(st)}$' increases as pier spacing increases and reaches to a maximum at pier spacing X_c/b=10. This maxima at X_c/b =10, occurs due to approachment of flow from

upstream piers to the downstream pier at 45° angle of attack which has maximum impact on local scour (Hannah, 1978).

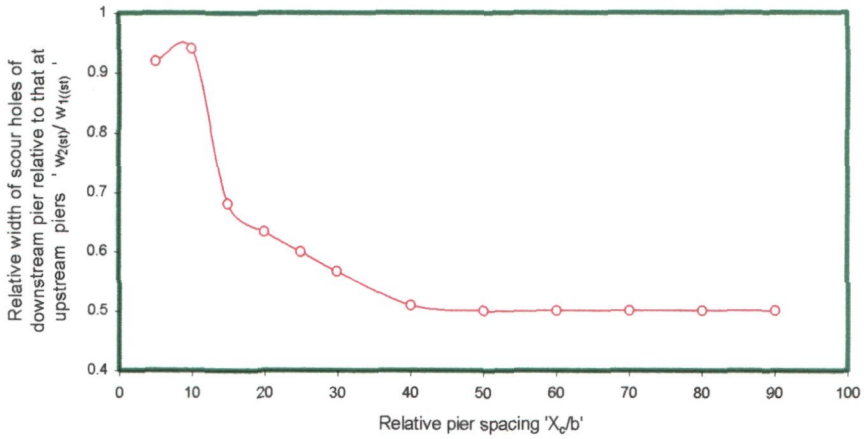

Fig. 5.90 Variation of width of scour hole of downstream pier relative to the scour hole width of upstream piers placed in staggered arrangement '$w_{2(st)}/w_{1(st)}$' with pier spacing X_c/b (where $w_{1(st)}$ and $w_{2(st)}$ are width of scour hole of upstream and downstream piers respectively).

At $10<X_c/b<15$, there is a steep reduction in the values of '$w_{2(st)}/w_{1(st)}$' which can be explained mainly due to two reasons. First reason is the shielding effect of wakes of upstream piers and the second reason is the steep reduction in the angle of attack of flow approaching to the downstream pier. At $15<X_c/b<40$, there is a gradual decrease in the values of 'w_2/w_1'. This gradual decrease can be attributed to a decrease in the effect of angle of attack at increasing 'X_c/b'. At $40<X_c/b<90$, the value of 'w_2/w_1' remain constant which indicates the disappearance of shielding effect of upstream piers and effect of angle of attack on downstream pier at these pier spacings.

(c) Variation of area of scour extents with pier spacing

Using the scour data collected in this study, areal extents of scour around the three staggered piers are plotted as shown in Appendix-II. Overlapping of areal extents around upstream and downstream piers at pier spacing 'X_c/b' as shown in Fig 5.91 indicates the existence of the effect of mutual interference of piers.

It can, however, be seen in Fig. 5.92 that the areal extents of scour become independent of each other at pier spacing $X_c/b=60$ which implies that the three piers have become free from the effect of mutual interference.

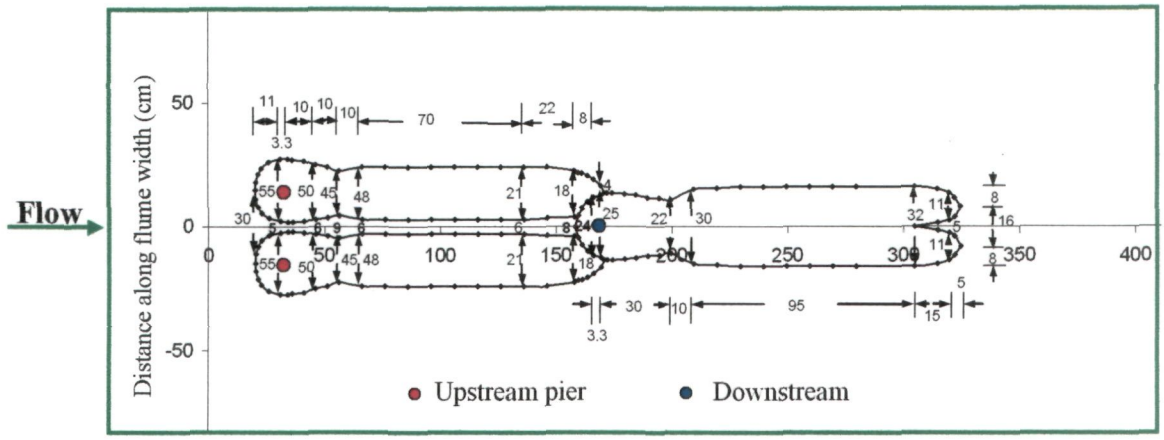

Fig.5.91 Areal extent of scour around upstream and downstream piers placed in staggered arrangement at X_c/b=40

In order to study the effect of pier spacing on areal extents of scour around the piers placed in staggered arrangement, the areas of the extent of scour are computed.

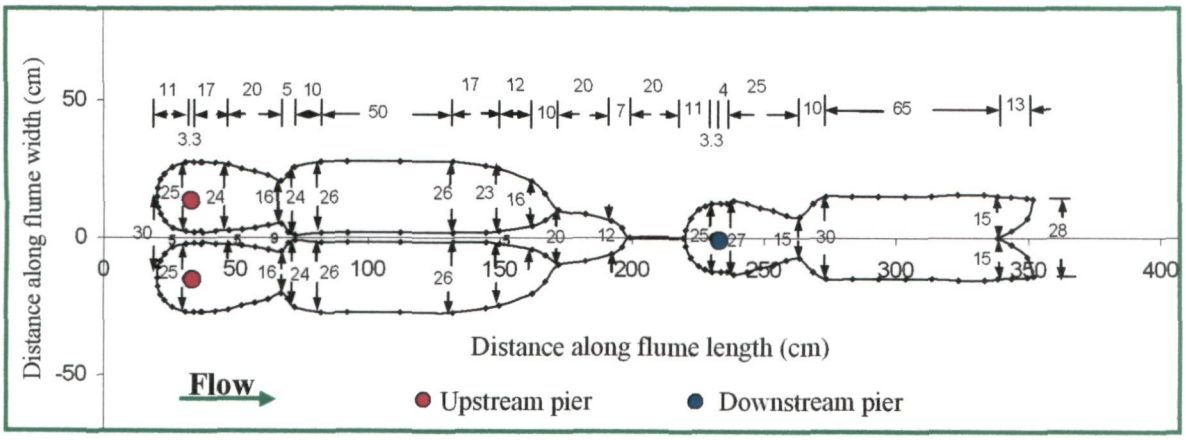

Fig. 5.92 Areal extent of scour around upstream and downstream piers placed in staggered arrangement at X_c/b=60

The computed values of areas of scour extent are divided by the area of scour extent of an isolated pier to obtain dimensionless area of scour extent '$A/3A_i$' and plotted against relative pier spacing 'X_c/b' as shown in Fig.5.93.

As can be seen in Fig. 5.93 there is no regular pattern in the variation of area of scour extent at varied pier spacing. The reason for such a variation is the change in the flow pattern with increasing pier spacing X_c/b. The increase in the area of extent at X_c/b=10 can be attributed to the strong interaction of flow approaching towards the downstream pier at 45° angle of attack with the wake vortices on downstream side of upstream piers.

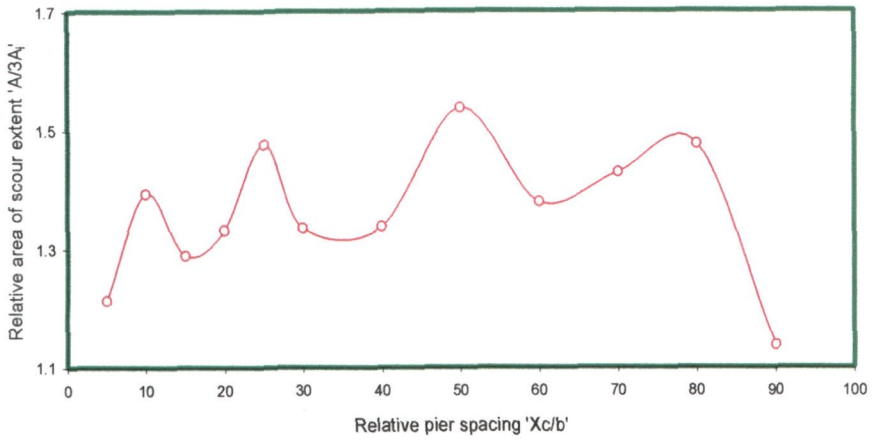

Fig. 5.93 Variation of relative area of scour extent around upstream and downstream piers placed in staggered arrangement *'$A/3A_i$'* with pier spacing *'X_c/b'* (where A = area of extent of scour around upstream and downstream piers, A_i = area around an isolated pier).

However, at X_c/b=15, the angle of attack sharply decreases which results in a weak interaction of flow approaching from upstream piers with wake vortices of upstream piers and this trend continues upto X_c/b=20. However, beyond X_c/b=20, the area of the extent of scour again increases at X_c/b=25, This increase in area of extent results from the change in flow pattern at downstream face of downstream pier where the bed material lifted by the wake vortices deposits over wider widths in the flow direction as shown in Fig. 5.94.

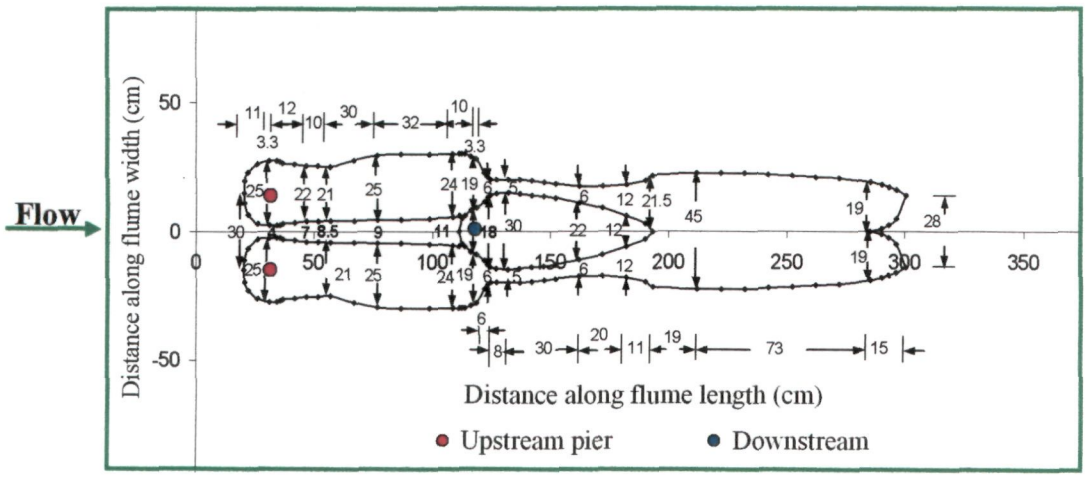

Fig. 5.94 Areal extent of scour around upstream and downstream piers placed in staggered arrangement at X_c/b=25

The area of scour extent decreases upto X_c/b=30. This decrease may be due to reduction in the strength of wake vortices of downstream pier due to which the bed material

deposits in a narrower width at the rear face of downstream pier along the flow direction as shown in Fig.5.95.

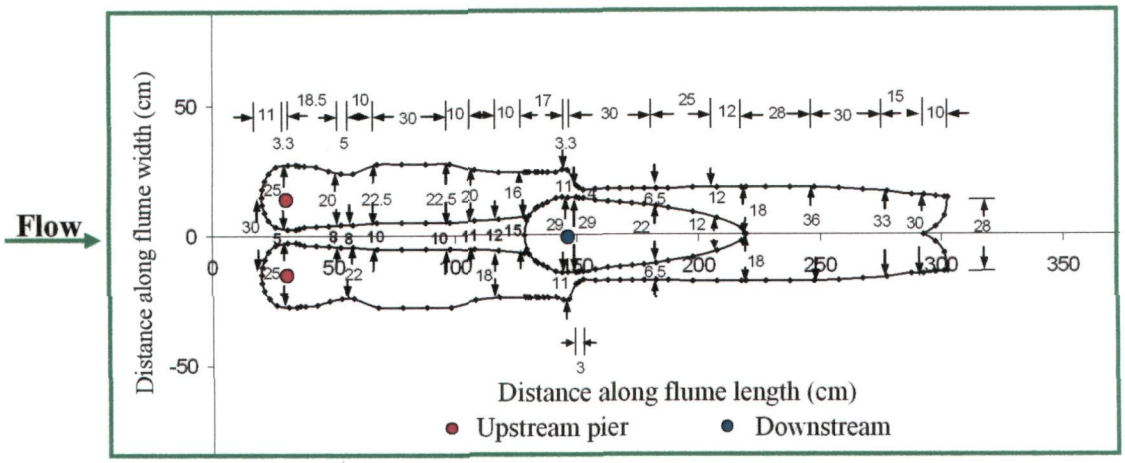

Fig. 5.95 Areal extent of scour around upstream and downstream piers placed in staggered arrangement at Xc/b=30

The area of scour extent at $30<X_c/b<40$ remains almost same due to the same flow pattern prevailing between pier spacing X_c/b=30 and 40. As evident from Appendix-IV, the areal extents of scour around upstream and downstream piers overlap each other upto X_c/b=40, however, at X_c/b=50, the areal extents of scour are just on the verge of being independent from one another as shown in Fig. 5.96, as a result of which the area of scour extent increases.

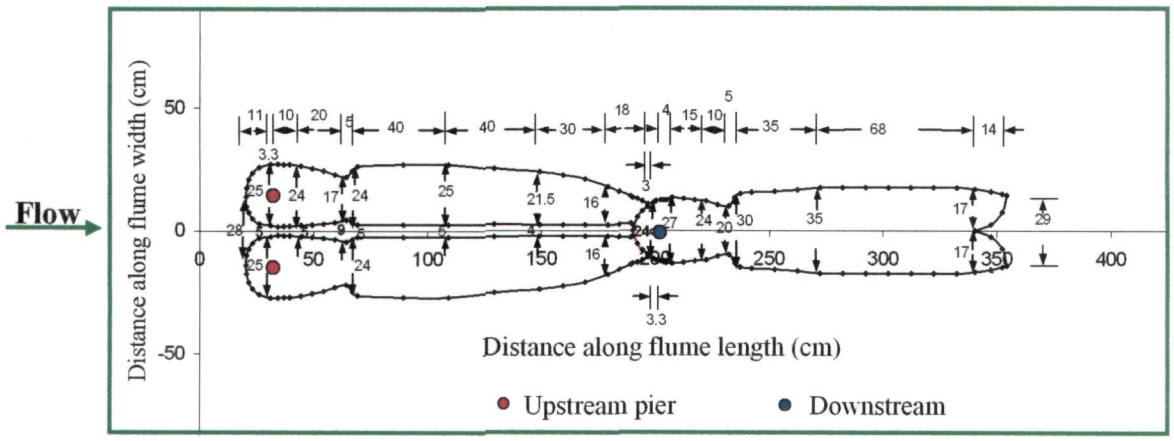

Fig. 5.96 Areal extent of scour around upstream and downstream piers placed in staggered arrangement at X_c/b=50

At X_c/b>50, Fig 5.97 shows that the area of the extent of scour decreases upto X_c/b=60 at which the areal extent of scour around upstream and downstream piers becomes completely independent of one another as revealed in Fig. 5.97.

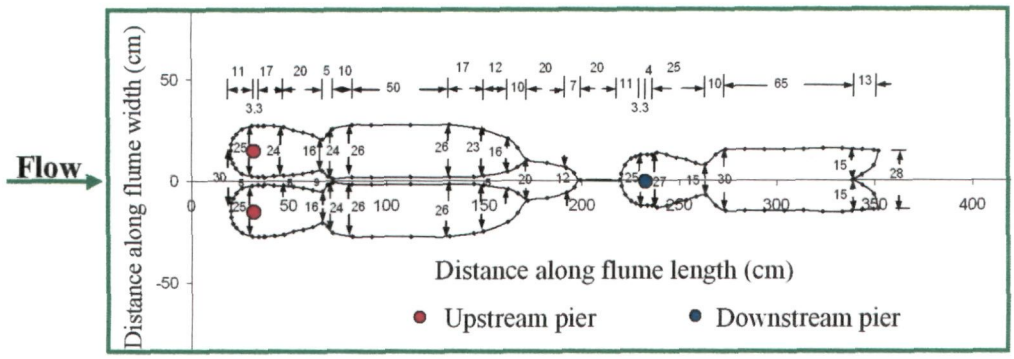

Fig.5.97 Areal extent of scour at X_c/b=60

As a result, a change in flow pattern occurs which causes the deposition of bed material over narrower width along the flume length as shown in Fig 5.97. At $60<X_c/b<80$, areas of extent of scour remain invariable because of stability in the flow pattern established around upstream and downstream piers. However, at X_c/b=90, the area of scour extent decreases and approaches to that around an isolated pier. This decrease and approachment of area of scour to the area of single pier scour extent point towards the fact that the flow pattern around the three piers has become free of mutual interference.

(d) Length of sediment deposition at downstream face of upstream and downstream piers

Fig. 5.98 shows the variation in the length of sediment deposition at the rear faces of upstream and downstream piers with pier spacing X_c/b. A decreasing trend in the average values of length of deposition at the downstream side of piers can be noticed in Fig.5.98 The reason for this decreasing trend can be explained by the fact that as the pier spacing X_c/b increases, the flow pattern at the downstream end of upstream and downstream piers changes due to the altering interaction of flow with piers and the sediment bed.

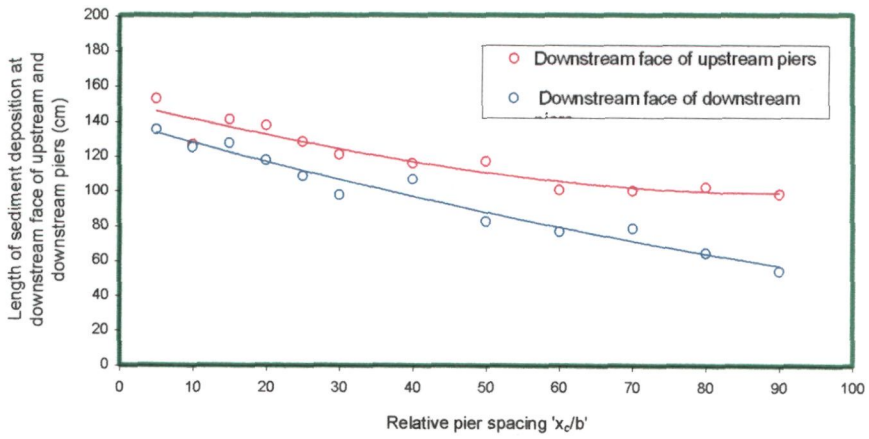

Fig.5.98 Variation of length of sediment deposition at rear faces of upstream and downstream piers placed in staggered arrangement with pier spacing X_c/b.

5.7.6 Variation of angle of attack with longitudinal pier spacing

The angles of attack 'α' are computed for lateral spacing between upstream piers Z_c/b=9 and varying longitudinal spacing between upstream and downstream piers X_c/b = 5 to 90 and are plotted against the longitudinal pier spacing X_c/b as shown in Fig. 5.99, An abrupt reduction in the angle of attack is observed in Fig. 5.99 upto X_c/b=20 followed by the gradual decrease as the pier spacing increases further. At X_c/b>60, the angle of attack remains under 7.5°, which has been found to be insignificant in affecting the scour depth (Chabert Engeldinger, 1956; Laursen and Toch, 1956; and Melville, 1997).

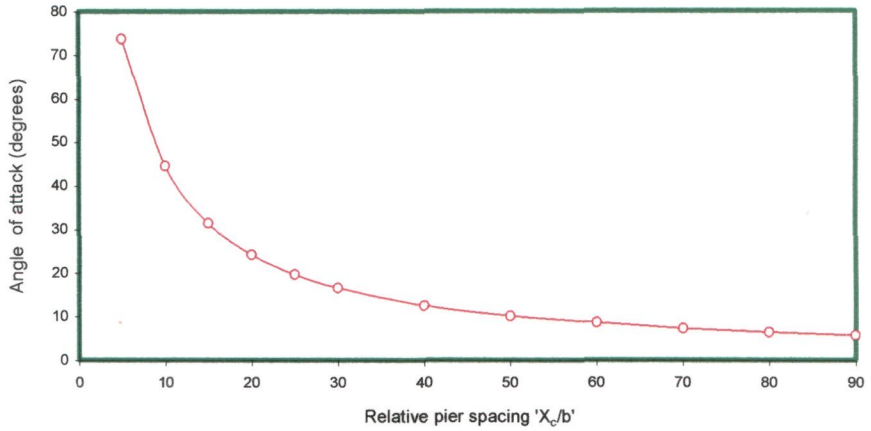

FIG. 5.99 Variation of angle of attack formed by three piers in staggered arrangements with longitudinal pier spacing 'X_c/b'.

5.7.7 Scour depth at downstream pier with respect to an isolated pier at varying angles of attack (*i.e.*, varying longitudinal pier spacing)

The relative scour depths at the downstream pier are plotted against angles of attack produced by the three piers located in staggered arrangement for varying longitudinal pier spacings 'X_c/b' as shown in Fig.5.100. It is observed that the relative scour depth is maximum at 44.5°≅45° *i.e.*, X_c/b=10) angle of attack, which verifies the experimental results of Hannah, 1978 It is also seen that at α <7.5°, relative scour depth remains constant which verifies the findings of (Laursen and Toch, 1956). The relative scour depth at downstream pier is smaller at an angle of attack 'α' = 73.74° than at 'α' = 44.5°. At angles of attack 12.52°<α< 44.5° the relative scour depth decreases due to the dominance of shielding effect of wakes of upstream piers on the effect of angle of attack. At angle of attack α =7.24° to12.52°, the relative scour depth increases which indicates the dominance of effect of angle of attack over the shielding effect of upstream piers.

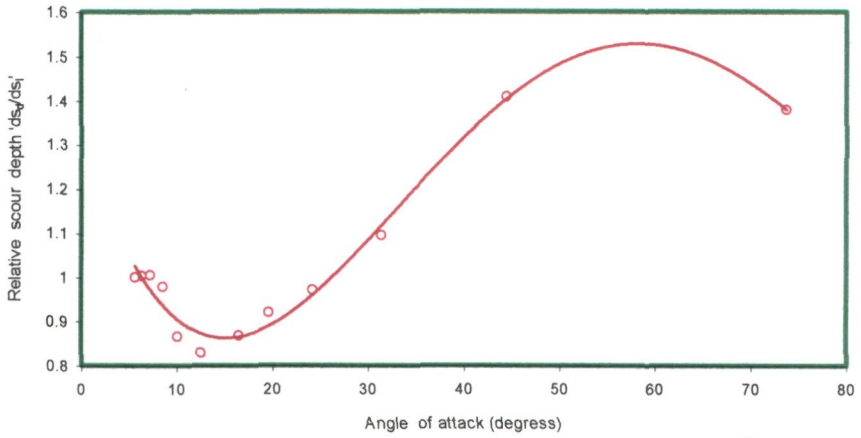

Fig.5.100 Variation of scour depth at downstream pier of piers group placed in staggered arrangement, with respect to that of an isolated pier '$ds_{st(d)}/ds_{(i)}$' at varying angles of attack 'α' formed by three piers in staggered arrangement.

Photographs shown in Figs. P9 & P10 authenticate the analysis of results on scour characteristics discussed above.

5.7.8 Temporal variation of scour

The data on temporal variation of scour depth colleted on three piers placed in staggered arrangement for varied longitudinal pier spacings are given in Appendix-I. The plots of these data (not shown here) reveal that the rate of scour at downstream pier is more than that at upstream piers due to the increased strength of horseshoe vortex caused by the approachment of flow from upstream piers to the downstream pier at some angle of attack. The data in Appendix reveal that the temporal scour depth variation curve for downstream pier lies above the temporal variation curve for upstream pier upto pier spacing X_c/b=20. However, in the range of 40>X_c/b >25, the temporal variation curve for downstream pier falls below the temporal variation curve for upstream piers. Beyond X_c/b>40, the temporal scour depth variation curve for downstream pier falls below that for the upstream one. At X_c/b= 90, the temporal variation of scour depth becomes identical to that at an isolated pier which implies that the three piers have become free of the effects of mutual interference.

5.7.9 Concluding remarks

It is observed that the scour depths at upstream and downstream piers are maximum at pier spacing X_c/b=10. The arrangement of two upstream piers at lateral pier spacing Z_c/b=9 and downstream pier at longitudinal pier spacing X_c/b=10 produces total

effective angle of attack equal to 45° which is identified as the most critical angle of attack producing severe effect on scour depth as found in present study and also reported by Hannah, 1978. At pier spacing X_c/b>10, the scour depth at the downstream is minimum at X_c/b=40. Thereafter, it increases upto pier spacing X_c/b=65 and then remains constant upto X_c/b=90.Based on the results achieved in this part of present investigation, it can be concluded that the downstream pier should be placed at X_c/b=40 since, at this pier spacing, the effect of upstream piers on at downstream pier local scour, is minimum.

5.8 Two Piers at Constant Angle of Attack but Varying Radial Spacing

5.8.0 Introduction

Scouring around two piers aligned in a direction transverse to the flow is affected by the compression of horseshoe vortices developed around the two piers. However, the scouring around two piers having their line of centres at an angle 45° to the approach flow is affected by all effects (reinforcing, sheltering shed vortices and compression of horseshoe vortices) and depending on the radial spacing between the piers, there is dominance of some effects over the others. It is experimentally observed that the striking strength of shed vortices of front pier is maximum at the rear pier when the two piers having their lines of centres at 45° to the direction of flow have centre to centre radial pier spacing R/b=5.

In order to analyze the results obtained from present experimental data on local scour around front and rear piers placed at varying radial pier spacing *'R/b'* and having their line of centres at 45° to the approach flow, the longitudinal profile of scour, lateral profile of scour and areal extent of scour are plotted for varied radial pier spacings *'R/b'* and are shown in Appendix-II, Appendix-III and Appendix-IV respectively. Some distinctive cases of longitudinal profiles of scour and areal extent of scour are considered in this section for analysis and discussion. In order to analyze the results, the photographs showing the scour and deposition patterns on the bed around the piers were taken at the end of each experiment. Photographs for some distinctive cases are shown in Fig. P11 & P12.

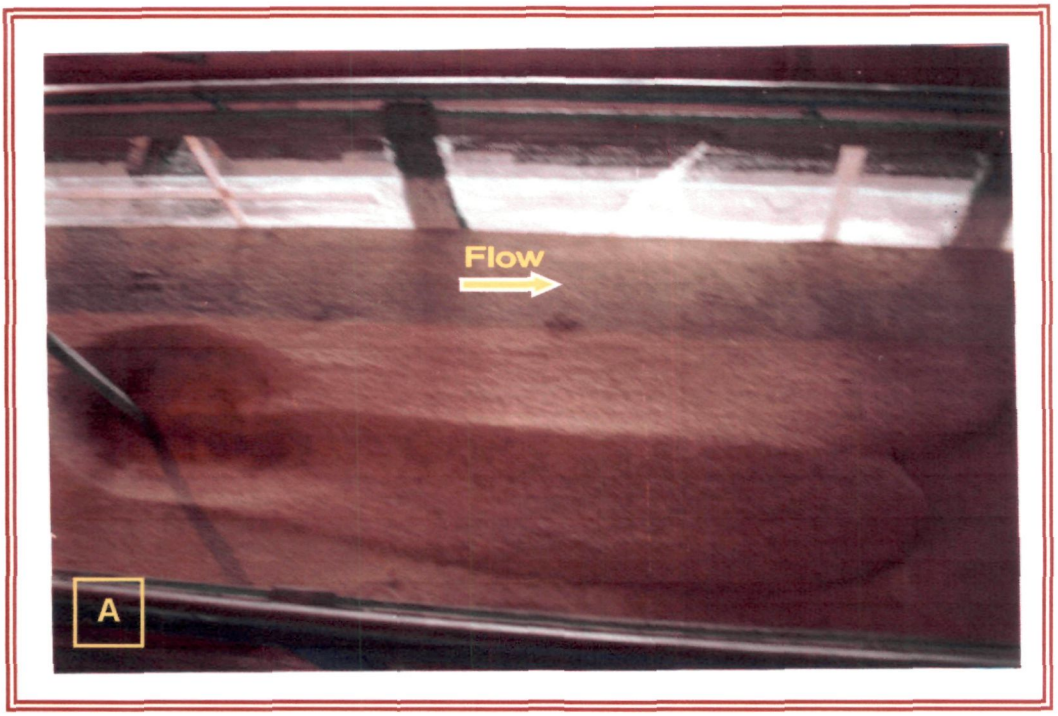

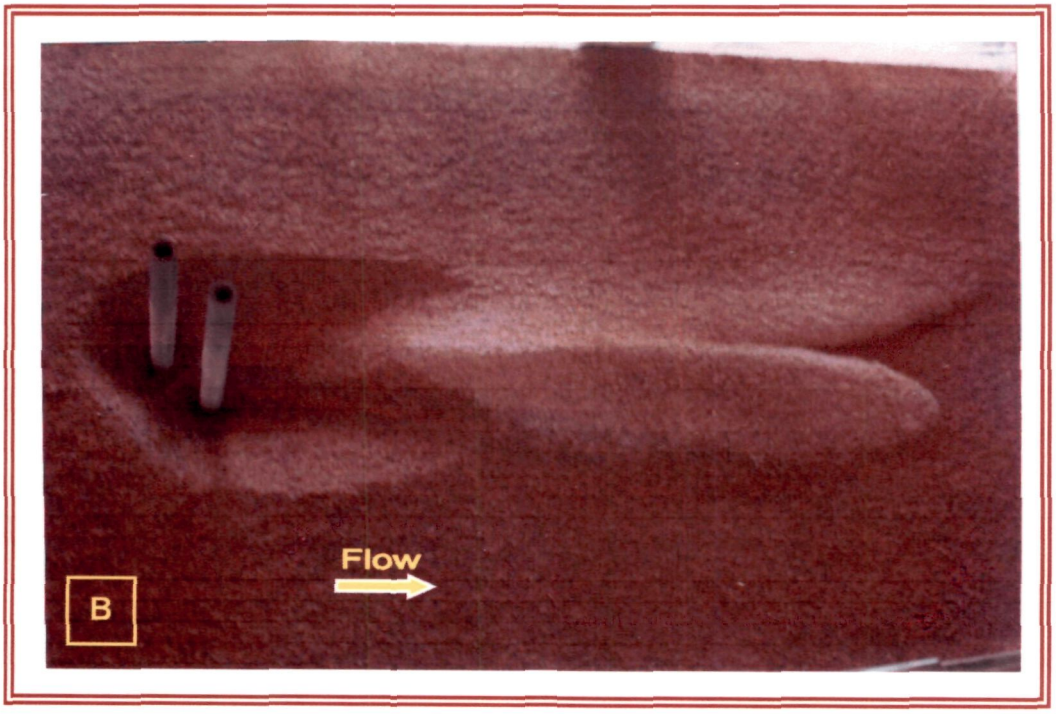

Fig. P11: Scour and deposition patterns around two piers aligned at constant angle 45° and varying radial pier spacings *R/b*
(A) *R/b*=0 (B) *R/b*=2

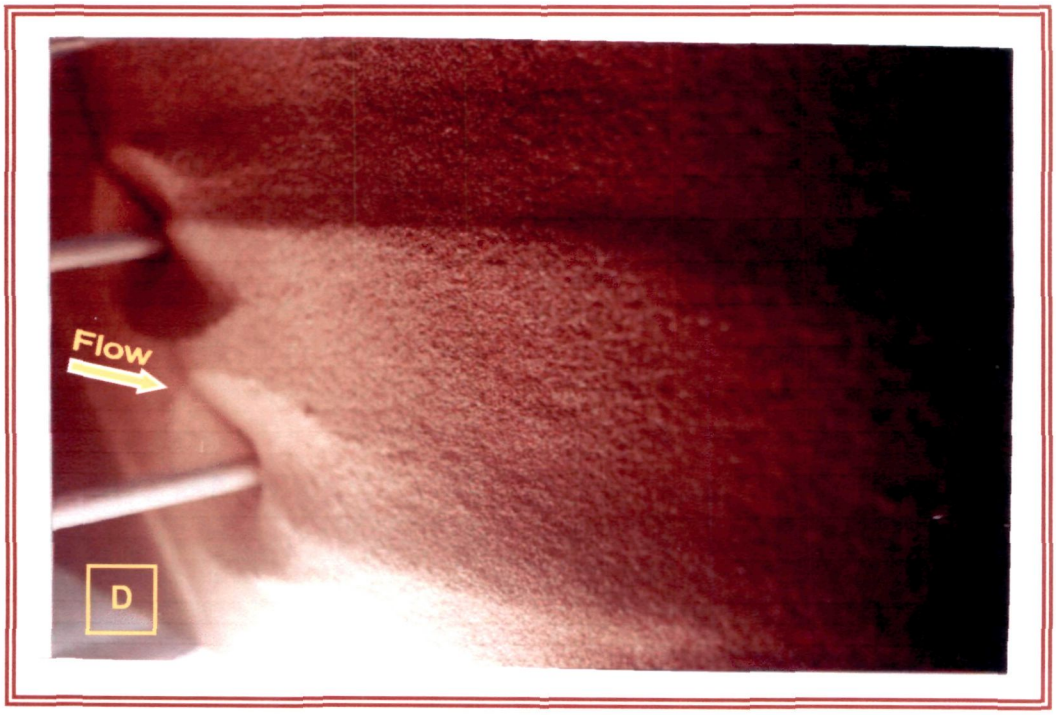

Fig. P12: Scour and deposition patterns around two piers aligned at constant angle 45° and varying radial pier spacings *R/b*
(C) *R/b*=8 (D) *R/b*=11

5.8.1 Variation of scour depth along flume length

Using the scour data collected in this study, the scour depths along the central line of flume in flow direction are plotted in longitudinal profiles of scour as shown in Appendix-II. It can be seen that the longitudinal profiles of scour start getting separated from one another at radial pier spacing R/b=11, however, the length of the profile of rear pier remains smaller than that of the front pier. As the radial pier spacing R/b approaches to 12, the lengths of longitudinal profiles become similar to that of an isolated pier indicating that the two piers being freed from mutual interference.

5.8.2 Scour depth at front and rear piers

Appendix-II shows the longitudinal profiles of scour in which the scour depths, length of scour holes, length of deposition and magnitudes of maximum deposit are marked.

The relative scour depths '$ds_{ca(f)}/ds_{(i)}$' and '$ds_{ca(r)}/ds_{(i)}$' observed at the upstream face of front and rear piers, having their line of centres at 45° to the approach flow and placed at varying radial spacings are plotted against radial pier spacing 'R/b' as shown in. Fig. 5.101. At radial pier spacing R/b=0 (*i.e.*, the two piers are touching each other), the maximum scour depth is observed as 2.012 $ds_{(i)}$. However, at radial pier spacing R/b=1, the scour depths at front and rear piers are observed as 1.35ds_i and 1.38ds_i respectively. This steep reduction in relative scour depths is due to a decrease in the frontal width caused by the free space between the two piers. At radial pier spacing R/b>1, the scour depths at rear pier are observed to be more than at the front pier for all radial pier spacings except R/b=12. The scour depths at this spacing approaches to that of an isolated pier. Increase in scour depths at rear pier are mainly due to the combined action of 'shed vortices' from the front pier and compression of the 'horseshoe vortices' between the piers. Evidently, the combined action of shed vortices and compression of horseshoe vortices between the front and rear piers dominate over the sheltering effect of front pier. As evident in Fig. 5.101, the maximum scour depth at rear pier occurs at radial pier spacing R/b=3.

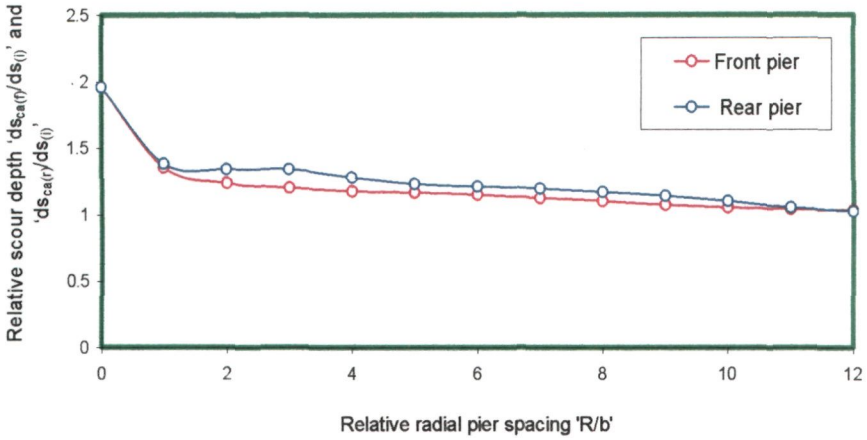

Fig.5.101 Variation of relative scour depth at front and rear piers placed at constant angle of attack α=45° '$ds_{ca(f)}/ds_{(i)}$' and '$ds_{ca(r)}/ds_{(i)}$' with radial pier spacing 'R/b'(where $ds_{ca(f)}/ds_{(i)}$= scour depth at front pier, $ds_{ca(r)}/ds_{(i)}$=scour depth at rear pier and $ds_{(i)}$ = scour depth at an isolated pier).

Also, maximum difference between the scour depths at front and rear piers is observed at radial pier spacing R/b=3. For spacing R/b>3, the difference between the scour depths at front and rear piers decreases and the scour depths merge into one another at R/b= 12 which equals to the scour depth that is observed at an isolated pier.

The details of ANN models applied to the present experimental data for the estimation of scour depths at front and rear piers placed at constant radial pier spacing R/b=5 and varying angles of attack 'α', are given in Tables.6.1 and 6.2 (Chapter VI) and are also shown in ANN architectures Fig 6.8 (Chapter VI). The scatter grams plotted between observed and ANN estimated scour depths are shown in Fig. 6.18 (Chapter VI). The closeness of data points to the line of best agreement indicates the accuracy of the ANN model in predicting the scour depths. The average values of correlation coefficient R^2 between observed and estimated scour depths at front and rear piers for training and testing data sets are 0.9740 and 0.9765 respectively. The values of *rmse* between observed and estimated scour depths for front and rear piers are 9.74×10^{-4} and 2.172×10^{-3} respectively. The higher values of R^2 and lower values of *rmse* indicate the accuracy of ANN models in predicting the scour depth.

5.8.3 Scour hole characteristics

Since the knowledge of scour whole dimensions is essential in determining the extent of countermeasures needed to prevent/control scour at piers, various parameters explained as under using present experimental data are determined.

(a) Scour hole characteristics at front and rear piers

Scour holes characteristics around front and rear piers are analyzed by plotting the longitudinal and lateral profiles of scour and areal extent of scour around the piers against radial pier spacing *'R/b'* as shown in Appendix-II, Appendix-III and Appendix-IV respectively. It is experimentally noticed that the spiral motion of flow takes place in a clockwise direction around two piers placed at zero radial pier spacing and having their line of centres at 45° to the approach flow. Two piers at zero spacing acts like a single round nosed rectangular pier having a length to width ratio equal to 2 and single horseshoe vortex develops around it. However, as the rear pier is separated from the front one, independent horseshoe vortices are developed around the piers. At short radial pier spacings, a strong interaction is observed between the flow patterns generated around the piers.

(b) Length of scour hole at upstream faces of front and rear pier

The length of scour holes at the upstream faces of front and rear pier relative to the length of scour hole of an isolated pier *'$Lsh_{cau(f)}/Lsh_{u(i)}$'* and *'$Lsh_{cau(r)}/Lsh_{u(i)}$'* are plotted against radial pier spacing *'R/b'* as shown in Fig. 5.102. The lengths of scour holes observed at the upstream face of front and rear piers at radial pier spacing *R/b*=0 are 1.64 and 1.59 times more than observed for an isolated pier respectively. While at pier spacing *R/b*=1, these lengths remain only 1.23 and 1.27 times more than the corresponding value observed for an isolated pier respectively.

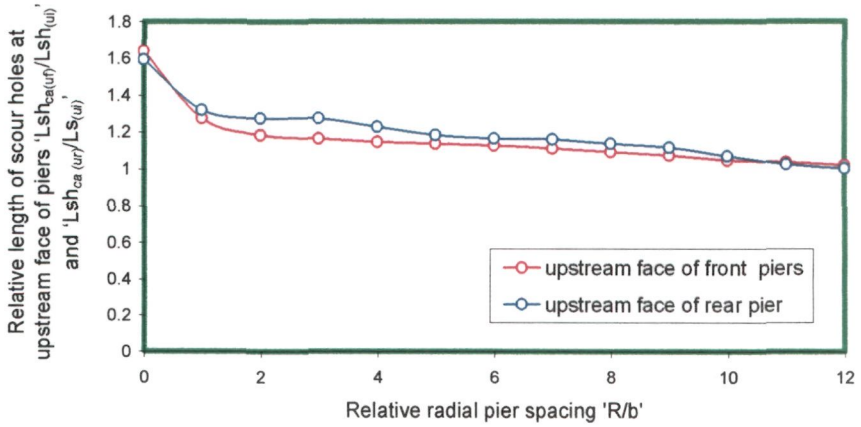

Fig. 5.102 Variation of length of scour holes at upstream faces of front and rear piers placed at constant angle of attack α=45° *'$Lsh_{cau(f)}/Lsh_{u(i)}$'* and *'$Lsh_{cau(r)}/Lsh_{u(i)}$'* with radial pier spacing *'R/b'* (where $Lsh_{cau(f)}$ = length of scour hole at upstream face of front pier , $Lsh_{cau(r)}$ = length of scour hole at upstream face of rear pier, $Lsh_{u(si)}$ = length of scour hole at upstream face of an isolated pier).

This rapid decrease in the values of '$Lsh_{cau(f)}/Lsh_{u(i)}$' and '$Lsh_{cau(r)}/Lsh_{u(i)}$' occurs due to the reduction in the scour depth due to increase in the free gap along flume width between the piers. For radial pier spacing R/b=2 and beyond, the effect of compression of horseshoe vortices and reinforcing effect of on front pier reduces consequent upon which the scour depth also decreases and results in decrement of. '$Lsh_{cau(f)}/Lsh_{u(i)}$' At radial pier spacing 'R/b' =10, the value of '$Lsh_{cau(f)}/Lsh_{u(i)}$' at the front pier decreases and approaches to unity. Thereafter, the front pier remains almost free from mutual interference and, as a result, the value of '$Lsh_{cau(f)}/Lsh_{u(i)}$' remains constant (*i.e.*,1.0) upto radial pier spacing R/b=12. However, at rear pier the combined effect of shed vortices and compression of horseshoe vortices between the piers is such that the value of '$Lsh_{cau(r)}/Lsh_{u(i)}$' remains constant between radial pier spacing R/b= 2 to 4 and thereafter, it decreases and approaches to unity at pier spacing R/b=12.

(c) Length of scour hole at downstream faces of front and rear piers

The length of scour holes at the downstream face of front and rear piers with respect to the length of scour hole of an isolated pier '$Lsh_{cad(f)}/Lsh_{d(i)}$' and '$Lhs_{cad(r)}/Lsh_{d(i)}$' are plotted against radial pier spacing 'R/b' as shown in Fig. 5.103. The lengths of scour holes at R/b=0 are observed as about 1.29 $Lsh_{d(i)}$ and 1.18 $Lsh_{d(i)}$ respectively. At R/b>0, the lengths decrease and approach to a value as observed for an isolated pier at radial pier spacing R/b=11 and remains the same upto R/b=12.As shown in Fig. 5.103, the values of '$Lsh_{cad(f)}/Lsh_{d(i)}$' and '$Lhs_{cad(r)}/L_{s(dsi)}$' decrease at a relatively higher rate upto R/b=1, due to a decrease in the frontal width of pier caused by separation of piers. However, at pier spacing R/b>1, the value of '$Lhs_{cad(r)}/L_{s(dsi)}$' at rear pier remains fairly constant upto R/b=3.

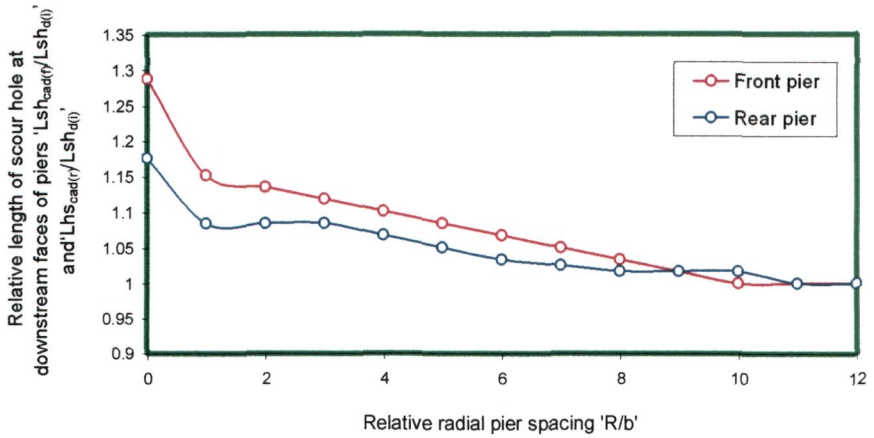

Fig. 5.103 Variation of length of scour holes at downstream faces of front and rear piers placed at constant angle of attack α=45° '$Lsh_{cad(f)}/Lsh_{d(i)}$' and '$Lhs_{cad(r)}/Lsh_{d(i)}$' with radial pier spacing 'R/b' (where $Lsh_{cad(f)}$ = length of scour hole at upstream face of front pier , $Lhs_{cad(r)}$= length of scour hole at upstream face of rear pier, $Lsh_{d(i)}$ = length of scour hole at upstream face of an isolated pier).

This constant variation is due to the balance maintained among the various flow mechanisms (*i.e.*, reinforcing, shed vortices and compression of horseshoe vortices) interplaying around two piers. The decrease in '$Lhs_{cad(r)}/Lsh_{d(i)}$' at rear pier at R/b>3 is attributed to the decrement in the effect of vortex shedding and compression of horseshoe vortices. However, the value of '$Lsh_{cad(f)}/Lsh_{d(i)}$' at front pier decreases due to decrement in the reinforcing effect of rear pier of front pier.

(d) Slope of scour holes

(i) Slope of scour holes on upstream of front and rear piers

The slope of scour holes observed at the upstream face of front and rear piers with respect to the slope observed at upstream face of an isolated pier '$S_{lcau(f)}/S_{lu(i)}$' and '$S_{lcau(r)}/S_{lu(i)}$' are plotted against radial pier spacing 'R/b' as shown in Fig. 5.104. As evident from this figure, the slope at upstream face of front and rear piers is maximum at R/b=0, however, it decreases rapidly upto R/b=1 and thereafter, a gradual decrement is observed upto R/b=12.

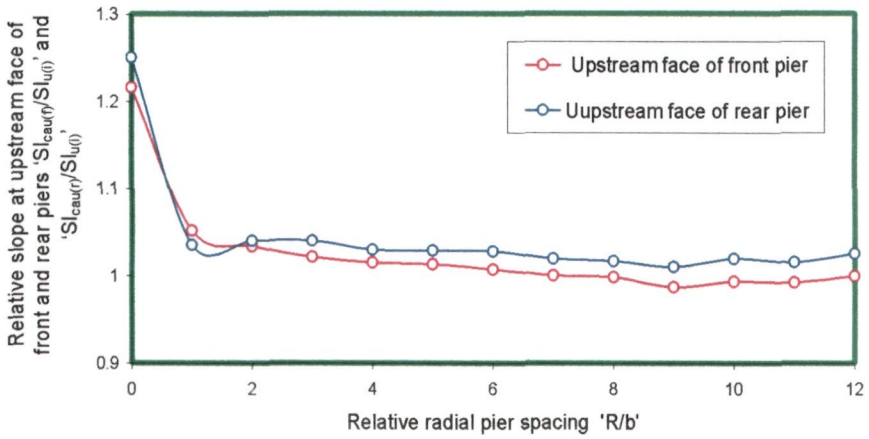

Fig.5.104 Variation of relative slope of scour hole at upstream faces of front and rear piers placed at constant angle of attack α=45° '$S_{lcau(f)}/S_{lu(i)}$' and '$S_{lcau(r)}/S_{lu(i)}$' with radial pier spacing 'R/b' (where $S_{lcau(f)}$ = slope of scour hole at upstream face of front pier, $S_{lcau(r)}$ = slope of scour hole at upstream face of rear pier and $S_{lu(i)}$=slope of scour hole at upstream face of an isolated pier).

This variation in the relative slope '$S_{lcau(f)}/S_{lu(i)}$' or '$S_{lcau(r)}/S_{lu(i)}$' suggests that, as the frontal width of two piers at R/b=0 is maximum, the scour depth, which is directly proportional to the frontal width, is maximum. As a result, the slope of scour hole at upstream face of front and rear piers is maximum. At R/b=1, however, the separate horseshoe vortices develop around front and rear piers, mutual interaction between horseshoe vortices and shed vortices occurring around the front and rear piers gets intensified which causes a rapid decrease in the slope at upstream face of front and rear

piers. At radial pier spacings ranging between R/b=1 to 3, scour depth at rear pier remains constant (see, Fig.5.101) due to which, the slope at '$S_{lcau(r)}/S_{lu(i)}$' remains constant. For radial pier spacing R/b>3, the intensity of interference between the horseshoe vortices around front and rear piers decreases as the radial pier spacing increases and causes a decrement in the values of '$S_{lcau(r)}/S_{lu(i)}$' upto radial pier spacing R/b=12. At the upstream face of front pier, a gradual decrease in the values of '$S_{lcau(f)}/S_{lu(i)}$' is observed at radial pier spacings 1<R/b<11. This decrement in the values of '$S_{lcau(f)}/S_{lu(i)}$' is attributed to the reduction in the reinforcing effect of rear pier. At radial pier spacing R/b=12, the slope remains nearly same as that of an isolated pier which implies that the front and rear piers become free from the effects of mutual interference.

(ii) Slope of scour holes at downstream faces of front and rear piers

The slope of scour holes observed at the downstream face of front and rear piers relative to the slope at the downstream face of an isolated pier '$S_{lcad(f)}/S_{ld(i)}$' and '$S_{lcad(r)}/S_{ld(i)}$' are plotted against radial pier spacing R/b as shown in Fig. 5.105. The slope '$S_{lcad(f)}/S_{ld(i)}$' is observed to be maximum at radial pier spacing R/b=0, since, the frontal width of piers being maximum at radial pier spacing R/b=0. However, as two pier are separated, the shed vortices of front pier interacts with the vortex system of rear pier resulting in the generation of a complex flow pattern around the two piers which causes the slopes '$S_{lcad(f)}/S_{ld(i)}$' and '$S_{lcad(r)}/S_{ld(i)}$' to decrease rapidly at radial pier spacing R/b=1. The slope at rear pier, '$S_{lcad(r)}/S_{ld(i)}$' remains constant between pier spacings R/b= 1 and 2 due to the balance maintained among the various effects (*i.e.*, effect of reinforcing, shed vortices and horseshoe vortex compression) interplaying around the two piers.

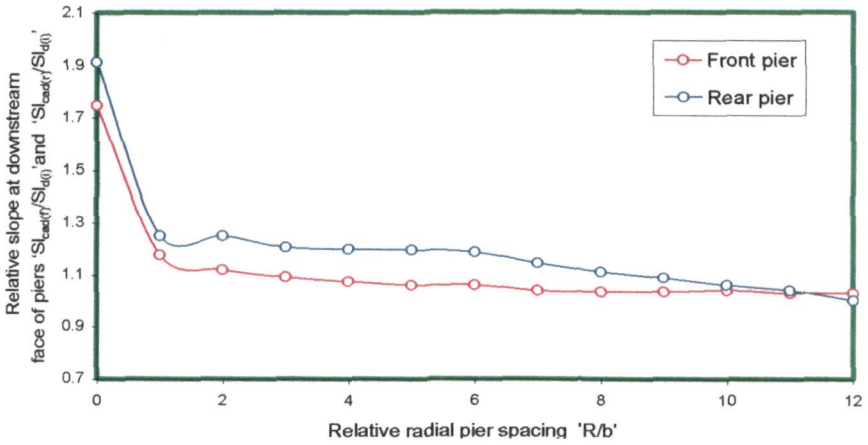

Fig. 5.105 Variation of relative slope of scour holes at downstream faces of front and rear piers placed at constant angle of attack α=45° '$S_{lcad(f)}/S_{ld(i}$' *and* '$S_{lcad(r)}/S_{ld(i)}$' with radial pier spacing 'R/b' (where $S_{lcad(f)}$ = slope of scour hole at downstream face of front pier, $S_{lcad(r)}$= slope of scour hole at downstream face of rear pier and $S_{ld(i)}$= slope of scour holes at downstream face of an isolated pier).

At radial pier spacing R/b>2, the effect of the mutual interaction of vortices around front and rear piers weakens resulting in a decrease in the value of slope '$S_{lcad(r)}/S_{ld(i)}$' at rear pier and reaches to that of an isolated pier at radial pier spacing R/b=12. In the case of front pier, as the radial pier spacings R/b increases beyond 1, the reinforcing effect on front pier caused by the presence of rear pier decreases and the value of slope '$S_{lcad(f)}/S_{ld(i)}$'at downstream face of front pier gradually decreases and reaches to that of an isolated pier at radial pier spacing R/b=12, which indicates diminishing state of mutual interference effect between the piers.

(e) Deposition of sediment at downstream faces of piers

The length of sediment deposition at the downstream face of front and rear piers with respect to the length of sediment deposition at downstream face of an isolated pier '$Ldep_{ca(f)}/Ldep_{(i)}$' and '$Ldep_{ca(r)}/Ldep_{(i)}$' are plotted against radial pier spacing R/b as shown in Fig.5.106. A decrement in the values of length of sediment deposition '$Ldep_{ca(f)}/Ldep_{(i)}$' and '$Ldep_{ca(r)}/Ldep_{(i)}$' at downstream face of front and rear piers is observed upto radial pier spacing R/b=3. It is observed that the bed material scoured from around the two piers deposit more along flume width than along the flow direction as shown in Appendix-II. This happens due to the interaction of wake vortices of front pier with horseshoe vortex of rear pier. These wake vortices of front pier lose their strength after interacting with the vortices at rear pier and are rendered unable to transport the scoured bed material further downstream.

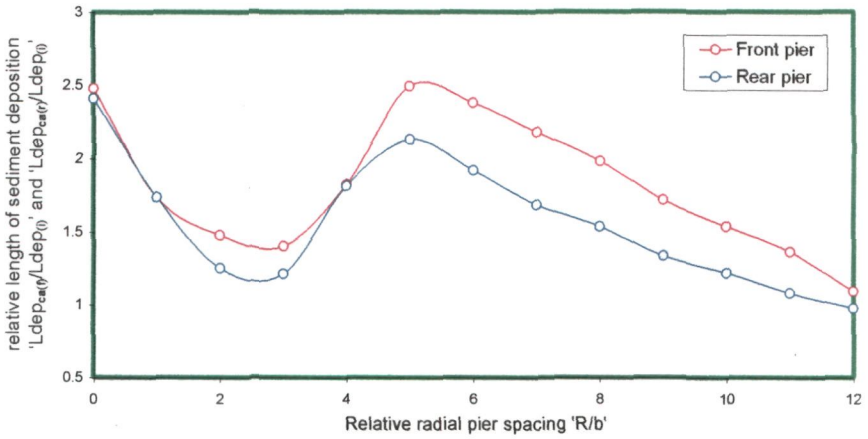

Fig. 5.106 Variation of relative length of sediment deposition at downstream faces of front and rear piers placed at constant angle of attack α=45° '$Ldep_{ca(f)}/Ldep_{(i)}$' and '$Ldep_{ca(r)}/Ldep_{(i)}$' with radial pier spacing 'R/b'(where $Ldep_{ca(f)}$= length of sediment deposition at downstream face of front pier, $Ldep_{ca(r)}$= length of sediment deposition at downstream face of rear pier and $Ldep_{(i)}$ = length of sediment deposition at downstream face of an isolated pier).

At pier spacing R/b=3 to 5, '$Ldep_{ca(f)}/Ldep_{(i)}$' and '$Ldep_{ca(r)}/Ldep_{(i)}$' increase as the shed vortices generating from front pier increases the strength of shed vortices of rear pier by striking more closely to the rear pier.

The maximum values of '$Ldep_{ca(f)}/Ldep_{(i)}$' and '$Ldep_{ca(r)}/Ldep_{(i)}$' occur at R/b=5 as shown in Fig. 5.106. The maximum in these values is validated by earlier studies. Hannah (1978), in his study has also reported scour depth at rear pier to be maximum when two piers with their line of centres at 45° to the direction of flow are placed at radial pier spacing R/b=5. Fig. 5.106 reveals that as the pier spacing 'R/b' increases beyond 5, a decrease in the values of '$Ldep_{ca(f)}/Ldep_{(i)}$' and '$Ldep_{ca(r)}/Ldep_{(i)}$' is observed upto pier spacing R/b=12.The values of '$Ldep_{ca(f)}/Ldep_{(i)}$' and '$Ldep_{ca(r)}/Ldep_{(i)}$' at radial pier spacing R/b=12 are observed to be nearly equal to those observed at an isolated pier, since the shed vortices from the front pier fail to approach near the rear pier.

(f) Variation of area of scour extent with radial pier spacings

The data on areal extents of scour collected in present study are plotted as shown in Appendix-IV for varied radial pier spacings R/b. It can be seen in Fig.107 (R/b=11) that the areal extents of scour around two piers overlap upto radial pier spacing R/b =11.

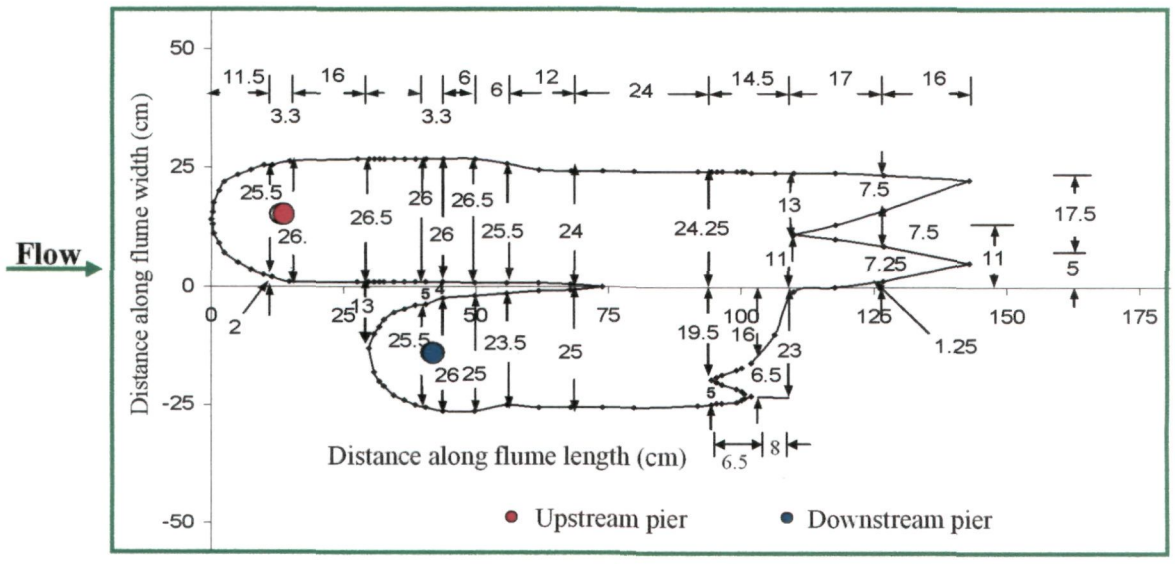

Fig.5.107 Areal extent of scour around front and rear pier placed at constant angle of attack α=45° and R/b=11

However, at radial pier spacing R/b=12, Fig. 5.108 shows that the areal extents of scour get separated from one another, nevertheless the size of areal extent around two piers remains quite different from one another.

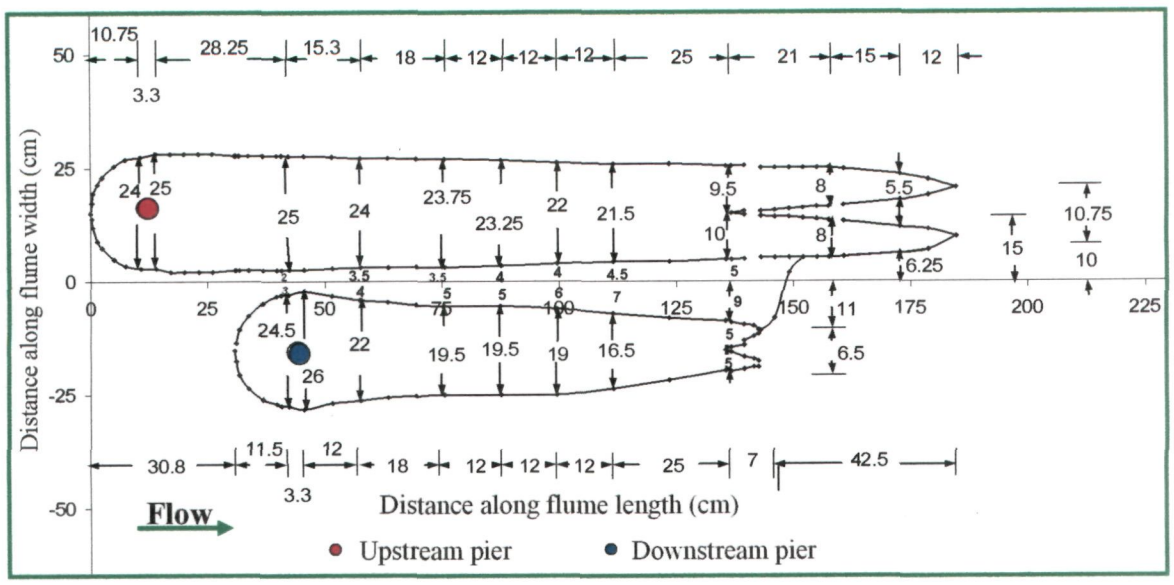

Fig.5.108 Areal extent of scour around front and rear piers placed at constant angle of attack α=45° and *R/b*=12

The areas of the extent of scour for varied radial pier spacings *'R/b'* with respect to the area of scour extent of an isolated pier *'$A_{ca}/2A_i$'* are plotted against radial pier spacing *'R/b'* as shown in Fig. 5.109.

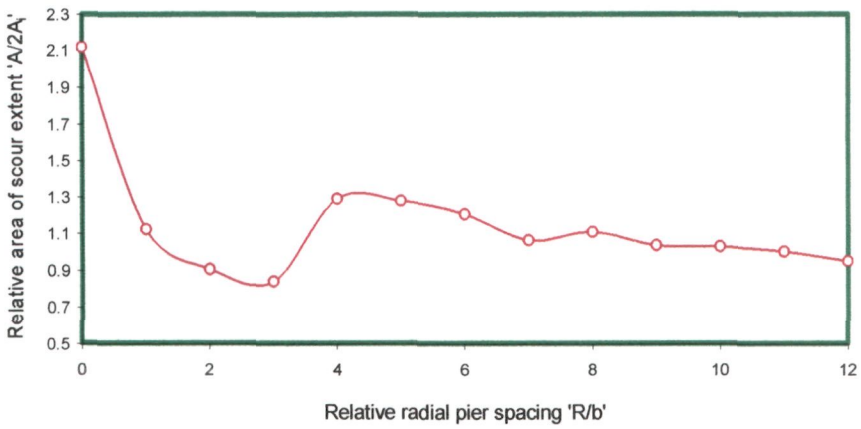

Fig. 5.109 Variation of relative area of scour extent around front and rear piers placed at constant angle of attack α=45° *'$A_{ca}/2A_i$'* with radial pier spacing *'R/b'* (where, A_{ca} = total area of scour around front and rear piers and A_i = area of scour extent around an isolated pier).

At radial pier spacing *R/b*= 0, two piers act together as a single pier having length to width ratio equal to 2. As observed in Fig.5.109, the value of *'$A/2A_i$'* = 2.12, is a maximum at radial pier spacing *R/b*=0 which is slightly more than 2.04, the frontal width of piers at zero degree angle of attack. This maxima in the value of area of extent is due to the increased strength of vortex system developed around the two

piers due to their alignment at an angle of 45° to the flow. As the radial pier spacing *'R/b'* increases to 1, a steep reduction in the value of *'$A/2A_i$'* is observed. At this radial pier spacing, the value of *'$A/2A_i$'* is equal to 1.12. The decrease in frontal width caused by the separation of two piers is the reason for this steep reduction in area of scour extent. During experiments it was noticed that as the radial pier spacing *'R/b'* exceeded 1, separate horseshoe vortices were observed to be forming at front and rear piers. Also an intensive interaction between the flow patterns occurring around the two piers was observed. In Fig. 5.109, a decrement in the values of *'$A/2A_i$'* is observed at radial pier spacing $1<R/b<3$and as pier spacing *'R/b'* reaches to 3, the value of *'$A/2A_i$'* approaches to 0.84, a minimum. This decrement in the value of *'$A/2A_i$'* at radial pier spacing $1<R/b<3$ occurs due to the balance maintained in mutual interaction of vortex system developed around the front and rear piers due to which the wake vortices do not remain able to transport the bed material scoured from the scour holes of the two piers to the larger extent of area.

It was observed during experiments that upto radial pier spacing $R/b=3$, shed vortices from the front pier pass very close to the rear pier. The maxima in Fig. 5.109 suggests that at radial pier spacing $R/b=4$, shed vortices generating from front pier approach directly at the nose of rear pier which enhances the transporting strength of wake vortices at rear pier. As a result the bed material scoured from the rear pier scour hole is transported at the downstream end and deposits over a large area. The decreasing trend in the values of *'$A/2A_i$'* indicates that at pier spacing $R/b=5$ and onward, the shed vortices of front pier deviate and pass away from the rear pier resulting in a decrease in the transporting strength of wake vortices of rear pier and a reduction in the area of the extent of scour. At pier spacing $R/b=12$, shed vortices pass away from the rear pier, and leads to a negligible influence on rear pier as such that the extent of scour around front and rear piers is nearly same as that of an isolated pier.

(g) Width of scour holes

Appendix-IV shows the areal extents of scour around piers to overlap each other along their inner sides at short radial pier spacing *R/b*. However, as *R/b* increases, areal extents of scour around front and rear piers starts separating from one another and gets completely separated from one another at $R/b=12$.

To examine the variation of width of scour holes with radial pier spacing *R/b*, scour profiles along the flume width across the nose of front and rear piers are plotted against *'R/b'* as shown in Appendix-III. The top width of scour hole *'w_1'* and *'w_2'* at front and rear piers respectively, are the horizontal distances measured between the extreme ends of scour extent across the nose of front and rear piers The top widths of scour holes across the respective noses of the piers relative to the top width of scour hole across nose of an isolated pier *'w_{1ca}/wi'* and *'w_{2ca}/w_i' are* plotted against radial pier spacing *R/b* as shown in Fig.5.110.

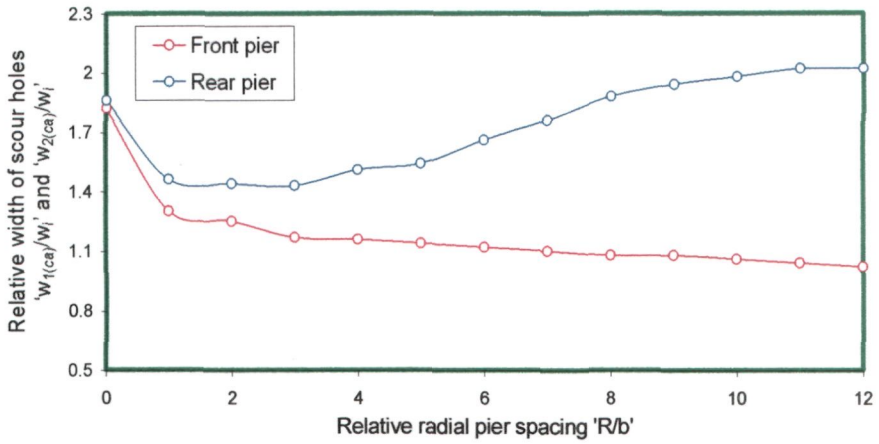

Fig. 5.110 Variation of relative width of scour holes of front and rear piers placed at constant angle of attack α=45° *'$w_{1(ca)}/w_i$'* and *'$w_{2(ca)}/w_i$'* with radial pier spacing *'R/b'*(where $w_{1(ca)}$=width of scour hole at front pier, $w_{2(ca)}$=width of scour hole at rear pier, w_i=width of scour hole at an isolated pier).

For pier spacing *R/b*=0 *'$w_{1(ca)}/w_i$'* and *'$w_{2(ca)}/w_i$'* are observed as 1.86 and 1.82 respectively. These values are slightly more than that would be suggested by a linear dependence of scour hole width on frontal width, namely, 1.64. The occurrence of maximum scour hole width at *R/b*=0 is attributed to an increased scour depth caused by large frontal width resulting from zero radial pier spacing. A steep reduction in the values of *'$w_{1(ca)}/w_i$'* and *'$w_{2(ca)}/w_i$'* is observed at *R/b*= 1, since, piers behave independently at *R/b*>0.

For radial pier spacing *R/b*≥1, (see, Fig. 5.110, the decreasing trend in the values of *'$w_{1(ca)}/w_i$'* at front pier continues upto pier spacing *R/b*=12. This decreasing trend can be explained in a way that, as *R/b* increases, the respective scour holes of front and rear piers in between, get separated from each other. As shown in Appendix-IV, the scour holes at upstream face of front and rear piers are observed to get separated completely at radial pier spacing *R/b*=11 but still overlap one another at downstream face of two piers.

At rear pier, a decreasing trend in the values of '$w_{2(ca)}/w_i$' continues up-to radial pier spacing R/b=3, increases upto pier spacing R/b=11 and then remains constant between pier spacing R/b=11 to 12. Fig.5.110 shows a minimal decrease in the values of '$w_{2(ca)}/w_i$' at rear pier spacing $1<R/b<3$, which indicates that the effect of shed vortices approaching to the rear pier dominates over the effect of compression of horseshoe vortices and sheltering effect offered by the front pier. The values of 'w_2/wi' remain nearly same in the range of radial pier spacing $1<R/b<3$ and a results in the same scour depths. As 'R/b' approaches to 4, the shed vortices from front pier approach directly to the rear pier as a result of which the scour depth at rear pier increases and hence the value of '$w_{2(ca)}/w_i$' increases. With further increase in pier spacing R/b, the shed vortices pass away from the rear pier and result in a decrease in the scour depth at rear pier. Furthermore, with an increase in pier spacing R/b, the overlapping of scour holes of front and rear piers decreases as a result of which the width of scour hole '$w_{2(ca)}/w_i$' increases and reaches to a maximum at pier spacing R/b=12 when the scour holes at front and rear piers are completely separated from one another.

The action of shed vortices of front pier causes an increase in the scour depth at rear pier but at the same time the bed material scoured from front pier gets transported into the rear pier scour hole which balances the increase in the scour depth. This process remains dominant in the range of pier spacing $1<R/b<3$ due to which the variation in the scour depth and scour hole width at rear pier '$w_{2\,(ca)}/w_i$' remains small in the range of radial pier spacing $1<R/b<3$.

The scour and deposition patterns captured in photographs shown in Fig. P11 & P12 authenticate the analysis of results on scour characteristics discussed above for piers placed at constant angle of attack and varying radial pier spacing.

5.8.4 Temporal variation of scour depth

The data on temporal variation of scour depth colleted on two piers having fixed radial pier spacing and varied longitudinal pier spacings are given in Appendix-I. The plots of these data (not shown here) reveal that the rate of scour at downstream pier is more than that at upstream piers due to the increased strength of horseshoe vortex caused by the approachment of flow from upstream piers to the downstream pier at some angle of

attack. The data in Appendix-I reveal that the temporal scour depth variation curve for downstream pier lies above the temporal variation curve for upstream pier up-to pier spacing X_c/b=20. However, in the range of 40>X_c/b >25, the temporal variation curve for downstream piers falls below the temporal variation curve for upstream piers. Beyond X_c/b>40, the temporal scour depth variation curve for downstream pier falls below that for the upstream one. At X_c/b=90, the temporal variation of scour depth becomes identical to that at an isolated pier which implies that the three piers have become free of the effects of mutual interference.

5.8.5 Concluding remarks

The scouring around two piers having their line of centres at an angle 45° to the approach flow is affected by several effects (reinforcing, sheltering shed vortices and compression of horseshoe vortices) and depending on the radial spacing between the piers, there is dominance of some effects over the others. The effect of shed vortices remains dominant between the two piers due to which scour depth at rear pier remains deeper at short radial pier spacings R/b. However, as R/b increases, shed vortices originating from the front pier fail to reach the rear pier and thus become ineffective in increasing the scour depth at rear pier. At R/b=0, scour depth is deeper than the twice of the scour depth at an isolated pier. However, at R/b=1, the scour depth at front and rear piers swiftly decreases but still remains 35% and 38% deeper than that at an isolated pier. At R/b >1, the scour depth at rear pier gradually decreases and approaches to that at isolated pier at R/b=12. Based on the results achieved in this part of present investigation, it can be concluded that the downstream pier should be placed at pier spacing in the range 6<R/b<12 since the effect of vortex shedding produced by upstream pier is reasonably less in this range of pier spacings.

5.9 Two Piers at Constant Radial Spacing but Varying Angles of Attack

5.9.0 Introduction

Using the data collected from experimental tests in this study on two piers placed at constant radial pier spacing R/b=5 and having their line of centres at varying angles to the flow direction, the longitudinal and lateral profiles of scour and areal extents of scour are plotted in Appendix-II, Appendix-III and Appendix-IV respectively to study the effect of

angle of attack on local scour. The experimental investigation reveals that the scouring process at two piers placed at constant radial pier spacing R/b=5 and varying angles of attack ranging between 0° and 90° involves various scouring mechanisms like, sheltering of rear pier by the front pier, shed vortices from front pier and compression of horseshoe vortices between the piers.

5.9.1 Variation of scour depth along flume length

The data on scour depths collected in this study around two piers placed at constant radial pier spacing R/b=5 and having their line of centres at varying angles to the flow direction are plotted along centre line of flume in flow direction as shown in Appendix-II. It can be seen that the longitudinal profiles of scour are highly unsymmetrical about the longitudinal axis of the flume except at angles of attacks $\alpha = 0°$ and 90°. The longitudinal profiles show that the effect of mutual interference remains at all angles of attack.

Some distinctive cases of longitudinal profile of scour and areal extent of scour are considered fro analysis and discussion in this part of present study. In order to have a better insight into the scouring at piers placed at constant radial pier spacing and varying angles of attack, the photographs showing scour and deposition features on the bed around the piers taken at the end of each experiment. The photographs for some distinctive cases are shown in Figs. P13 & P14.

5.9.2 Scour depth at front and rear piers

The scour depths around front and rear piers are marked in the longitudinal scour profiles as shown in Appendix-II. The scour depths observed at the upstream face of piers relative to the scour depth observed at upstream face of an isolated pier 'ds/ds_i' are plotted against angle of attack of flow 'α' as shown in Fig.5.111. It is observed that the scour depth at the front pier is not very sensitive to the angle of attack and varies by less than 6% of its value at α=0°. However, scour depth at rear pier is more sensitive to the change in angle of attack 'α' due to the various scouring mechanisms, described above, and being dominant.

At small angles of attack, (α<15), the scour depth at front pier is affected by the reinforcing effect of rear pier whereas the dominant effect at the rear pier is sheltering by the front pier. As the angle of attack increases, sheltering of rear pier is reduced and the

rear pier is affected by the shed vortices, which approach it from the front pier. Consequently, scour depth increases reaching to a maximum at 'α' equal to 45°. Scour depth reduces when rear pier moves clear of the influence of shed vortices due to an increase in angle of attack and approach approximately to that observed at an isolated pier as 'α' approaches to 90°.

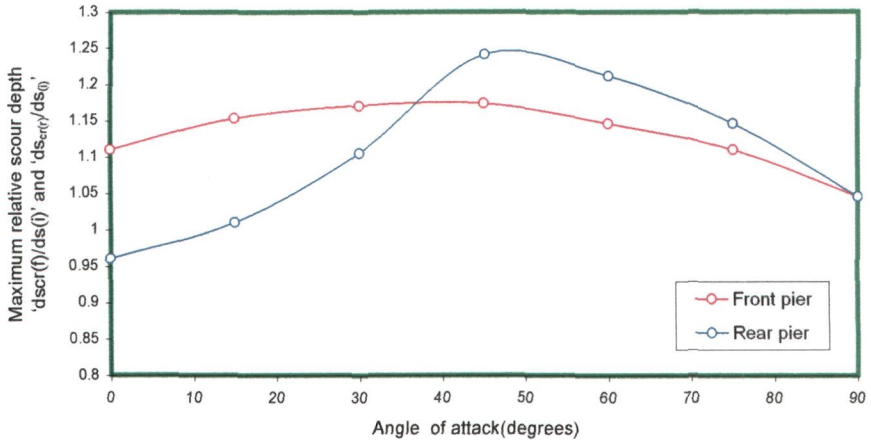

Fig. 5.111 Variation of scour depth at front and rear piers '$ds_{cr(f)}/ds_{(i)}$' and '$ds_{cr(r)}/ds_{(i)}$' with angle of attack 'α' (where $ds_{cr(f)}$ = scour depth at front pier, $ds_{cr(r)}$ = scour depth at rear pier and $ds_{(i)}$= scour depth at an isolated pier).

As shown in Fig. 5.111, the scour depths at the front and rear piers at α=0°, are about 1.1 and 0.96 times, the scour depth of a single pier respectively. The increase in scour depth at front pier is due to reinforcing effect of rear pier whereas the sheltering of the rear pier causes the decrease in scour depth at rear pier. As the angle of attack increases the scour depth at both the piers increases and reaches a maximum at α=45°, however, the scour depth at rear pier remains more than that at the front pier. This feature indicates the dominance of shed vortices effect on rear pier. At α>45°, scour depth at both the piers decreases. This decrement in scour depth occurs as the rear pier moves clear of the influence of shed vortices due to an increase in angle of attack. At 'α'=90°, the scour depths at front and rear piers are equal but about 4.5% higher than that of an isolated pier. The increment in the scour depth at α=45° indicates the dominance of effect of compression of horseshoe vortices between the two piers.

5.9.3 Variation of bed level between the piers

The maximum scour depth observed between front and rear piers relative to that at an isolated pier are plotted against angles of attack as shown in Fig.5.112. As shown in Fig.

5.112, maximum scour depth between the two pier is observed at an angle of attack α=45° which decreases thereafter. This increase in scour depth is attributed to the enhancement in the scouring strength at rear pier by shed vortices approaching to the rear pier. Decrement in the scour depth at angles of attack greater than 45° takes place as the rear pier moves clear of the influence of shed vortices. However, the decrement in scour depth at an angle of attack equal to 90° is attributed to the disappearance of all effects except the effect of compression of horseshoe vortices between the piers.

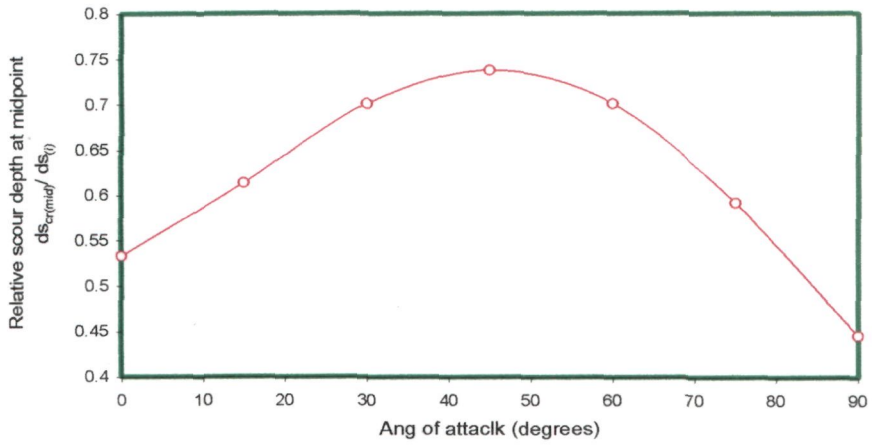

Fig. 5.112 Variation of relative scour depth at midway between the front and rear piers '$ds_{cr(mid)}/ds_{(i)}$' with angle of attack (where $ds_{cr(mid)}$ = scour depth at middle of the two piers, $ds_{(i)}$ = scour depth at an isolated pier).

For the estimation of scour depths at front and rear piers placed at constant angle of attack 'α' and varying radial pier spacing R/*b*, ANN models are applied to the present experimental data. The details of ANN models are given in Tables.6.1 and 6.2 (Chapter VI) and are also shown in ANN architectures Fig. 6.8 (Chapter VI). The scatter grams plotted between observed and estimated scour depths are shown in Fig.6.17 (Chapter VI). The closeness of data points to the line of best agreement as shown in scatter grams indicates the accuracy of the ANN model in predicting the scour depths. The average values of correlation coefficient R^2 between observed and estimated scour depths at front and rear piers for training and testing data sets are 0.9994and 0.9982 respectively. The values of *rmse* between observed and ANN estimated scour depths for front and rear piers are $2.499\text{x}10^{-3}$ and $7.625\text{x}10^{-4}$ respectively. The higher values of R^2 and lower values of *rmse* indicate the accuracy of ANN models in predicting the scour depth.

5.9.4 Characteristics of scour holes

Since the knowledge of scour whole dimensions is significant in determining the extent of countermeasures needed to prevent/control scour at piers, various parameters explained as under using present experimental data are determined.

To study the scour hole characteristics, upstream length of scour holes at the upstream and downstream faces of front and rear piers with respect to the corresponding length of scour hole at an isolated pier '$Lsh_{cru(f)}/Lsh_{u(i)}$' and '$Lsh_{cru(r)}/Lsh_{u(i)}$' are plotted against angle of attack 'α' as shown in Fig.5.113 and 5.114.

(a) Length of scour hole at upstream faces of piers

Fig. 5.113 shows the variation in the length of scour holes at upstream face of front and rear piers '$Lsh_{cru(f)}/Lsh_{u(i)}$' and '$Lsh_{cru(r)}/Lsh_{u(i)}$' relative to that at an isolated pier with angle of attack 'α'. It is observed that the length of scour hole at upstream face of front pier at zero degree angle of attack is 2.23% more than the corresponding value for an isolated pier. This slight increase in the value of '$Lsh_{cru(f)}/Lsh_{u(i)}$' is mainly due to the reinforcing effect of rear pier. At 15° and 30° angles, the values of '$Lsh_{cru\ (f)}/Lsh_{u(i)}$' are 4.5% and 9.1% more, than that at an isolated pier.

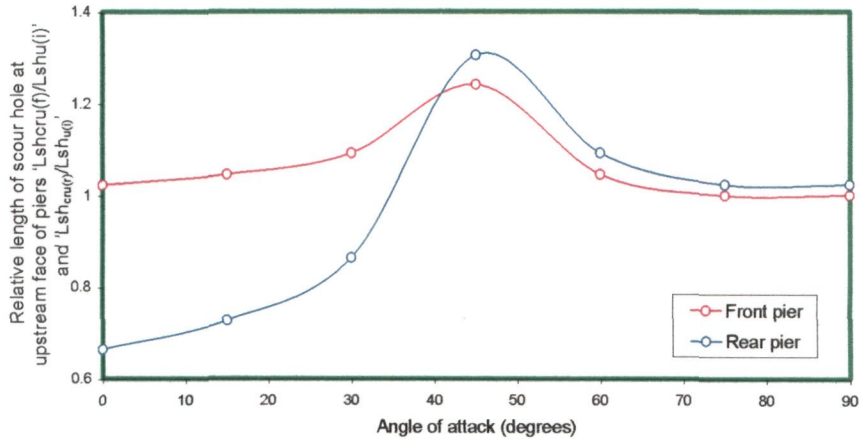

Fig. 5.113 Variation of relative length of scour holes at upstream faces of front and rear piers '$Lsh_{cru(f)}/Lsh_{u(i)}$' and '$Lsh_{cru(r)}/Lsh_{u(i)}$' with angle of attack (where $Lsh_{cru(f)}$= length of scour hole at upstream face of front pier, $Lsh_{cru(r)}$= length of scour hole at upstream face of rear pier and $Lsh_{u(i)}$ = length of scour hole at upstream face of an isolated pier).

To explore the reason behind this increase in the values of '$Lsh_{cru(f)}/Lsh_{u(i)}$' and '$Lsh_{cru(r)}/Lsh_{u(i)}$' at angles 15° and 30°, it is experimentally observed that when the two piers are misaligned to the flow, a clockwise spiral motion of flow around the line of their centres takes place due to which the strength of horseshoe vortex at front pier slightly increases. As a result, an additional force driving the flow in forward direction on the side of piers which are exposed to the flow, is generated which causes an increase in scour depth and the corresponding length of scour hole at the upstream face of front pier. The intensity of this force increases with an increase in the angle of attack and reaches to a maximum at an angle of 45°. Consequently, as shown in Fig. 5.113, the values of '$Lsh_{cru(f)}/Lsh_{u(i)}$' and '$Lsh_{cru(r)}/Lsh_{u(i)}$' are maximum at an angle of 45°. However, as the angle of attack further increases, the intensity of this force at front pier decreases and the scour depth along with the corresponding length of scour hole at upstream face of front pier decreases.

The relative length of scour hole at rear pier is more sensitive to the angle of attack than the front one. As can be seen in Fig.5.113, the value of '$Lsh_{cru(r)}/Lsh_{u(i)}$' at rear pier for zero degree angle, is about 66.36% of that at an isolated pier. This decrease in the value of '$Lsh_{cru(r)}/Lsh_{u(i)}$' is due to sheltering of rear pier by the front pier. At angles of attack greater than zero degree, the value of '$Lsh_{cru(r)}/Lsh_{u(i)}$' increases and reaches to a maximum at α=45°. The shed vortices approaching and striking the rear pier tend to increase the strength of horseshoe vortex at rear pier and result in an increase in the value of '$Lsh_{cru(r)}/Lsh_{u(i)}$'. At α=45°, the length of scour hole at the upstream face of rear pier is observed as about 30.4% more, than at an isolated pier. At α>45° the length of scour hole at upstream face of rear pier decreases and reaches to that of an isolated pier at α = 75°; whereas between α =75° to 90°, the length of scour hole remains unchanged.

(b) Length of scour hole at downstream faces of piers

The length of scour holes observed at the downstream face of front and rear piers relative to that at an isolated pier '$Lsh_{crd(f)}/Lsh_{d(i)}$' and '$Lsh_{crd(r)}/Lsh_{d(i)}$' are plotted against the angles of attack 'α' as shown in Fig. 5.114. It is observed that the values of '$Lsh_{crd(f)}/Lsh_{d(i)}$' and '$Lsh_{crd(r)}/Lsh_{d(i)}$' at the downstream face of piers at zero degree angle is 0.31 times of that at an isolated pier. This decrease in the value of '$Lsh_{crd(f)}/Lsh_{d(i)}$' and '$Lsh_{crd(r)}/Lsh_{d(i)}$' suggests the dominance of sheltering effect of rear pier by the front pier.

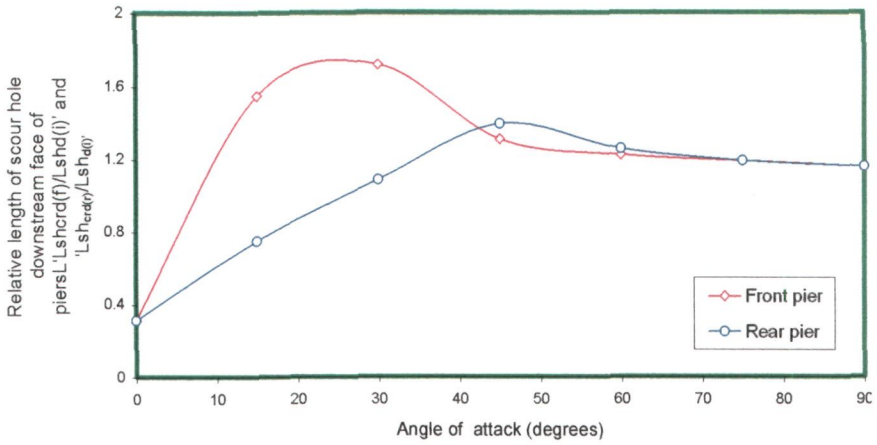

Fig. 5.114 Variation of relative length of scour holes at downstream face of front and rear piers '$Lsh_{crd(f)}/Lsh_{d(i)}$' and '$Lsh_{crd(r)}/Lsh_{d(i)}$' with angle of attack (where $Lsh_{crd(f)}$= length of scour hole at downstream face of front pier, $Lsh_{crd(r)}$= length of scour hole at downstream face of rear pier and $Lsh_{d(i)}$=length of scour hole at downstream face of an isolated pier).

As shown in Fig.5.114, the occurrence of longer length of scour hole at the upstream face of front pier than that at the upstream face of rear pier for angles of attack in the range $0°<\alpha<30°$, indicates that the point of initiation of maximum force driving the flow towards downstream on exposed side of the line joining the centres of front and rear piers, lies at the front pier (also evident in Fig. 5.111) in which the scour depths at front pier are more than the rear pier at $0°<\alpha<30°$. As the angle of attack reaches to 45°, the point of occurrence of maximum scour depth shifts towards the exposed side of rear pier as a result of which the value of '$Lsh_{crd(r)}/Lsh_{d(i)}$' increases at the rear pier than the front pier. This trend of shifting in the occurrence of maximum scour depth continues upto angle α=60°. Between α =75° to 90°, the two piers remain almost free from the effect of angle of attack of flow which is evident from the occurrence of same value of '$Lsh_{crd(f)}/Lsh_{d(i)}$' and '$Lsh_{crd(r)}/Lsh_{d(i)}$' at these angles.

(c) Slope of scour holes at upstream faces of front and rear piers

The slope of scour holes at the upstream face of front and rear piers with respect to an isolated pier '$S_{lcr(uf)}/S_{l(ui)}$' and '$S_{lcr(ur)}/S_{l(ui)}$' are plotted against angle of attack 'α' as shown in Fig. 5.115. A mild increase in the values of '$S_{lcr(uf)}/S_{l(ui)}$' is observed upto 30° angle. The values of '$S_{l(u)}/S_{l(ui)}$' at α=30° are about 10% more than that of an isolated pier. This increase is due to a slight increase in the scour depths and lengths of scour holes at the upstream face of front pier.

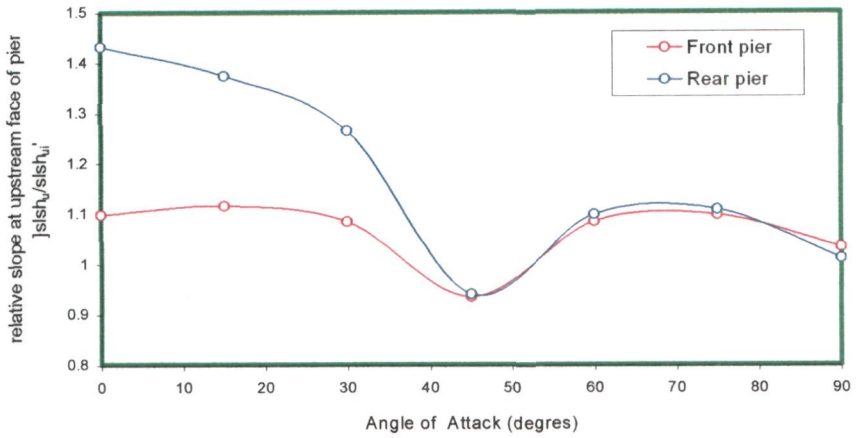

Fig. 5.115 (chart 8) Variation of slope at upstream faces of front and rear piers '$S_{lcr(uf)}/S_{l(ui)}$' and '$S_{lcr(ur)}/S_{l(ui)}$' with angles of attack (where $S_{lcr(uf)}$ = slope of scour hole at upstream face of front pier, $S_{lcr\ (ur)}$ = slope of scour hole at upstream face of rear pier and $S_{l\ (ui)}$ = slope at upstream face of an isolated pier).

Fig.5.109 also indicates that with an increases in 'α' upto 45°, the scour depth at front pier slightly increases but the length of scour hole, as observed in Fig. 5.113, considerably increases, as a result, the value of $S_{lcr(uf)}/S_{l(ui)}$ decreases but remains very close to that of an isolated pier. At rear pier, the scour depth and length of scour hole simultaneously increases in the same proportion as a result of which the resulting slope '$S_{lcr(ur)}/S_{l(ui)}$' at the upstream face of rear pier is less but very close to that of an isolated pier. It is observed in Fig. 5.115 that at angles greater than 45°, the slope of scour holes '$S_{lcr(uf)}/S_{l(ui)}$' and '$S_{lcr(ur)}/S_{l(ui)}$' at upstream face of both the piers decrease and reach to slightly greater than that of an isolated pier at angle α=90°.

Table 5.5 Relative Scour Depth, Length of Scour Hole and Slope of Scour Hole at Upstream Face of Piers

Angle of attack	Front Pier			Rear Pier		
	Relative scour depth	Relative length of scour holes at upstream face	Slope of scour hole at upstream face	Relative scour depth	Relative length of scour hole at upstream face	Relative slope of scour hole at upstream face
0	1.109489	1.022727	1.097204	0.960584	0.663636	1.431427
15	1.153285	1.045455	1.115169	1.010219	0.727273	1.37367
30	1.170803	1.090909	1.083934	1.105109	0.863636	1.265431
45	1.173723	1.240909	0.935383	1.240876	1.304545	0.940661
60	1.145985	1.045455	1.084022	1.211679	1.090909	1.098407
75	1.109489	1.000000	1.097204	1.145985	1.022727	1.108111
90	1.045255	1.000000	1.033681	1.045255	1.022727	1.010711

(d) Slope of scour holes at downstream faces of front and rear piers

The slopes of scour holes at the downstream face of the piers relative to that of an isolated pier '$S_{lcr(du)}/S_{l(di)}$' and '$S_{lcr(dr)}/S_{l(di)}$' are plotted against angles of attack 'α' as shown in Fig. 5.116. A large difference in the values of '$S_{lcr(du)}/S_{l(di)}$' and '$S_{lcr(dr)}/S_{l(di)}$' for front and rear piers at zero degree angle indicates that '$S_{lcr(du)}/S_{l(di)}$' and '$S_{lcr(dr)}/S_{l(di)}$' are more sensitive to the angle of attack. At downstream faces of the piers, the values of '$S_{l\,(d)}/S_{l\,(di)}$' are about 3.3 and 2.68 times more than at an isolated pier respectively. Appendix-II shows the scoured portion between piers for zero degree angle of attack.

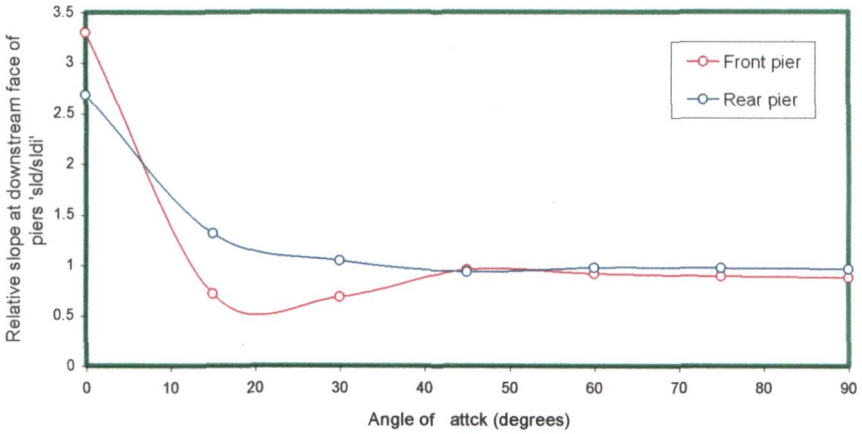

Fig. 5.116 Variation of slope at downstream faces of front and rear piers '$S_{lcr(df)}/S_{l(di)}$' and '$S_{lcr(dr)}/S_{l(di)}$' with angles of attack (where $S_{lcr(df)}$ = slope of scour hole at downstream stream face of front pier, $S_{lcr(dr)}$ = slope of scour hole at downstream stream face of rear pier and $S_{l\,(di)}$ = slope at downstream stream face of an isolated pier).

The peak formed by the sediment deposited on the bed between piers separates the boundary between the scour holes at downstream face of front and upstream face of rear piers. The length of scour holes at the downstream face of front and rear piers is observed to be same Fig 5.114 but the scour depth at downstream face of front pier is greater than at downstream face of rear pier Fig 5.111. As a result, the value of '$S_{lcr(df)}/S_{l(di)}$' at the downstream face of front pier is more than the rear pier and thus the value of '$S_{l(df)}/S_{l\,(di)}$' at front pier is noticed to be more than the corresponding value at rear pier. As the angle reaches to 15°, the length of scour hole observed at the downstream face of front pier becomes more than the rear pier (see, Fig. 5.114). As a result, the value of '$S_{lcr(df)}/S_{l(di)}$' at front pier is less than that at rear pier. Similar trend is observed at angle of 30°. However, at 45° angle and onward, the values of '$S_{lcr(df)}/S_{l(di)}$' remain constant and are close to that of an isolated pier.

(e) Length of sediment deposition at downstream faces of front and rear piers

The lengths of sediment deposition at the downstream face of front and rear piers with respect to that occurring on downstream face of an isolated pier '$L_{depcr(f)}/L_{dep(i)}$' and '$L_{depcr(r)}/L_{dep(i)}$' are plotted against angles of attack as shown in Fig. 5.117.

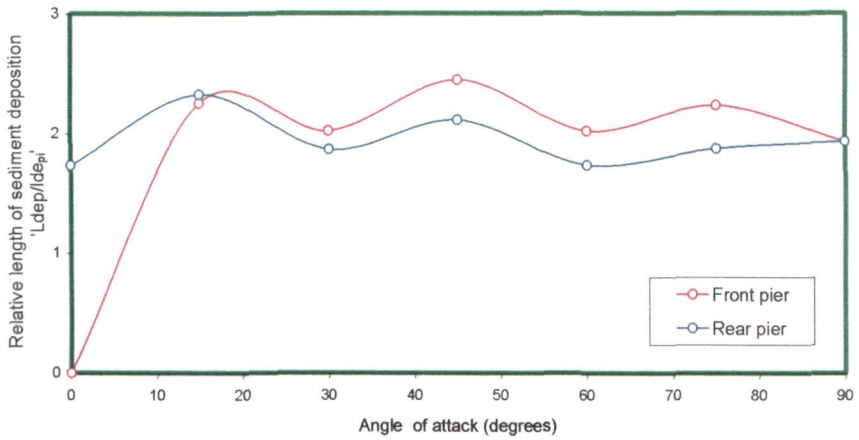

Fig.5.117 Variation of length of sediment deposition at downstream faces of front and rear piers relative to that at an isolated pier '$L_{depcrr(f)}/L_{dep(i)}$' and '$L_{depcr(r)}/L_{dep(i)}$' with angle of attack (where $L_{depcr(f)}$= length of sediment deposition at downstream face of front pier, $L_{depcr(r)}$= length of sediment deposition at downstream face of rear pier and $L_{dep(i)}$ = length of sediment deposition at the downstream face of an isolated pier).

The sediment deposition at $\alpha = 0°$ does not occur at the downstream face of front pier however, the length of sediment deposition at downstream face of rear pier is about 12.5% more than at an isolated pier. Fig.5.117 illustrates the length of sediment deposition to be more at 15°, 45°, and 75° (*i.e.*, odd angles) and less at 30°, 60° and 90° (*i.e.*, even angles) and the maximum length of sediment deposition is observed at 45° angle. At the downstream face of rear pier, the length of sediment deposition at angles $0 \leq \alpha \leq 90$ remains more than those occurring at an isolated pier. The length of sediment deposition at the downstream face of rear pier remains less upto 15°, more in between angles $15° < \alpha < 75°$ and becomes equal at $\alpha = 90°$ when compared to an isolated pier. These variations in length of sediment deposition occur due to changes occurring in the flow pattern in accordance to the change in angle of attack.

(f) Area of scour extent around the front and rear piers

Using the data collected in this study, the areal extents of scour around two piers are plotted as shown in Appendix-IV. It can be seen that except at $\alpha = 0°$ and 90°, the areal

extents are unsymmetrical about the longitudinal axis of the flume. As an example, the areal extent of scour for angle of attack of 30° is presented in Fig. 5.118 which is unsymmetrical about the longitudinal axis of the flume.

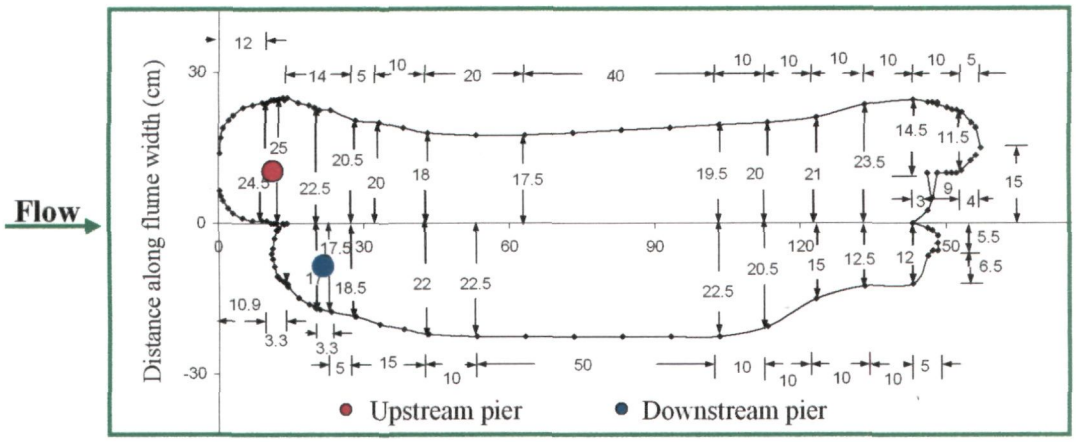

Fig. 5.118 Areal of extent of scour around front and rear piers placed at constant radial pier spacing *R b* and angle of attack=60°

The areas of scour extent relative to the area of scour extent around an isolated pier *'A/Ai'* are plotted against angles of attack *'α'* as shown in Fig. 5.119.

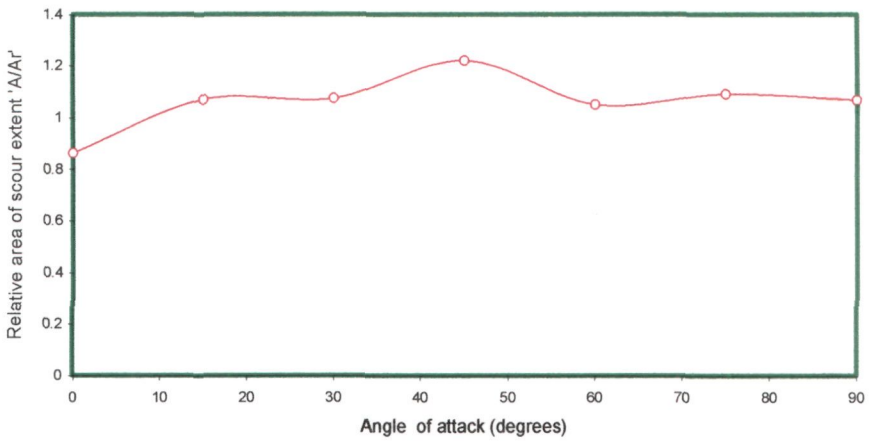

Fig. 5.119 Variation of relative area of scour extent around front and rear piers *'A_{cr}/A_i'* with angle of attack (where A_{cr} = area of extent of scour around front and rear piers, A_i = area of extent of scour around an isolated pier).

It is observed that the relative area of scour extent *'A/Ai'* at zero degree angle is about 86% of that at an isolated pier. This decrease in the area of scour extent is due to the interplay of reinforcing effect of rear pier and sheltering effect of front pier. Upstream pier shelters the downstream pier and causes a decrease in velocity of flow approaching to the rear pier. As a result, the wake vortices become weak in transporting scoured bed

material to a larger extent. At α=15°, the area of scour extent increases to about 7% more than that of an isolated pier. This increase is attributed to the flow mechanism that occurs at two piers misaligned to the flow. When the flow approaches the two misaligned piers, the shed vortices passing from front pier strike the rear pier and cause an increase in the velocity of flow approaching to the rear pier. As a result, the strength of vortex system at rear pier increases and the scoured bed material is transported to a larger extent by the wake vortices. Between 15° and 30° angles, there occurs a minimal increase in area of extent as compared to that at 15° angle. This shows a small increment in the strength of wake vortices as compared to that at 15° angle. The area of scour extent is found to be maximum (about 22% more than of an isolated pier) at α=45°. This increase is the result of enhancement in the strength of wake vortices caused by approachment of shed vortices directly to the rear pier. Between 60° and 90°, the area of scour extent fluctuates around about 1.06. This reduction beyond 45° angle indicates the decrease in strength of wake vortices as the shed vortices pass away from the rear pier.

(g) Width of scour holes at front and rear piers

The widths of scour holes at upstream face of front and rear piers relative to that an isolated pier '$w_{1cr(f)}/w_i$' and '$w_{2cr(r)}/w_i$' are plotted against angle of attack 'α' as shown in Fig. 5.120. At zero degree angle, the width of scour hole at front pier '$w_{1cr(f)}/w_i$' is slightly more than that of an isolated pier. This slight increase in the value of $w_{1cr(r)}/w_i$ is due to an increase in the scour depth caused by the reinforcing effect induced by the rear pier. However, at rear pier, the value of w_2/w_i is 0.98 times of that for an isolated pier. This decrease in the value of '$w_{2cr(r)}/w_i$' is caused due to a decrease in the scour depth resulting from the sheltering of rear pier. When the piers are misaligned to the flow, the shed vortices of front pier pass closer to the rear pier due to which the velocity of flow approaching the rear pier increases and thus the strength of horseshoe vortex increases. When α=45°, the shed vortices of front pier approaches straightforwardly to the rear pier and causes the maximum increase in strength of horseshoe vortex thereby resulting in a maximum increase in scour depth at rear pier. The values of w_1/w_i and w_2/w_i increase with an increase in the angles of attack and reaches to a maximum at angle 45°. At angles between 45° and 75°, the shed vortices pass relatively away from the rear pier due to which strength of horseshoe vortex at rear pier decreases.

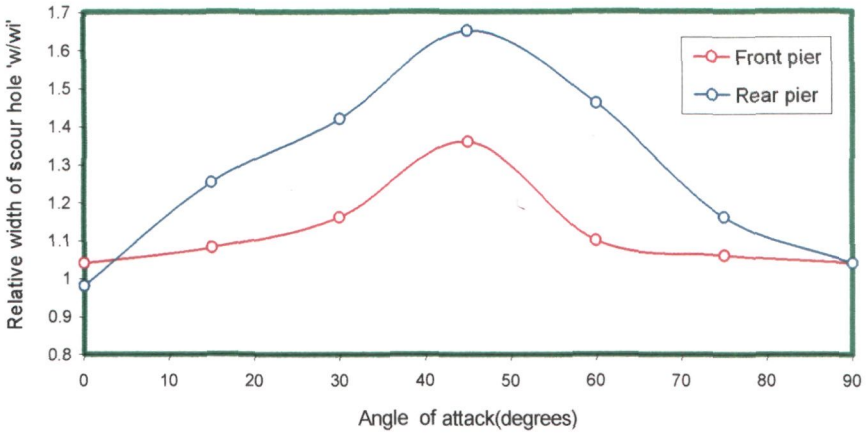

Fig.5.120 Variation of relative width of scour holes of front and rear piers '$w_{1cr(f)}/w_i$' and '$w_{2cr(r)}/w_i$' with angles of attack (where $w_{1cr(f)}$ = width of scour hole of front pier, $w_{2cr(r)}$ = width of scour hole of rear pier *and* w_i = width of scour hole of an isolated pier).

Consequently the value of '$w_{2cr(r)}/w_i$' w_2/w_i decreases but remains more than that of an isolated pier. At α=90°, the values of w_1/w_i and w_2/w_i become equal but remain 4% more than that of an isolated pier. This slight increase in the values of w_1/w_i or w_2/w_i is caused due to compression of horseshoe vortices between two piers.

The facial appearance of the bed around the piers shown in Figs. P13 & P14 validate the analysis of results on scour characteristics discussed above for the piers placed at constant radial pier spacing and varying angles of attack.

5.9.5 Temporal variation of scour depth

The data on temporal variation of scour depth colleted on two piers placed at constant angle of attack and varied longitudinal pier spacings re given in Appendix-I. The plots of these data (not shown here) reveal that the rate of scour at downstream pier remains more than that at upstream pier due to the increased strength of horseshoe vortex caused by the approachment of flow from upstream piers to the downstream pier at some angle of attack. The data in Appendix-I reveal that the temporal scour depth variation curve for downstream pier lies above the temporal variation curve for upstream pier up-to pier spacing R/b=11. However, at R/b=12, the temporal variation curves for upstream and downstream piers almost coincide with each other signaling that the two piers become free of the mutual interference.

5.9.6 Concluding remark

The scouring process at two piers placed at constant radial pier spacing R/b=5 and varying angles of attack ranging between 0° and 90° involves various scouring mechanisms like, reinforcing effect of rear pier, sheltering of rear pier by the front pier, shed vortices from front pier and compression of horseshoe vortices between the piers. Depending on the angles of attack, there is dominance of some effects over the others. At zero degree angle, the reinforcing, vortex shedding and sheltering effects affect the local scour at front and rear piers. At $\alpha>0°$, all the effects (*i.e.*, reinforcing, sheltering, shed vortices and compression of horseshoe vortices) play their roll in influencing the local scour at front and rear piers. At $\alpha=90°$, however, front and rear piers are influenced mutually by the compression of horseshoe vortices only. Based on the results achieved in this part of present study, it can be concluded that the rear pier can be placed at angle of attack $\alpha<15°$ as various hydraulic effects interplaying between the two piers have little impact on scour depth at rear pier, however, the scour depth at front pier leftovers about 10 % higher than that at an isolated pier owing to reinforcing effect induced by the rear pier. Placement of rear pier at angle of attack greater than 45° in any case should, however, be avoided as the scour depth at front and rear pier remains maximum at this angle of attack.

5.10 Local Scour at a Group of Circular Piers of Varying Sizes

5.10.0 Experimental depiction of local scour around a group of circular piers of varied sizes aligned at different angles of attack (α).

(a) Piers group without collar

At zero degree angle of attack, flow was symmetrical about the longitudinal axis of the piers group and, throughout the test duration, the depth of scour remained maximum at the nose of upstream smallest diameter pier. At $\alpha>0°$, however, approach flow was asymmetrical about longitudinal axis of piers group and the sediment scoured from around the piers group was observed moving around the piers group in clockwise direction. The location of occurrence of maximum scour depth around the piers group without a collar, was also changing with angle of attack as shown in Fig.5.121 The maximum scour depth at 7.5° and 10° angles of attack, occurred at points *'A'* and *'B'* respectively in the vicinity of right face of upstream smallest diameter pier, whereas at

15°angle, the maximum scour depth was observed at point *'C'* in close vicinity of right face of largest pier diameter. At angle of attack of 30°, the maximum scour depth was observed at point *'D'* towards the right face of upstream smallest diameter pier at a distance of 2.5 cm from nose of smallest diameter pier.

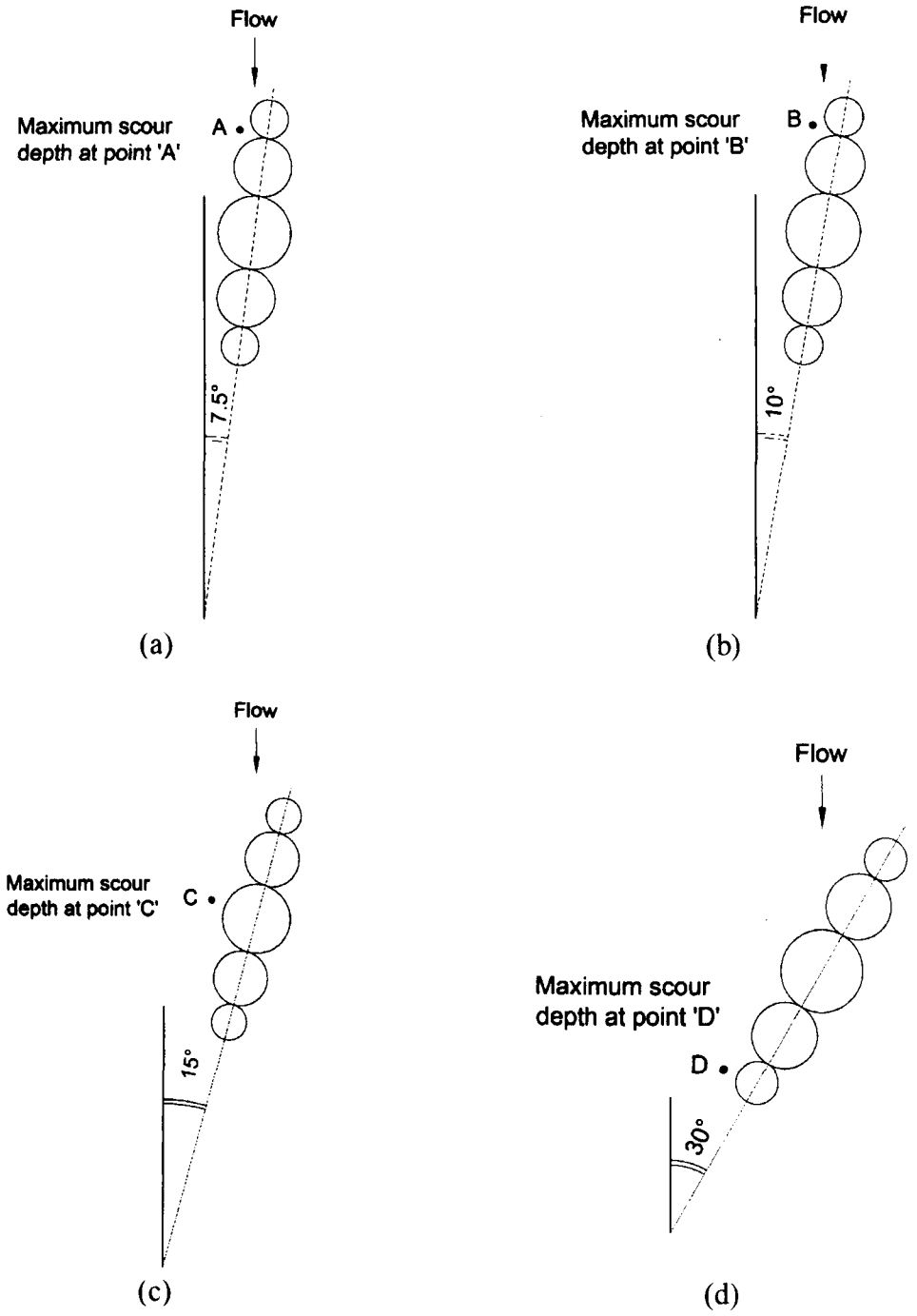

Fig. 5.121 Location of maximum scour depth around piers group without collar aligned at different angles of attack.

The facial appearance developed on the bed around the piers group without a collar at the end of tests at angles of attack 0°, 7.5°, 10°, 15° and 30°, is shown in Figs. P15, P16, P17 and P18 respectively. Fig. PI shows scour and deposition patterns around an isolated 415 mm pier.

(b) Piers group with collar

The piers group with collar aligned at an angle of attack 'α' is shown in Fig. 5.122

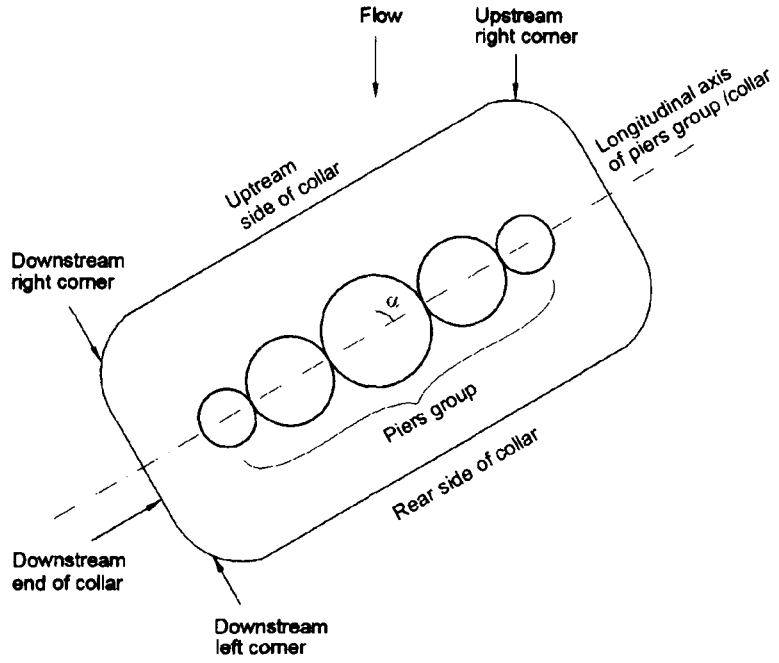

Fig. 5.122 Piers group with collar aligned at an angle of attack 'α'

Experimental depiction of local scour around a group of circular cylindrical piers of varied sizes with collar aligned at different angles of attack 'α'is summarized below.

5.10.1 Angle of attack (α) = 0°

During ten hours experimental run at 0° angle of attack, no sign of scour around the collar was noticed which indicates complete shielding of sediment bed by the collar against the action of down flow, horseshoe vortex and wake vortices. The facial appearance of the sediment bed around the piers group with a collar at the end of test is shown in Fig. P15. It is noteworthy that the sediment bed around the collar remained perfectly plain till the end of the test.

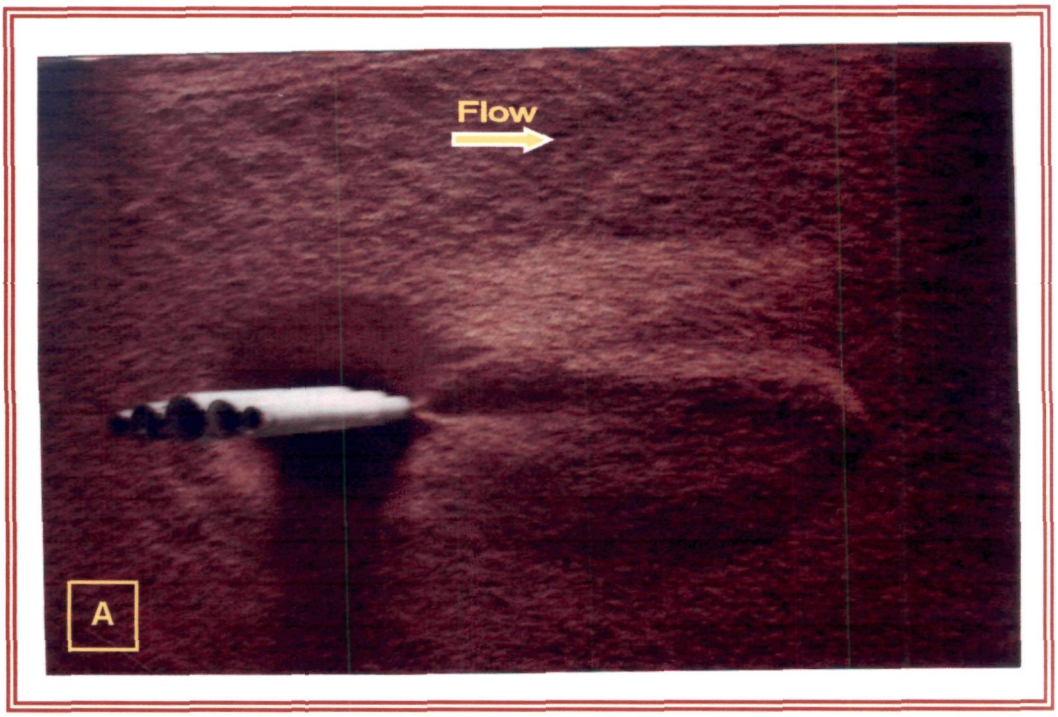

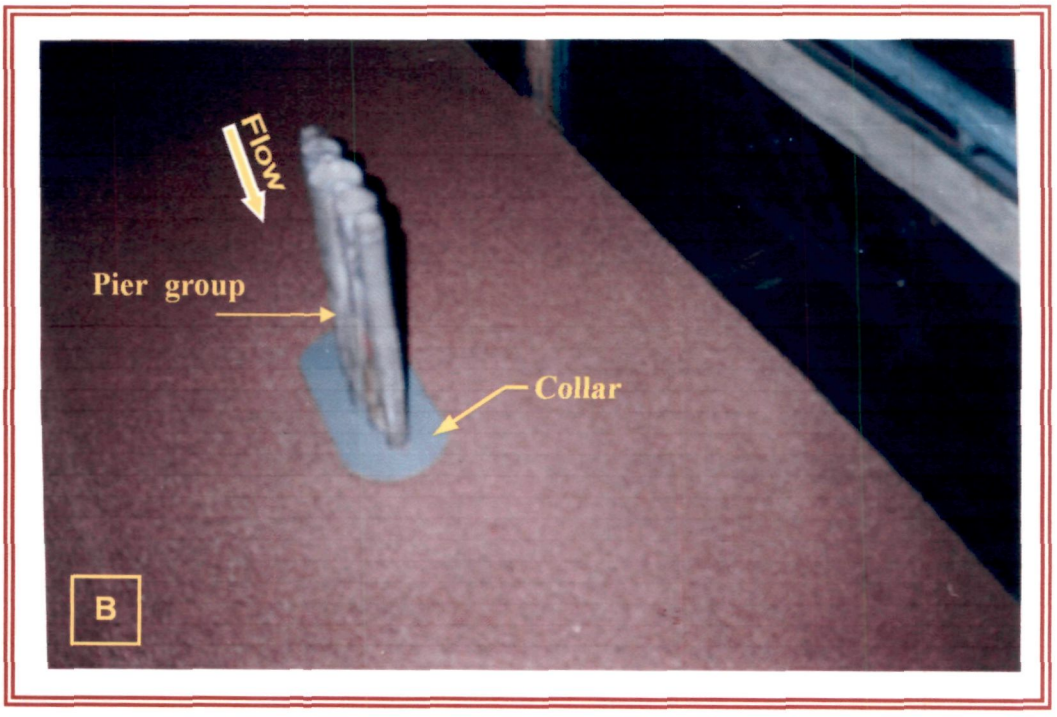

Fig. P15: Scour and deposition patterns around a group of piers of varying sizes at $\alpha=0°$ (A) Without collar (B) With collar

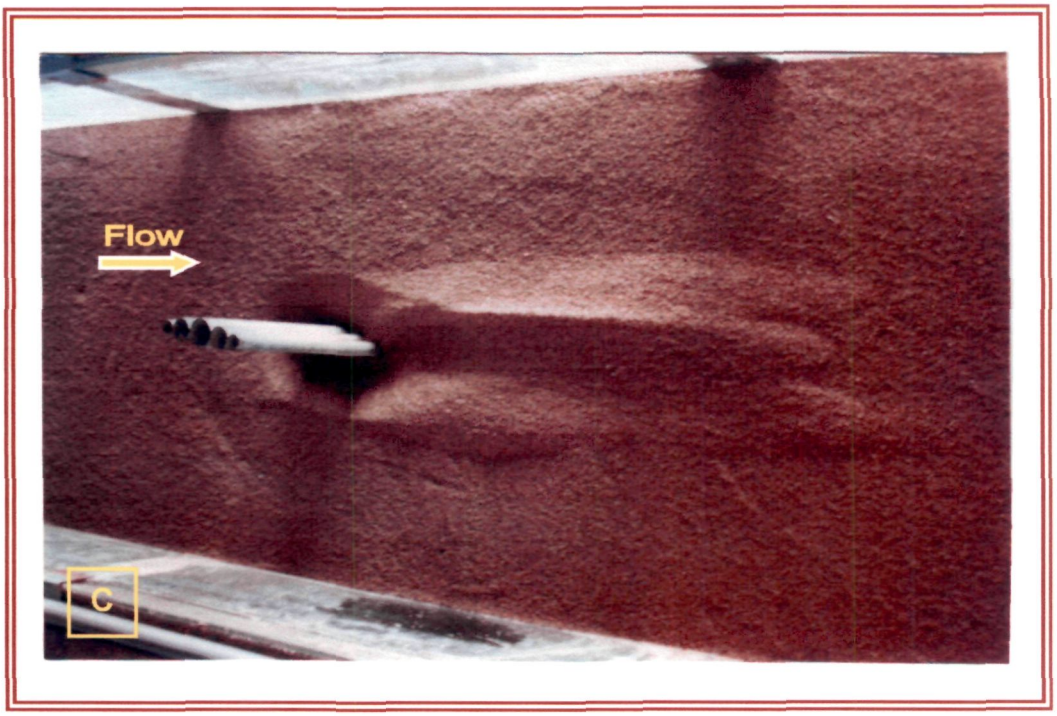

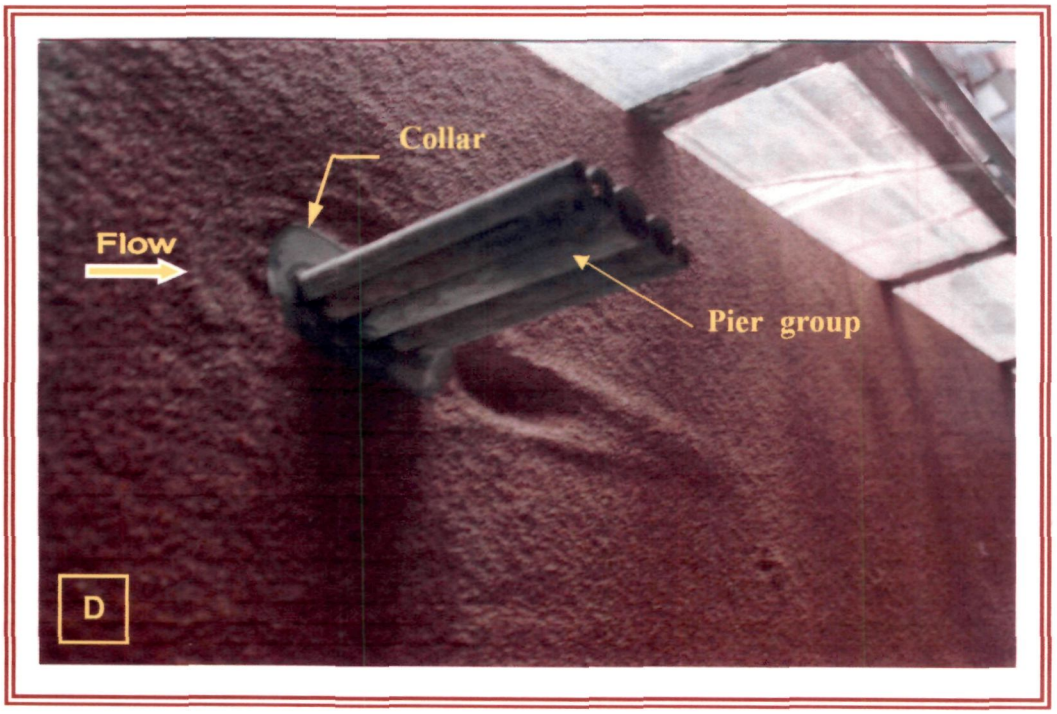

Fig. P16: Scour and deposition patterns around a group of piers of varying sizes at α=10° (C) Without collar (D) With collar

5.10.2 Angle of attack (α) =7.5°

Upto 60 minutes from the commencement of experiment at 7.5° angle of attack scour did not occur, however, soon after, a few sediment particles got eroded at the downstream edge of collar by the incoming flow due to which thickness of collar was slightly exposed in a length segment *'L'* as shown in Fig. 5.123. In next 60 minutes, scour did not progress further, however, thereafter, thickness of collar in length segment *'L_1'* on either end of length *'L'*, got partially visible. No scour hole of any depth around the collar was noticed till the end of experimental run.

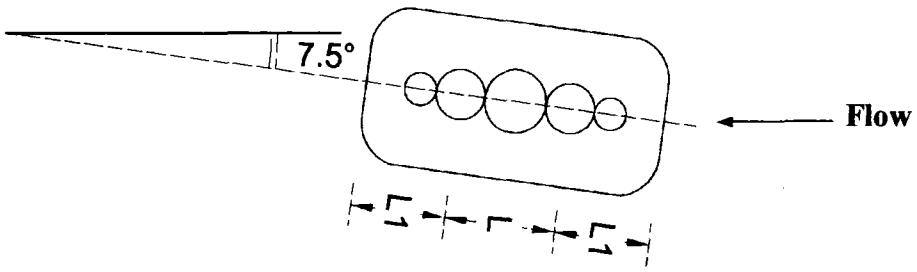

Fig. 5. 123 Piers group with collar at 7.5° angle of attack

5.10.3 Angle of attack (α=10°)

Upto 60 minutes from the start of experiment, no sign of scour around the collar were noticed, however, thickness of collar got exposed only at point *'A'* shown in Fig.5.124

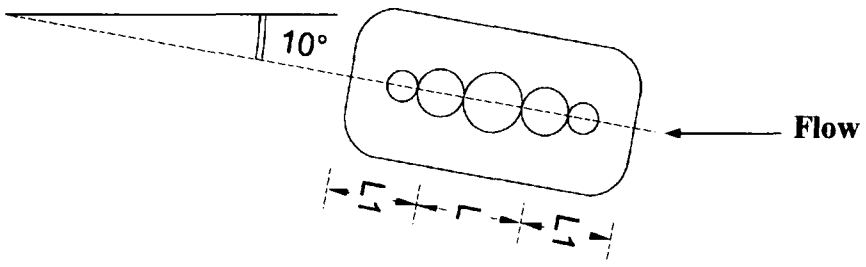

Fig.5. 124 Piers group with collar at 10° angle of attack

At the end of experiment, maximum scour depth was noticed at downstream side of collar at a distance of 1.5 cm from 33 mm diameter pier of piers group. The areal extents of scour developed around the piers group without and with collar are shown in Fig. 5.125.

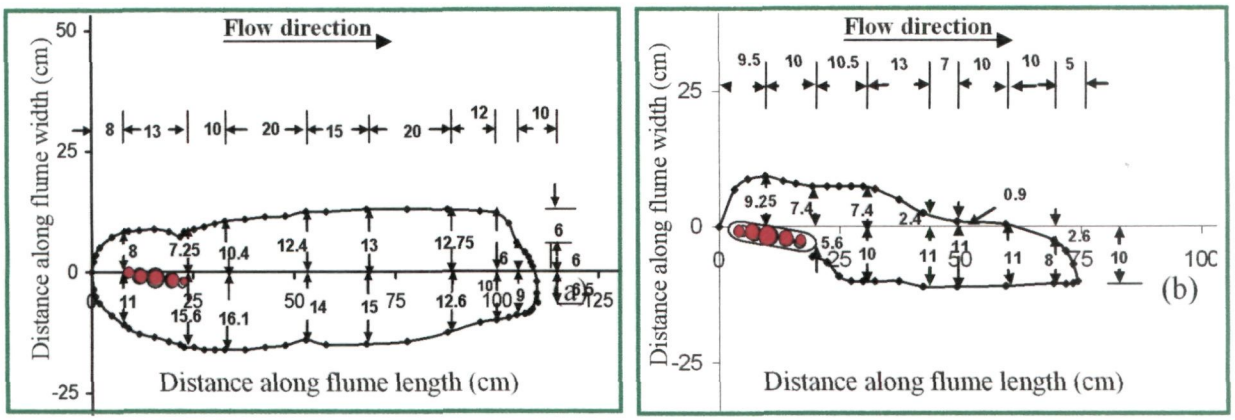

Fig.5.125 areal extent of scour at α= 10° (a) without collar (b) with collar

It can be noticed that the application of collar to the piers group causes significant reduction in the area of scour extent which in turn, causes considerable reduction in the cost to be incurred on the scour countermeasures for the safety of piers group against local scour. The photograph showing scour and deposition patterns developed around the piers group with and without collar at the end of experimental runs can be seen in Fig.P16. These photographs corroborate the analysis of results discussed in the section 5.10.3.

5.10.4 Angle of attack (α) =15°

Fig. 5.126 shows piers group with collar aligned at 15° angle of attack. When the experiment started, scour commenced and after 10 minutes, and a small scour hole formed on downstream side of collar.

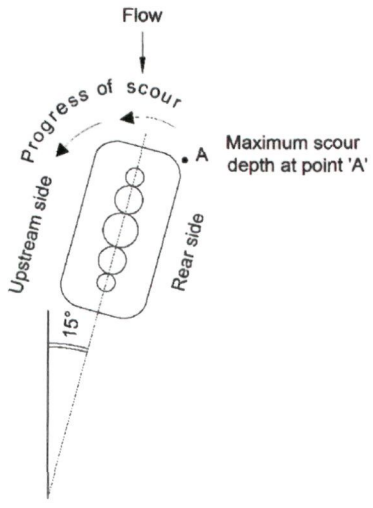

Fig. 5.126 Piers group with collar at 15° angle of attack

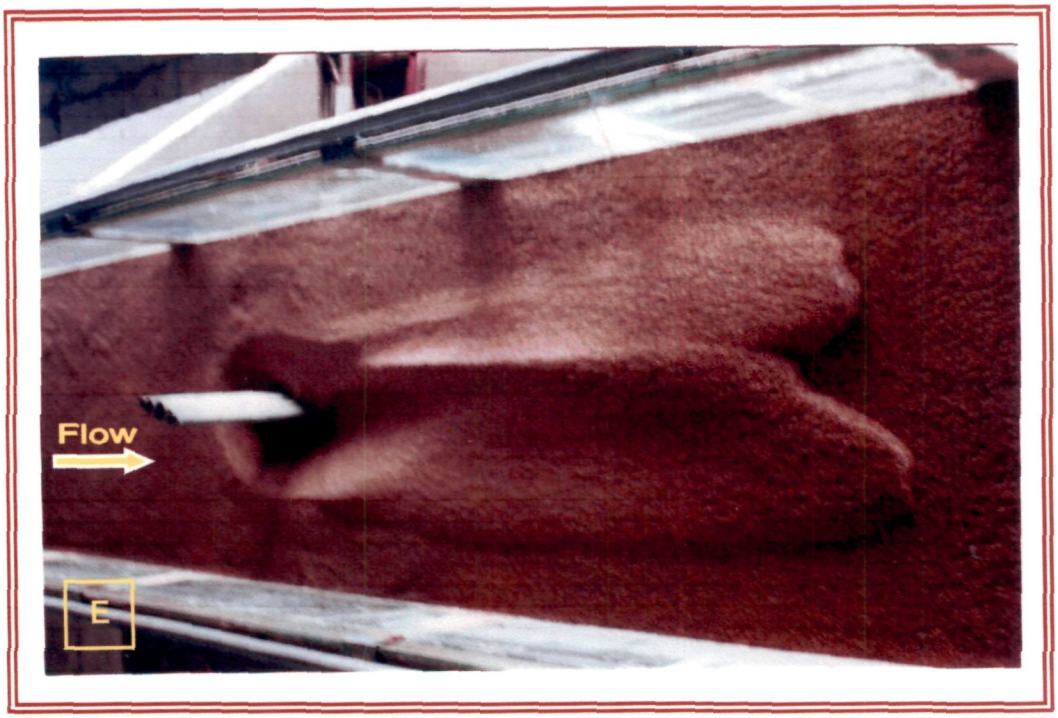

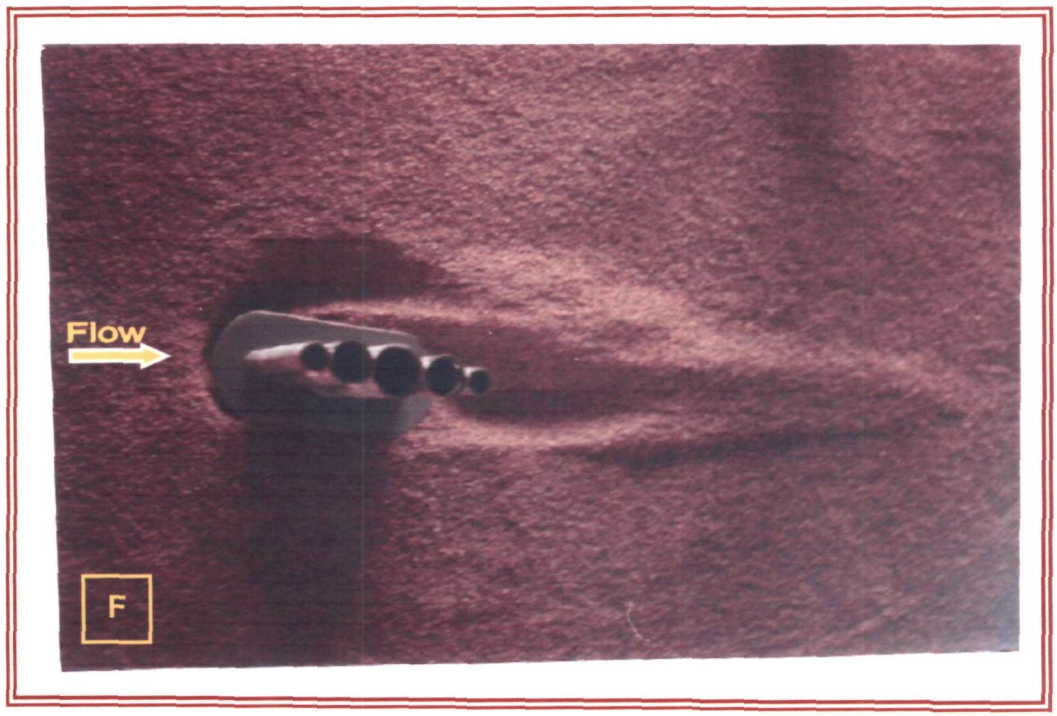

Fig. P17: Scour and deposition patterns around a group of piers of varying sizes at α=15° (E) Without collar (F) With collar

The bed material scoured from this scour hole got deposited on left side this scour hole. With the passage of time, scour progressed from downstream side of collar towards the upstream side of collar. After 90 minutes, scour then progressed towards downstream end of collar.

At the end of test run, the maximum scour depth was observed at downstream end of collar (point *A*) at a distance of 2 cm from 33 mm diameter pier of piers group. The areal extents of scour developed around piers group without and with collar at the end of experimental run are shown in Fig. 5.127

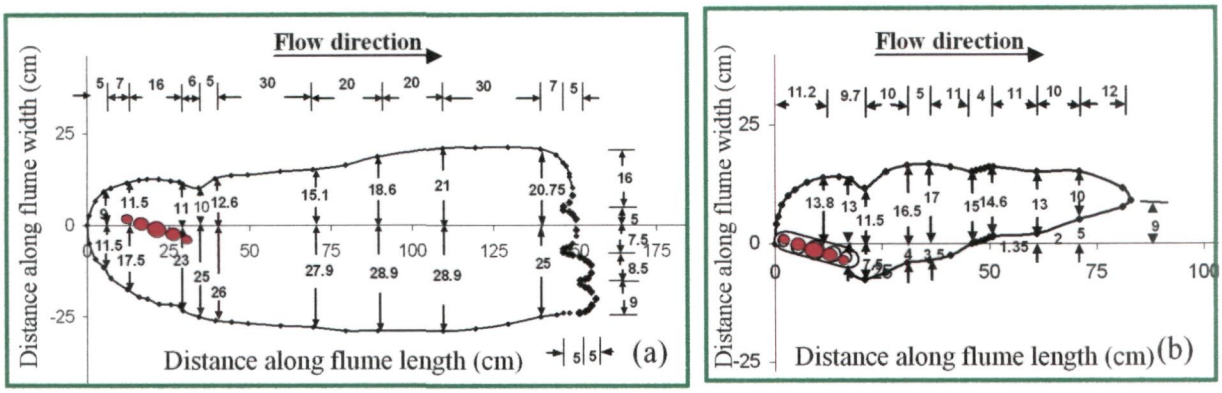

Fig. 5.127 Areal extent of scour at α = 15° (a) without collar (b) with collar

This figure shows that how the areal extent around piers group with a collar differs from that without a collar, in shape and size. As appears in Fig.5.127 area of scour extent around the piers group gets reduced considerably due to application of collar.

The scour and deposition features developed around the piers group with and without collar at the end of experiment can be noticed in Fig. P17. As observed in Figs. 127(a, b) and Fig. P17 the application of collar at piers group at α = 15°, causes considerable reduction in the area of extent of scour, which in turn causes significant reduction in the cost of scour countermeasures required for pier protection.

5.10.5 Angle of attack (α) = 30°

Initially, scour commenced at three points, namely, along 1/3rd length of downstream side of collar (point B), at upstream right corner of collar (point A) and at downstream right corner of collar (point C) as shown in Fig 5.128 Then after, scour progressed towards downstream side of collar (point F). Within 5 minutes of starting the experiment, bed material from the immediate vicinity of the edge of collar al-around its perimeter except the downstream left side corner, was scoured; however,

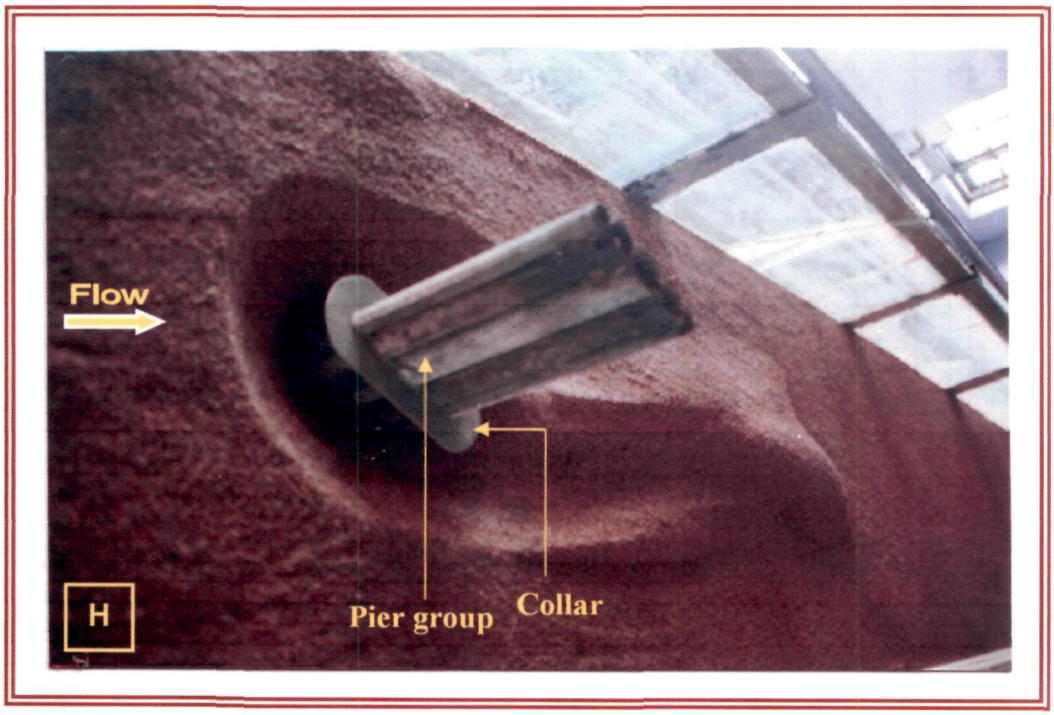

Fig. P18: Scour and deposition patterns around a group of piers of varying sizes at $\alpha=30°$ (G)Without collar (H)With collar

the consequential scour depth was of the order of collar thickness. After one hour, two small scour holes, one on right side of collar (points G) and other on left side of collar (point H), were developed. At the end of test run, scour hole developed al-around the collar except downstream right corner of collar (point K), where the material scoured from around the collar was deposited. Nevertheless, the sediment in the close vicinity of piers group beneath the collar was not removed. The maximum scour depth at the end of experiment was observed at Point A Photographs shown in Fig. P18 taken at the end of experimental run depict a scour hole all around the collar except downstream end of collar where material beneath the collar was not disturbed.

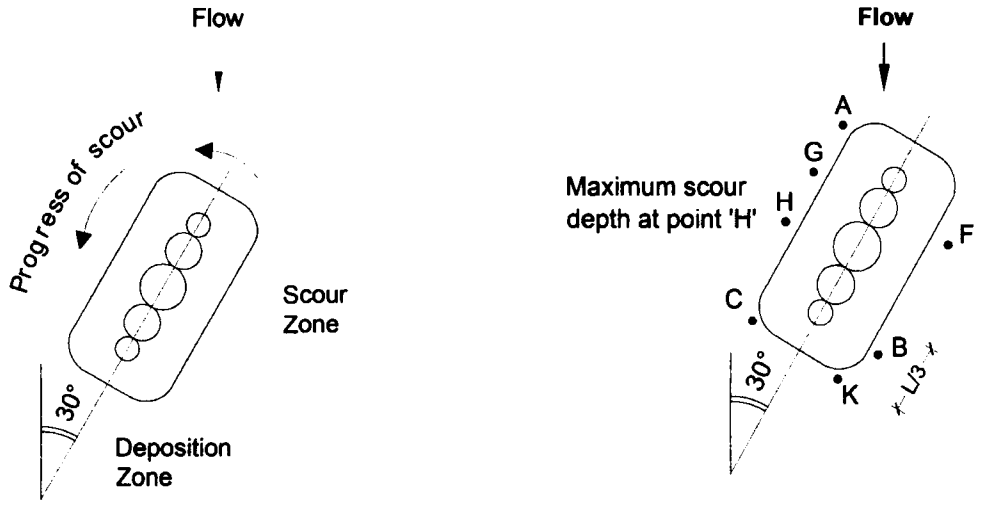

Fig. 5.128 Piers group with collar at 30° angle of attack

The areal extents of scour developed around piers group without and with collar plotted after the completion of experimental run are shown in Fig. 5.129 which reveals that, though, the effectiveness of collar relatively gets reduced at larger angle of attack, nevertheless, the area of scour extent remains less than that without collar.

In order to analyze the experimental results obtained in present study on the application of collar around a group of piers of varying diameters, important elements of scour like, temporal development of scour depth, lateral profile of scour depth, areal extent of scour, length and height of sediment deposition and the maximum scour depth and location of its occurrence around the group of piers with and without collar aligned at varying angles of attack, are studied. Also, scour depth reduction efficiency of the collar applied to the group of piers, is analyzed.

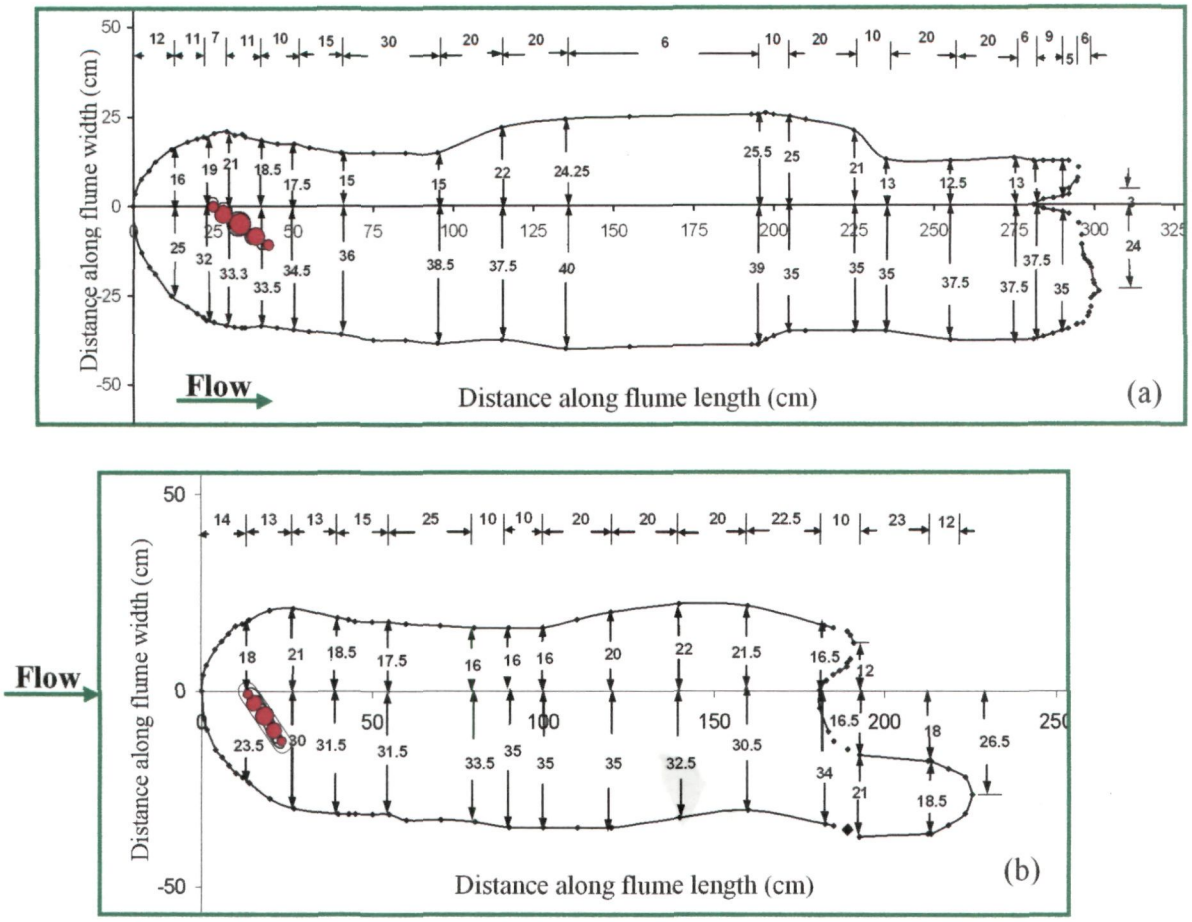

Fig.5.129 areal extent of scour at α= 30° (a) without collar (b) with collar

5.10.6 Scour depth at piers group without collar

As the objective of this part of research is to provide a cost-effective design of a pier, an alternative to a round-nose rectangular pier (L/b=4) is examined by using a group of circular piers of varying sizes (Fig. 5.130) in which the maximum diameter of pier is equal to the width of pier (b=4.15cm) and the length of piers group is equal to the length of round-nose rectangular pier (L=4b).

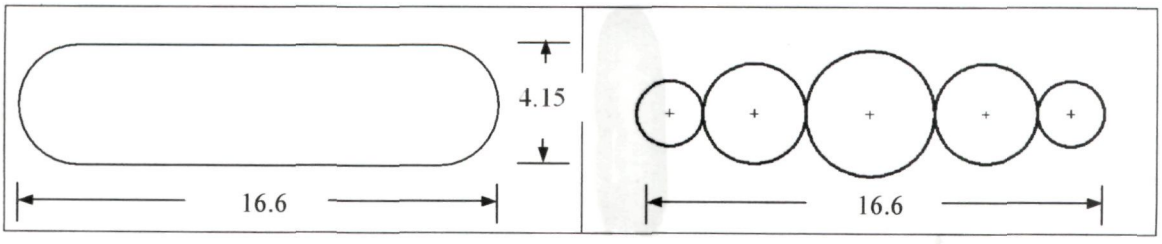

Fig.5.130 Round-nose rectangular pier and a group of t circular piers of varying diameters, both of same length to width ratio 4:1.

The results are analyzed by plotting scour depths observed around piers group with respect to the scour depths around a round-nose rectangular pier against angles of attack as shown in Fig. 5.131

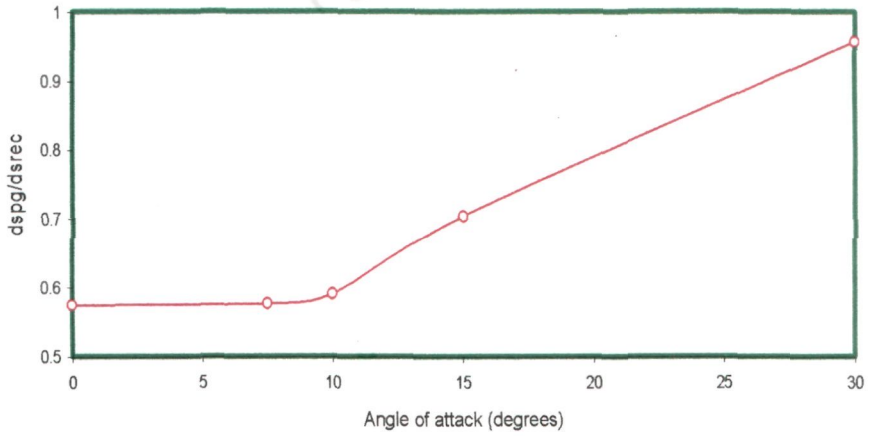

Fig. 5.131 Variation of maximum scour depth at piers group without collar relative to the scour depth at round-nosed rectangular pier '$ds_{pg(woc)}/ds_{(rectp)}$' with angles of attack (where $ds_{pg(woc)}$ = maximum scour depth at group of piers without collar, $ds_{(rectp)}$= scour depth at round-nose rectangular pier.)

It is noteworthy that at an angle α =0°, the relative scour depth '$ds_{pg(woc)}/ds_{(rectp)}$' is 62 % of that at round-nose rectangular pier. Between 0° and 7.5° angles, the relative scour depth remains nearly constant, however, beyond 7.5°, it increases linearly and at 15° angle. The maximum scour depth observed at this angle is about 85% of that at round-nose rectangular pier. At 30° angle, the scour depth at piers group nearly equals to that of round-nosed rectangular pier.

The reduction in relative scour depth shown in Fig. 5.131 suggests that upto 7.5° angle, the smallest diameter pier at upstream end of the piers group acts like a sharp edge object which breaks the vortex tube approaching to the piers group in two parts and results in the development of a weak horseshoe vortex around the piers group model and thereby results in shallower scour depths. However, as angle of attack increases, the bluntness of piers group increases and hence scour depth increases. At α =30°, piers group loses significance of its shape in reducing the scour depth as compared to that of round-nosed rectangular pier.

5.10.7 Scour depth at piers group with collar

The scour depths at piers group with collar relative to that of without collar; 'ds_{wc}/ds_{woc}' are plotted against angles of attack as shown in Fig. 5.132 It is noticed that the value of scour depths ratio 'ds_{wc}/ds_{woc}' remains unchanged viz., zero, and upto 7.5° angle. Thereafter, it increases with angle of attack. Nonetheless, at 30° angle the value of 'ds_{wc}/ds_{woc}' remains as low as 0.58.

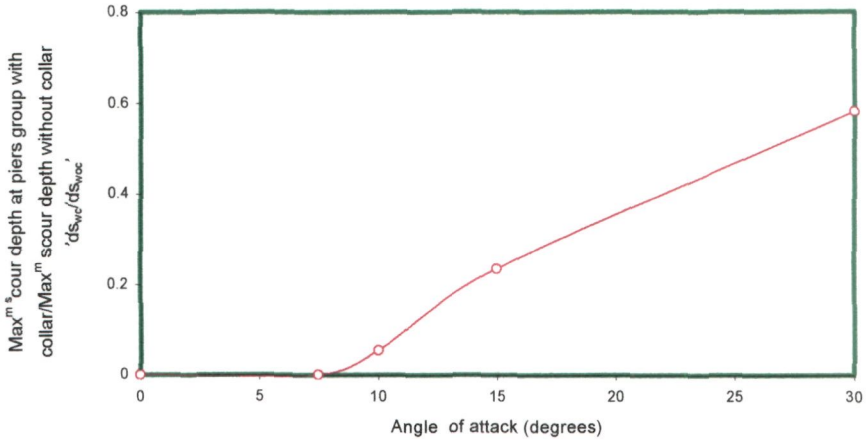

Fig. 5.132 Variation of maximum scour depth at piers group with collar relative to the maximum scour depth without collar '$ds_{g(wc)}$ $ds_{g(woc)}$' with angles of attack (where $ds_{g(woc)}$ = maximum scour depth at piers group without collar, $ds_{g(wc)}$ = maximum scour depth at piers group with collar).

The variation of scour depth shown in Fig. 5.132 indicates that upto 7.5° angle, the collar completely shields the sediment bed around piers group against the impinging of down-flow and deflects the flow, results in the formation of horseshoe vortex on the rigid surface of the collar plate which does not allow the horseshoe vortex to sink into the sediment bed in the vicinity of piers group and thus causes zero scour depth around the piers group. As the angle of attack increases, the upstream end of piers group becomes relatively blunter due to which the size of the horseshoe vortex increases and causes more scouring around the collar plate. With further increase in angle of attack, size of the horseshoe vortex goes on increasing, as a result, the shielding effects of the collar goes on reducing and scour depth around the piers group goes on increasing.

As regards to the prediction of the scour depth around the piers group, an ANN model with details given in Tables 5.1 and 5.2 (Chapter 5-II), has been applied to the observed

experimental data for the estimation of scour depth at this group of piers with & without collar and aligned at varied angles of attack. Scatter grams shown in Fig.6.20 (Chapter VI) and ANN architectures shown in Fig.6.9 (Chapter VI) reveal an excellent agreement between observed and ANN estimated scour depths. Higher values of the correlation coefficient R^2 and lower values of *rmse* mentioned in Tables 6.1 and 6.2 Chapter VI) also indicate the goodness of ANN models in predicting the scour depth.

5.10.8 Efficiency of collar in the reduction of scour depth at piers group

Fig.5.133 shows percent reduction in the scour depth at varied angles of attack due to the application of collar to piers group. Upto 7.5° angle, a 100% reduction in the scour depth is observed. To ascribe a reason for this, it is worth mentioning that the smallest diameter piers at upstream end of the piers group acts like a sharp edge object and breaks the vortex tube approaching to the piers group which results in the formation of a weak horseshoe vortex around the piers group. Also, as the down-flow impinges on the collar plate, the down flow is incapable to scour the sediment bed. As the angle of attack increases beyond 7.5°, the percent reduction in scour depth goes down and reaches to 42% at 30°angle. This decrease is credited to the increase in the size of horseshoe vortex with an increase in bluntness of piers group at larger angle of attack.

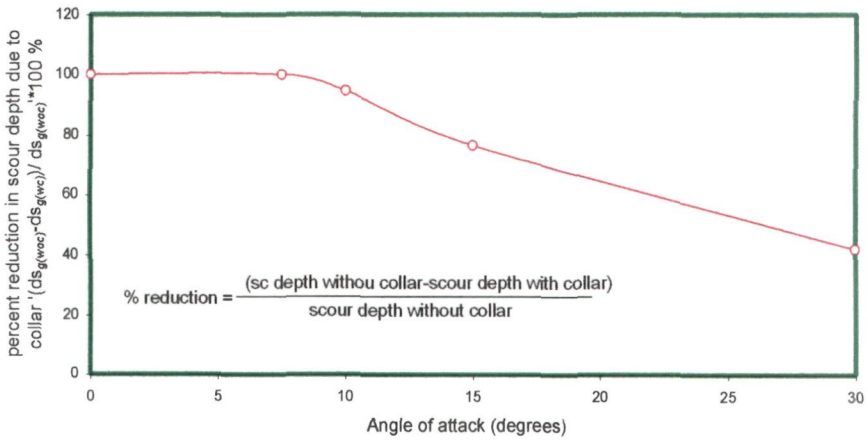

Fig. 5.133 Variation of percentage reduction in the maximum scour depth at piers group due to the application of collar $[(ds_{pg(woc)}-ds_{pg(wc)})/ds_{gp(woc)}]_{x100}$ % with angle of attack (where $ds_{pg(woc)}$ = scour depth at piers group without collar, $ds_{pg(wc)}$ scour depth at piers group with collar).

5.10.9 Location of occurrence of maximum scour depth around piers group with and without collar

Throughout the experimental run, the maximum scour depth at piers group without collar at 0° angle occurred at the upstream face of piers group. However, at angles of attack α=7.5° and 10°, the maximum scour depth occurred in the vicinity of smallest diameter pier near the side of piers group facing towards the flow. At α =15°, the maximum scour depth occurred in the vicinity of largest size pier near the piers group side facing towards the flow. At α =30°, the maximum scour depth occurred at the piers group side facing towards the flow, at a distance of 2.5 cm from the largest diameter pier.

5.10.10 Characteristics of scour hole

Since the knowledge of scour hole dimensions is important in determining the extent of countermeasures needed to reduce scour at piers, various relevant parameters are analyzed using present experimental data.

In order to study the scour and deposition patterns around the piers group, the length of scour holes at upstream and downstream faces of the piers group, width of scour holes, length of sediment deposition, maximum height and location of sediment deposition are analyzed herein.

(a) Length of scour holes at upstream and downstream faces of piers group without collar

The relative length of scour holes at upstream face of piers group '$L_{shu}/L_{shu(0°)}$' and downstream face of piers group '$L_{shd}/L_{shd(0°)}$' without a collar are plotted against angles of attack as shown in Fig. 5.133. It is noticed that as the angle of attack increases, the values of '$L_{shu}/L_{shu(0°)}$' and '$L_{shd}/L_{shd(0°)}$' increases on upstream and downstream sides of piers group respectively.

This increase is attributed to the increase in the frontal width (projected width) of piers group with an increase in angle of attack.

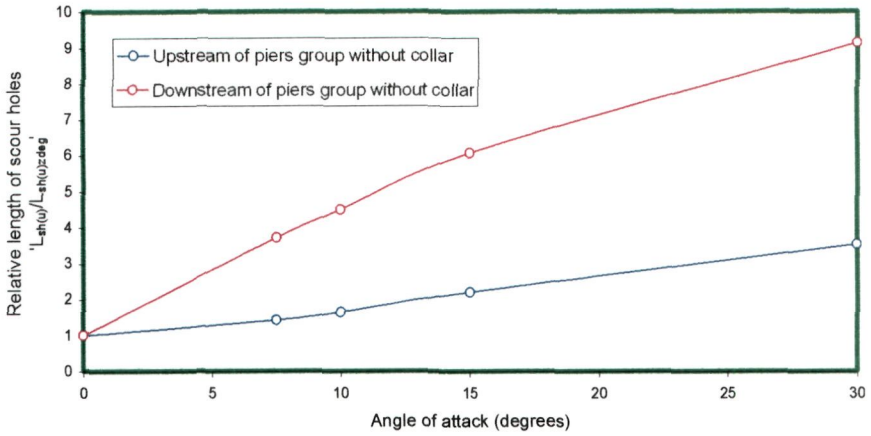

Fig.5.134 Length of Scour Holes on Upstream and Downstream of Piers group Without Collar (where L_{shu} and L_{shd}= Length of scour holes at upstream and downstream ends of piers group at an angle of attack respectively and $L_{shu(0°)}$ = Length of scour hole at upstream face of piers group at zero degree angle of attack).

At upstream end of piers group, the relative length of scour hole '$L_{shu}/L_{shu(0°)}$' at 30° angle is 3.53 times more than that is observed at 0° angle, while the relative length of scour hole '$L_{shd}/L_{shd(0°)}$' at downstream end of piers group, is about 9.14 times more than that is observed at 0° angle of attack. As shown in Fig.5.134 the values of '$L_{shu}/L_{shu(0°)}$' and '$L_{shd}/L_{shd(0°)}$' at upstream and downstream ends of piers group are same at 0° angle .

(b) Length of scour hole at downstream end of piers group with collar

The length of scour hole at piers group with collar with respect to that without collar '$L_{sh(wc)}/L_{sh(woc)}$' are plotted against angles of attack as shown in Fig. 5.135.

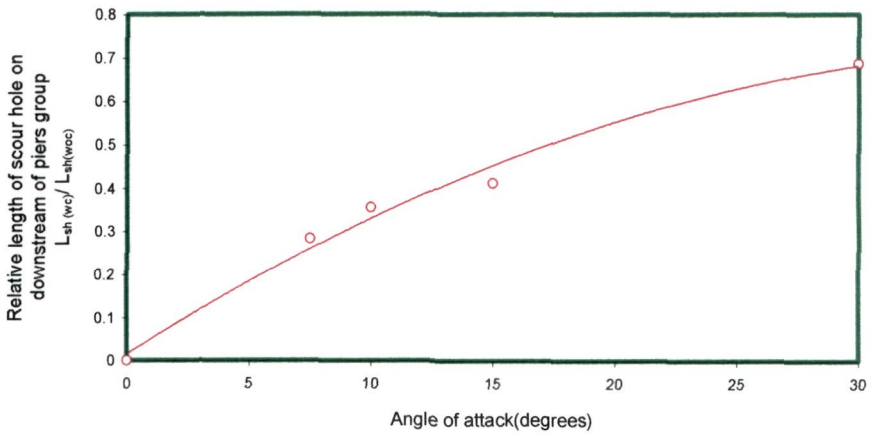

Fig. 5.135 Variation of Length of scour holes at downstream end of piers group with collar relative to the corresponding length without collar '$L_{sh(wc)}/L_{sh(woc)}$' with angles of attack(where, $L_{sh(wc)}$= length of scour hole at downstream end of piers group with collar, $L_{sh(wc)}$ = length of scour hole at downstream end of piers group without collar).

An increasing trend in the value of '$L_{sh(wc)}/L_{sh(woc)}$' with angle of attack is observed; however, as compared to the length of scour hole at downstream end of piers group without collar, the length of scour holes at downstream end of piers group with collar, reduces considerably. Even, at 30° angle, the length of scour hole at downstream of piers group with collar is 70% less than that of without collar. This decrease is attributed to reduction in strength of wake vortices due to the shielding of sediment bed by the collar.

(c) Length of sediment deposition at downstream end of piers group with and without collar

The lengths of sediment deposition at downstream end of piers group with and without collar are plotted against angle of attack as shown in Fig.5.136 It is observed that the length of sediment deposition at downstream end of piers group with and without collar increases with angle of attack, however, the lengths of sediment deposition with collar are less than that of without collar at all angles of attack. Comparison of two curves in Fig 5.136 clearly shows that the application of collar has significant effect in the reduction of length of sediment deposition.

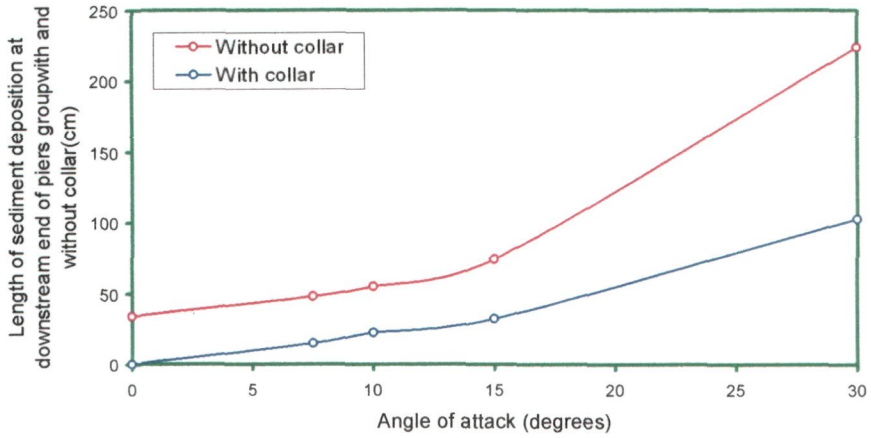

Fig. 5.136 Variation of length of sediment deposition at downstream end of piers group without collar with angles of attack 'α'.

The length of sediment deposition at piers group aligned at various angles of attack with respect to that aligned at 0° angle '$L_{dep(ang)}/L_{dep(zang)}$' are plotted against angles of attack as shown in Fig.5.137 In general, an increasing trend in the relative length of sediment deposition is observed. The reason for this increment is the increase in the frontal width of piers group at higher angles of attack. The relative length of sediment deposition at 30° angle is as high as 6.9 times more as that at 0° angle.

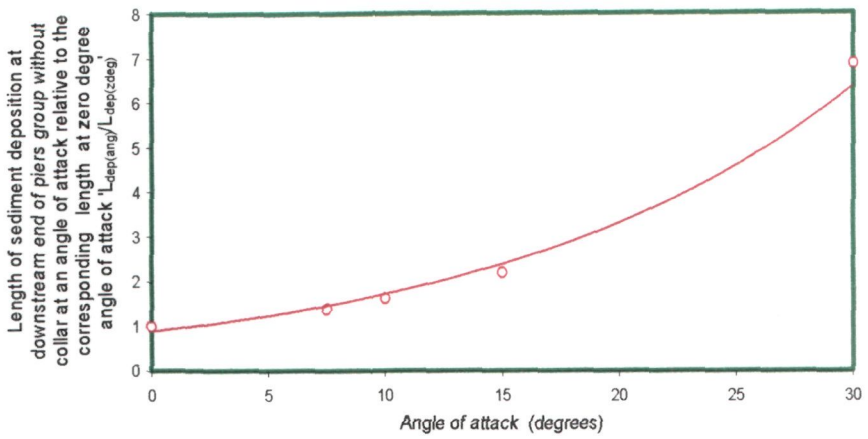

Fig. 5.137 Variation of length of sediment deposition at downstream end of piers group without collar at an angle of attack relative the corresponding length at zero degree angle of attack '$L_{dep(ang.)}/L_{dep(zdeg)}$' (where, $L_{dep(ang)}$=length of sediment deposition at downstream end of piers group at an angle of attack, $L_{dep(zdeg)}$= length of sediment deposition at downstream end of piers group at zero degree angle of attack).

(d) Length of sediment deposition at downstream end of piers group with collar

The percent reduction in the length of sediment deposition at downstream end of piers group with collar is plotted against angles of attack in Fig. 5.138 As discussed in section 5.10.1 of this Chapter; the collar plate at 0° angle completely shields the sediment bed around piers group against scouring. As a result, a 100% reduction in the length of sediment deposition is observed. However, as the angle of attack increases, percent reduction in length of sediment deposition decreases. As the angle of attack approaches to 10°, percent reduction goes down to 59.1%. The rate of this decrement is comparatively more upto 10° angle. Beyond 10° angle, the rate of percent reduction gradually slowed down upto 30° angle. This decrease in percent reduction is ascribed to the increase in frontal width of piers group at angles of attack larger than zero degree.

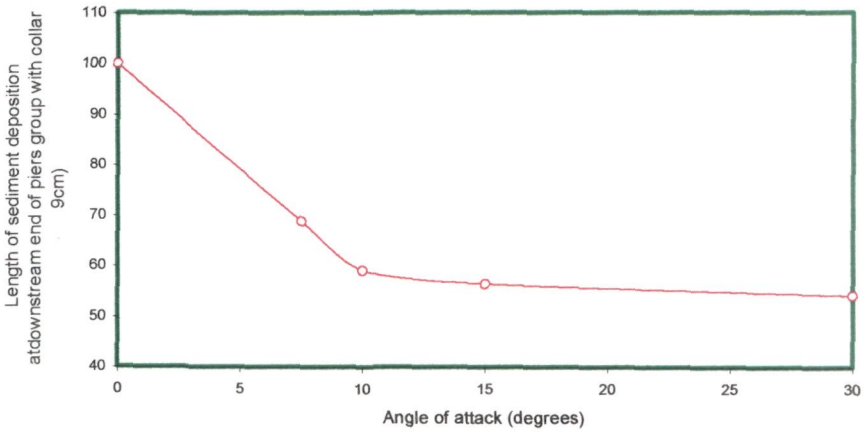

Fig.5.138 Variation of length of sediment deposition at downstream end of piers group with collar versus angle of attack 'α'

(e) Height of sediment deposition at downstream end of piers group with and without collar

For no collar around piers group, the maximum heights of sediment deposition at downstream end of piers group at varied angles of attack are plotted with respect to that at 0° angle as shown in Fig. 5.139 It can be seen that the height of sediment deposition increases with an increase in angles of attack. The reason for this increment is the increase in frontal width of piers group at larger angle of attack which causes more scouring and sediment deposition around the piers group.

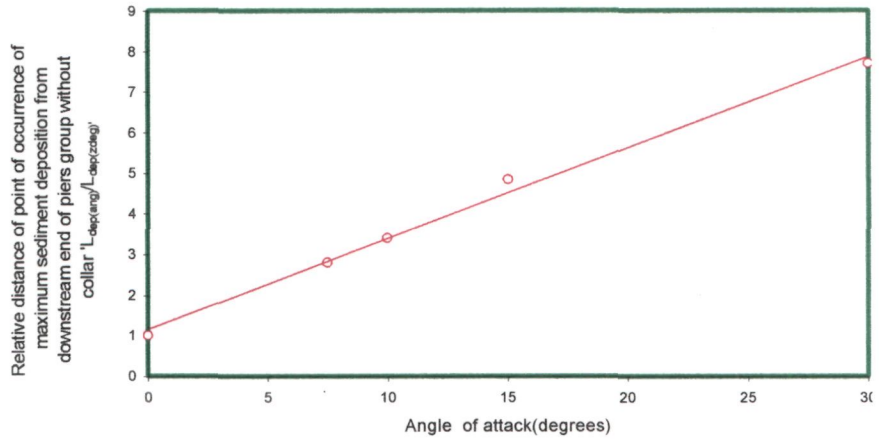

Fig. 5.139 Variation of relative distance of occurrence of maximum sediment deposition '$L_{dep(ang)}$ /$L_{dep(zdeg)}$' at downstream end of piers group with collar at an angle of attack (where, $L_{dep(ang)}$= distance of point of occurrence of maximum sediment deposition at angle of attack and $L_{dep(zdeg)}$ = distance of point of occurrence of maximum sediment deposition at zero angle of attack)

(f) Location of occurrence of maximum deposition of sediment at downstream end of piers group without collar

The distances of point of occurrence of maximum height of sediment deposition from the downstream end of piers group are plotted against angles of attack as shown in Fig. 5.140 It is observed that the distance of occurrence of maximum height of sediment deposition increases with angle of attack. The reason for this is the more scouring around the piers group resulting from increased frontal width of piers group at larger angles of attack.

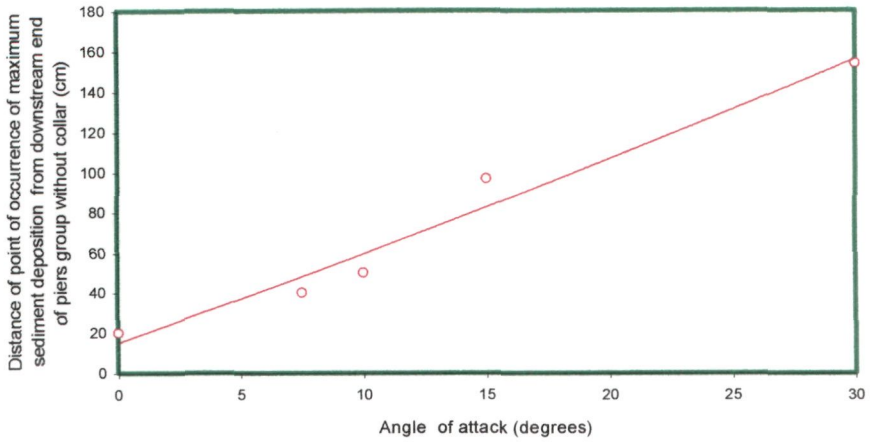

Fig. 5.140 Variation of point of maximum deposition of sediment at downstream end of piers group without collar with angles of attack.

(g) Location of occurrence of maximum deposition of sediment with collar

The distances of point of occurrence of maximum height of sediment deposition from the downstream end of piers group with collar, are plotted against angles of attack as shown in Fig. 5.141. It is observed that as the angle of attack increases, the location of occurrence of maximum height of sediment deposition shifts downstream. This is attributed to the formation of strong wake vortices due to the increase in the frontal width of piers group at larger angles of attack.

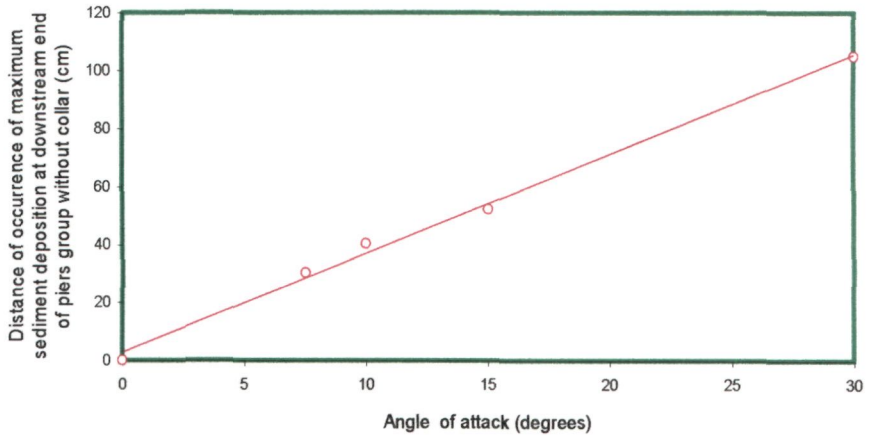

Fig. 5.141 Variation of point of occurrence of maximum sediment deposition at downstream end of piers group with collar corresponding to without collar with angles of attack (where, $Dismax_{dep\ (wc)}$ = distance of point of maximum sediment deposition with collar and $Dismax_{dep\ (woc)}$ = distance of point of maximum sediment deposition without collar).

The distance of occurrence of maximum sediment deposition at downstream end of piers group with collar '$H_{dep\ (wc)}$' with respect to that without collar, '$H_{dep\ (wc)}$'/'$H_{dep\ (woc)}$' are plotted against angles of attack as shown in Fig. 5.142. It is observed that the value of this ratio increases with angle of attack; however, it remains much below unity, which is

indicative of the shielding effect of collar plate on the sediment bed due to which lesser amount of sediment gets scoured from the sediment bed and deposited on the bed downstream of piers group.

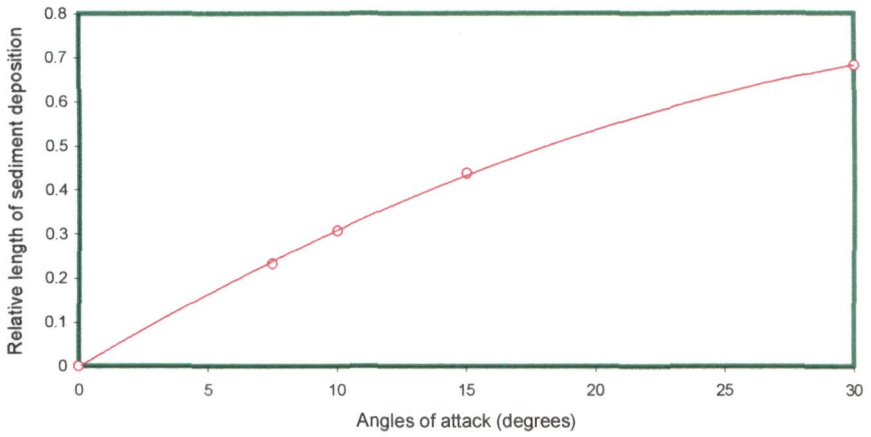

Fig. 5.142 Variation of maximum height of sediment deposition at downstream end of piers group with collar relative to the corresponding height without collar '$H_{dep(wc)}$'/ '$H_{dep(woc)}$' with angles of attack (where, $H_{dep(wc)}$ = maximum height of sediment deposition at downstream end of piers group with collar and $H_{dep(woc)}$ = maximum height of sediment deposition at downstream end of piers group without collar).

(h) Areal extents of scour

The areal extents of scour for various angles of attack are plotted as shown in Appendix-IV. It can be seen that the areal extent of scour is symmetrical about the piers group at α =0°. However, the areal extents of scour developed at α >0°, are asymmetrical in shape.

The percent reduction in the areas of extent due to the application of collar is plotted against angles of attack as shown in Fig. 5.143 It is observed that the application of collar at piers group aligned at 0°angle shields completely the sediment bed around the piers group against the action of down-flow and the horseshoe vortex and causes, therefore, 100% reduction in the area of scour extent. At α>0° angle, the frontal width of piers group increases which results in the formation of larger size horseshoe vortex and stronger wake vortices around the piers group that erodes the sediment bed around the piers group and causes sediment deposition over a larger area. As a result, the area of scour extent around the piers group with collar, increases and percent reduction in area of scour extent caused by the collar, decreases and reaches to about 38% at 30° angle of attack.

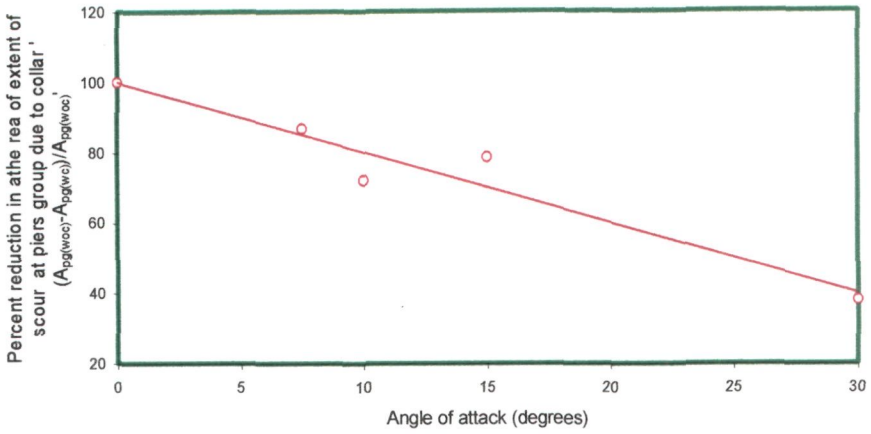

Fig.5.143 Angles of attack versus percent reduction in areas of extent with collar '$(A_{pg(woc)}-A_{pg(wc)})/A_{pg(woc)}$' with angle of attack(where, $A_{pg(woc)}$ =area of scour extent around piers group without collar and $A_{pg(woc)}$ = area of scour extent around piers group with collar).

(i) Width of scour holes

The widths of scour holes at upstream and downstream ends of piers group without collar are plotted against angles of attack as sown in Fig. 5.144 It is observed that the widths of scour hole at downstream end of piers group are more than that at upstream end at all angles of attack. This increase in scour hole widths at downstream end of piers group is ascribed to the increased scouring strength of wake vortices, which shed from both sides of largest size pier in piers group.

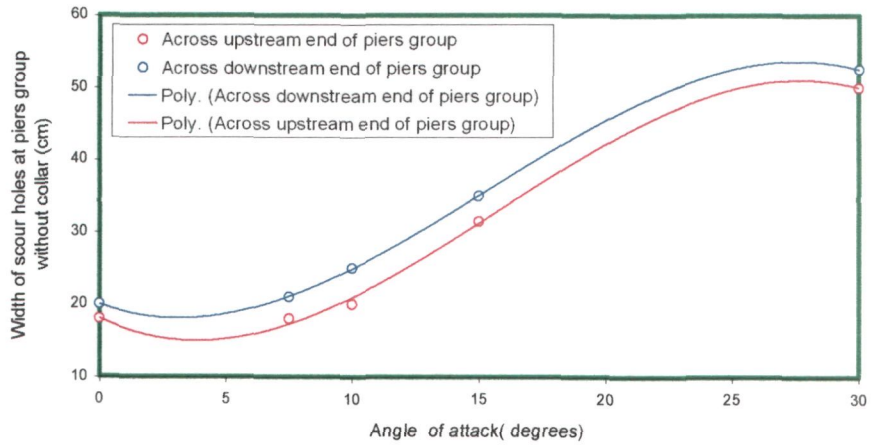

Fig.5.144 Angle of attack versus width of scour hole without collar.

The widths of scour holes at upstream and downstream ends of piers group with collar are plotted against angles of attack as shown in Fig. 5.145 It can be seen that the scour hole at upstream end of piers group has zero width upto 15° angle; however, at 30° angle, the width of scour hole at upstream end increases, nevertheless, remains slightly less than that at downstream end. This is because of increased intensity of

scouring at downstream end than the upstream end of piers group at larger angles of attack. At downstream end of piers group with collar, the width of scour hole increases with angle of attack. This is because of the enhancement in the scouring intensity at downstream end with angle of attack.

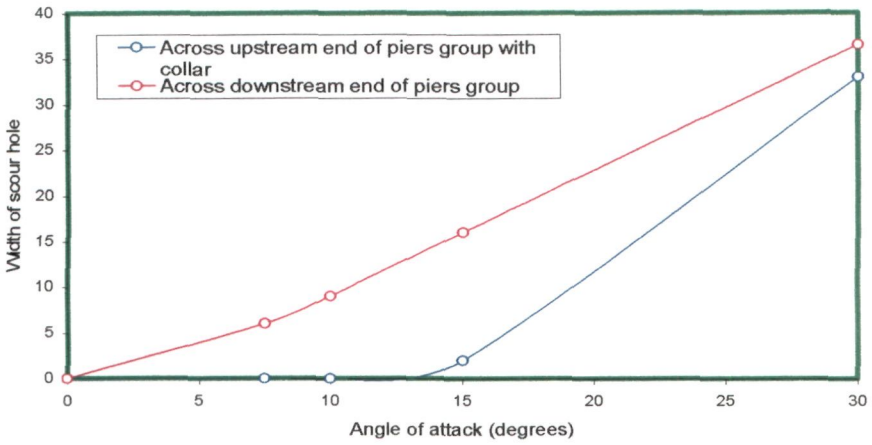

Fig.5.145 Angle of attack versus width of scour hole with collar.

5.10.11 Temporal development of scour at piers group with and without collar

The temporal development of scour depth at piers group without collar for varied angles of attacks is presented in Fig.5.146 It is observed that for a given time, the scour depth increases with angle of attack. This increment is due to the increase in the frontal width of piers group with angle of attack *'α'*.

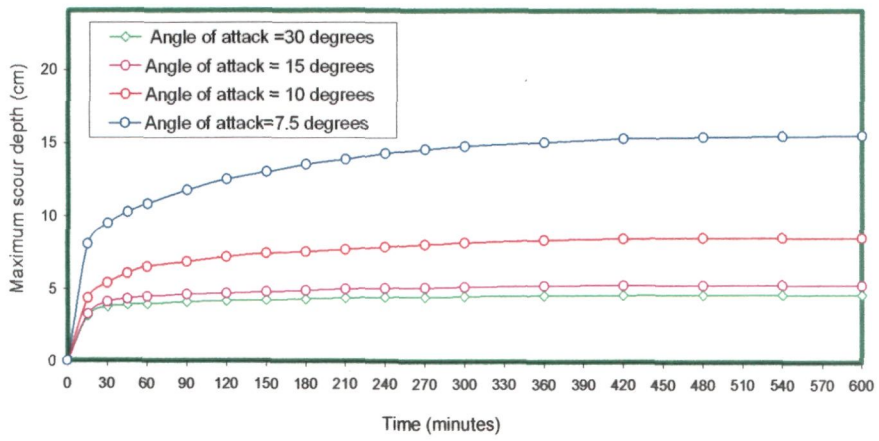

Fig.5.146 Temporal variation of scour depth at piers group without collar.

The temporal development of scour depth at piers group with collar for varied angles of attacks is shown in Fig.5.147 It is evident from this figure that for the same flow conditions and angles of attack, the application of collar around piers group, not only

causes reduction in the maximum scour depth but also the rate of scouring gets reduced considerably. This happens because the collar diverts the down-flow and protects the sediment bed from its direct impact. Reduction in the rate of scouring is important as it reduces the risk of pier failure when the duration of flood is low.

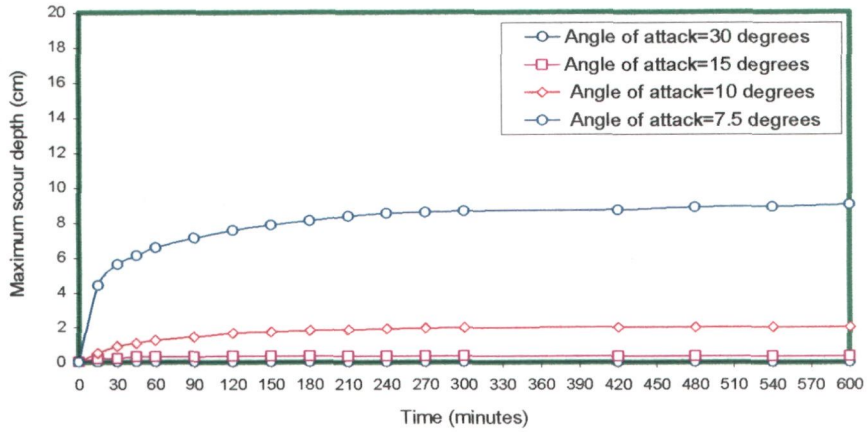

Fig. 5.147 Temporal variation of scour hole with collar.

5.11 Local Scour at a Group of two Piers with and without Collar

5.11.0 Introduction

This section of present study analyses the experimental observations obtained by using a group of two circular piers of 41.5 mm diameter with clear spacing of twice the pier diameter; in place of a round-nosed rectangular pier of width 41.5 mm and same length to width ratio as that of group of two 41.5 mm diameter piers viz., 4:1(Fig. 148). The motive of using a group of two circular piers was to provide an alternative to a round-nosed rectangular pier so as to have cost effective construction of piers and in addition, bears less impact of approaching flow. Raudkivi (1986) in discussing effects of pier alignment also states that the use of cylindrical columns would produce a shallower scour as compared to a solid pier.

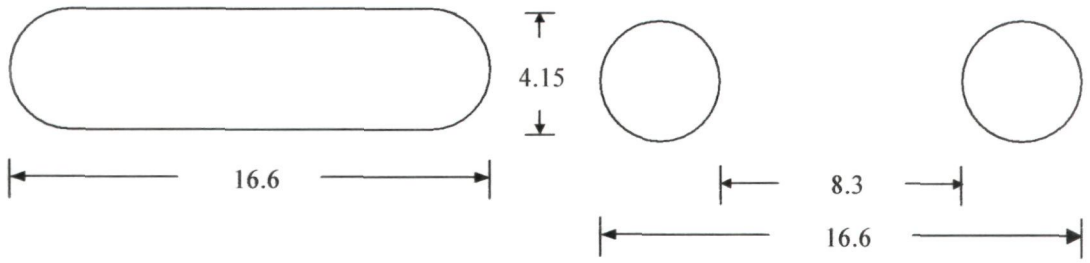

(a) Round nose rectangular pier (b) Group of two circular piers

Fig.5.148 Round-nose rectangular pier and a group of two circular piers, both of same length to width ratio 4:1

When scour commences at this group of piers two piers placed at varied alignments with respect to the flow direction ranging from 0° to 90°, the reinforcing effect of rear pier, sheltering effect of front pier, effect of shed vortices from front pier and effect of compression of horseshoe vortices between the two piers, come into action. However, some of these effects dominate on the other when alignment of piers with respect to flow, changes. The spiral flow, which takes place in clockwise direction around this group of piers aligned at an angle of attack, induces an additional tractive force on the bed material at the base of front pier due to which the scour depth at front pier increases.

In order to analyze the results obtained for scouring around the group of these two piers with and without a collar and aligned at varied angles of attack, the longitudinal and lateral profiles of scour and the areal extent of scour around the piers, are plotted as shown in Appendix-II, Appendix-III and Appendix-IV. The longitudinal profiles are drawn through front and rear piers along the flume length for different angles of attack. Lateral profiles are drawn at nose of the piers group. Some distinctive cases of longitudinal and lateral profile of scour and areal extent of scour are discussed in this part of study.

The photographs showing the scour and deposition patterns on the bed around the piers taken at the end of experiments are shown in Figs. P19 to P25. Throughout the test period, the location and magnitude of maximum scour depth was noticed, measured and recorded. The analysis of the results achieved in this part of present study has been carried out in three phases namely, phase-I experiments with single pier, phase-II experiments using group of two piers without a collar and phase-III experiments using group of two piers with collar.

5.11.1 Phase-I: Experiments with single pier

Experiments were first conducted on a single pier to form a basis for the evaluation of effect of mutual interference of two piers of this pier group on scour depth due to their proximate location. The scour and deposition patterns around 41.5 mm isolated pier are shown in Fig. PI.

5.11.2 Experiments on group of two piers with and without collar

As the motive behind the use of this group of two circular piers with and without a collar is to replace a round-nosed rectangular pier of the same width as that of the pier diameter (*i.e.*, 41.5 mm), the results are compared with the scour depths computed for the round-nosed rectangular pier using existing published method of (Zarrati *et al.*, 2004).

5.11.3 Phase II: Experiments without collar

In this phase, 7 tests were conducted on a group of two piers with no collar installed around it and aligned at 0°, 15°, 30°, 45°, 60°, 75°, and 90° angles of attack to the flow keeping the clear spacing between the two piers equal to twice the diameter of pier used in the group The results obtained in this phase of experiments are analyzed under the following heads:

5.11.4 Experiments on piers group aligned with the flow (α= 0°)

At the start of experiment, the scouring was first noticed at the front pier and deposition of the scoured material in the wake of the front pier *i.e.*, at the upstream faces of the rear pier. However, when the scour hole of the front pier grew in size, the sediment deposited at the upstream face of the rear pier, was observed moving downstream and a scour hole was observed forming around the rear pier.

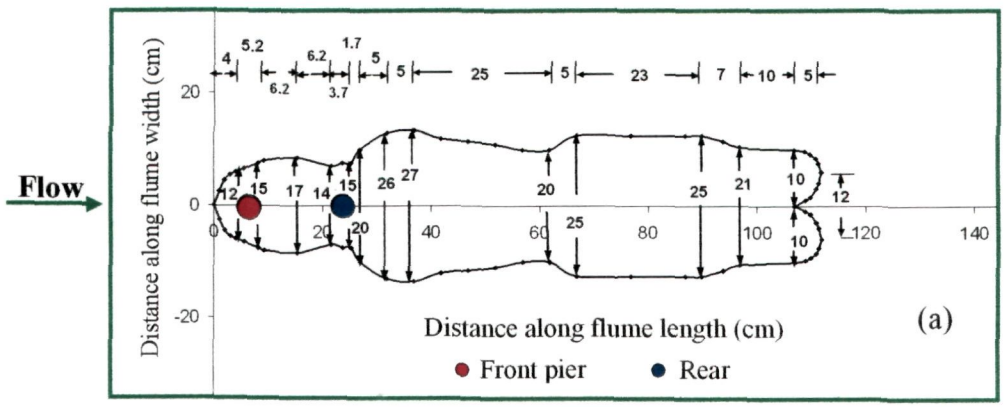

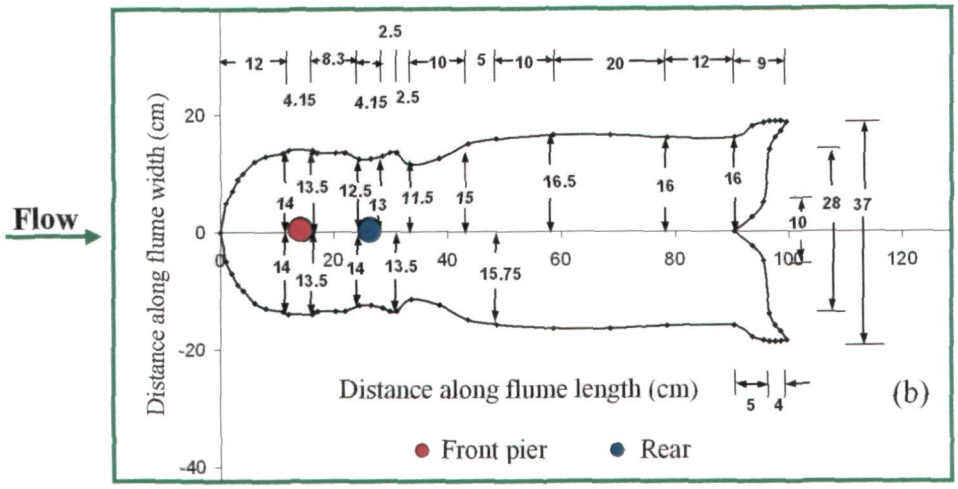

Fig.5.149 Areal extents of scour at α=0° (a) without collar (b) with collar

Thereafter, the sediment deposited in front of the rear pier was observed sliding down into the scour hole of the rear pier. Initially, the rate of scour in front pier scour hole was fast, however, when the scour hole of front pier grew in size and the scour hole around the rear pier was formed, the scour rate in front pier scour hole slowed down and the rate of scour in the rear pier scour hole increased. After 18 hours of the test run, variation in scour depth at front and rear piers was negligible, and about 90 % of scouring at the two piers occurred in the first four hours. The maximum scour depths measured at the front and rear piers were in good agreement with the published results (Hannah, 1978). The maximum scour depth occurring at the front and the rear piers were 9.1 cm and 7.37 cm respectively. The reason of occurrence of shallower scour depth at the rear pier is ascribed to the shielding effect of front pier and the deposit of scoured bed material on upstream of rear pier.

The areal extents of scour plotted around the piers group after test run can be depicted in Fig. 5.149. It can be seen that areal extents of scour with and without collar are quite different in shape, however, lengthwise; the areal extent of scour around piers group without collar is longer. Widthwise, the areal extent of scour around piers group with collar is wider. The net effect of collar on area of scour extent is insignificant at $\alpha = 0°$.

5.11.5 Experiments with the piers group aligned at ($\alpha = 15°$)

At the initial stage of experiment, scouring of sediments was noticed from upstream and downstream piers both; however, the rate of scour at the front pier was more than the rear pier. After one hour of commencement of experiment, the scour depth was observed more at the side of the front pier exposed to the flow as compared to its nose, while the scour depth at the rear pier was observed to remain maximum at its nose throughout the test duration.

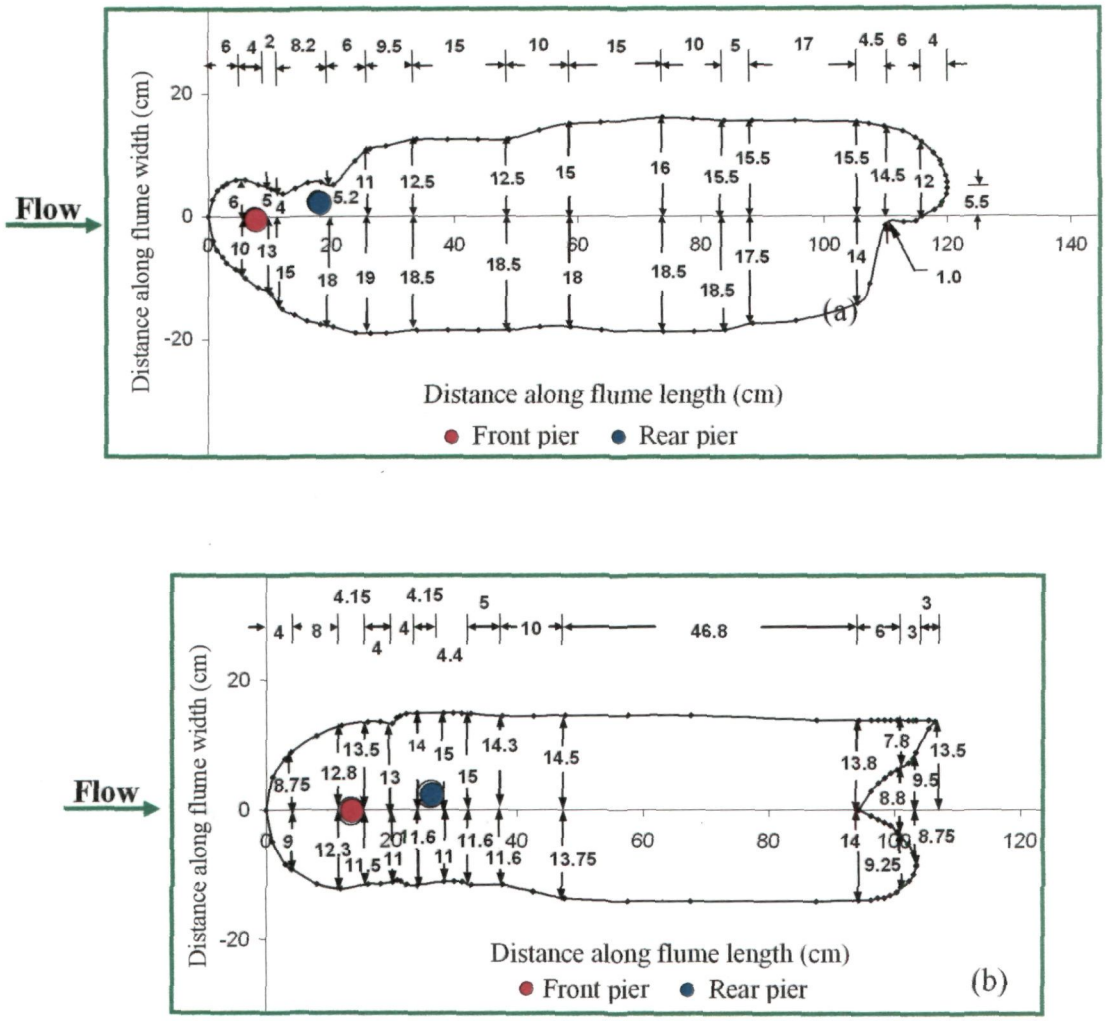

Fig. 5.150 Areal extents of scour at α=15° (a) without collar (b) with collar

The maximum scour depths at the upstream and downstream piers were 9.5 cm and 9.35 cm respectively. The deeper scour depth at the downstream pier is caused due to the increase in scouring strength around rear pier due striking action of vortices shedding from the upstream pier.

Areal extents of scour around piers group with and without collar are shown in Fig. 5.150. It can be noticed that as compared to the piers group without collar, the scour extent around piers group with collar is shorter in length and narrower in width. The collar, therefore, is effective in reducing the cost of scour countermeasure required for the safety of piers group against local scour.

5.11.6 Experiments with the piers group aligned at ($\alpha = 30°$)

At the start of experiment, scouring was observed at upstream and downstream piers both, however, upto 3 hours from starting the experiment, the observed scour depth at the front pier remained higher than that at the rear pier. The reason for this is the transport of the scoured sediment into the scour hole of the downstream scour hole. Thereafter, the scour depth was observed increasing at the downstream pier as compared to the upstream pier. The maximum scour depths observed at the upstream and the down stream piers were 9.7cm and 10.15 cm respectively.

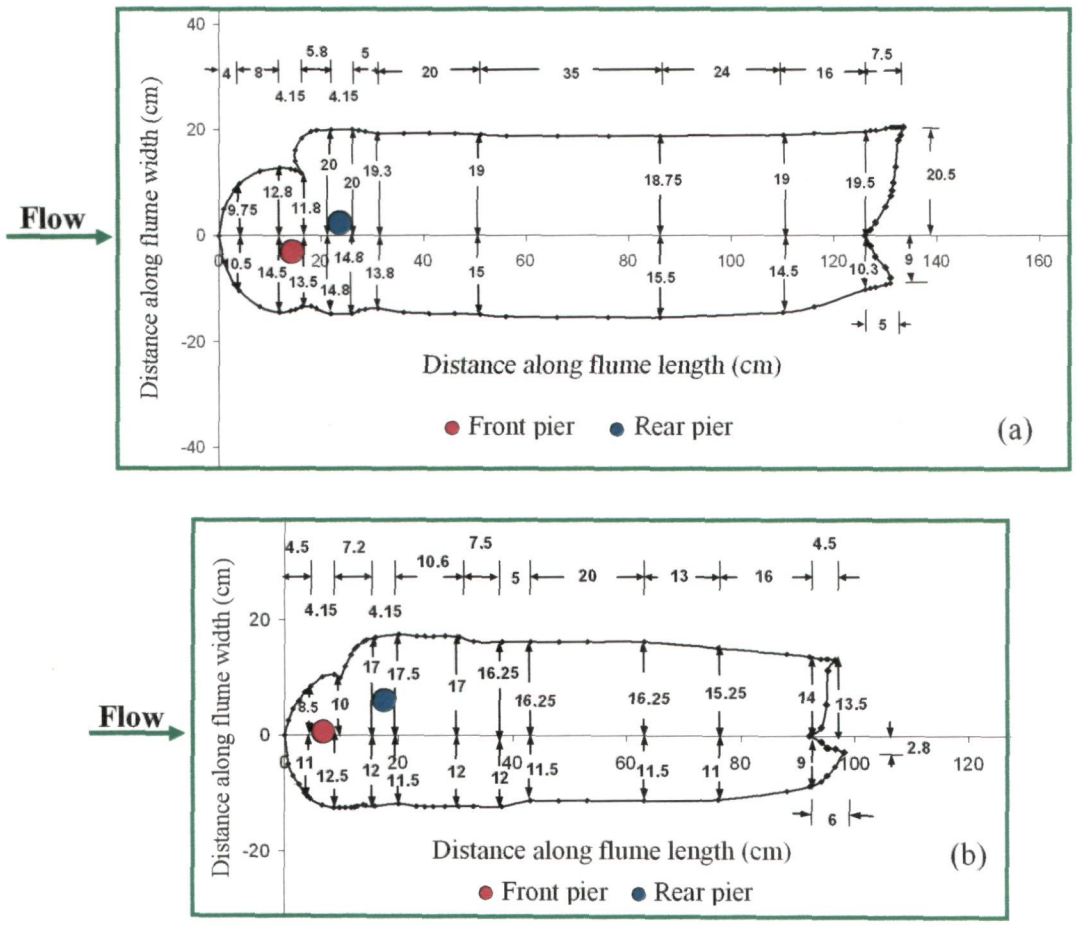

Fig. 5.151 Areal extents of scour at α=30° (a) without collar (b) with collar

Though the scour depth at the rear pier was deeper than the front pier, however, the difference was not much. The marginal difference between scour depths at front and rear piers is indicative of the reduction in the strength of vortices shedding from upstream pier.

The areal extents of scour around the piers group with and without collar measured after test run can be depicted in Fig. 5.151 As regard to the piers group without collar, the areal extent of scour around piers group with collar is smaller in area and hence cost effective for scour countermeasures required for the safety of piers group against local scour.

5.11.7 Experiments with the piers group aligned at ($\alpha = 45°$)

Initially, two separate scour holes around the two piers were developed. But after two hours from the start of experiment, these two scour holes overlapped each other, however these scour holes were discernible by a rim formed between them.

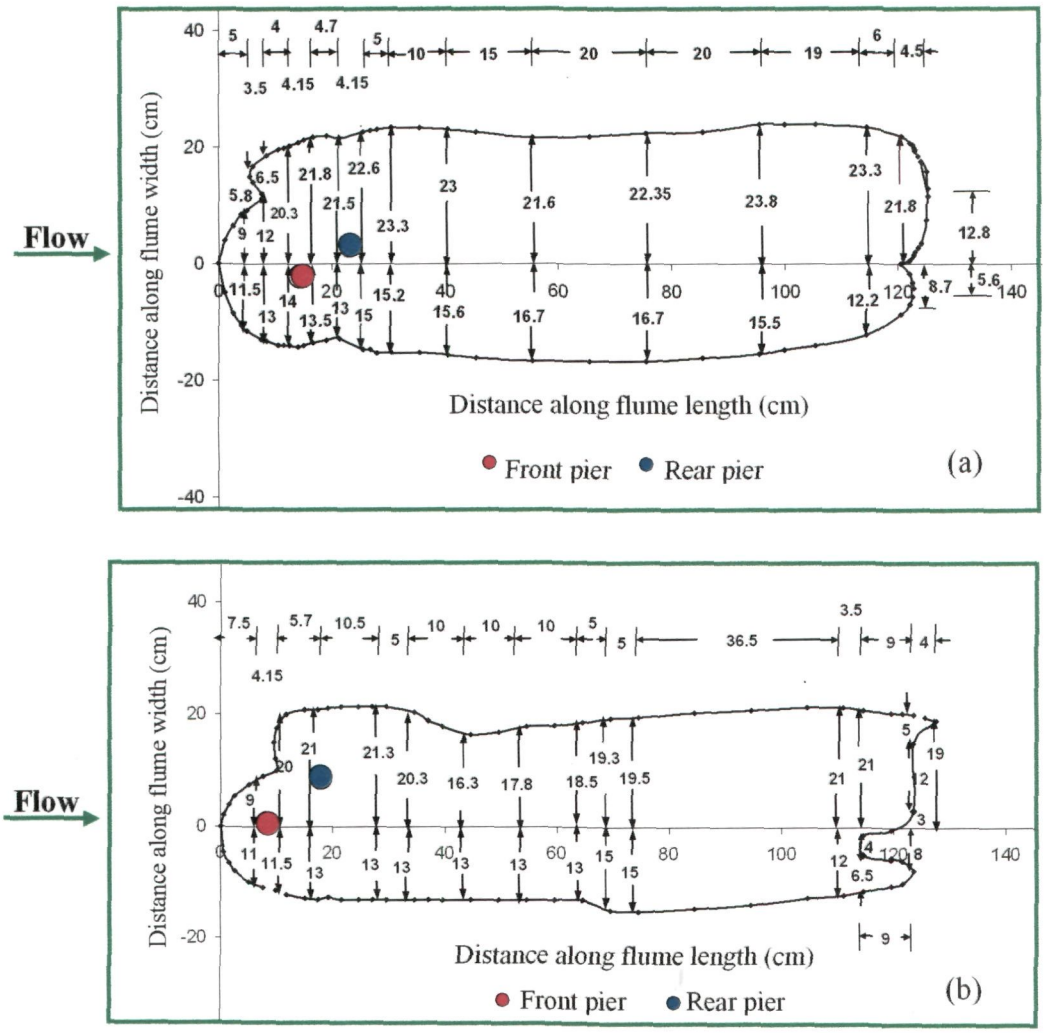

Fig.5.152 Areal extents of scour at α=45° (a) without collar (b) with collar

The elevation of the rim, between the two scour holes, was lower than the outer edges of the two scour holes. The scour depth observed at the rear pier remained higher than the

front pier throughout the test duration. The maximum scour depths observed at the upstream and downstream piers were 9.75 cm and 10.3 cm respectively.

The areal extents of scour around the piers group measured after completion of the test are plotted as shown in Fig. 5.152. The areal extent of scour around piers group with collar is narrower in width but slightly smaller in length and hence smaller in area and economical from protection point of view.

5.11.8 Experiments with the piers group aligned at ($\alpha = 60°$)

As the experiment commenced, two separate scour holes around the upstream and downstream piers were developed.

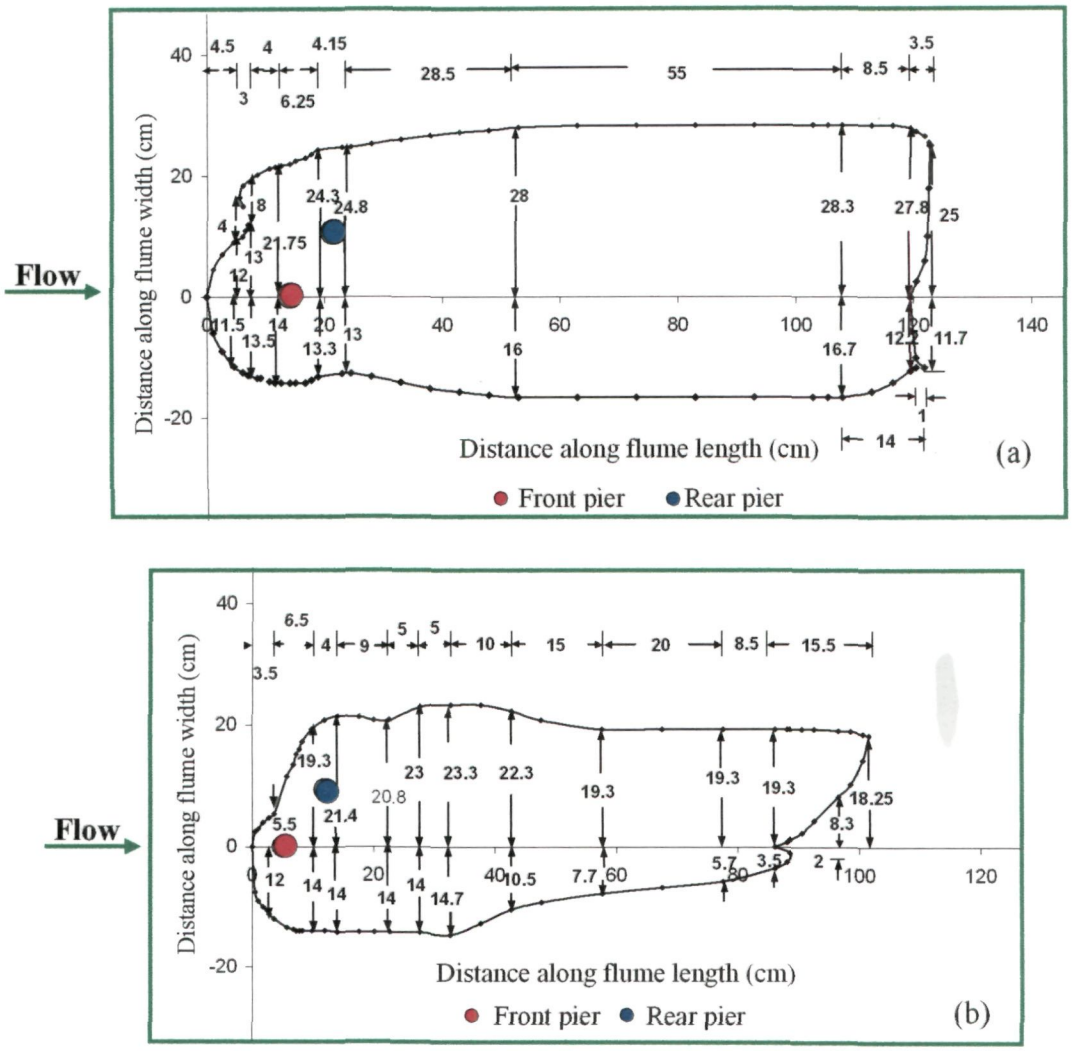

Fig. 5.153 Areal extents of scour at α=60° (a) without collar (b) with collar

However, the elevation of the rim formed between the two scour holes, was lower than the level of the outer edges of scour holes. The scour depth observed at the downstream pier

remained higher than the front pier throughout the experimental run. The maximum scour depths observed at the upstream and downstream piers were 8.75 and 10.15 respectively.

The areal extents of scour around the piers group with and without collar after test run are plotted and shown in Fig 5.153 As the area of scour extent around piers group with collar is significantly smaller than that without collar, collar is considerably economical from protection point of view.

5.11.9 Experiments with the piers group aligned at ($\alpha = 75°$)

As the experiment commenced, scouring of the sediment was observed at upstream and the downstream piers. The scour depth observed at the downstream pier remained higher than that at the upstream pier throughout the duration of experimental run. The maximum scour depths measured at upstream and downstream piers were 9 cm and 10.0 cm respectively.

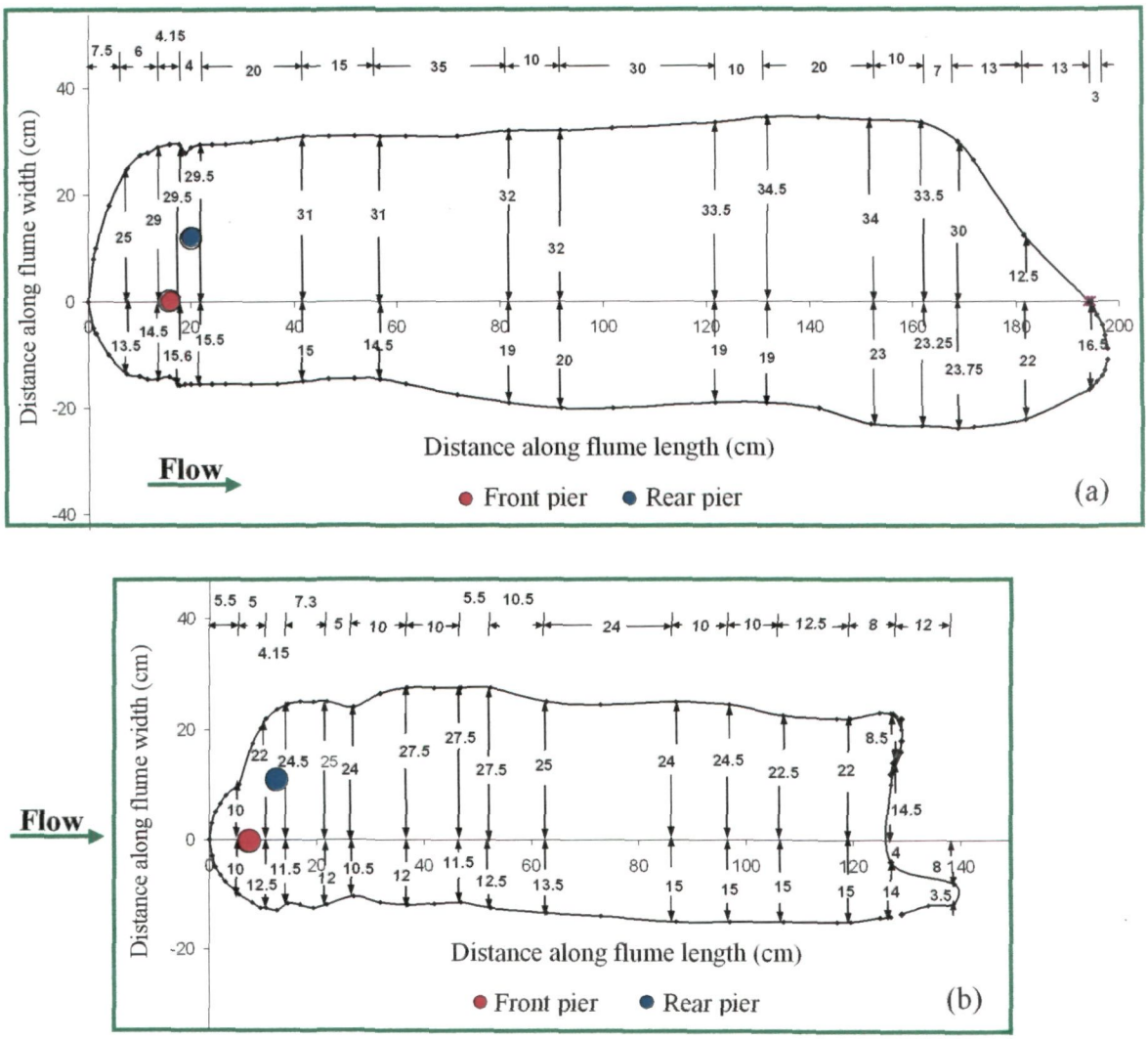

Fig.5.154 Areal extents of scour at α=75° (a) without collar (b) with collar

The areal extents of scour around the piers group plotted at the end of experiment can be depicted in Fig.5.154. As the area of scour extent around piers group with collar is considerably smaller than that without collar, the use of collar is cost effective in piers group protection against local scour.

5.11.10 Experiments with the piers group aligned at ($\alpha = 90°$)

The inner arms of the horseshoe vortices around two piers were observed more active in removing the material as compared to the outer arms. The reason ascribed for this is the compression of inner arms of horseshoe vortices of the two piers. The material from the outer side of the piers was observed moving towards the center of the gape between piers and then moving out of the scour hole towards the downstream.

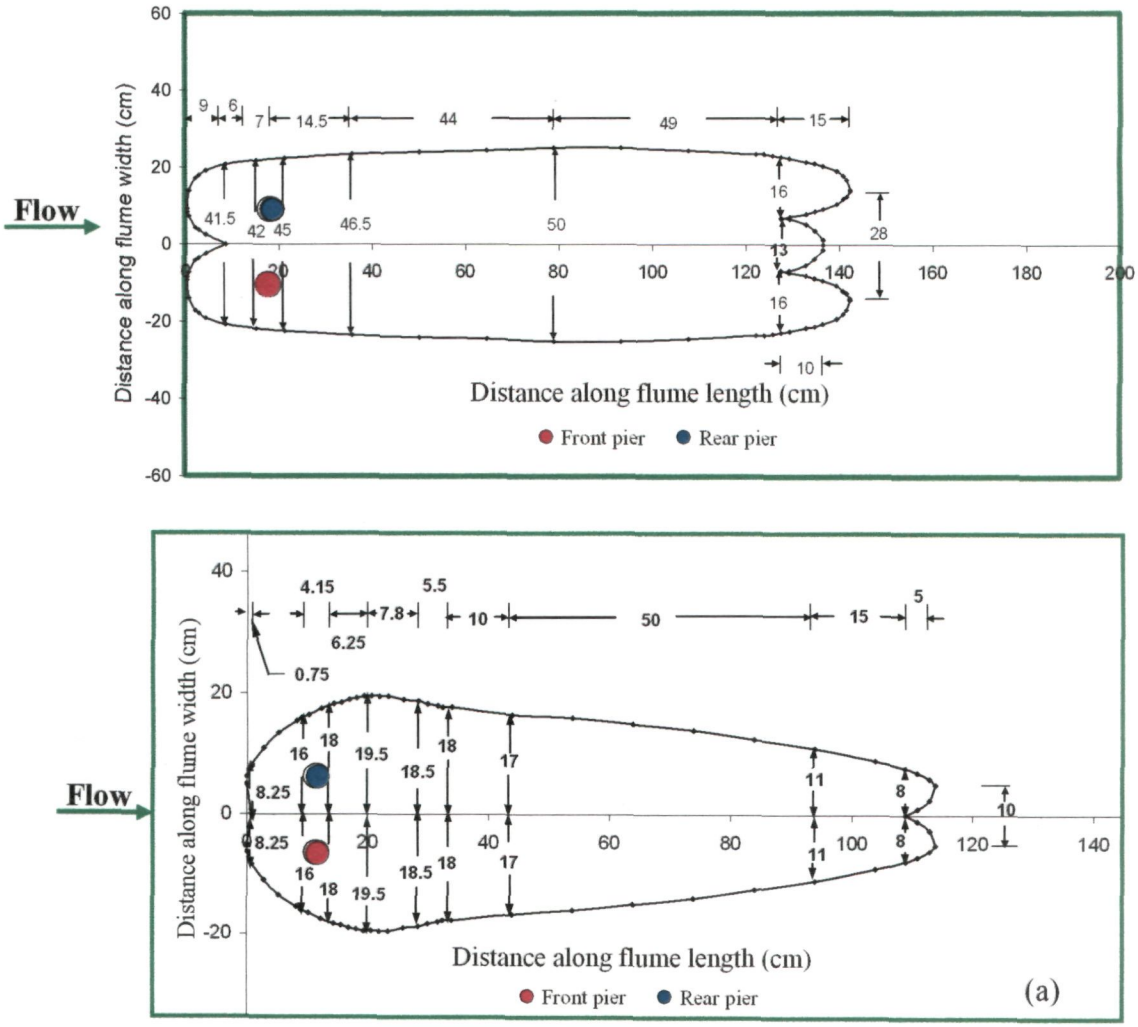

Fig. 5.155 Areal extents of scour at α=90° (a) without collar (b) with collar

After one hour of the commencement of experiment, the sediment particles stopped moving towards the center and sediment started dislodging and moving directly from their existing position in the scour hole. The maximum measured scour depth was 9.6 cm at left pier and 9.6 cm at right pier.

The areal extents of scour around the piers group at the end of test are plotted as shown in Fig.5.155. The effectiveness of collar at 90° angle of attack considerably reduces, as the areal extents of scour around piers group with and without collar are similar in area.

The maximum scour depths and location of their occurrence around the piers group for varied angles of attack are given in Table 5.6.

Table 5.6 Maximum scour depth and location of its occurrence around group of two piers without collar for varied angles of attack.

Angle of attack α	Maximum scour depth (cm)	Location of occurrence of maximum scour depth
0°	9.10	Nose of Upstream pier
15°	9.50	Nose of Upstream pier
30°	10.15	Nose of Downstream pier
45°	10.30	Nose of Downstream pier
60°	10.15	Nose of Downstream pier
75°	10.00	Nose of Downstream pier
90°	9.60	Nose of Upstream and downstream piers

5.11.11 Phase III: Experiments with Collar

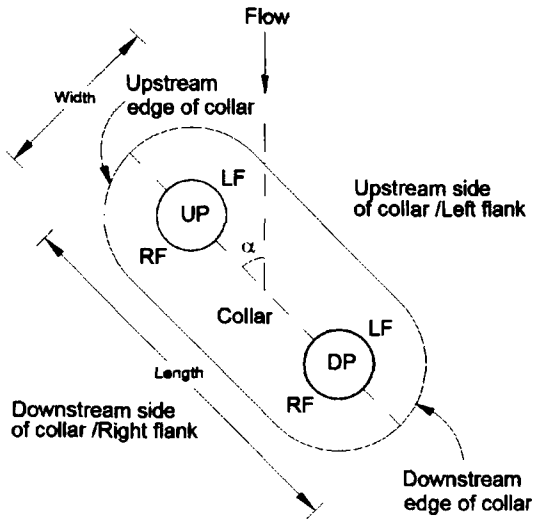

RF: Right face, LF : Left face, α : Angle of attack of flow
UP : Upstream pier, DP : Downstream pier,

Fig.5.156 Group of two circular piers with collar

In this phase of experiments, a collar as shown in Fig.5.156, was installed around the piers group and seven tests were conducted with this collar fitted piers group aligned at 0°, 15°, 30°, 45°, 60°, 75°, and 90° angles of attack to the flow, keeping the clear spacing between the two piers same as that in the experiments with no collar. The experimental results are analyzed under the following heads:

5.11.12 Experiments with collar at an angle of attack at ($\alpha = 0°$)

At an angle of attack 'α' = 0; two scour holes, identical in shape and size, were observed forming at downstream end of the collar which were symmetrical about the mid point of the downstream edge of the collar. Thereafter, two small scour holes symmetrical in shape and size on either side of the collar along the mid points of the collar length were formed. The scour holes on sides and downstream of the collar grew in size with the passage of time and joined each other Fig. 5.157.

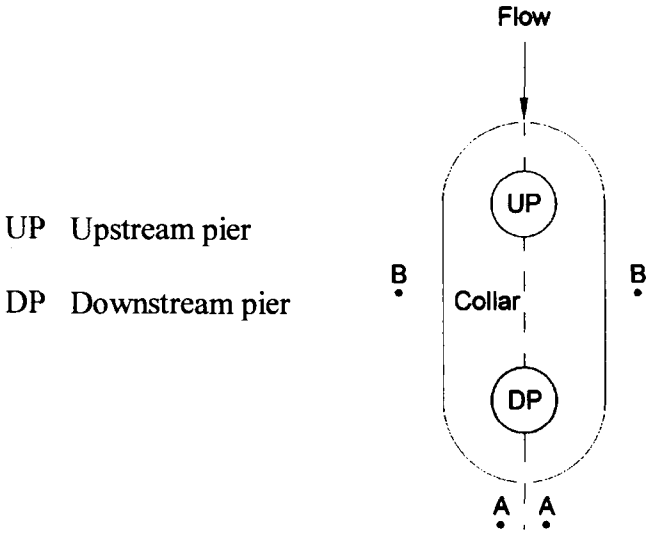

Fig.5.157 Group of two piers with collar at $\alpha = 0°$

The scour holes formed on sides of collar propagated towards the upstream end of the collar and towards the rear pier, but these scour holes did not join each other upto three and half hours from starting of the experiment.

At 3 hours 50 minutes of start of the experiment, these scour holes on sides and downstream of the collar joined each other and the edges of the collar on its longer sides, near the downstream pier, were exposed. The material scoured from the side scour holes was observed transporting and depositing along the longer edges of the collar near the side faces of downstream pier. At the end of the experiment, the downstream edge of the

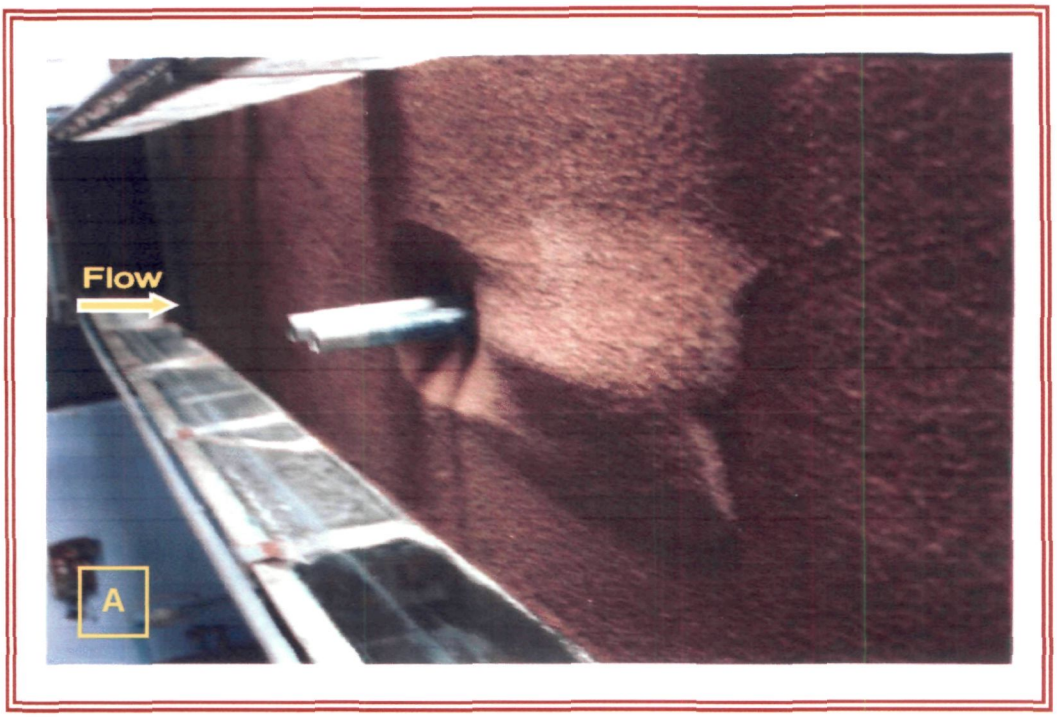

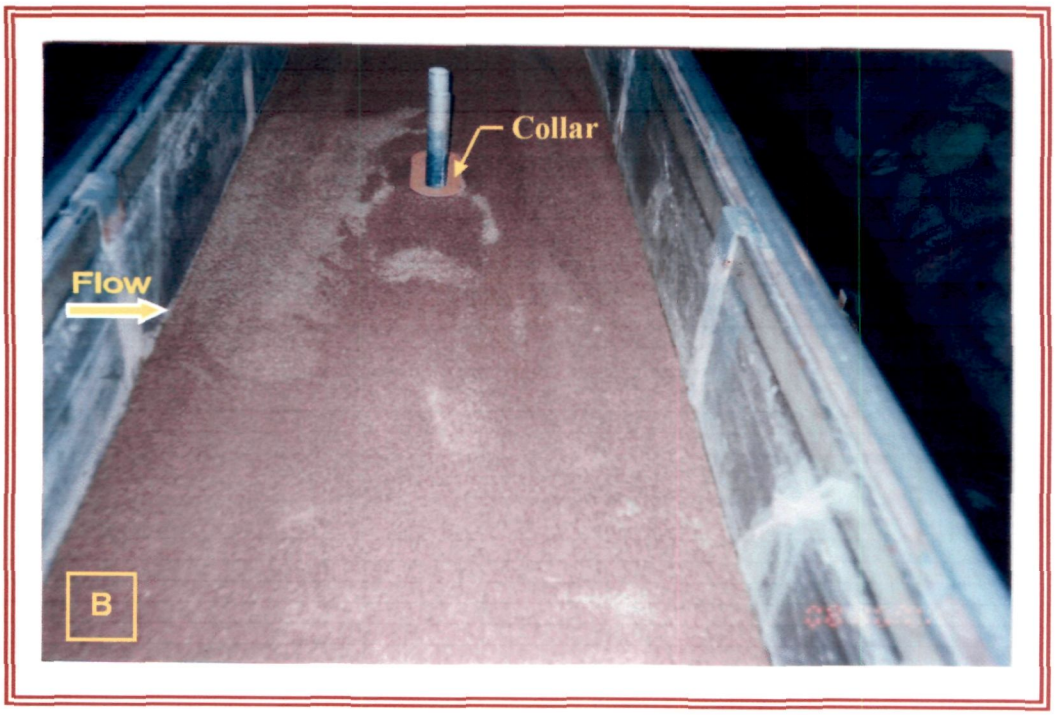

Fig. P19: Scour and deposition patterns around a group of two piers of same sizes at $\alpha=0°$ (A) Without collar (B) With collar

collar was in perfect contact with the bed and the scour depth was 1.95 cm at upstream pier and zero cm at downstream pier respectively.

The areal extents of scour measured around the piers group after the test was over, can be depicted in Fig. 5.149. In order to substantiate the analysis of the results, photographs shown in Fig. P19 were taken at the end of experiments. It is evident from Fig. 5.149 and Fig. P19 that area of scour extent with collar gets reduced due to application of collar at group of two piers.

5.11.13 Experiments with collar at an angle of attack at ($\alpha = 15°$)

As α increases to 15°, two scour holes, one on right flank of collar (point B) and one near downstream edge of collar point A, were formed and after 30 minutes, the scour holes propagated on left and right flanks up to points C and D respectively as shown in Fig.5.158. On left flank, scour progressed upto point E after one hour of start. At the end of 3 hours and 25 minutes, no exposure of the pier was observed and the scour depth was same as at after one hour of starting of experiment. The erosion of material beneath the corner of collar downstream of the downstream pier was observed at the end of 4 hours and 25 minutes. The portion of collar from point E to point C remained in perfect contact with the bed up to 5 hours and 30 minutes of start. The collar at point F was hanging slightly in the air. The maximum scour depth was observed on right flank of the collar near the downstream pier. The scour at the end of 6 hours and 30 minutes progressed up to point G. At this stage, portion of collar from point G to C was in contact with the bed. At the end of experiment, the maximum scour depth was measured as 3.4 cm at upstream pier and zero cm at downstream pier respectively.

UP Upstream pier

DP Downstream pier

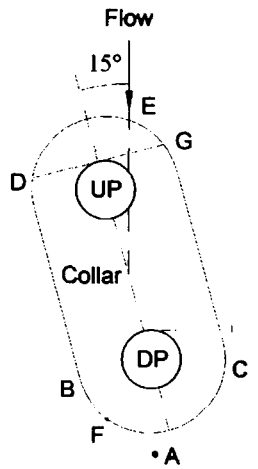

Fig.5.158 Group of two piers with collar at $\alpha = 15°$

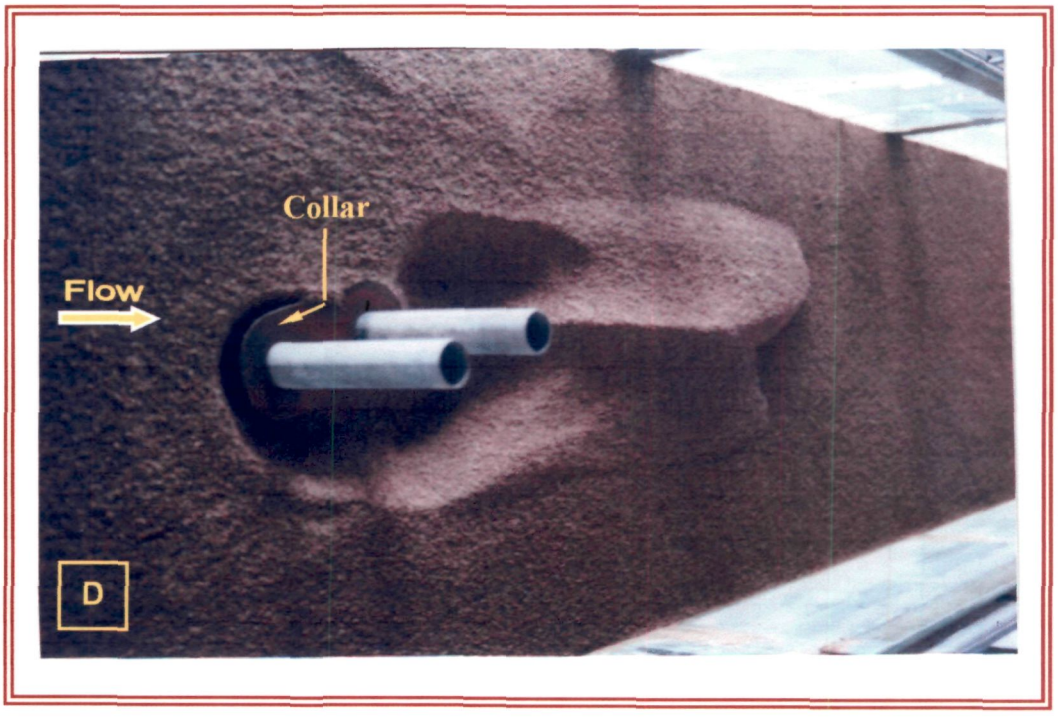

Fig. P20: Scour and deposition patterns around a group of two piers of same sizes at α=15° (C) Without collar (D) With collar

The areal extents of scour measured around the piers group after the test was over, can be depicted in Fig. 5.150. The photographs showing scour and deposition patterns developed on the bed around the piers group with and without collar taken at the end of experiments can be depicted in Fig. P20. Fig. 150 and Fig. P20 show how the application of collar to a group of two piers is effective in reducing the area of scour extent and hence the costs of scour countermeasures.

5.11.14 Experiments with collar at angle of attack (α= 30°)

Fig. 5.159 shows the piers group with collar aligned at 30° angle. Scour initiated near the downstream edge of the collar at point A and on right flank of the collar plate at point B. At 30 minutes of start, scour progressed up to point C where collar edge was exposed only upto its thickness. At point E, there was deposition of sediment and collar was resting completely on the bed. On right flank of the collar, scour from point B propagated to point F. The scour on left flank progressed up to point G and after 2.5 hours of start, progressed up to point H. At the end of 5.5 hours of start, the scour propagated to point K from right and to point H from left. The depth of scour along the left flank of the collar remained same between 2.5 and 3.5 hours of start. At 4 hours from starting the test, scour progressed up to point I (*i.e.*, mid point of collar length). Nevertheless, downstream corner of collar was resting on the bed. The scour progressed towards the left side of rear pier upto point D near the longer edge of collar but not on right side of the rear pier. The right side of the upstream pier was slightly exposed but left side of upstream pier was not exposed at all. Scour did not propagate beyond points J and K even after 7 hours of start. At the end of experiment, the maximum scour depth was measured as 3.95 cm on upstream pier and 1.05 cm at downstream pier respectively.

UP Upstream pier

DP Downstream pier

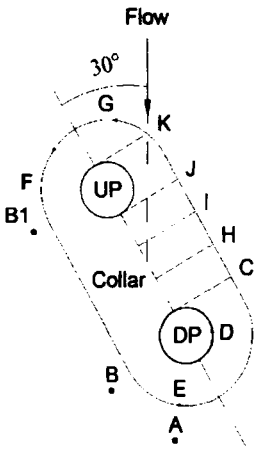

Fig.5.159 Group of two piers with collar at α = 30°

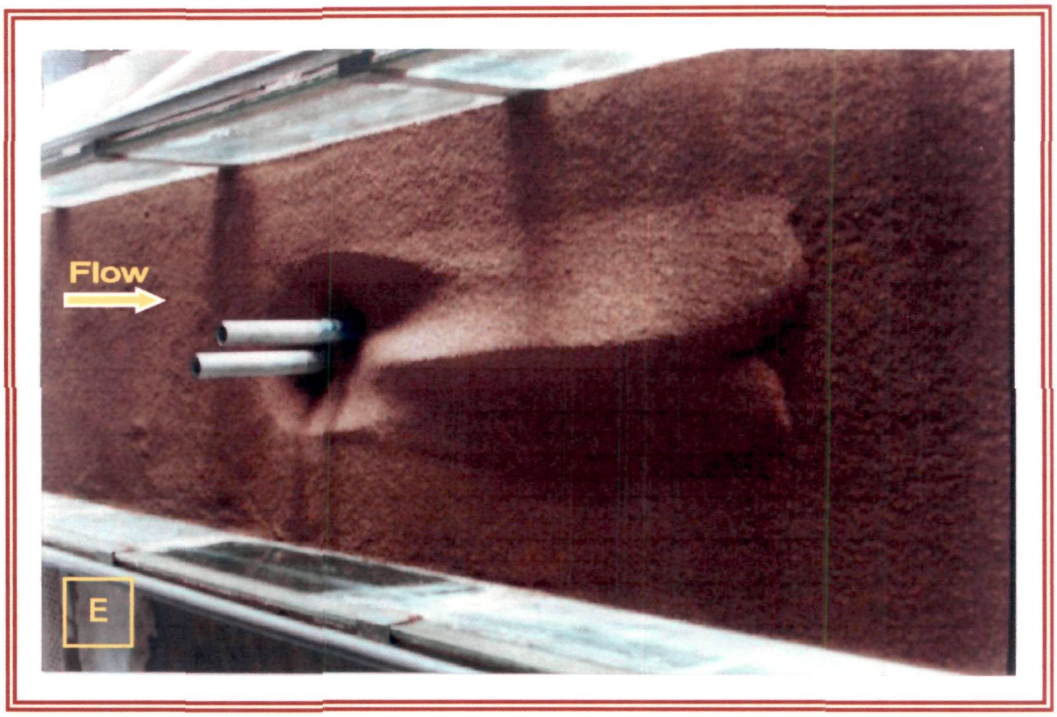

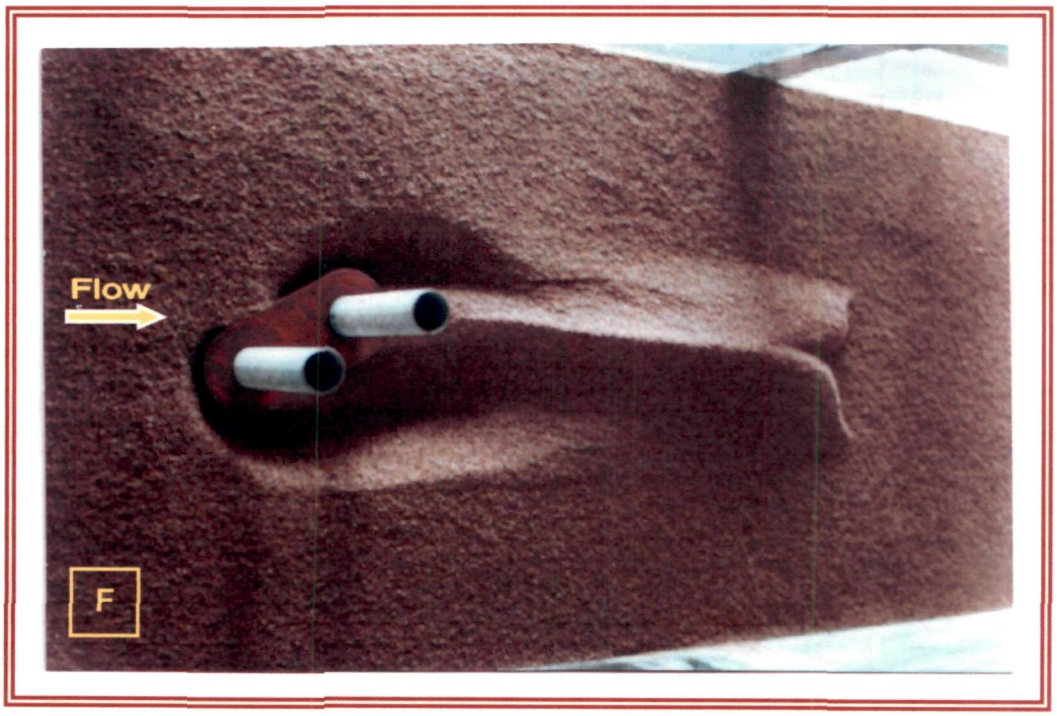

Fig. P21: Scour and deposition patterns around a group of two piers of same sizes at α=30° (E) Without collar (F) With collar

The areal extents of scour measured around the piers group after the test was over, can be seen in Fig. 5.151. The scour and deposition patterns developed on the bed around the piers group at the end of experiments can be depicted in Fig. P21. As compared to the piers group without collar, the areal extent of scour around piers group with collar is smaller in area and hence cost effective for scour countermeasures.

5.11.15 Experiments with collar at angle of attack at (α= 45°)

Fig 5.160 shows the piers group with collar aligned at 45° angle. A scour hole was developed at point A and then immediately after this a scour hole started forming at point B, however, the removal of sediment was quicker from point B as compared to point A. Scour progressed towards upstream from point A. At 10 minutes of the start, scour progressed upto the middle of the collar length on upstream. The material from beneath the collar was removed by the flow; however, the scour did not reach the piers. The scoured material deposited on downstream of the rear pier and on the collar just downstream of the rear pier. The corner of collar on downstream of the rear was in perfect contact with the bed. At 25 minutes of start, scour progressed along the edge of the collar up to point D along the edge of the collar.

UP Upstream pier

DP Downstream pier

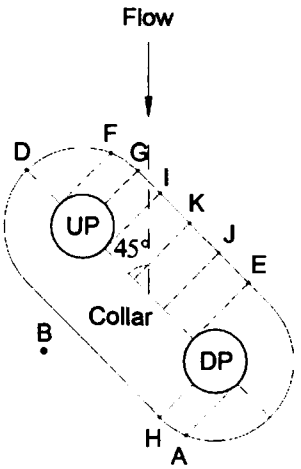

Fig.5.160 Group of two piers with collar at α = 45°

At this stage, portion of collar between points D and E was in contact with the bed and the thickness of the collar plate in this portion was not exposed. At 45 minutes of start, portion of bed along edge of the collar between points D and F was scoured. Between points E and F and at downstream of the rear pier, the collar was in perfect contact with the bed. Sediment was deposited on corner of the collar downstream of the rear pier.

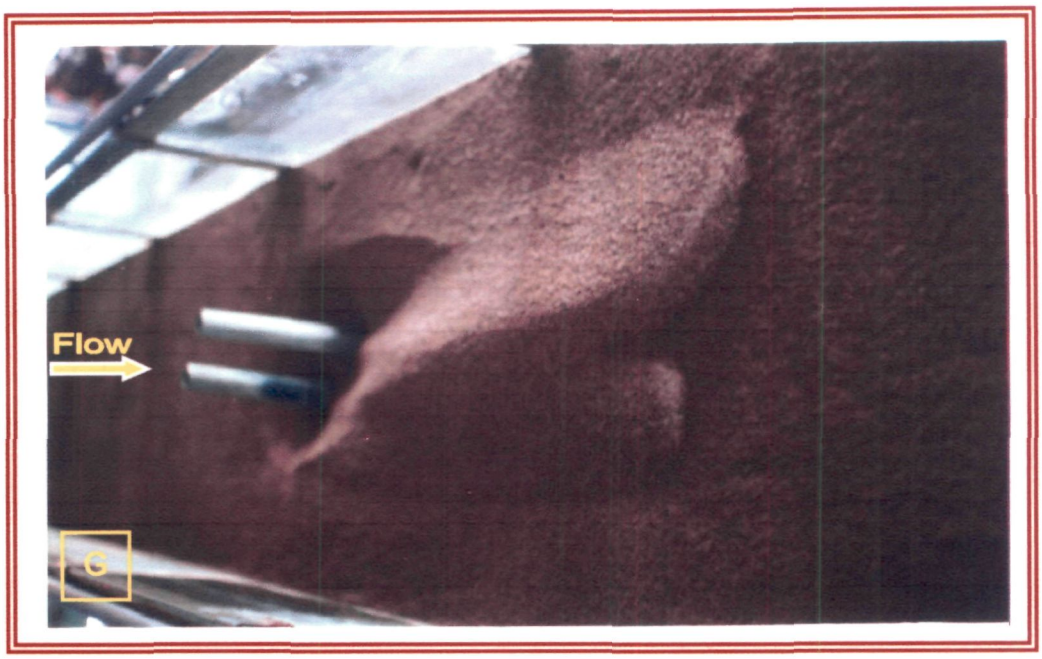

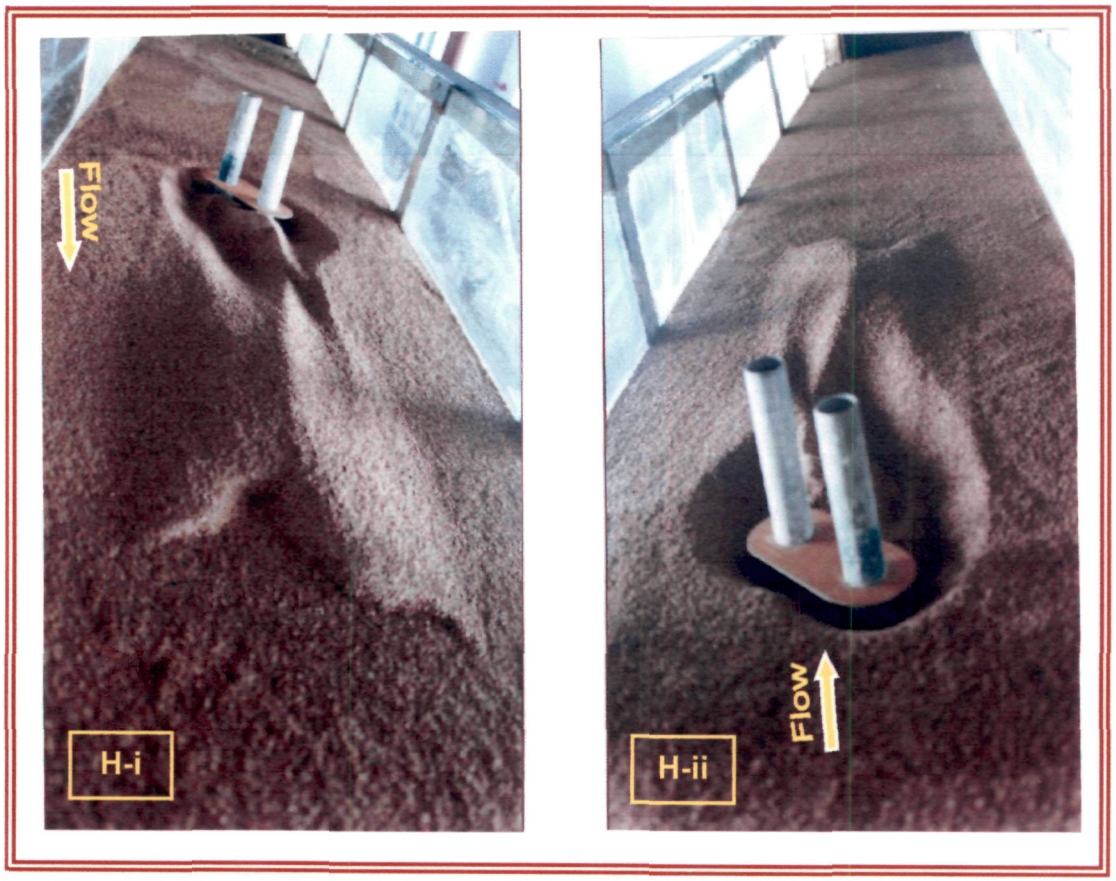

Fig. P22: Scour and deposition patterns around a group of two piers of same sizes at α=45° (G) Without collar (H) [i & ii] With collar

Scour at one hour of start, the bed between points F and G was scoured along the edge of collar, however no scour was observed from point E towards point G at this stage, the piers were not exposed though the collar edge was clearly exposed from point H to point G and from point H to point E and material beneath the collar was also removed but not from the close vicinity of the piers. Scour reached up to points J and I after 90 minutes of start. Scour progressed at K after 2 hours and piers on their sides were slightly exposed. After 3 hours of start, the downstream face of upstream pier and upstream face of the downstream pier were exposed. Then the scour progressed all along the collar except at the downstream corner of the collar just downstream of the rear pier. Beneath the collar, the scour was more at front pier as compared to the scour at rear pier; however, the scour depth was maximum at B. After 4 hours of start, the corner of the collar downstream of the rear pier was touching the bed. Except this point, the entire collar was free. After 5 hours, the total collar was hanging and the material beneath the collar was removed. At the completion of experiment, the maximum scour depth was observed as 4.75 cm at front pier and 5.65 cm at rear pier respectively.

The areal extents of scour measured around the piers group after the test was over, can be depicted in Fig. 5.152. The scour and deposition patterns developed on the bed around the piers group at the end of experiments can be depicted in Fig. P22. It is discernible that the areal extent of scour around piers group with collar is narrower in width but slightly smaller in length and hence smaller in area and economical from protection point of view.

5.11.16 Experiments with collar at angle of attack at ($\alpha = 60°$)

Fig. 5.161 shows the piers group with collar aligned at 60° angle. Scour started from point C and A simultaneously. At 15 minutes of start, the scour progressed up to point D. The collar at point E was hanging in the air at this stage. At 30 minutes of start, scour progressed up to point F. At 60 minutes of start, scour depth was increased by one cm and progressed up to point G, however, this scour depth remained constant and piers were not exposed at all on any side upto 2 hours of start. At 1.5 hour of start, scour progressed to just 1 cm short of middle *i.e.*, upto point J. On upstream, scour progressed up to point H in the initial stages of experiment. The maximum scour depth was observed 4.9 cm on front pier and 0.0 cm at rear pier respectively.

The areal extents of scour measured around the piers group after the test was over, can be depicted in Fig. 5.153.

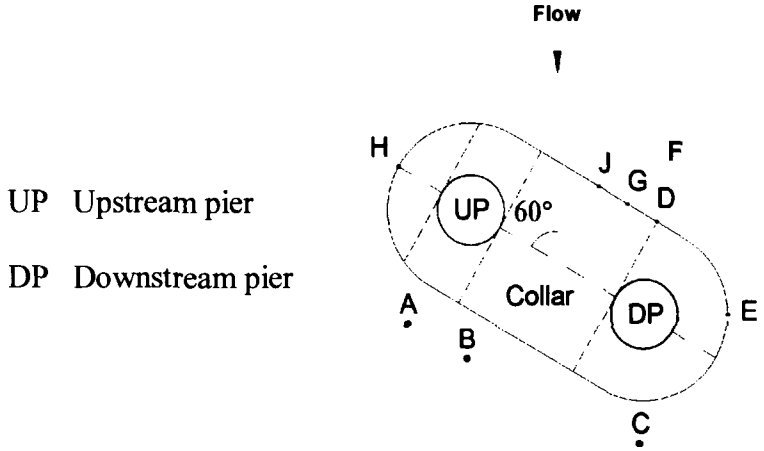

Fig.5.161 Group of two piers with collar at $\alpha = 60°$

The scour and deposition patterns developed on the bed around the piers group at the end of experiments can be depicted in Fig. P23. It is noticeable that the area of scour extent around piers group with collar is significantly smaller than that without collar; collar is considerably economical from protection point of view.

5.11.17 Experiments with collar at angle of attack ($\alpha = 75°$)

Fig. 5.162 shows the piers group with collar aligned at 75° angle. At this angle of attack, scour started from point A and B and progressed towards point C at 55 minutes from starting the test and the scour depth was same at points A, B and C. However, after 2 hours of start the observed scour depth at point C was more. Then after, the material scoured from points A and B started depositing at point C and scour depth at point C started decreasing while scour depth at point A was held constant but scour depth at point B continued to increasing and was maximum at 6.55 cm at front pier and 41.5 mm at rear pier respectively at the end of the experiment.

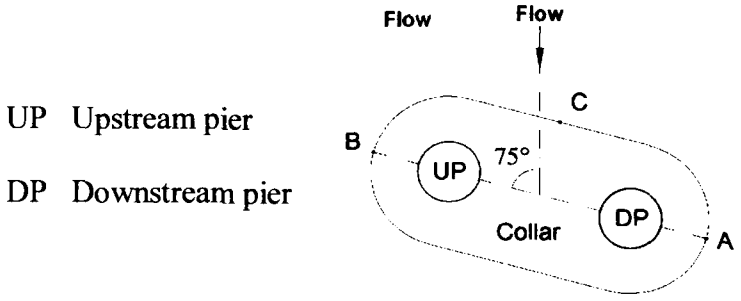

Fig.5.162 Group of two piers with collar at $\alpha = 75°$

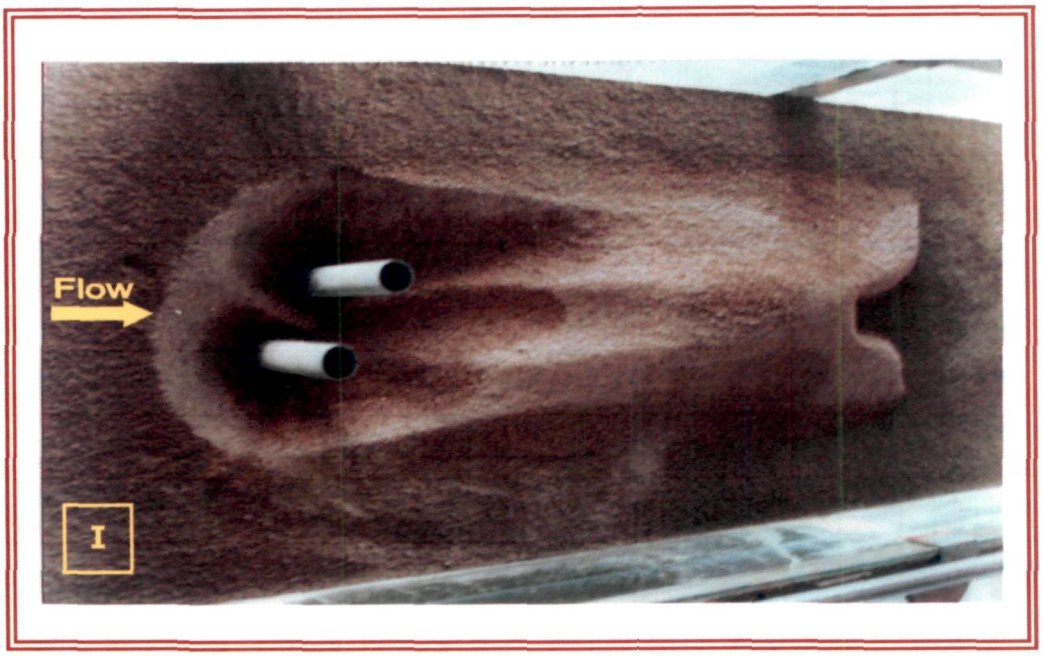

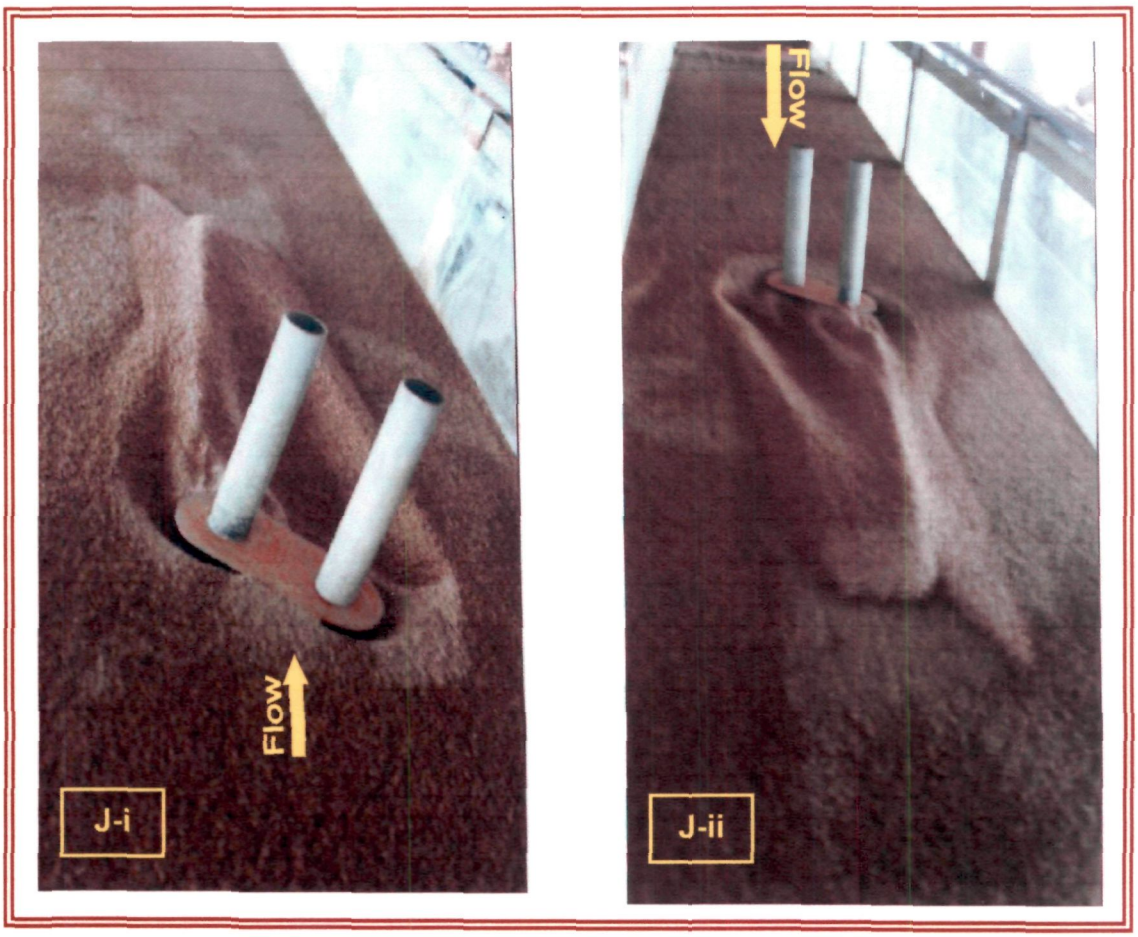

Fig. P23: Scour and deposition patterns around a group of two piers of same sizes at α=60° (I) Without collar (J) [i & ii] With collar

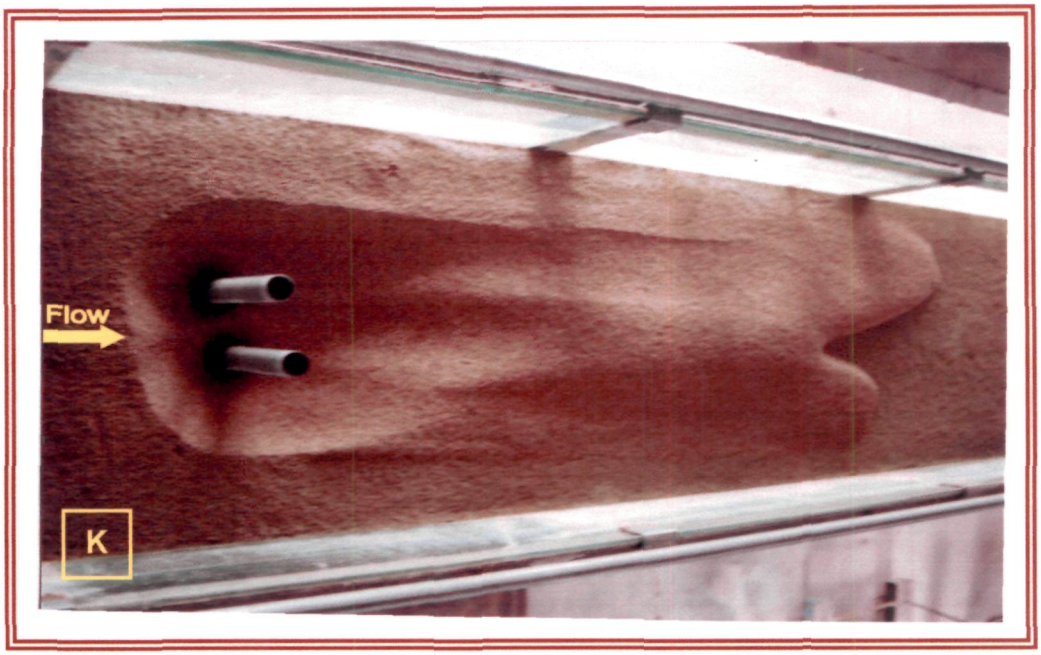

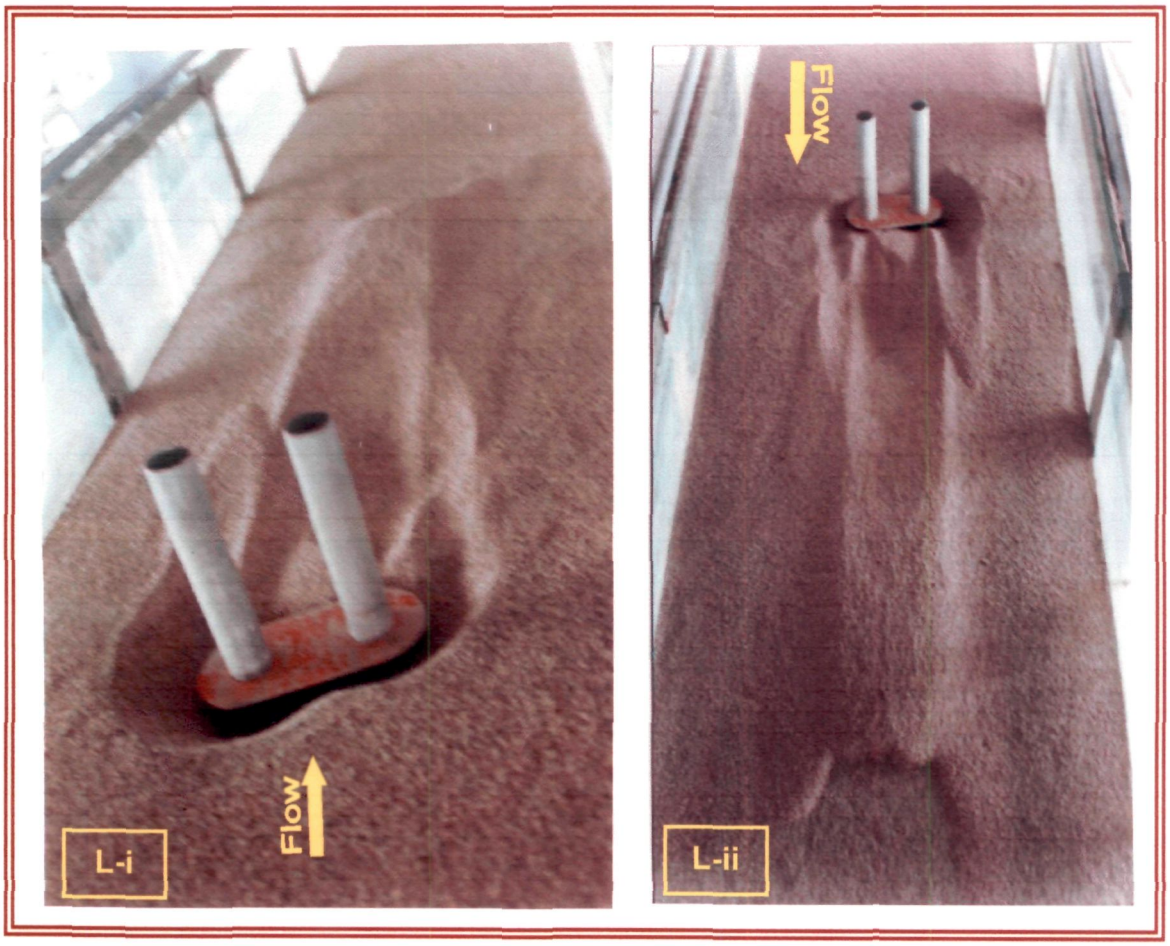

Fig. P24: **Scour and deposition patterns around a group of two piers of same sizes at α=75° (K) Without collar (L) [i & ii] With collar**

The areal extents of scour measured around the piers group after the test was over, can be depicted in Fig.5.154. The scour and deposition features developed on the bed around the piers group at the end of experiments can be depicted in Fig. P24. It is evident that the area of scour extent around piers group with collar is considerably smaller than that without a collar. Hence the use of collar is cost effective in piers group protection against local scour.

5.11.18 Experiments with collar at an angle of attack at ($\alpha = 90°$)

Fig. 5.163 shows the piers group with collar aligned at 90° angle. As the flow started, initially scour started just in front of the pier on upstream of the front edge of the collar plate. Then scour progressed towards the nose of the piers and after about 4 hours, the material beneath the collar edge was removed. Then a stage came when the collar plate was hanging, however, when beam of light from upstream was passed beneath the collar, the light did not pass through the gap between the two piers beneath the collar. The maximum scour depth measured at the end of experiment was as 7 cm on upstream of collar (point A) and 7.5 cm on downstream of the collar (point B.)

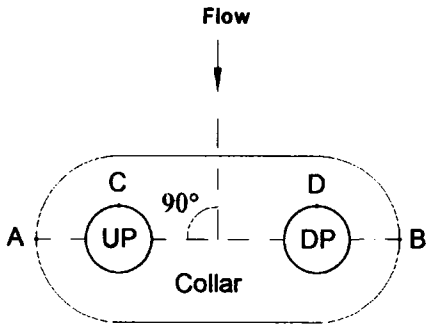

UP Upstream pier DP Downstream pier

Fig.5.163 Group of two piers with collar at $\alpha = 90°$

The areal extents of scour measured around the piers group after the test was over, can be depicted in Fig. 5.155. The scour and deposition patterns developed on the bed around the piers group at the end of experiments can be depicted in Fig. P25. As visible in Fig. P25, the effectiveness of collar at 90° angle of attack gets considerably lost, because the areal extents of scour around piers group with and without collar are similar in area.

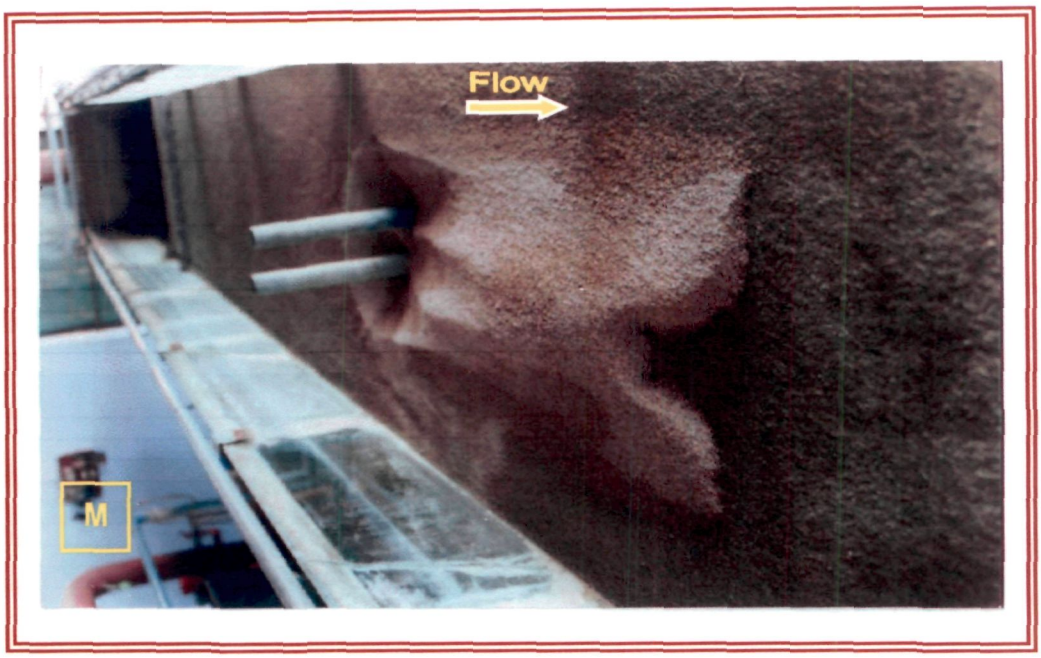

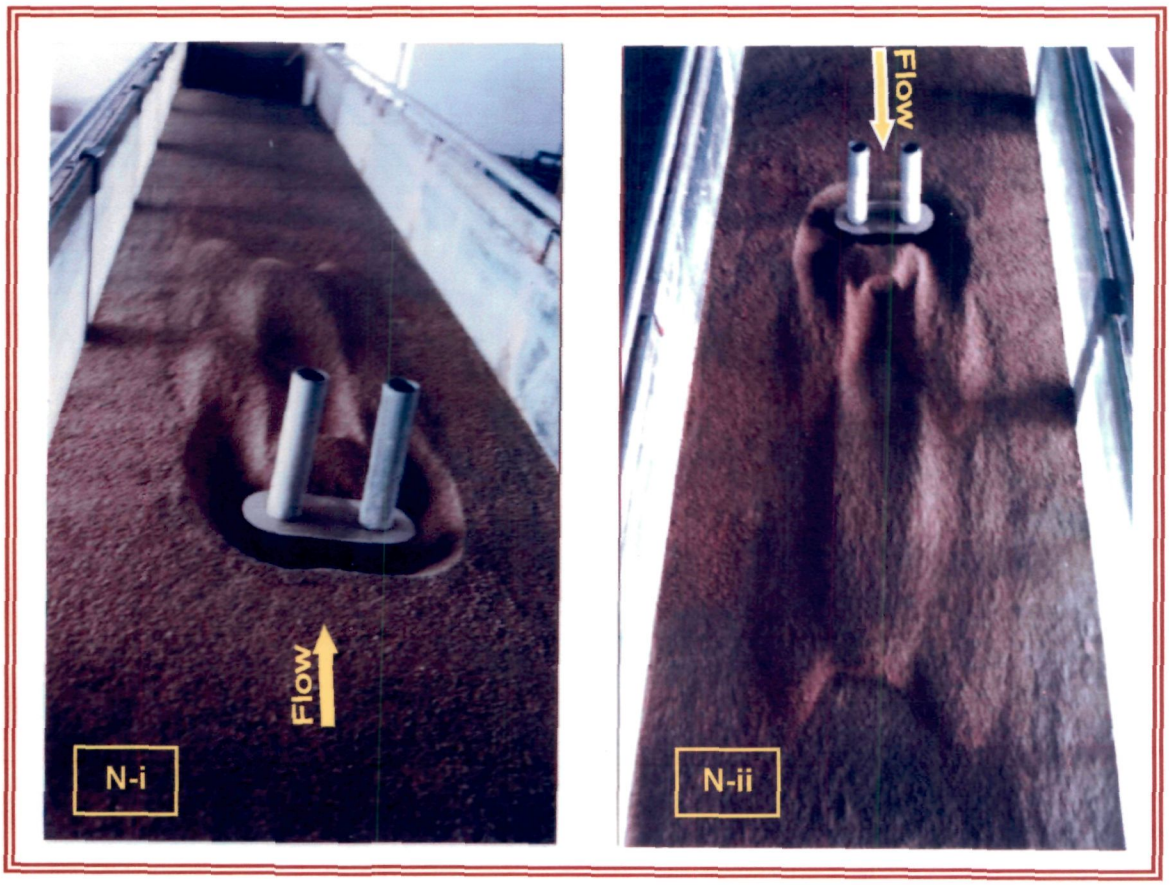

Fig. P25: Scour and deposition patterns around a group of two piers of same sizes at α=90° (M) Without collar (N) [i & ii] With collar

Vautier, E.W. (1972). Flow around a cylindrical pier with scour hole formation, M.E. Thesis, Auckland University.

Venkatadri, C., Rao, A.M., Hussain, S.T. and Asthana, K.C., (1065). Scour around bridge piers and abutments, Irrigation and Power, January, pp. 35-42.

Veronese, A. (1937). Erosion de fond en aval d'une decharge. In: IAHR, meeting for hydraulic works, Berlin.

Verstappen, E.L. (1978). Non-steady local scour at a cylindrical pier, M.E. Thesis, University of Canterbury, Christ Church.

Vischer, G.S. (1969). Grain size distributions and depositional process, Journal of Sedimentary Petrology, Vol. 39, pp. 1074-1106.

Vittal, N., Kothyari, U.C. and Haghighat, M. (1994). Clear water scour around bridge piers group, J. Hydr. Engrg, ASCE, 120(11), 1309-1318.

Walker, B.F.G. (1975). Scour at a cylindrical pier by translation waves, M.E. Thesis, University of Canterbury, Christchurch.

Wang, F. (1994). The use of artificial neural networks in a geographical information system for agricultural land-suitability assessment. Environment and Planning A, 26, 265-284.

Wang, T.W. (1994). A study of pier scouring and scour reduction, Proc. 9th Congr. Asia Pacific Div. IAHR. Int. Assoc. for Hyd. Res., Delft. The Netherlands, Singapore, 18-28.

Wardhana, Kumalasari, and Fabian C. Hadipriono. (2003). Analysis of Recent Bridge Failures in the United States. Journal of Performance of Constructed Facilities 17.3, pp. 144-150.

Wasserman, P.D. (1993). Advanced methods in neural computing, New York: Van. Nostrand Reinhold.

Werbos, P. J., (1995) Backpropagation: basics and new developments, In The Handbook of Brain Theory and Neural Networks, edited by M. A. Arbib. (London: The MIT Press), 134-139.

White, W.R. (1975). Scour around bridge piers in steep streams, Proceedings of the 16th I.A.H.R. Congress, Sao Paulo, Vol. 2, pp. 279-284.

Wilby, R.L., Abrahart, R.J. and Dawson C.W. (2003). Detection of conceptual model rainfall runoff processes inside an artificial neural network. Hydrol Sci. J, 48 (2), pp. 163-81.

Worman, A. (1989). Riprap protection without filter layers, J. Hydr. Engrg., ASCE, 115(12), 1615-1630.

Wu, C.M. (1973). Scour at downstream end of dams in Taiwan, In: International symposium on river mechanics, Bangkok, Thailand, Vol. I, A 13, pp. 1–6.

Yalin, M.S. (1972). Mechanics of sediment transport, published by pergammon Press.

Yalin, M.S. and Karahan, E. (1979), Inception of sediment transport, J. Hydr. Div., ASCE, 105(11), pp. 1433-1443.

Yanmaz, A.M. and Altinbilek, D. (1991). Study of time-dependent local scour around bridge piers, J. Hydr. Engrg., ASCE, 117(10), 1247-1268.

Yanmez, A.M. and Altinbilek, H.D. (1991). Study of time-dependent local scour around bridge piers, J. of Hydr. Engrg., ASCE, 117(10), 1247-1268.

Yaroslavtziev, J.A. (1954). Protection of bridge supports from scour, Moscow Mintranosfoj, U.S.S.R.

Yoon, T.H., Yoon, S.B. and Yoon, K.S. (1995). Design of riprap for scour protection around bridge piers, 26th IAHR Congress, UK, Vol. 1, pp. 105-110.

Zarrati, A.M., Gholami, H. and Mashahir, M.B. (2004). Application of collar to control scouring around rectangular bridge piers, Journal of Hydraulic Research, IAHR, 42 (1) 97-103.

Zarrati, A.M., Nazariah, M. and Mashahir, M.B. (2006). Reduction of local scour in the vicinity of bridge pier group using collars and riprap, Journal of Hydraulic Engineering, ASCE, 132(2), pp. 154-162.

Zarrati, A.R., Gholami, H. and Azizi, M. (1999). Simultaneous application of collar and riprap to control scouring around bridge piers, 2nd Iranian Hydraulics Conference, University of Science and Industry, Vol. 1, pp. 233-240, (in Persian).

Zdravkovich, M.M. (1977 a). Interference between two circular cylinders, series of unexpected discontinuities, J. of industrial aerodynamics, Vol. 2, pp. 255-270.

Zdravkovich, M.M. (1977 b). Review of flow Interference between two circular cylinders in various arrangements, Trans. A.S.M.E. Journal of Fluid Engineering, Vol. 100, pp. 618-633.

Zdravkovich, M.M. (1987). The effects of interference between circular cylinders in cross flow, J. Fluids structures, 1, pp. 235-261.

Zdravkvich, M.M., (1977a). Interference between two circular cylinders, Series of unexpected discontinuities, Journal of Industrial Aerodynamics, Vol. 2, pp. 255-270.

Zulhilmi Ismail (2001). Scour Investigation around Multiple Bridge Piers, Unpublished Master Thesis, Universiti Teknologi Malaysia.

APPENDIX – I

TEMPORAL VARIATION OF SCOUR

Table I-1: Temporal variation of scour depth around a single pier

Time (minutes)	ds (observed)	ds (Kothyari *et.al.*, 1992 a)
0	0.00	0.00
15	4.30	4.29
30	5.00	4.98
45	5.25	5.25
60	5.45	5.44
90	5.75	5.74
120	5.97	5.96
150	6.11	6.10
180	6.28	6.27
210	6.40	6.39
240	6.50	6.49
270	6.60	6.58
300	6.67	6.65
330	6.73	6.73
360	6.77	6.75
420	6.80	6.80
480	6.82	6.83
540	6.84	6.84
600	6.85	6.86

Table I-2: Data on temporal variation of scour depth around bridge piers placed in different pier arrangements

Two piers of same size placed in tandem arrangement at varied pier spacings *x/b*													
$\frac{x}{b}=0$			$\frac{x}{b}=1$			$\frac{x}{b}=2$			$\frac{x}{b}=4$			$\frac{x}{b}=6$		
time (min)	FP	RP	time (min)	FP	RP	time (min)	FP	RP	time (min)	FP	RP	time (min)	FP	RP
0	0.00	0.00	0	0.00	0.00	0	0.00	0.00	0	0.00	0.00	0	0.00	0.00
15	4.35	4.35	15	2.80	1.70	15	3.50	1.80	15	3.15	1.50	15	3.40	2.15
30	4.97	4.97	30	5.30	3.25	30	5.24	3.16	30	5.20	2.75	30	5.00	3.50
45	5.15	5.15	45	6.00	3.45	45	5.70	4.30	45	5.84	3.50	45	5.42	3.87
60	5.30	5.30	60	6.25	3.57	60	5.91	5.00	60	6.15	3.96	60	5.55	3.97
90	5.56	5.56	90	6.60	3.90	90	6.23	5.04	90	6.40	4.05	90	5.80	4.00
120	5.75	5.75	120	6.83	4.30	120	6.40	5.15	120	6.56	4.50	120	6.00	4.13
150	5.92	5.92	150	6.95	4.61	150	6.60	5.25	150	6.67	4.85	150	6.10	4.35
180	6.05	6.05	180	7.12	4.77	180	6.77	5.35	180	6.77	5.06	180	6.27	4.65
210	6.18	6.18	210	7.24	4.88	210	6.90	5.45	210	6.87	5.20	210	6.40	5.00
240	6.29	6.29	240	7.35	4.98	240	7.00	5.55	240	7.00	5.40	240	6.52	5.46
270	6.40	6.40	270	7.45	5.06	270	7.11	5.67	270	7.05	5.60	270	6.60	5.75
300	6.50	6.50	300	7.50	5.21	300	7.23	5.72	300	7.13	5.80	300	6.75	5.95
330	6.58	6.55	330	7.55	5.33	330	7.30	5.81	330	7.23	5.92	330	6.90	6.10
360	6.62	6.62	360	7.62	5.42	360	7.45	5.92	360	7.27	6.01	360	6.95	6.18
420	6.70	6.70	420	7.80	5.62	420	7.60	6.05	420	7.42	6.23	420	7.10	6.30
480	6.78	6.78	480	7.85	5.75	480	7.77	6.12	480	7.53	6.35	480	7.27	6.43
540	6.72	6.72	540	7.90	5.90	540	7.87	6.18	540	7.65	6.45	540	7.40	6.53
600	6.85	6.85	600	7.98	5.96	600	7.94	6.23	600	7.70	6.50	600	7.48	6.64

$\frac{x}{b}$=8			$\frac{x}{b}$=10			$\frac{x}{b}$=12.5			$\frac{x}{b}$=15			$\frac{x}{b}$=20		
time (min)	FP	RP	time (min)	FP	RP	time (min)	FP	RP	time (min)	FP	RP	time (min)	FP	RP
0	0.00	0.00	0	0.00	0.00	0	0.00	0.00	0	0.00	0.00	0	0.00	0.00
15	3.40	2.2	15	3.60	2.20	15	3.40	2.20	15	3.30	2.45	15	3.05	2.10
30	5.25	3.6	30	5.00	3.50	30	4.45	3.30	30	4.80	4.00	30	4.35	3.10
45	5.68	3.73	45	5.39	3.25	45	4.95	3.34	45	5.35	4.53	45	4.95	3.70
60	5.90	3.75	60	5.55	3.00	60	5.12	3.32	60	5.64	4.80	60	5.21	4.12
90	6.10	3.85	90	5.85	3.00	90	5.43	4.00	90	5.91	5.04	90	5.64	4.63
120	6.20	4.10	120	6.04	3.00	120	5.62	4.38	120	6.05	5.08	120	5.84	4.88
150	6.35	4.43	150	6.25	3.10	150	5.80	4.46	150	6.10	4.98	150	6.00	5.10
180	6.47	4.65	180	6.35	3.50	180	5.86	4.48	180	6.15	4.75	180	6.10	5.25
210	6.50	4.82	210	6.50	4.24	210	6.00	4.50	210	6.20	4.50	210	6.18	5.27
240	6.60	4.85	240	6.62	4.80	240	6.08	4.42	240	6.30	4.30	240	6.27	5.30
270	6.68	4.90	300	6.78	5.35	270	6.15	4.38	270	6.38	4.21	270	6.35	5.27
300	6.75	5.00	330	6.80	5.47	300	6.28	4.42	300	6.47	4.28	300	6.40	5.26
330	6.80	5.12	360	6.85	5.60	330	6.35	4.43	330	6.53	4.68	330	6.47	5.22
360	6.90	5.25	420	6.90	5.85	360	6.48	4.46	360	6.70	5.14	360	6.58	5.10
420	7.00	5.68	460	6.95	6.00	420	6.65	4.50	420	6.82	5.45	420	6.70	5.00
480	7.12	6.25	480	7.02	6.08	480	6.80	4.67	480	6.93	5.65	480	6.80	5.50
540	7.24	6.48	540	7.12	6.24	540	6.95	4.90	540	7.00	5.75	540	6.90	5.80
600	7.30	6.54	600	7.18	6.30	600	7.00	5.00	600	7.00	5.75	600	6.97	5.89

$\frac{x}{b}=25$			$\frac{x}{b}=30$			$\frac{x}{b}=40$			$\frac{x}{b}=50$		
time (min)	FP	RP	time (min)	FP	RP	time (min)	FP	RP	time (min)	FP	RP
0	0.00	0.00	0	0.00	0.00	0	0.00	0.00	0	0.00	0.00
15	3.70	2.90	15	3.70	2.20	15	3.70	2.20	15	3.70	2.20
30	5.02	4.30	30	4.65	4.10	30	5.05	4.30	30	4.95	4.25
45	5.35	4.68	45	5.06	4.62	45	5.43	4.80	45	5.35	4.80
60	5.52	4.82	60	5.22	4.80	60	5.60	4.95	60	5.58	5.05
90	5.72	5.03	90	5.48	4.98	90	5.75	5.12	90	5.80	5.25
120	5.88	5.22	120	5.64	5.15	120	5.90	5.28	100	5.85	5.35
150	6.02	5.29	150	5.75	5.24	150	6.00	5.35	120	5.95	5.40
180	6.14	5.38	180	5.90	5.30	180	6.07	5.42	150	6.01	5.47
210	6.22	5.42	210	5.98	5.39	210	6.15	5.50	180	6.08	5.57
240	6.33	5.48	240	6.09	5.44	240	6.23	5.60	210	6.14	5.63
270	6.38	5.53	270	6.20	5.50	270	6.30	5.65	240	6.19	5.68
300	6.45	5.55	300	6.30	5.58	300	6.36	5.67	270	6.25	5.75
330	6.50	5.60	330	6.35	5.65	330	6.42	5.72	300	6.34	5.80
360	6.52	5.62	360	6.43	5.68	360	6.46	5.78	330	6.39	5.85
420	6.60	5.60	420	6.55	5.77	420	6.55	5.88	360	6.45	5.92
480	6.75	5.70	480	6.72	5.85	480	6.66	6.04	420	6.55	6.04
540	6.81	5.83	540	6.84	5.90	540	6.80	6.17	480	6.68	6.15
600	6.85	5.85	600	6.90	6.00	600	6.85	6.25	540	6.80	6.30

$\frac{x}{b}=60$			$\frac{x}{b}=70$			$\frac{x}{b}=80$			$\frac{x}{b}=90$		
time (min)	FP	RP	time (min)	FP	RP	time (min)	FP	RP	time (min)	FP	RP
0	0.00	0.00	0	0.00	0.00	0	0.00	0.00	0	0.00	0.00
15	3.70	2.20	15	3.70	3.20	15	3.70	2.75	15	2.50	2.48
30	4.75	4.15	30	4.96	4.50	30	4.97	4.65	30	4.94	4.95
45	5.28	4.80	45	5.35	5.00	45	5.44	5.16	45	5.40	5.38
60	5.50	5.07	60	5.63	5.26	60	5.65	5.39	60	5.55	5.53
90	5.81	5.40	90	5.83	5.52	90	5.88	5.64	90	5.67	5.66
120	5.95	5.54	120	5.95	5.65	120	6.00	5.75	120	5.76	5.74
150	6.06	5.65	150	6.03	5.74	150	6.12	5.84	150	5.85	5.86
180	6.12	5.75	180	6.12	5.81	180	6.20	5.95	180	5.95	5.93
210	6.21	5.81	210	6.21	5.89	210	6.29	6.05	210	6.05	6.02
240	6.27	5.85	240	6.26	5.96	240	6.36	6.10	240	6.10	6.08
270	6.32	5.92	270	6.31	6.01	270	6.42	6.16	270	6.20	6.18
300	6.37	5.94	300	6.35	6.06	300	6.48	6.21	300	6.25	6.21
330	6.45	5.99	330	6.40	6.09	330	6.52	6.25	330	6.31	6.30
360	6.50	6.08	360	6.46	6.16	360	6.55	6.30	360	6.37	6.34
420	6.60	6.19	420	6.57	6.28	420	6.63	6.39	420	6.52	6.50
480	6.73	6.30	480	6.68	6.37	480	6.70	6.48	480	6.65	6.62
540	6.83	6.40	540	6.79	6.50	540	6.8	6.55	540	6.77	6.77
600	6.87	6.45	600	6.86	6.54	600	6.85	6.6	600	6.85	6.80

Three piers of same size placed in tandem arrangement at varied pier spacings *x/b*																			
$\frac{x}{b}=5$				$\frac{x}{b}=10$				$\frac{x}{b}=15$				$\frac{x}{b}=30$				$\frac{x}{b}=60$			
Time	FP	MP	RP	Time	FP	MP	RP	Time	FP	MP	RP	Time	FP	MP	RP	Time	FP	MP	RP
0	0.00	0.00	0.00	0	0.00	0.00	0.00	0	0.00	0.00	0.00	0	0.00	0.00	0.00	0	0.00	0.00	0.00
15	5.05	2.45	1.25	15	3.88	3.00	2.87	15	3.00	3.00	2.80	15	4.25	4.00	3.95	15	4.30	3.80	3.30
30	5.18	3.80	2.38	30	4.50	3.28	3.32	30	5.40	4.93	4.37	30	4.75	4.50	4.37	30	5.05	4.40	4.05
45	5.28	4.12	2.42	45	4.82	3.35	3.32	45	5.40	4.90	4.40	45	4.95	4.72	4.57	45	5.27	4.64	4.26
60	5.42	4.33	2.40	60	5.10	3.37	3.32	60	5.60	4.60	4.28	60	5.10	4.85	4.70	60	5.42	4.78	4.38
90	5.70	4.50	2.45	90	5.45	3.60	3.38	90	5.73	4.18	4.04	90	5.30	5.07	4.90	90	5.62	4.95	4.52
120	6.00	4.48	3.47	120	5.65	4.10	3.50	120	5.80	4.10	3.97	120	5.47	5.24	5.04	120	5.78	5.08	4.70
150	6.35	5.47	4.13	150	5.70	5.88	3.68	150	5.88	4.12	3.87	150	5.58	5.35	5.15	150	5.93	5.23	4.83
180	6.60	6.14	4.50	180	5.75	6.10	3.80	180	5.90	4.12	3.82	180	5.68	5.44	5.24	180	6.02	5.35	4.90
210	6.85	6.53	4.79	210	5.90	6.04	3.95	210	5.94	4.10	3.78	210	5.77	5.48	5.30	210	6.12	5.40	4.98
240	7.05	6.76	5.00	240	6.00	6.02	4.05	240	5.98	4.10	3.76	240	5.85	5.54	5.35	240	6.25	5.48	5.03
270	7.21	6.95	5.18	270	6.10	6.00	4.14	270	6.00	4.10	3.90	270	5.91	5.58	5.40	270	6.36	5.55	5.10
300	7.33	7.05	5.38	300	6.20	6.00	4.30	300	6.02	4.10	4.20	300	6.00	5.61	5.45	300	6.46	5.60	5.10
360	7.51	7.25	5.60	360	6.42	6.01	4.55	360	6.10	4.20	4.75	360	6.15	5.67	5.50	360	6.60	5.70	5.20
420	7.58	7.41	5.67	420	6.68	6.00	4.80	420	6.28	4.48	4.87	420	6.30	5.70	5.56	420	6.72	5.77	5.22
480	7.58	7.43	5.75	480	6.80	6.05	5.00	480	6.35	4.70	4.86	480	6.35	5.75	5.65	480	6.75	5.80	5.25
540	7.62	7.44	5.76	540	6.80	6.05	5.00	540	6.40	4.90	4.80	540	6.35	5.75	5.65	540	6.75	5.80	5.25
600	7.65	7.45	5.85	600	6.80	6.05	5.00	600	6.40	4.90	4.80	600	6.35	5.75	5.65	600	6.75	5.80	5.25

Big pier (66 mm pier) at front and small pier (33 mm pier) at rear placed in tandem arrangement at varied pier spacings x/b															
$\frac{x}{b}=0$				$\frac{x}{b}=1$				$\frac{x}{b}=2$				$\frac{x}{b}=4$			
Time (min)	66mm pier at front	Mid point	33mm pier at rear	Time (min)	66mm pier at front	Mid point	33mm pier at rear	Time (min)	66mm pier at front	Mid point	33mm pier at rear	Time (min)	66mm pier at front	Mid point	33mm pier at rear
0	0.00	0.00	0.00	0	0.00	0.00	0.00	0	0.00	0.00	0.00	0	0.00	0.00	0.00
15	6.00	3.10	3.10	15	5.95	3.00	3.00	15	5.65	2.80	3.20	15	5.25	1.50	1.60
30	7.50	5.00	5.00	30	7.80	5.00	5.00	30	6.85	3.90	4.50	30	8.00	2.20	2.50
60	8.30	6.12	6.12	60	8.50	6.08	6.08	60	7.88	5.10	5.70	60	8.20	2.50	3.00
90	8.80	6.62	6.62	90	8.85	6.64	6.64	90	8.38	5.77	6.30	90	8.86	3.80	4.30
120	9.13	6.67	6.67	120	9.05	6.85	6.85	120	8.80	6.20	6.80	120	9.40	4.52	5.14
150	9.40	6.90	6.90	150	9.18	6.90	6.90	150	9.15	6.55	7.10	150	9.90	5.13	5.75
180	9.65	7.20	7.20	180	9.32	6.97	6.97	180	9.48	6.70	7.13	180	10.27	5.60	6.13
210	9.95	7.60	7.60	210	9.49	7.16	7.16	210	9.73	6.80	7.20	210	10.75	5.96	6.50
240	10.22	7.95	7.95	240	9.60	7.28	7.28	240	10.00	7.00	7.40	240	11.10	6.22	6.80
270	10.60	8.40	8.40	270	10.17	7.52	7.52	270	10.42	7.35	7.75	270	11.35	6.47	7.03
300	10.83	8.65	8.65	300	10.88	7.76	7.76	300	10.80	7.45	8.06	300	11.54	6.67	7.22
360	11.15	8.96	8.96	360	11.22	8.16	8.16	360	11.15	7.70	8.30	360	11.75	6.97	7.58
420	11.22	9.05	9.05	420	11.38	8.62	8.62	420	11.40	7.75	8.35	420	11.90	7.30	7.85
480	11.31	9.17	9.17	480	11.50	9.15	9.15	480	11.50	7.70	8.35	480	12.15	7.50	8.15
540	11.33	9.19	9.19	540	11.53	9.18	9.18	540	11.53	7.73	8.38	540	12.18	7.52	8.18
600	11.35	9.20	9.20	600	11.55	9.20	9.20	600	11.55	7.75	8.40	600	12.20	7.55	8.20

$\frac{x}{b}$=6				$\frac{x}{b}$=8				$\frac{x}{b}$=10				$\frac{x}{b}$=12			
Time (min)	66mm pier at front	Mid point	33mm pier at rear	Time (min)	66mm pier at front	Mid point	33mm pier at rear	Time (min)	66mm pier at front	Mid point	33mm pier at rear	Time (min)	66mm pier at front	Mid point	33mm pier at rear
0	0.00	0.00	0.00	0	0.00	0.00	0.00	0	0.00	0.00	0.00	0	0.00	0.00	0.00
15	5.20	0.15	0.75	15	5.70	-0.55	2.05	15	7.25	-1.75	1.75	15	5.15	-1.70	1.75
30	7.95	0.50	1.45	30	7.97	-0.30	3.00	30	8.90	-0.20	1.98	30	8.25	-2.00	2.56
45	8.80	1.20	3.12	45	8.72	0.40	3.60	45	9.38	0.50	2.15	45	9.1	-1.25	2.77
60	9.28	2.10	4.75	60	9.15	1.16	4.00	60	9.70	0.92	2.45	60	9.65	-0.50	2.95
90	9.90	3.75	4.80	90	9.60	2.30	4.48	90	10.15	1.60	3.40	90	10.25	0.90	3.75
120	10.20	4.06	5.10	120	9.85	3.00	4.87	120	10.55	2.05	4.12	120	10.7	1.85	4.25
150	10.56	4.29	5.54	150	10.10	3.62	5.12	150	10.90	2.60	4.67	150	11.1	2.57	4.77
180	10.91	4.87	5.97	180	10.36	3.85	5.35	180	11.25	3.05	5.25	180	11.33	3.02	5.17
210	11.14	5.28	6.17	210	10.58	3.90	5.43	210	11.50	3.55	5.65	210	11.6	3.30	5.47
240	11.40	5.65	6.36	240	10.8	3.97	5.56	240	11.72	4.00	6.00	240	11.75	3.55	5.78
270	11.60	5.95	6.54	270	11.00	3.98	5.65	270	11.87	4.16	6.23	270	11.9	3.76	6.10
300	11.68	6.16	6.97	300	11.12	3.95	5.87	300	12.05	4.40	6.5	300	12	3.90	6.30
360	12.00	6.60	7.08	360	11.36	4.33	6.55	360	12.35	4.75	6.85	360	12.1	4.00	6.64
420	12.10	6.92	7.10	420	11.53	4.65	6.80	420	12.60	4.72	7.05	420	12.15	4.00	6.91
480	12.12	6.93	7.15	480	11.55	4.75	6.82	480	12.62	4.70	7.07	480	12.16	4.00	6.92
540	15.13	6.94	7.18	540	11.58	4.78	6.83	540	12.63	4.68	7.08	540	12.18	4.00	6.93
600	12.15	6.95	7.20	600	11.60	4.80	6.85	600	12.65	4.70	7.09	600	12.2	4.00	6.95

$\frac{x}{b}$=14				$\frac{x}{b}$=15				$\frac{x}{b}$=16				$\frac{x}{b}$=18			
Time (min)	66mm pier at front	Mid point	33mm pier at rear	Time (min)	66mm pier at front	Mid point	33mm pier at rear	Time (min)	66mm pier at front	Mid point	33mm pier at rear	Time (min)	66mm pier at front	Mid point	33mm pier at rear
0	0.00	0.00	0.00	0	0.00	0.00	0.00	0	0.00	0.00	0.00	0	0.00	0.00	0.00
15	7.20	-2.25	2.00	15	7.70	-3.40	2.60	15	6.15	-3.45	4.05	15	6.70	-4.00	3.60
30	8.62	-2.30	2.22	30	8.95	-3.50	3.22	30	7.90	-3.10	4.13	30	8.60	-4.25	4.15
45	9.20	-1.90	2.21	45	9.25	-2.90	3.30	45	8.65	-2.64	4.00	45	8.90	-3.78	4.00
60	9.50	-1.40	2.21	60	9.50	-2.30	3.36	60	9.00	-2.00	3.96	60	8.90	-3.30	3.80
90	10.00	-0.55	2.30	90	9.80	-1.10	3.55	90	9.60	-0.75	3.70	90	8.97	-2.36	3.80
120	10.35	0.15	3.15	120	10.08	-0.30	3.65	120	9.95	0.30	3.45	120	9.18	-1.75	4.00
150	10.67	0.85	3.75	150	10.3	0.30	4.04	150	10.33	0.85	3.80	150	9.37	-1.25	4.12
180	10.87	1.48	4.30	180	10.52	0.70	4.42	180	10.60	1.12	4.15	180	9.65	-0.78	4.30
210	11.06	1.88	4.60	210	10.65	1.05	4.62	210	10.90	1.35	4.35	210	9.89	-0.47	4.47
240	11.30	2.30	5.00	240	10.86	1.30	4.85	240	11.20	1.55	4.55	240	10.10	-0.15	4.55
270	11.50	2.68	5.25	270	11.02	1.42	5.10	270	11.40	1.70	4.70	270	10.30	0.00	4.65
300	11.68	3.00	5.48	300	11.15	1.60	5.18	300	11.61	1.90	4.90	300	10.47	0.18	4.80
360	11.90	3.50	5.85	360	11.36	1.90	5.38	360	11.90	2.40	5.22	360	10.77	0.48	5.08
420	12.13	3.83	6.12	420	11.50	2.05	5.45	420	12.15	3.05	5.75	420	11.05	0.75	5.35
480	12.25	3.85	6.25	480	11.70	2.18	5.60	480	12.20	3.06	5.76	480	11.10	0.95	5.40
540	12.23	3.88	6.28	540	11.65	2.30	5.61	540	12.23	3.05	5.77	540	11.13	0.98	5.42
600	12.25	3.90	6.30	600	11.70	2.35	5.65	600	12.25	3.07	5.8	600	11.15	1.00	5.45

$\frac{x}{b}=20$				$\frac{x}{b}=22$				$\frac{x}{b}=25$				$\frac{x}{b}=30$			
Time (min)	66mm pier at front	Mid point	33mm pier at rear	Time (min)	66mm pier at front	Mid point	33mm pier at rear	Time (min)	66mm pier at front	Mid point	33mm pier at rear	Time (min)	66mm pier at front	Mid point	33mm pier at rear
0	0.00	0.00	0.00	0	0.00	0.00	0.00	0.	0.00	0.00	0.00	0	0.00	0.00	0.00
15	5.45	-3.32	2.25	15	5.75	-2.60	2.80	15	5.80	-0.10	3.20	15	7.40	0	4.10
30	7.70	-4.05	3.60	30	8.50	-3.90	4.20	30	8.20	-3.20	4.05	30	8.70	-0.20	5.06
45	8.48	-3.95	3.80	45	9.33	-3.89	4.20	45	9.02	-3.80	3.96	45	9.20	-0.80	5.20
60	8.90	-3.80	3.80	60	9.75	-3.65	4.10	60	9.40	-3.60	3.80	60	9.55	-1.33	5.22
90	9.35	-3.20	3.80	90	10.07	-3.20	3.80	90	9.86	-3.20	3.58	90	10.02	-2.63	5.18
120	9.72	-2.67	3.65	120	10.30	-2.53	3.47	120	10.12	-2.70	3.16	120	10.35	-2.75	4.65
150	9.95	-2.10	3.40	150	10.50	-2.00	3.15	150	10.40	-2.27	2.85	150	10.62	-2.65	4.00
180	10.20	-1.60	3.45	180	10.62	-1.40	3.18	180	10.60	-1.82	3.00	180	10.90	-2.38	3.50
210	10.40	-1.10	3.45	210	10.67	-1.03	3.33	210	10.82	-1.30	3.25	210	11.1	-2.05	3.45
240	10.64	-0.65	3.65	240	10.74	-0.65	3.49	240	11.00	-0.90	3.53	240	11.30	-1.80	3.48
270	10.81	-0.33	3.96	270	10.92	-0.43	3.67	270	11.17	-0.50	3.75	270	11.54	-1.47	3.50
300	10.96	0.00	4.25	300	11.05	-0.22	3.85	300	11.35	-0.25	3.95	300	11.69	-1.20	3.50
360	11.24	0.30	4.60	360	11.26	0.17	4.17	360	11.55	0.25	4.22	360	11.97	-0.60	4.06
420	11.47	0.70	4.80	420	11.40	0.30	4.23	420	11.68	0.65	4.40	420	12.13	0.30	4.16
480	11.53	0.88	4.83	480	11.42	0.28	4.26	480	11.71	0.80	4.50	480	12.16	1.05	4.20
540	11.57	1.00	4.84	540	11.43	0.29	4.28	540	11.73	0.84	4.53	540	12.18	1.08	4.22
600	11.60	1.00	4.85	600	11.45	0.30	4.30	600	11.75	0.85	4.55	600	12.20	1.10	4.25

$\frac{x}{b}=35$				$\frac{x}{b}=40$				$\frac{x}{b}=50$				$\frac{x}{b}=60$			
Time (min)	66mm pier at front	Mid point	33mm pier at rear	Time (min)	66mm pier at front	Mid point	33mm pier at rear	Time (min)	66mm pier at front	Mid point	33mm pier at rear	Time (min)	66mm pier at front	Mid point	33mm pier at rear
0	0.00	0.00	0.00	0	0.00	0.00	0.00	0	0.00	0.00	0.00	0	0.00	0.00	0.00
15	7.25	0.00	4.00	15	5.50	0.15	2.90	15	6.80	0.00	3.68	15	6.55	0.00	3.85
30	8.65	-0.40	5.00	30	8.25	-1.05	4.35	30	8.50	0.00	4.75	30	8.20	0.00	4.70
45	9.35	-0.95	5.15	45	8.95	-2.15	4.74	45	9.13	0.00	4.95	45	8.70	-0.10	4.90
60	9.73	-1.30	5.15	60	9.30	-2.80	4.75	60	9.50	0.00	5.10	60	9.03	0.00	5.00
90	10.18	-2.00	5.22	90	9.78	-2.82	4.90	90	9.97	0.00	5.22	90	9.45	-0.60	5.00
120	10.38	-2.23	5.30	120	10.05	-2.85	4.95	120	10.33	-0.58	5.36	120	9.80	-0.85	5.35
150	10.63	-2.30	4.68	150	10.36	-2.70	5.00	150	10.68	-1.82	5.46	150	10.10	-0.90	5.70
180	10.75	-2.20	3.95	180	10.62	-2.50	5.13	180	10.90	-2.65	5.58	180	10.40	-1.00	5.85
210	10.85	-2.08	3.62	210	10.82	-2.35	5.22	210	11.10	-2.83	5.75	210	10.65	-1.28	6.00
240	10.97	-1.90	3.47	240	11.04	-2.20	4.96	240	11.25	-2.96	5.40	240	10.93	-1.50	6.00
270	11.3	-1.63	3.48	270	11.22	-2.10	4.28	270	11.38	-2.87	4.65	270	11.13	-1.70	6.00
300	11.7	-1.40	3.62	300	11.40	-2.00	3.65	300	11.52	-2.80	3.85	300	11.35	-1.88	6.00
360	12.00	-1.20	3.65	360	11.65	-1.80	3.00	360	11.70	-2.72	3.68	360	11.75	-2.20	6.00
420	12.08	-0.70	3.75	420	11.92	-1.60	3.28	420	11.82	-2.13	3.57	420	12.00	-2.30	6.02
480	12.11	0.60	3.78	480	12.05	-1.40	3.50	480	11.95	-2.00	3.55	480	12.16	-2.40	6.03
540	12.13	-0.50	3.81	540	12.10	-1.10	3.65	540	12.00	-1.85	3.55	540	12.18	-2.45	6.04
600	12.15	0.00	3.83	600	12.10	0.00	3.85	600	12.00	-1.85	3.55	600	12.20	-2.50	6.05

$\frac{x}{b}=70$				$\frac{x}{b}=80$				$\frac{x}{b}=90$			
Time (min)	66mm pier at front	Mid point	33mm pier at rear	Time (min)	66mm pier at front	Mid point	33mm pier at rear	Time (min)	66mm pier at front	Mid point	33mm pier at rear
0	0.00	0.00	0.00	0	0.00	0.00	0.00	0	0.00	0.00	0.00
15	6.30	0.00	3.60	15	5.60	0.00	2.50	15	7.40	0.00	3.60
30	8.20	0.00	4.65	30	9.25	0.00	4.85	30	9.25	0.00	4.60
45	8.95	0.00	5.00	45	10.17	0.00	5.54	60	10.4	0.00	5.15
60	9.30	0.00	5.20	60	10.55	0.00	5.75	90	10.85	0.00	5.35
90	9.72	0.00	5.40	90	11.10	0.00	5.95	120	11.20	0.00	5.54
120	10.00	0.00	5.55	120	11.40	0.00	6.05	150	11.35	0.00	5.70
150	10.30	0.00	5.65	150	11.60	0.00	6.14	180	11.47	0.00	5.75
180	10.44	-0.32	5.72	180	11.83	-0.15	6.20	210	11.60	0.00	5.80
210	10.68	-1.40	5.82	210	11.97	-0.66	6.30	240	11.70	0.00	5.90
240	10.78	-2.18	5.90	240	12.08	-1.70	6.42	270	11.80	-2.30	6.08
270	11.00	-2.60	6.00	270	12.20	-1.90	6.40	300	11.83	-2.55	6.12
300	11.17	-2.80	6.03	300	12.25	-2.00	6.50	330	11.90	-2.60	6.15
360	11.35	-3.00	6.15	360	12.40	-1.95	6.57	360	11.90	-2.55	6.12
420	11.50	-2.80	6.18	420	12.50	-1.90	6.76	420	12.10	-2.60	6.20
480	11.51	-2.60	6.24	480	12.52	-2.05	6.77	480	12.12	-2.60	6.25
540	11.53	-2.52	6.28	540	12.53	-2.08	6.78	540	12.13	-2.60	6.25
600	11.55	-2.50	6.30	600	12.55	-2.10	6.80	600	12.15	-2.60	6.25

Small pier (33 mm pier) at front and Big pier (66 mm pier) at rear placed in tandem arrangement at varied pier spacings *x/b*

$\frac{x}{b}=0$				$\frac{x}{b}=1$				$\frac{x}{b}=2$				$\frac{x}{b}=3$			
Time (min)	33mm pier at front	Mid point	66mm pier at rear	Time (min)	33mm pier at front	Mid point	66mm pier at rear	Time (min)	33mm pier at front	Mid point	66mm pier at rear	Time (min)	33mm pier at front	Mid point	66mm pier at rear
0	0.00	0.00	0.00	0	0.00	0.00	0.00	0	0.00	0.00	0.00	0	0.00	0.00	0.00
15	4.40	4.40	4.15	15	4.75	4.10	5.00	15	4.12	2.40	4.25	15	4.00	1.25	4.50
30	5.70	5.70	5.45	30	5.65	5.20	5.85	30	5.00	3.10	5.15	30	5.10	1.98	5.60
60	6.33	6.33	6.04	60	6.40	5.90	6.53	60	5.70	3.80	5.85	60	5.75	2.80	6.30
90	6.80	6.80	6.45	90	6.80	6.20	6.98	75	5.90	4.00	6.10	90	6.00	3.35	6.60
120	7.10	7.10	6.80	120	7.00	6.46	7.20	90	6.15	4.20	6.35	120	6.16	3.75	6.80
150	7.48	7.48	7.10	150	7.30	6.60	7.27	120	6.38	4.60	6.67	150	6.15	3.70	6.92
180	7.75	7.75	7.38	180	7.55	6.68	7.35	150	6.55	4.90	6.95	180	6.30	3.95	6.75
210	8.00	8.00	7.68	210	7.65	6.76	7.50	180	6.76	5.00	7.12	210	6.59	4.25	6.79
240	8.25	8.25	7.93	240	7.75	6.90	7.55	210	6.85	5.22	7.30	240	6.90	4.56	7.19
270	8.42	8.42	8.07	270	7.85	7.17	7.68	240	7.12	5.50	7.45	270	7.06	4.80	7.48
300	8.62	8.62	8.30	300	8.00	7.45	7.80	270	7.40	5.75	7.75	300	7.20	5.05	7.80
360	8.85	8.85	8.55	360	8.28	7.90	8.14	300	7.55	6.15	8.04	360	7.40	5.40	8.20
420	9.00	9.00	8.75	420	8.65	8.15	8.45	360	7.70	6.55	8.65	400	7.45	5.45	8.35
480	9.05	9.10	8.80	480	8.90	8.25	8.60	420	7.80	6.60	8.80	480	7.47	5.45	8.37
540	9.08	9.08	8.83	540	8.93	8.27	8.67	480	7.83	6.63	8.83	540	7.48	5.45	8.38
600	9.10	9.10	8.85	600	8.95	8.30	8.70	540	7.85	6.65	8.85	600	7.50	5.45	8.40

$\frac{x}{b}$=4				$\frac{x}{b}$=6				$\frac{x}{b}$=10				$\frac{x}{b}$=12			
Time (min)	33mm pier at front	Mid point	66mm pier at rear	Time (min)	33mm pier at front	Mid point	66mm pier at rear	Time (min)	33mm pier at front	Mid point	66mm pier at rear	Time (min)	33mm pier at front	Mid point	66mm pier at rear
0	0.00	0.00	0.00	0	0.00	0.00	0.00	0	0.00	0.00	0.00	0	0.00	0.00	0.00
15	4.50	1.30	5.05	15	4.00	-0.88	4.60	15	3.50	-0.60	4.20	15	4.00	-1.10	4.75
30	5.35	2.15	5.7	30	4.70	-0.53	5.50	30	4.67	-1.50	5.40	30	4.88	-1.66	5.72
60	5.67	3.60	5.9	60	5.25	0.85	6.35	60	5.38	-1.15	6.34	60	5.15	-1.95	6.32
90	5.87	4.68	6.00	90	5.65	1.75	6.90	90	5.80	-0.60	6.90	90	5.34	-1.90	6.69
120	6.10	5.35	6.25	120	5.84	2.27	7.20	120	6.10	0.07	7.22	120	5.48	-1.80	6.90
150	6.33	4.77	6.80	150	6.10	2.60	7.43	150	6.33	0.61	7.38	150	5.58	-1.60	7.12
180	6.55	4.25	7.25	180	6.25	2.80	7.65	180	6.45	1.09	7.56	180	5.65	-1.46	7.27
210	6.78	4.22	7.55	210	6.38	2.95	7.77	210	6.60	1.50	7.70	210	5.65	-1.35	7.35
240	6.90	4.25	7.70	240	6.53	3.13	7.90	240	6.70	1.88	7.85	240	5.72	-1.18	7.40
270	7.03	4.33	7.79	270	6.60	3.30	8.00	270	6.88	2.18	7.95	270	5.75	-1.05	7.50
300	6.92	4.44	7.90	300	6.75	3.43	8.08	300	6.90	2.40	8.00	300	5.81	-0.90	7.55
360	7.18	4.73	8.22	360	6.90	3.65	8.10	360	7.13	2.93	8.40	360	5.86	-0.70	7.69
420	7.47	4.98	8.47	420	7.00	3.75	8.17	420	7.27	3.36	9.33	420	5.95	0.15	6.90
480	7.60	5.02	8.60	480	7.02	3.80	8.20	480	7.48	3.63	9.68	480	5.97	0.20	7.96
540	7.63	5.03	8.63	540	7.03	3.80	8.23	540	7.48	3.64	9.69	540	5.98	0.20	7.69
600	7.65	5.05	8.65	600	7.05	3.80	8.25	600	7.50	3.65	9.70	600	6.00	0.20	7.70

$\frac{x}{b}$=14				$\frac{x}{b}$=15				$\frac{x}{b}$=16				$\frac{x}{b}$=18			
Time (min)	33mm pier at front	Mid point	66mm pier at rear	Time (min)	33mm pier at front	Mid point	66mm pier at rear	Time (min)	33mm pier at front	Mid point	66mm pier at rear	Time (min)	33mm pier at front	Mid point	66mm pier at rear
0	0.00	0.00	0.00	0	0.00	0.00	0.00	0	0.00	0.00	0.00	0	0.00	0.00	0.00
15	4.20	0.90	5.4	15	4.50	0.00	5.85	15	3.65	-1.10	5.00	15	3.95	-0.50	5.4
30	4.88	0.23	6.4	30	5.34	-0.50	7.00	30	5.12	-1.70	6.40	30	4.70	-0.98	6.36
60	5.16	-1.10	7.00	60	6.00	-1.33	7.85	60	5.77	-1.38	7.10	60	5.15	-1.55	7.05
90	5.36	-1.28	7.32	90	6.25	-1.95	8.40	90	6.25	-1.00	7.45	90	5.40	-1.80	7.50
120	5.48	-1.25	7.58	120	6.50	-1.82	8.58	120	6.50	-0.70	7.72	120	5.56	-1.50	7.80
150	5.58	-1.22	7.74	150	6.74	-1.33	8.62	150	6.75	-0.38	7.93	150	5.65	-1.00	8.00
180	5.70	-1.10	7.84	180	6.82	-0.96	8.75	180	6.88	-0.14	8.12	180	5.74	-0.99	8.12
210	5.78	-1.00	7.88	210	6.97	-0.80	8.82	210	7.00	0.15	8.27	210	5.80	-0.99	8.20
240	5.83	-0.90	7.90	240	7.05	-0.65	8.84	240	7.15	0.37	8.35	240	5.90	-1.00	8.30
270	5.80	-0.80	8.00	270	7.22	-0.60	8.95	270	7.20	0.57	8.43	270	6.00	-0.93	8.34
300	5.90	-0.60	8.10	300	7.30	-0.55	8.95	300	7.25	0.67	8.50	300	6.12	-0.80	8.38
360	6.00	0.22	8.16	360	7.40	-0.45	8.45	360	7.40	1.00	8.65	360	6.37	-0.50	8.44
420	6.00	0.82	8.22	420	7.43	-0.40	8.50	420	7.43	1.30	8.82	420	6.57	-0.35	8.47
480	6.25	1.05	8.25	480	7.50	-0.35	8.52	480	7.45	1.42	8.83	480	6.60	-0.40	8.54
540	6.38	1.08	8.28	540	7.53	-0.35	8.53	540	7.48	1.43	8.84	540	6.60	-0.45	8.60
600	6.40	1.10	8.30	600	7.55	-0.35	8.55	600	7.50	1.45	8.85	600	6.60	-0.45	8.60

$\frac{x}{b}$=20				$\frac{x}{b}$=25				$\frac{x}{b}$=27.5				$\frac{x}{b}$=30			
Time (min)	33mm pier at front	Mid point	66mm pier at rear	Time (min)	33mm pier at front	Mid point	66mm pier at rear	Time (min)	33mm pier at front	Mid point	66mm pier at rear	Time (min)	33mm pier at front	Mid point	66mm pier at rear
0	0.00	0.00	0.00	0	0	0.00	0	0	0.00	0.00	0.00	0	0.00	0.00	0.00
15	4.30	0.20	5.00	15	4.5	-0.40	6.5	15	3.80	0.00	5.30	15	3.50	0.00	5.8
30	5.55	0.25	6.70	30	5.12	-0.65	7.36	30	5.05	0.00	7.40	30	4.46	-0.30	7.00
60	6.00	0.20	7.55	60	5.49	-1.25	7.9	60	5.45	-0.86	7.950	60	5.00	-0.80	7.96
90	6.20	-0.25	8.00	90	5.72	-1.60	8.13	90	5.70	-1.60	8.30	90	5.35	-1.20	8.40
120	6.35	-0.90	8.25	120	5.87	-1.85	8.3	120	5.93	-1.66	8.60	120	5.60	-1.45	8.70
150	6.48	-1.72	8.39	150	6.01	-2.00	8.44	150	6.18	-1.68	8.80	150	5.84	-1.75	8.90
180	6.53	-1.26	8.45	180	6.12	-2.05	8.58	180	6.30	-1.70	8.95	180	6.00	-1.87	9.05
210	6.67	-0.90	8.50	210	6.23	-2.09	8.7	210	6.42	-1.70	9.05	210	6.14	-1.90	9.15
240	6.80	-0.70	8.52	240	6.32	-2.12	8.8	240	6.60	-1.71	9.22	240	6.27	-1.87	9.18
270	6.90	-0.40	8.58	270	6.42	-2.12	8.87	270	6.67	-1.70	9.32	270	6.40	-1.81	9.18
300	7.00	-0.30	8.62	300	6.5	-2.00	8.95	300	6.80	-1.67	9.38	300	6.48	-1.73	9.12
360	7.15	-0.05	8.60	360	6.65	-1.85	9.08	360	7.00	-1.63	9.50	360	6.65	-1.60	9.10
420	7.30	0.15	8.60	420	6.8	-1.60	9.2	420	7.12	-1.50	9.32	420	6.75	-1.55	9.2
480	7.35	0.15	8.60	480	6.93	-1.45	9.25	480	7.16	-1.27	9.12	480	6.77	-1.55	9.22
540	7.35	0.15	8.60	540	7.03	-1.30	9.33	540	7.18	-1.20	9.03	540	6.78	-1.55	9.23
600	7.35	0.15	8.60	600	7.05	-1.20	9.34	600	7.20	-1.20	9.00	600	6.80	-1.55	9.25

$\frac{x}{b}=20$				$\frac{x}{b}=25$				$\frac{x}{b}=27.5$				$\frac{x}{b}=30$			
Time (min)	33mm pier at front	Mid point	66mm pier at rear	Time (min)	33mm pier at front	Mid point	66mm pier at rear	Time (min)	33mm pier at front	Mid point	66mm pier at rear	Time (min)	33mm pier at front	Mid point	66mm pier at rear
0	0.00	0.00	0.00	0	0	0.00	0	0	0.00	0.00	0.00	0	0.00	0.00	0.00
15	4.30	0.20	5.00	15	4.5	-0.40	6.5	15	3.80	0.00	5.30	15	3.50	0.00	5.8
30	5.55	0.25	6.70	30	5.12	-0.65	7.36	30	5.05	0.00	7.40	30	4.46	-0.30	7.00
60	6.00	0.20	7.55	60	5.49	-1.25	7.9	60	5.45	-0.86	7.950	60	5.00	-0.80	7.96
90	6.20	-0.25	8.00	90	5.72	-1.60	8.13	90	5.70	-1.60	8.30	90	5.35	-1.20	8.40
120	6.35	-0.90	8.25	120	5.87	-1.85	8.3	120	5.93	-1.66	8.60	120	5.60	-1.45	8.70
150	6.48	-1.72	8.39	150	6.01	-2.00	8.44	150	6.18	-1.68	8.80	150	5.84	-1.75	8.90
180	6.53	-1.26	8.45	180	6.12	-2.05	8.58	180	6.30	-1.70	8.95	180	6.00	-1.87	9.05
210	6.67	-0.90	8.50	210	6.23	-2.09	8.7	210	6.42	-1.70	9.05	210	6.14	-1.90	9.15
240	6.80	-0.70	8.52	240	6.32	-2.12	8.8	240	6.60	-1.71	9.22	240	6.27	-1.87	9.18
270	6.90	-0.40	8.58	270	6.42	-2.12	8.87	270	6.67	-1.70	9.32	270	6.40	-1.81	9.18
300	7.00	-0.30	8.62	300	6.5	-2.00	8.95	300	6.80	-1.67	9.38	300	6.48	-1.73	9.12
360	7.15	-0.05	8.60	360	6.65	-1.85	9.08	360	7.00	-1.63	9.50	360	6.65	-1.60	9.10
420	7.30	0.15	8.60	420	6.8	-1.60	9.2	420	7.12	-1.50	9.32	420	6.75	-1.55	9.2
480	7.35	0.15	8.60	480	6.93	-1.45	9.25	480	7.16	-1.27	9.12	480	6.77	-1.55	9.22
540	7.35	0.15	8.60	540	7.03	-1.30	9.33	540	7.18	-1.20	9.03	540	6.78	-1.55	9.23
600	7.35	0.15	8.60	600	7.05	-1.20	9.34	600	7.20	-1.20	9.00	600	6.80	-1.55	9.25

$\frac{x}{b}=40$				$\frac{x}{b}=50$				$\frac{x}{b}=60$			
Time (min)	33mm pier at front	Mid point	66mm pier at rear	Time (min)	33mm pier at front	Mid point	66mm pier at rear	Time (min)	33mm pier at front	Mid point	66mm pier at rear
0	0.00	0.00	0.00	0	0.00	0.00	0.00	0	0.00	0.00	0.00
15	4.55	0.00	6.50	15	3.90	0.10	5.85	15	4.10	0.00	5.10
30	5.50	0.00	7.83	30	4.80	0.15	6.95	30	5.00	0.00	6.35
60	5.90	0.00	8.54	60	5.50	0.15	8.10	60	5.55	0.00	7.50
90	6.17	-0.35	8.87	90	5.86	0.15	8.75	90	5.85	0.00	8.21
120	6.34	-0.90	9.12	120	6.14	0.15	9.35	120	6.00	0.00	8.65
150	6.47	-1.33	9.30	150	6.34	0.15	9.75	150	6.08	0.00	9.00
180	6.52	-1.47	9.40	180	6.53	0.15	10.08	180	6.20	0.00	9.15
210	6.55	-1.57	9.50	210	6.65	-0.05	10.30	210	6.30	0.00	9.35
240	6.65	-1.63	9.58	240	6.80	-0.60	10.45	240	6.44	0.00	9.54
270	6.72	-1.65	9.66	270	6.92	-1.00	10.62	270	6.54	0.00	9.70
300	6.75	-1.65	9.70	300	7.00	-1.12	10.65	300	6.60	0.00	9.80
360	6.87	-1.69	9.80	360	7.24	-1.28	10.64	360	6.76	0.00	9.98
420	7.00	-1.69	9.82	420	7.30	-1.40	10.65	420	6.90	0.00	10.15
480	7.34	-1.42	10.66	480	6.95	0.00	10.15	480	7.34	-1.42	10.66
7540	7.15	-1.70	9.85	540	6.98	0.00	10.18	540	7.10	-0.50	10.21
600	7.15	-1.70	9.85	600	7.00	0.00	10.20	600	7.10	-0.50	10.25

$\frac{x}{b}=70$				$\frac{x}{b}=80$				$\frac{x}{b}=90$			
Time (min)	33mm pier at front	Mid point	66mm pier at rear	Time (min)	33mm pier at front	Mid point	66mm pier at rear	Time (min)	33mm pier at front	Mid point	66mm pier at rear
0	0	0.00	0.00	0	0.00	0.00	0.00	0	0.00	0.00	0.00
15	4.00	0.00	5.55	15	3.50	0.00	5.50	15	3.75	0.00	5.60
30	5.25	0.00	6.92	30	4.80	0.00	7.25	30	4.60	0.00	6.90
60	5.80	0.00	7.80	60	5.58	0.00	8.00	60	5.30	0.00	7.90
90	5.98	0.00	8.35	90	5.80	0.00	8.25	90	5.70	0.00	8.43
120	6.10	0.00	8.60	120	5.95	0.00	8.45	120	5.90	0.00	8.68
150	6.25	0.00	8.85	150	6.00	0.00	8.66	150	6.00	0.00	8.95
180	6.35	0.00	9.00	180	6.16	0.00	8.85	180	6.13	0.00	9.13
210	6.41	0.00	9.15	210	6.24	0.00	8.95	210	6.25	0.00	9.25
240	6.55	0.00	9.28	240	6.35	0.00	9.05	240	6.35	0.00	9.41
270	6.67	0.00	9.40	270	6.45	0.00	9.15	270	6.40	0.00	9.50
300	6.75	0.00	9.50	300	6.55	0.00	9.27	300	6.50	0.00	9.60
360	6.90	0.00	9.65	360	6.65	0.00	9.48	360	6.60	0.00	9.85
420	7.00	0.00	9.90	420	6.80	0.00	9.75	420	6.70	0.00	9.97
480	7.10	0.00	10.00	495	6.85	0.00	9.95	480	6.77	0.00	10.00
540	7.10	0.00	10.00	4.95	6.85	0.00	9.98	540	6.79	0.00	10.17
600	7.10	0.00	10.00	4.95	6.85	0.00	10.00	600	6.80	0.00	10.20

Two piers of same size placed in transverse arrangement at varied lateral pier spacings Z_c/b																	
$\frac{Z_c}{b}=0$		$\frac{Z_c}{b}=1$		$\frac{Z_c}{b}=2$		$\frac{Z_c}{b}=3$		$\frac{Z_c}{b}=4$		$\frac{Z_c}{b}=5$		$\frac{Z_c}{b}=6$		$\frac{Z_c}{b}=7$		$\frac{Z_c}{b}=8$	
Time (min)	LP/ RP	Time (min)	LP/ RP	Time (min)	LP/ RP	Time (min)	LP/ RP	Time (min)	LP/ RP	Time (min)	LP/ RP	Time (min)	LP/ RP	Time (min)	LP/ RP	Time (min)	LP/ RP
0	0.00	0	0.00	0	0.00	0	0.00	0	0.00	0	0.00	0	0.00	0	0.00	0	0.00
15	4.45	15	5.20	15	3.65	15	4.45	15	4.30	15	2.55	15	3.14	15	3.50	15	3.90
30	7.64	30	6.10	30	4.75	30	5.37	30	5.00	30	4.80	30	4.85	30	4.45	30	4.60
60	9.50	60	6.80	60	5.60	60	6.10	60	5.45	60	5.60	60	5.32	60	5.22	60	5.10
90	10.40	90	7.18	90	6.09	90	6.66	90	5.78	90	5.87	90	5.60	90	5.55	90	5.40
120	11.00	120	7.50	120	6.50	120	7.06	120	6.00	120	6.05	120	5.82	120	5.80	120	5.66
150	11.55	150	7.72	150	6.82	150	7.37	150	6.19	150	6.20	150	5.99	150	5.95	150	5.84
180	11.90	180	7.90	180	7.10	180	7.65	180	6.33	180	6.30	180	6.08	180	6.05	180	6.04
210	12.15	210	8.10	210	7.30	210	7.83	210	6.48	210	6.40	210	6.23	210	6.18	210	6.20
240	12.35	240	8.20	240	7.50	240	8.00	240	6.56	240	6.50	240	6.35	240	6.31	240	6.34
270	12.46	270	8.28	270	7.62	270	8.12	270	6.64	270	6.60	270	6.44	270	6.42	270	6.45
300	12.54	300	8.35	300	7.70	300	8.18	300	6.72	300	6.65	300	6.53	300	6.51	300	6.52
360	12.75	360	8.45	360	7.79	360	8.26	360	6.79	360	6.80	360	6.66	360	6.63	360	6.66
420	12.94	420	8.51	420	7.83	420	8.30	420	6.84	420	6.87	420	6.75	390	6.70	420	6.72
480	13.00	480	8.55	480	7.86	480	8.34	480	6.88	480	6.92	480	6.81	480	6.76	480	6.78
540	13.03	540	8.57	540	7.89	540	8.37	540	6.92	540	6.96	540	6.85	540	6.82	540	6.82
600	13.05	600	8.59	600	7.92	600	8.40	600	6.95	600	6.98	600	6.86	600	6.85	600	6.85

Two piers placed at constant radial distance but varied angles of attack α										
α=0°			α=15°			α=30°			α=45°		
time (min)	FP	RP	time (min)	FP	RP	time (min)	FP	RP	time (min)	FP	RP
0	0.00	0.00	0	0.00	0.00	0	0.00	0.00	0	0.00	0.00
15	4.27	3.27	15	1.83	1.87	15	4.38	4.67	15	4.40	4.60
30	5.05	3.75	30	3.40	3.30	30	4.95	5.30	30	4.70	5.00
60	5.58	4.00	60	4.68	4.60	60	5.34	5.63	60	5.35	5.75
90	5.87	4.56	90	5.31	5.37	90	5.50	5.80	90	5.73	6.22
120	6.02	4.98	120	5.67	5.68	120	5.64	5.93	120	6.05	6.60
150	6.21	5.30	150	5.88	5.90	150	5.74	6.06	150	6.35	6.96
180	6.36	5.50	180	6.04	6.08	180	5.84	6.15	180	6.64	7.25
210	6.50	5.70	210	6.17	6.2	210	5.95	6.26	210	6.82	7.51
240	6.64	5.80	240	6.30	6.32	240	6.07	6.36	240	6.95	7.73
270	6.69	5.90	270	6.42	6.45	270	6.12	6.42	270	7.06	7.90
300	6.78	6.05	300	6.52	6.55	300	6.25	6.51	300	7.10	8.09
360	6.91	6.25	360	6.65	6.68	360	6.40	6.63	360	7.20	8.27
420	6.95	6.35	420	6.74	6.77	420	6.53	6.75	420	7.23	8.37
480	6.97	6.36	480	6.80	6.81	480	6.64	6.82	480	7.25	8.40
540	6.98	6.38	540	6.82	6.84	540	6.78	6.87	540	7.28	8.43
600	7.00	6.40	600	6.86	6.88	600	6.82	6.90	600	7.30	8.45

α=60°			α=75°			α=90°		
time (min)	FP	RP	time (min)	FP	RP	time (min)	FP	RP
0	0.00	0.00	0	0	0	0	0	0
30	2.60	2.65	15	3.30	3.33	15	4.50	4.50
30	4.60	5.00	30	5.17	5.47	30	5.00	5.05
60	5.25	5.75	60	5.70	6.00	60	5.36	5.38
90	5.54	6.10	90	5.72	6.03	90	5.65	5.66
120	5.75	6.30	120	5.75	6.10	120	5.83	5.84
150	5.85	6.40	150	5.87	6.15	150	5.96	5.98
180	5.98	6.70	180	6.12	6.40	180	6.10	6.11
210	6.14	7.00	210	6.38	6.70	210	6.28	6.30
240	6.28	7.18	240	6.56	6.87	240	6.38	6.40
270	6.45	7.45	270	6.68	7.08	270	6.54	6.55
300	6.57	7.65	300	6.78	7.20	300	6.62	6.63
360	6.72	7.88	360	6.87	7.36	360	6.80	6.80
420	6.86	8.04	420	7.03	7.53	420	6.89	6.90
480	6.90	8.10	480	7.18	7.62	480	6.98	6.99
540	6.93	8.13	540	7.28	7.72	540	7.02	7.04
600	6.95	8.15	600	7.32	7.77	600	7.04	7.06

Two piers placed at constant angle of attack but varied radial pier spacings *R/b*											
$\frac{R}{b}=0$			$\frac{R}{b}=1$			$\frac{R}{b}=2$			$\frac{R}{b}=3$		
time (min)	FP	RP	time (min)	FP	RP	time (min)	FP	RP	time (min)	FP	RP
0	0.00	0.00	0	0.00	0.00	0	0.00	0.00	0	0.00	0.00
15	4.30	3.50	15	4.60	5.10	15	3.85	4.35	15	3.00	3.45
30	7.15	6.40	30	5.65	6.03	30	4.93	5.20	30	4.50	5
45	8.00	7.55	45	6.04	6.45	45	5.30	5.58	45	5.17	5.72
60	8.53	8.10	60	6.33	6.73	60	5.65	5.90	60	5.60	6.2
90	9.25	8.90	90	6.85	7.20	90	6.07	6.35	90	6.14	6.75
120	9.73	9.40	120	7.18	7.60	120	6.43	6.70	120	6.55	7.15
150	10.10	9.80	150	7.45	7.85	150	6.68	7.00	150	6.80	7.45
180	10.40	10.10	180	7.72	8.08	180	6.86	7.19	180	7.05	7.7
210	10.60	10.35	210	7.93	8.27	210	7.00	7.35	210	7.20	7.89
240	10.88	10.56	240	8.09	8.50	240	7.13	7.51	240	7.40	8.09
270	11.10	10.82	270	8.30	8.70	270	7.25	7.68	270	7.50	8.21
300	11.32	11.00	300	8.49	8.83	300	7.36	7.85	300	7.65	8.38
360	11.65	11.35	360	8.80	9.13	360	7.50	8.19	360	7.86	8.7
420	11.87	11.60	420	8.93	9.27	420	7.62	8.45	420	8.00	8.85
480	11.98	11.70	480	8.97	9.35	495	7.73	8.65	480	8.08	8.95
540	12.00	11.72	540	8.99	9.37	540	7.75	8.67	540	8.10	8.97
600	12.02	11.73	600	9.00	9.38	600	7.77	8.68	600	8.12	8.98

$\frac{R}{b}=4$			$\frac{R}{b}=5$			$\frac{R}{b}=6$			$\frac{R}{b}=7$		
time (min)	FP	RP	time (min)	FP	RP	time (min)	FP	RP	time (min)	FP	RP
0	0.00	0.00	0	0.00	0.00	0	0.00	0.00	0	0.00	0.00
15	3.70	4.3	15	3.90	4.60	15	3.90	4.50	15	3.20	3.55
30	4.75	5.0	30	5.23	5.70	30	4.90	5.42	30	4.82	5.25
45	5.10	5.70	45	5.70	6.10	45	5.25	5.72	45	5.47	5.85
60	5.25	5.85	60	5.90	6.35	60	5.43	5.90	60	5.75	6.15
90	5.57	6.20	90	6.27	6.74	90	5.75	6.30	90	6.10	6.55
120	5.75	6.40	120	6.54	7.00	120	5.88	6.50	120	6.38	6.8
150	5.84	6.60	150	6.75	7.20	150	6.10	6.75	150	6.57	7.00
180	6.05	6.77	180	6.90	7.38	180	6.24	6.87	180	6.70	7.20
210	6.15	6.93	210	7.05	7.50	210	6.36	7.00	210	6.86	7.35
240	6.28	7.10	240	7.20	7.70	240	6.51	7.13	240	6.95	7.47
270	6.45	7.25	270	7.30	7.82	270	6.6	7.25	270	7.10	7.59
300	6.57	7.35	300	7.32	7.852	300	6.68	7.35	300	7.15	7.68
360	6.80	7.70	360	7.50	8.00	360	6.83	7.53	360	7.25	7.85
420	7.00	7.90	420	7.60	8.13	420	6.90	7.60	420	7.40	7.94
480	7.14	8.10	480	7.65	8.17	480	7.00	7.70	480	7.47	8.03
540	7.34	8.30	540	7.67	8.26	540	7.07	7.77	540	7.49	8.05
600	7.40	8.35	600	7.68	8.27	600	7.08	7.78	600	7.50	8.06

$\frac{R}{b}$=8			$\frac{R}{b}$=9			$\frac{R}{b}$=10			$\frac{R}{b}$=11			$\frac{R}{b}$=12		
time (min)	FP	RP	time (min)	FP	RP	time (min)	FP	RP	time (min)	FP	RP	time (min)	FP	RP
0	0.00	0.00	0	0.00	0.00	0	0.00	0.00	0	0.00	0.00	0	0.00	0.00
15	4.20	4.60	15	3.10	3.40	15	4.20	4.50	15	4.60	4.60	15	4.30	4.30
30	5.00	5.40	30	4.90	5.30	30	5.00	5.25	30	5.32	5.34	30	5.24	5.25
45	5.35	5.70	45	5.55	5.90	45	5.20	5.50	45	5.63	5.64	45	5.62	5.64
60	5.50	5.90	60	5.90	6.30	60	5.43	5.72	60	5.75	5.75	60	5.80	5.82
90	5.80	6.20	90	6.20	6.70	90	5.68	5.95	90	6.04	6.05	90	6.05	6.10
120	6.02	6.40	120	6.40	6.90	120	5.88	6.16	120	6.18	6.21	120	6.28	6.29
150	6.20	6.60	150	6.55	7.05	150	6.08	6.35	150	6.32	6.34	150	6.42	6.44
180	6.35	6.80	180	6.64	7.14	180	6.25	6.52	180	6.43	6.45	180	6.56	6.58
210	6.52	6.92	210	6.75	7.25	210	6.38	6.68	210	6.55	6.57	210	6.70	6.72
240	6.58	7.00	240	6.82	7.32	240	6.52	6.75	240	6.65	6.70	240	6.81	6.83
270	6.70	7.12	270	6.90	7.42	270	6.70	6.90	270	6.76	6.78	270	6.90	6.90
300	6.80	7.28	300	6.92	7.44	300	6.75	7.00	300	6.80	6.80	300	7.00	7.01
360	6.97	7.47	360	7.12	7.6	360	6.85	7.12	360	6.90	6.95	360	7.06	7.08
420	7.18	7.67	420	7.20	7.70	420	7.05	7.24	420	7.03	7.03	420	7.10	7.10
480	7.35	7.80	480	7.22	7.73	480	7.15	7.40	480	7.10	7.10	480	7.12	7.12
540	7.42	7.87	540	7.24	7.75	540	7.17	7.42	540	7.12	7.12	540	7.14	7.14
600	7.43	7.88	600	7.25	7.76	600	7.19	7.43	600	7.14	7.14	600	7.16	7.16

Three piers placed in staggered arrangement at varied longitudinal pier spacings X_c/b																	
$\frac{X_c}{b}=5$			$\frac{X_c}{b}=10$			$\frac{X_c}{b}=15$			$\frac{X_c}{b}=20$			$\frac{X_c}{b}=25$			$\frac{X_c}{b}=30$		
Time (min)	U/S Piers	D/S Pier	Time (min)	U/S Piers	D/S Pier	Time (min)	U/S Piers	D/S Pier	Time (min)	U/S Piers	D/S Pier	Time (min)	U/S Piers	D/S Pier	Time (min)	U/S Piers	D/S Pier
0	0.00	0	0.00	0	0.00	0	0.00	0	0.00	0	0.00	0	0.00	0	0.00	0	0.00
15	4.45	15	5.20	15	3.65	15	4.45	15	4.30	15	2.55	15	3.14	15	3.50	15	3.90
30	7.64	30	6.10	30	4.75	30	5.37	30	5.00	30	4.80	30	4.85	30	4.45	30	4.60
60	9.50	60	6.80	60	5.60	60	6.10	60	5.45	60	5.60	60	5.32	60	5.22	60	5.10
90	10.40	90	7.18	90	6.09	90	6.66	90	5.78	90	5.87	90	5.60	90	5.55	90	5.40
120	11.00	120	7.50	120	6.50	120	7.06	120	6.00	120	6.05	120	5.82	120	5.80	120	5.66
150	11.55	150	7.72	150	6.82	150	7.37	150	6.19	150	6.20	150	5.99	150	5.95	150	5.84
180	11.90	180	7.90	180	7.10	180	7.65	180	6.33	180	6.30	180	6.08	180	6.05	180	6.04
210	12.15	210	8.10	210	7.30	210	7.83	210	6.48	210	6.40	210	6.23	210	6.18	210	6.20
240	12.35	240	8.20	240	7.50	240	8.00	240	6.56	240	6.50	240	6.35	240	6.31	240	6.34
270	12.46	270	8.28	270	7.62	270	8.12	270	6.64	270	6.60	270	6.44	270	6.42	270	6.45
300	12.54	300	8.35	300	7.70	300	8.18	300	6.72	300	6.65	300	6.53	300	6.51	300	6.52
360	12.75	360	8.45	360	7.79	360	8.26	360	6.79	360	6.80	360	6.66	360	6.63	360	6.66
420	12.94	420	8.51	420	7.83	420	8.30	420	6.84	420	6.87	420	6.75	390	6.70	420	6.72
480	13.00	480	8.55	480	7.86	480	8.34	480	6.88	480	6.92	480	6.81	480	6.76	480	6.78
540	13.03	540	8.57	540	7.89	540	8.37	540	6.92	540	6.96	540	6.85	540	6.82	540	6.82
600	13.05	600	8.59	600	7.92	600	8.40	600	6.95	600	6.98	600	6.86	600	6.85	600	6.85

$\frac{X_c}{b}=40$			$\frac{X_c}{b}=50$			$\frac{X_c}{b}=60$			$\frac{X_c}{b}=70$			$\frac{X_c}{b}=80$			$\frac{X_c}{b}=90$		
Time (min)	U/S Piers	D/S Pier	Time (min)	U/S Piers	D/S Pier	Time (min)	U/S Piers	D/S Pier	Time (min)	U/S Piers	D/S Pier	Time (min)	U/S Piers	D/S Pier	Time (min)	U/S Piers	D/S Pier
0	0.00	0.00	0	0.00	0.00	0	0.00	0.00	0	0.00	0.00	0	0.00	0.00	0	0.00	0.00
15	4.10	4.7	15	3.50	3.7	15	4.35	4.75	15	3.55	3.50	15	4.40	4.55	15	4.00	4.00
30	4.85	5.45	30	5.15	5.58	30	5.06	5.32	30	4.90	4.95	30	5.18	5.20	30	5.15	5.15
45	5.07	5.72	45	5.63	5.99	45	5.26	5.55	45	5.26	5.30	45	5.38	5.42	50	5.45	5.50
60	5.23	5.9	60	5.82	6.17	60	5.43	5.70	60	5.50	5.55	60	5.57	5.60	60	5.55	5.55
90	5.48	6.18	90	6.00	6.35	90	5.64	5.91	90	5.75	5.80	90	5.77	5.80	90	5.80	5.80
120	5.70	6.35	120	6.12	6.47	120	5.80	6.05	120	5.92	5.97	120	5.90	5.93	120	5.95	5.95
150	5.85	6.52	150	6.23	6.55	150	5.90	6.18	150	6.04	6.10	150	6.03	6.05	150	6.10	6.10
180	6.00	6.62	180	6.33	6.6	180	6.05	6.30	180	6.15	6.20	180	6.19	6.20	180	6.18	6.18
210	6.10	6.63	210	6.40	6.68	210	6.17	6.38	210	6.23	6.26	210	6.30	6.32	210	6.25	6.28
240	6.20	6.45	240	6.50	6.71	240	6.28	6.50	240	6.30	6.34	240	6.38	6.43	240	6.35	6.37
270	6.30	5.85	270	6.54	6.75	270	6.35	6.55	270	6.40	6.38	270	6.50	6.55	270	6.43	6.45
300	6.36	5.45	300	6.62	6.8	300	6.45	6.58	300	6.46	6.50	300	6.55	6.60	300	6.52	6.53
360	6.55	5.7	360	6.70	6.85	360	6.55	6.67	360	6.60	6.65	360	6.72	6.75	360	6.65	6.65
420	6.65	5.85	420	6.76	6.9	420	6.64	6.75	420	6.77	6.82	420	6.80	6.85	420	6.77	6.76
480	6.70	5.9	480	6.80	6.94	480	6.72	6.80	480	6.85	6.86	480	6.85	6.88	480	6.83	6.82
540	6.80	6	540	6.83	6.97	540	6.78	6.84	540	6.87	6.89	540	6.87	6.90	540	6.86	6.86
600	6.85	6.1	600	6.86	6.98	600	6.85	6.88	600	6.89	6.92	600	6.89	6.92	600	6.89	6.89

Two piers placed at fixed spacing without collar and varied angles of attack α										
α=0°			α=15°			α=30°			α=45°		
time (min)	FP	RP	time (min)	FP	RP	time (min)	FP	RP	time (min)	FP	RP
0	0.00	0.00	0	0.00	0.00	0	0.00	0.00	0	0.00	0.00
15	4.25	2.40	15	3.55	3.20	15	4.92	4.10	15	5.03	5.50
30	5.10	3.25	30	4.35	4.15	30	5.70	5.20	30	5.76	6.10
45	5.48	3.62	45	4.39	4.60	45	5.86	5.70	45	5.96	6.30
60	5.72	3.95	60	4.50	5.05	60	6.00	5.90	60	6.15	6.48
90	6.05	4.30	90	5.38	5.58	90	6.50	5.90	90	6.42	6.74
120	6.30	4.50	120	5.87	5.87	120	6.85	6.20	120	6.65	7.00
150	6.50	4.65	150	6.20	6.07	150	7.10	6.50	150	6.85	7.20
180	6.65	4.80	180	6.34	6.13	180	7.25	6.75	180	7.05	7.40
210	6.78	4.95	210	6.55	6.20	210	7.37	6.96	210	7.13	7.60
240	6.85	5.05	240	6.75	6.25	240	7.53	7.16	240	7.20	7.75
270	6.95	5.21	270	6.89	6.32	270	7.60	7.35	270	7.35	7.90
300	7.08	5.35	300	7.00	6.35	300	7.74	7.54	300	7.50	8.10
360	7.28	5.57	360	7.20	6.55	360	7.99	7.82	360	7.64	8.40
420	7.40	5.75	420	7.30	6.70	420	8.24	8.15	420	7.77	8.60
480	7.50	5.85	480	7.35	6.80	480	8.40	8.40	480	7.80	8.70
540	7.64	6.00	540	7.42	6.90	540	8.55	8.70	540	7.90	8.80
600	7.75	6.25	600	7.50	6.98	600	8.65	8.90	600	8.05	8.90
720	8.08	6.48	720	7.65	7.25	720	8.90	9.30	720	8.20	9.20
900	8.60	6.94	900	8.20	8.00	900	9.25	9.80	900	8.75	9.65
1080	9.10	7.37	1080	9.50	9.35	1080	9.70	10.15	1080	9.75	10.30

α=60°			α=75°			α=90°		
time (min)	FP	RP	time (min)	FP	RP	time (min)	FP	RP
0	0.00	0.00	0	0.00	0.00	0	0.00	0.00
15	4.60	5.40	15	5.30	5.15	15	4.76	4.76
30	5.62	6.20	30	6.20	5.90	30	6.16	6.16
45	6.04	6.56	45	6.45	6.20	45	6.61	6.61
60	6.50	6.90	60	6.73	6.43	60	6.83	6.83
90	6.90	7.20	90	7.15	6.85	90	7.11	7.11
120	7.10	7.50	120	7.47	7.17	120	7.28	7.28
150	7.28	7.65	150	7.77	7.45	150	7.39	7.39
180	7.43	7.80	180	8.04	7.70	180	7.50	7.50
210	7.55	7.90	210	8.30	7.90	210	7.61	7.61
240	7.62	8.00	240	8.55	8.13	240	7.67	7.67
270	7.70	8.10	270	8.75	8.30	270	7.73	7.73
300	7.75	8.15	300	8.95	8.50	300	7.80	7.80
360	7.85	8.20	360	9.30	8.80	360	7.95	7.95
420	7.85	8.40	420	9.60	9.10	420	8.00	8.00
480	7.90	8.50	480	9.70	9.25	480	8.10	8.10
540	7.95	8.60	540	9.70	9.25	540	8.28	8.28
600	8.05	8.70	600	9.70	9.25	600	8.40	8.40
720	8.13	8.90	720	9.55	9.40	720	8.68	8.68
900	8.25	9.30	900	9.30	9.60	900	9.10	9.10
1080	8.75	10.15	1080	9.00	10.00	1080	9.60	9.60

Two piers placed at fixed spacing with collar and varied angles of attack α											
α=0°			α=15°			α=30°			α=45°		
Time (min)	FP	RP	Time (min)	FP	RP	Time (min)	FP	RP	Time (min)	FP	RP
0	0.00	0.00	0	0.00	0.00	0	0.00	0.00	0	0.00	0.00
15	1.18	0.32	15	1.20	1.70	15	1.45	1.45	15	1.25	2.10
30	1.90	0.75	30	1.60	2.20	30	1.20	1.95	30	1.40	2.45
45	1.00	1.20	45	1.75	2.01	45	1.13	2.16	45	1.45	2.75
60	0.95	1.35	60	1.85	1.85	60	1.10	2.25	60	1.50	2.85
90	1.10	1.50	90	1.77	2.50	90	1.20	1.85	90	2.00	3.15
120	1.20	1.58	120	1.63	3.25	120	1.20	1.95	120	2.30	3.25
150	1.32	1.55	150	1.65	3.84	150	1.20	2.10	150	2.50	3.40
180	1.44	1.54	180	1.75	4.27	180	1.50	2.48	180	2.60	3.55
210	1.54	1.50	210	1.95	4.60	210	1.60	2.70	210	2.65	3.60
240	1.60	1.45	240	2.20	4.90	240	2.00	2.85	240	2.70	3.65
270	1.73	1.42	270	2.30	5.00	270	2.25	3.05	270	2.75	3.70
300	1.82	1.40	300	2.35	5.15	300	2.35	3.25	300	2.75	3.75
360	1.90	1.37	360	2.43	5.25	360	2.40	3.42	360	2.75	3.78
420	1.90	1.36	420	2.45	5.35	420	2.45	3.60	420	2.75	3.80
480	1.90	1.35	480	2.50	5.35	480	2.45	3.65	480	2.73	3.80
540	1.90	1.35	540	2.50	5.35	540	2.45	3.70	540	2.70	3.80
600	1.90	1.35	600	2.50	5.35	600	2.45	3.70	600	2.70	3.80
720	1.90	1.35	720	2.50	5.35	720	2.45	3.70	720	2.70	3.80
900	1.90	1.35	900	2.50	5.35	900	2.45	3.70	900	2.70	3.80
1080	1.90	1.35	1080	2.50	5.35	1080	2.45	3.70	1080	2.70	3.80

α=60°			α=75°			α=90°		
time (min)	FP	RP	time (min)	FP	RP	time (min)	FP	RP
0	0.00	0.00	0	0.00	0.00	0	0.00	0.00
15	1.25	1.65	15	2.10	2.00	15	1.60	1.60
30	1.75	1.85	20	2.25	2.30	30	2.10	2.10
60	2.35	1.55	30	2.25	2.40	60	2.52	2.52
90	2.60	1.55	60	2.52	2.60	90	2.80	2.80
120	2.75	1.60	90	2.95	3.00	120	3.05	3.05
150	2.80	1.56	120	3.20	3.50	150	3.27	3.27
180	2.97	1.53	150	3.35	3.70	180	3.49	3.49
210	3.10	1.60	180	3.60	3.60	210	3.65	3.65
240	3.20	1.60	210	3.80	3.10	240	3.80	3.80
270	3.28	1.56	240	4.00	2.81	270	4.25	4.25
300	3.35	1.55	270	4.25	2.65	300	4.60	4.60
360	3.65	1.55	300	4.55	2.60	360	5.00	5.00
385	3.70	1.60	360	4.85	2.67	390	5.45	5.45
420	3.80	1.60	420	5.15	2.75	420	5.85	5.85
480	3.80	1.60	480	5.50	2.75	480	6.25	6.25
540	3.80	1.60	540	5.90	2.75	540	6.67	6.67
600	3.80	1.60	600	6.15	2.75	600	7.15	7.15
720	3.80	1.60	720	6.40	2.75	720	7.35	7.35
900	3.80	1.60	900	6.50	2.75	900	7.45	7.45
1080	3.80	1.60	1080	6.55	2.75	1080	7.50	7.50

FP = Front Pier; MP = Middle Pier; RP = Rear Pier

APPENDIX–II

LONGITUDINAL PROFILES OF SCOUR

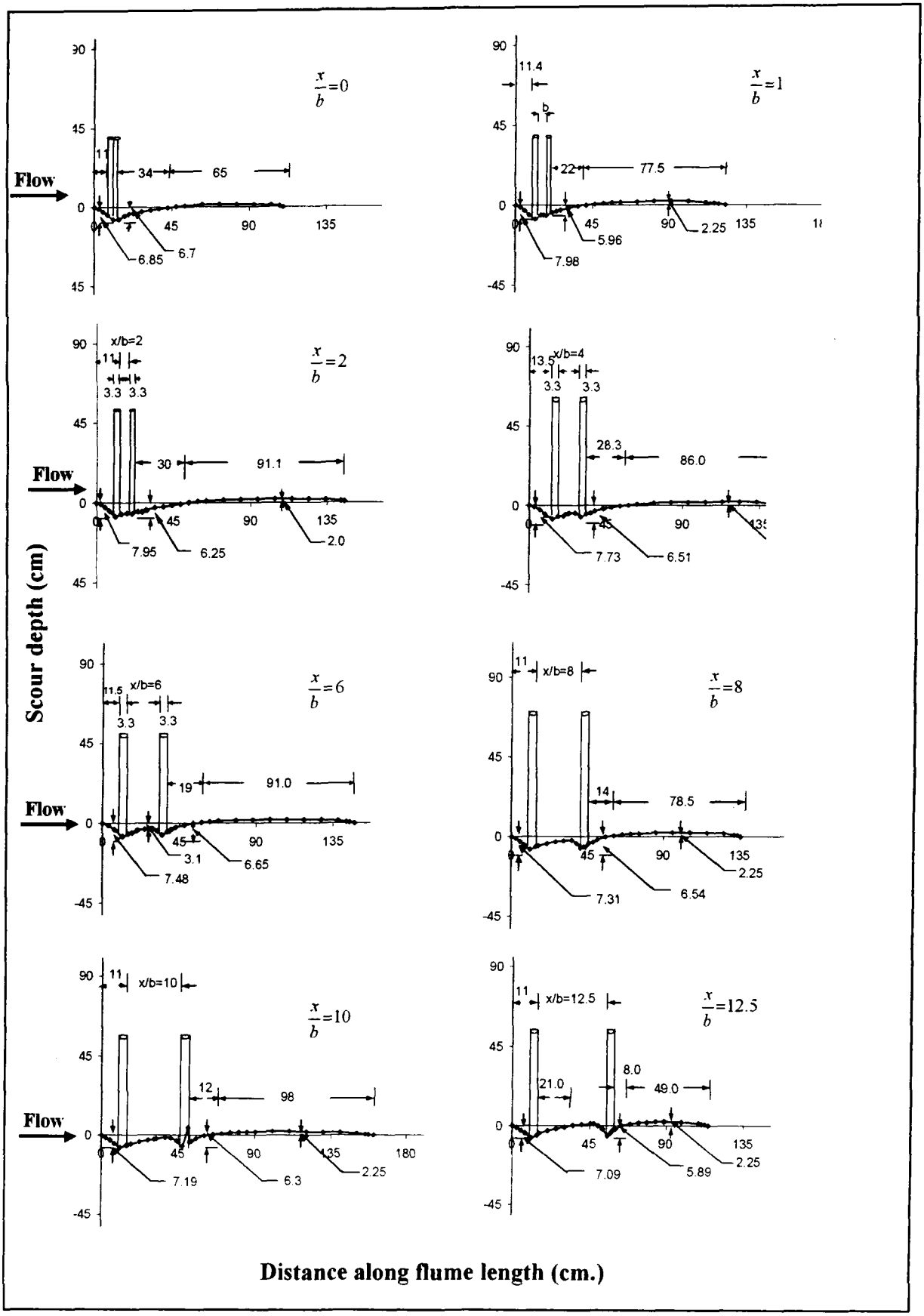

Longitudinal profiles for two piers of same size in tandem arrangement for varied pier spacing x/b.

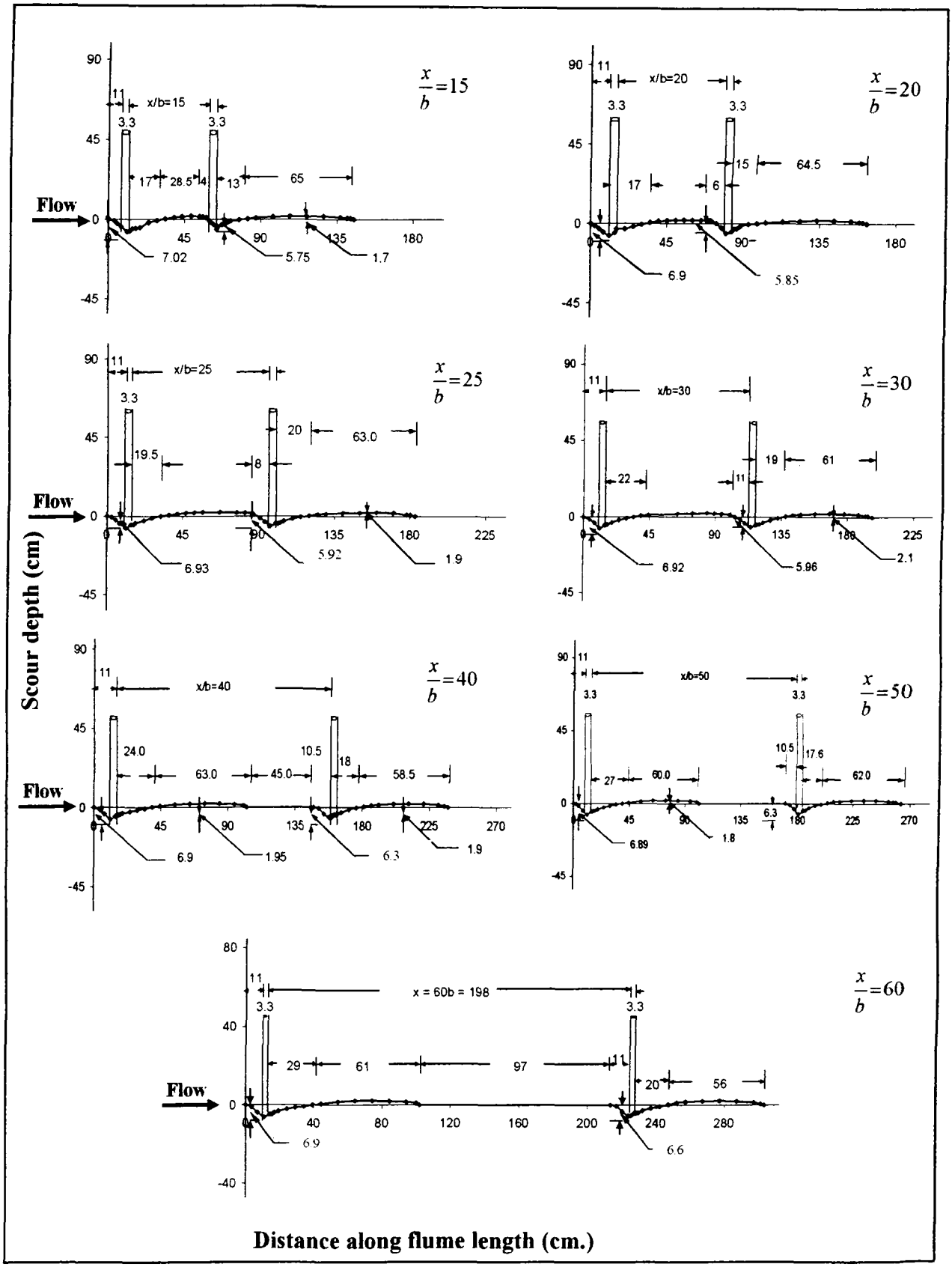

Longitudinal profiles for two piers of same size in tandem arrangement for varied pier spacing x/b.

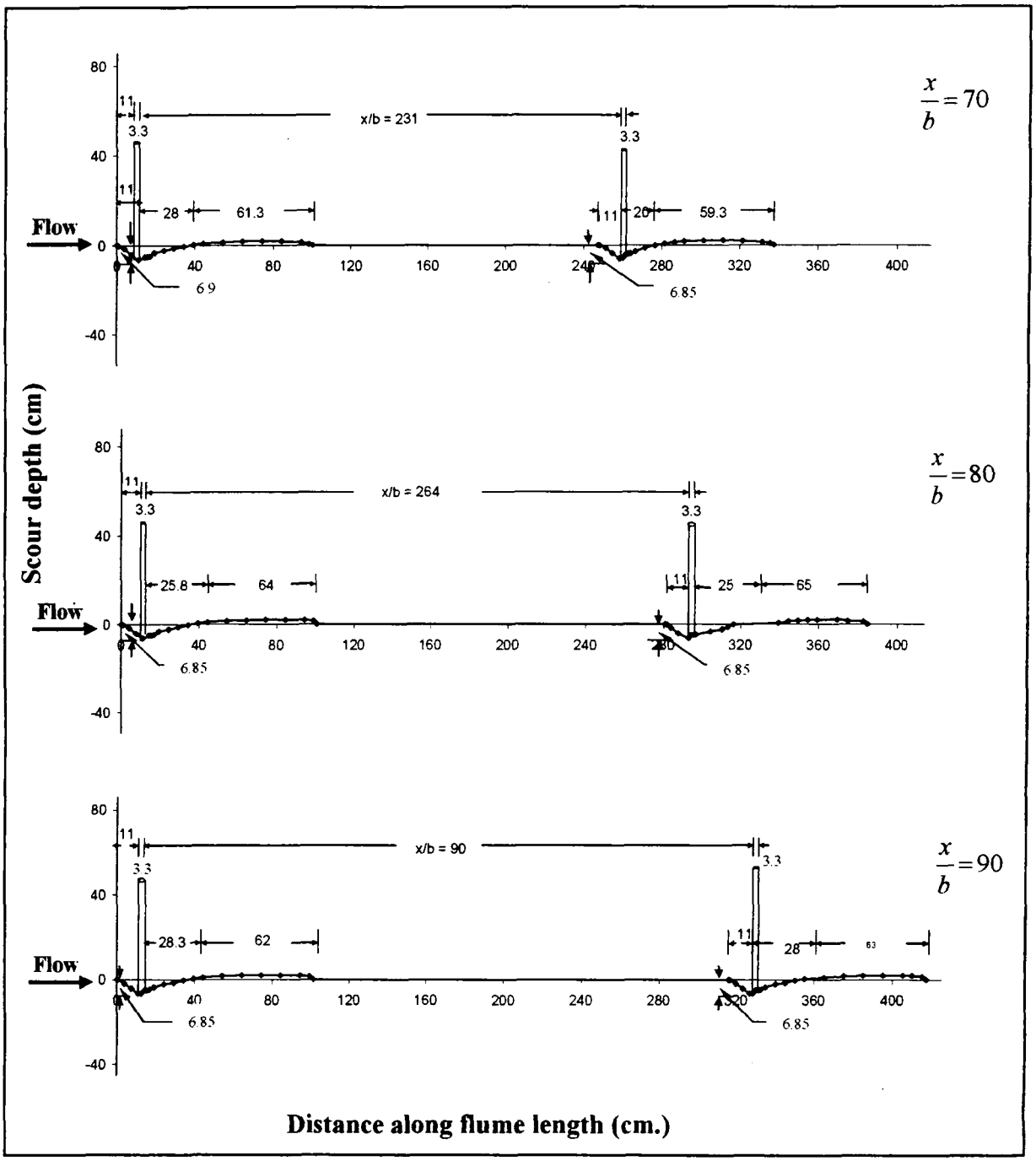

Longitudinal profiles for two piers of same size in tandem arrangement for varied pier spacing x/b.

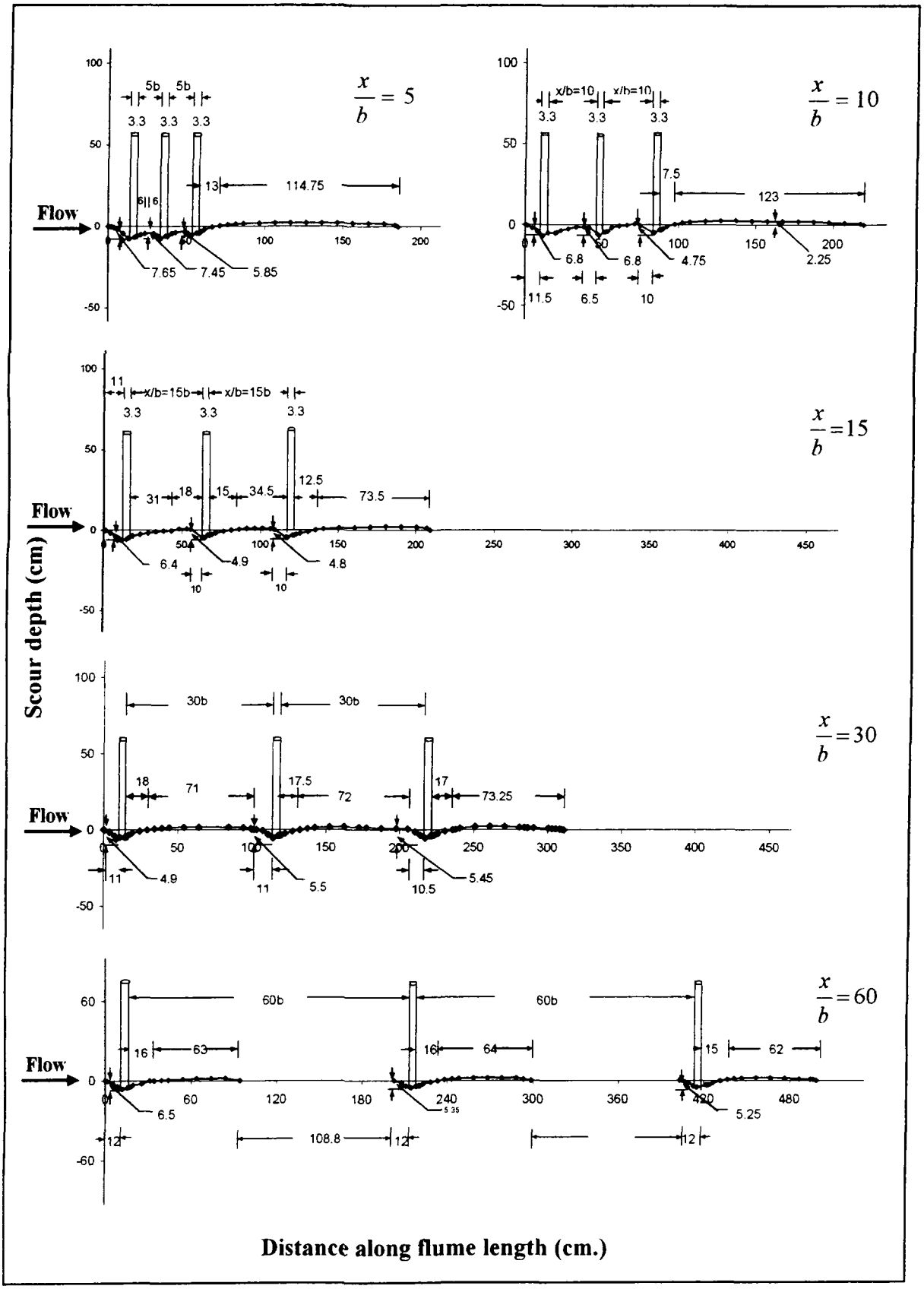

Longitudinal profiles for three piers of same size in tandem arrangement for varied pier spacing x/b.

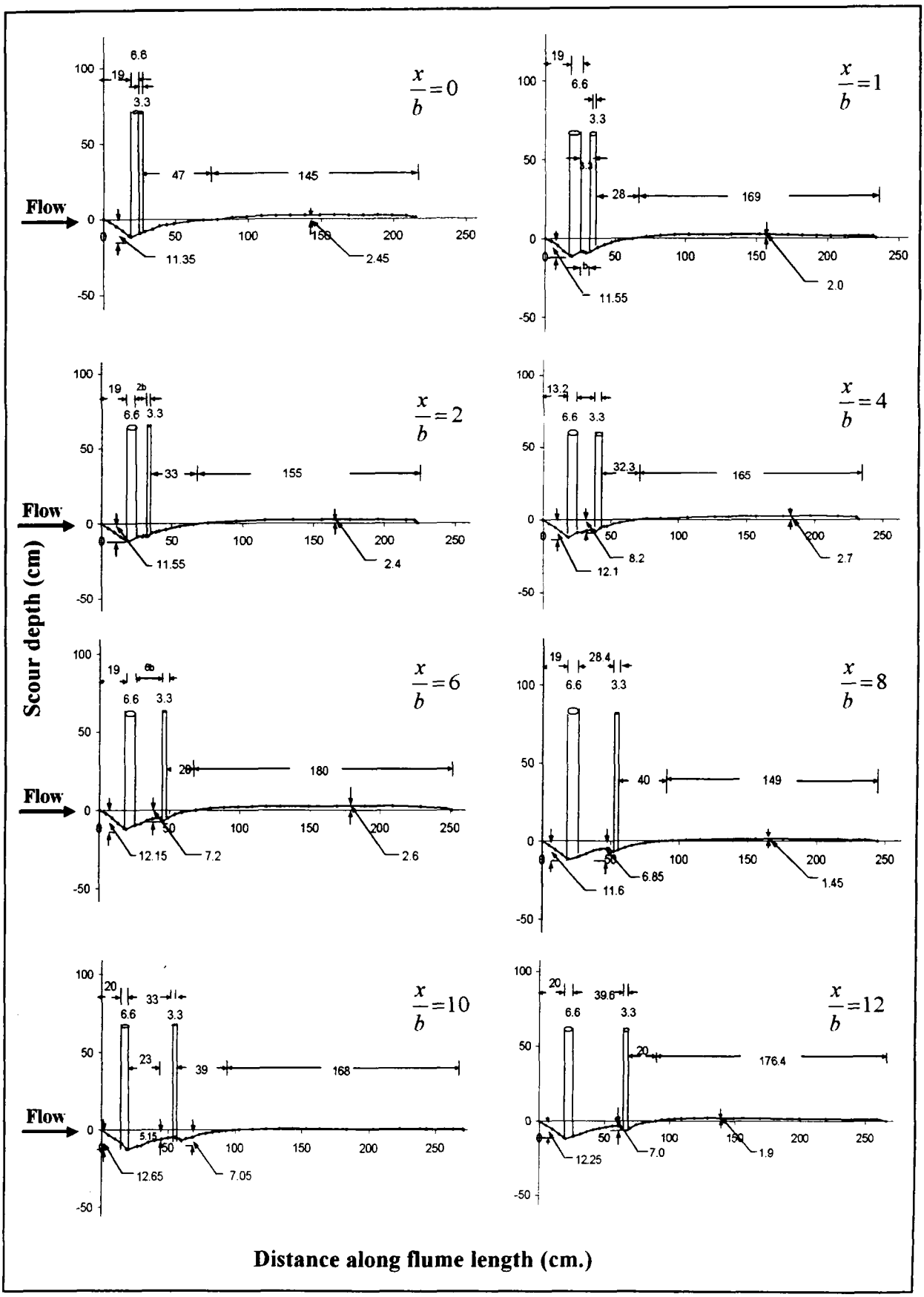

Longitudinal profiles for big pier at front and small pier at rear in tandem arrangement for varied pier spacing x/b.

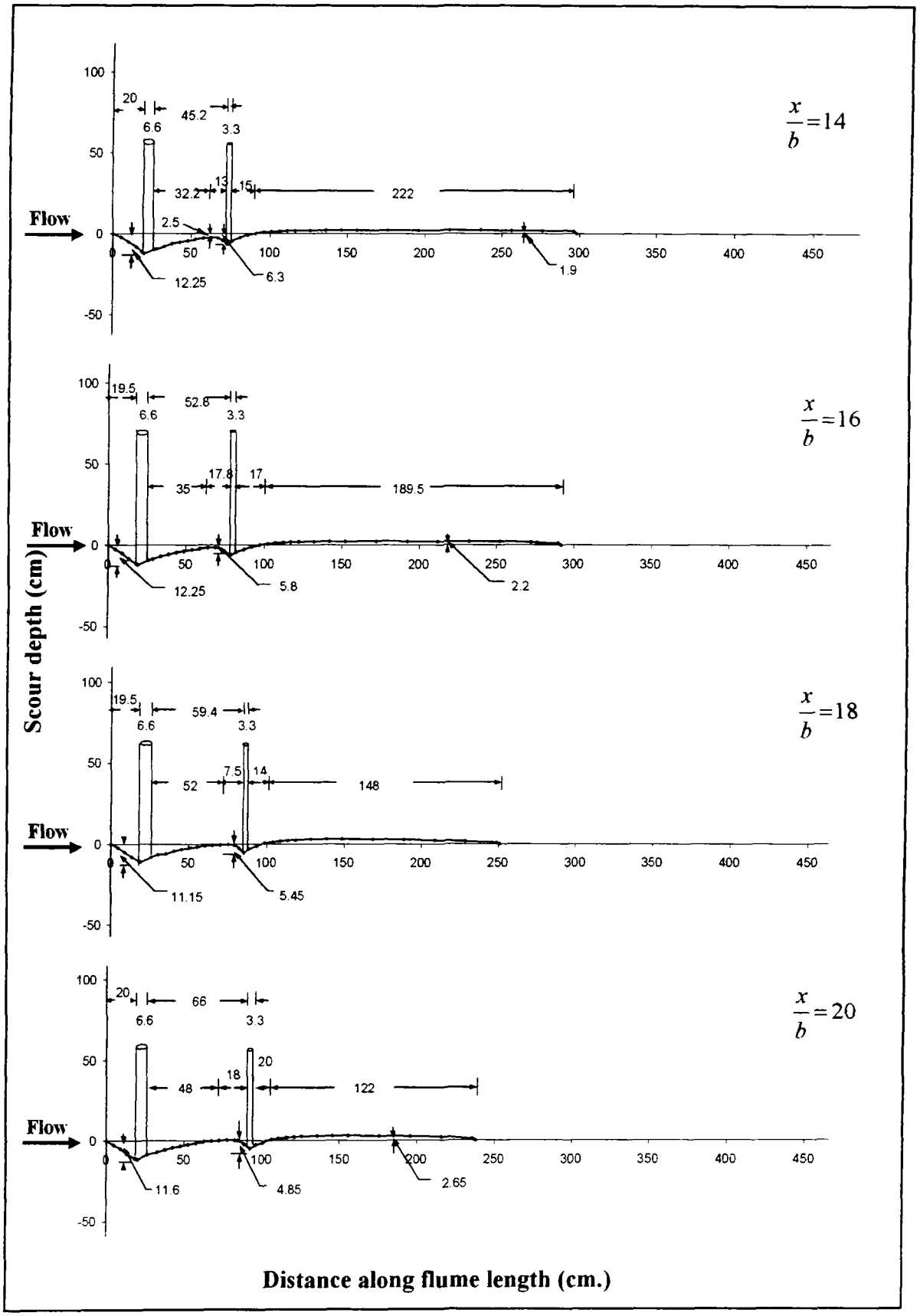

Longitudinal profiles for big pier at front and small pier at rear in tandem arrangement for varied pier spacing x/b.

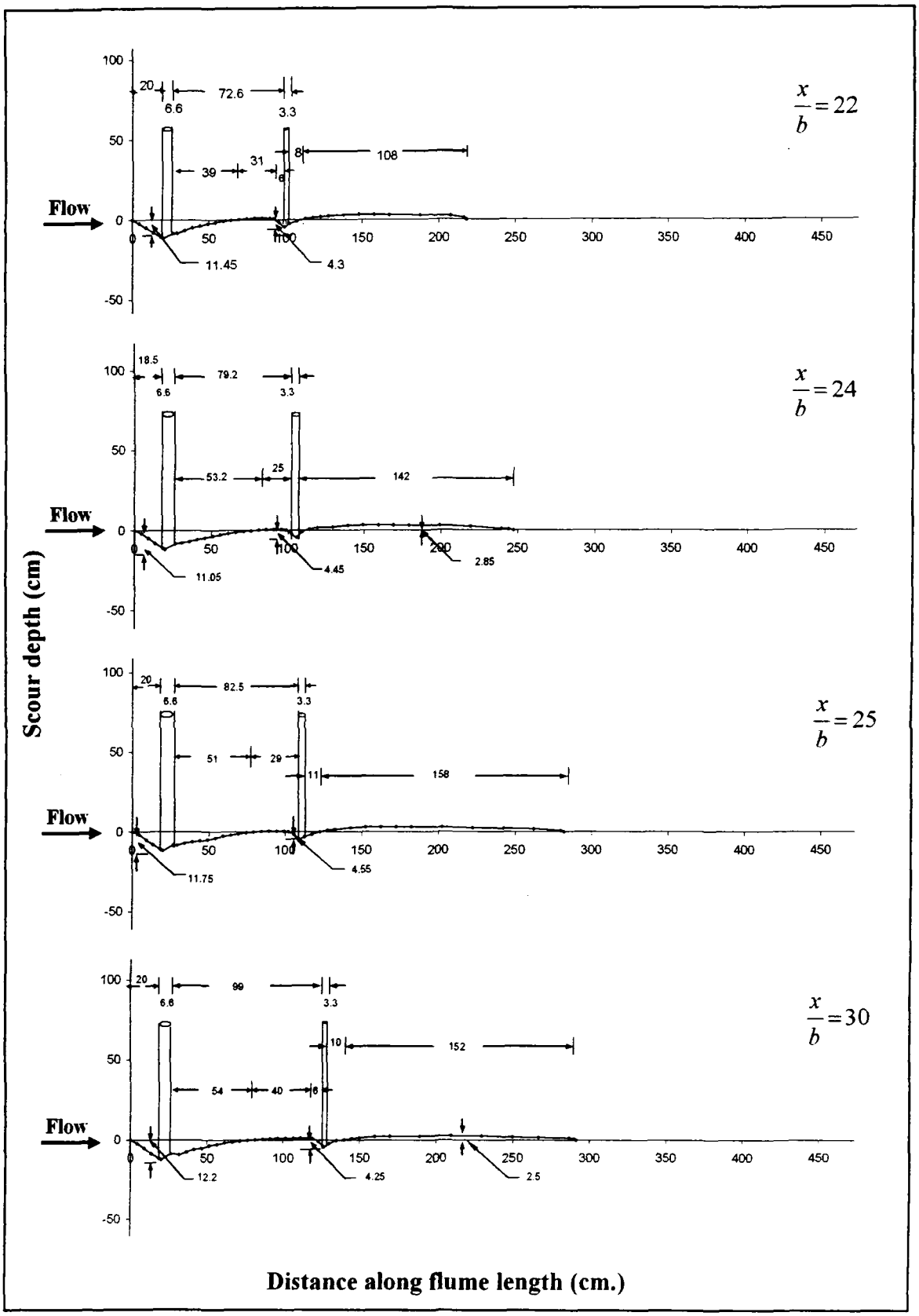

Longitudinal profiles for big pier at front and small pier at rear in tandem arrangement for varied pier spacing x/b.

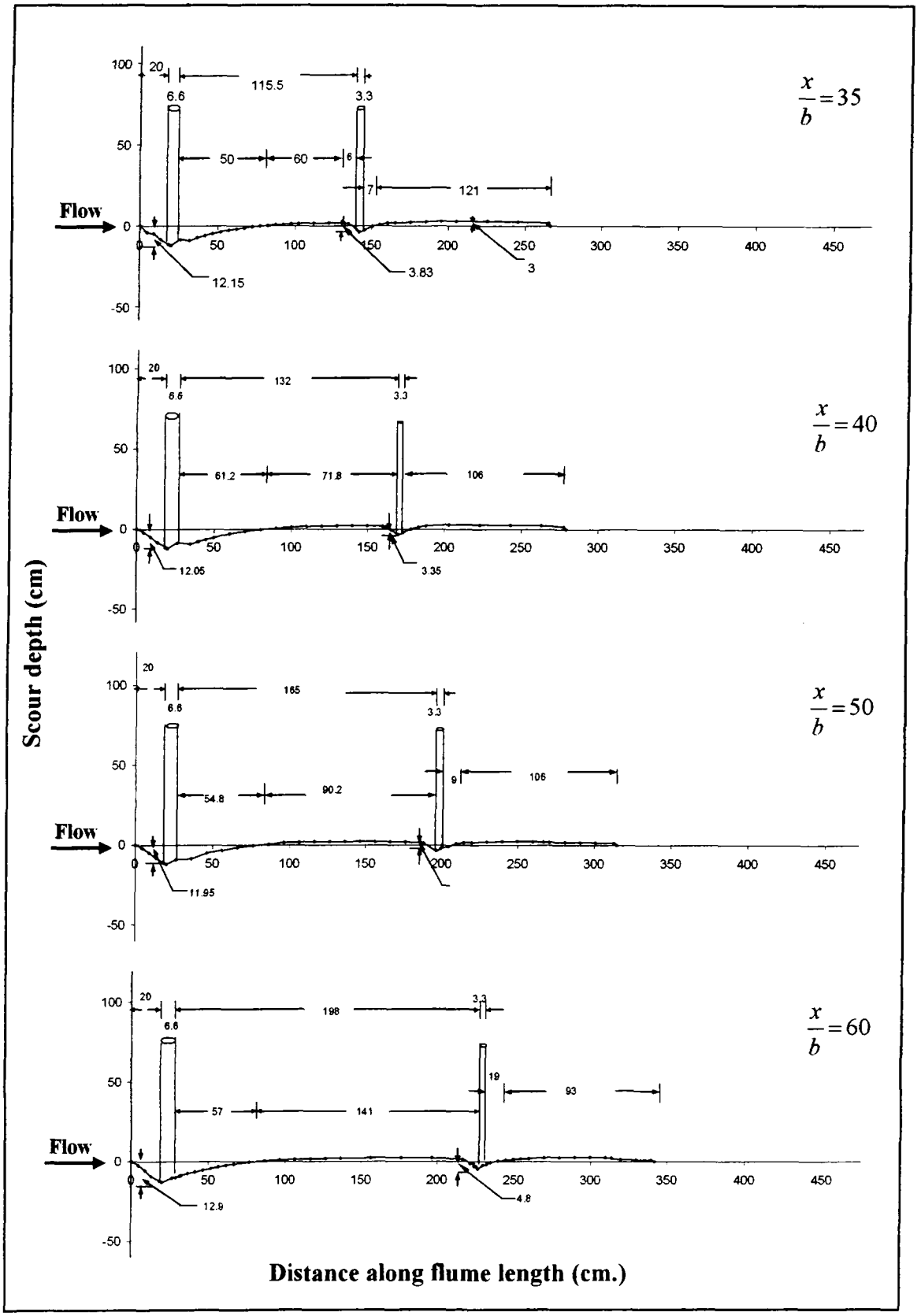

Longitudinal profiles for big pier at front and small pier at rear in tandem arrangement for varied pier spacing x/b.

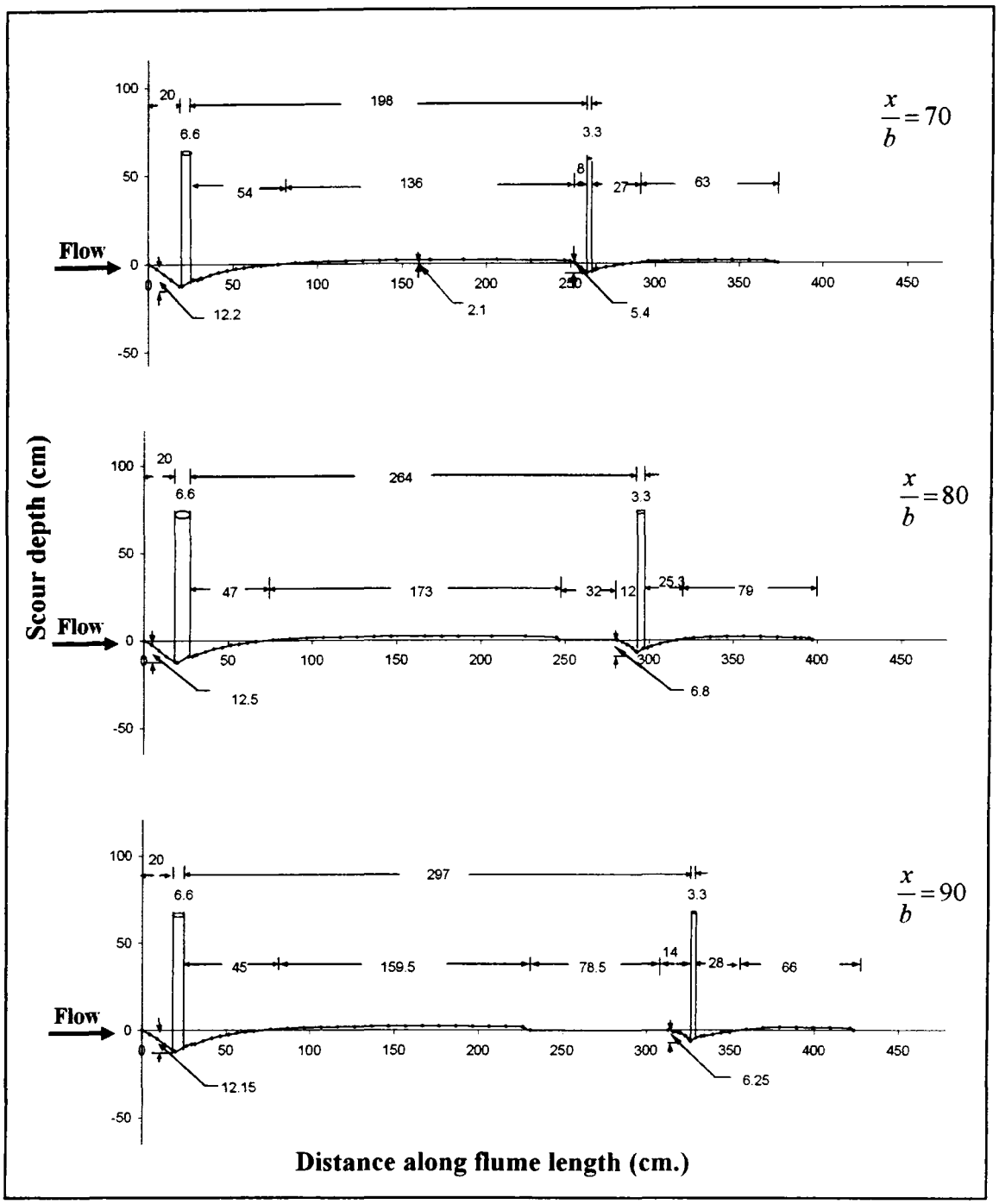

Longitudinal profiles for big pier at front and small pier at rear in tandem arrangement for varied pier spacing x/b.

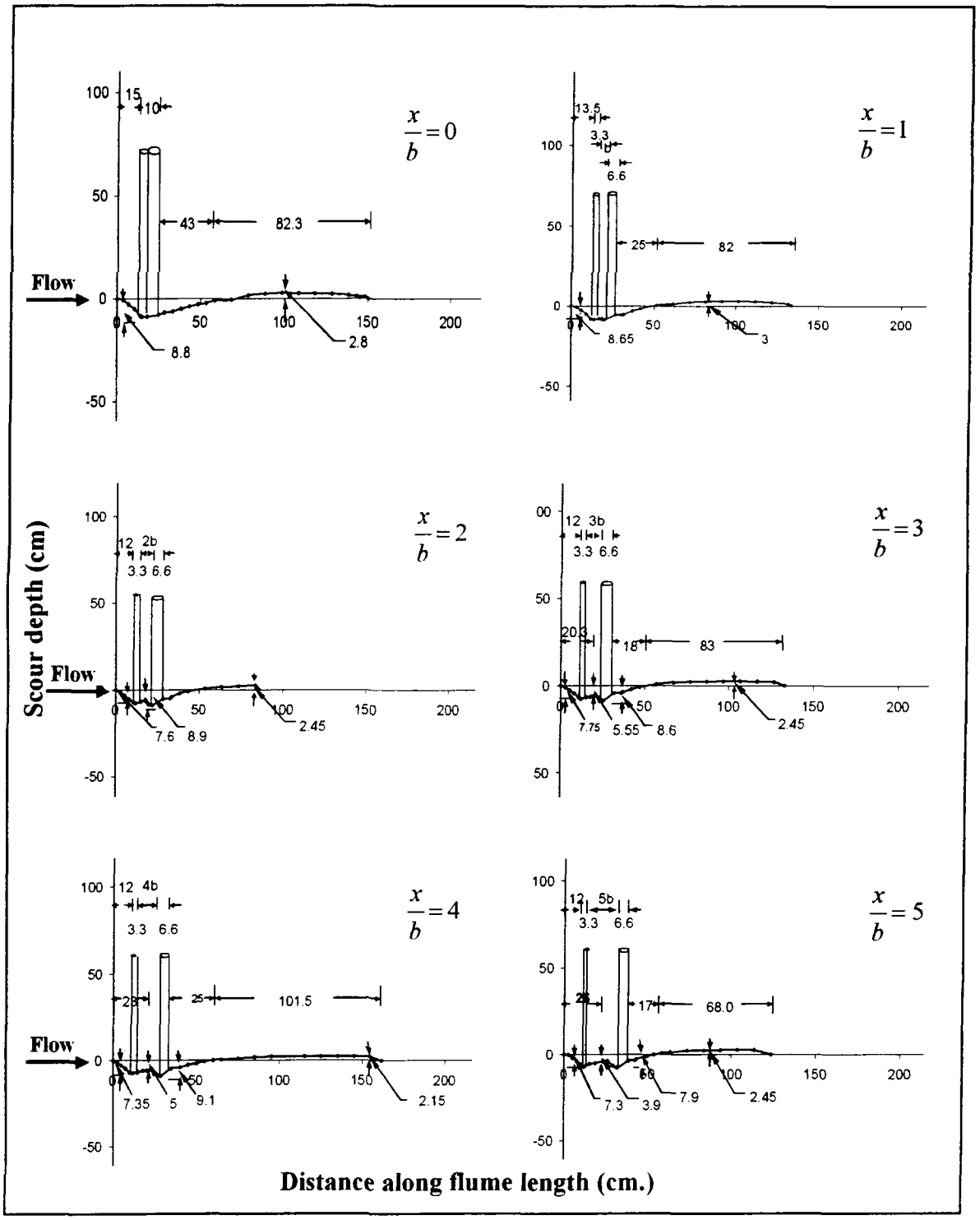

Longitudinal profiles for small pier at front and big pier at rear in tandem arrangement for varied pier spacing x/b.

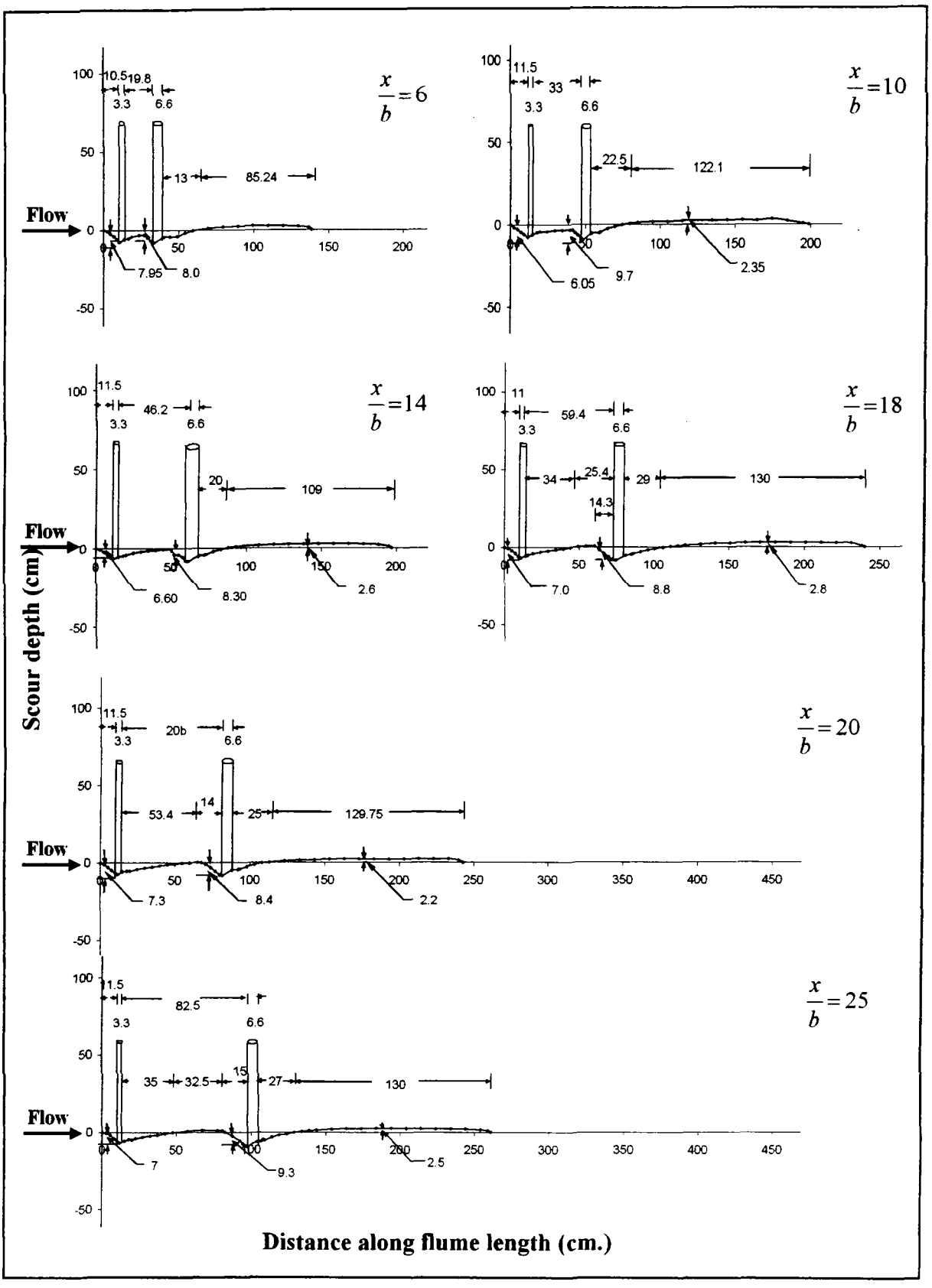

Longitudinal profiles for small pier at front and big pier at rear in tandem arrangement for varied pier spacing x/b.

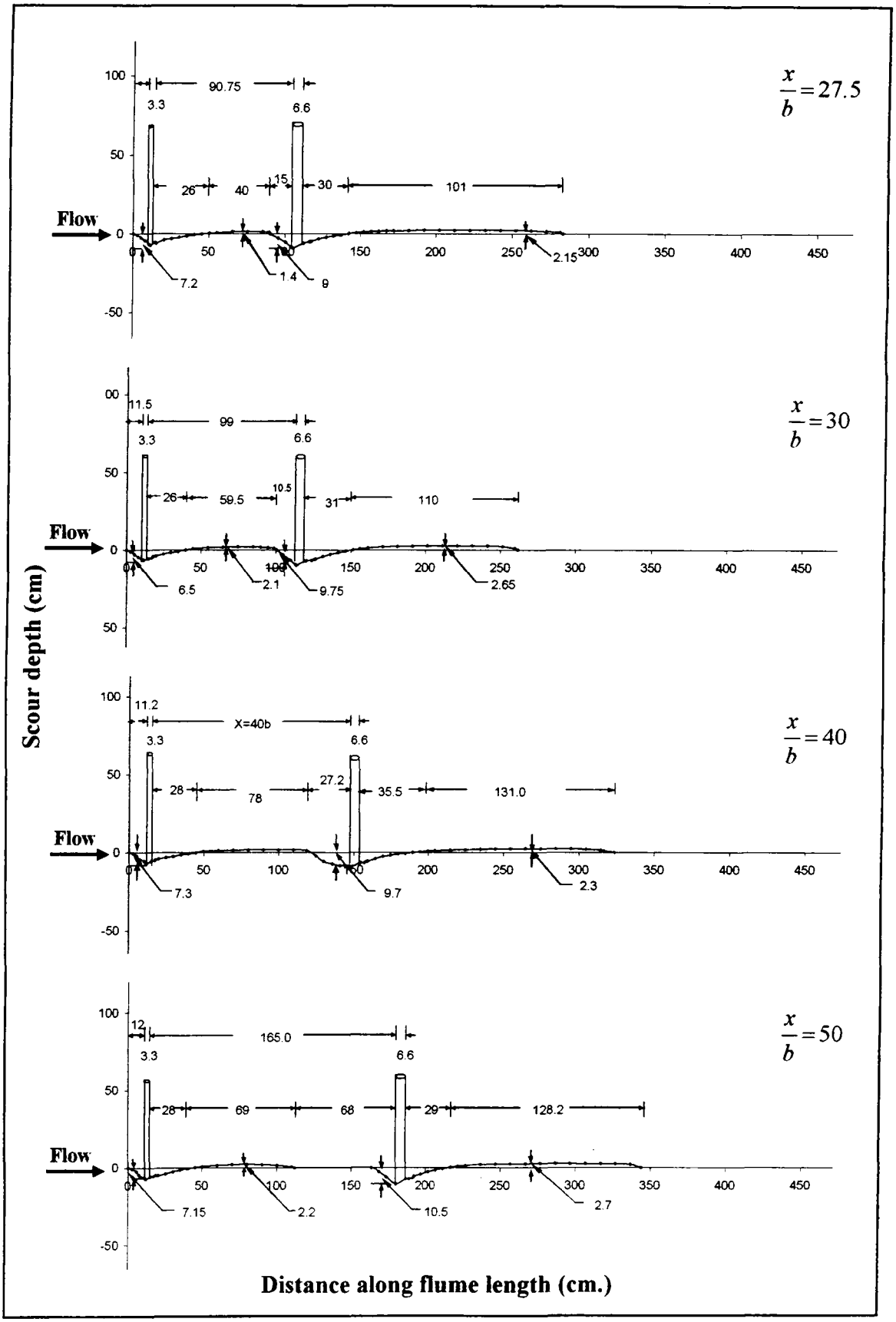

Longitudinal profiles for small pier at front and big pier at rear in tandem arrangement for varied pier spacing x/b.

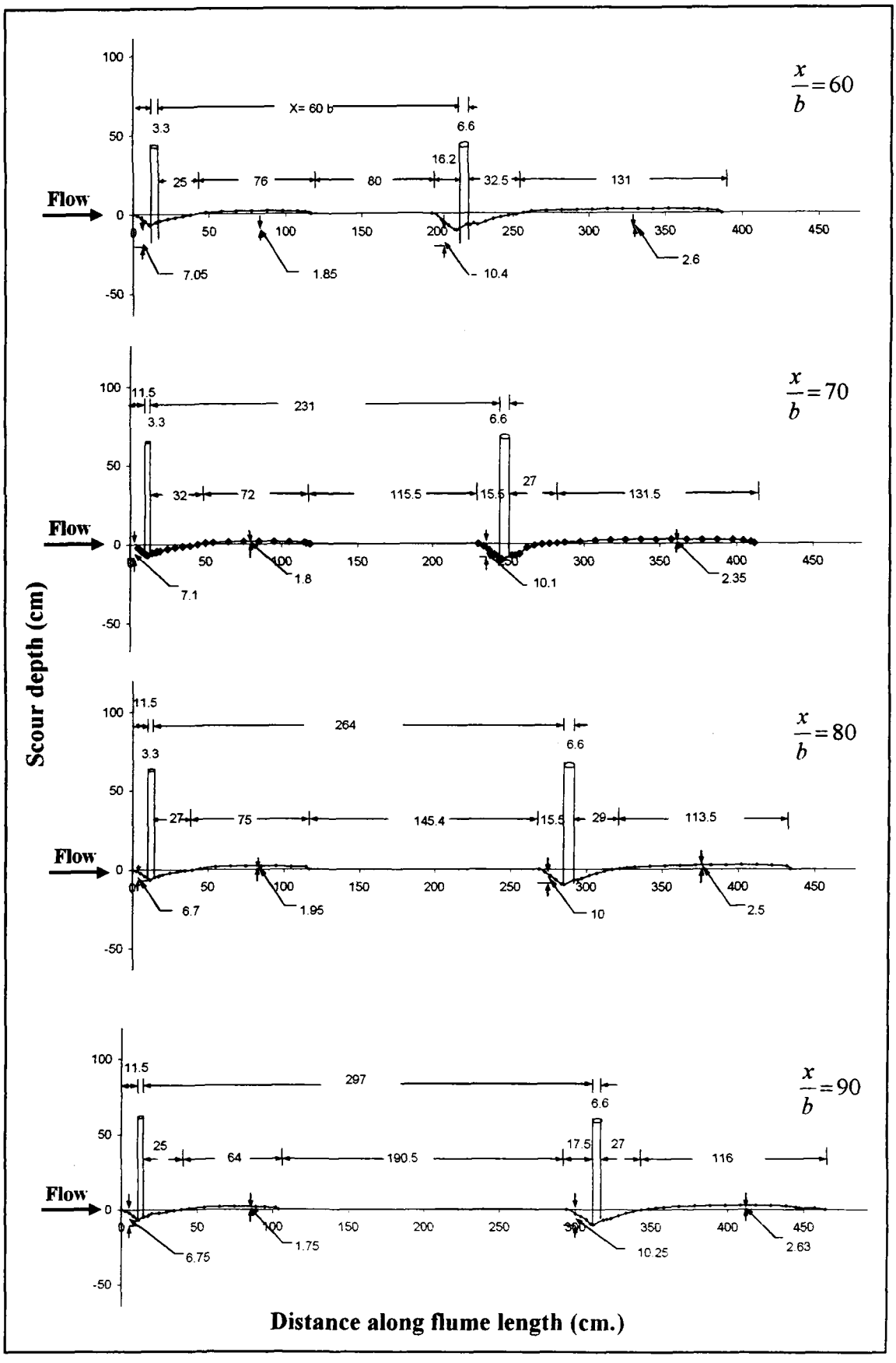

Longitudinal profiles for small pier at front and big pier at rear in tandem arrangement for varied pier spacing x/b.

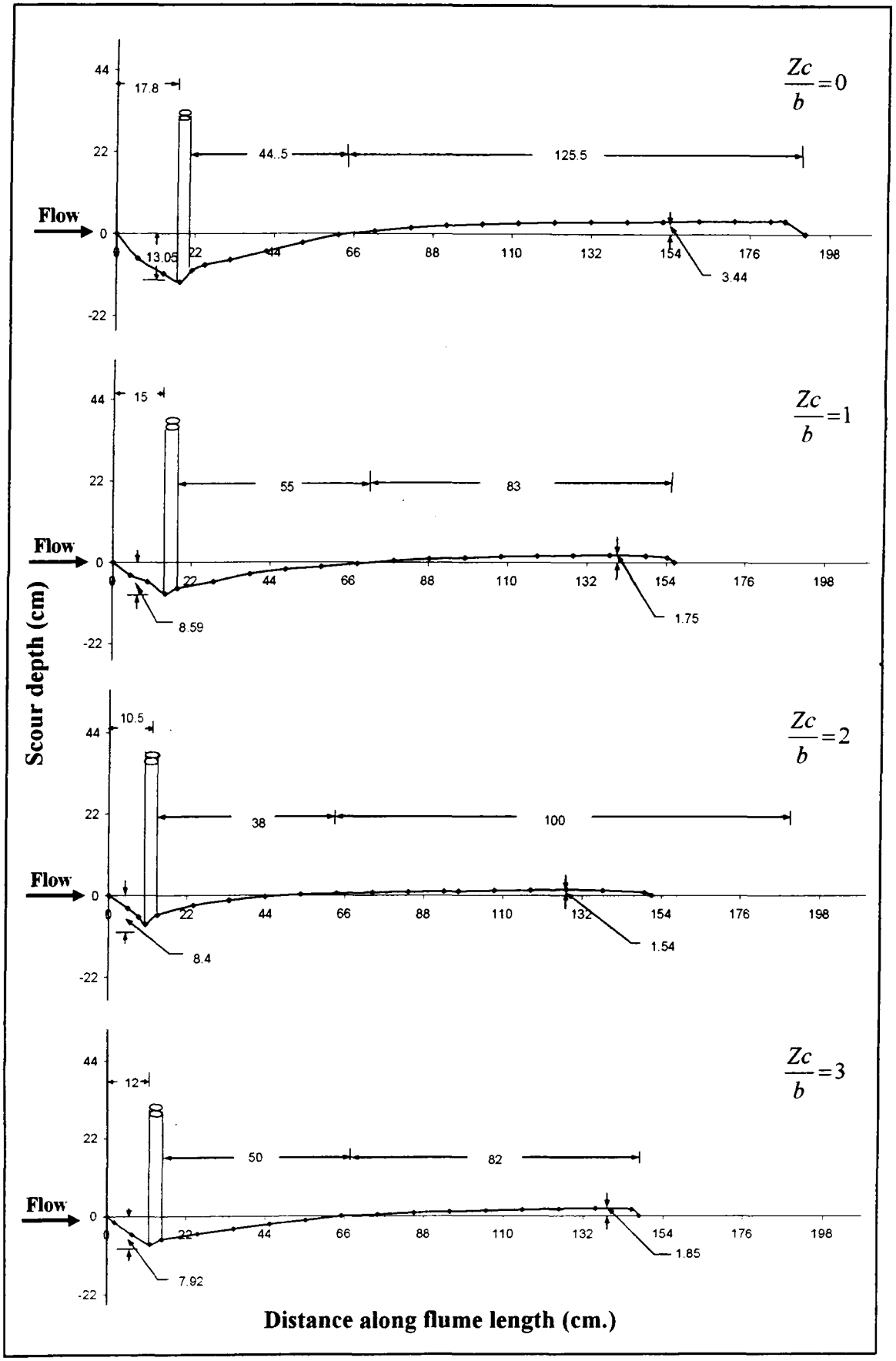

Longitudinal profiles for two piers of same size in transverse arrangement for varied lateral pier spacing Zc/b.

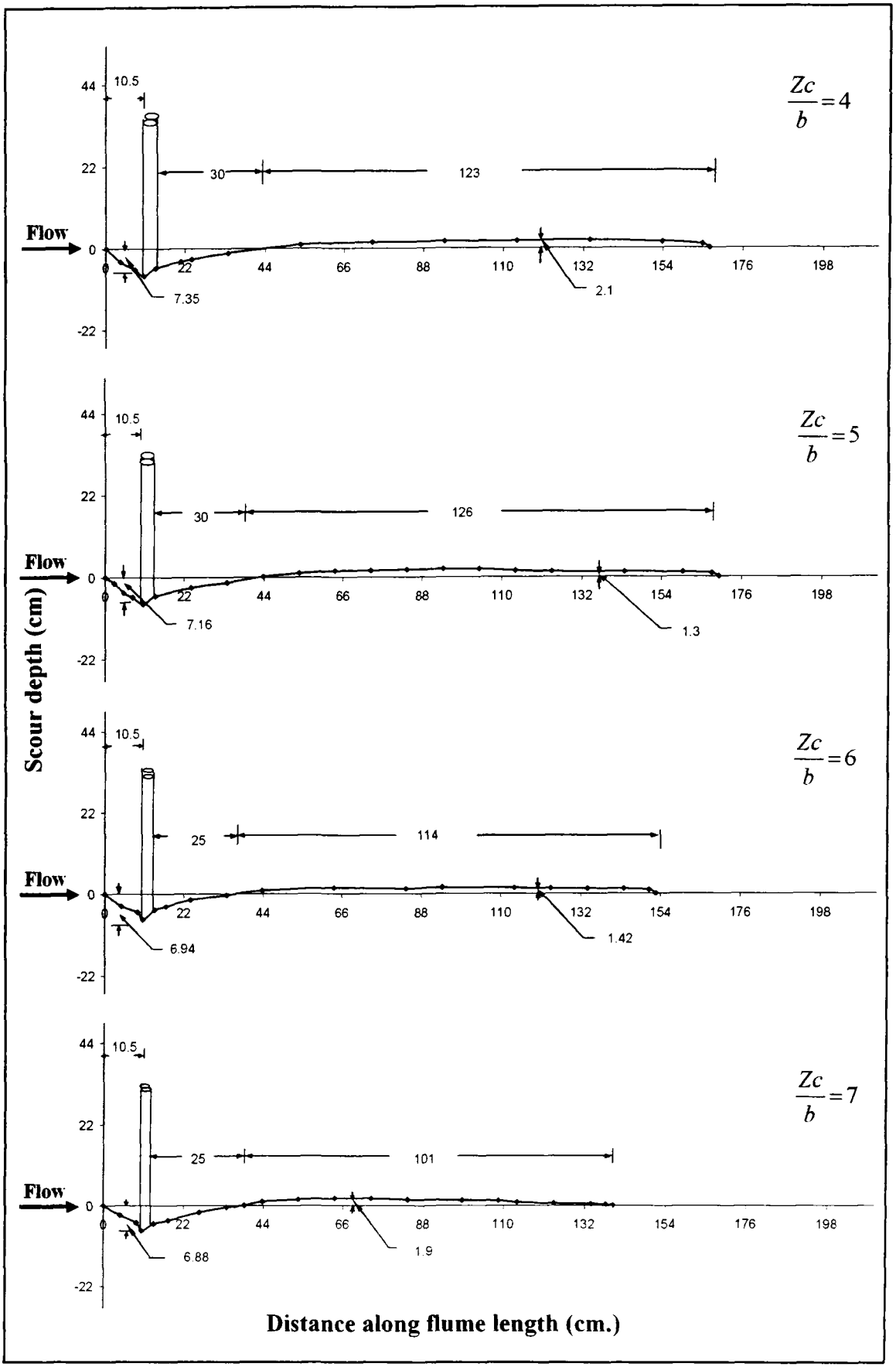

Longitudinal profiles for two piers of same size in transverse arrangement for varied lateral pier spacing Zc/b.

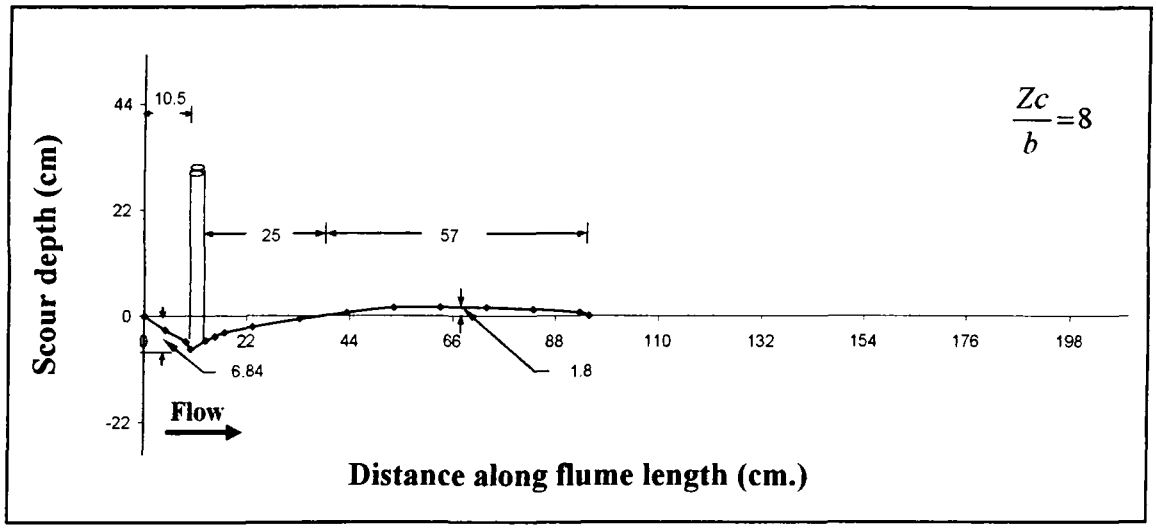

Longitudinal profiles for two piers of same size in transverse arrangement for varied lateral pier spacing Zc/b.

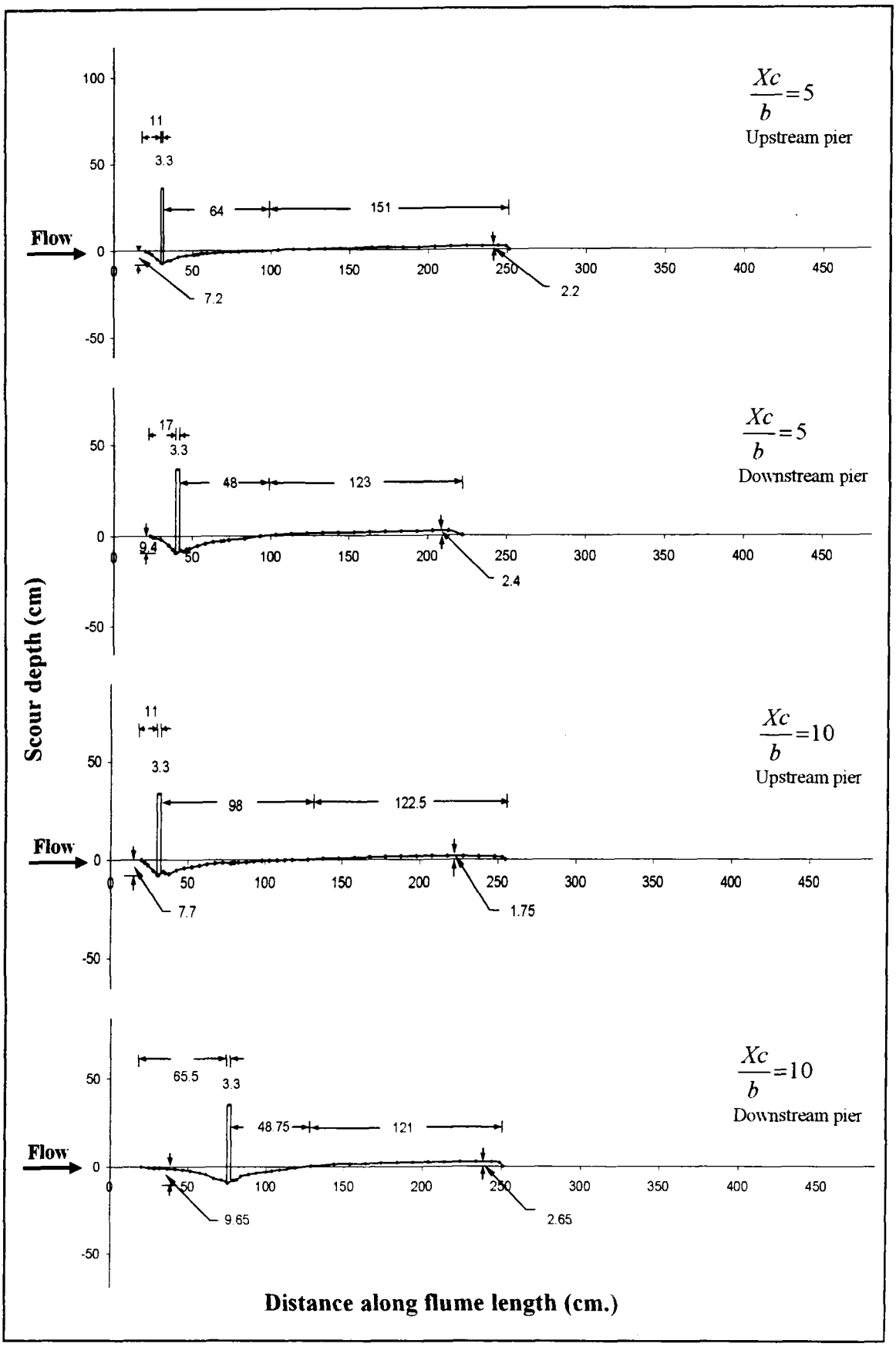

Longitudinal profiles for three piers of same size in staggered arrangement for varied pier spacing Xc/b.

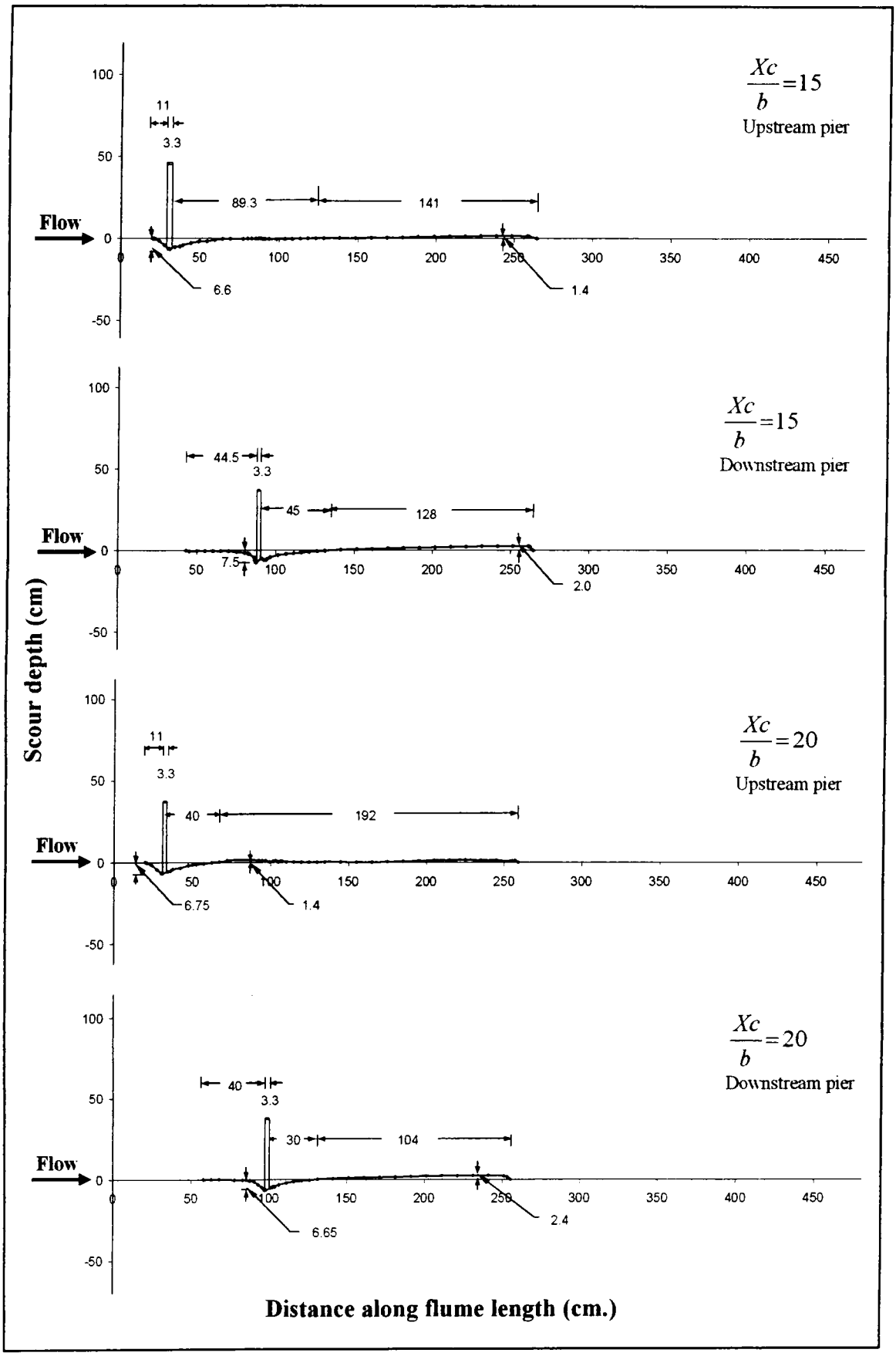

Longitudinal profiles for three piers of same size in staggered arrangement for varied pier spacing Xc/b.

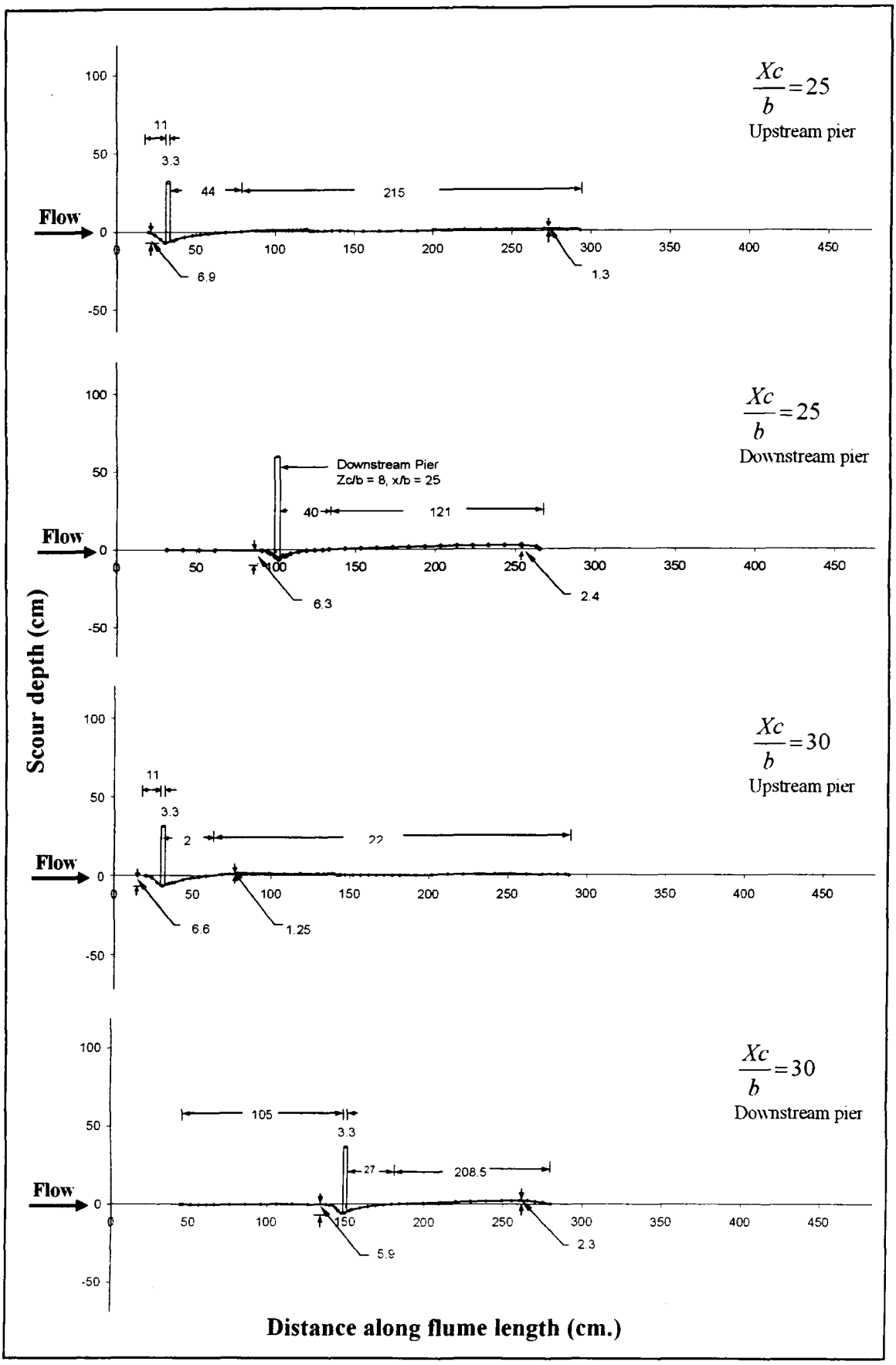

Longitudinal profiles for three piers of same size in staggered arrangement for varied pier spacing Xc/b.

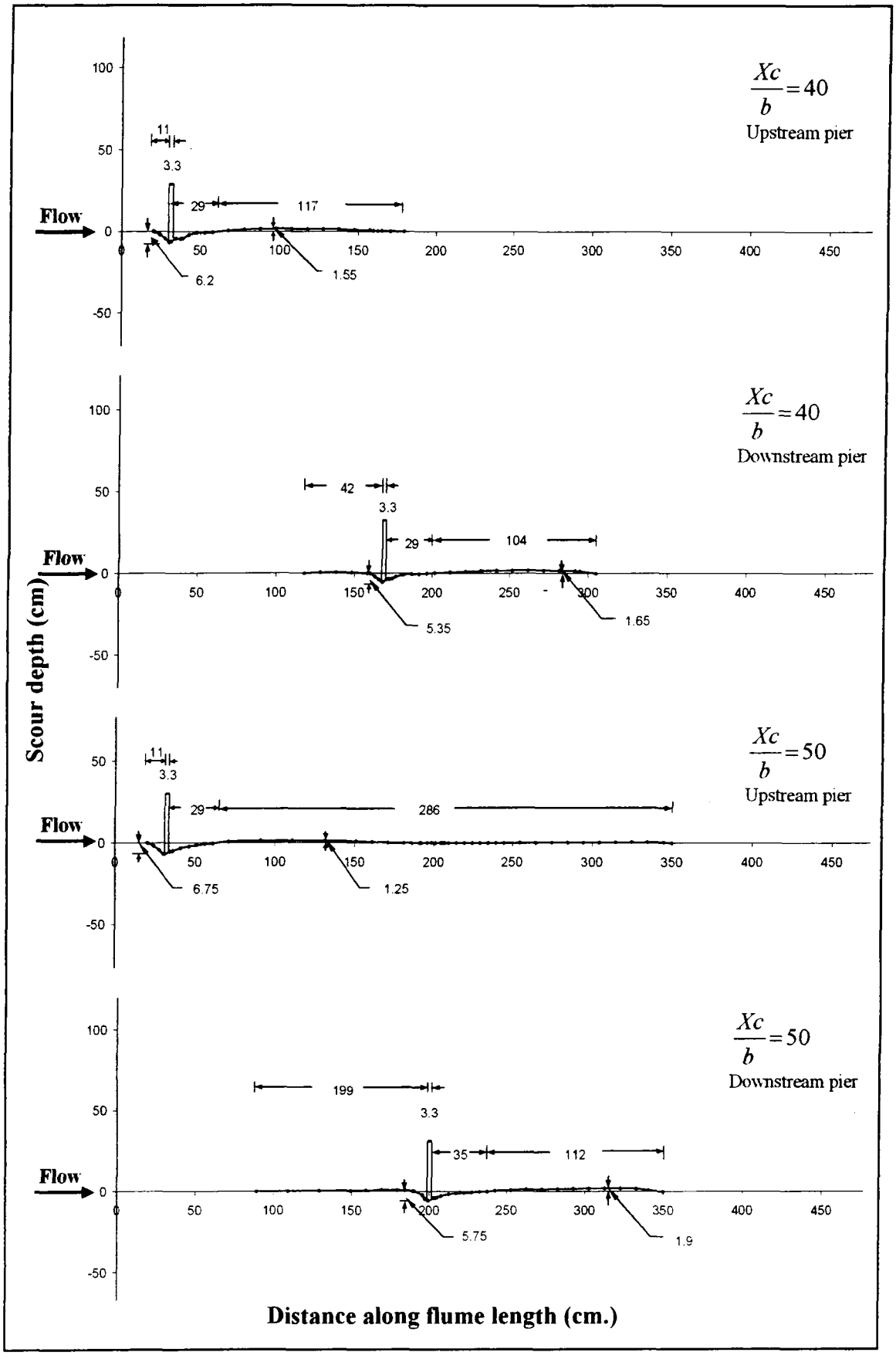

Longitudinal profiles for three piers of same size in staggered arrangement for varied pier spacing Xc/b.

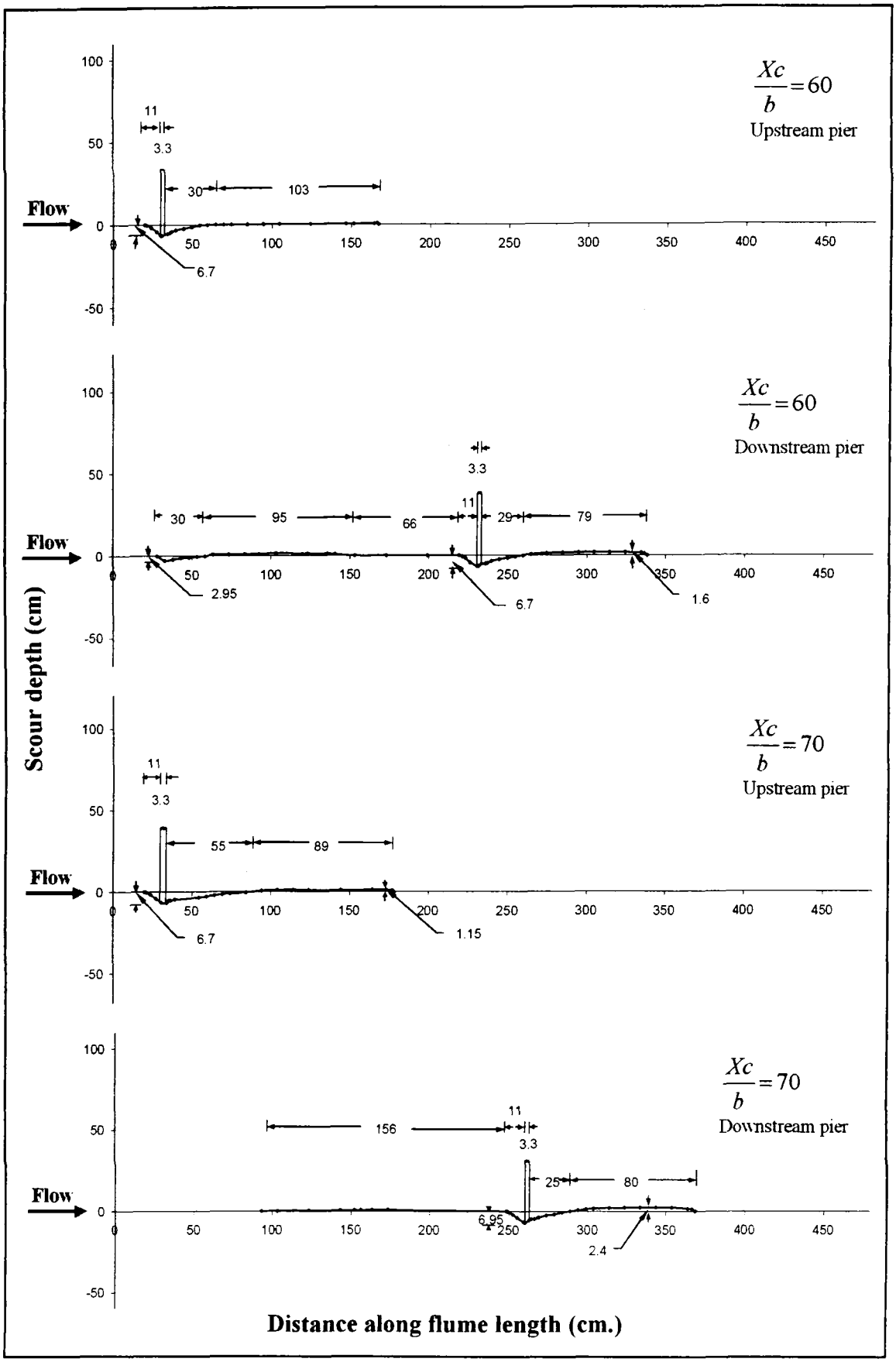

Longitudinal profiles for three piers of same size in staggered arrangement for varied pier spacing Xc/b.

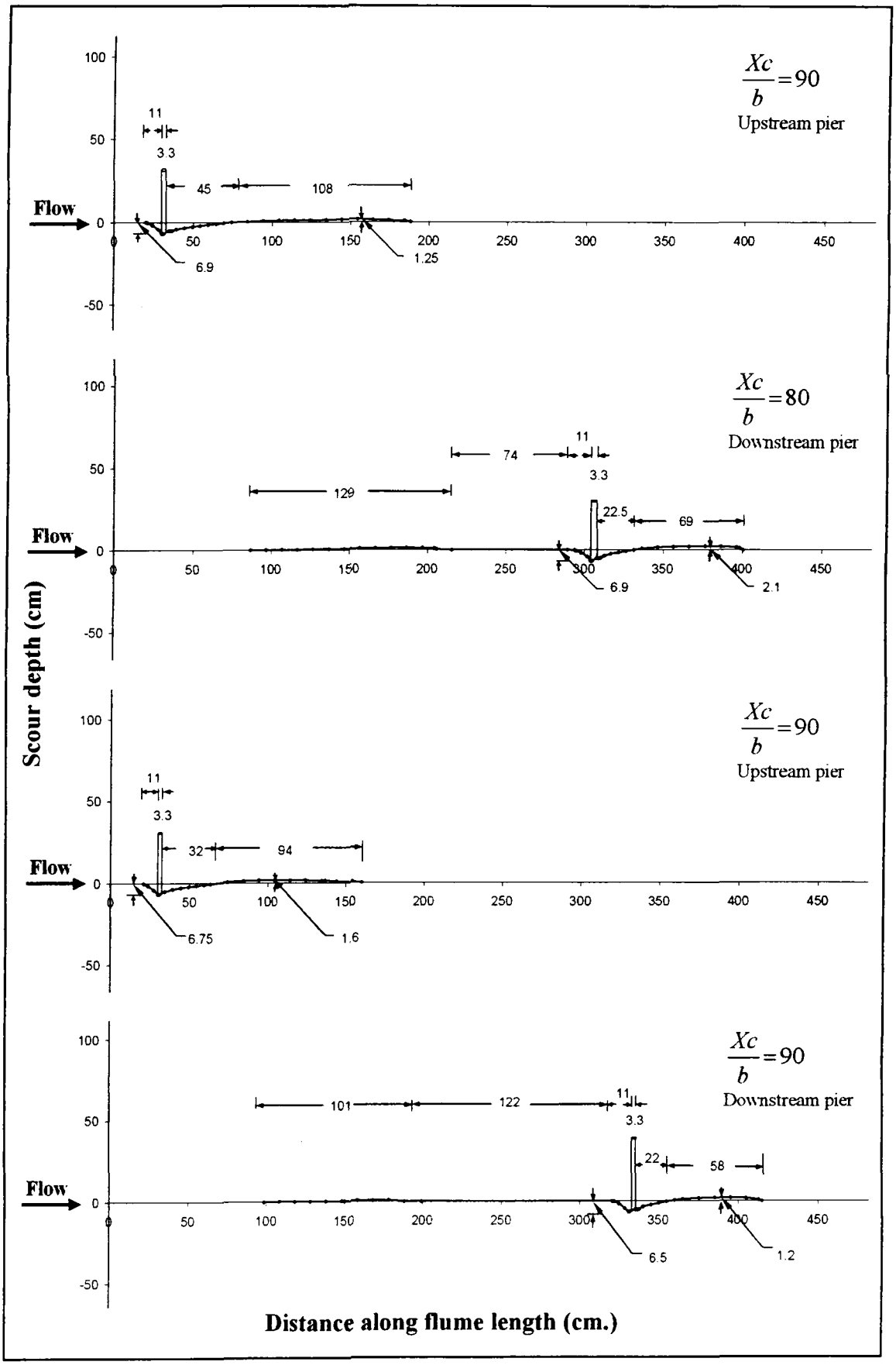

Longitudinal profiles for three piers of same size in staggered arrangement for varied pier spacing Xc/b.

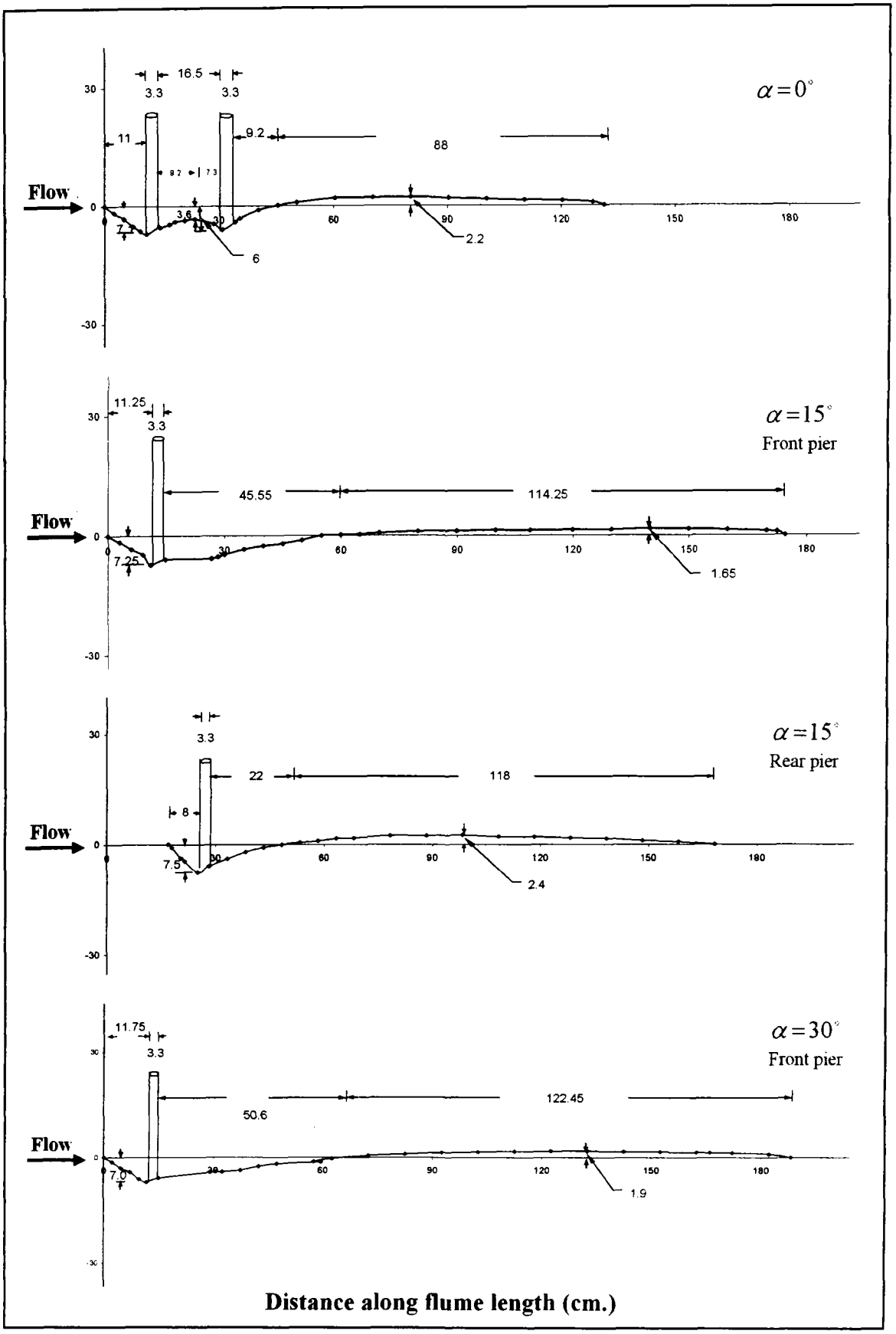

Longitudinal profiles for two piers of same size at constant radial spacings and variable angles of attack 'α'.

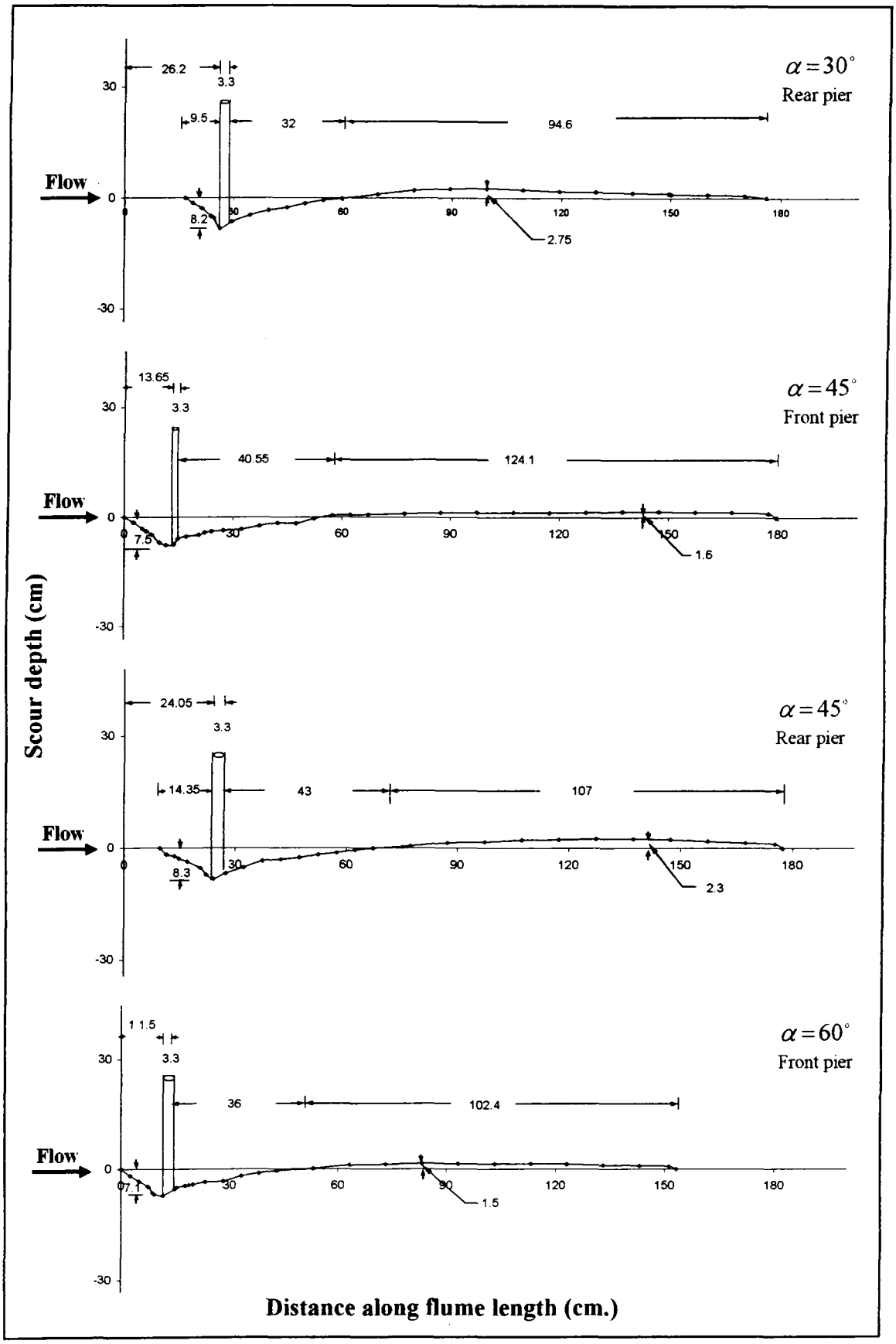

Longitudinal profiles for two piers of same size at constant radial spacings and variable angles of attack 'α'.

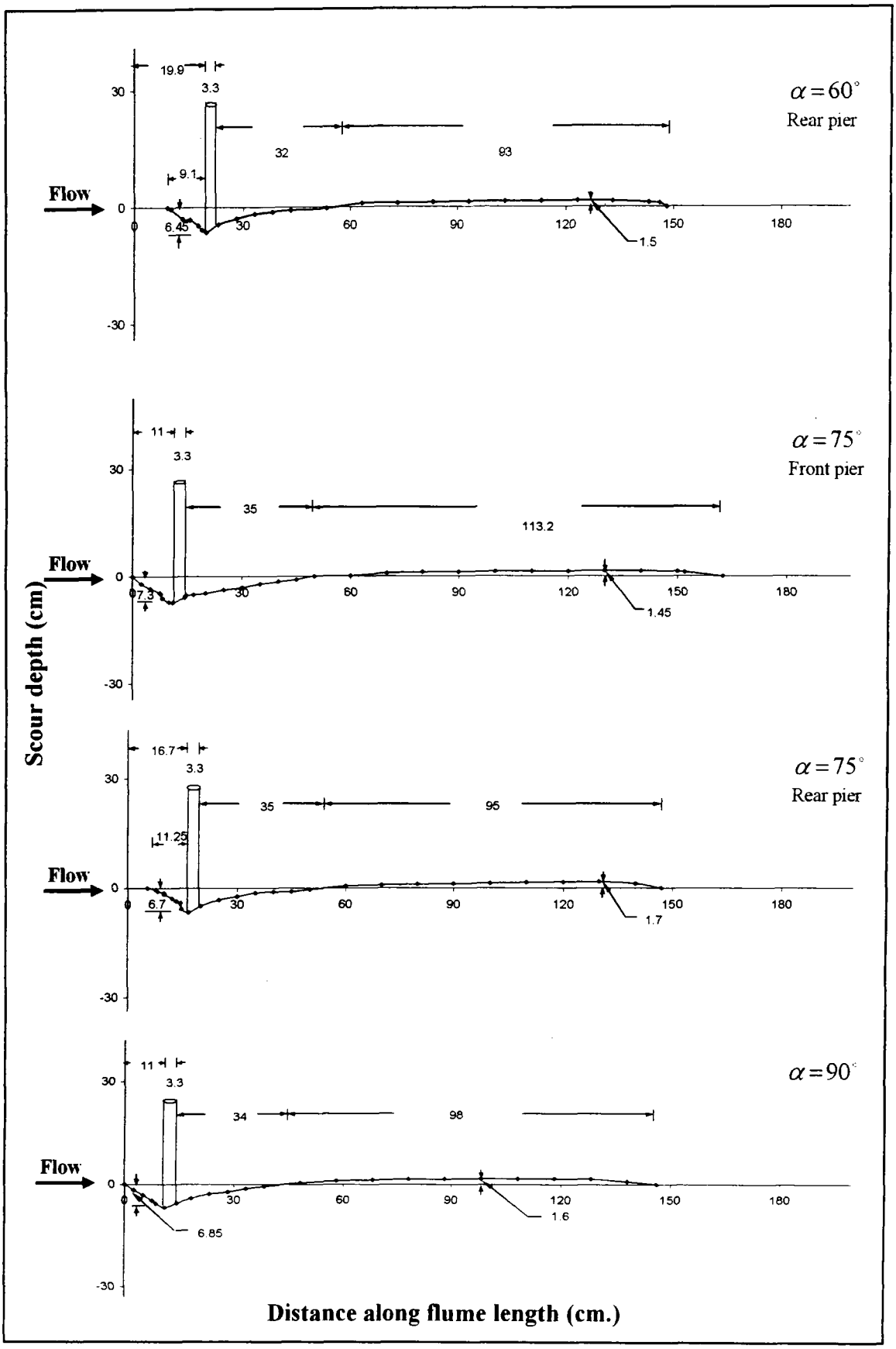

Longitudinal profiles for two piers of same size at constant radial spacings and variable angles of attack 'α'.

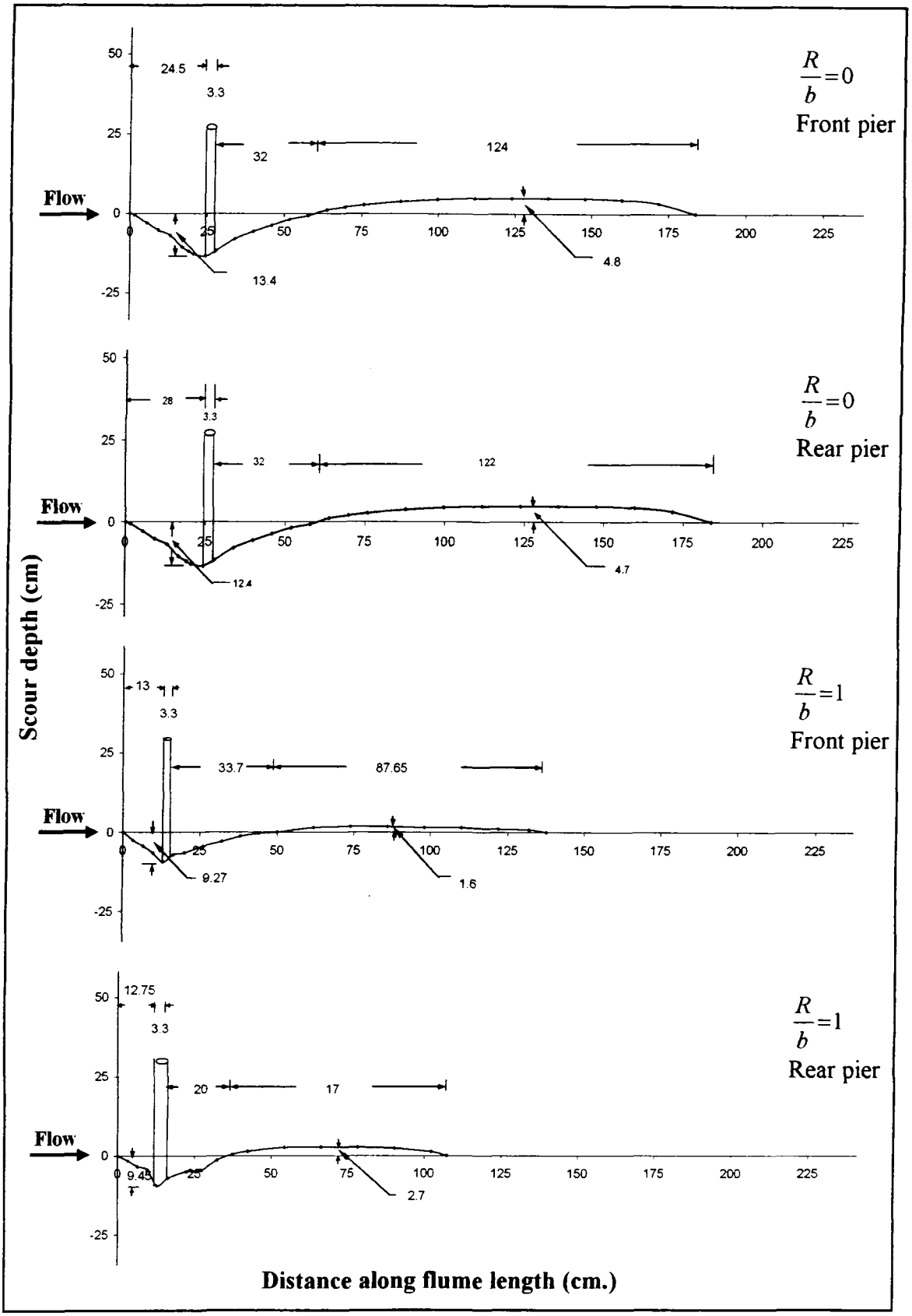

Longitudinal profiles for two piers of same size at constant angle of attack and variable radial sapcings 'R/b'.

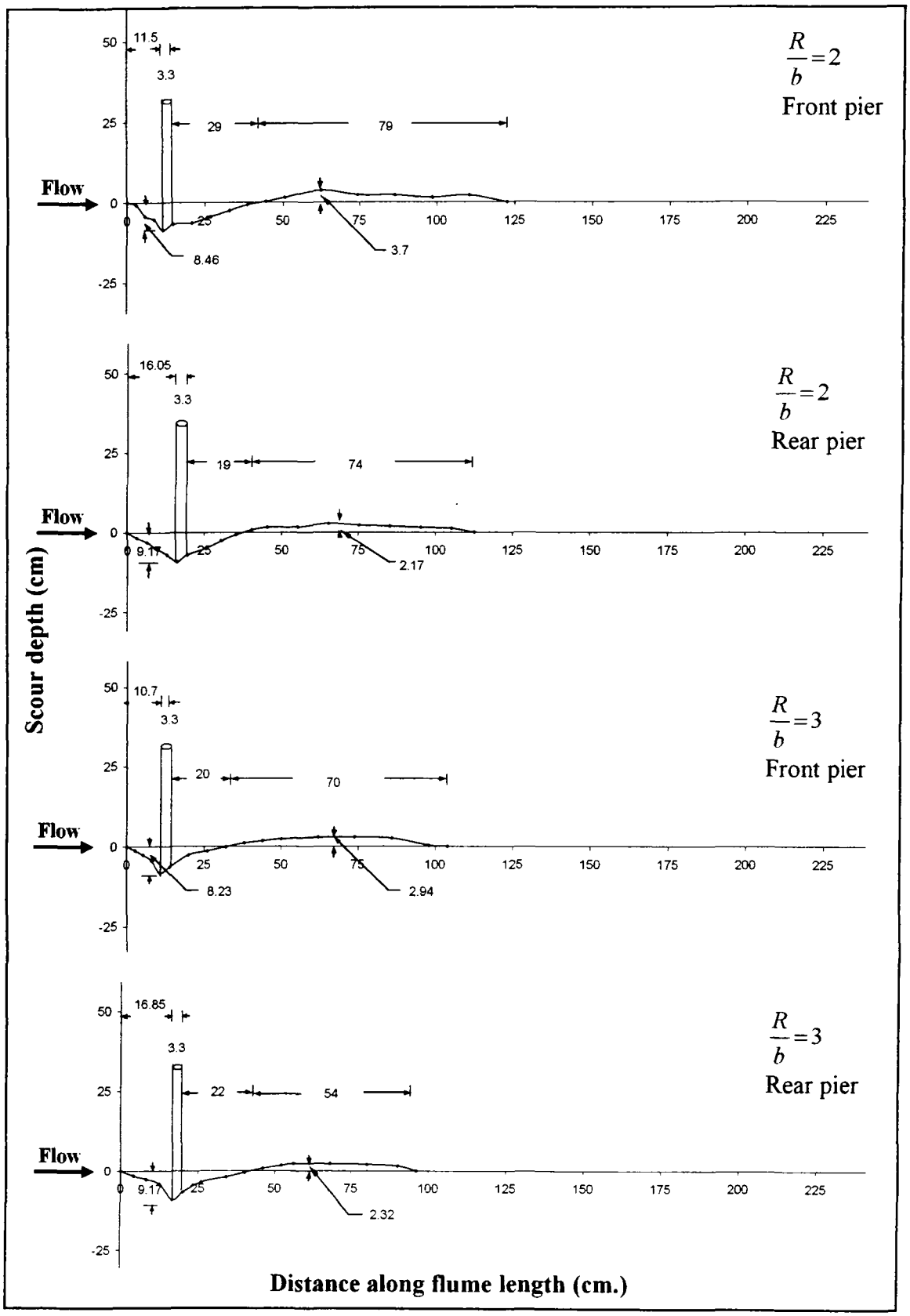

Longitudinal profiles for two piers of same size at constant angle of attack and variable radial sapcings 'R/b'.

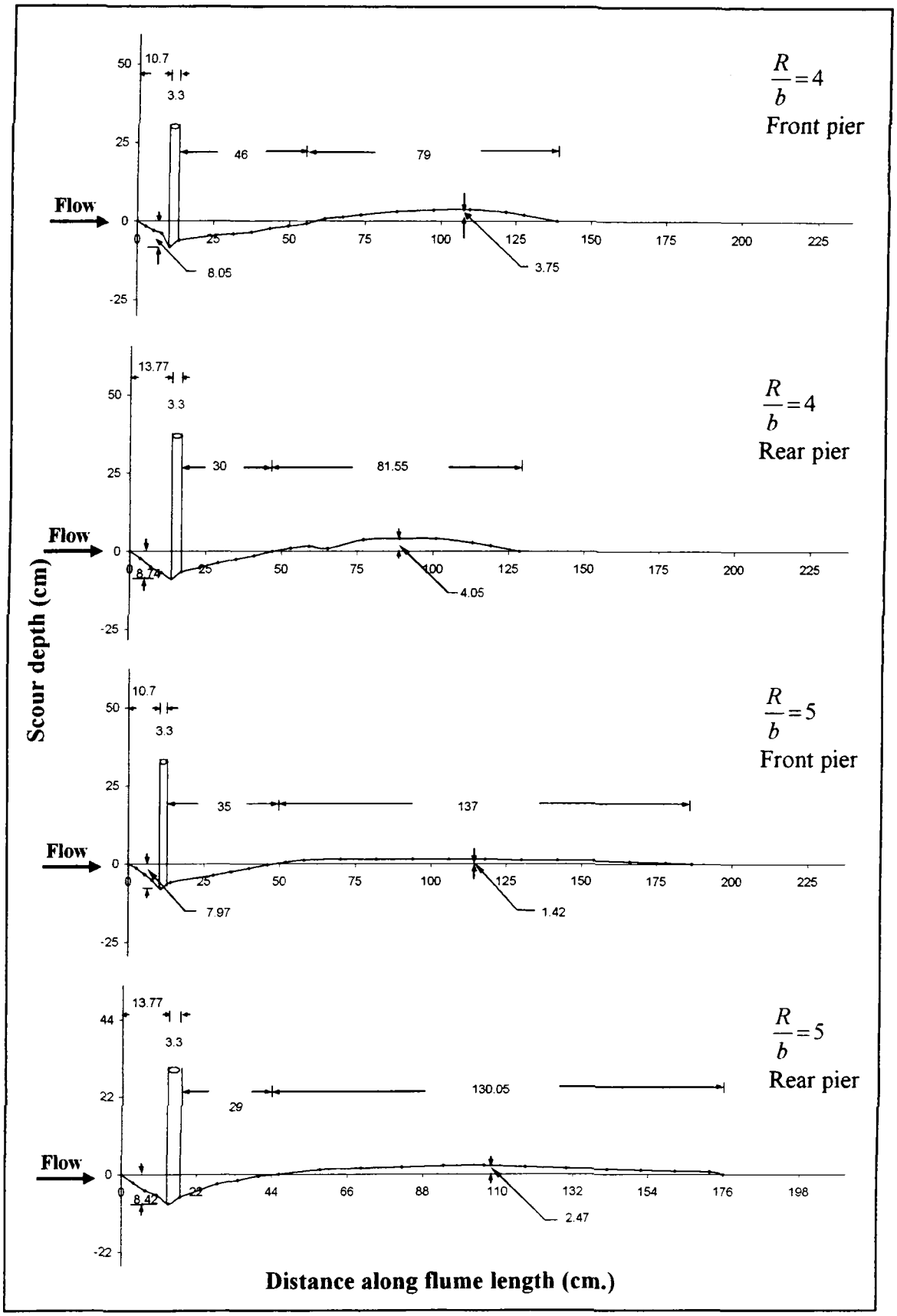

Longitudinal profiles for two piers of same size at constant angle of attack and variable radial spacings 'R/b'.

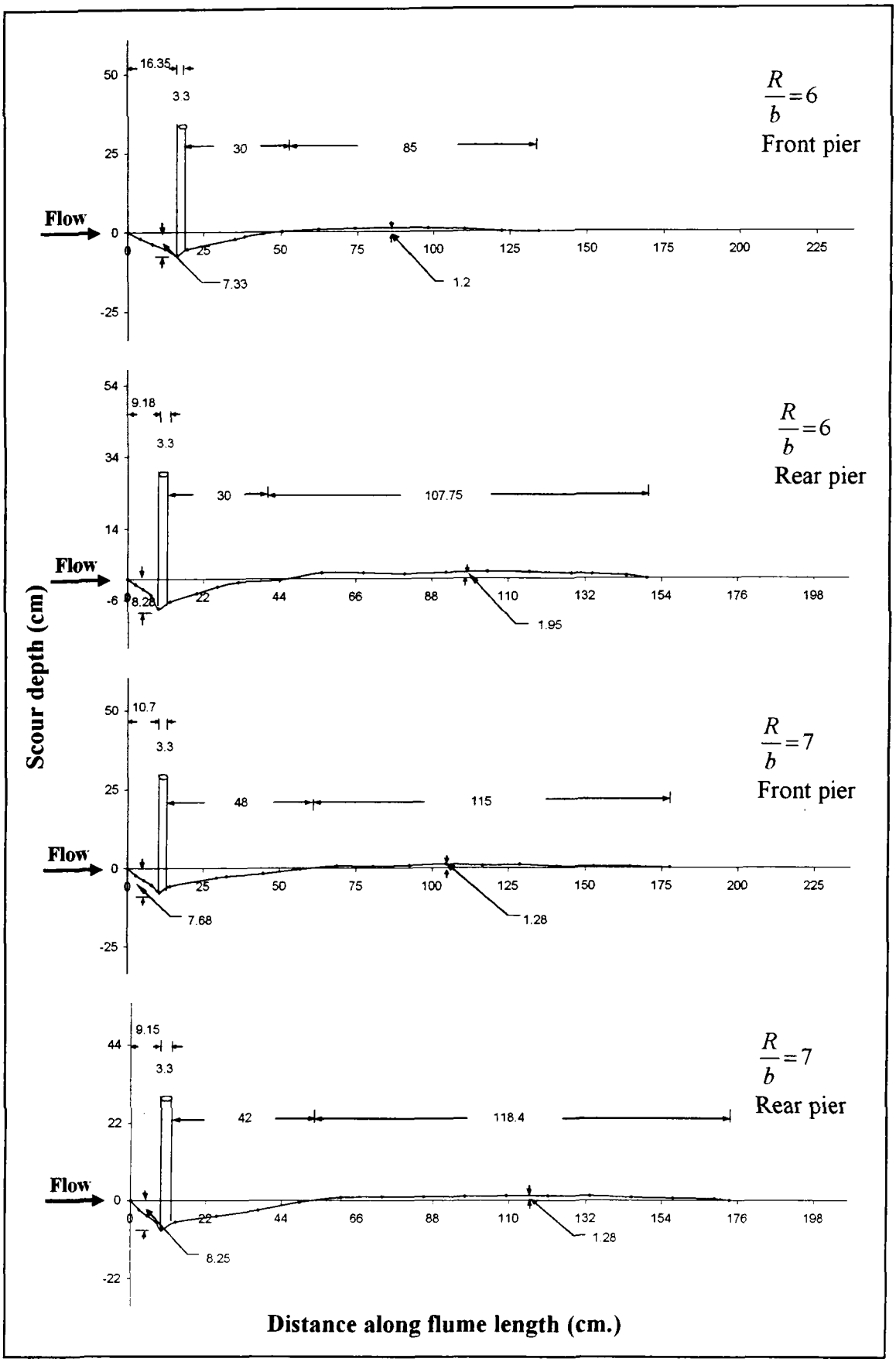

Longitudinal profiles for two piers of same size at constant angle of attack and variable radial spacings 'R/b'.

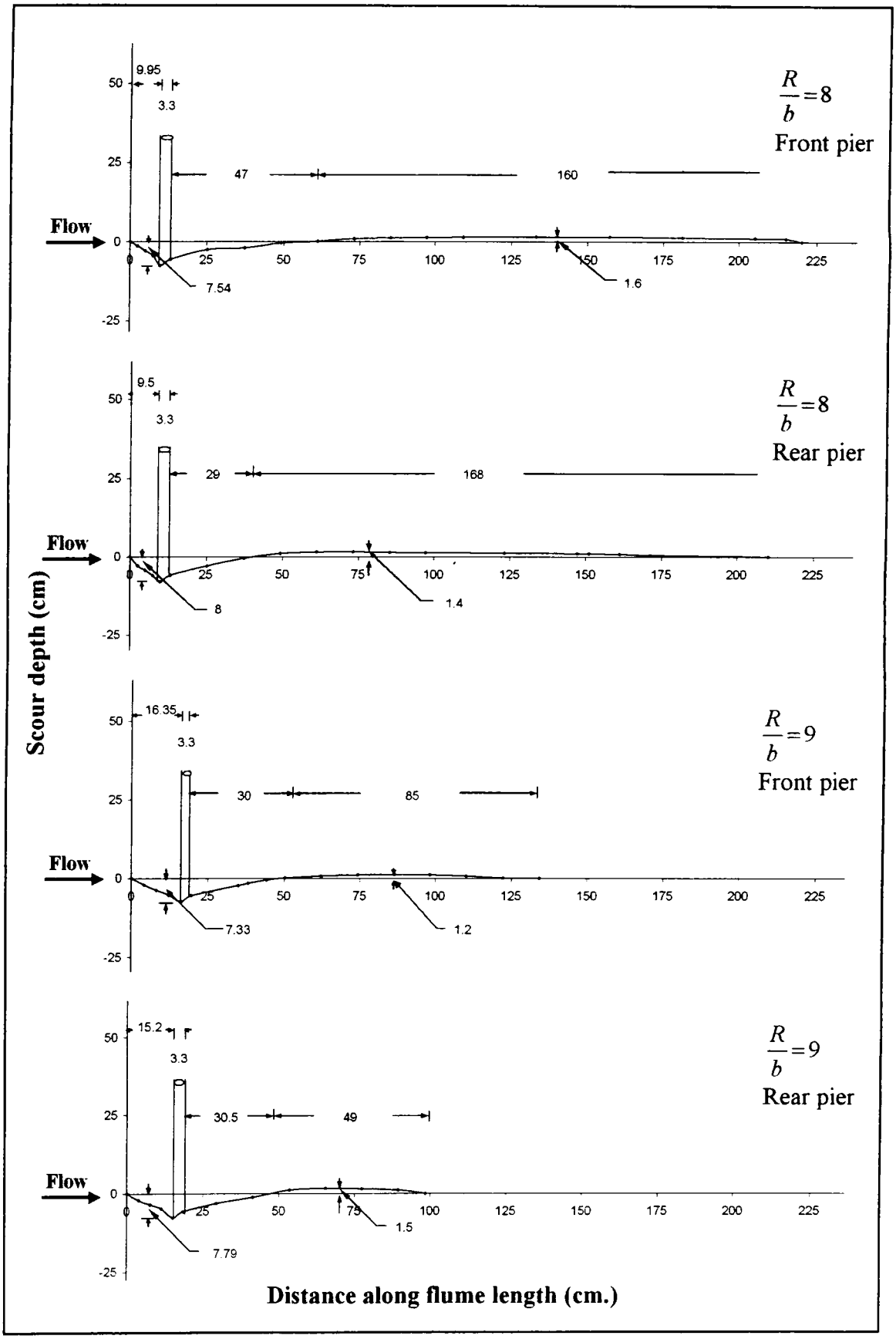

Longitudinal profiles for two piers of same size at constant angle of attack and variable radial spacings 'R/b'.

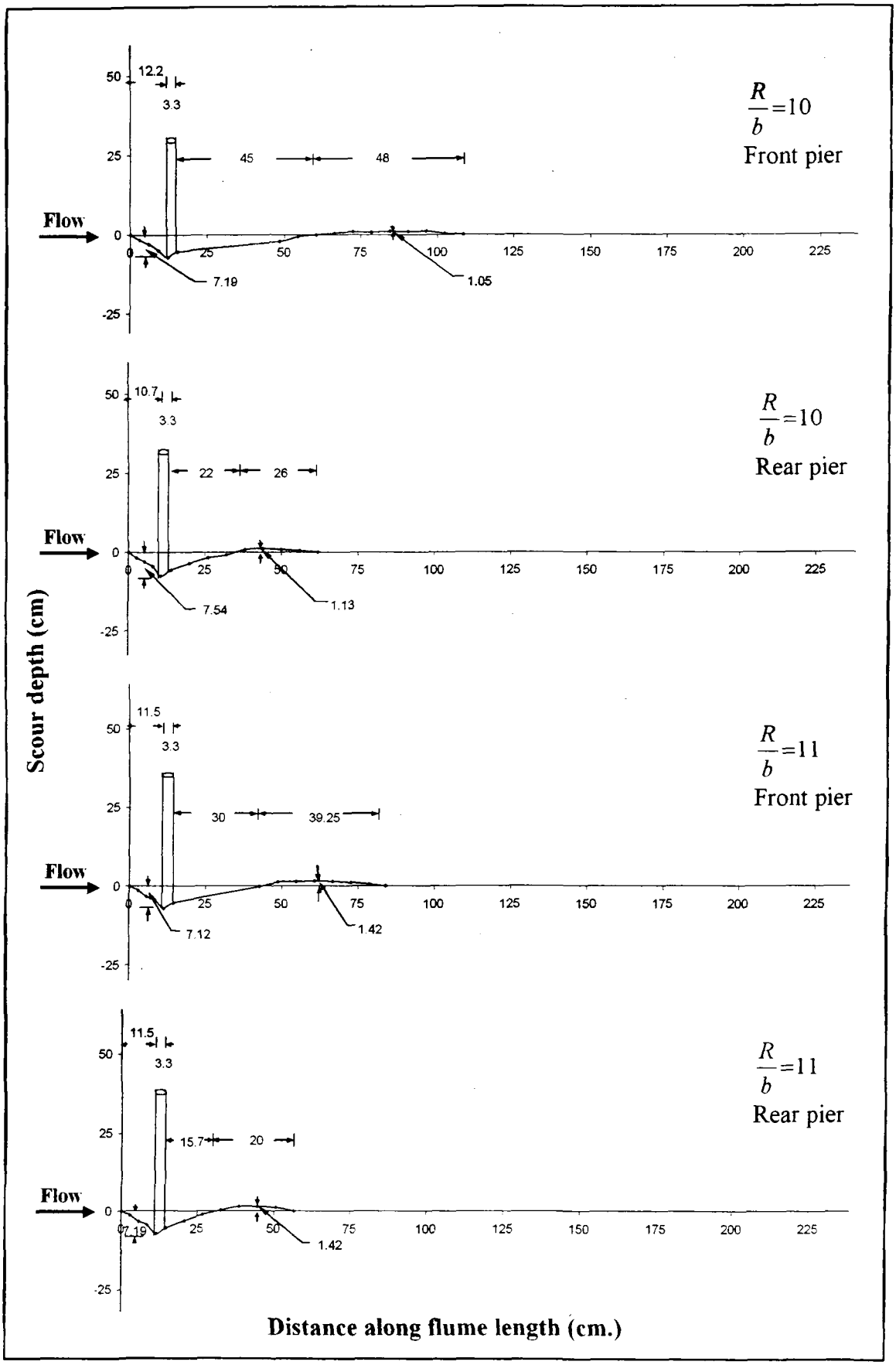

Longitudinal profiles for two piers of same size at constant angle of attack and variable radial spacings 'R/b'.

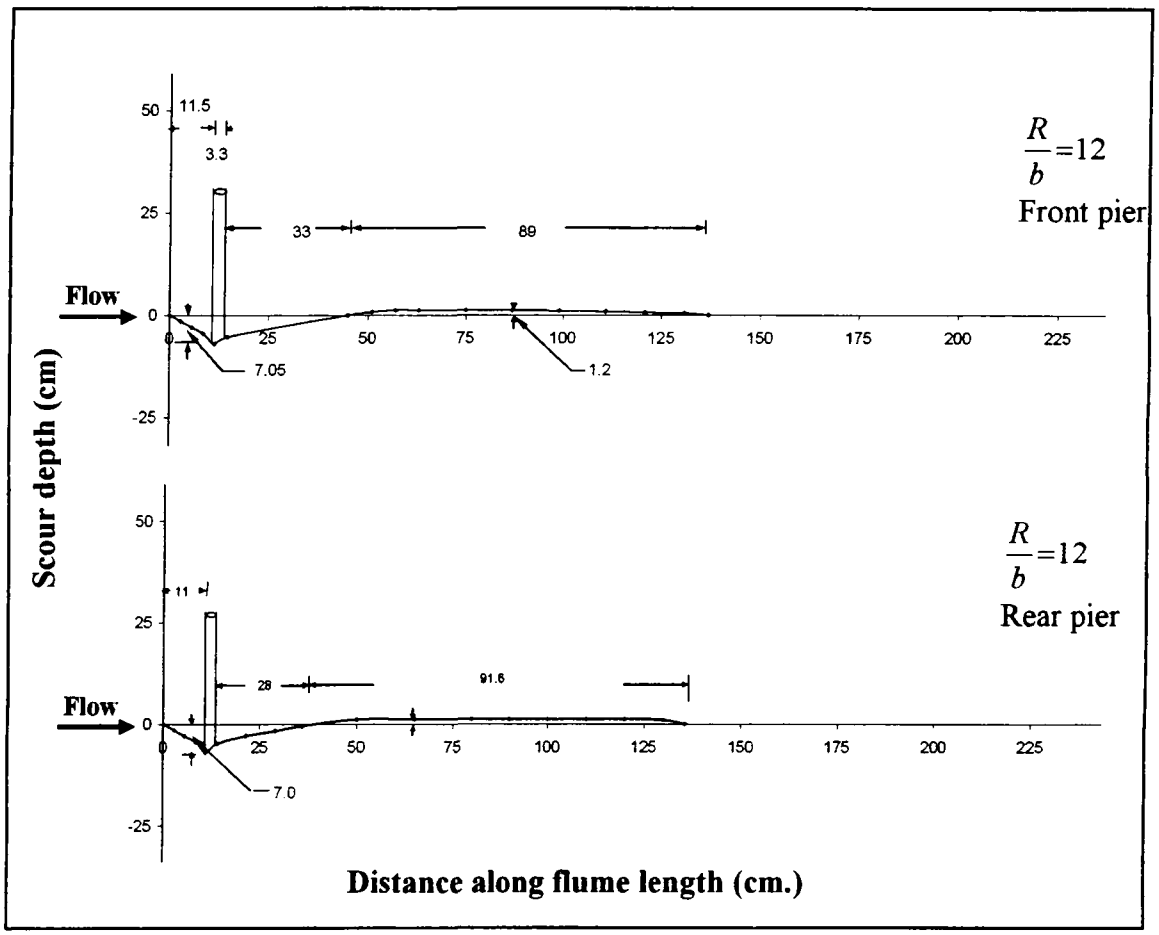

Longitudinal profiles for two piers of same size at constant angle of attack and variable radial spacings 'R/b'.

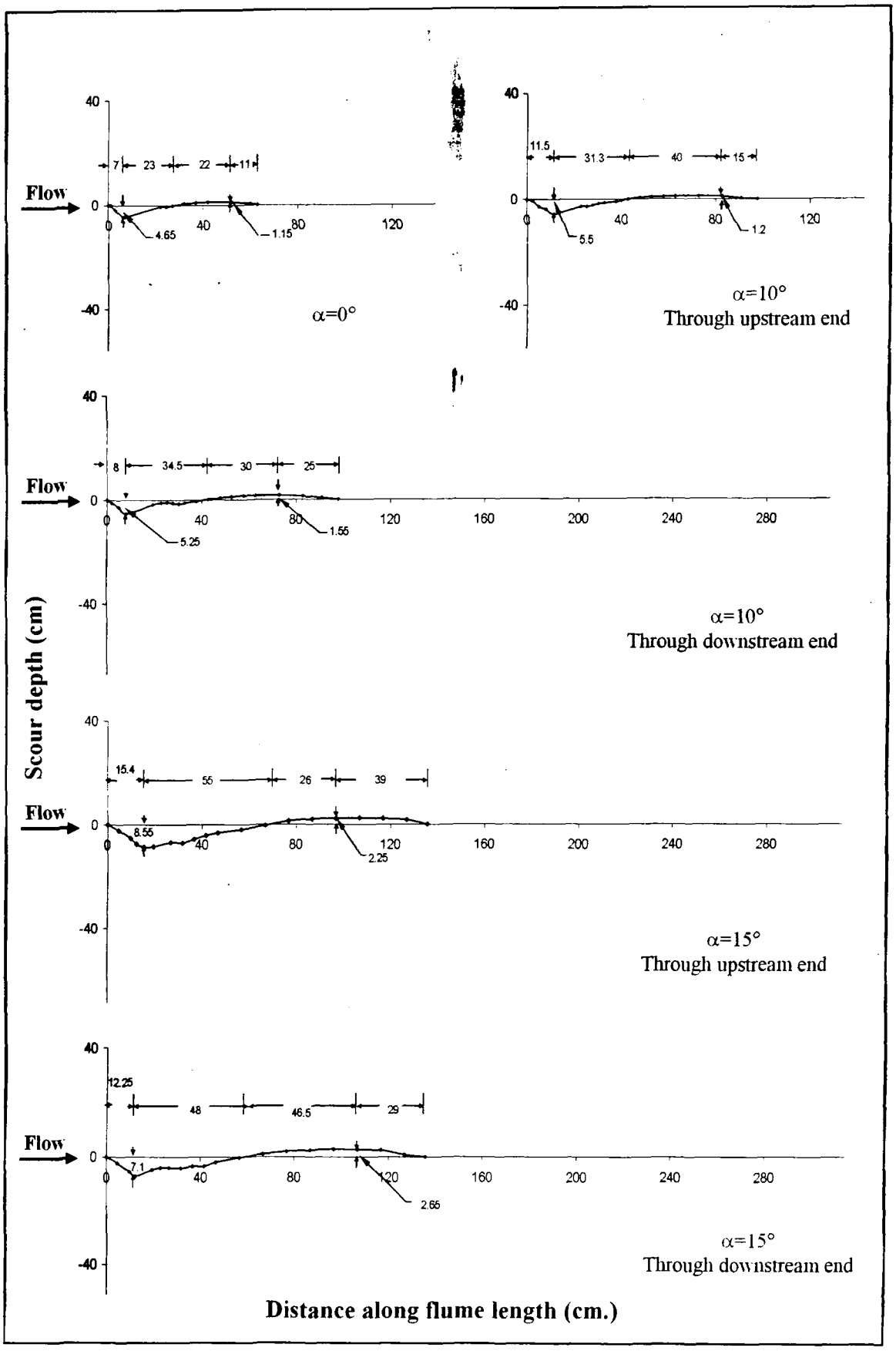

Longitudinal profiles for piers group without collar comprising on different size of piers for varied angles of attack 'α'.

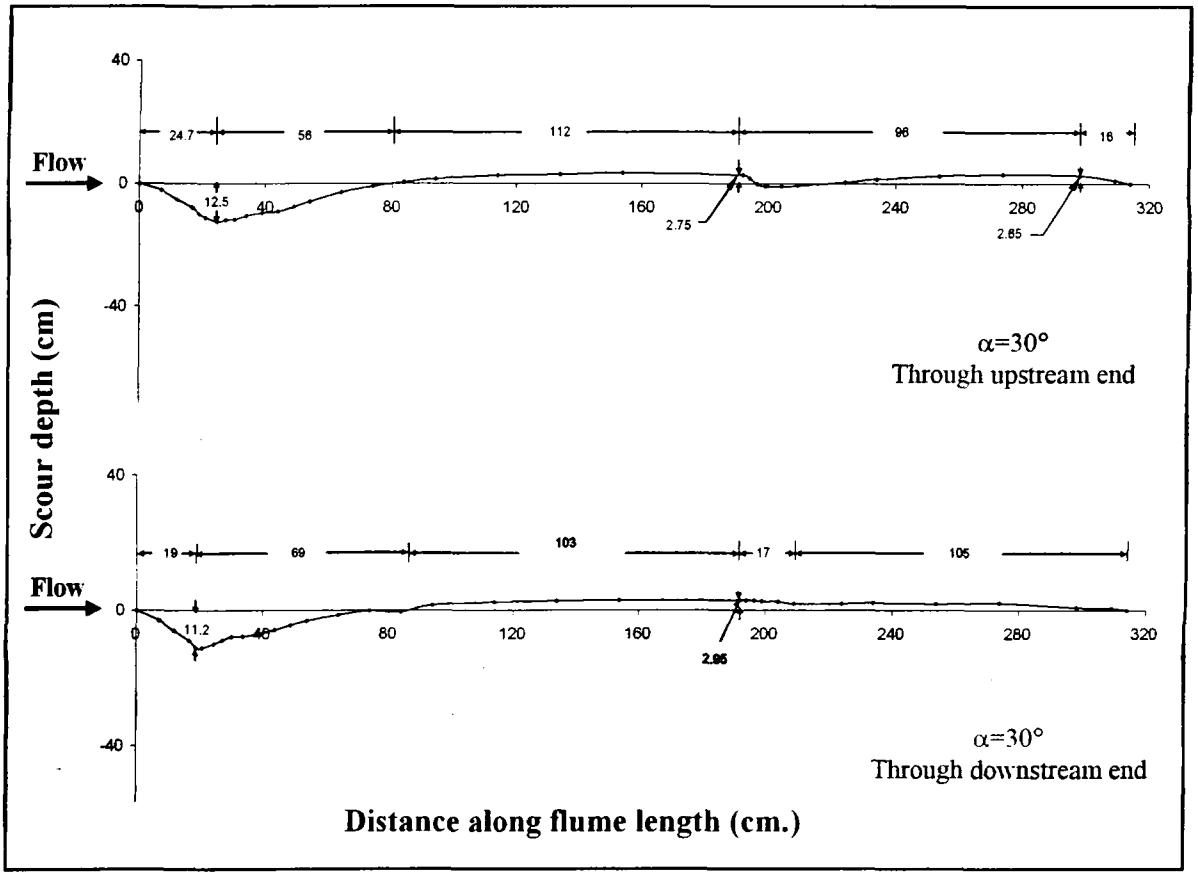

Longitudinal profiles for piers group comprising of cylinders of varying sizes without collar for varied angles of attack 'α'.

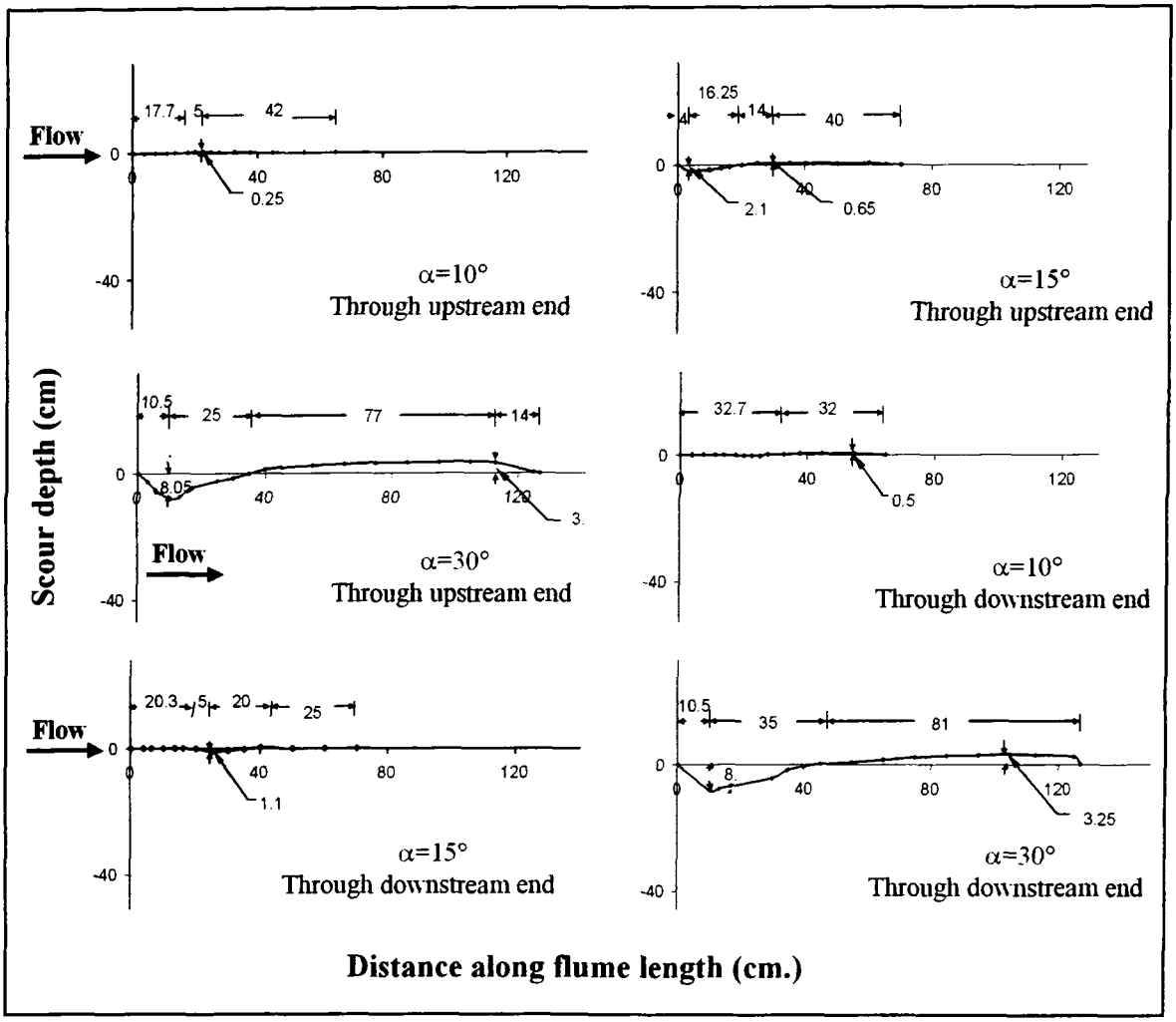

Longitudinal profiles for piers group with collar comprising on different size of piers for varied angles of attack 'α'.

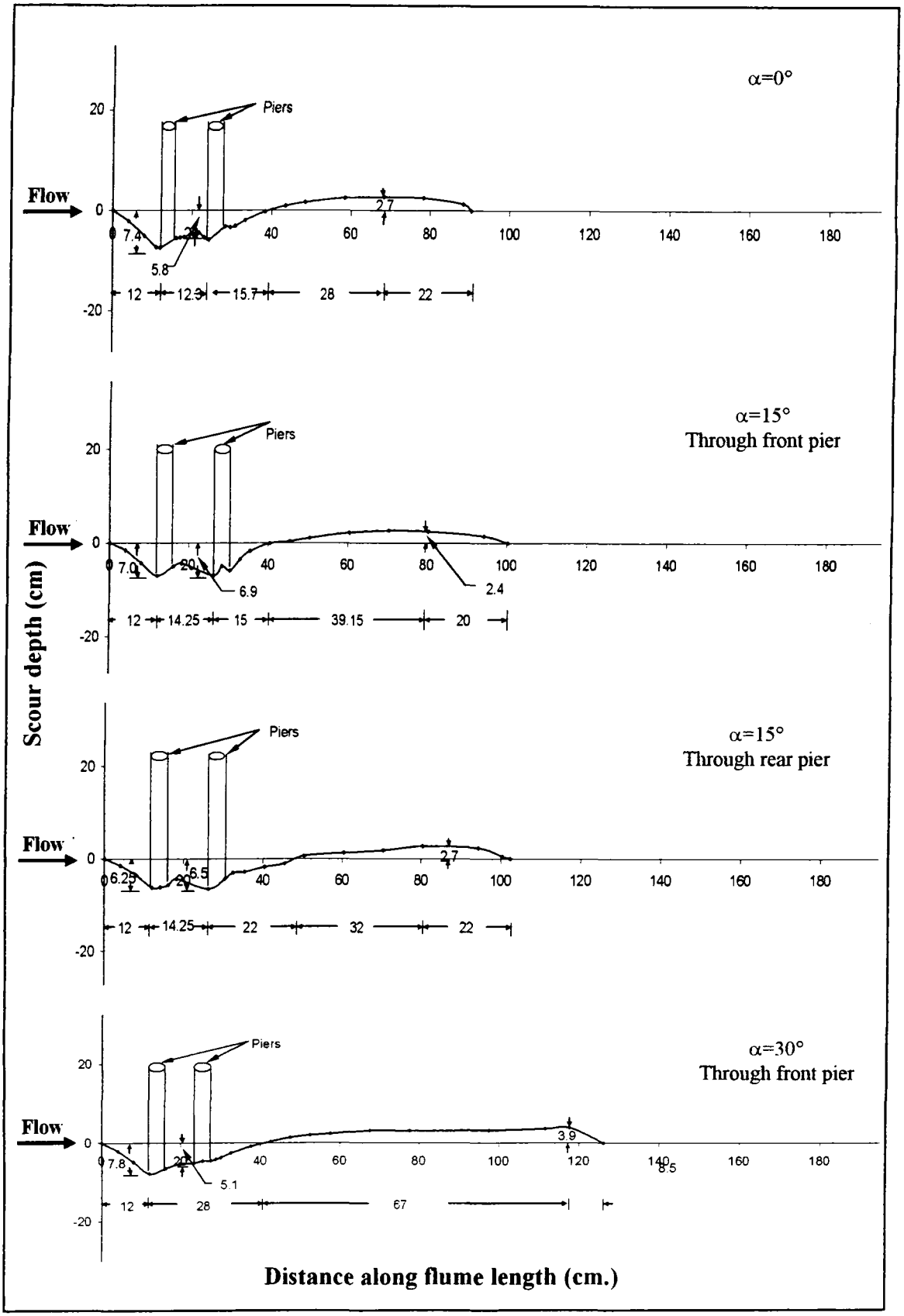

Longitudinal profiles for group of two piers with & without collar for varied angles of attack 'α'.

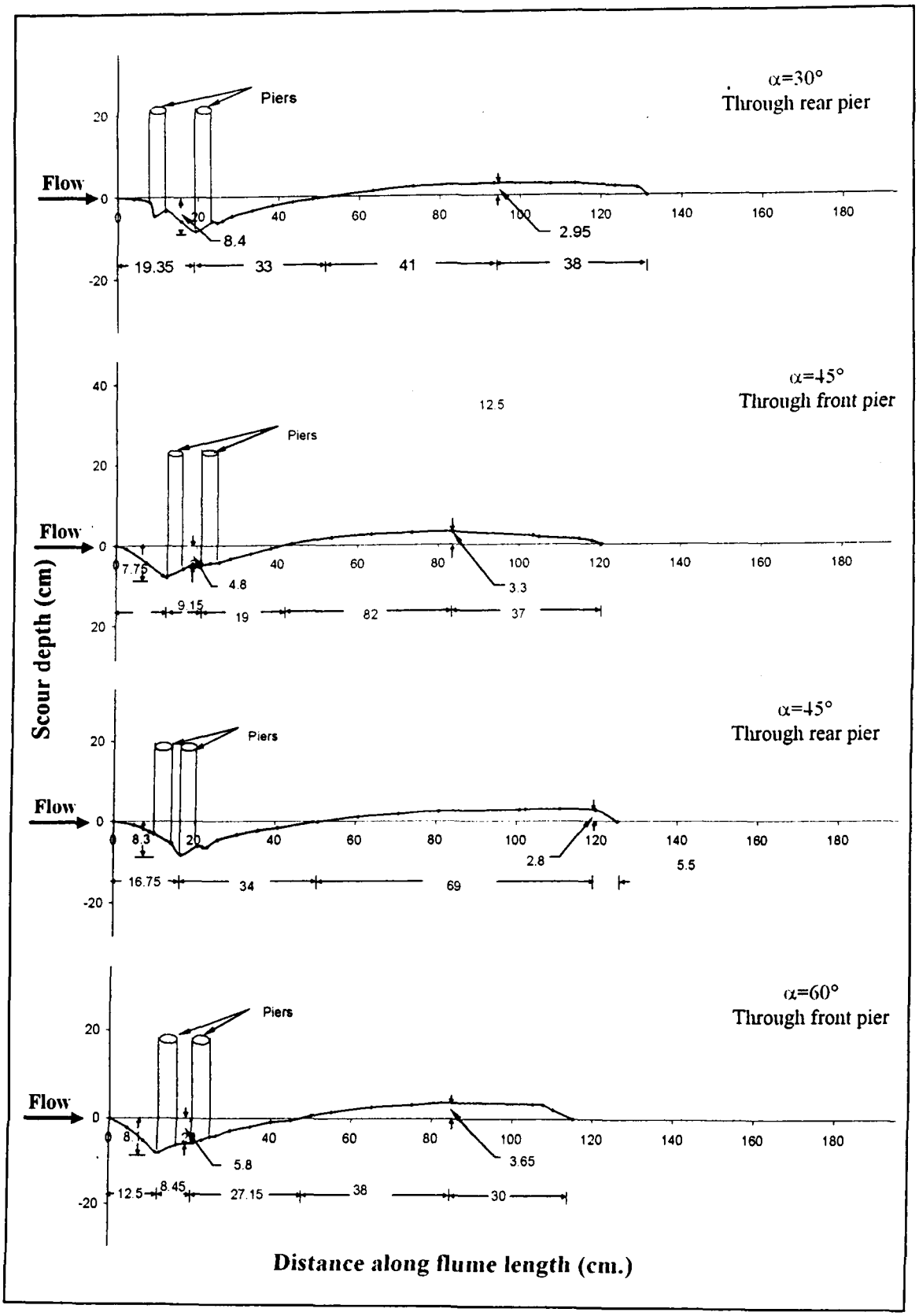

Longitudinal profiles for group of two piers with & without collar for varied angles of attack 'α'.

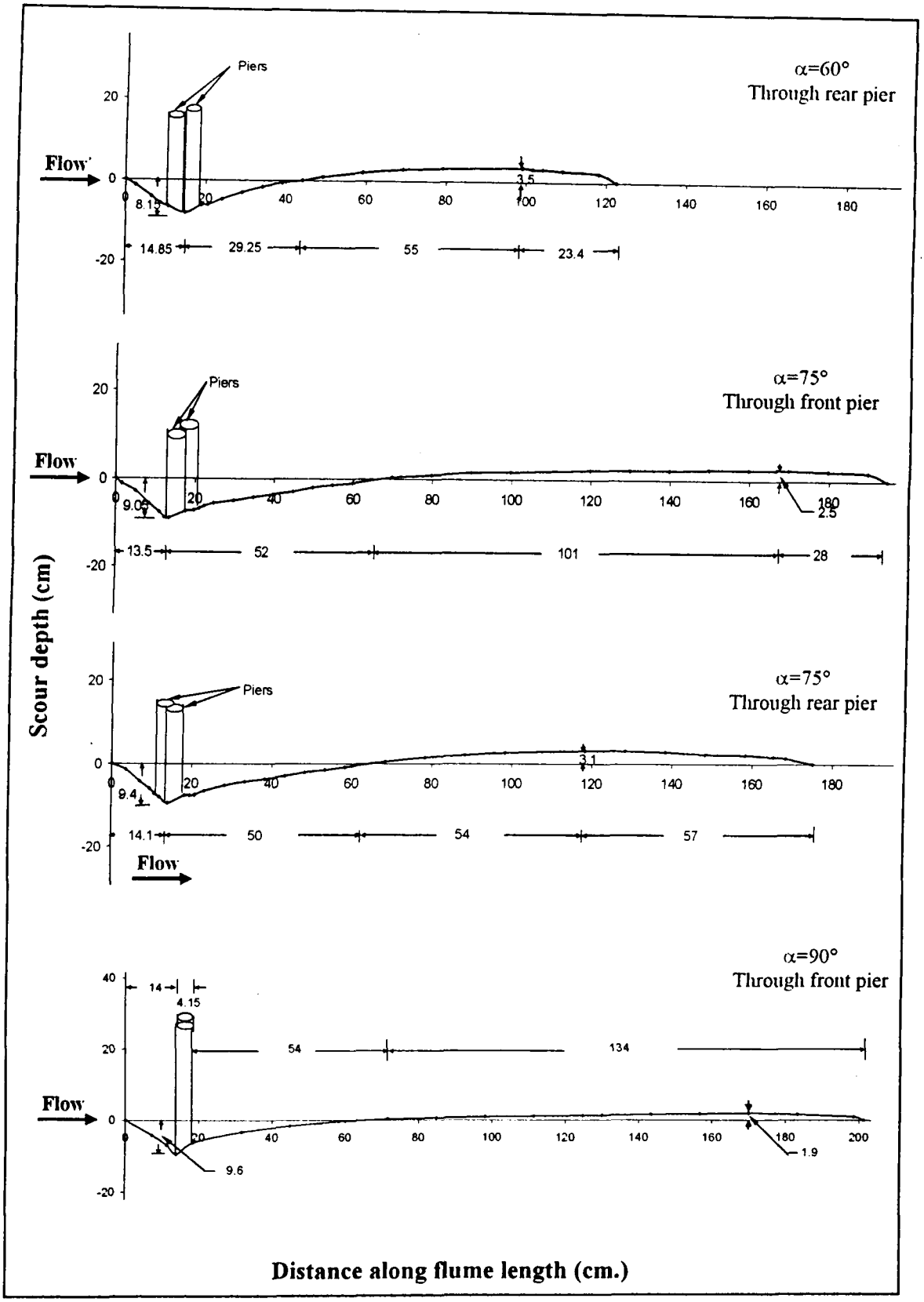

Longitudinal profiles for group of two piers with & without collar for varied angles of attack 'α'.

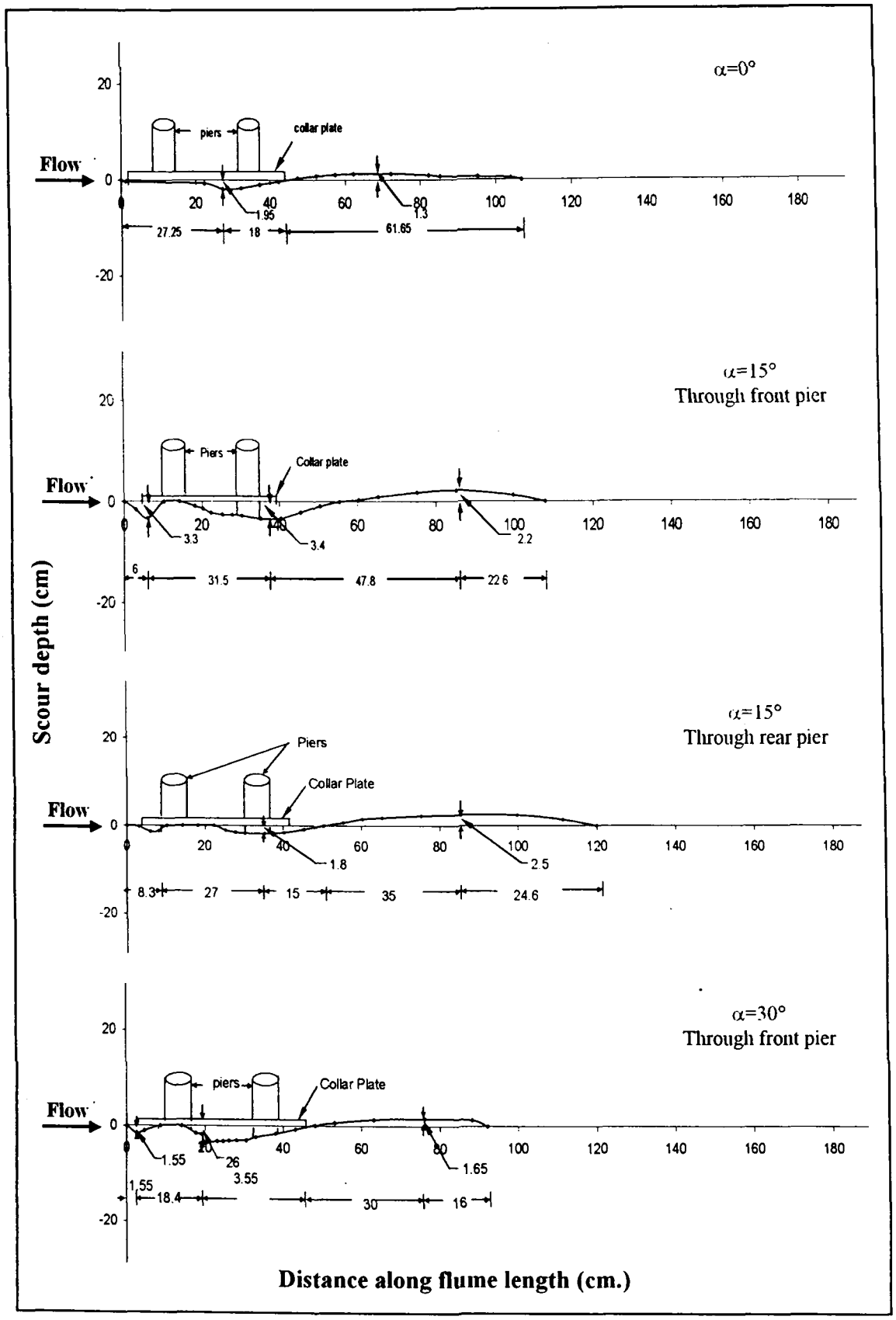

Longitudinal profiles for group of two piers with & without collar for varied angles of attack 'α'.

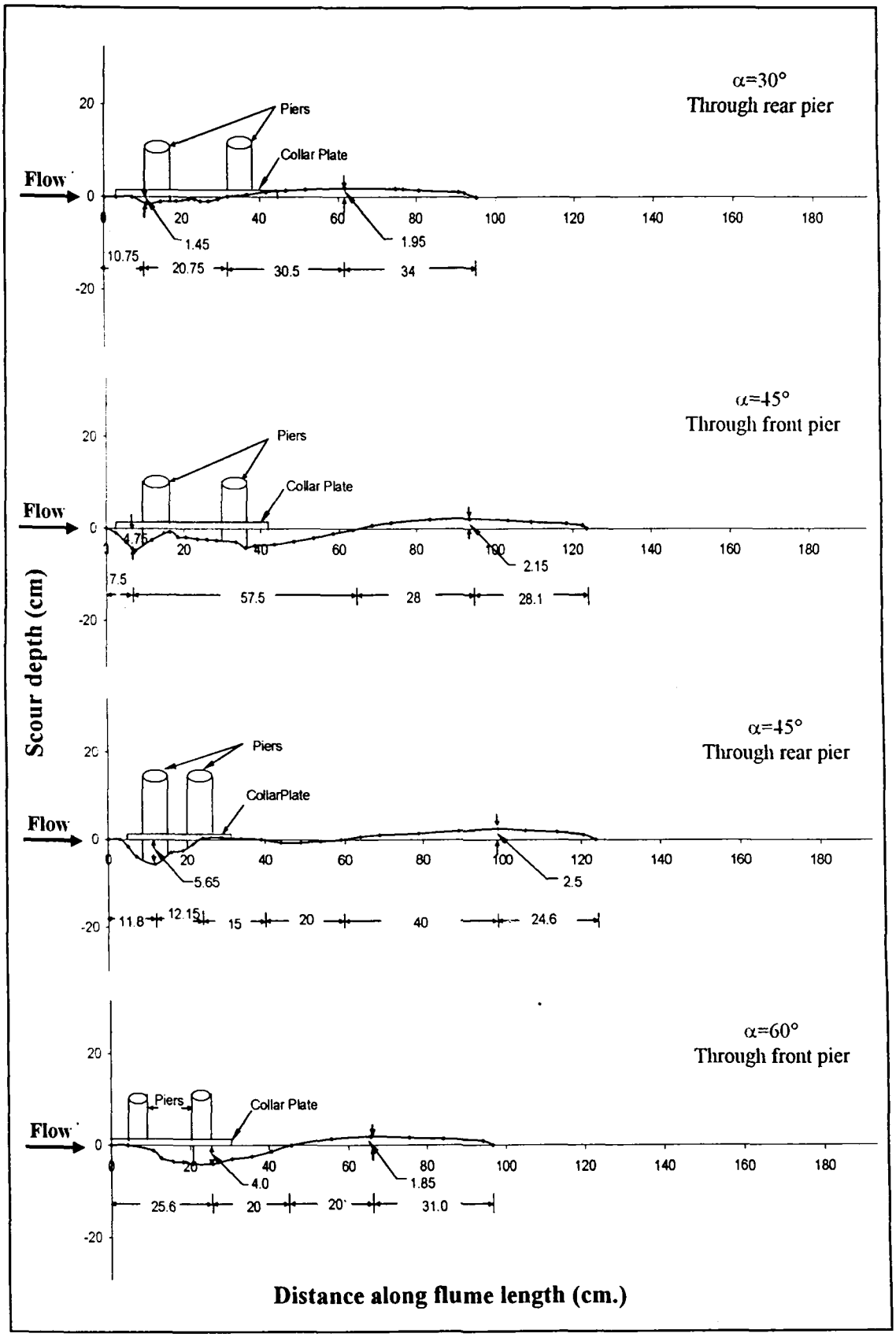

Longitudinal profiles for group of two piers with & without collar for varied angles of attack 'α'.

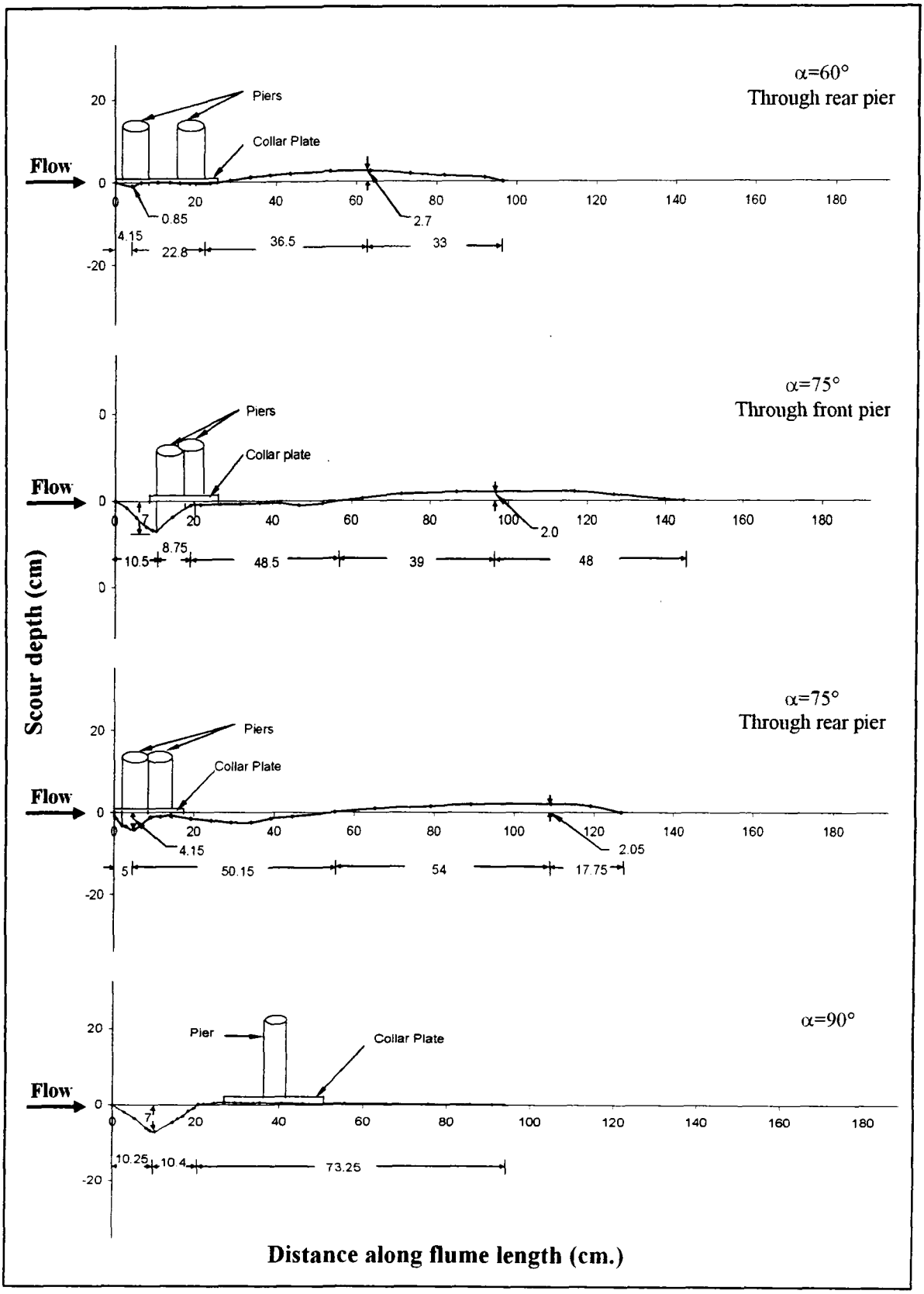

Longitudinal profiles for group of two piers with & without collar for varied angles of attack 'α'.

APPENDIX – III

LATERAL PROFILES OF SCOUR

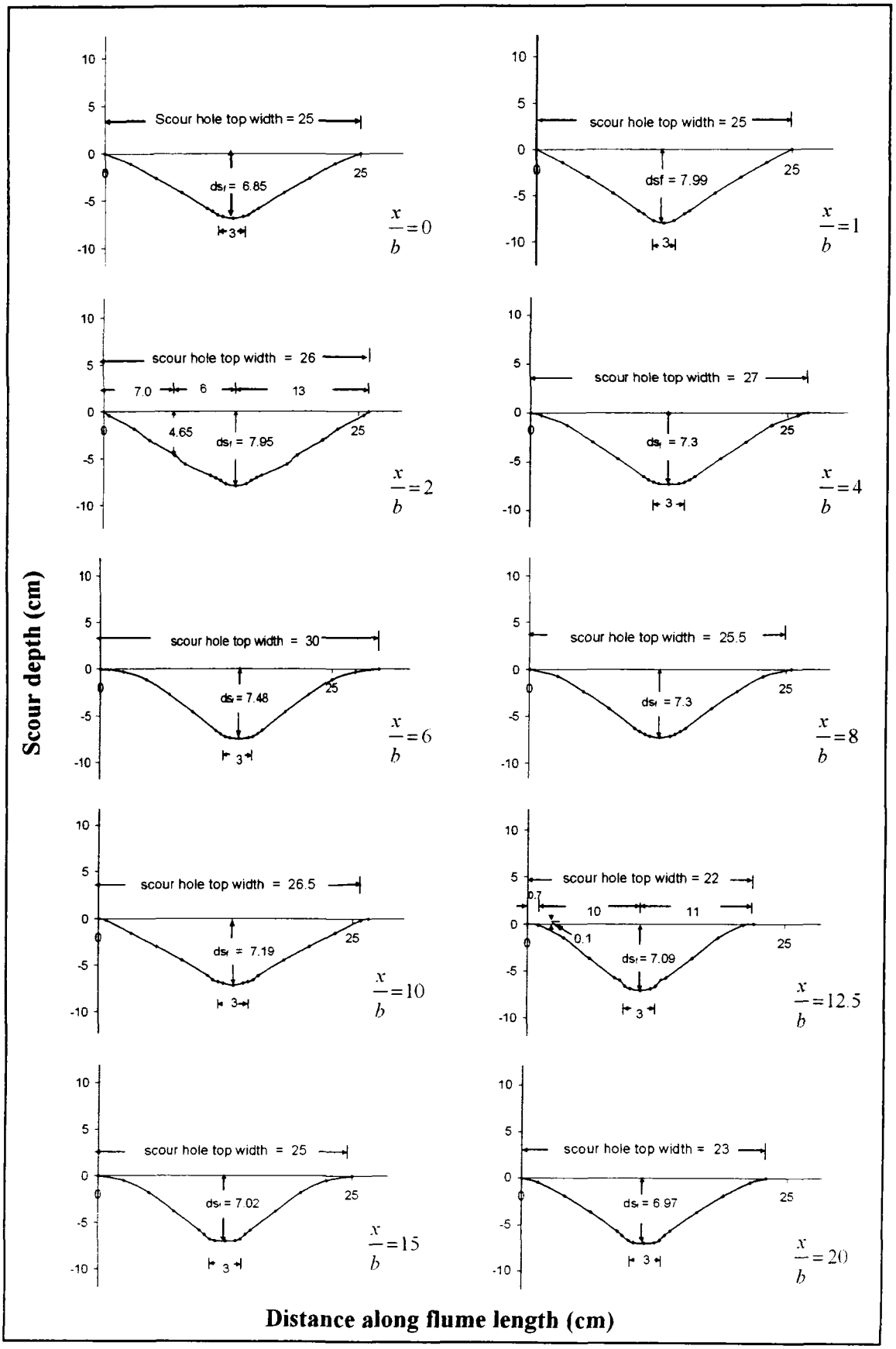

Lateral profiles around front pier for two piers of same size in tandem arrangement for varied pier spacing x/b.

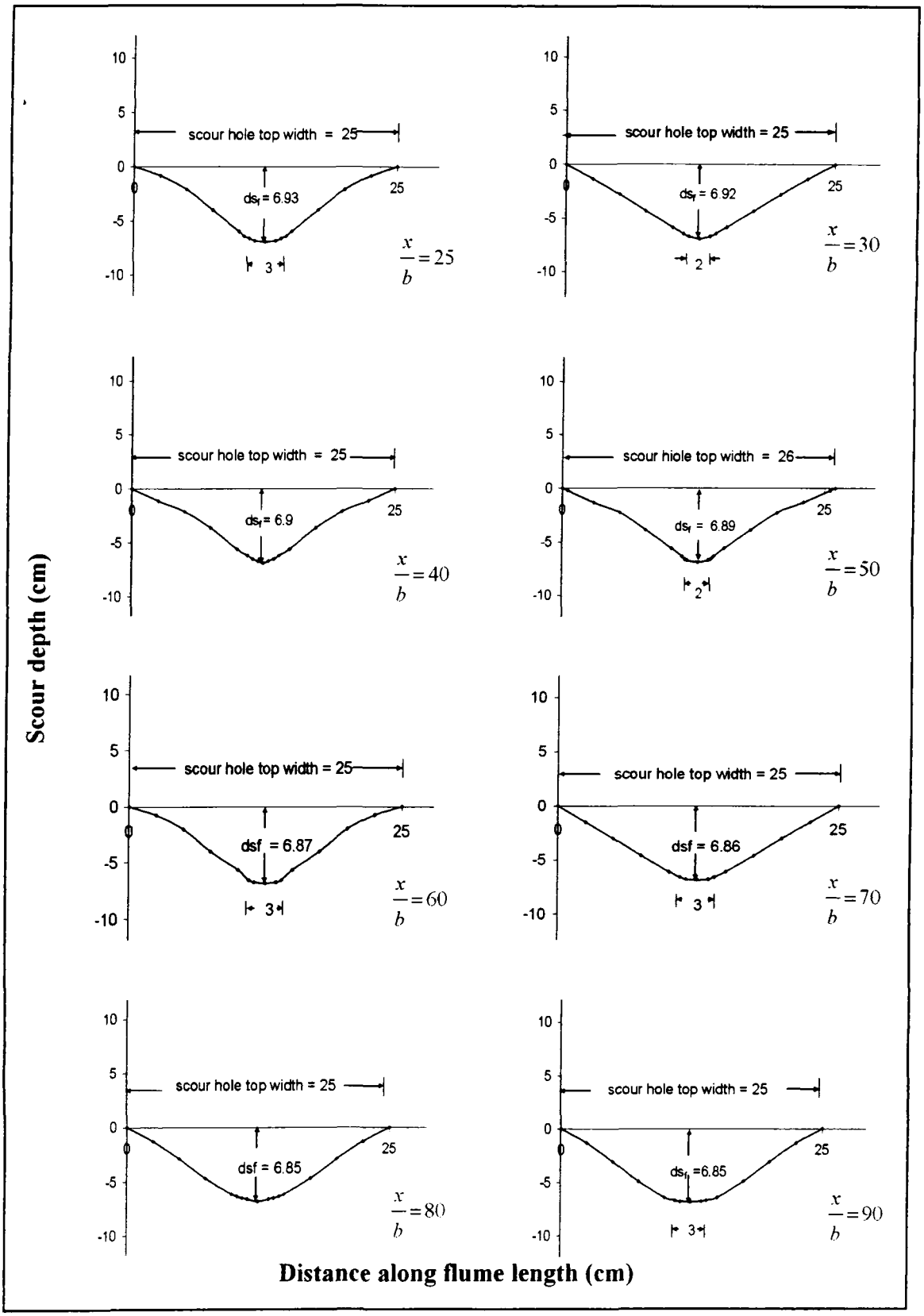

Lateral profiles around front pier for two piers of same size in tandem arrangement for varied pier spacing x/b.

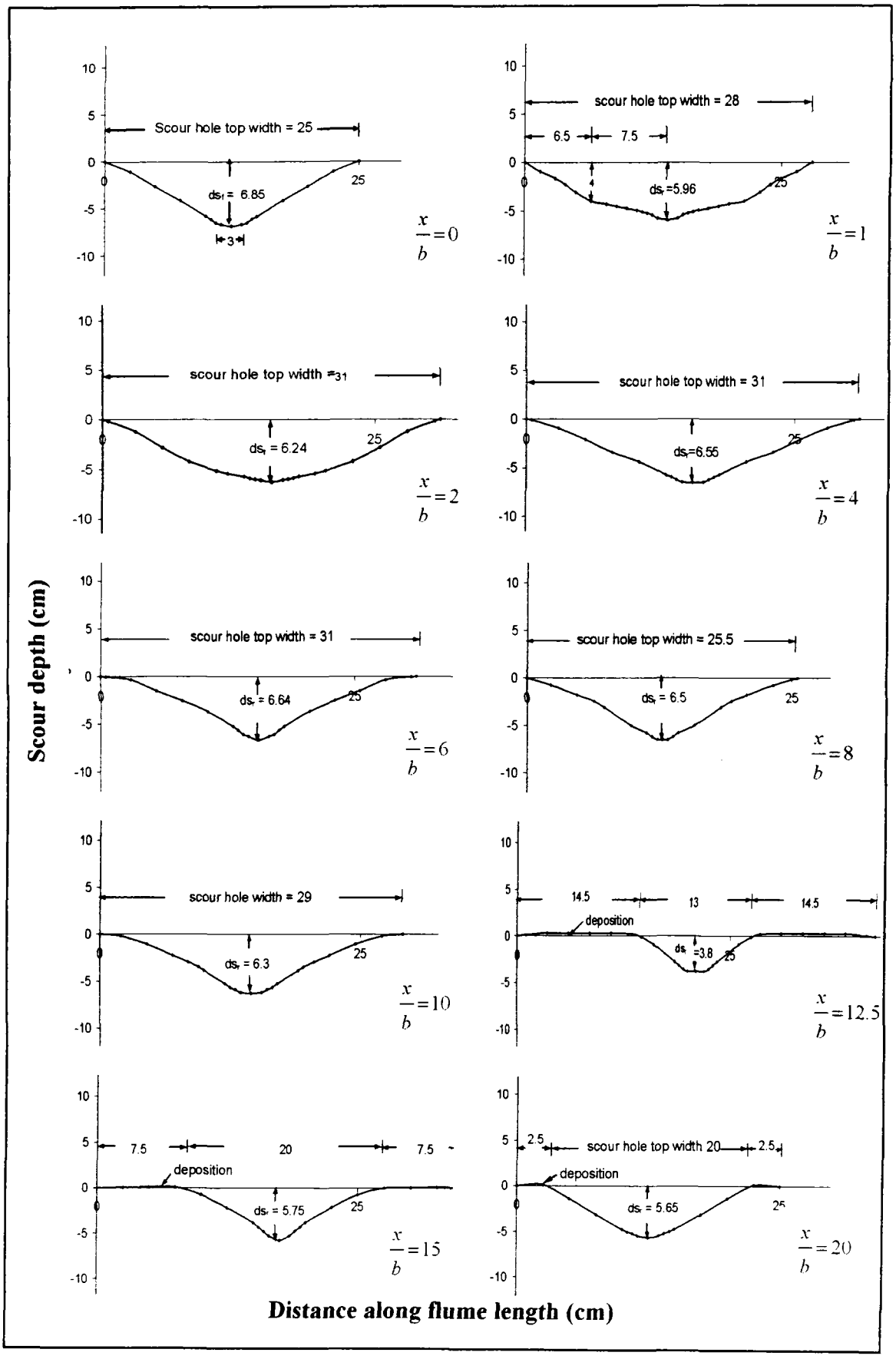

Lateral profiles around rear pier for two piers of same size in tandem arrangement for varied pier spacing x/b.

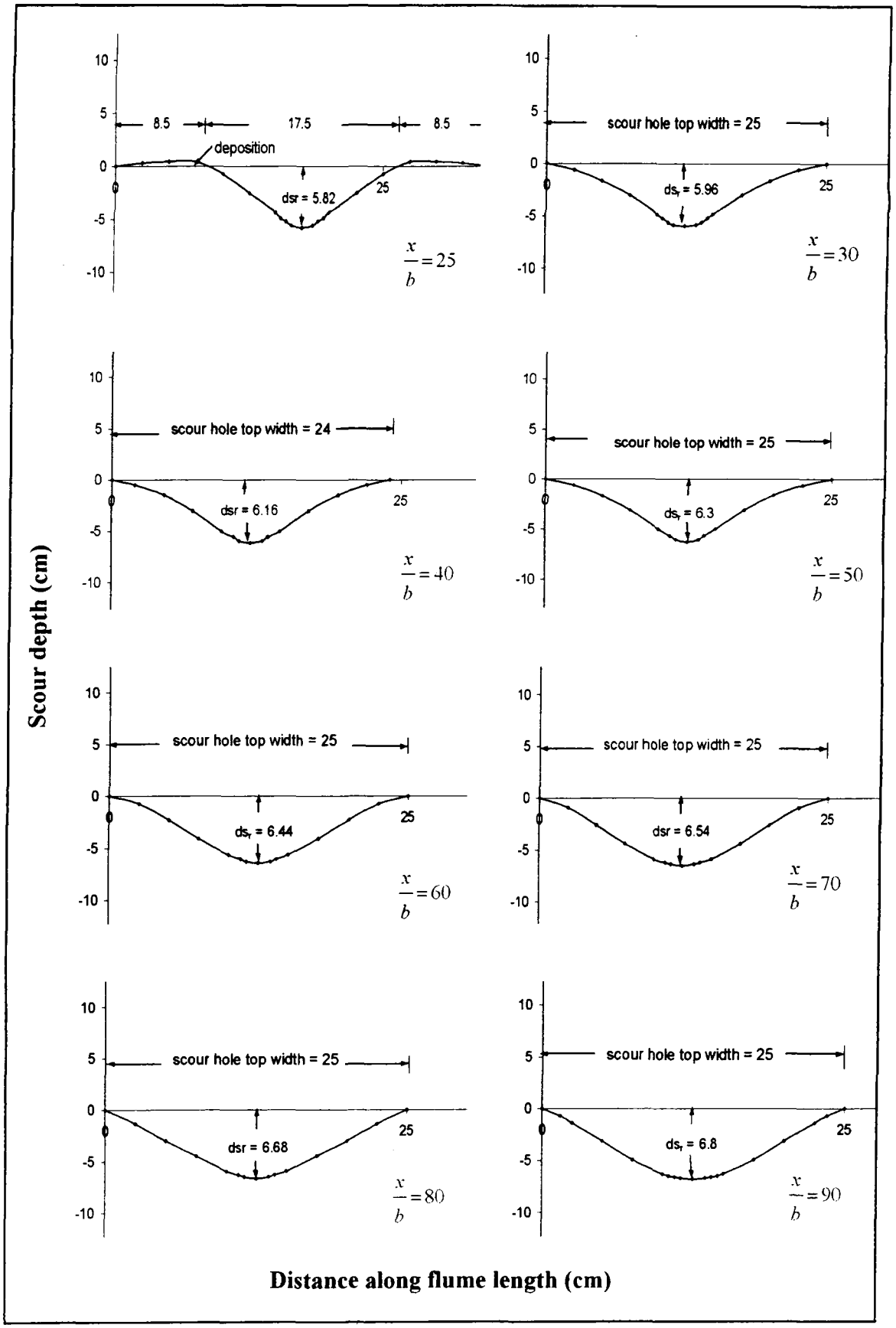

Lateral profiles around rear pier for two piers of same size in tandem arrangement for varied pier spacing x/b.

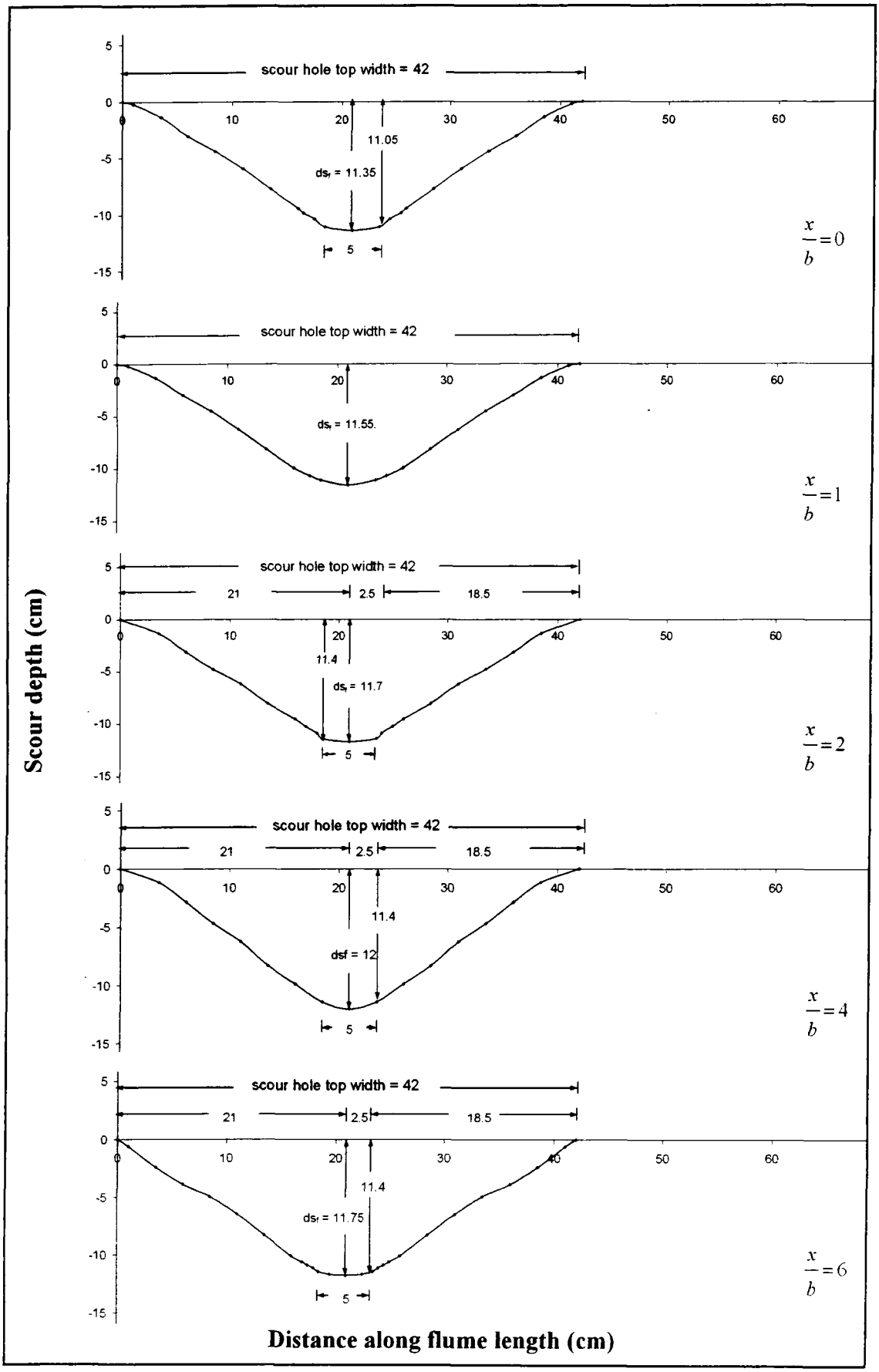

Lateral profiles around 6.6 cm front pier (big pier) for two piers of different size in tandem arrangement for varied pier spacing x/b

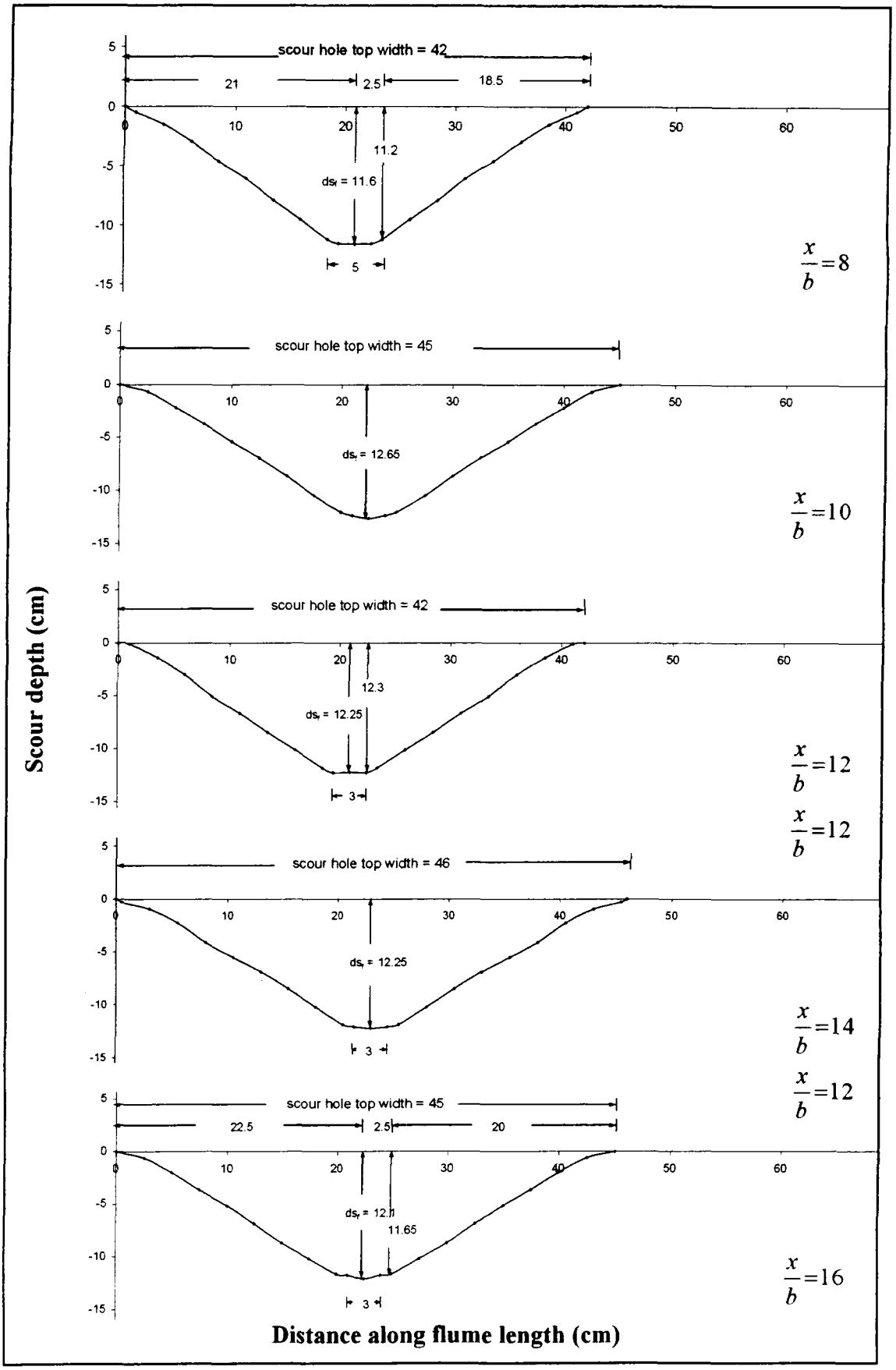

Lateral profiles around 6.6 cm front pier (big pier) for two piers of different size in tandem arrangement for varied pier spacing x/b

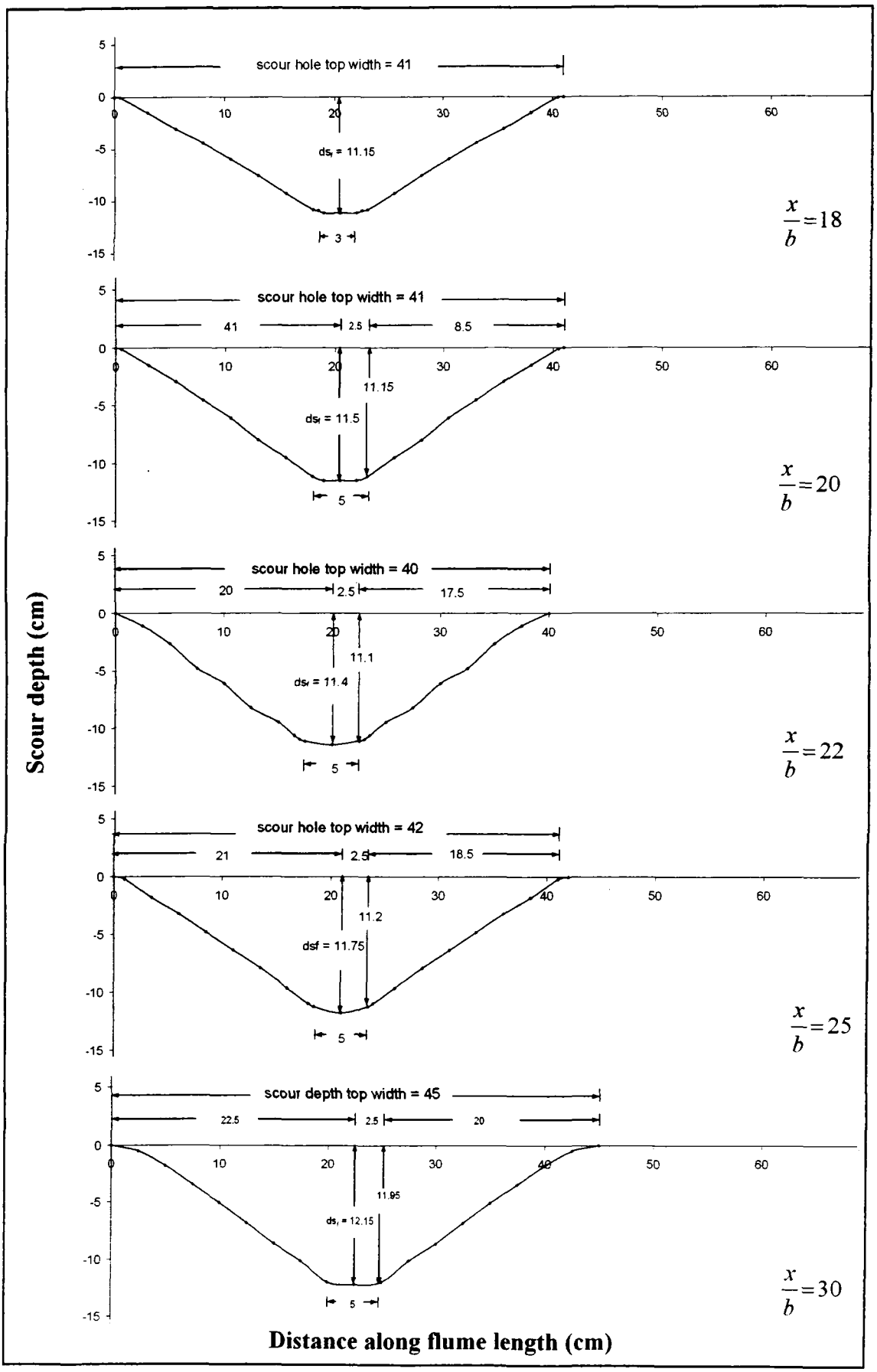

Lateral profiles around 6.6 cm front pier (big pier) for two piers of different size in tandem arrangement for varied pier spacing x/b

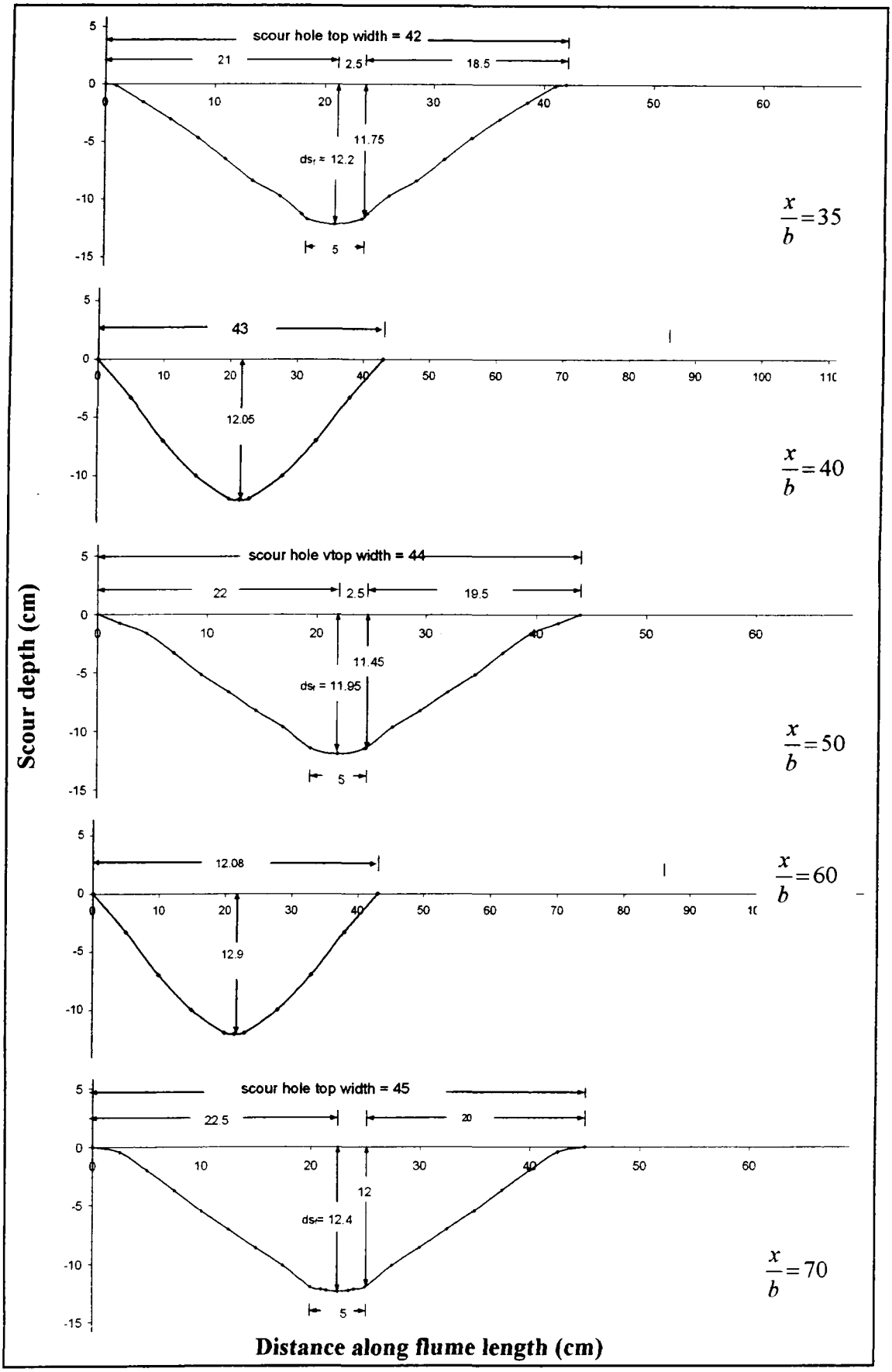

Lateral profiles around 6.6 cm front pier (big pier) for two piers of different size in tandem arrangement for varied pier spacing x/b

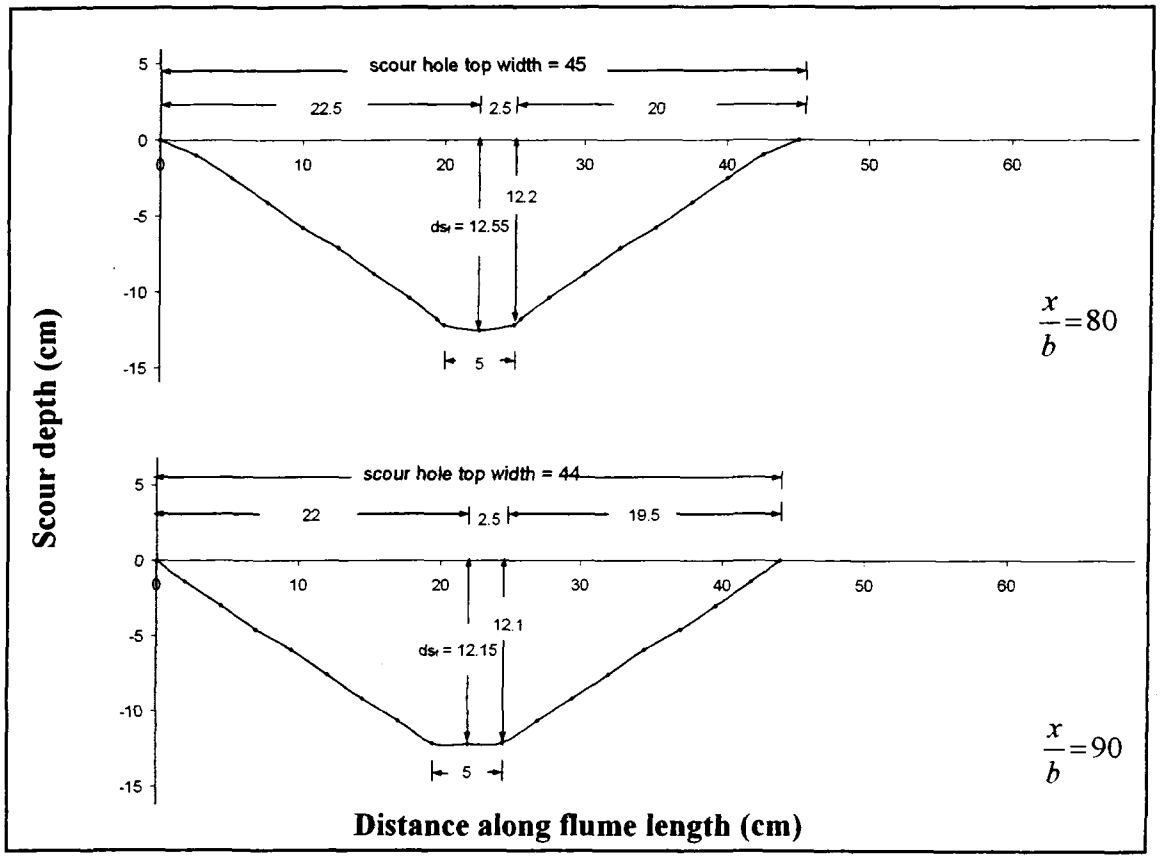

Lateral profiles around 6.6 cm front pier (big pier) for two piers of different size in tandem arrangement for varied pier spacing x/b

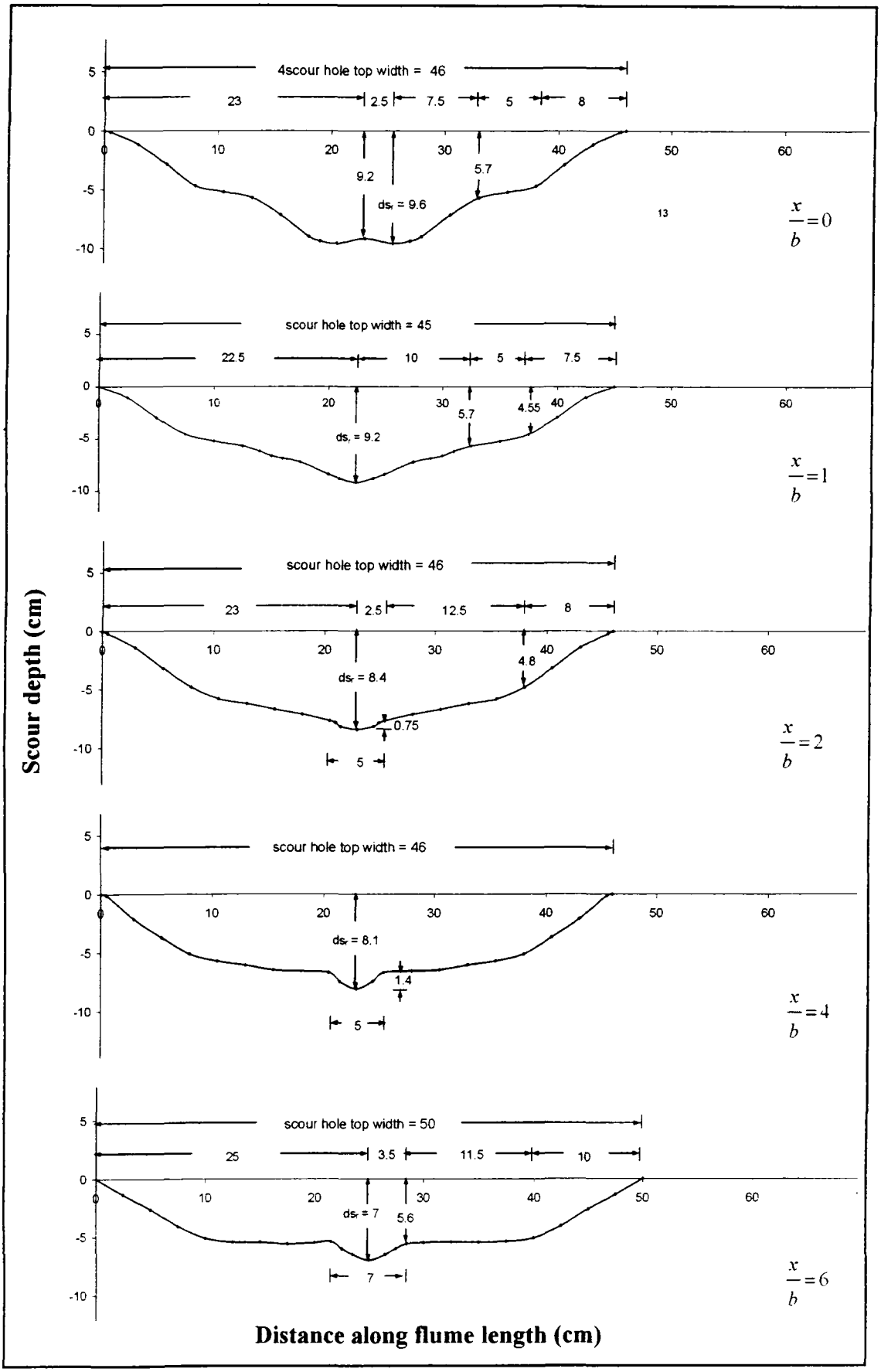

Lateral profiles around 3.3 cm rear pier (small pier) for two piers of different size in tandem arrangement for varied pier spacing x/b

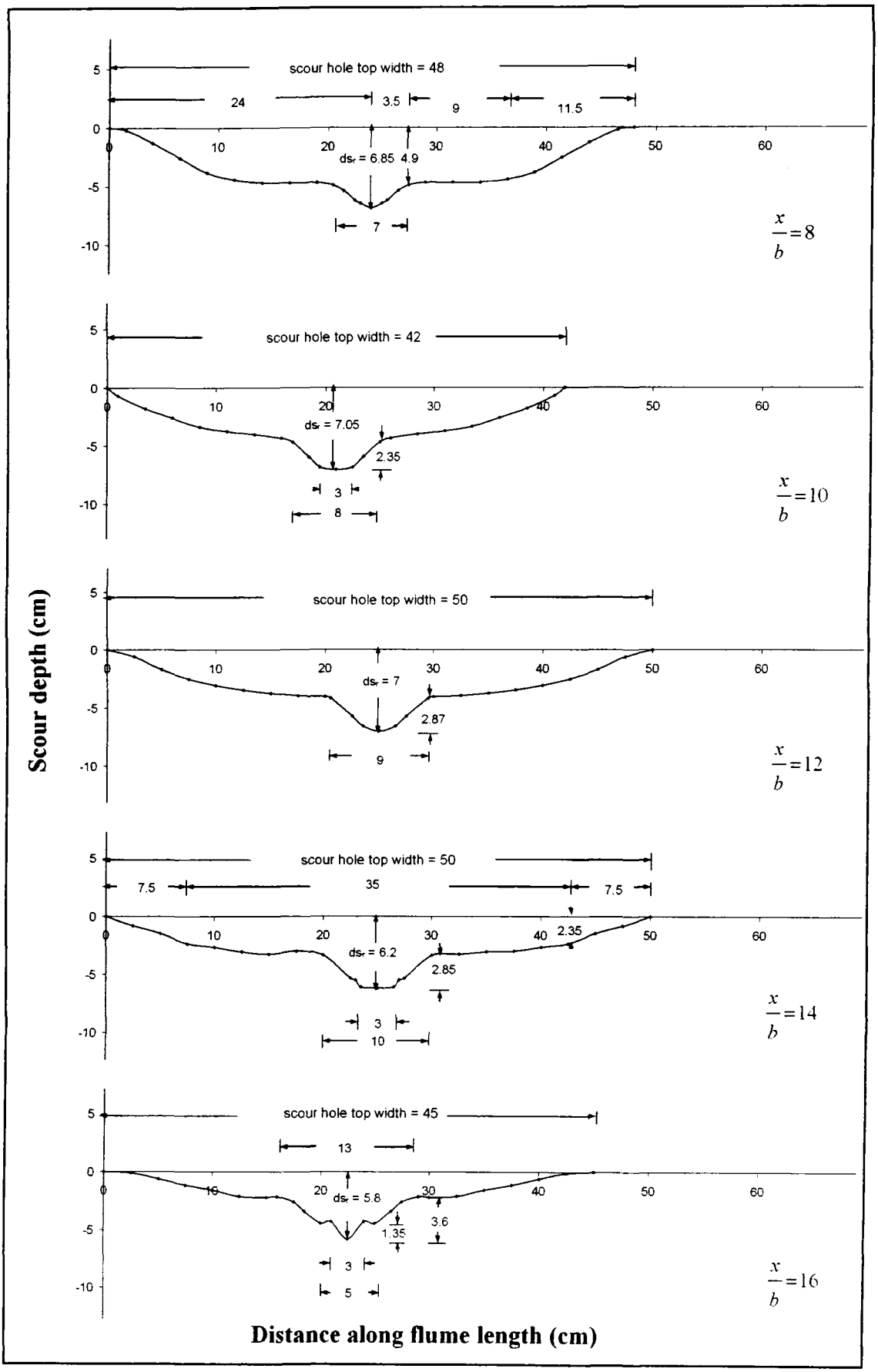

Lateral profiles around 3.3 cm rear pier (small pier) for two piers of different size in tandem arrangement for varied pier spacing x/b

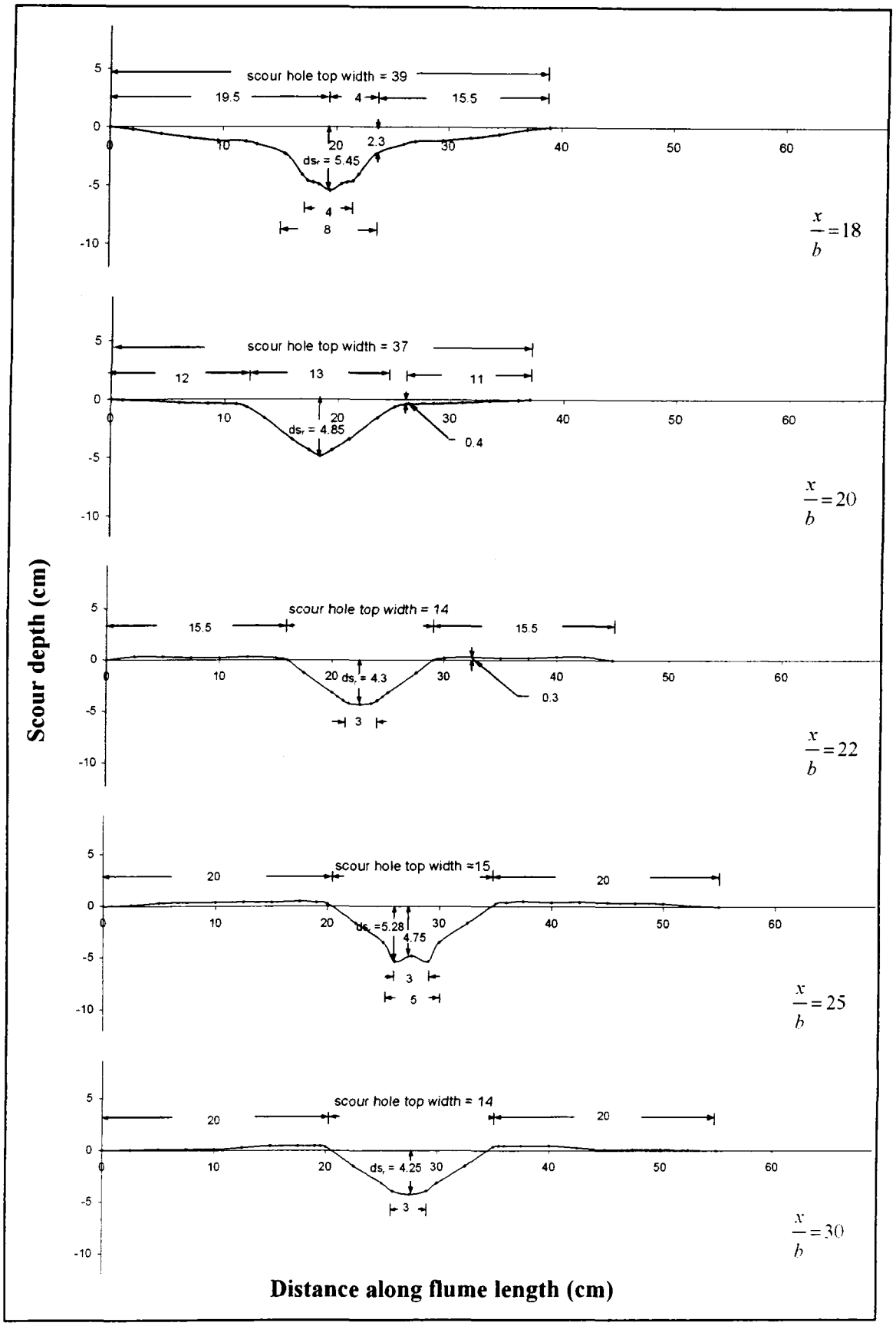

Lateral profiles around 3.3 cm rear pier (small pier) for two piers of different size in tandem arrangement for varied pier spacing x/b

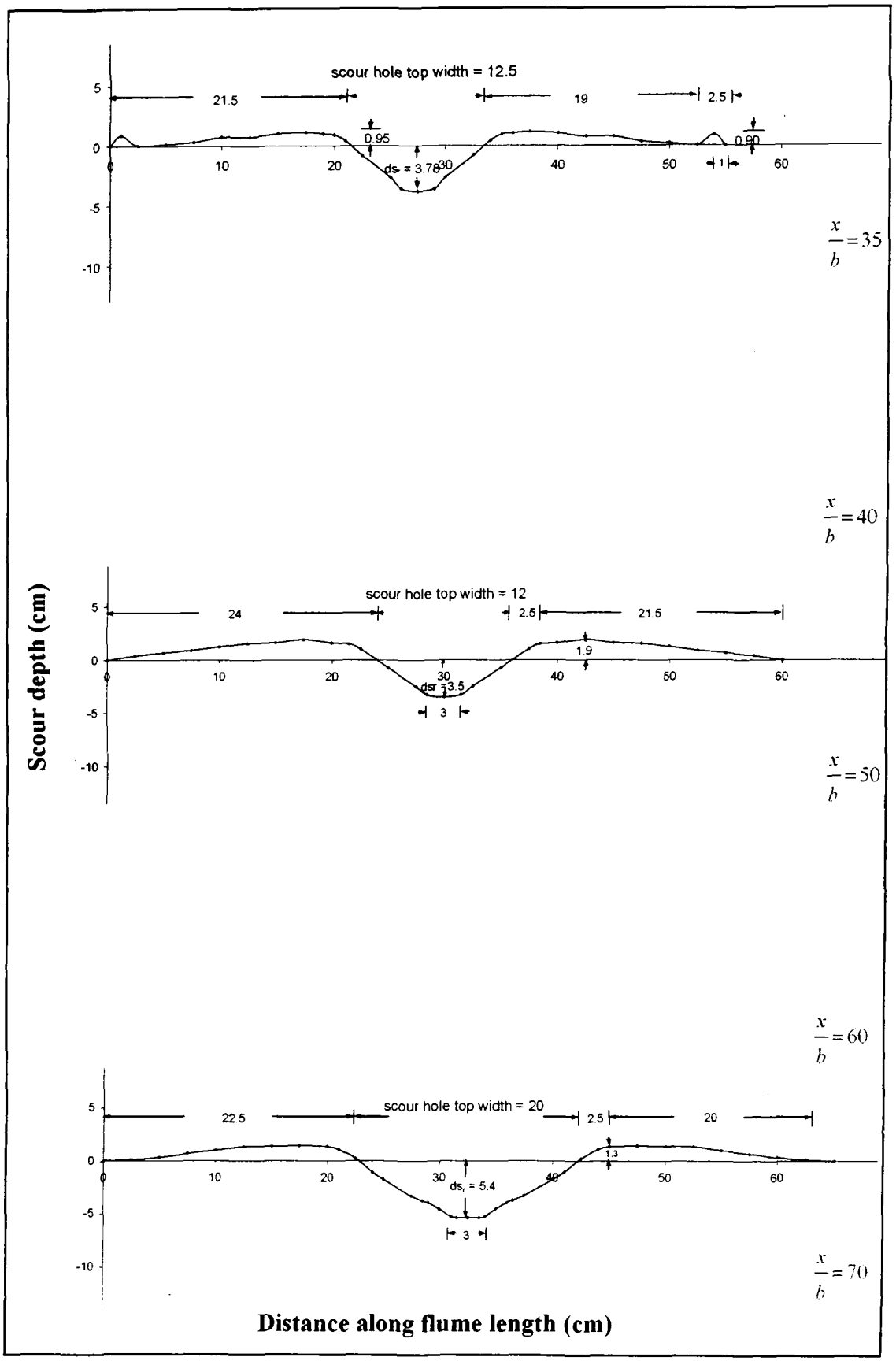

Lateral profiles around 3.3 cm rear pier (small pier) for two piers of different size in tandem arrangement for varied pier spacing x/b

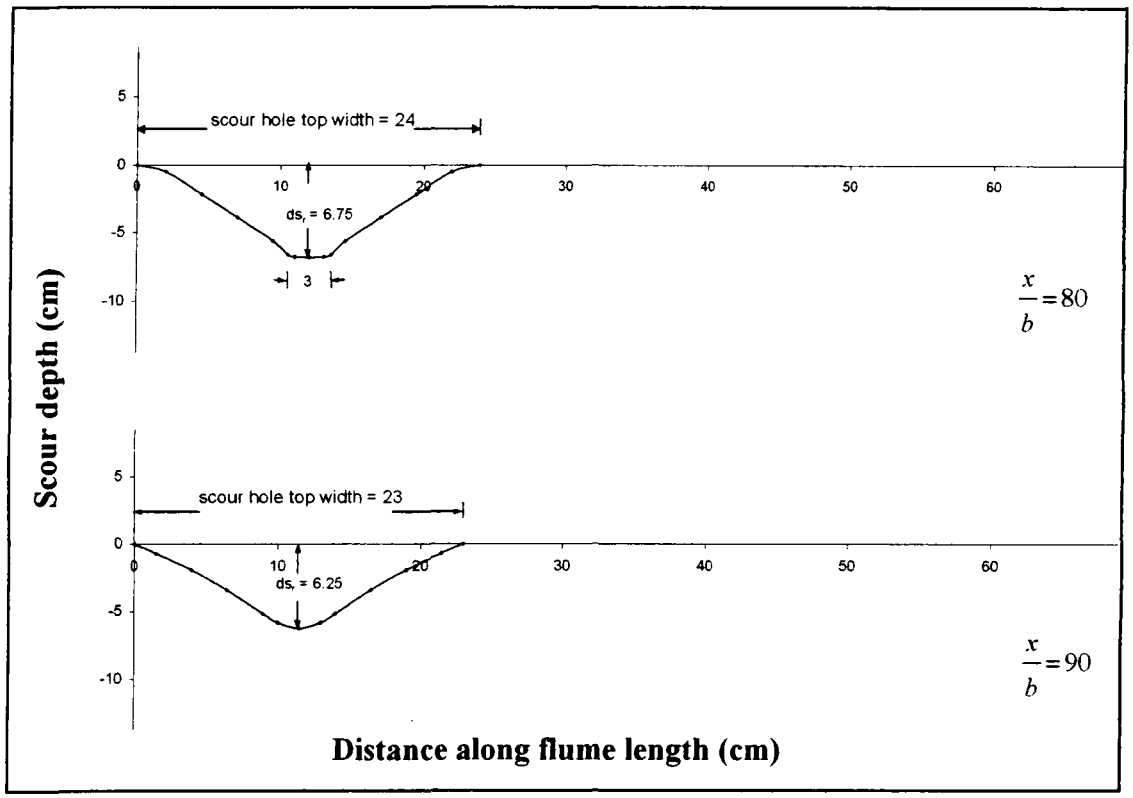

Lateral profiles around 3.3 cm rear pier (small pier) for two piers of different size in tandem arrangement for varied pier spacing x/b

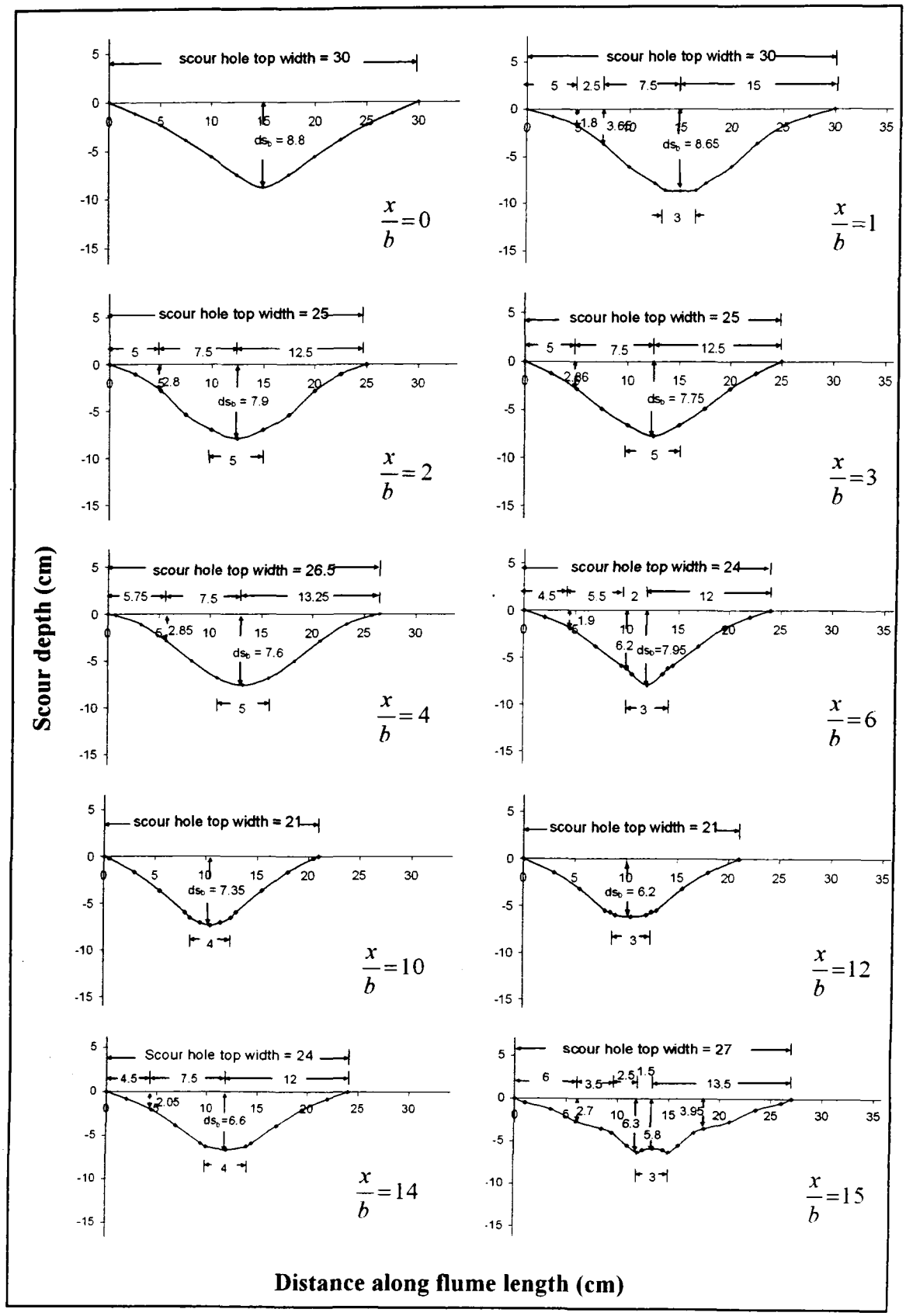

Lateral profiles around 3.3 cm front pier (small pier) for two piers of different size in tandem arrangement for varied pier spacing x/b

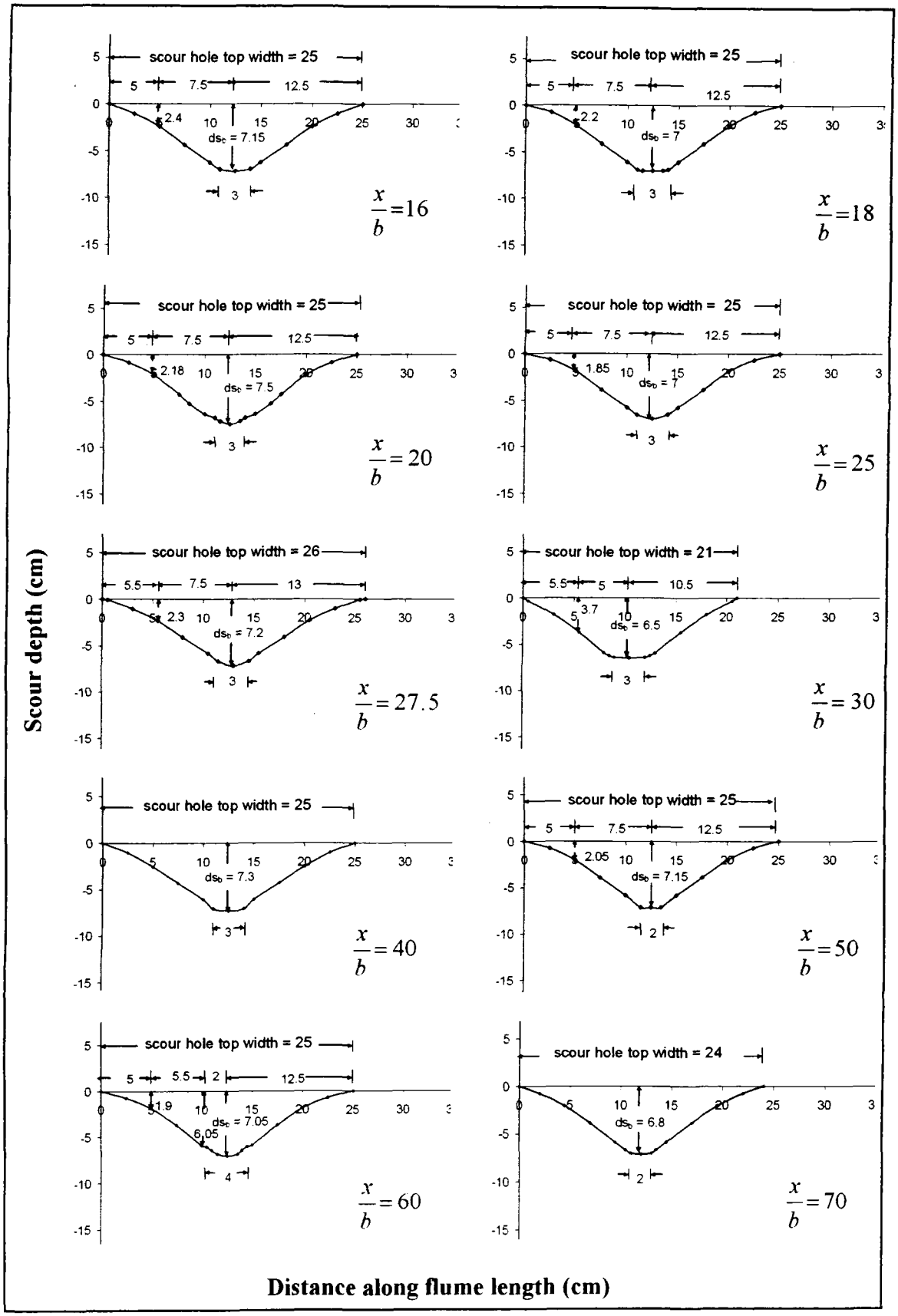

Lateral profiles around 3.3 cm front pier (small pier) for two piers of different size in tandem arrangement for varied pier spacing x/b

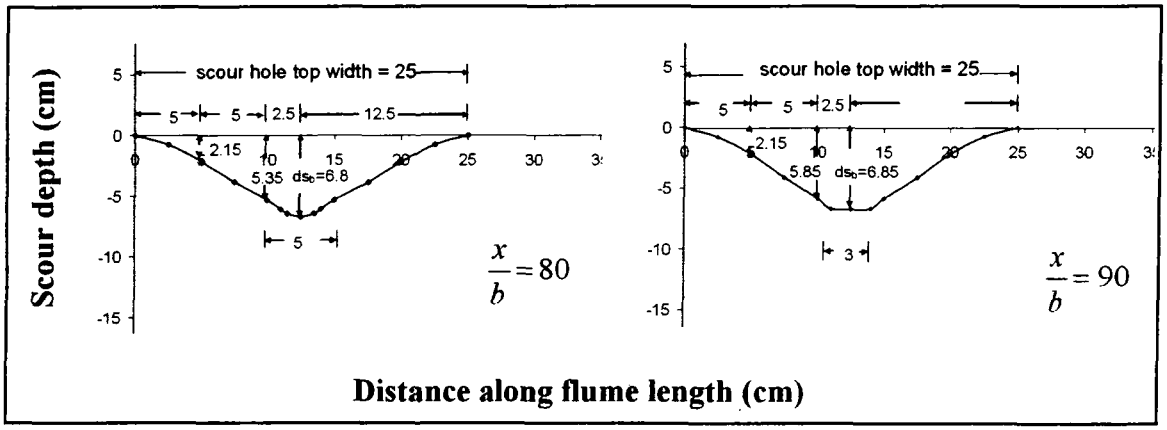

Lateral profiles around 3.3 cm front pier (small pier) for two piers of different size in tandem arrangement for varied pier spacing x/b

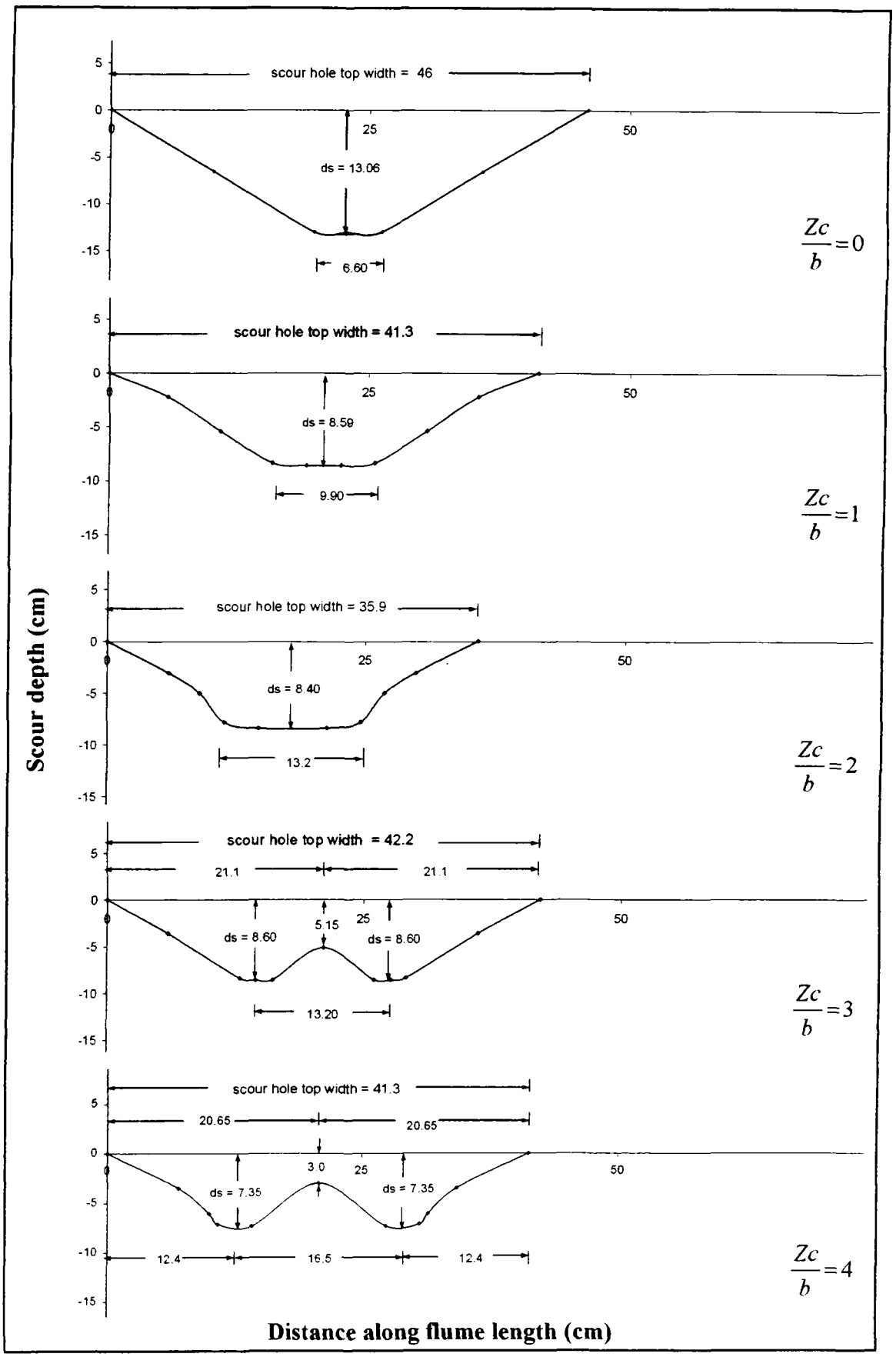

Lateral profiles around two piers of same size in transverse arrangement for varied pier spacing Zc/b

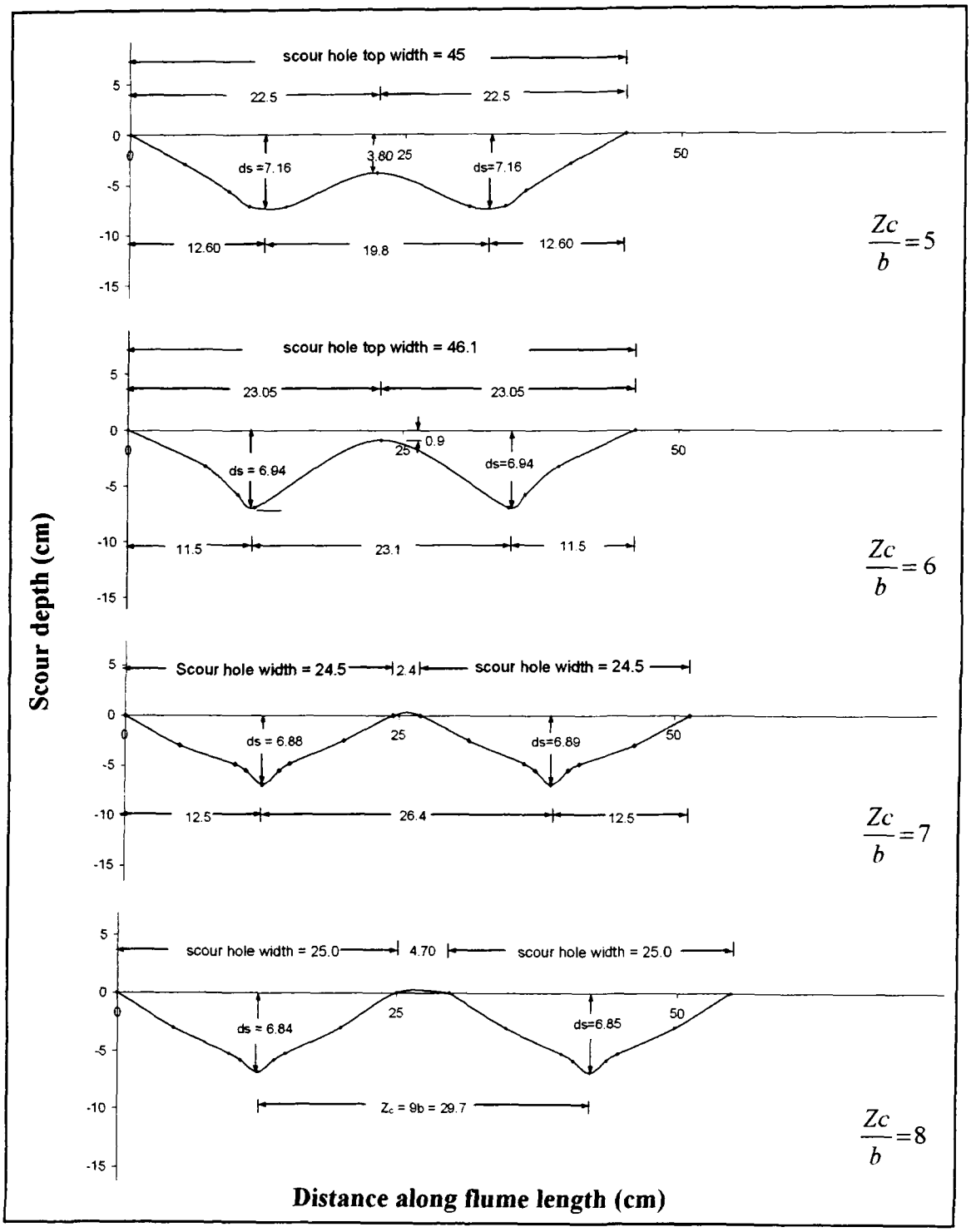

Lateral profiles around two piers of same size in transverse arrangement for varied pier spacing Zc/b

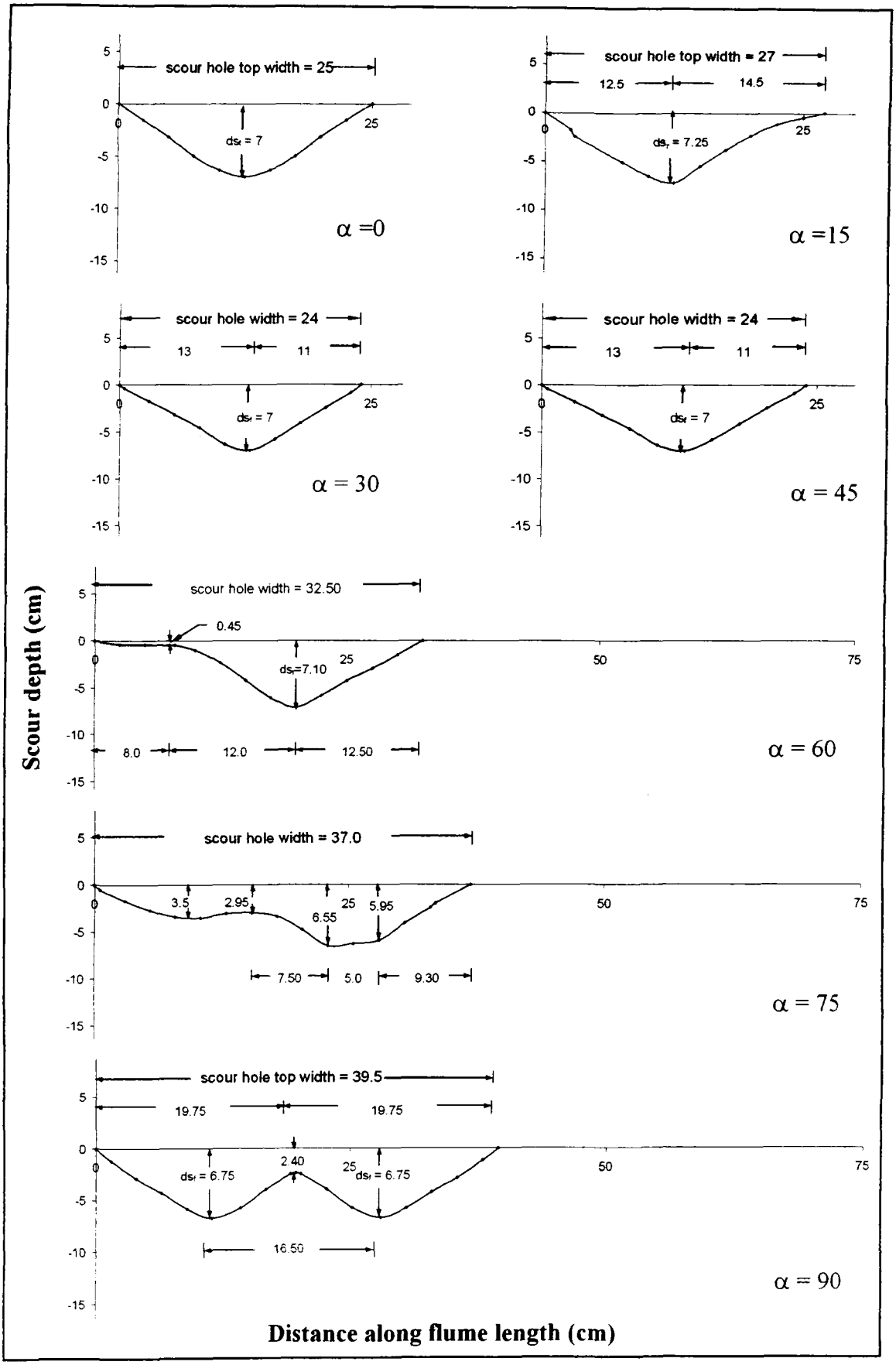

Lateral profiles around front pier of a group of two piers of same size at constant radial pier spacing R/b = 5 and various angles of attack 'α'

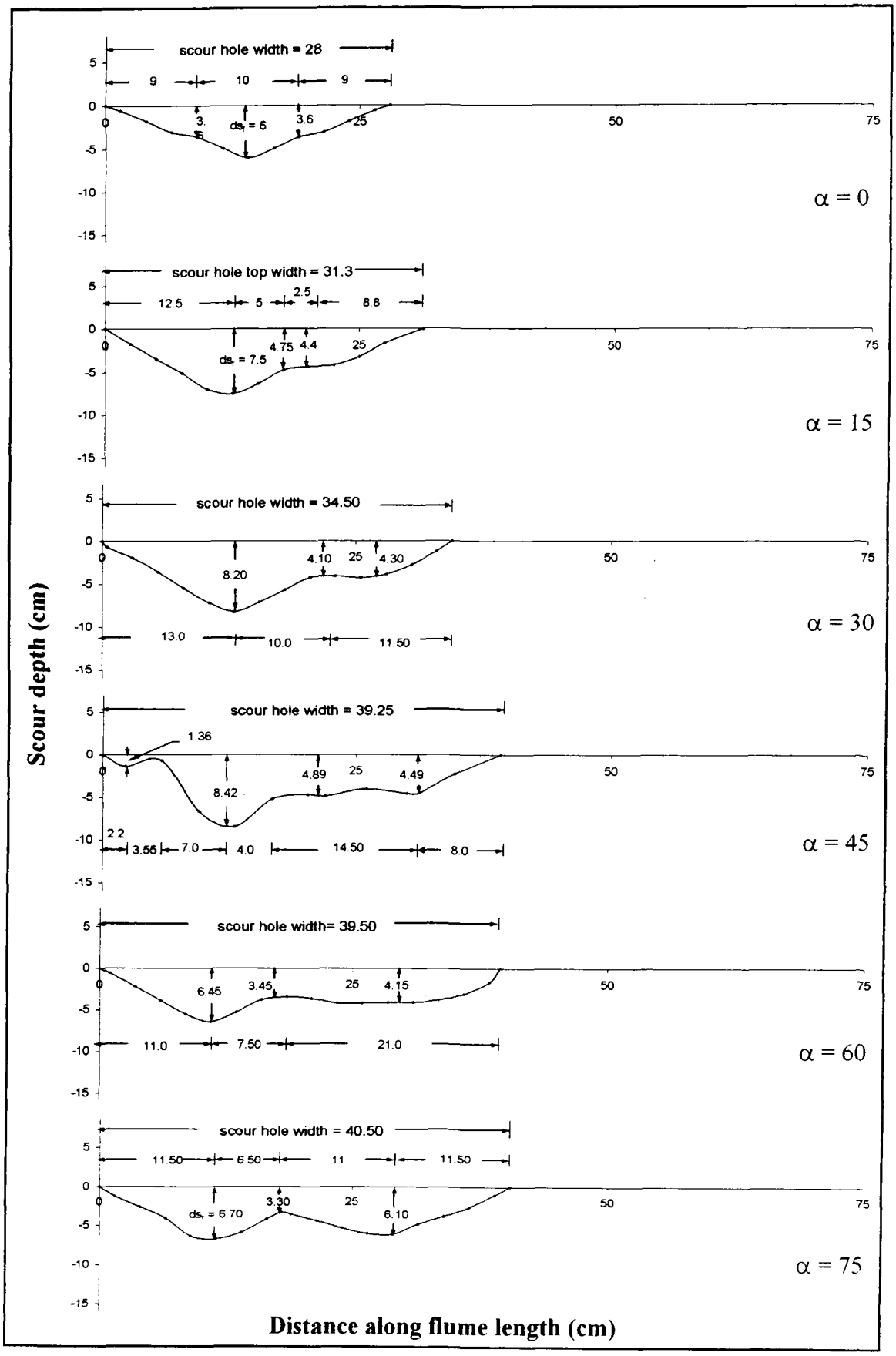

Lateral profiles around rear pier of a group of two piers of same size at constant radial pier spacing R/b = 5 and various angles of attack 'α'

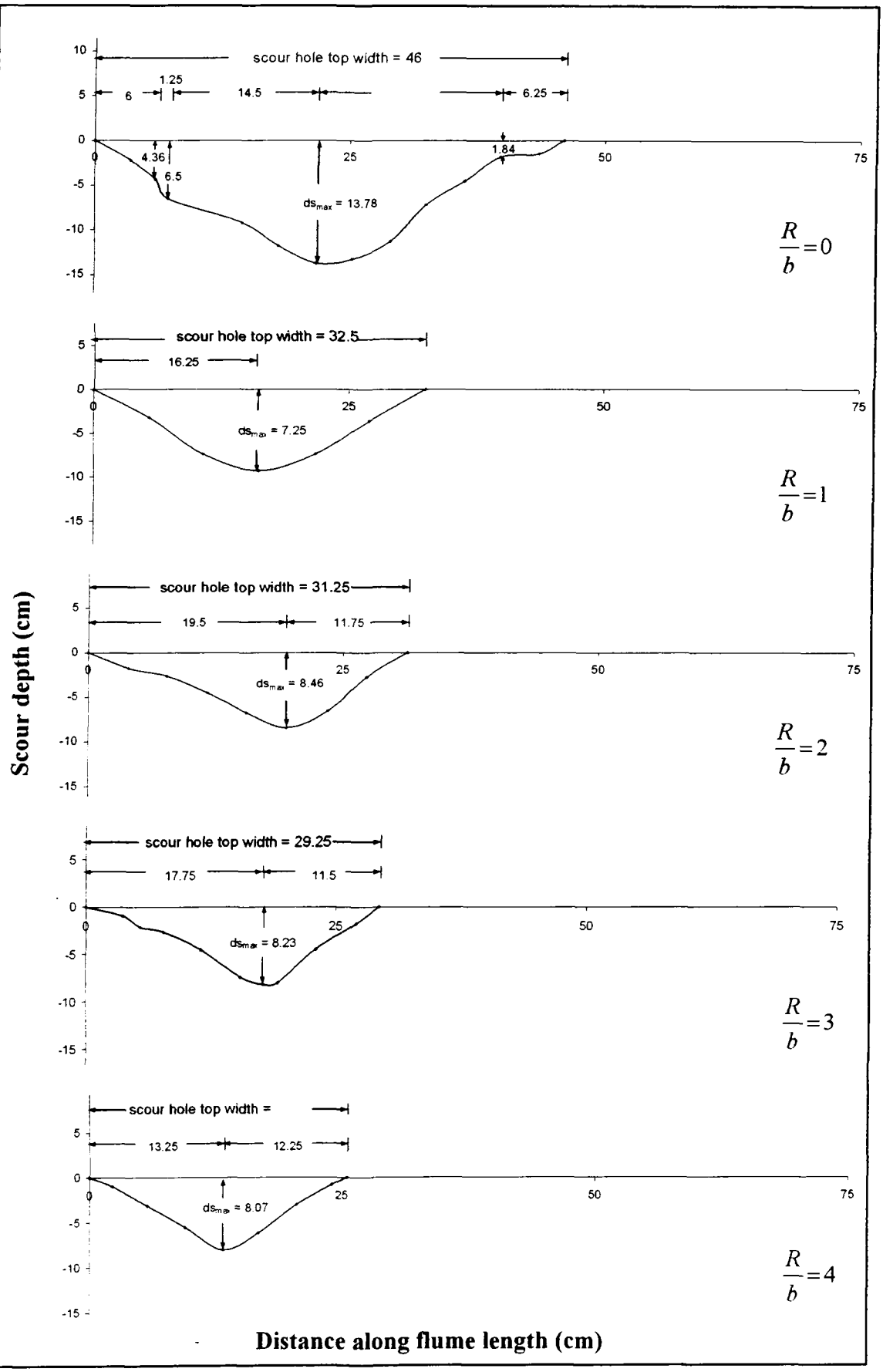

Lateral profiles around front pier of a group of two piers of same size at constant angle of attack α = 45 and varied radial pier spacing R/b

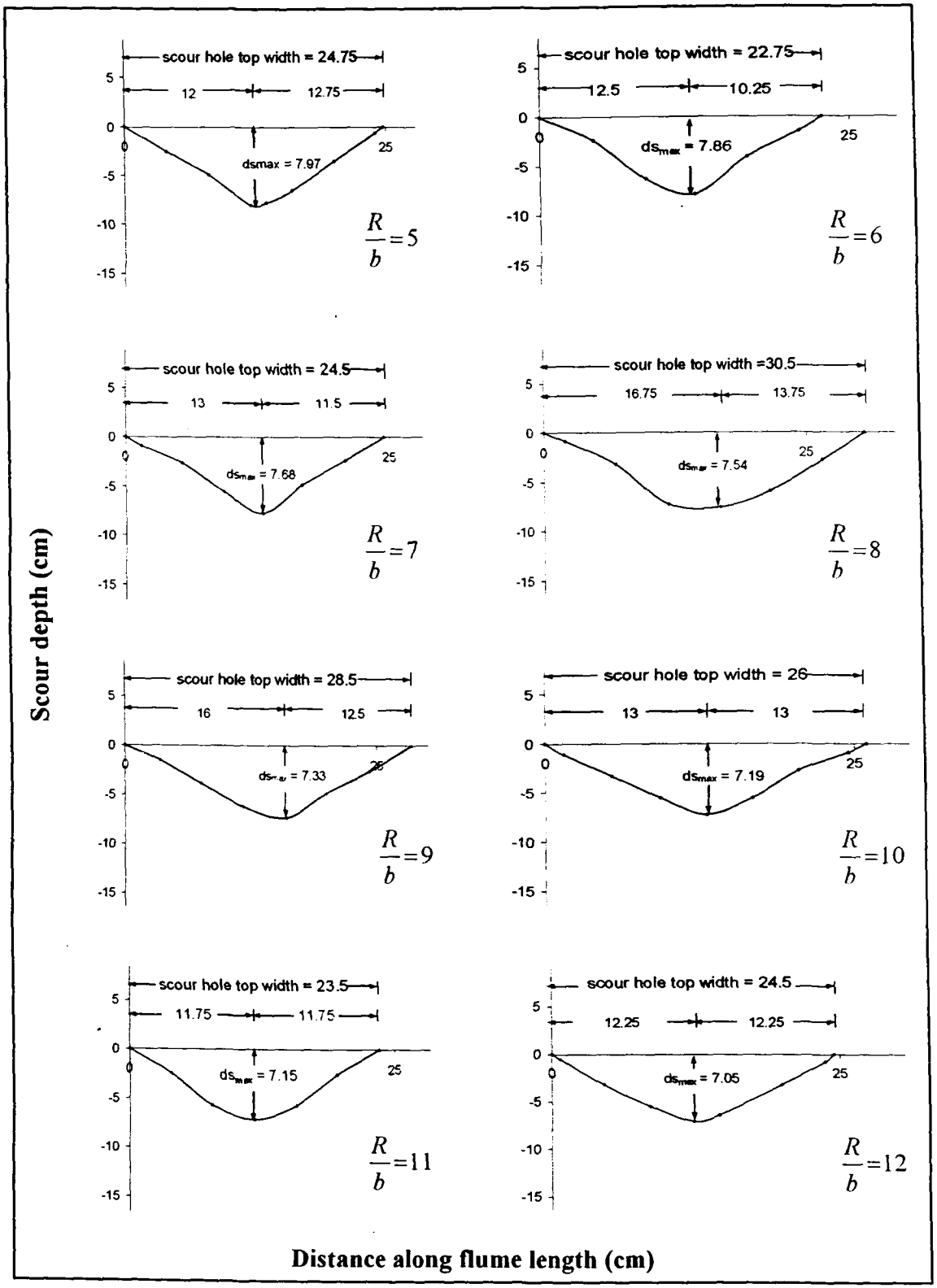

Lateral profiles around front pier of a group of two piers of same size at constant angle of attack α = 45 and varied radial pier spacing R/b

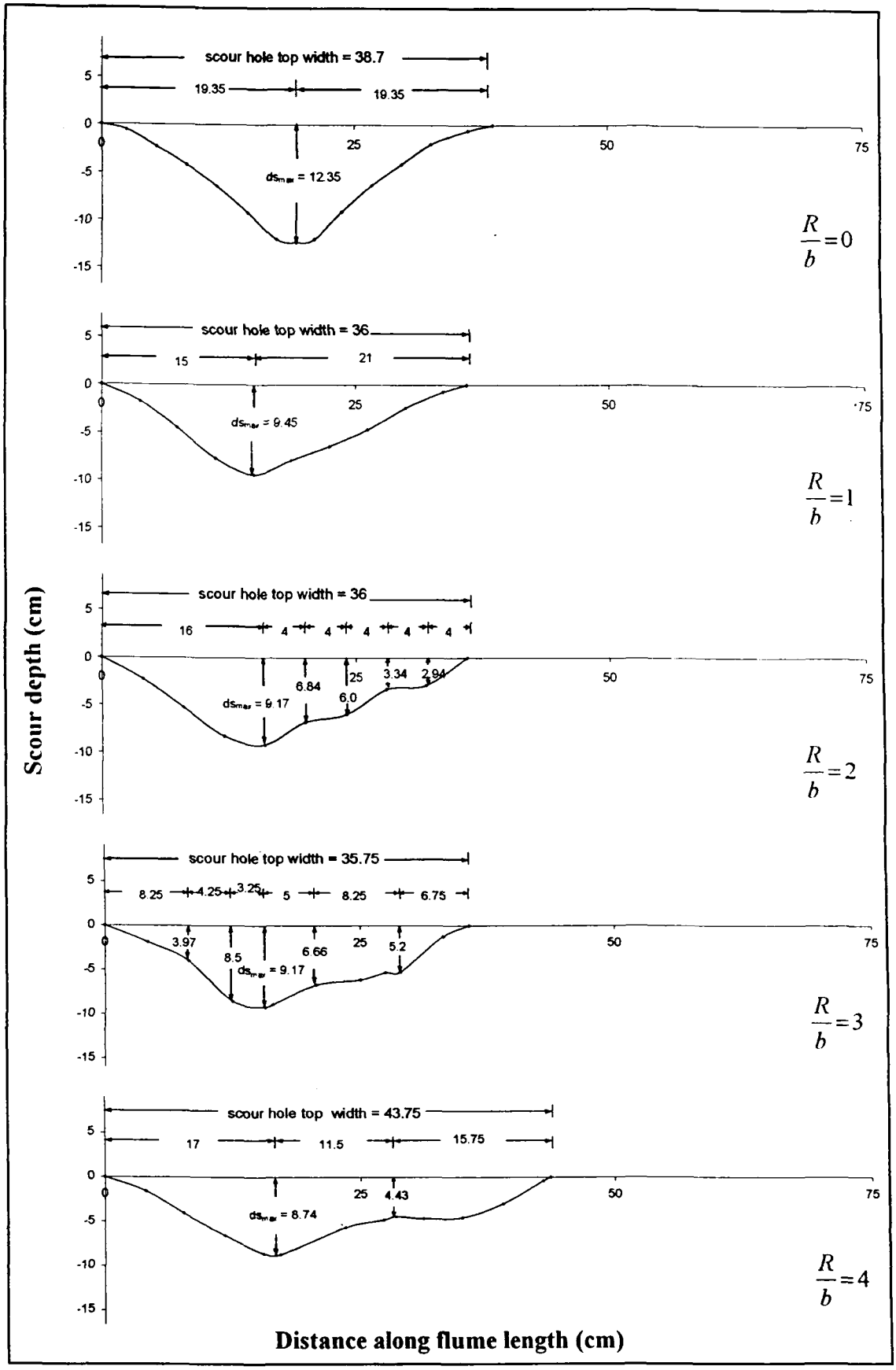

Lateral profiles around rear pier of a group of two piers of same size at constant angle of attack α = 45 and varied radial pier spacing R/b

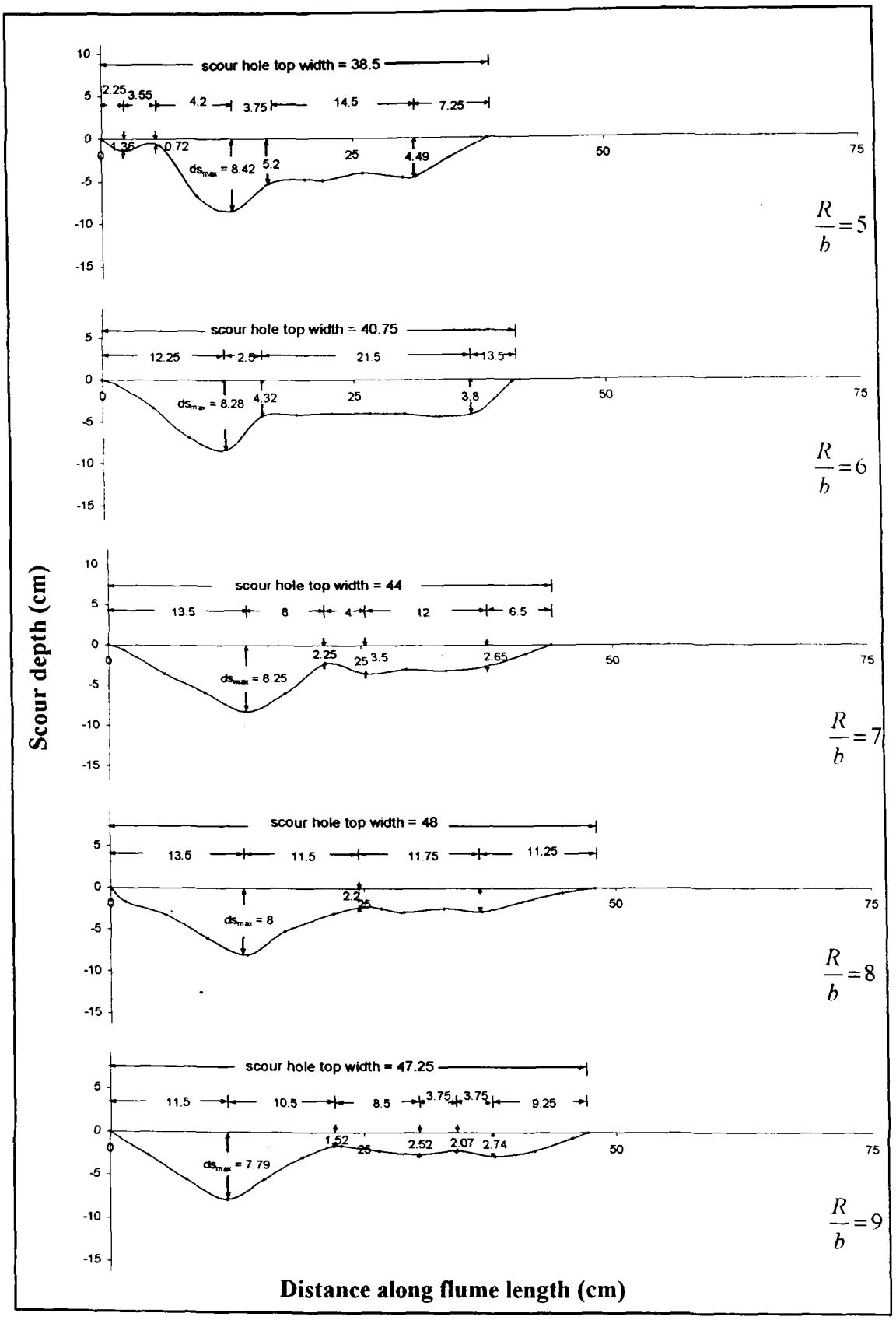

Lateral profiles around rear pier of a group of two piers of same size at constant angle of attack α = 45 and varied radial pier spacing R/b

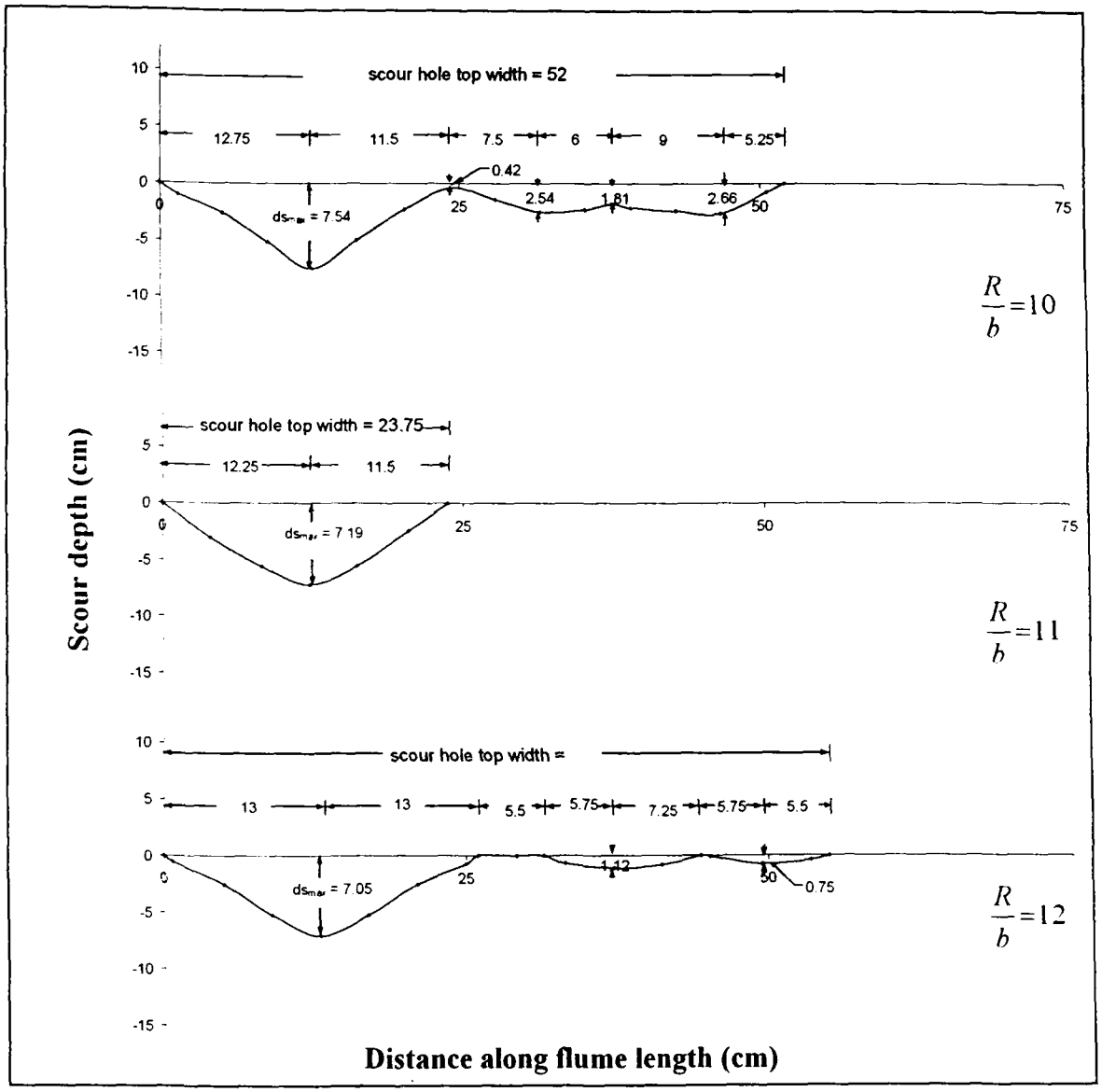

Lateral profiles around rear pier of a group of two piers of same size at constant angle of attack α = 45 and varied radial pier spacing R/b

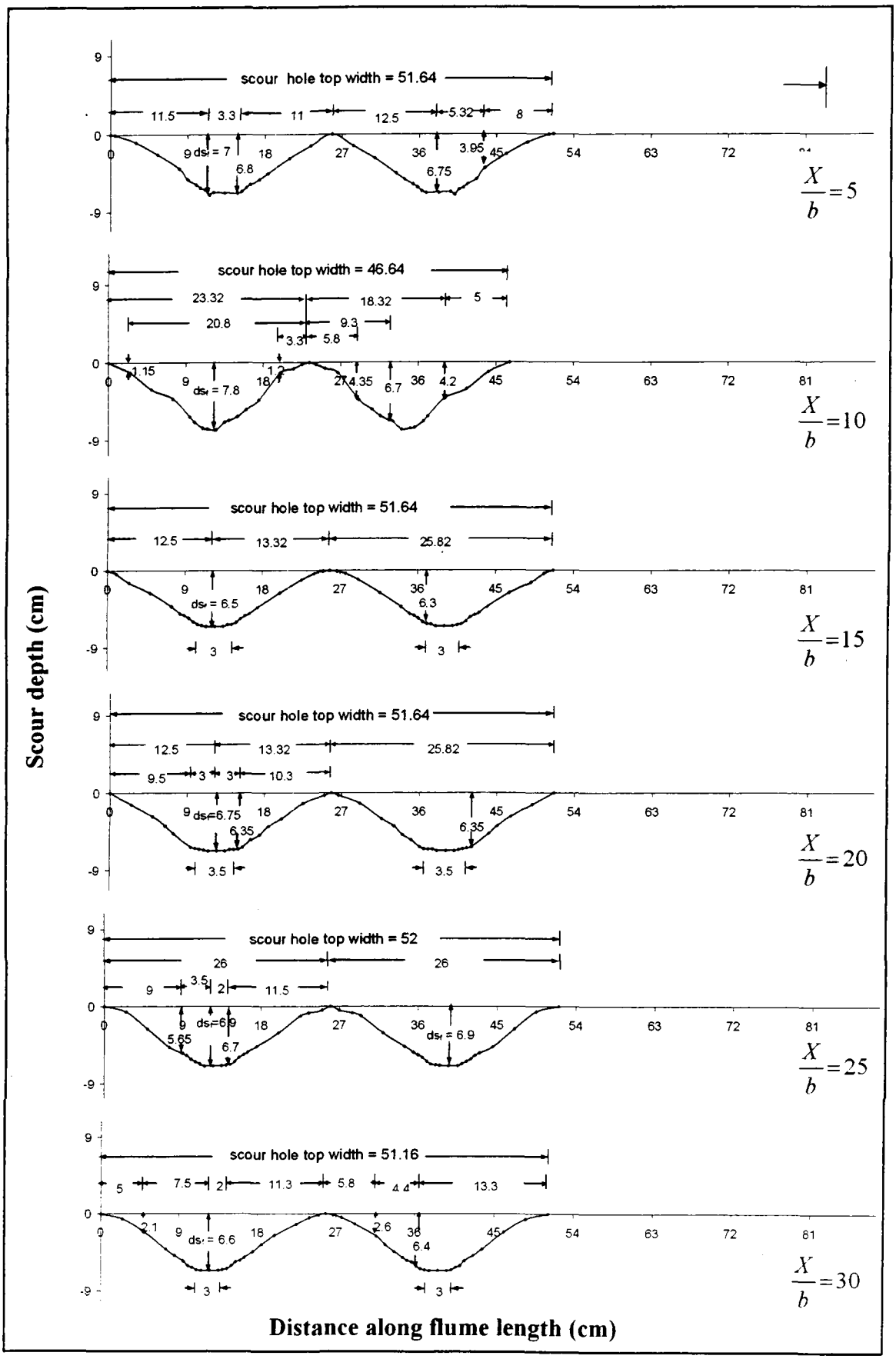

Lateral profiles around upstream piers of a group of three piers of same size in staggered arrangement at varied pier spacing X/b

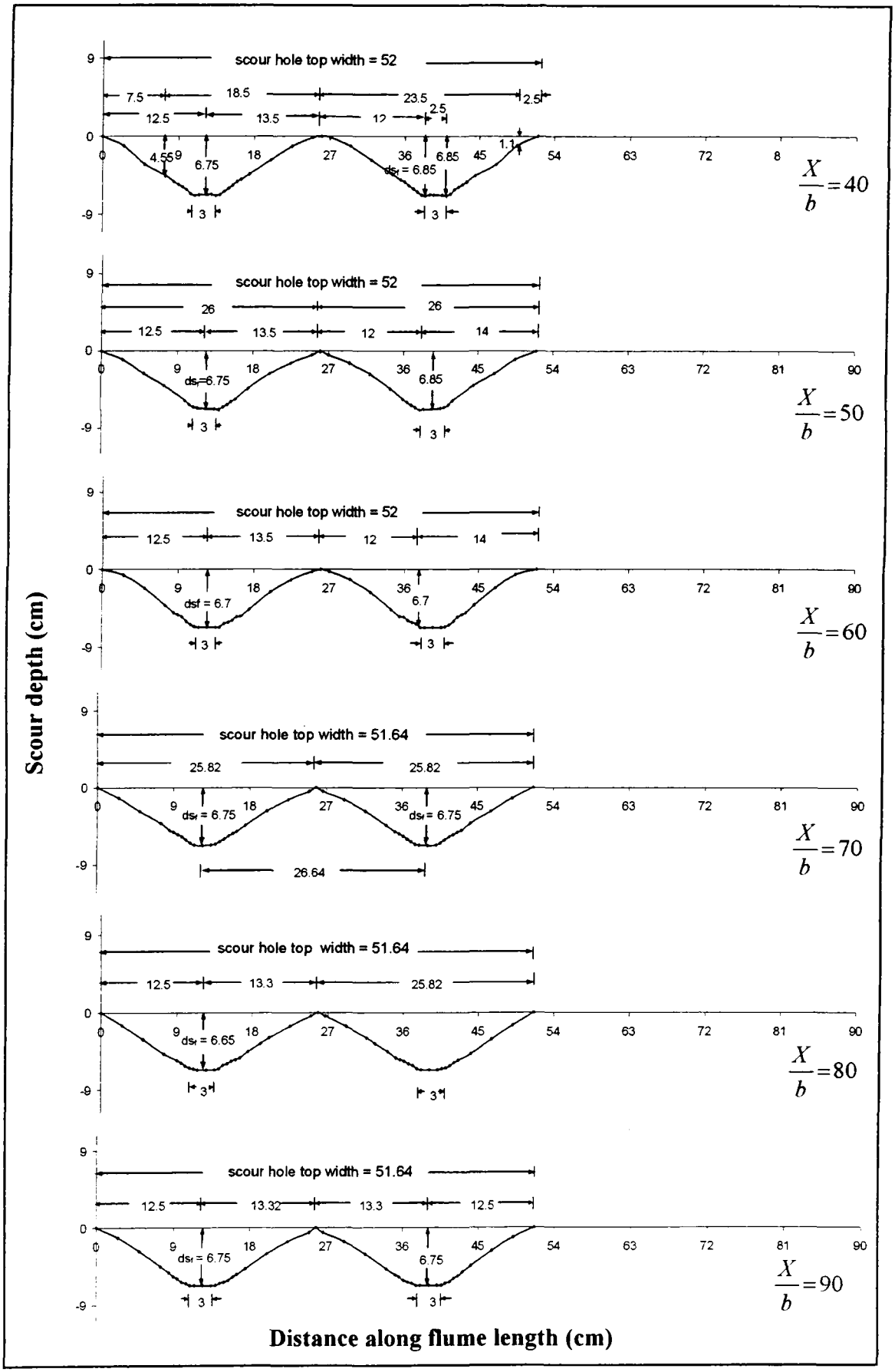

Lateral profiles around upstream piers of a group of three piers of same size in staggered arrangement at varied pier spacing X/b

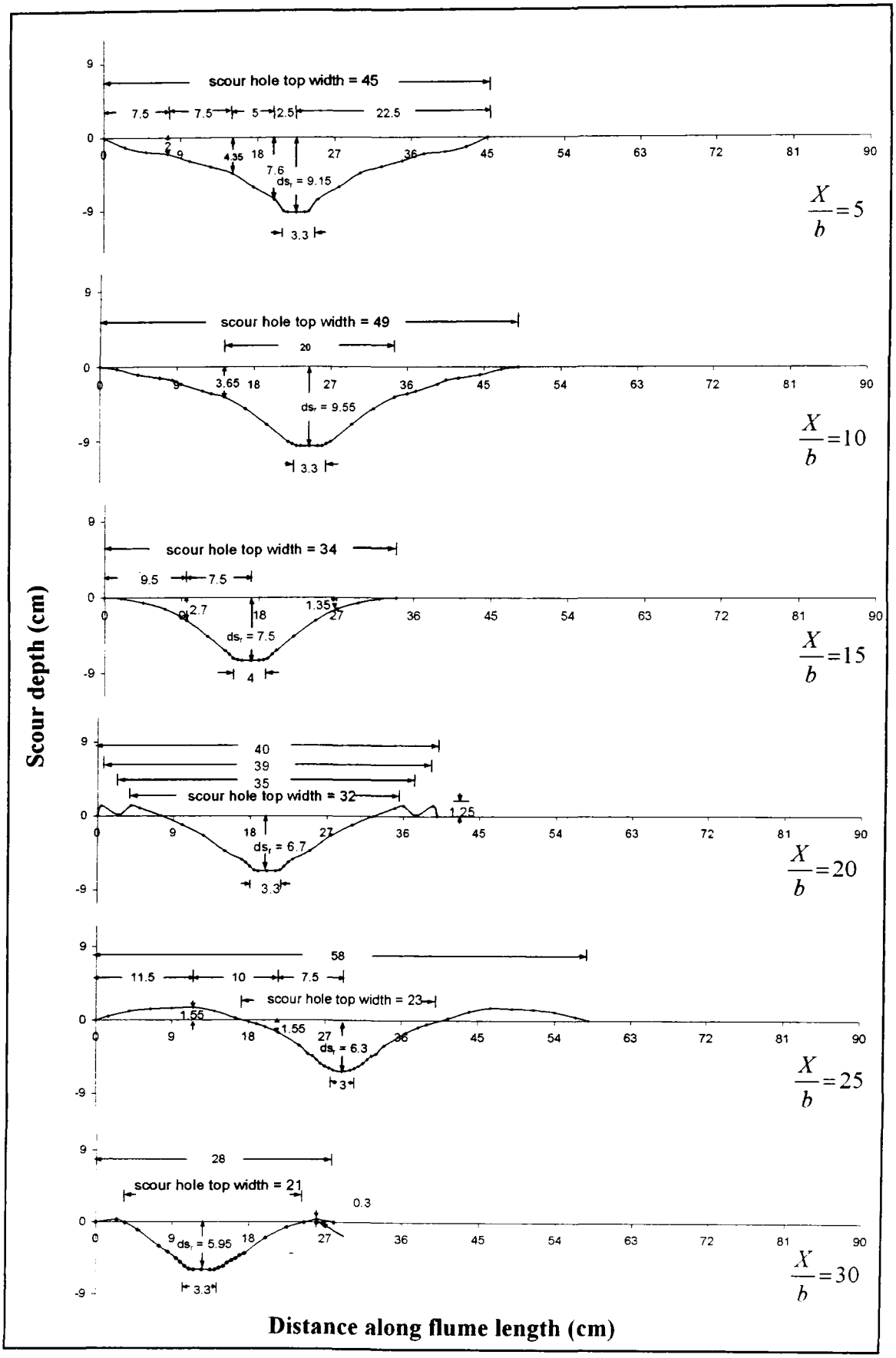

Lateral profiles around downstream pier of a group of three piers of same size in staggered arrangement at varied pier spacing X/b

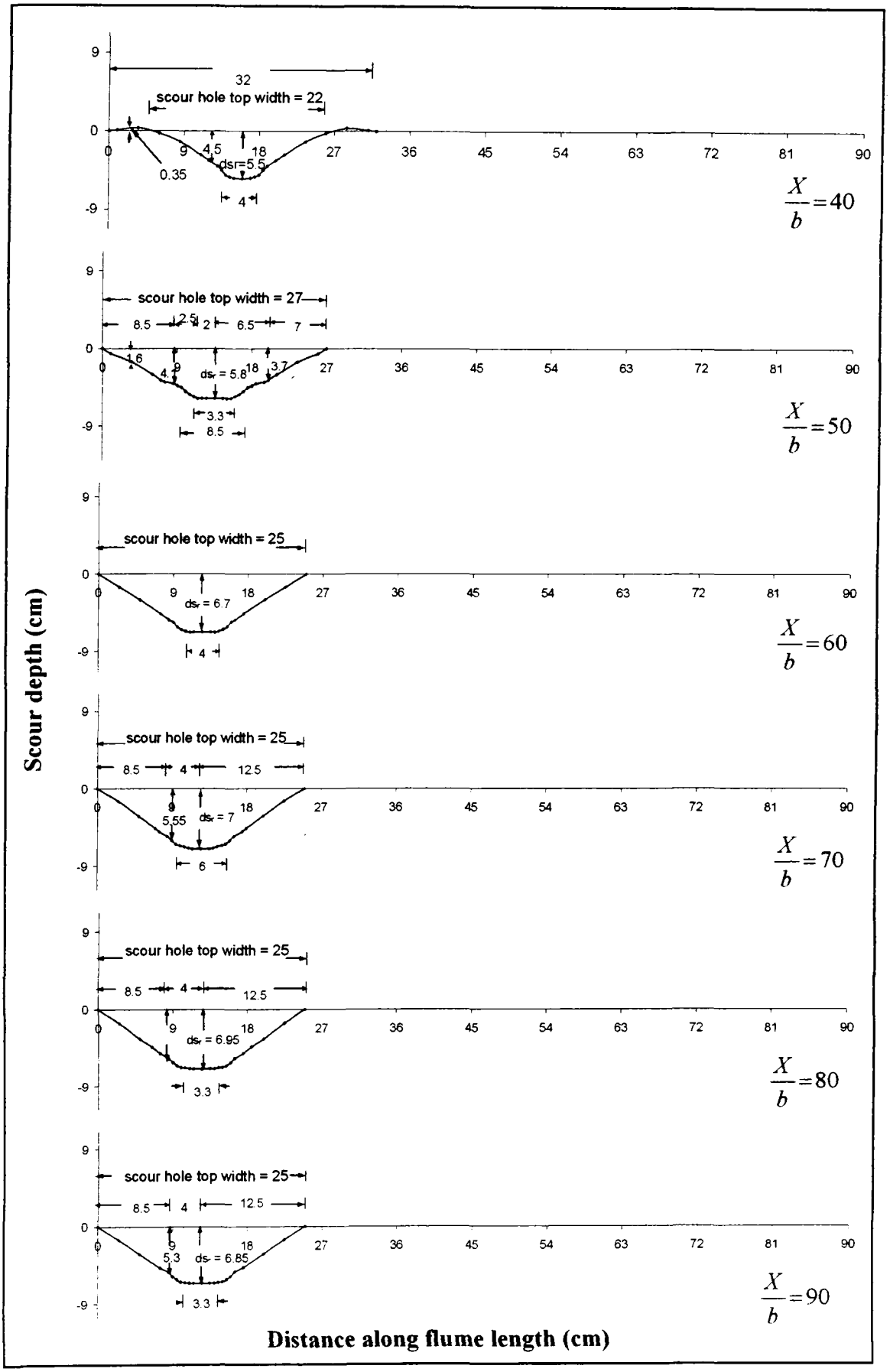

Lateral profiles around downstream pier of a group of three piers of same size in staggered arrangement at varied pier spacing X/b

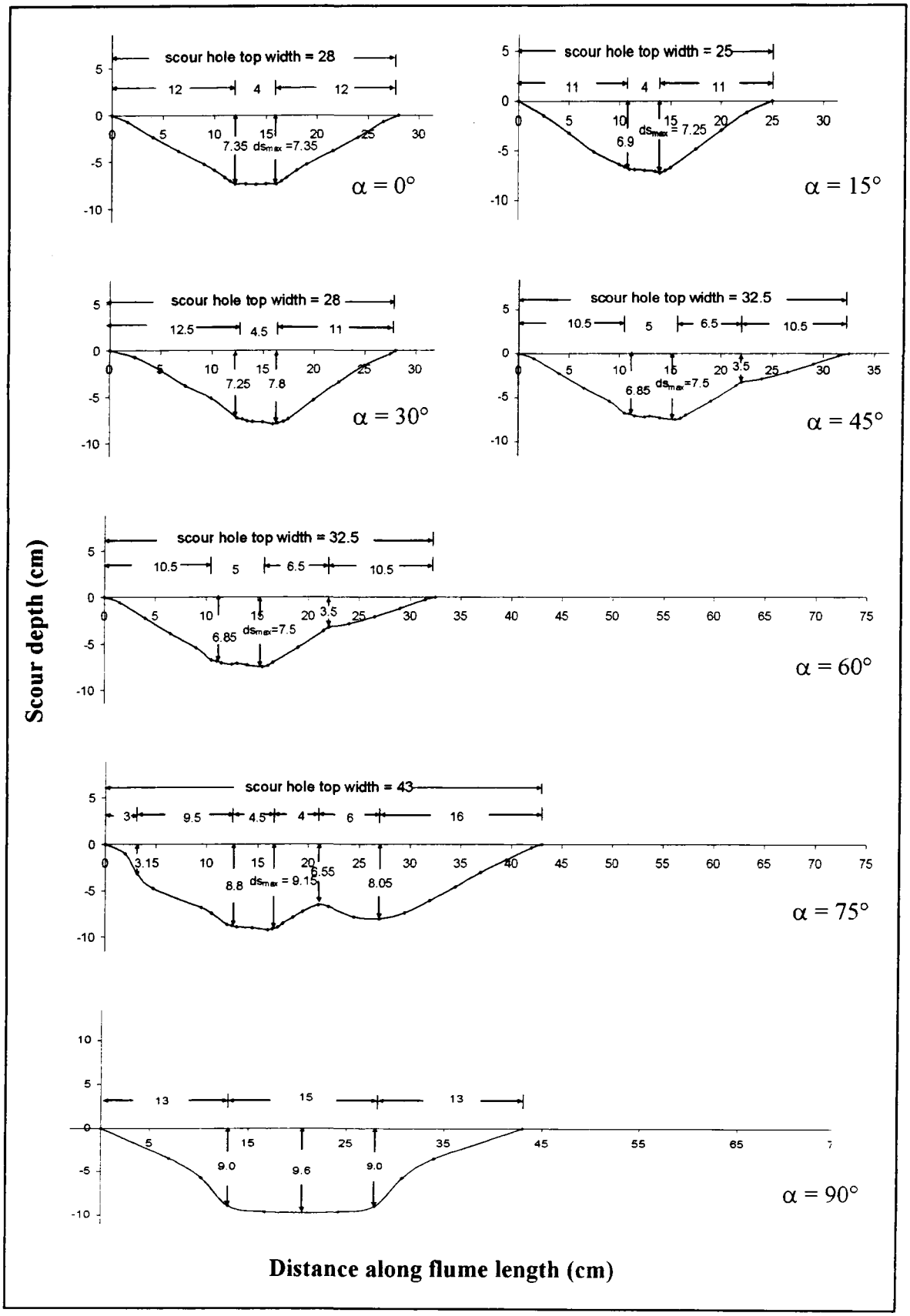

Lateral profiles around front pier of a group of two piers of same size at fixed pier spacing X/b = 2 without collar

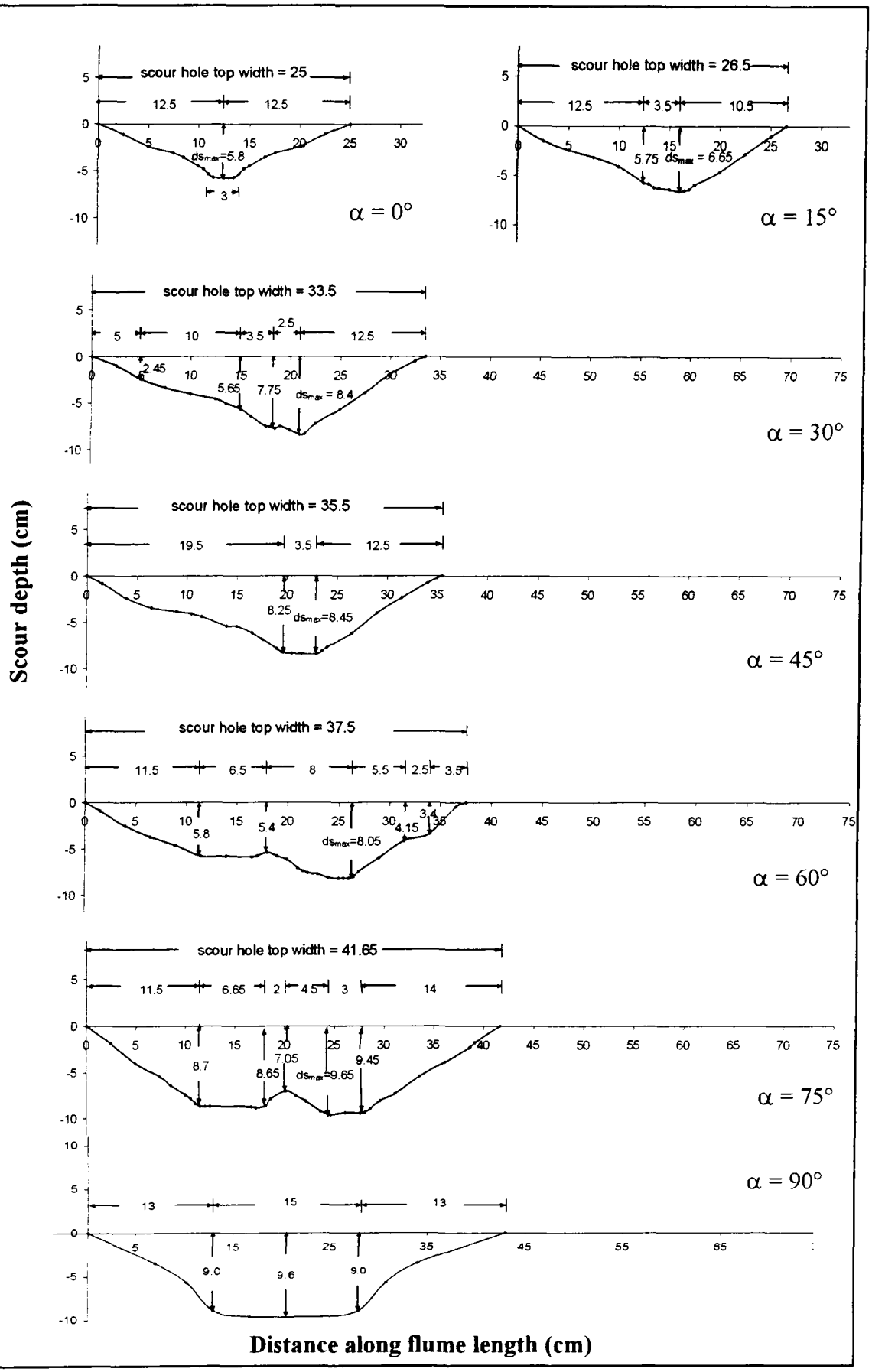

Lateral profiles around rear pier of a group of two piers of same size at fixed pier spacing X/b = 2 without collar

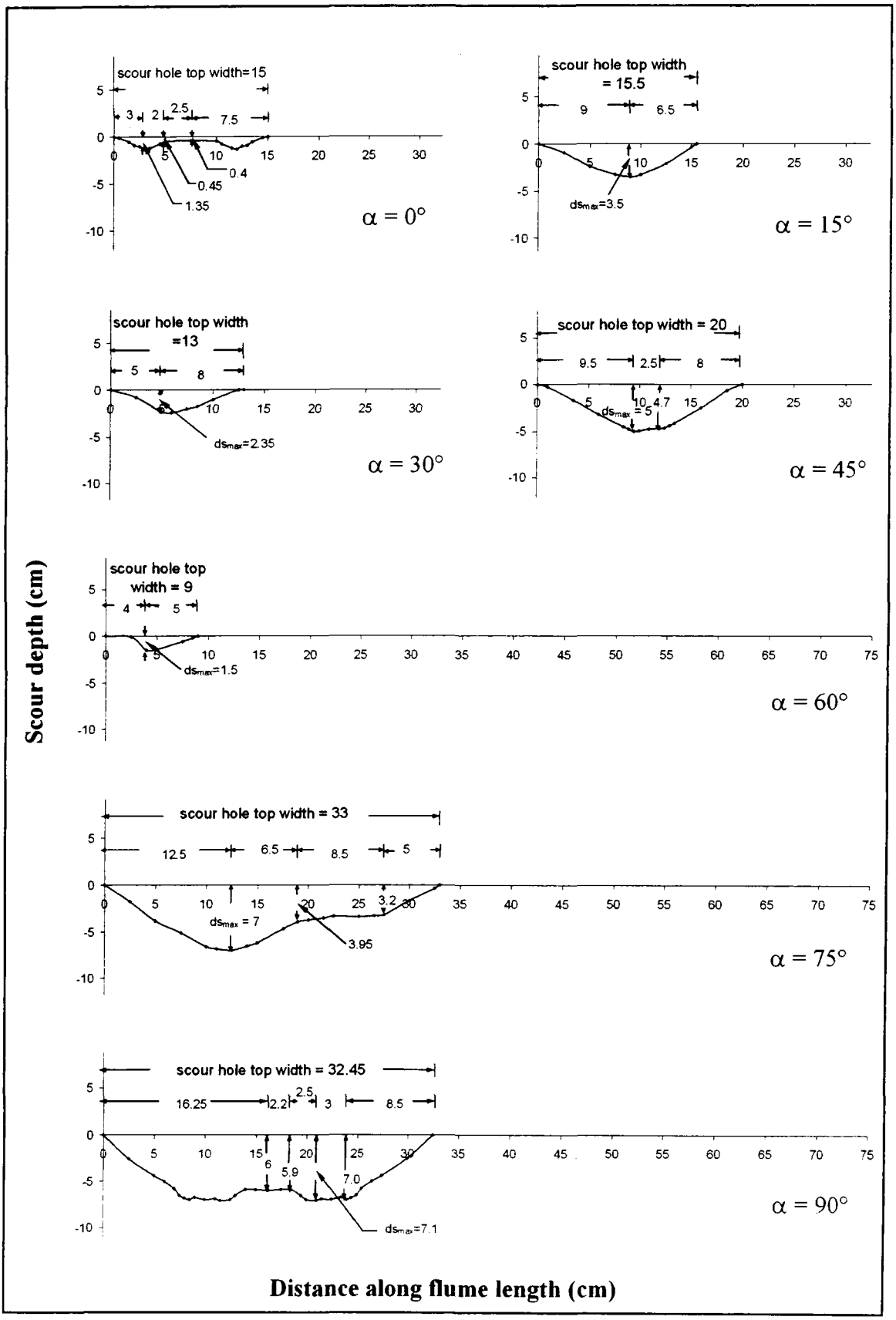

Lateral profiles around front pier of a group of two piers of same size at fixed pier spacing X/b = 2 with collar

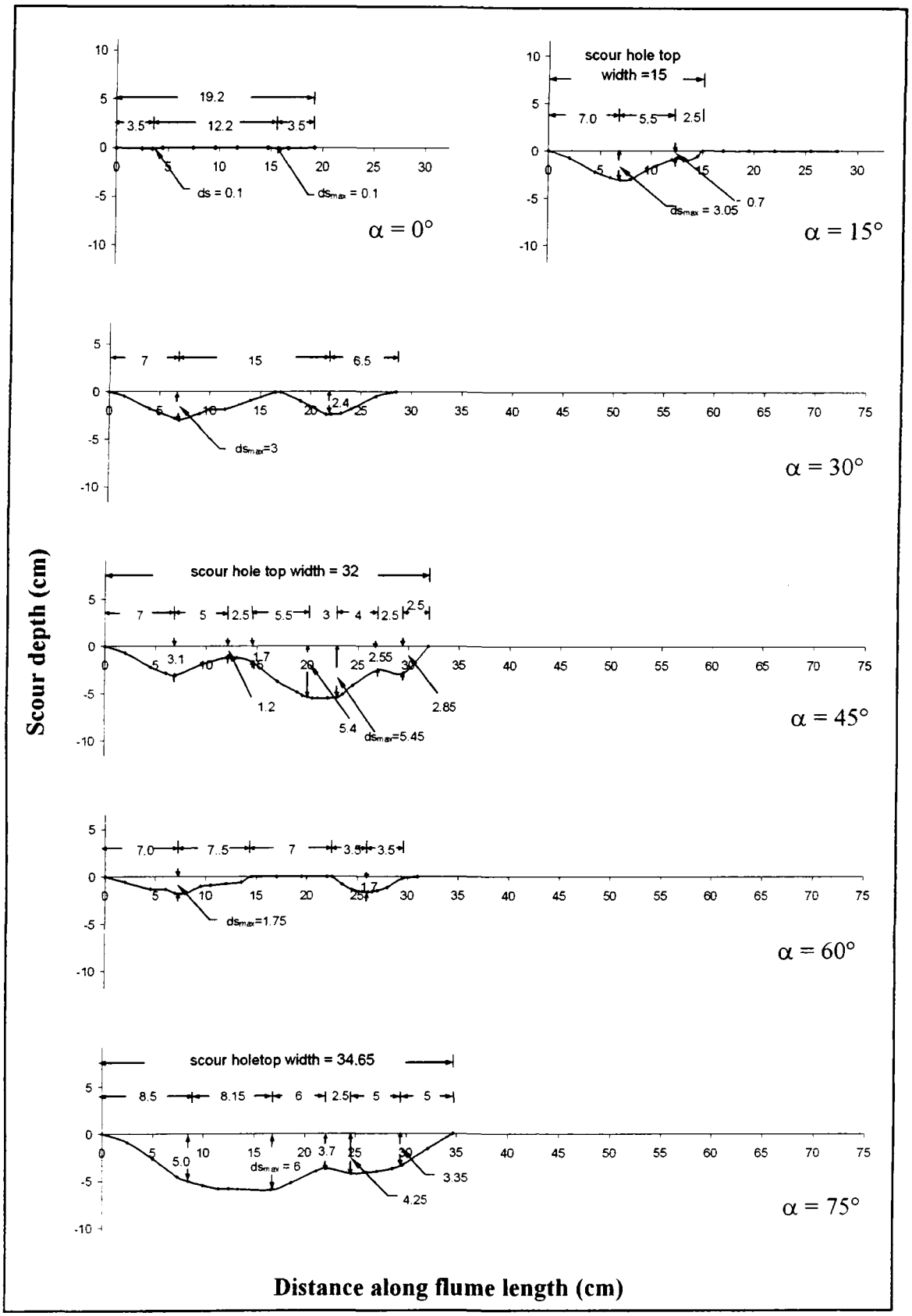

Lateral profiles around front pier of a group of two piers of same size at fixed pier spacing X/b = 2 with collar

APPENDIX – IV

AREAL EXTENTS OF SCOUR

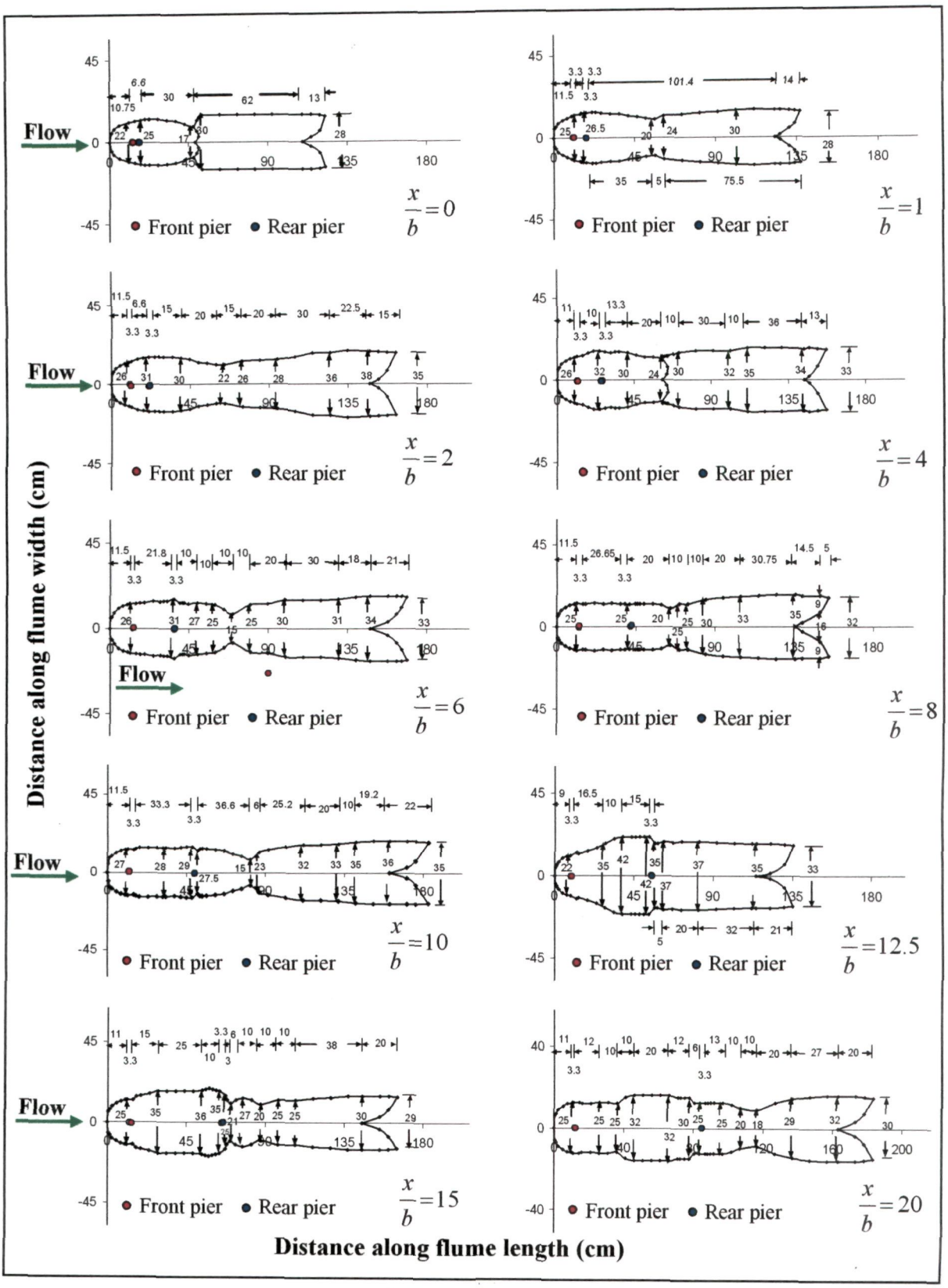

Areal extents of scour for two pears in tandem arrangement for varied pier spacings x/b.

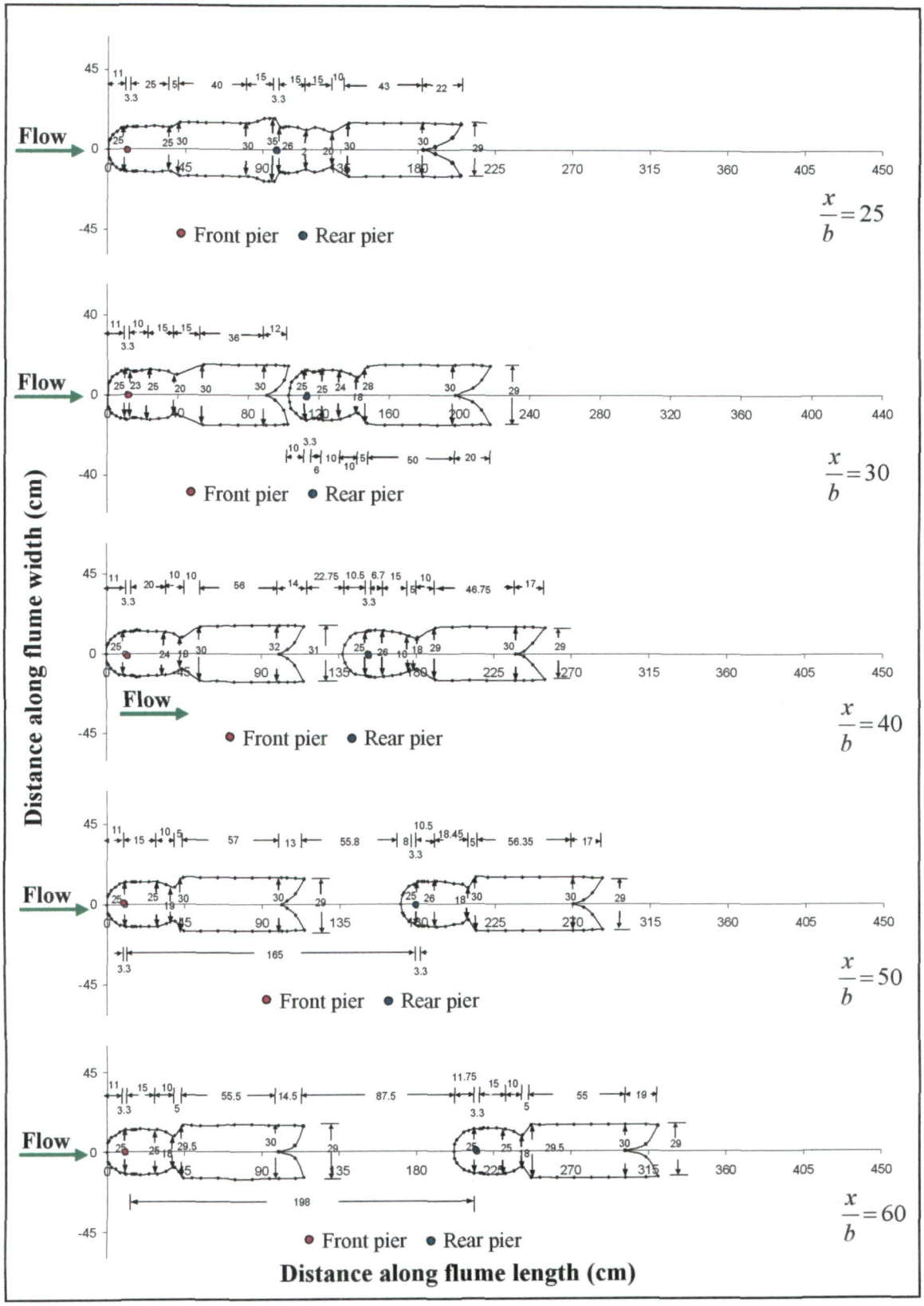

Areal extents of scour for two pears in tandem arrangement for varied pier spacings x/b.

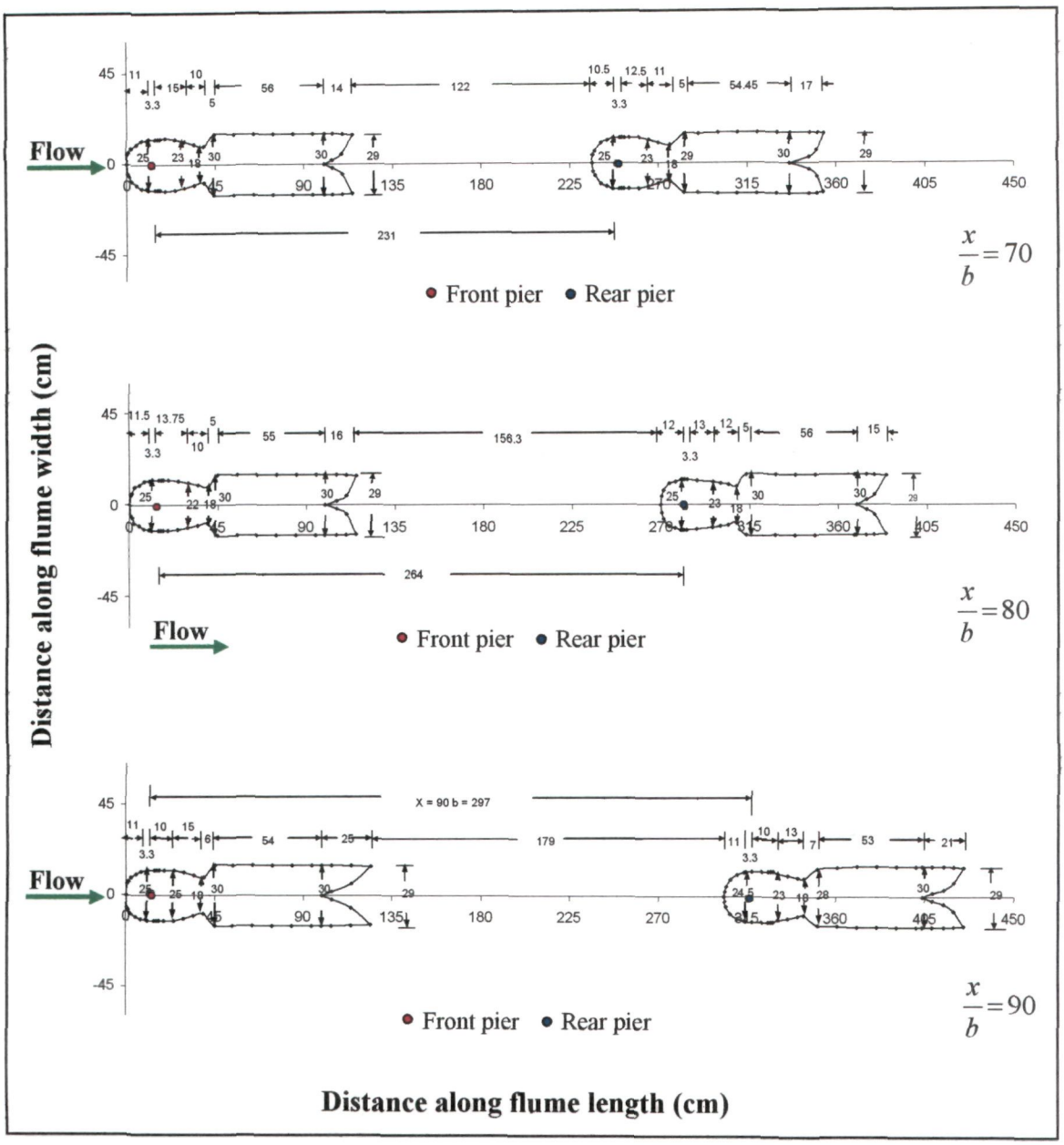

Areal extents of scour for two pears in tandem arrangement for varied pier spacings x/b.

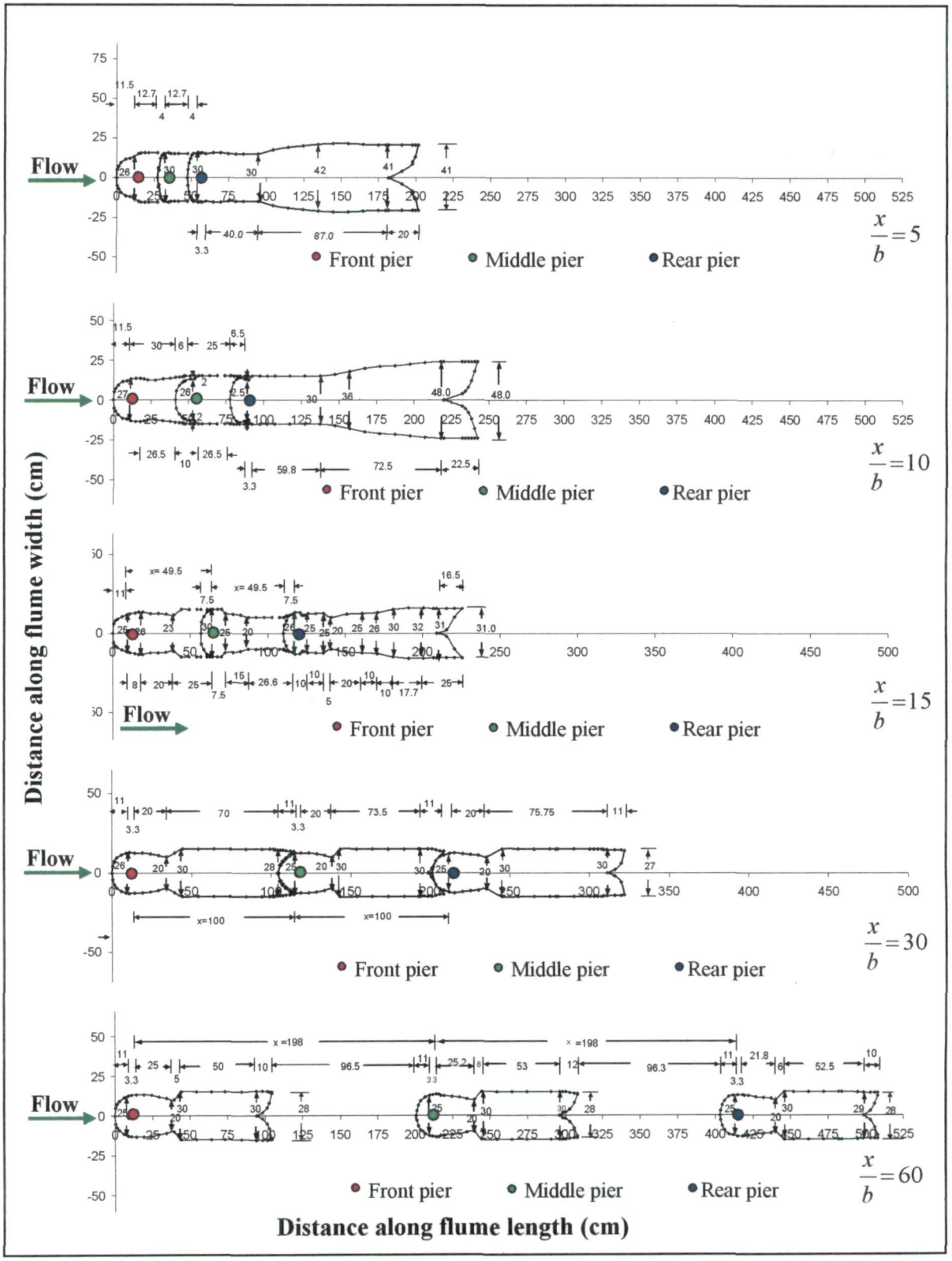

Areal extents of scour for three pears in tandem arrangement for varied pier spacings x/b.

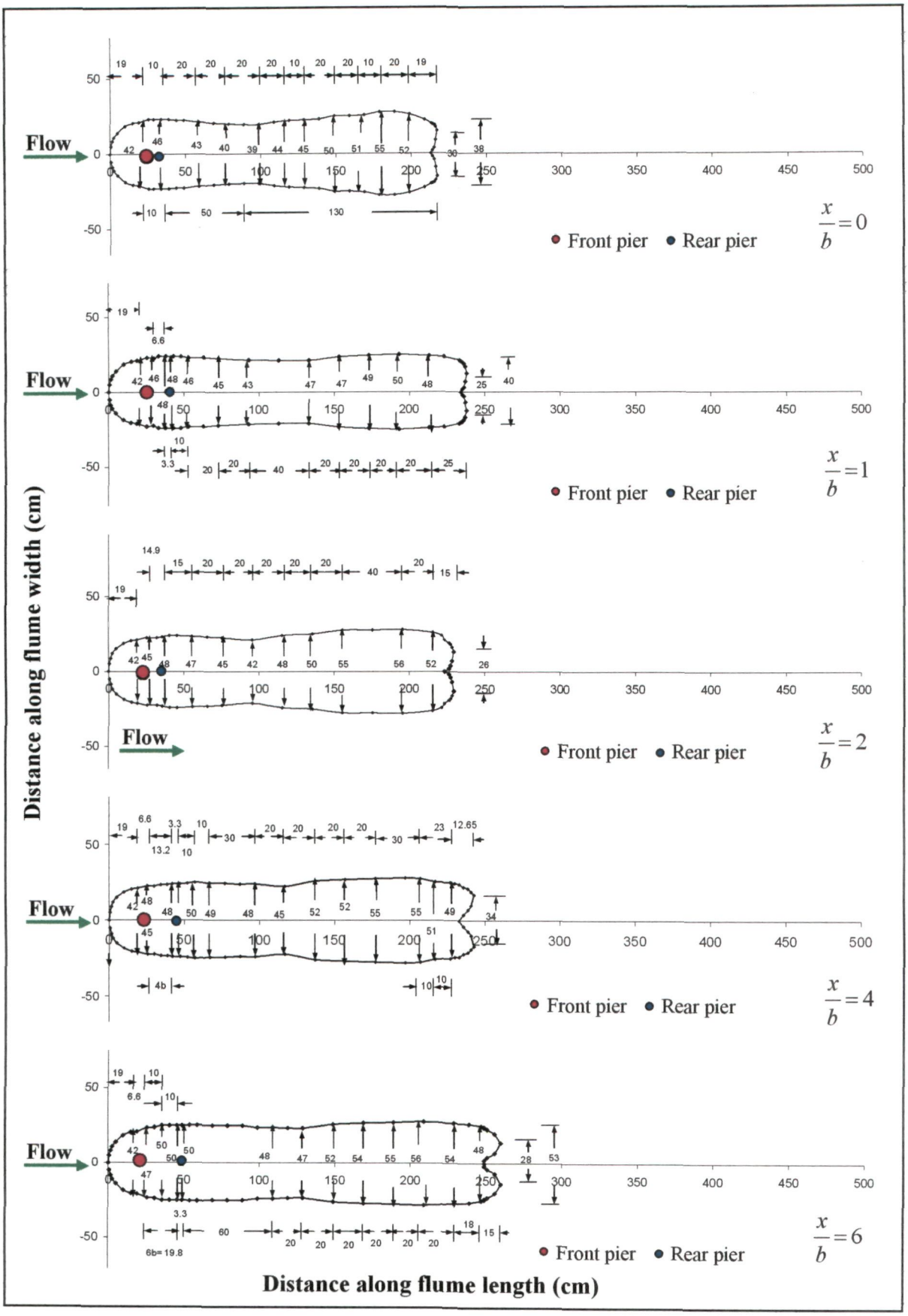

Areal extents of scour for two piers of unequal size (big pier at front and small pier at rear) in tandem arrangement for varied pier spacings x/b.

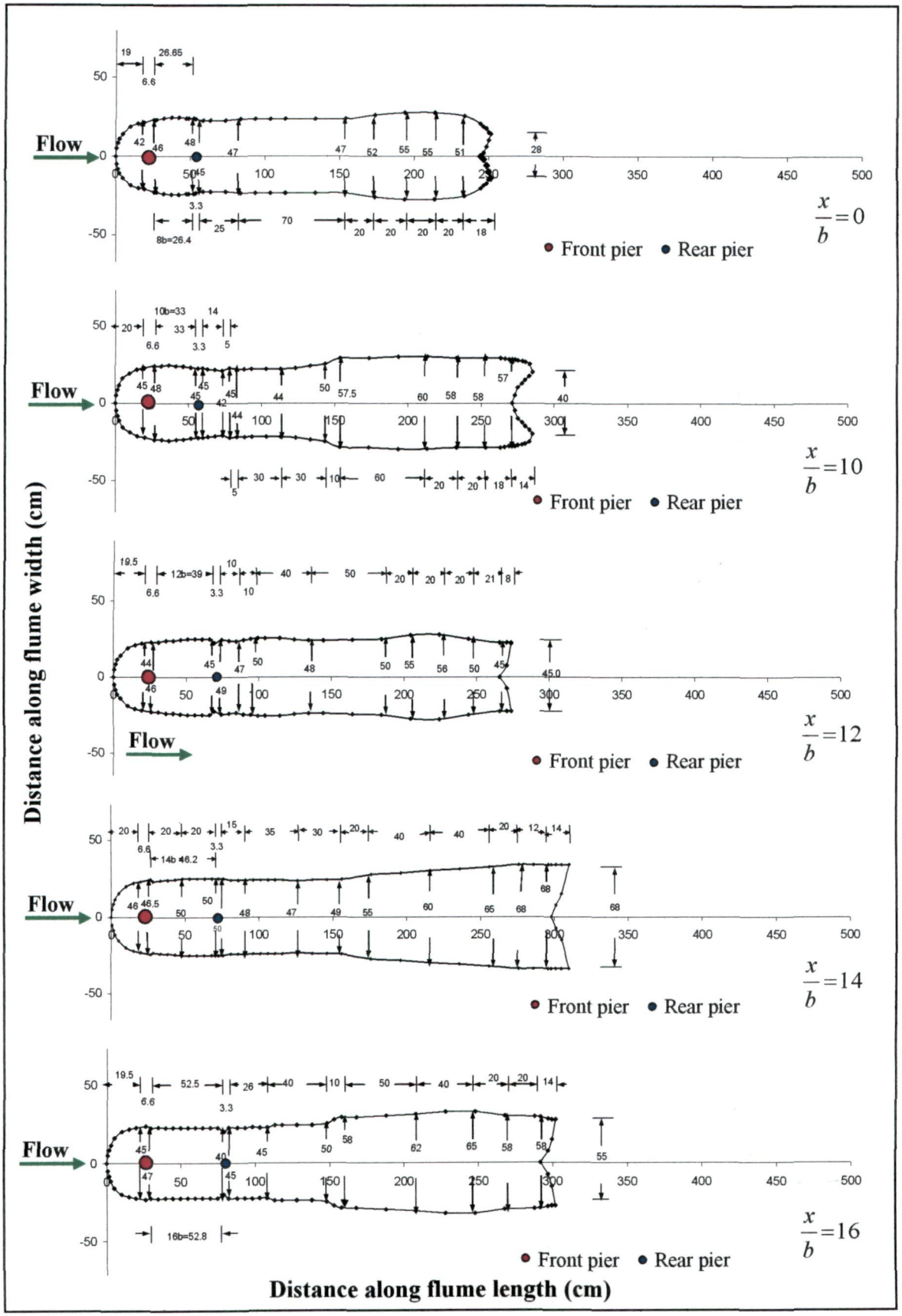

Areal extents of scour for two piers of unequal size (big pier at front and small pier at rear) in tandem arrangement for varied pier spacings x/b.

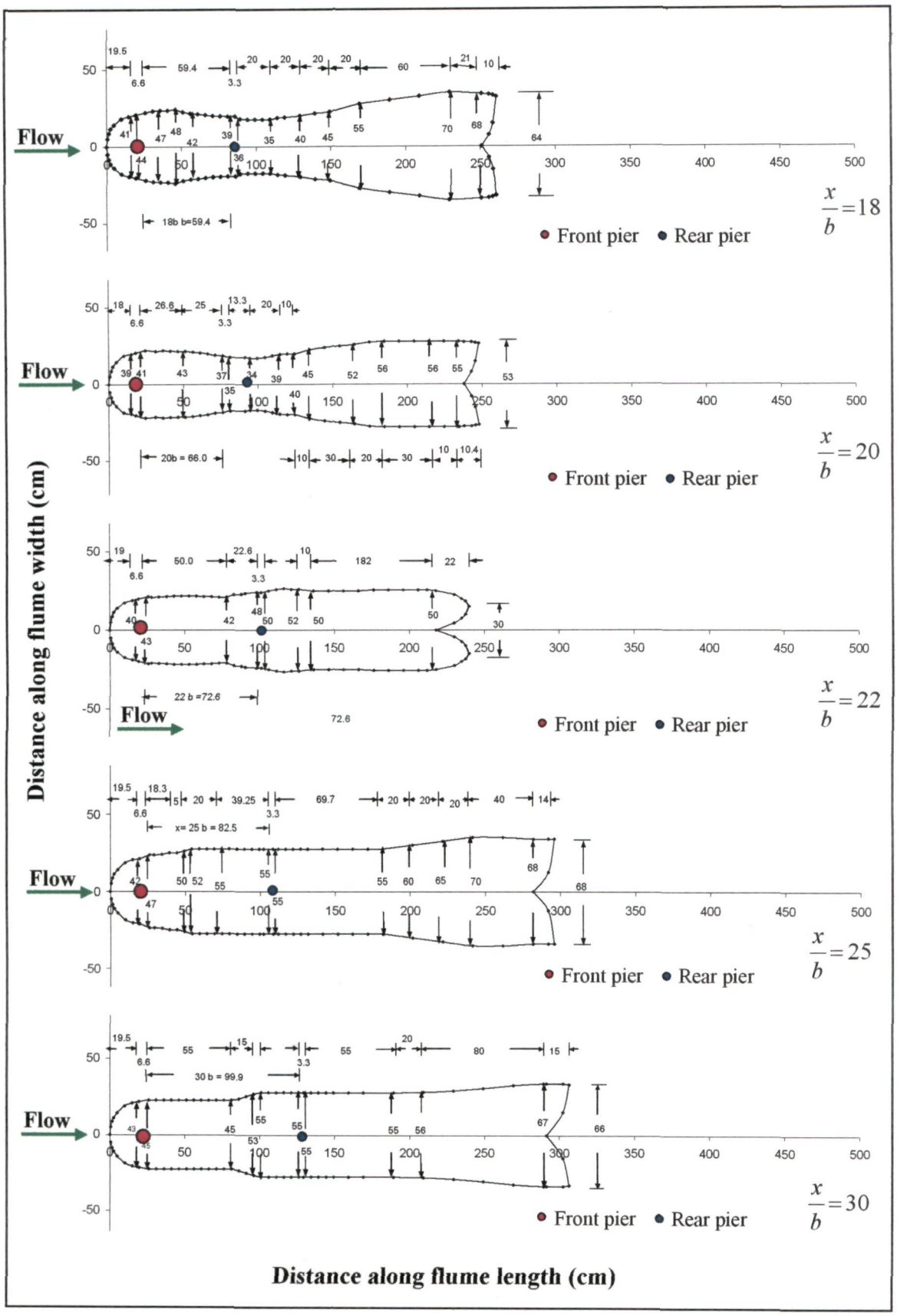

Areal extents of scour for two piers of unequal size (big pier at front and small pier at rear) in tandem arrangement for varied pier spacings x/b.

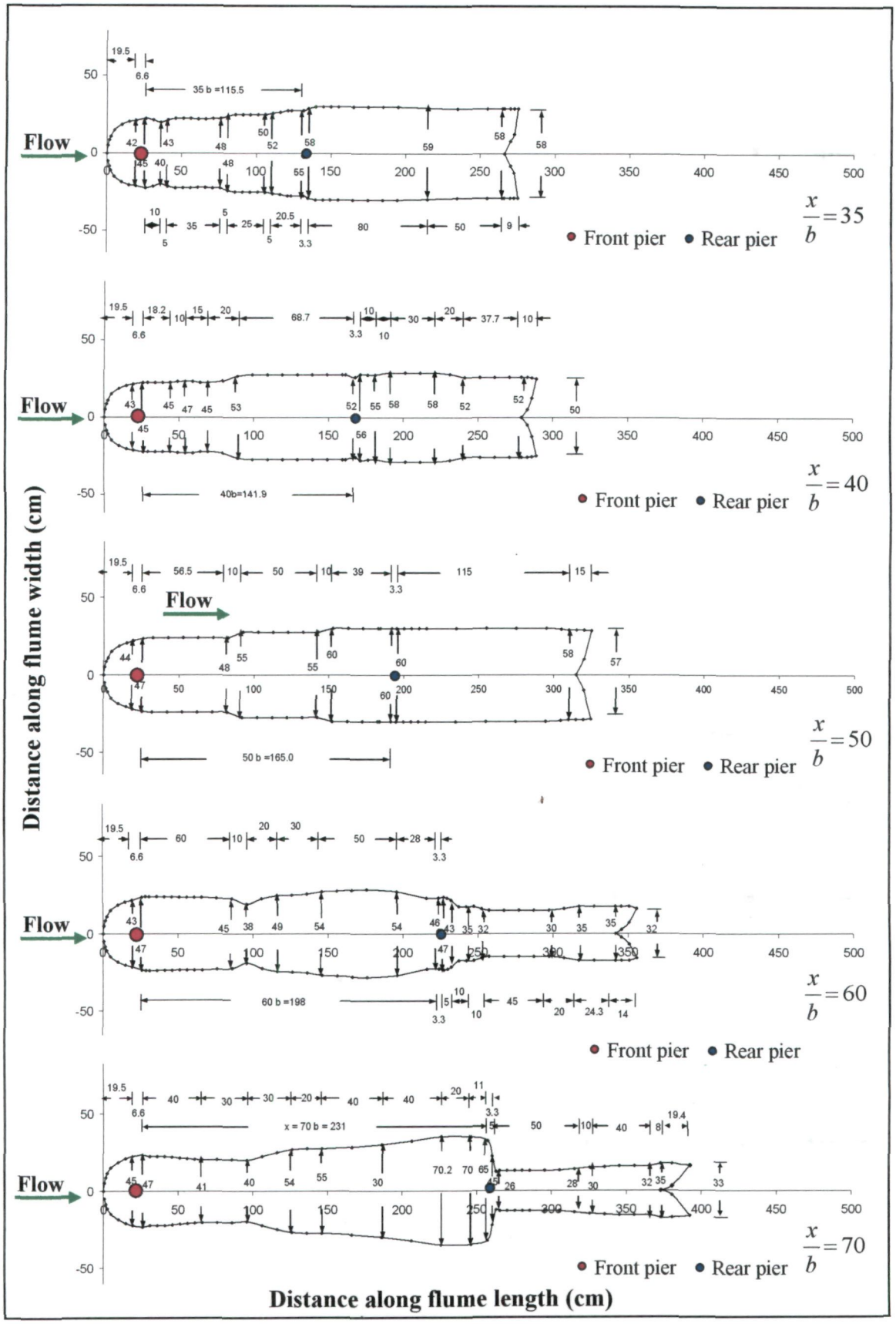

Areal extents of scour for two piers of unequal size (big pier at front and small pier at rear) in tandem arrangement for varied pier spacings x/b.

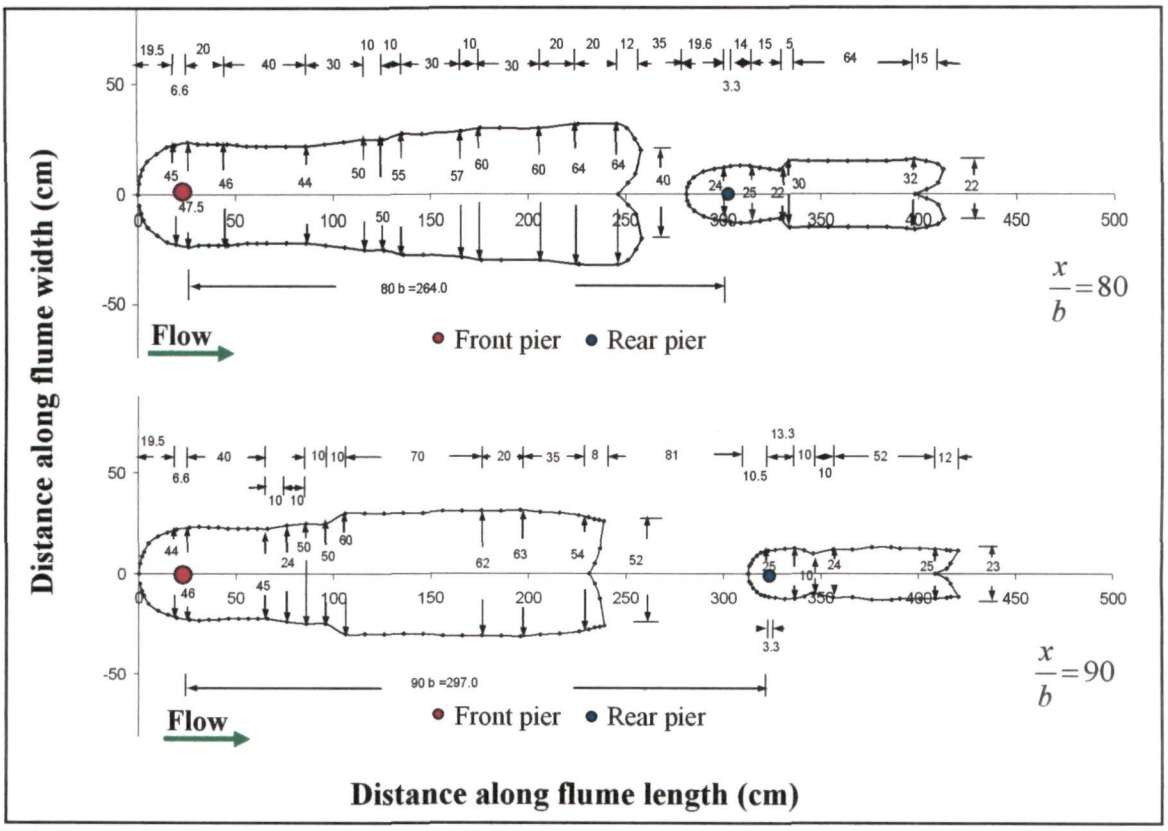

Areal extents of scour for two piers of unequal size (big pier at front and small pier at rear) in tandem arrangement for varied pier spacings x/b.

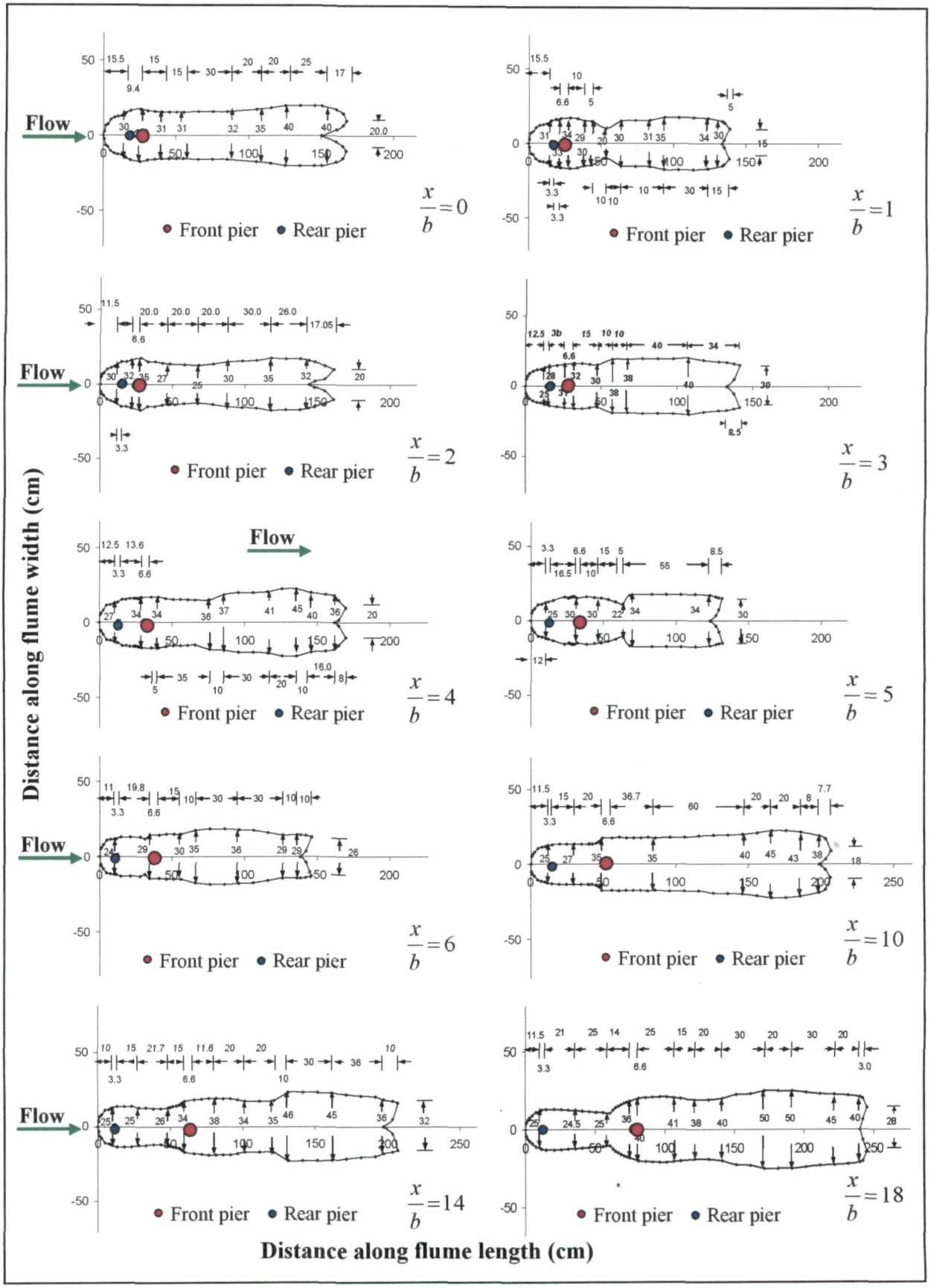

Areal extents of scour for two piers of unequal size (small pier at front and big pier at rear) in tandem arrangement for varied pier spacings x/b

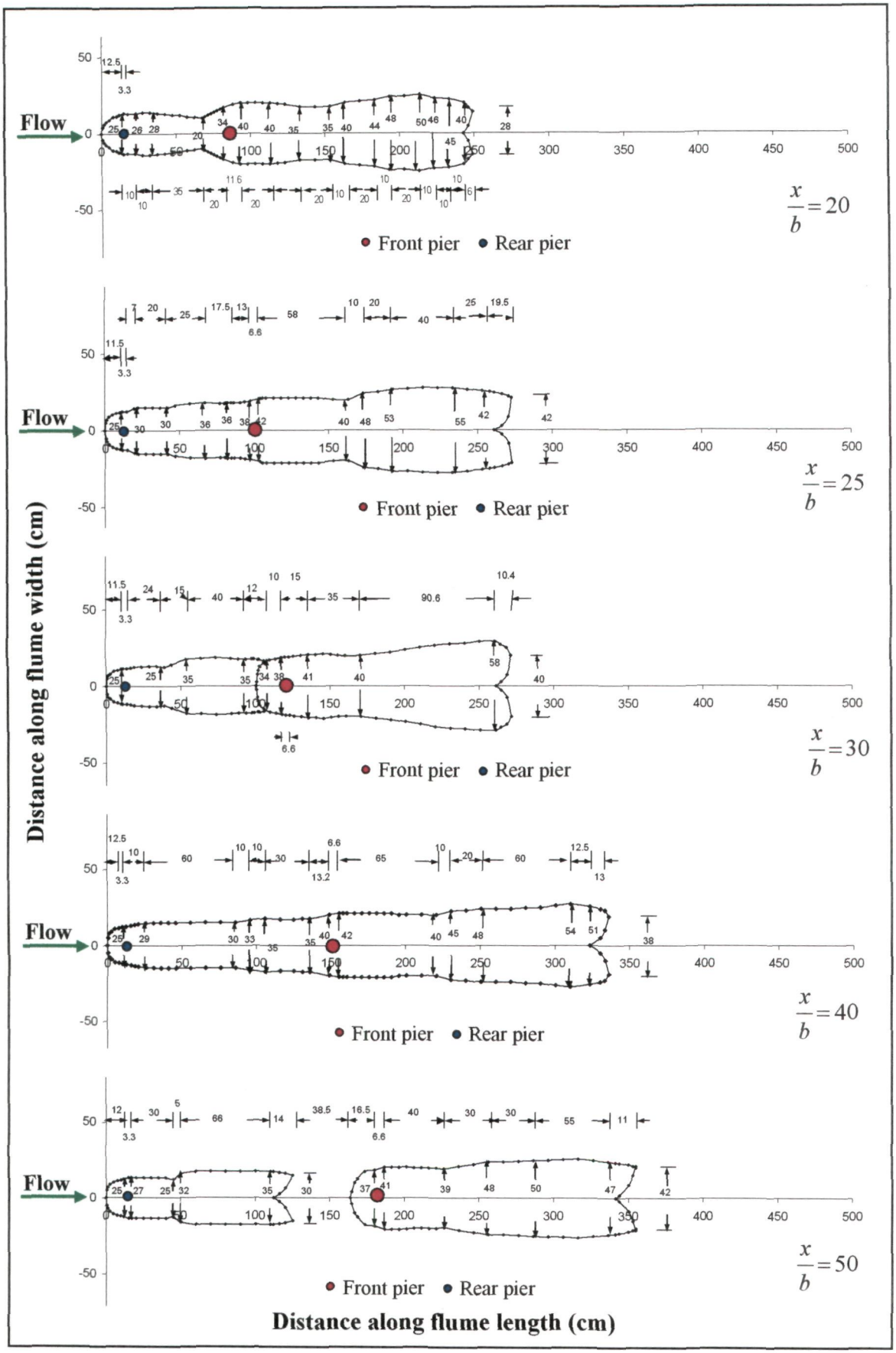

Areal extents of scour for two piers of unequal size (small pier at front and big pier at rear) in tandem arrangement for varied pier spacings x/b

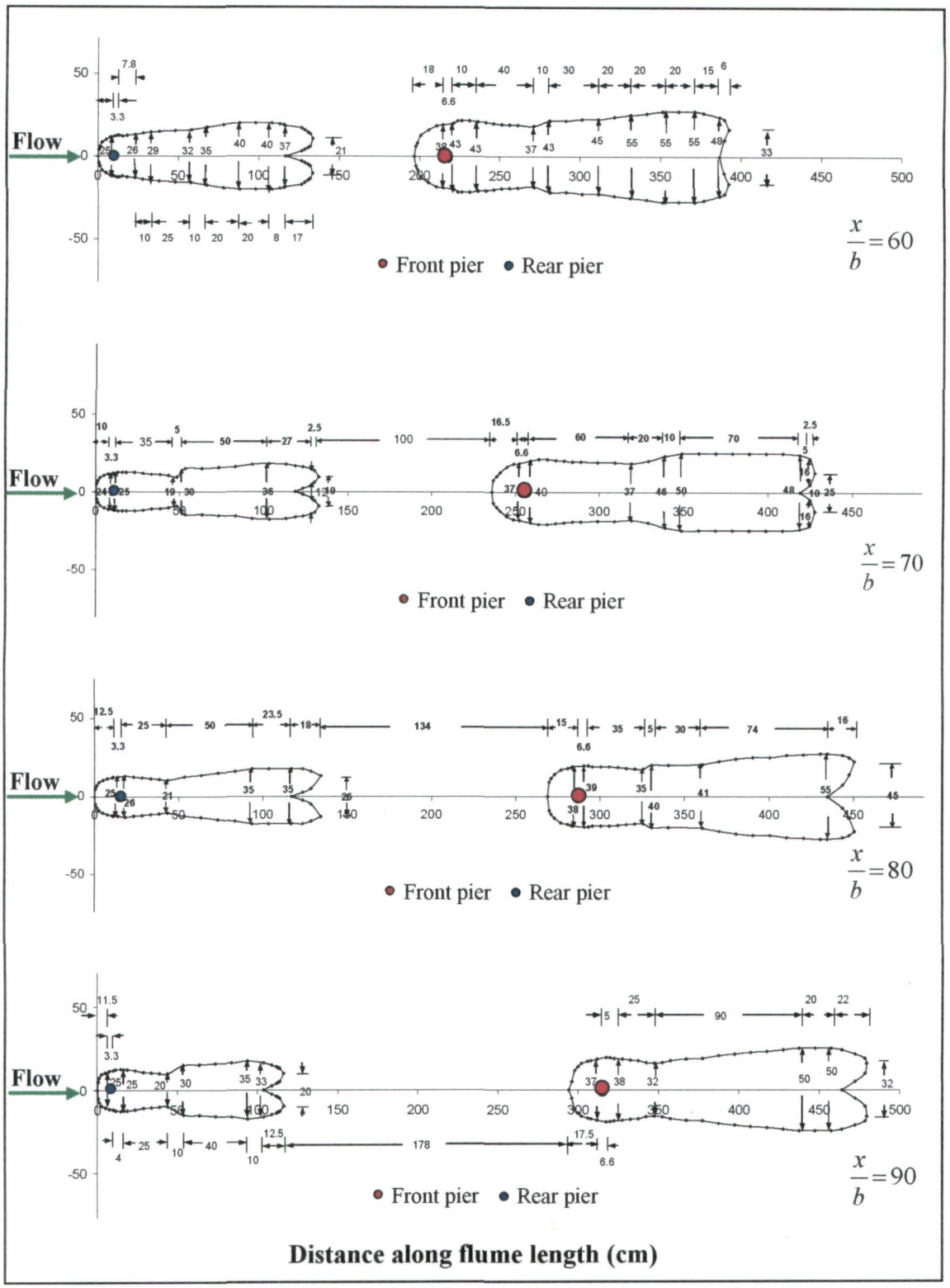

Areal extents of scour for two piers of unequal size (small pier at front and big pier at rear) in tandem arrangement for varied pier spacings x/b

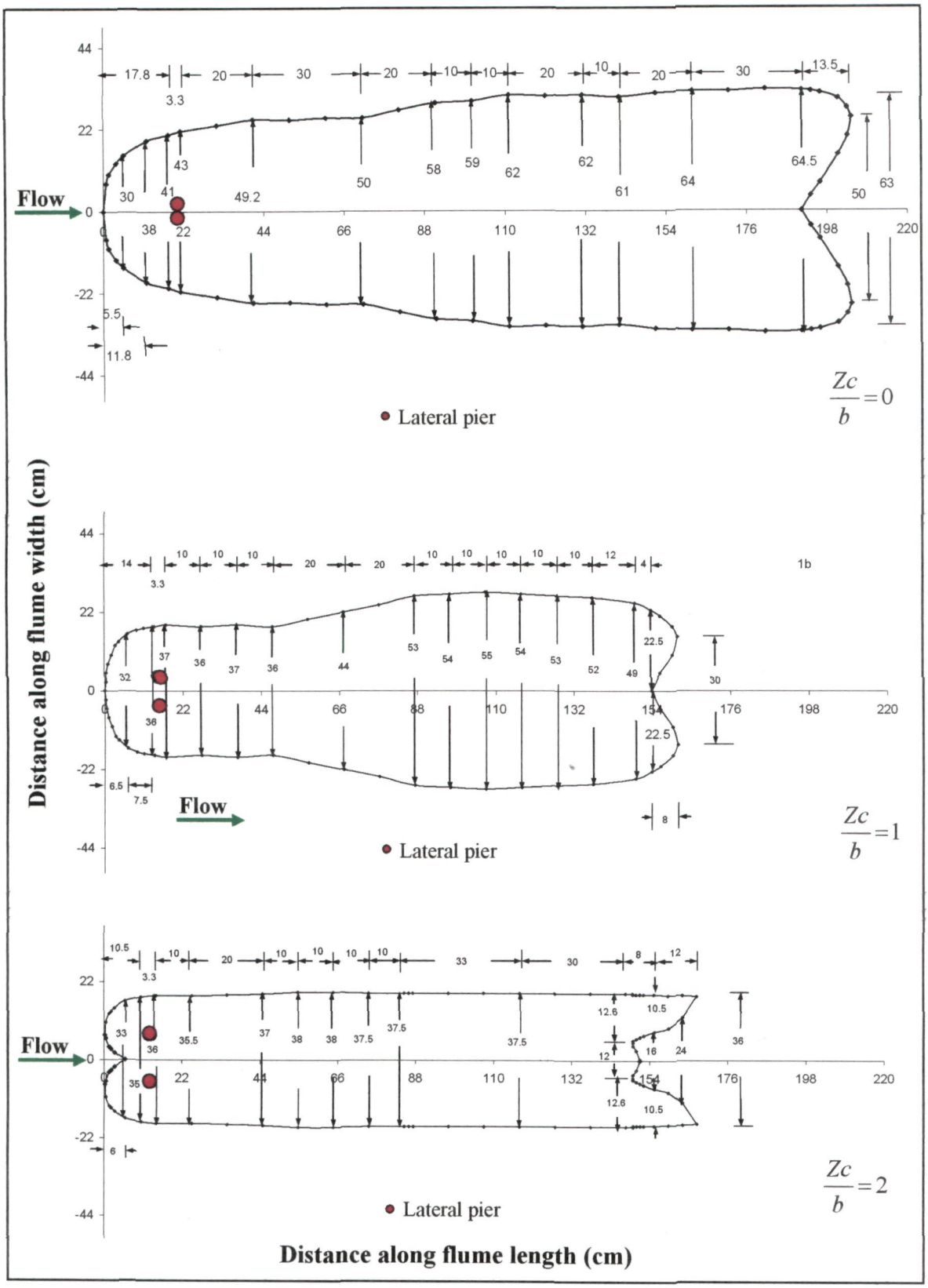

Areal extents of scour for two piers in transverse arrangement for varied lateral pier spacings Zc/b

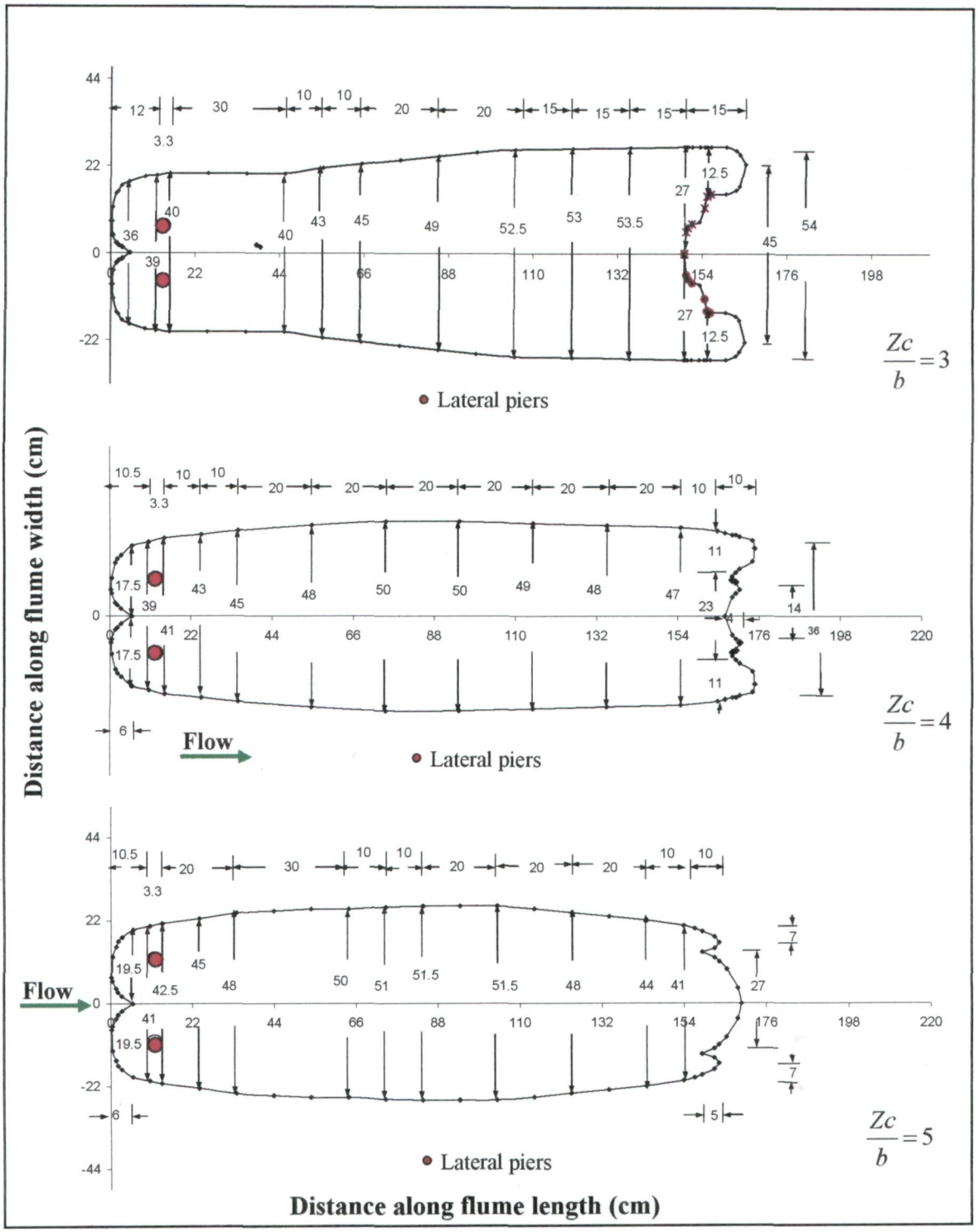

Areal extents of scour for two piers in transverse arrangement for varied lateral pier spacings Zc/b

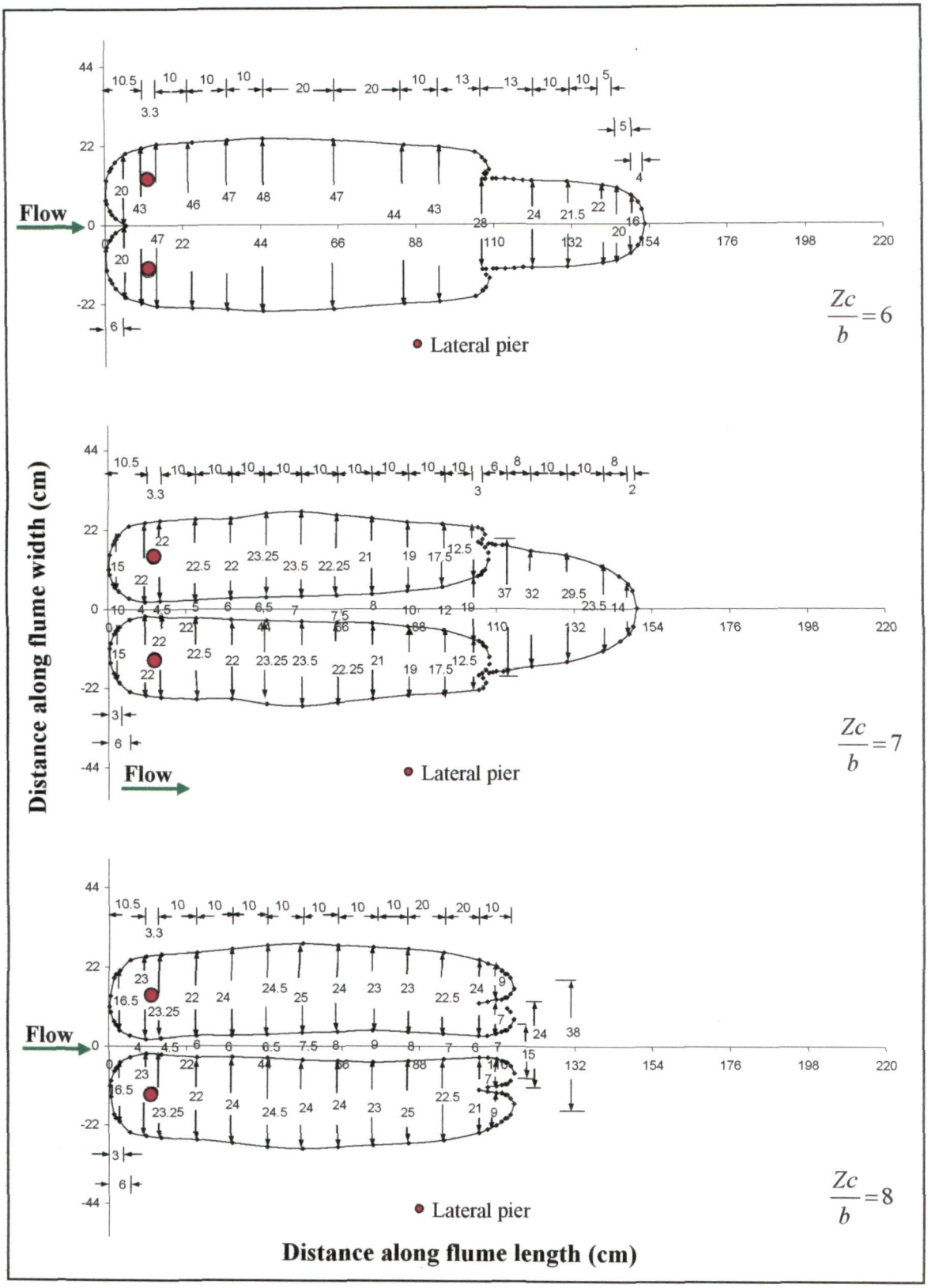

Areal extents of scour for two piers in transverse arrangement for varied lateral pier spacings Zc/b

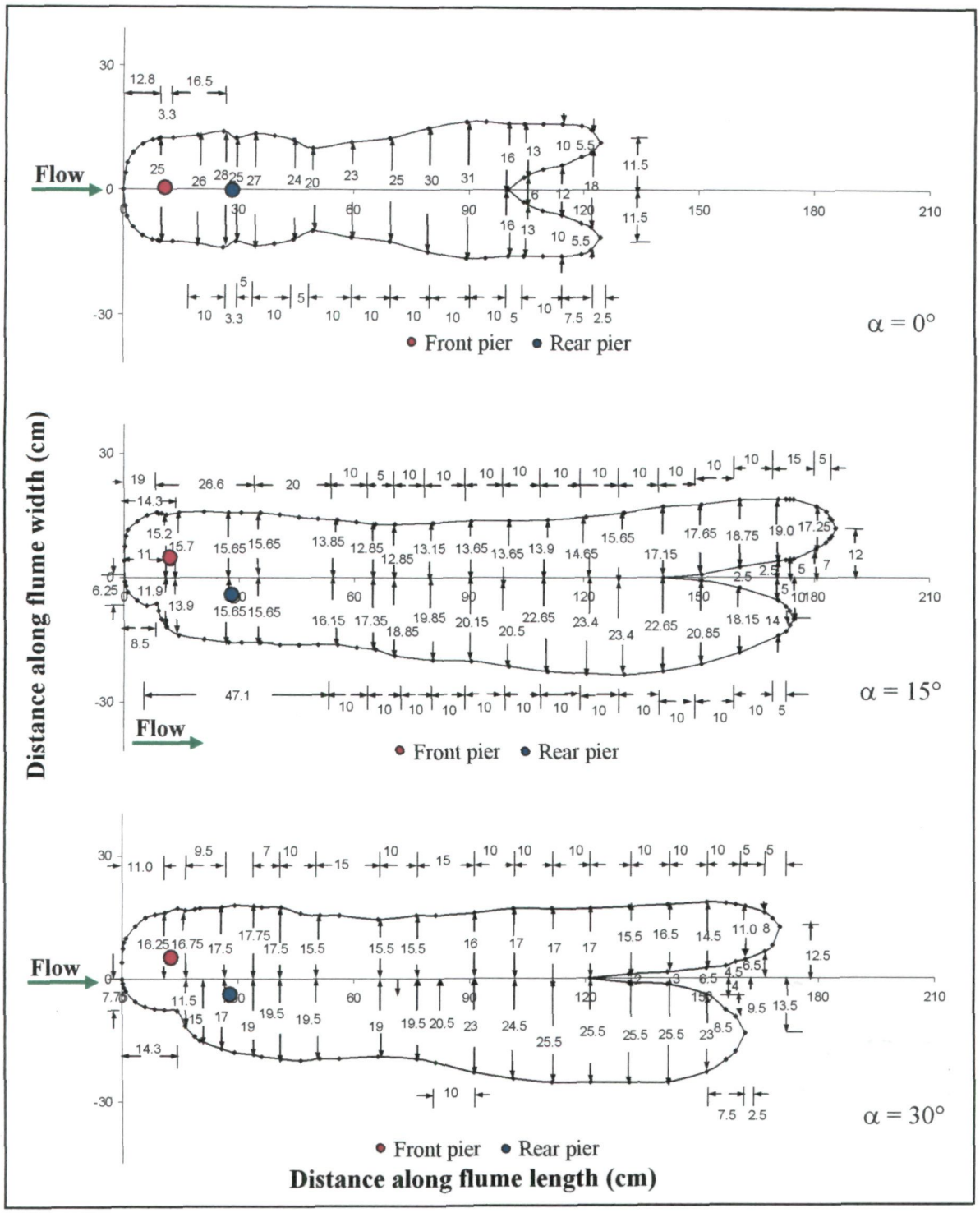

Areal extents of scour for two piers at constant radial pier spacing and varied angle of attack α

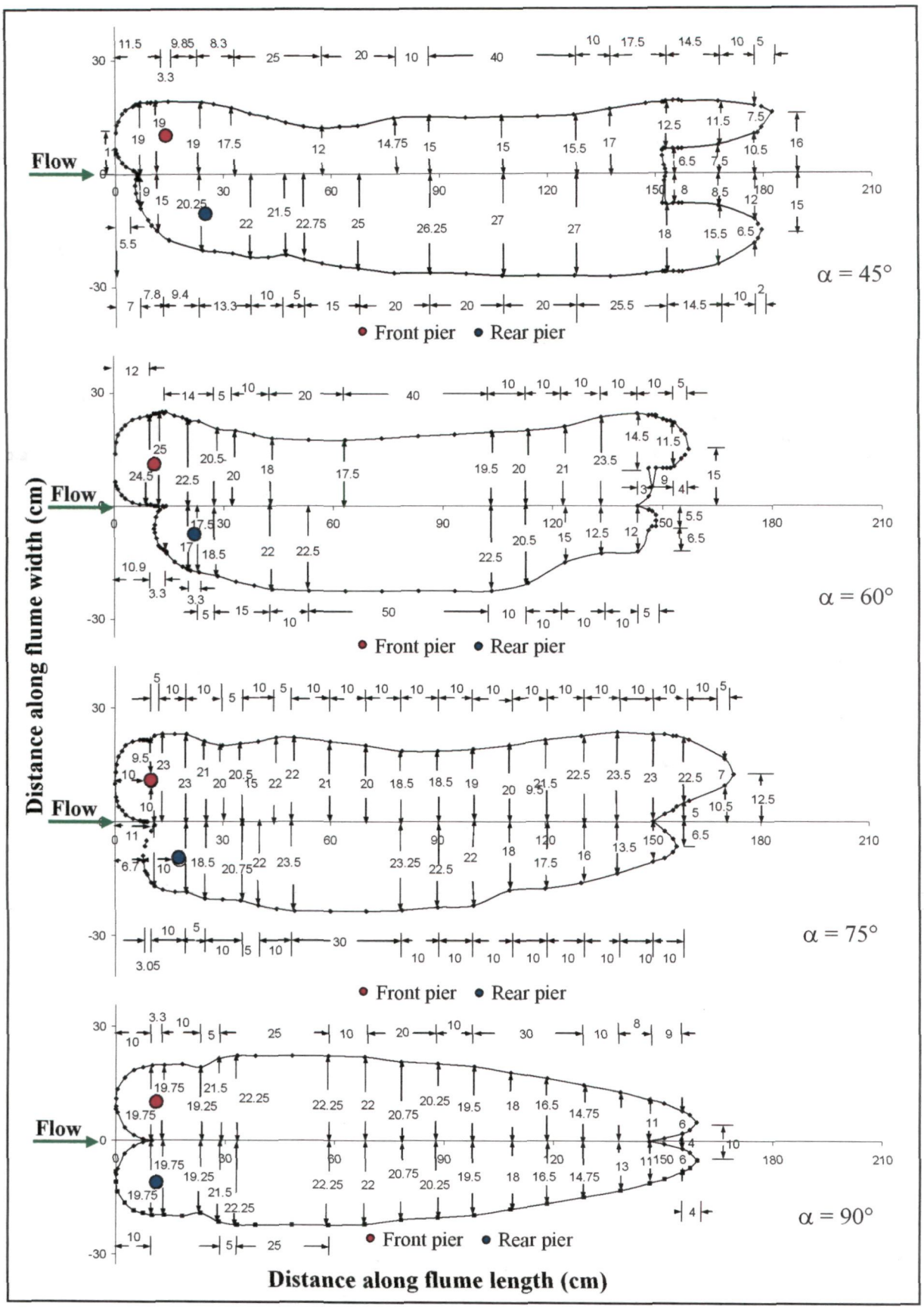

Areal extents of scour for two piers at constant radial pier spacing and varied angle of attack α

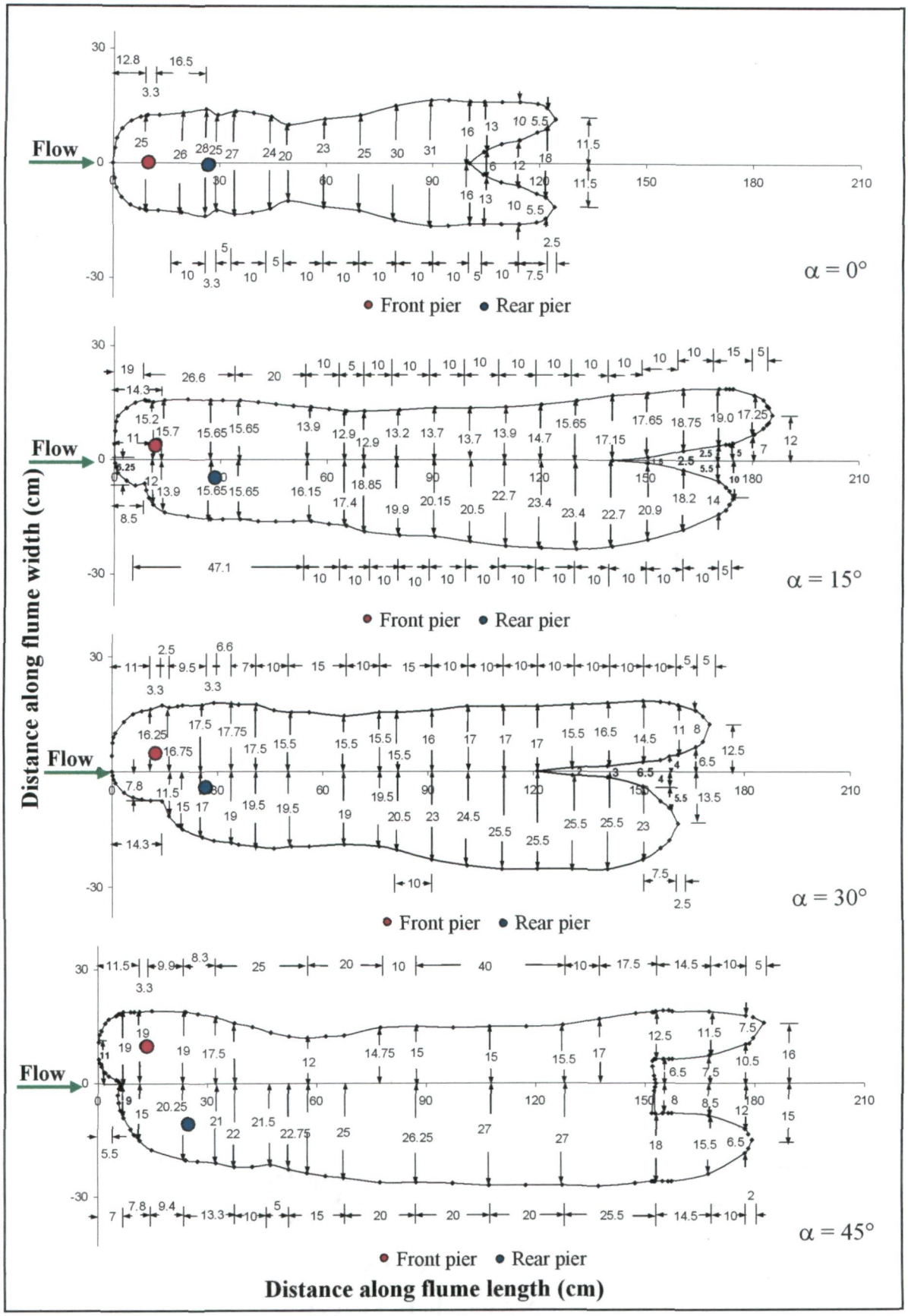

Areal extents of scour for two piers at constant radial pier spacing and varied angle of attack α

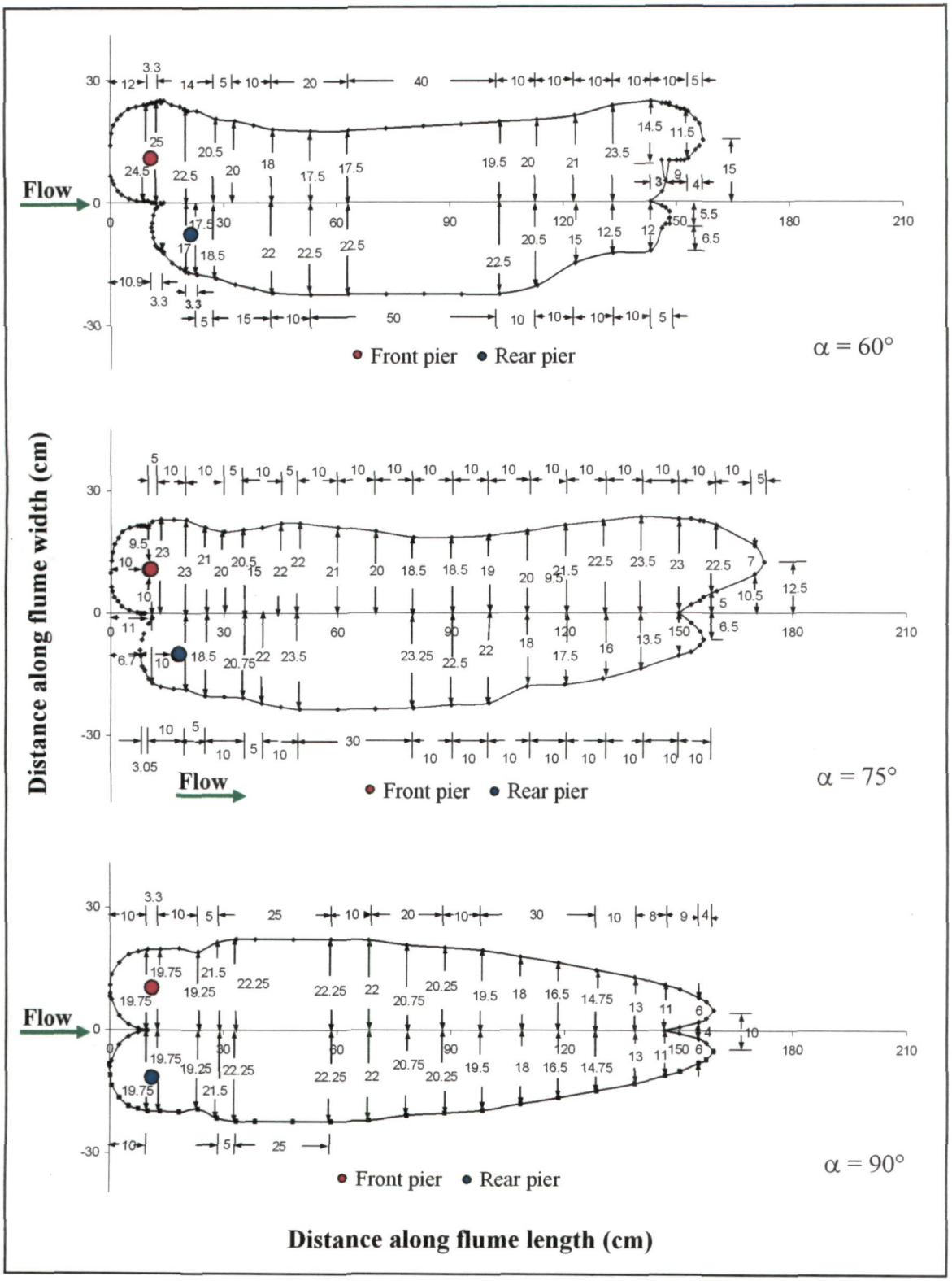

Areal extents of scour for two piers at constant radial pier spacing and varied angle of attack α

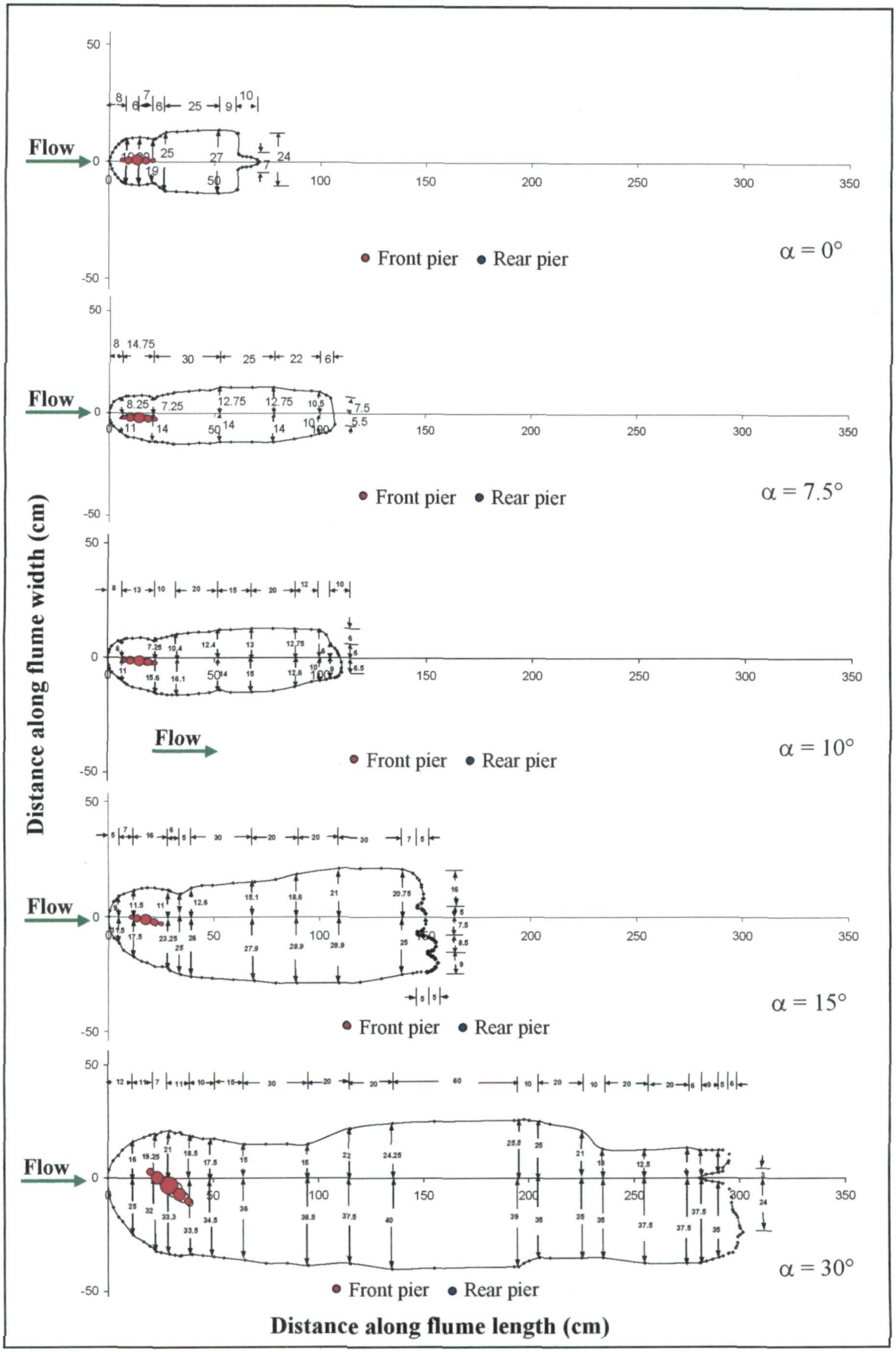

Areal extents of scour for a group of varying sizes of piers without collar at different angles of attack α

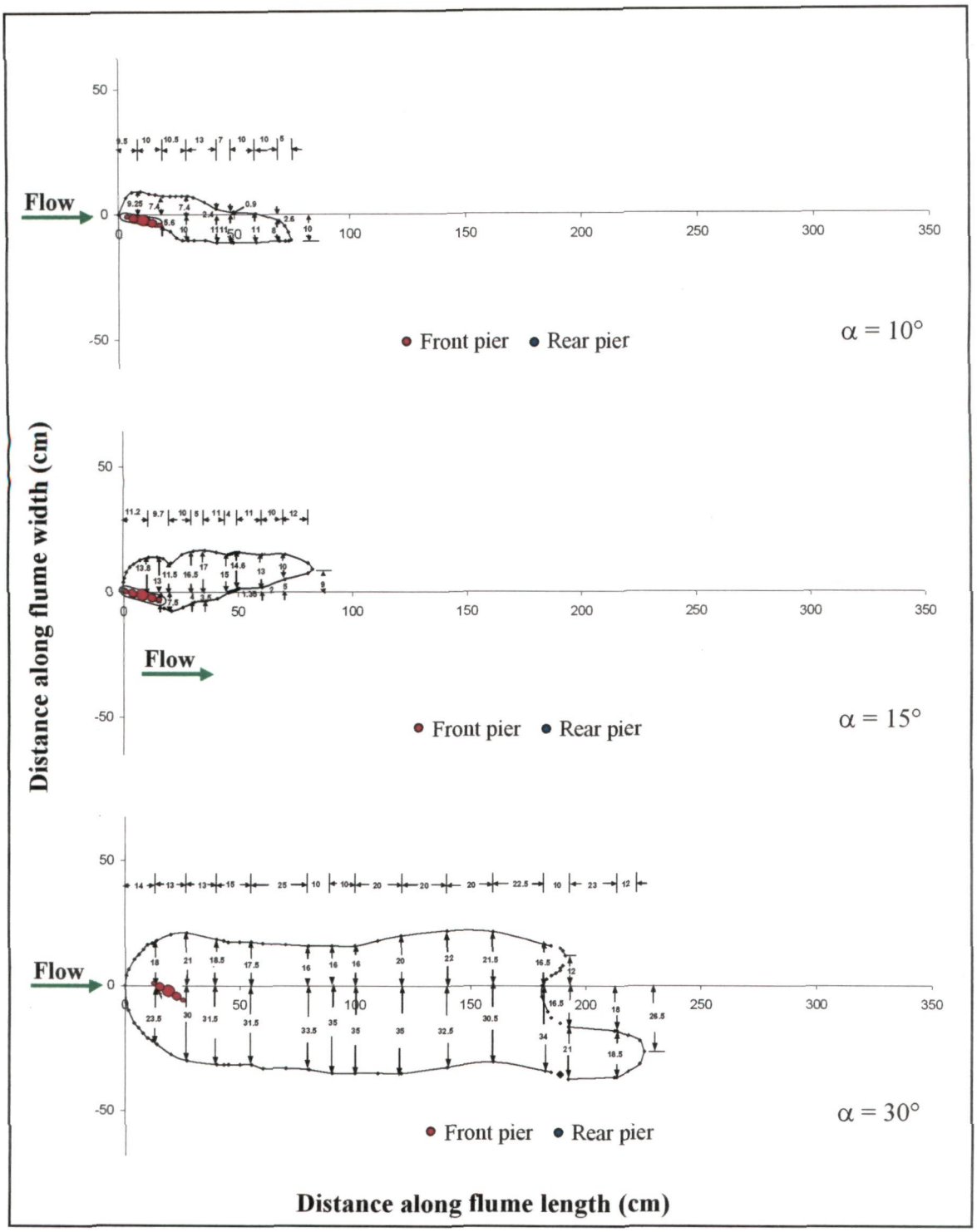

Areal extents of scour for a group of varying sizes of piers with collar at different angles of attack α

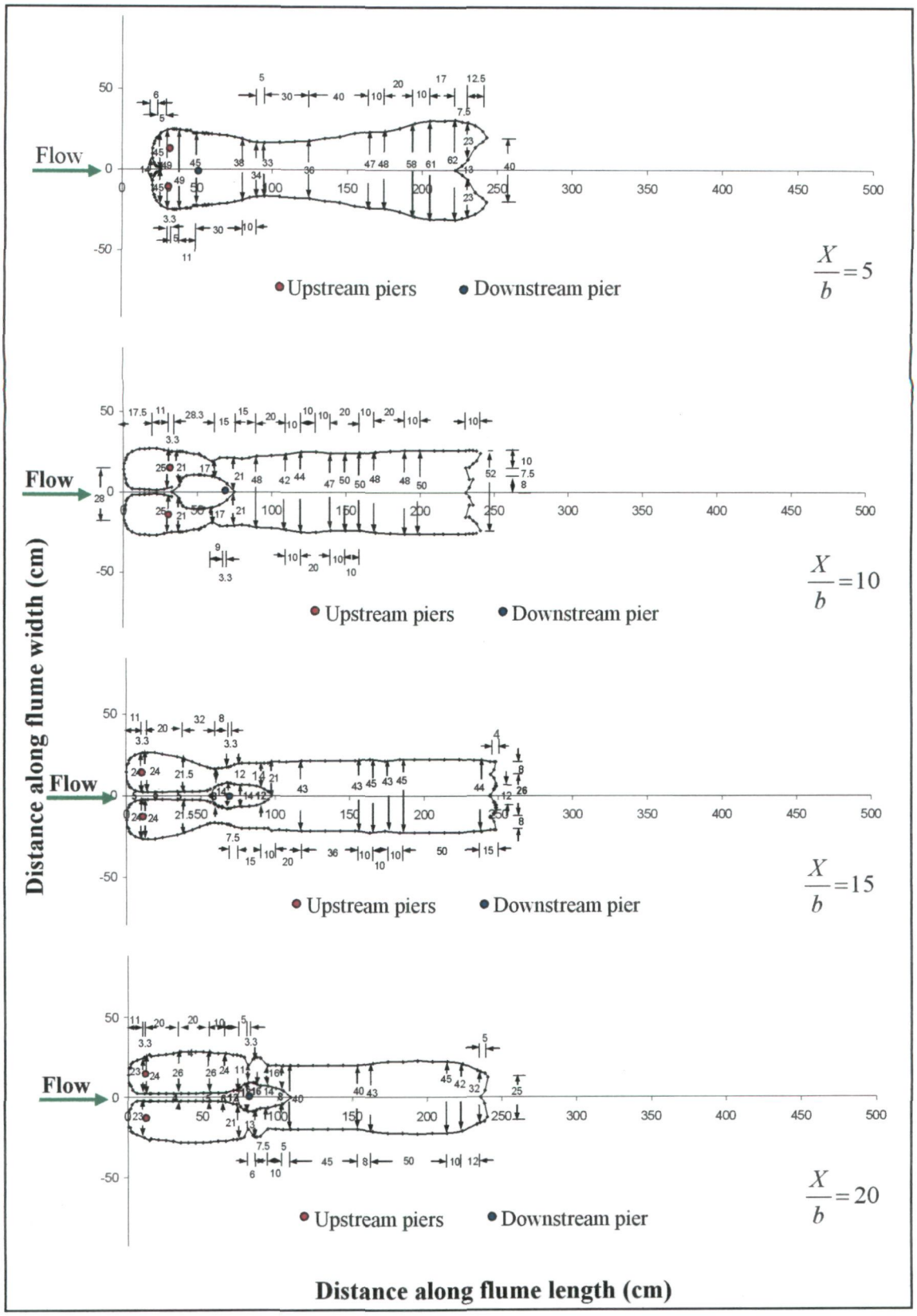

Areal extents of scour for three piers placed in staggered arrangement at varied longitudinal pier spacings X/b

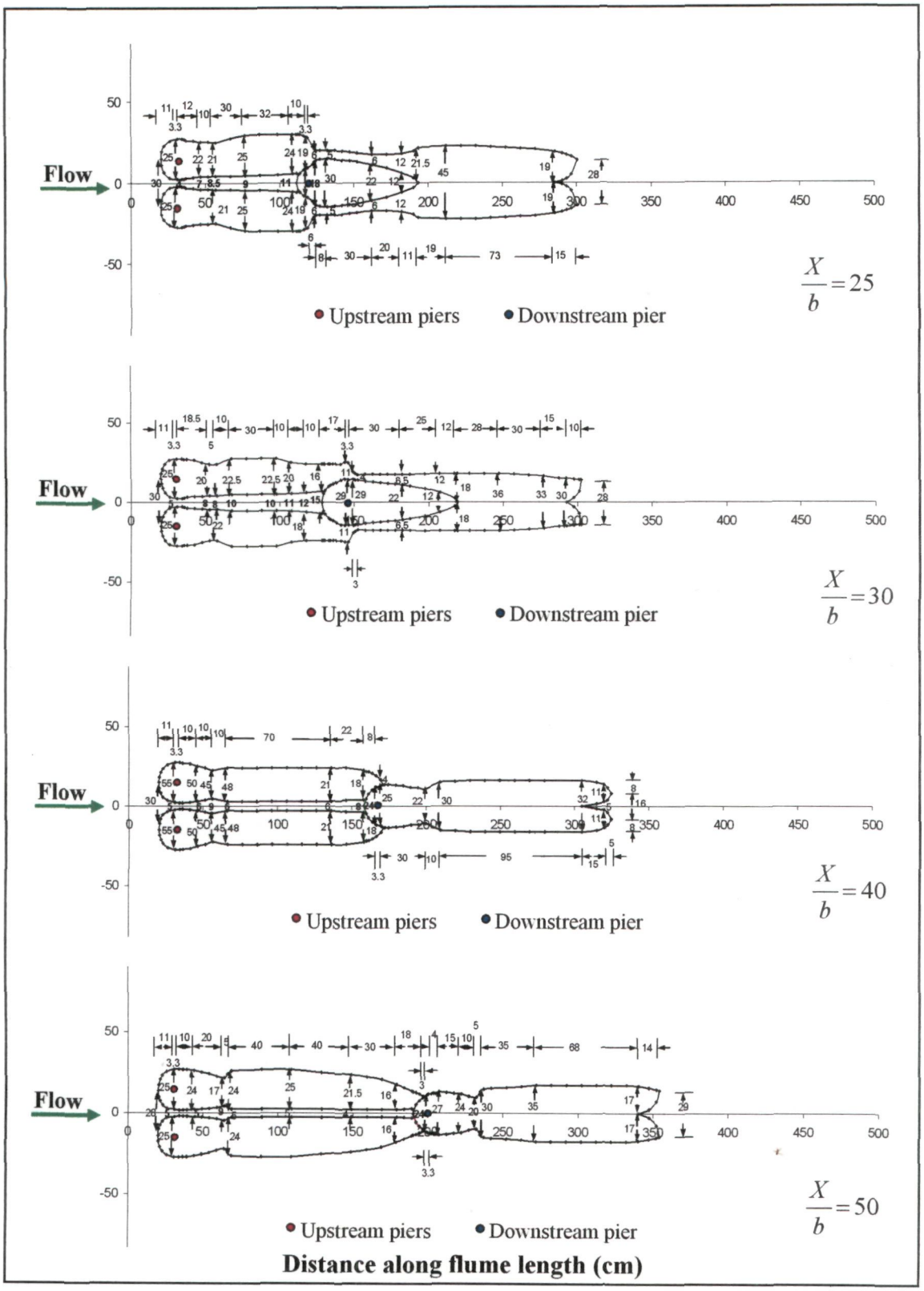

Areal extents of scour for three piers placed in staggered arrangement at varied longitudinal pier spacings X/b

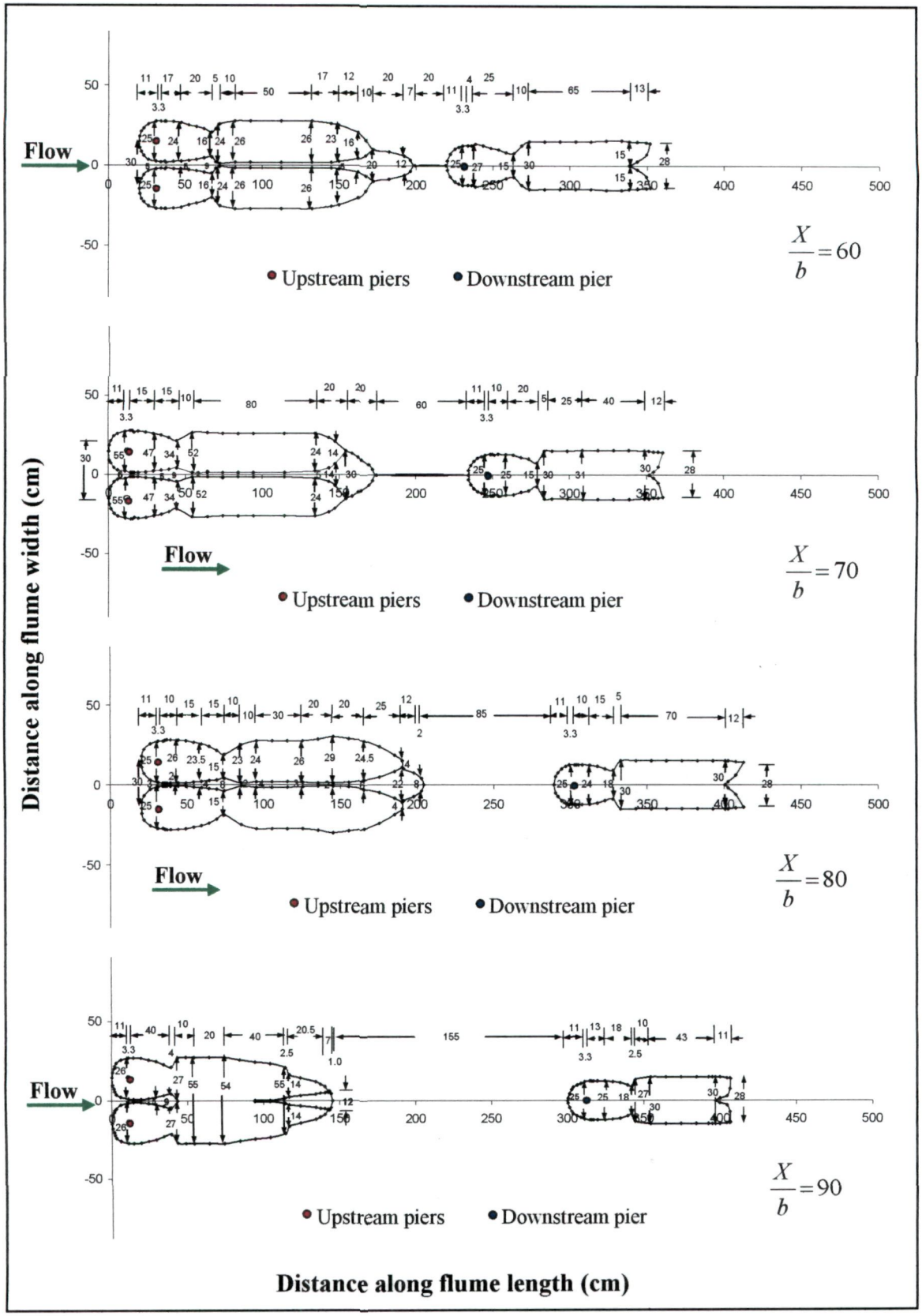

Areal extents of scour for three piers placed in staggered arrangement at varied longitudinal pier spacings X/b

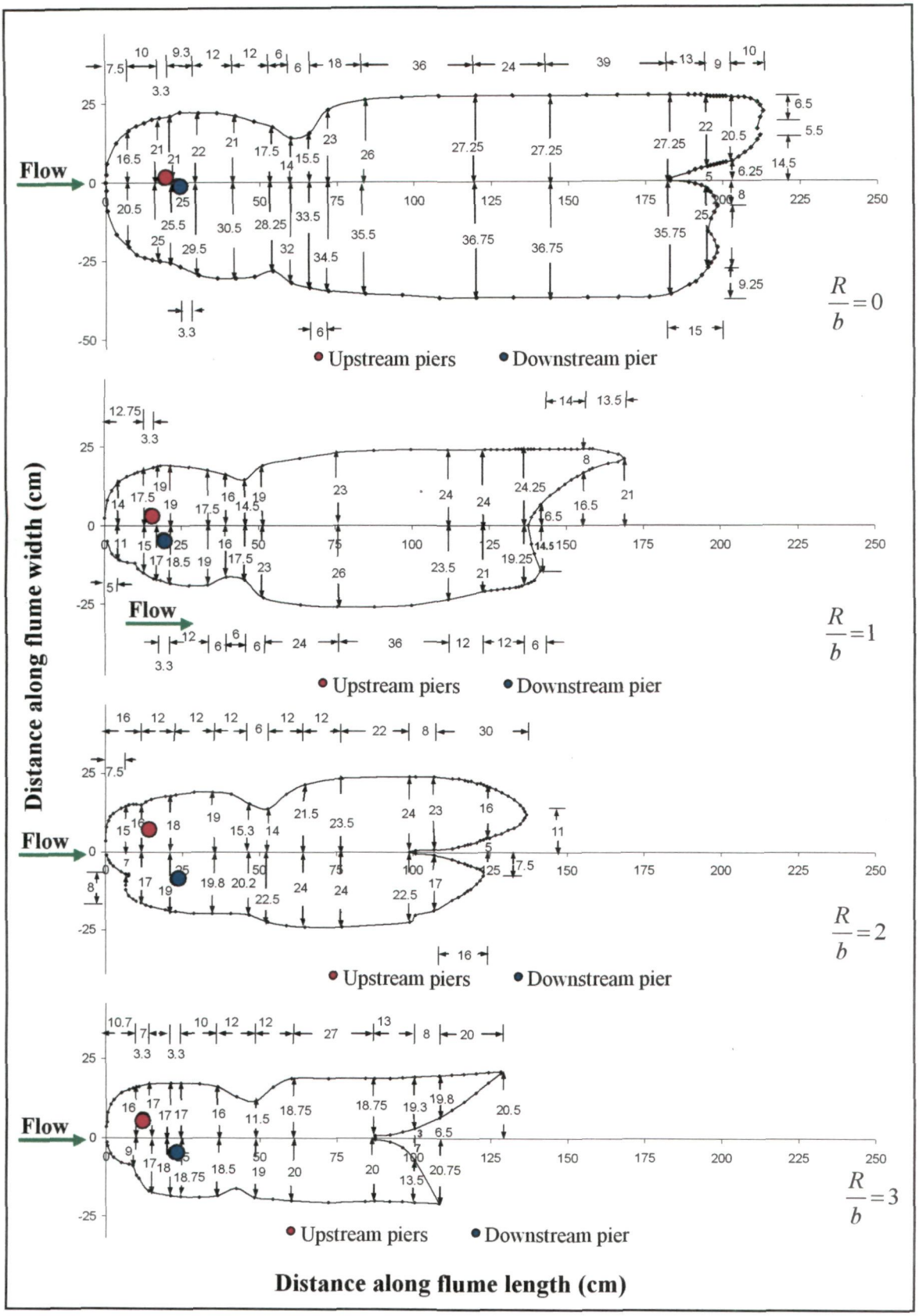

Areal extents of scour for two piers placed at constant angle of attack and varied radial pier spacing R/b

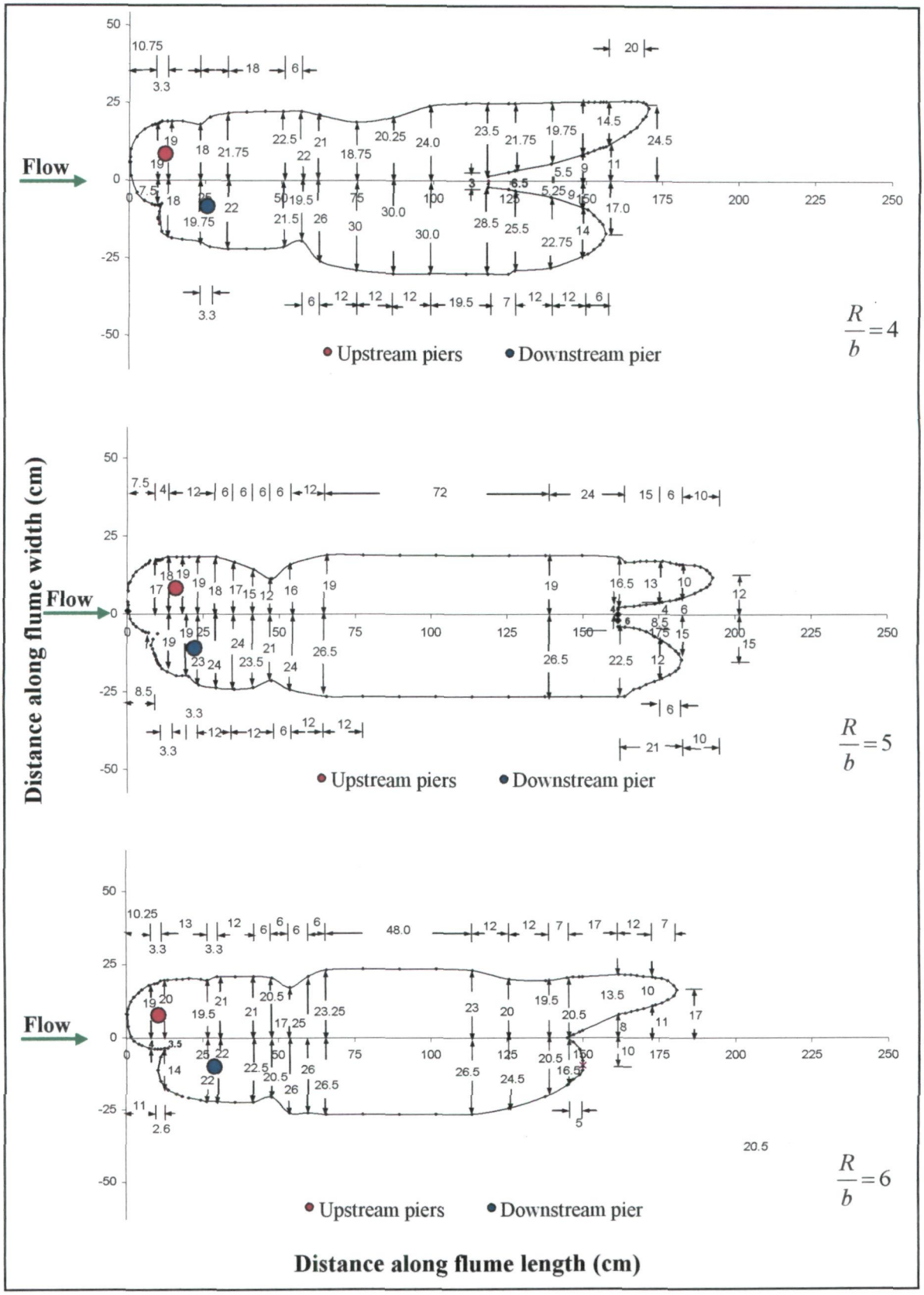

Areal extents of scour for two piers placed at constant angle of attack and varied radial pier spacing R/b

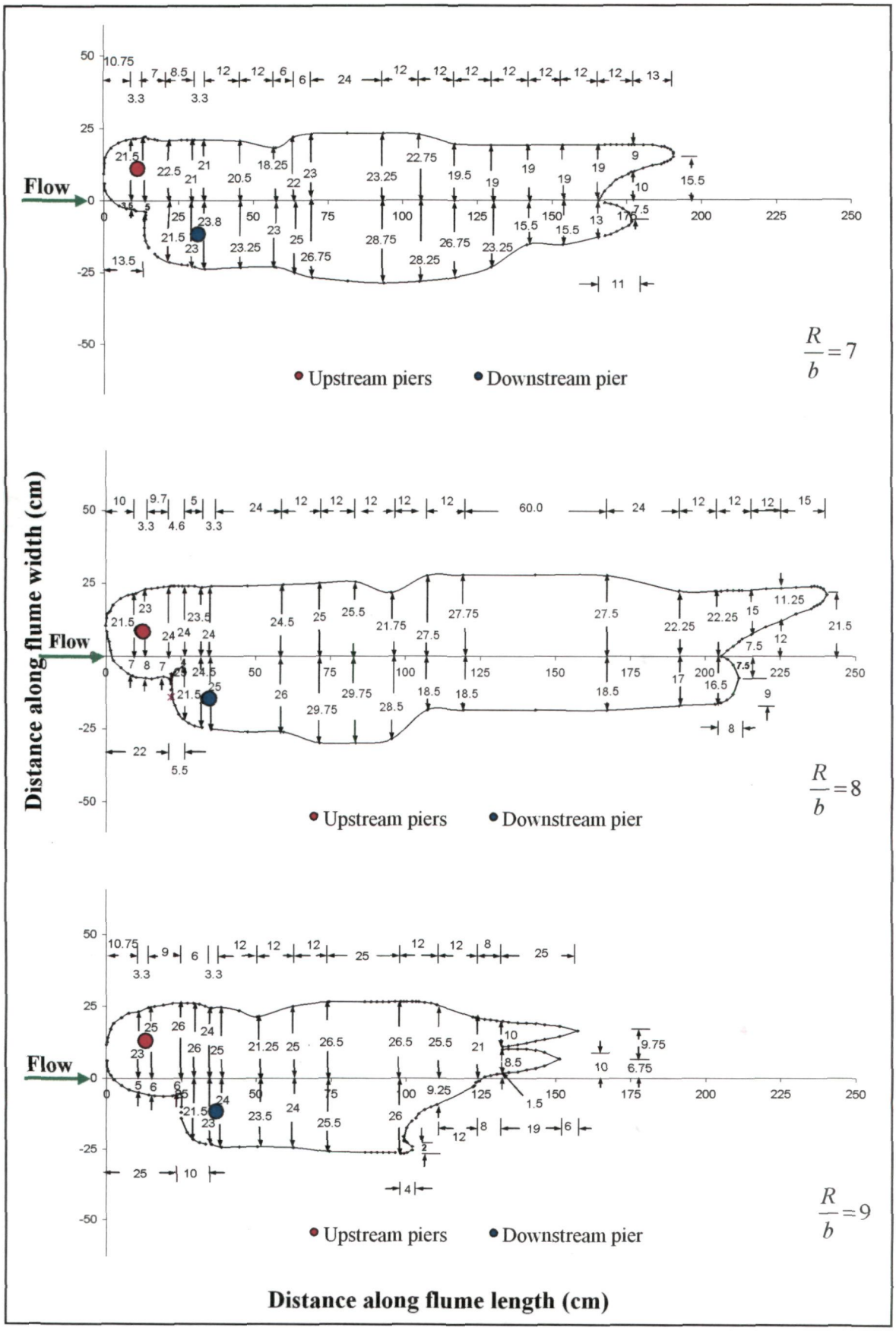

Areal extents of scour for two piers placed at constant angle of attack and varied radial pier spacing R/b

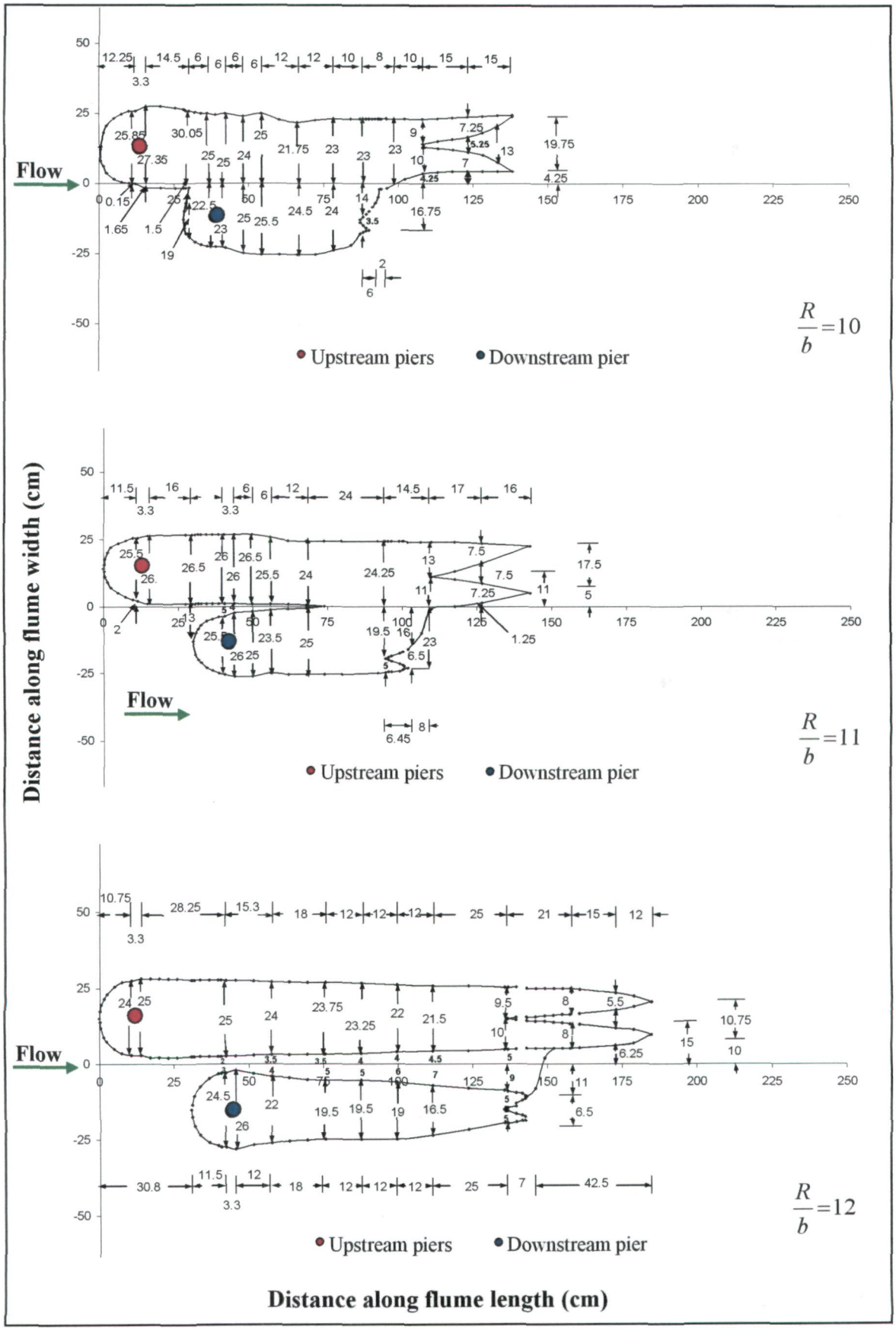

Areal extents of scour for two piers placed at constant angle of attack and varied radial pier spacing R/b

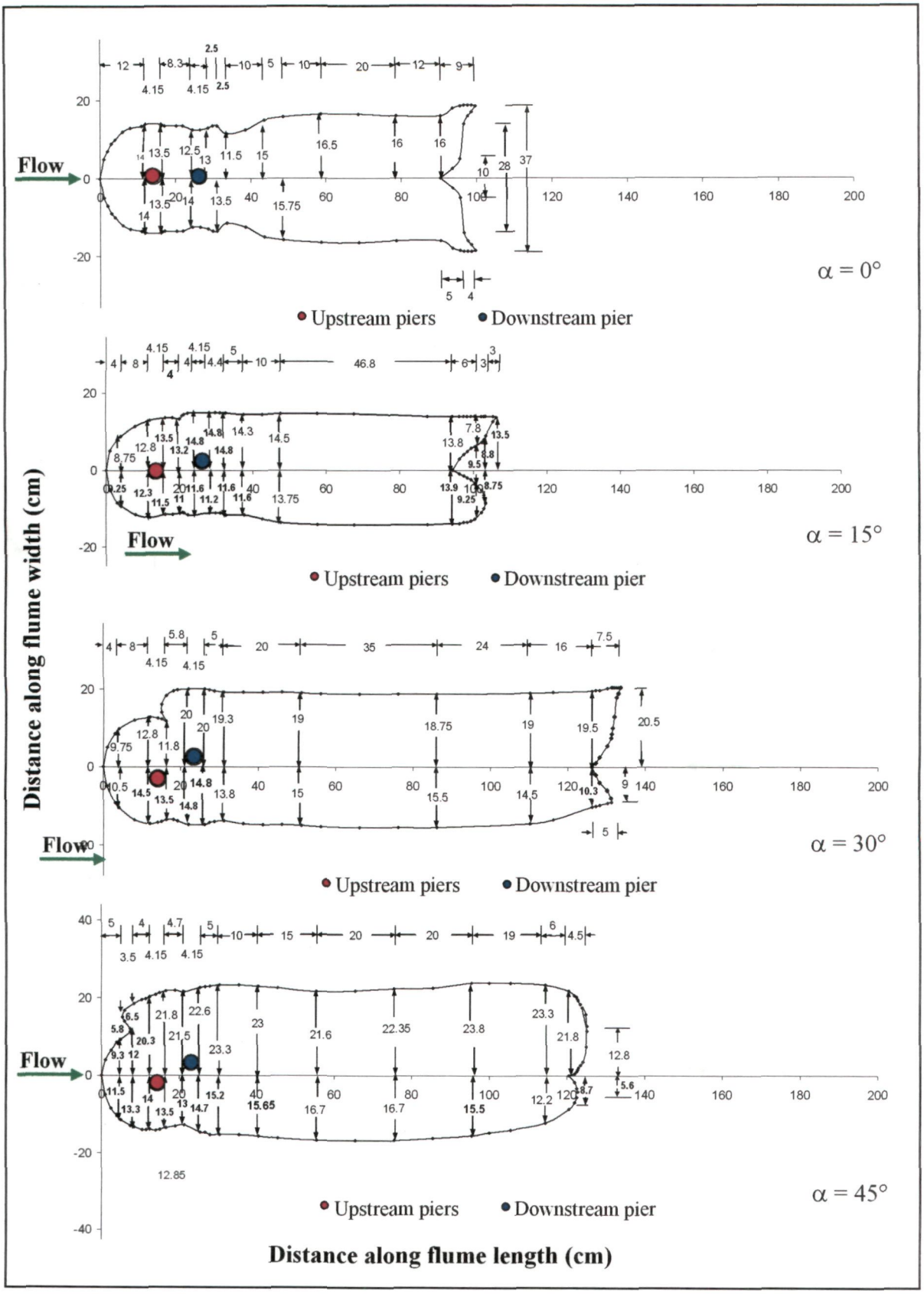

Areal extents of scour for two piers placed at fixed pier spacing without collar at varied angles of attack α

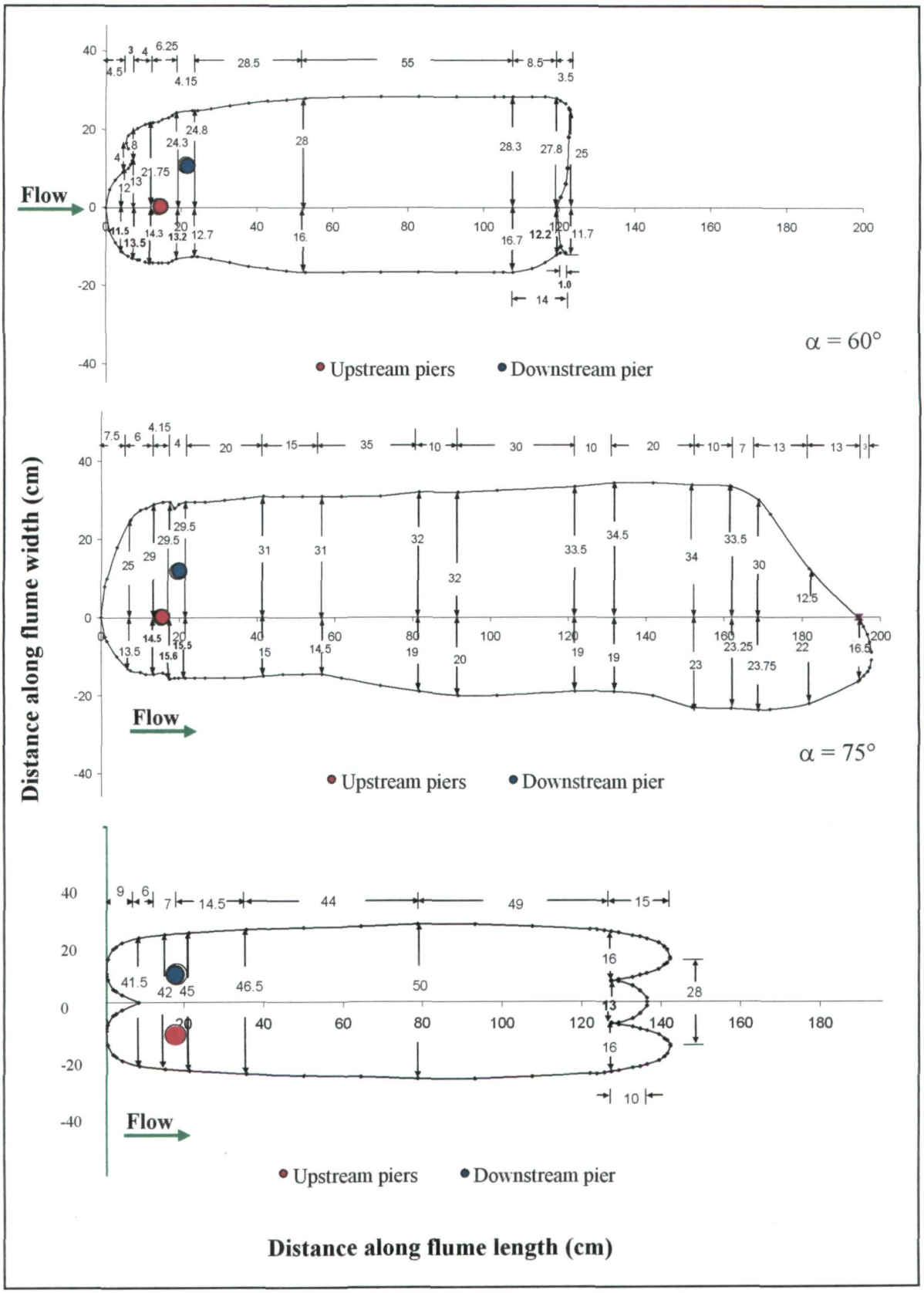

Areal extents of scour for two piers placed at fixed pier spacing without collar at varied angles of attack α

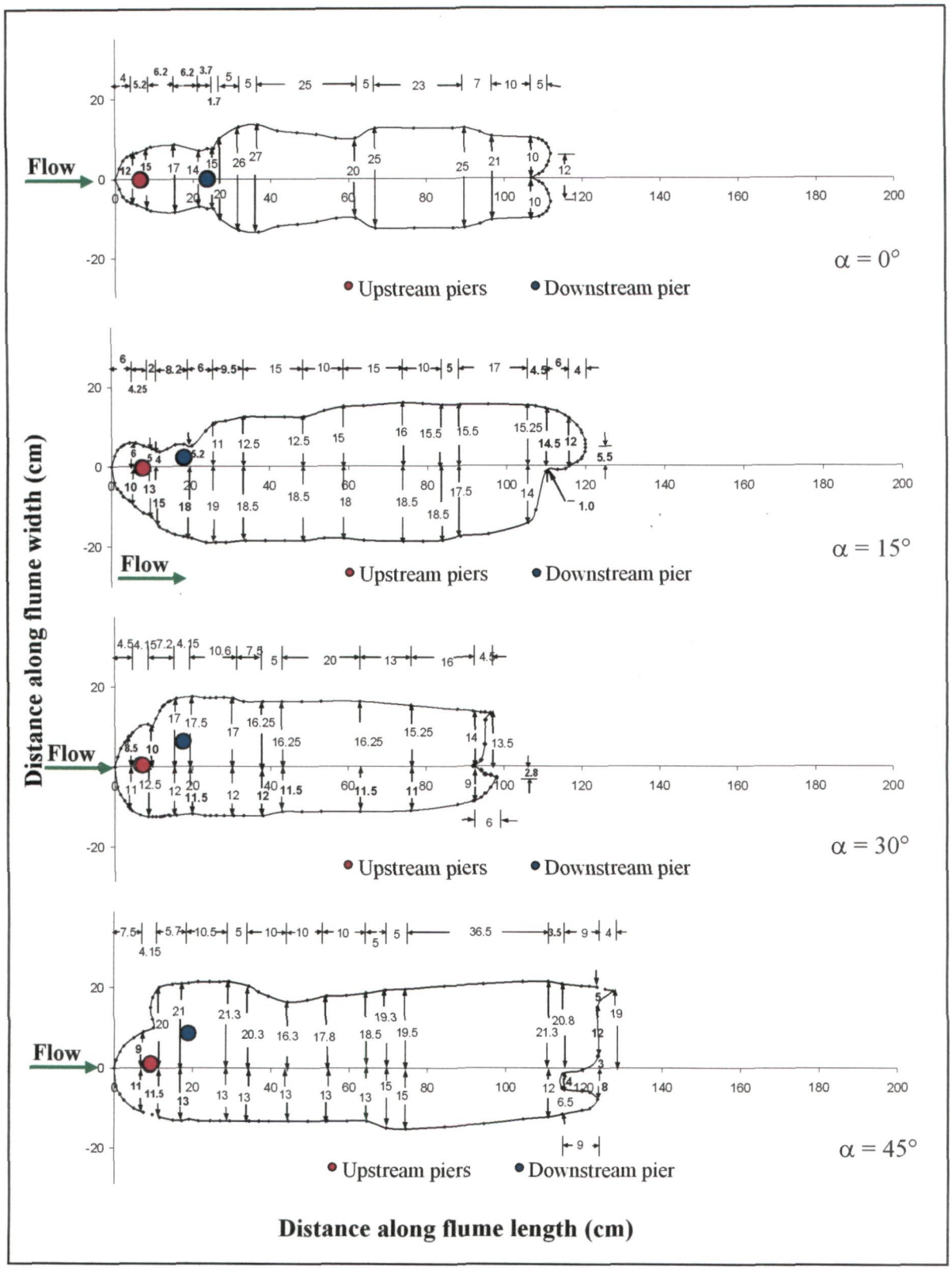

Areal extents of scour for two piers placed at fixed pier spacing with collar at varied angles of attack α

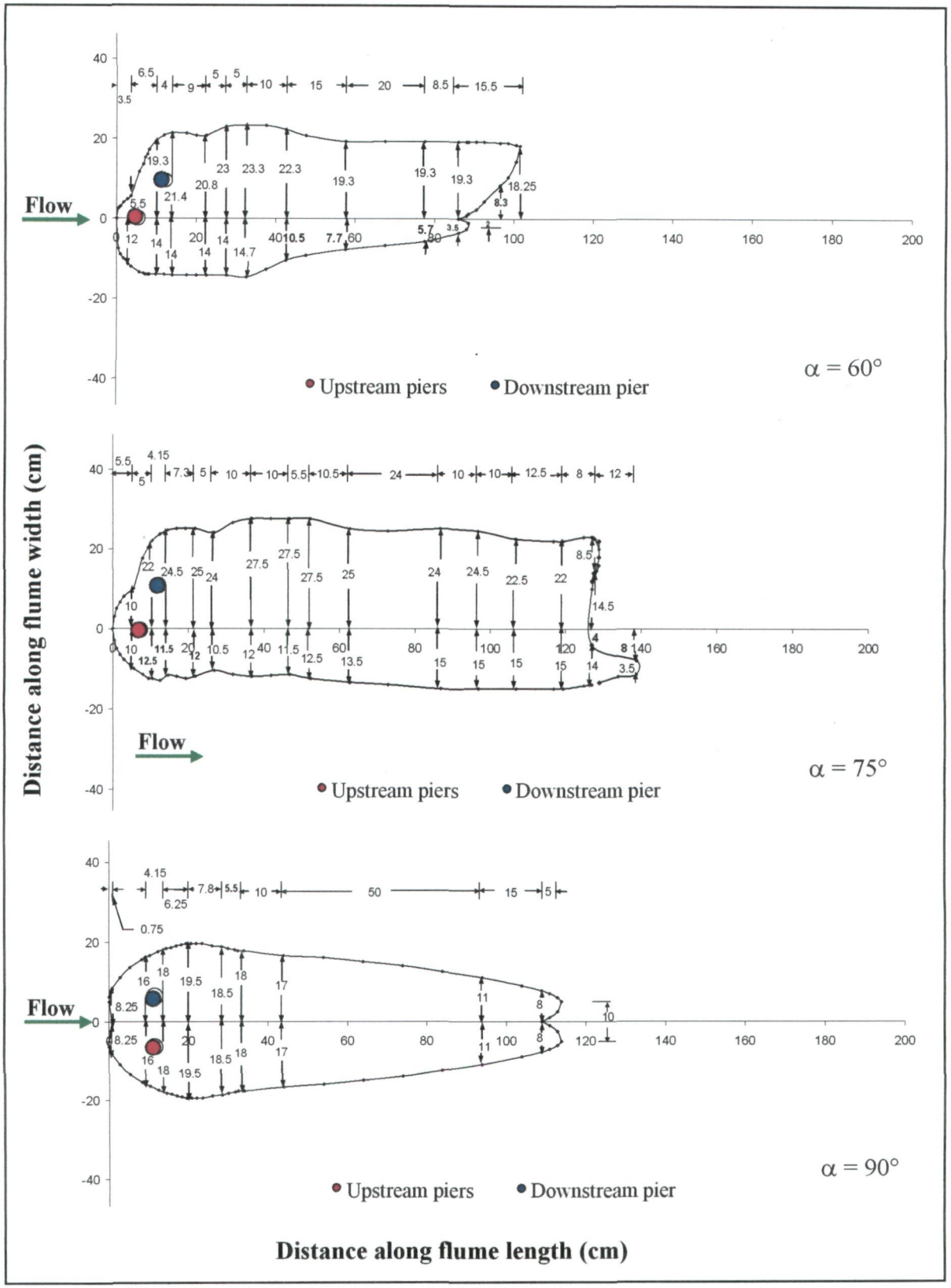

Areal extents of scour for two piers placed at fixed pier spacing with collar at varied angles of attack α

APPENDIX – V

CALCULATION OF FLOW CONDITIONS

In a laboratory flume with glass walls and sand bed, the roughness varies over the perimeter. In such a case the hydraulic radius for bed, R_b instead of R, in the resistance relations is used. Further, for the given sediment size it is intended to maintain flow conditions corresponding to bed shear equal to the critical shear for the given sediment *i.e.*, $\tau_0 = \tau_c$ where τ_0 is the bed shear stress and τ_c is the critical shear stress. Referring to Shields criterion,

$$\frac{\tau_c}{(\gamma_s - \gamma_f) d_{50}} = 0.06 \qquad \text{(AV-1)}$$

Critical shear velocity,

$$U_{*c} = \left(\frac{\tau_c}{\rho} \right)^{1/2} \qquad \text{(AV-2)}$$

The bed hydraulic radius at threshold condition,

$$R_{bc} = \frac{\tau_c}{(\gamma_f S_0)} \qquad \text{(AV-3)}$$

The Strickler's equation for Manning' coefficient of grain roughness,

$$n_s = \frac{d^{1/6}}{21} \qquad \text{(AV-4)}$$

Uniform velocity of flow,

$$U_0 = \frac{1}{n_s} R_{bc}^{\,2/3} S_0^{\,1/2} \qquad \text{(AV-5)}$$

Dimensionless critical shear stress,

$$\tau_{*c} = \frac{\tau_c}{(\gamma_s - \gamma_f) d_{50}} \qquad \text{(AV-6)}$$

Critical shear Reynolds number,

$$R_{*c} = \frac{(U_{*c}\, d_{50})}{\nu} \qquad \text{(AV-7)}$$

Flow Reynolds number,

$$R_{eh} = \frac{(U_0 y_0)}{\nu} \qquad \text{(AV-8)}$$

Particle Reynolds number,

$$R_{ed} = \frac{(U_0 d_{50})}{\nu} \tag{AV-9}$$

Flow Froude number,

$$F_r = \frac{U_0}{\sqrt{g y_0}} \tag{AV-10}$$

Critical flow Froude number,

$$F_{rc} = \frac{U_c}{\sqrt{g y_0}} \tag{AV-11}$$

APPENDIX – VI

SEDIMENT ENTRAINMENT

As per BS1377:1975 and (Vanoni, 1975), the sediment used in present investigation was cohesion-less coarse sand. The sediment normally consists of a distribution of particle sizes. Fig. Ap-VI shows the two common presentations of the particle size distribution, the cumulative distribution curve as the log-normal and the log-probability plot. The 50 % diameter on the log-probability plot is called the geometric mean diameter d_g and the geometric standard deviation σ_g is defined as

$$\sigma_g = \left(\frac{d_{84.1}}{d_{15.9}}\right)^{1/2} \quad or \quad \sigma_g = \frac{d_{84.1}}{d_{50}} = \frac{d_{50}}{d_{15.9}} \qquad \text{(AVI-1)}$$

the mean diameter, $\overline{d}$, is given by arithmetic mean of the size distribution. The values of $\overline{d}$ and d_g are related by

$$\overline{d} = d_g \exp\,[0.5 \log_n \sigma_g] \qquad \text{(AVI-2)}$$

The mean grain size can be determined as

$$\overline{d} = \frac{\sum_{p=0}^{100\%} \overline{di}\,pi}{\sum_{p=0}^{100\%} pi}\;;\; \overline{di} = \frac{1}{2}(di + di + 1) \qquad \text{(AVI-3)}$$

where p_i is the percentage weight of size d_i.

The size of the sample for analysis depends on the size of the large particles present. The ASTM recommends a sample size M in kg

$$M = 0.082\ b^{1.5} \qquad \text{(AVI-4)}$$

Where b is the maximum intermediate tri-axial dimension in mm.

If $\frac{d_{95}}{d_5} <$ 4 or 5, the sediment is uniform from the hydraulic point of view, and similarly, if σ_g <1.5, the sediment may be considered uniform.

The initiation or threshold of movement of a particle due to the action of fluid flow is defined as the instant when the applied forces due to fluid drag and lift, causing the particle to move, exceed the stabilizing force due to gravity. For uniform sediments in unidirectional flow this condition is best defined by Shields curve shown in Fig.1, which defines the threshold in terms of the entrainment function.

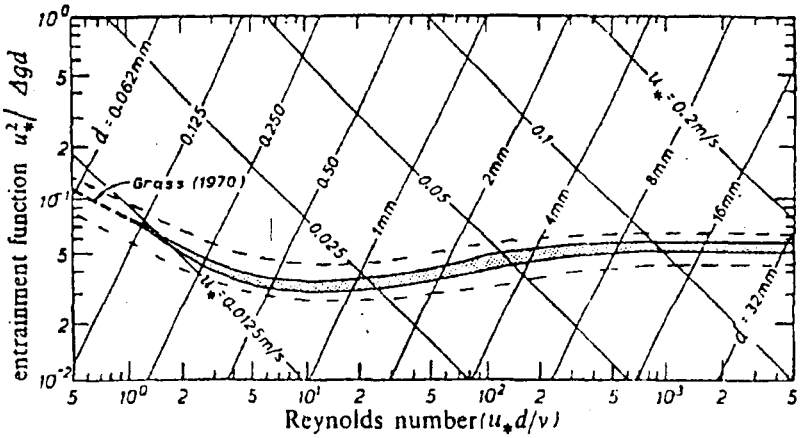

Fig. Ap-VI Sediment entrainment as a function of Reynolds number according to Shields. The shaded band indicates the spread of data by Shields, the dashed lines the envelope to most of the published data.

$$\theta_c = \frac{\tau_c}{(\rho g \Delta d)} = \frac{U_{*_c}^2}{(g \Delta d)} \qquad \text{(AVI-5)}$$

Which is a dimensionless shear stress, and the particle Reynolds number $R_{e*} = U_* d/\nu$ where $U_* = (\tau_0/\rho)^{1/2}$ is the shear velocity, and τ_0 and τ_c are the bed shear stress and its critical value respectively, *i.e.*, $\tau_0 = \rho g y_0 S$ where y_0 is the depth of flow and S is the energy slope.

The critical velocity can be calculated for given conditions from the critical shear stress or shear velocity. Thus mean critical velocity is

$$\frac{U_{*_c} C}{\sqrt{g}} \text{ or } U_c = U_{*_c}\left(5.75 \log \frac{y_0}{2d} + 6\right) \qquad \text{(AVI-6)}$$

or at a given elevation

$$U_c = 5.75 U_{*_c} \log \frac{y}{y'} \qquad \text{(AVI-7)}$$

Where C is the Chezy coefficient and y' is the elevation at which the logarithmic velocity distribution has zero velocity.

APPENDIX – VII

CALCULATION OF HYDRAULIC RADIUS FOR GLASS SIDED LABORATORY FLUME

In a laboratory flume with glass walls and sand bed, the roughness varies over the perimeter. In such a case, the hydraulic radius of the bed, R_b instead of R in the resistance relations. The hydraulic radius of the bed, R_b can be calculated by the following procedure (Einstein, H.A., 1942. In this analysis it is assumed that the velocity is uniformly distributed over the whole cross section.

Assuming that the total flow area can be divided into areas corresponding to the bed and sides,

$$A=A_w+A_b \qquad \text{(AVII-1)}$$

Where A_w is the area corresponding to the sides and A_b the area corresponding to the bed.

Using Manning's equation for the sides,

$$U=\frac{1}{n_w}R_w^{2/3}S^{1/2} \qquad \text{(AVII-2)}$$

R_w, the hydraulic radius corresponding to the walls can be calculated, if n_w, the Manning's coefficient for the side walls, is known. For rectangular channel, from equation (AVII-3),

$$R_b=D\left(1-2\frac{R_w}{B}\right) \qquad \text{(AVII-3)}$$

In case the sides are smooth, Vanoni and Brooks (1957) have suggested a procedure based on the resistance equation for a smooth boundary. They wrote

$$R_{ew}=R_e\,(R_w/R) \qquad \text{(AVII-4)}$$

Where R_{ew} and R_e are Reynolds numbers for the side walls and the complete cross section, respectively. Also

$$gR_wS = (f_w/8)U^2 \qquad \text{(AVII-5)}$$

$$gRS = (f/8)U^2 \qquad \text{(AVII-6)}$$

$$R_w/R = f_w/f \qquad \text{(AVII-7)}$$

And $R_{ew}/f_w = R_e/f$ from equation (AVII-4)

Where, $f = 8gRS/U^2$, f_w and f are the friction factors for the sides and the whole cross-section, respectively. Since both R_e and f are known, R_{ew}/f_w can be calculated. Using the Karman-Prandtl equation, Vanoni and Brooks plotted a graph Fig. Ap-VII between f_w and R_{ew}/f_w which can be used to find f_w. Thus,

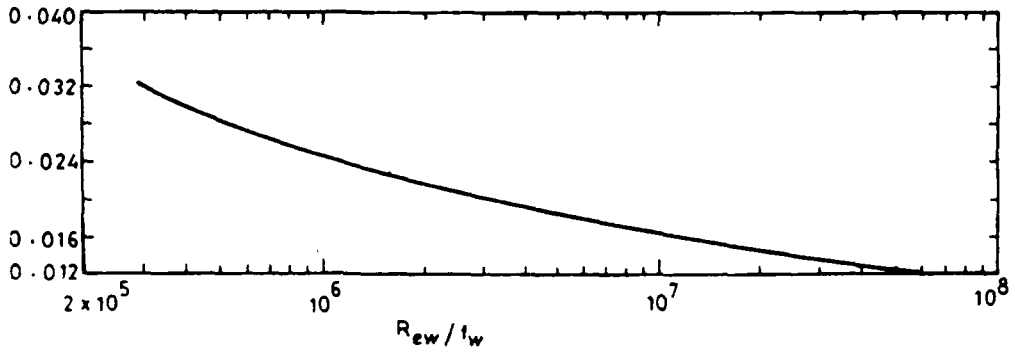

Fig. Ap-VII Relation between f_w and R_{ew}/f_w for smooth-walled channels (Vanoni and Brooks, 1957)

$$A_w = \frac{P_w f_w U^2}{8gS},\quad A_b = \frac{P_b f_b U^2}{8gS},\quad A = \frac{PfU^2}{8gS},\quad \text{and } A = A_b + A_w \qquad \text{(AVII-8)}$$

Hence,

$$Pf = P_b f_b + P_w f_w \qquad \text{(AVII-9)}$$

Since f_b, the friction factor of the bed is the only unknown in the above equation, f_b can be found and R_b determined from the following equation:

$$R_b = \frac{f_b U^2}{8gS} \qquad \text{(AVII-10)}$$

APPENDIX VIII

LIST OF PUBLICATIONS

(1) Mubeen Beg and Mohd. Adil Husain, (2002). **A Critical Study of Bed form Height Predictors**, *Water and Energy International Journal*, Central Board of irrigation and Power, Volume 59, No. 4, October-December 2002, pp. 41-49.

(2) Mubeen Beg, (2004). **Mutual Interference of bridge Piers on Local Scour**, paper presented in *Second International Conference on Scour and Erosion (ICES–2)*, held at Meritus Mandarin Hotel, **Singapore** from November 14 to November 17,2004., pp. 111-118, Vol. I.

(3) Mubeen Beg, (2004). Discussion on the paper, **Scour Reduction Around Non-Cylindrical Bridge Piers at High Angle of Attack Using Collar**, in the *ISH Journal of hydraulic Engineering*, India, pp.131-132. Vol.10, (1), No.2 Sep.-2004.

(4) Mohammad Jamil & Mubeen Beg, (2005). **A Critical Study of Bridge Pier Scour Depth Predictors**, *National Conference on Hydraulics & Water Resources with Special Emphasis on Tsunami*, organized by SiddaGanga Institute of technology and Indian society For Hydraulics, Tumkur, and Karnataka held at SiddaGanga Institute of technology, Tumkur, Karnataka, Dec. 8-9, 2005. , pp. 626-635

(5) Mubeen Beg and Mohammad Jamil, (2006). **Scour Reduction Using Collar around Piers Group**, *Third International Conference on Scour and Erosion (ICES – 3)*, held from November 1 to 3, 2006 in **Amsterdam, The Netherlands.**

(6) Mubeen Beg, (2008). **Scour Reduction By Using A Collar Around A Pier Group**, *4th International Conference on Scour and Erosion (ICES–4)* sponsored by The Japanese Geotechnical Society, ISSMGE Technical Committee TC33 on Geotechnics of Soil Erosion, **Japan Society of Civil Engineers,** Japan Society of Erosion Control Engineering and The Japan Landslide Society, to be held at Surugadai Memorial Hall, Chuo University, **Tokyo, Japan**, 5-7 November, 2008.

The maximum depths of scour and their location of occurrence around the collar are given in Table 5.7.

Table 5.7 Maximum scour depth at group of two piers with collar

Angle of Attackα	Maximum scour depth (cm)	Location of maximum scour depth
0°	1.95	5 cm from downstream edge of collar
15°	3.4	5 cm from downstream edge of collar and 10 cm on right side
30°	3.95	1.5 cm from downstream edge of collar and 10 cm on right side
45°	5.65	0.5 cm from right face of downstream pier
60°	4.9	5 cm from downstream edge of collar and 12.5 cm on right side
75°	6.55	Nose of front pier
90°	7.5	Nose of front pier

5.11.19 Variation of scour depth

(a) Maximum scour depth at front and rear piers without collar

In order to check the effectiveness of piers group in reducing scour depth, the maximum scour depths observed at front and rear piers without collar are made dimensionless by dividing them by the scour depth observed at an isolated pier of 41.5 mm diameter and are plotted against angles of attack as shown in Fig 5.164.

(i) Maximum scour depth at front pier

It is observed in Fig. 5.164 that at 0° angle, the scour depth at front pier is about 1.1 times more than that of an isolated pier. This increase in scour depth is caused by the reinforcing effect of rear pier. As the angle of attack increases, the effect of compression of horseshoe vortices assists the scour potential of flow at front pier due to which the scour depth at front pier further increases. In Fig 5.164 it can be seen that as angle of attack approaches to 45°, the scour depth approaches to maximum at 1.177 times more than that of an isolated pier indicating that the reinforcing effect is maximum at 45° angle. At angles of attack 45° $<\alpha<$ 90°, the scour depth at front pier

decreases but remains more than that of an isolated pier. This decrease in scour depth occurs due to a decrease in the reinforcing effect. At α = 90°, the scour depth is about 1.16 times more than that of an isolated pier. This increase in scour depth is caused only by the compression of horseshoe vortices between the two piers.

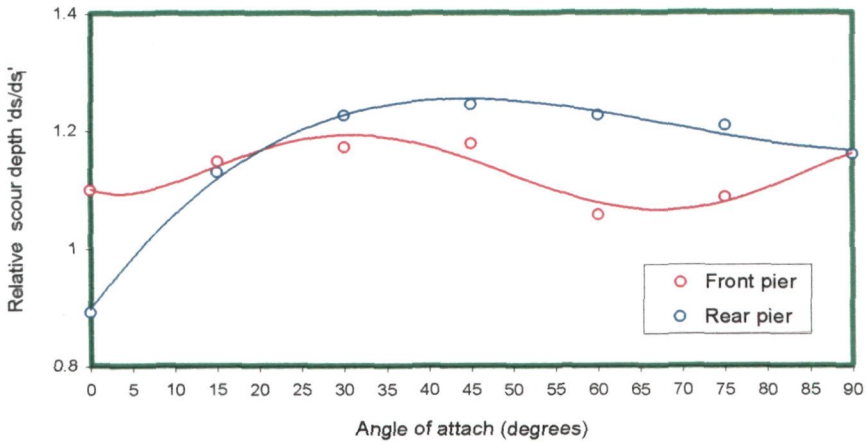

Fig. 5.164 Angle of attack versus relative scour depth without collar (where ds = scour depth at front or rear pier, ds_i = scour depth at 41.5 mm isolated pier).

(ii) Maximum scour depth at rear pier

Fig. 5.164 shows that the scour depth at rear pier is affected by the sheltering effect of front pier, compression of horseshoe vortices between the two piers and shed vortex effect of the front pier. It can be noticed that the scour depth at rear pier at 0° angle, is about 0.89 times of that observed at an isolated pier. This reduction in scour depth at rear pier is caused due to the sheltering effect of front pier. With an increase in angle of attack, the scour depth increases and reaches to a maximum at an angle α =45°. This increase in scour depth at rear pier suggests the predominance of the effects of compression of horseshoe vortices between the two piers and the shed vortices of front pier over the sheltering effect of front pier. The combined effect of horseshoe vortices compression and shed vortices is maximum at angle of α =45°. At angles of attack α>45°, it is observed that the effect of shed vortices reduces while the effect of compression horseshoe vortices still exists due to which the scour depth reduces, but remains more than that of an isolated pier. At an angle α =90°, the scour depth at two piers is affected only by the compression of horseshoe vortices between the piers and the scour depth that occurs at two piers is about 1.16 times more than that of an isolated pier.

(iii) Maximum scour depth at group of two piers with collar

The maximum scour depth observed at piers group with collar are plotted against angles of attack *'α'* as shown in Fig. 5.165. The scour depths without collar are also shown in Fig. 5.165. The comparison of two curves shows that how a collar is effective in reducing the scour depth. It is observed that the effectiveness of collar in the reduction of scour depth reduces as the angle of attack increases.

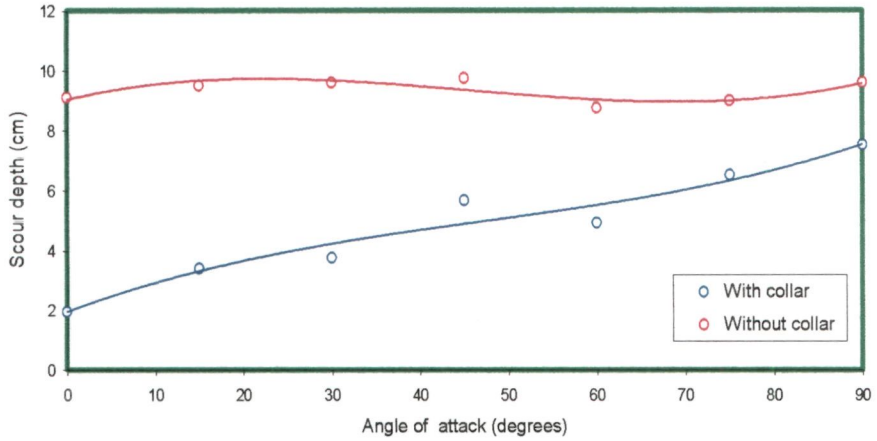

Fig. 5.165 angle of attack versus relative scour depth with collar.

In order to model the scour depth, ANN models the details of which are given in Tables 5.1 and 5.2 (Chapter 5-II) and ANN architectures Fig. 5.10 (Chapter 5-II), are applied to the present experimental data for the estimation of scour depths at upstream and downstream piers with and without collar placed at varying angles of attack 'α'. The scatter grams plotted between observed and ANN estimated scour depths are shown in Fig.5.20 (Chapter 5-II). The closeness of data points to the line of best agreement indicates the accuracy of the ANN model in predicting the scour depths. The average values of correlation coefficient R^2 between observed and estimated scour depths at front and rear piers for training and testing data sets are 0.9825 and 0.97 respectively. The values of *rmse* between observed and estimated scour depths for front and rear piers are 7.975×10^{-5} and 4.61×10^{-5} respectively. The higher values of R^2 and lower values of *rmse* indicate the accuracy of ANN models in predicting the scour depth.

(iv) Comparison of maximum scour depth at group of two piers and round-nose rectangular pier aligned at varied angles of attack without collar.

Fig. 5.166 compares the maximum scour depths observed around the group of two piers without collar with those computed for round-nose rectangular pier without collar using the equation of Richardson and Davis (2001). It is noticed that except at zero degree angle of attack, group of two piers produces scour depths significantly shallower than those at round-nose rectangular pier at angles of attack ranging in

between 15° to 90°. The reason for the occurrence of deeper scour depth at group of two piers at zero angle of attack is the reinforcing effect of downstream pier, while the reason behind the occurrence of shallower scour depths at angles of attack ranging in between 15°to 90°, is the gape between the two piers which behaves like a slot through the pier in reducing the scour depth. It can also be observed that the scour depth at round-nose rectangular pier increases with angle of attack while at group of two piers, scour depth after approaching to a maximum at 45°angle of attack, decreases with an increase in angle of attack. The reasons for this variation of scour depth at group of two piers are the reinforcing effect of downstream pier, vortex shedding effect of upstream pier, effect of compression of horseshoe vortices between the two piers and sheltering effect of upstream pier. The combined effect, however, is maximum at angle of attack of 45°.

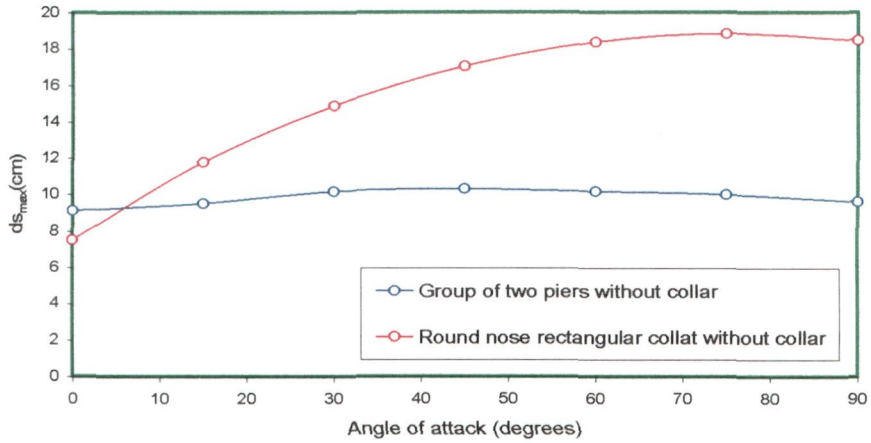

Fig. 5.166 Comparison of scour depths at a group of two piers and a round nose rectangular pier without collar at varying angles of attack.

Percent reduction in scour depth caused by the use of group of two piers as an alternative to a round-nose rectangular pier is plotted against angles of attack as shown in Fig. 5.167.

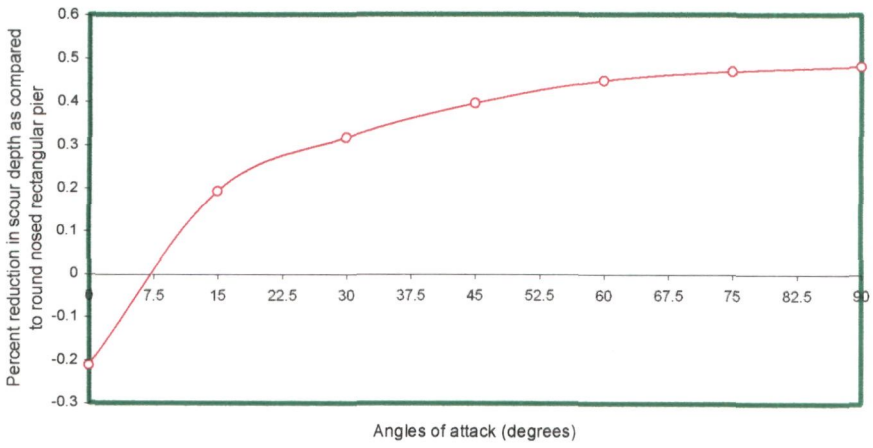

Fig. 5.167 Percent reduction in scour depth at group of two piers with respect to that at round-nose rectangular pier without collar.

It can be noticed that at zero degree angle of attack, round-nose rectangular pier produces a scour depth about 21% lesser than that of group of two piers. However, as angle of attack increases beyond 15°, group of two piers as compared to round-nose rectangular pier, causes reasonably high percent reduction in scour depth.

5.11.20 Efficiency of collar in scour depth reduction around a group of two piers

The percentile of scour depth reduction due to the application of collar to the group of two piers is plotted against angles of attack 'α' as shown in Fig.5.168.

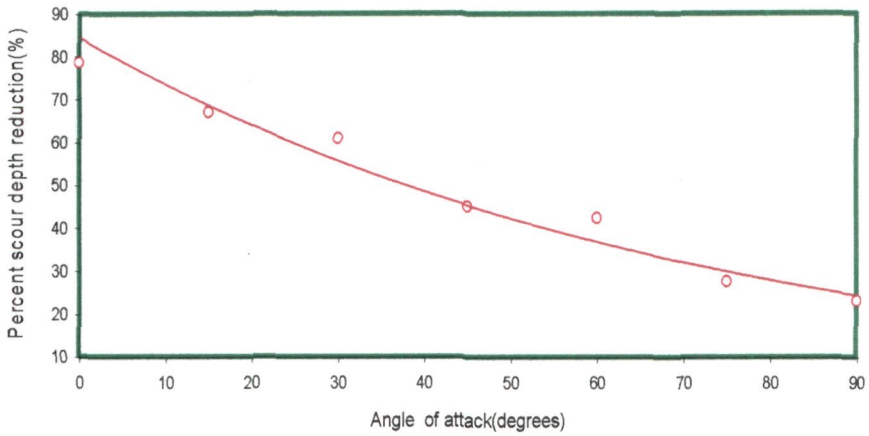

Fig. 5.168 Percent reduction in scour depth with collar.

The percent reduction in scour depth at front and rear piers with collar aligned at 0° angle of attack are 78.5% and 97.86% respectively. This reduction is mainly due to the fact that collar extends around the two piers which protects the bed from scouring effect of down-flow at the base of the piers and the associated vortex action around the base of the piers. Moreover, as angle of attack approaches to 15°, the percent reduction at front and rear piers leftovers 64.89% and 74.86% respectively. Fig.5.168 shows that the percent reduction in scour depth decreases with angle of attack and leftovers only 21.88% when angle of attack approaches to 90°.

5.11.21Comparison between studies of Zarrati *et. al.* 2006 and present study on scour depth reduction efficiency of collar around two piers aligned in line with flow

Zarrati *et. al.* (2006) applied a collar to a group of two circular piers. In comparison to the scour depths reported by Hannah (1978) for a group of two piers with x/b=2 (where x is clear spacing between the piers and b is the pier diameter) unprotected by collar and

aligned with the flow (see, Fig. 2.31, Chapter II), Zarrati *et al.* (2006) reported maximum reduction in scour depth at front and rear piers as 25% and 35% respectively. In present study the percent reduction in scour depth at front and rear piers with collar aligned at 0° angle of attack are achieved as 78.5% and 97.86% respectively. The percent reductions in scour depth in present study are higher than that of Zarrati *et al.*(2006). The reason for these percentiles being higher than Zarrati *et al.* (2006) is ascribed firstly to the fact that the space between two piers which was covered with rip-rap by Zarrati *et. al.*(2006), in present case is shielded by collar against the action of horseshoe vortices around the piers and wake vortices of front pier. Secondly, the test duration in present case is shorter as compared to that used by Zarrati *et. al.* (2006) in their experiments. Fig.5.168 indicates that the percent reduction in scour depth decreases with angle of attack and leftovers only 21.88% when angle of attack approaches to 90°. Zarrati *et al.* (2006) also reported lowest scour depth reduction efficiency of collar at an angle of 90°. Moreover, for two piers aligned transverse to the flow, they observed slight increase in scour depth.

5.11.22 Comparison of efficiency of collar applied to a group of two piers and a round nose rectangular pier

Zarrati *et al.* (2004) studied the efficiency of collars on a round-nose rectangular pier. The reduction in the effectiveness of collar around a round-nose rectangular pier with an increase in angle of attack is reported by Zarrati *et al.* (2004). For a round-nose rectangular pier at 0° angle of attack with collar to pier width ratios W/b=2 and W/b=3, Zarrati *et al.* (2004) reported 17 % and 74% reduction in scour depth respectively. However, at 10°angle of attack the percentage of scour depth reduction corresponding to W/b=2 and W/b=3 is reported by Zarrati *et al.* (2004) as 10.5% and 35% respectively. Nonetheless, as angle of attach increases to 15°, the percent reduction in present case remains only 64.21% as compared to maximum reduction of 35% reported by Zarrati *et al.* (2006) at 10° angle of attack with W/b=3.

5.11.23 Areal extent of scour

Using the data collected in present study the areal extent of scour around two piers with and without collar are plotted as shown in Fig.5.169. It can be seen that areal extent around two piers is unsymmetrical except at α=0° and 90°.

The ratios of the areas of scour extent with collar to that without collar *'Ac/A'* are plotted against angles of attack as shown in Fig. 5.169.

It is observed that the area of scour extent with collar at 0° angle is about 67.5 % of that without collar. It is clear from Fig.5.169 that as the angle of attack increases, the effectiveness of collar in reduction of area of extent decreases. The lowest effect of application of collar on the reduction of area of scour extent is observed at an angle of 45° where the area of scour extent with collar is 78.05% of that without collar. Beyond 45° angle, the effectiveness of collar in the reduction of area of scour extent increases upto 75° angle.

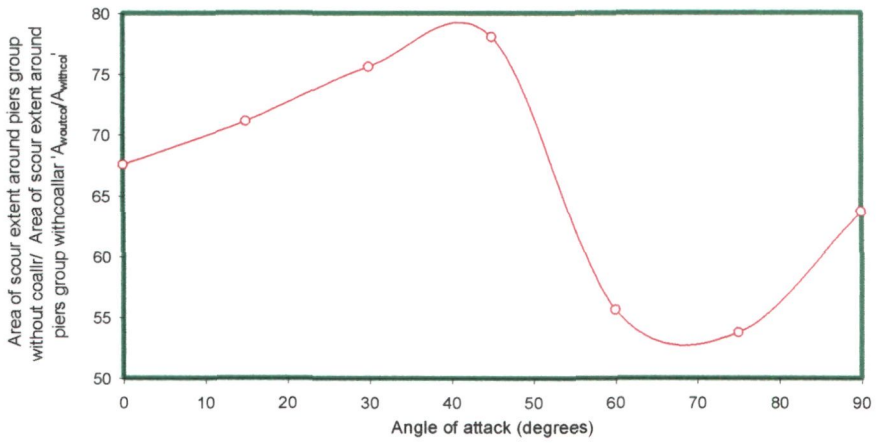

Fig. 5.169 Variation of area of scour extent around group of 41.5 mm diameter piers without collar relative to the corresponding area with collar *'$A_{woutcol}/A_{withcol}$'* with angle of attack(where, $A_{woutcol}$ = (area of scour extent around 41.5 mm diameter piers group without collar and $A_{withcol}$ = area of scour extent around 41.5 mm diameter piers group with collar).

At angle of 90°, the effect of collar on the reduction of area of scour extent decreases where the area of scour extent with collar is 63.68% of that without collar. To understand the cause of variation in the relative values of area of scour extent, it is worth mentioning that the flow mechanism which changes with a change in the angle of attack is responsible. At 0° angle, the reinforcing effect of rear pier affects flow mechanism while at 90° angle; compression of horseshoe vortices between the two piers affects the flow mechanism. Between 0° and 90° angles, the flow mechanism is affected by the reinforcing effect of rear pier, shed vortex and shedding effects from front pier and compression of horseshoe vortices between the two piers, where some of these effects overcome the other in accordance with the change alignment of piers group.

5.11.24 Length of scour holes

The lengths of scour hole at upstream face of two piers without collar are divided by the corresponding quantity of an isolated pier to obtain the relative length of scour hole and the same are plotted against angles of attack 'α' as shown in Fig. 5.170.

It is observed that the length of scour hole at upstream face of front pier increases with angle of attack and reaches to a maximum at 45° angle. This increment in the length of scour holes is in accordance with the increase in scour depth, and the occurrence of maxima at 45° angle is due to the occurrence of maximum scour depth at this angle.

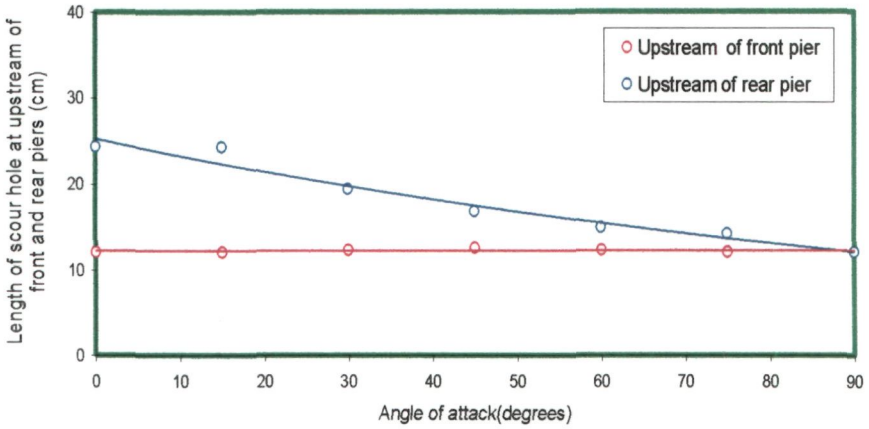

Fig. 5.170 Angle of attack versus relative length of scour hole at upstream face of 4.15 piers group without collar.

Beyond angle 45°, the length of scour hole decreases and reaches to a minimum at 90°. This decrement is in accordance with the decrement of scour depth at angles greater than 45°.

The relative lengths of scour holes at upstream face of rear pier decrease with angle of attack and reaches to a minimum at 90°. This decrease takes place due to the shifting of rear pier towards upstream due to an increase in angle of attack. At 90° angle, the lengths of scour holes at upstream faces of two piers are same.

5.11.25 Length of scour hole at downstream face of two piers without collar

To assess the effectiveness of use of piers group in reducing the length of scour hole, the lengths of scour holes at downstream face of two piers without collar are made dimensionless by dividing them by the corresponding quantity of an isolated pier of 4:1 length width ratio to obtain the relative length of scour hole and the same are plotted against angles of attack as shown in Fig.5.171.

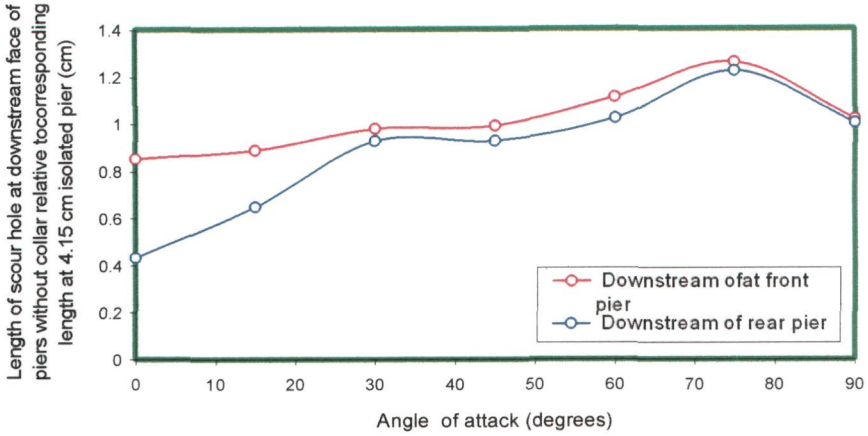

Fig. 5.171 Variation of length of scour hole at downstream face of piers in 41.5 mm piers group without collar with angles of attack '$L_{sh(d)}/L_{sh(di)}$' (where $L_{sh(d)}$ = length of scour hole at downstream of piers without collar, $L_{sh(di)}$ = length of scour hole at downstream of an isolated pier).

It is observed that the relative length of scour hole at the downstream face of the two piers increases with angle of attack. It is also observed that the values of relative length of scour holes of front pier are more than that of rear pier. The reason of such variation in the values of relative length of scour holes is the shifting of the location of rear pier with increasing angles of attack. At 90° angle, the lengths of scour holes at the downstream faces of two piers are same.

5.11.26 Length of sediment deposition at the downstream faces of front and rear piers without collar

The length of sediment deposition occurring at the downstream faces of front and rear piers with respect to the corresponding quantity at an isolated pier are plotted against angles of attack as shown in Fig. 5.172.

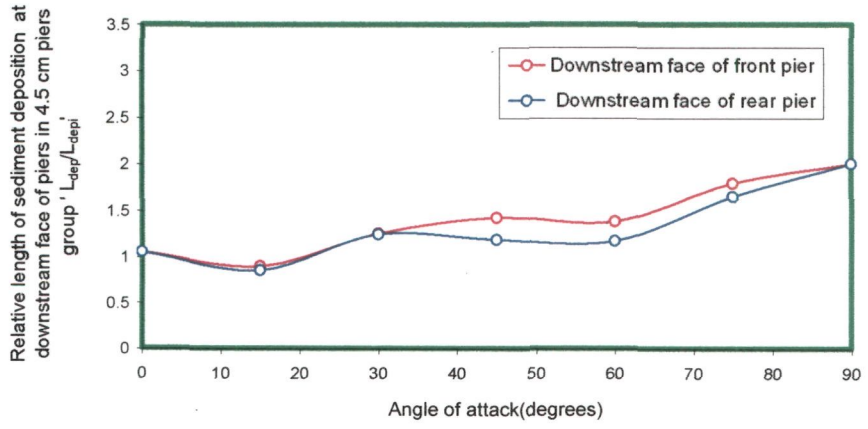

Fig. 5.172 Variation of length of sediment deposition at downstream face of piers in 41.5 mm piers group without collar relative to the corresponding length at downstream face of a 4.15 isolated round-nosed rectangular pier '$L_{dep}/L_{depi(rec)}$' (where L_{dep} = length of sediment deposition at downstream of piers without collar, $L_{depi(rec)}$ = length of sediment deposition at downstream of an isolated round nosed rectangular pier).

It is observed that upto 90° angle; the length of sediment deposition is same at two piers. As shown in Fig.5.172, the length of sediment deposition at the downstream face of front pier after increasing upto 45° angle, decreases upto 60° angle and then increases upto 90° angle.

The length of sediment deposition occurring at downstream face of rear pier, after increasing upto 30° angle, decreases upto 60° angle and then increases upto 90° angle. It can be seen that the length of sediment deposition at downstream faces of front and rear piers are same at angles of 90°. It is also observed that the length of deposition remains more at the downstream face of front pier than that at downstream face of rear pier at all angles of attack except 0° and 90° angles.

5.11.27 Length of Sediment Deposition at Downstream Face of Piers Group with Collar

The length of sediment deposition occurring at downstream faces of front and rear piers with collar relative to the corresponding quantity without collar are plotted against angles of attack as shown in Fig.5.173. The length of sediment deposition occurring at downstream face of front and rear piers with collar is smaller than that without collar at all angles of attack. The change in flow mechanism with increasing angles of attack causes the variation in the length of deposition occurring at downstream face of front and rear piers with collar as shown in Fig.5.173.

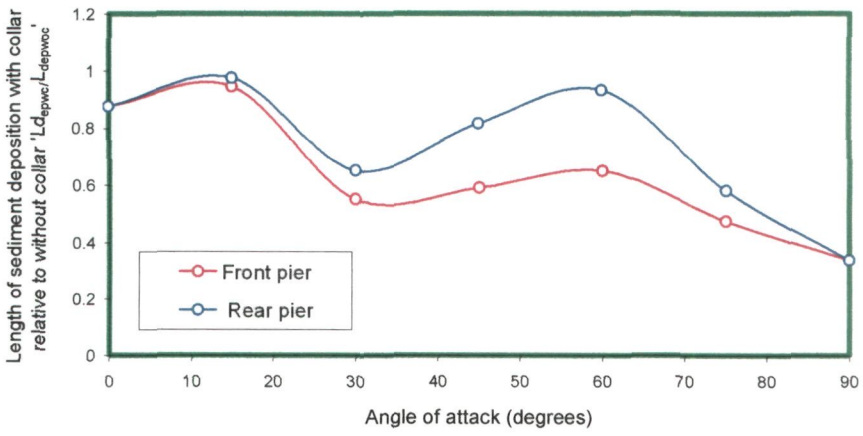

Fig. 5.173 Variation of length of sediment deposition at downstream face of piers group relative to that of without collar 'L_{depwc}/L_{depwoc}' with angles of attack (where $L_{dep(wc)}$ = length of sediment deposition with collar, $L_{dep\ (woc)}$ = length of sediment deposition without collar).

5.11.28 Concluding remarks

A bridge engineer has direct control over the geometry of his bridge foundation. He should, therefore, have an appreciation of the consequences of using different configurations, such as a circular, round-nose rectangular, streamlined piers or piers group.

The combined results of all the experiments support very definitely the viewpoint that the depth of scour is strongly related to the degree of disturbance of the flow. Together with the length-width ratio, the angle between pier and flow is most important geometrical characteristic of a pier or pier groups. Only for piers or pier groups truly aligned with the flow can streamlining of shape of piers or pier groups be fully effective

Analysis regarding the variation of scour depth, area of scour extent, length and width of scour holes, slope of scour holes, length of sediment deposition, temporal variation of scour depth, and other scour details has been presented using the data obtained in present study and the data available for studies of earlier investigators. ANN models formulated in (Chapter VI) for the estimation of scour depth variation are verified with the help of experimental data. Using experimental data graphical relationships are established for the computation of above mentioned scour elements around bridge piers located in different arrangements.

Though the group of two piers with collar as compared to a round nose rectangular pier produces significantly shallower scour depth at angles of attack greater than 0°, however, the debris may pose a problem at this group of two piers having two diameter spacing between them. Raudkivi and Ettema (1977) pointed out that debris might create a problem if spacing between the piers is less than five diameters. Moreover, in general, angles of attack greater than 15° should be avoided.

CHAPTER – VI

ANALYSIS OF RESULTS AND DISCUSSION BASED ON ARTIFICIAL NEURAL NETWORK APPROACH

6.1 Evaluation of Mutual Interference of Bridge Piers on Scour Depth around Group of Piers Using *ANN* Based Modeling Approach

The main objective of the present investigation is to evaluate the effect of mutual interference of bridge piers on local scour. In this chapter the various parameters affecting scour around pier groups are identified first. Then the functional relationships are worked out for the equilibrium depth around group of bridge piers located in different configurations at varying spacing between them. Functional relationships are also worked out for the equilibrium scour depth at group of piers comprising of circular cylinders of varying sizes with and without a collar plate skirted around them. Finally, based on artificial neural network modeling approach, scour depth estimation has been implemented. In order to prove the present experimental conditions, the data on local scour collected in the present study are compared with the values of depth of scour predicted from the available sources under comparable conditions.

6.2 Parameters Affecting Local Scour around Group of Piers

The relationship between the depth of local scour and the parameters which determine it, can be stated as

$ds = f$ [(fluid) (flow) (pier) (sediment) (time) (pier spacing) (angle of attack)]

1 2 3 4 5 6 7

(1) In mechanics a fluid is defined by its density ρ, kinematics viscosity ν and temperature T.

(2) The flow of a fluid is determined by its mean depth y_0, flow velocity U, energy slope S_0, and the acceleration of gravity g which generates the flow. The slope S_0, which produces, through the component of gravity, the shear stress τ_0 to maintain the flow, is more suitably replaced by the shear velocity $U_* = \sqrt{(gy_0S_0)}$.

(3) The action of the pier is determined by the effective blockage it presents to the flow. A cylindrical pier is defined by its diameter b. Other shaped piers are specified relative to b in terms of a shape factor η. The angle of the approach flow to the pier α modifies the effective width of the pier. The flow around a pier is also modified by the aspect ratio η_4 of the pier to channel width. The extent of the secondary flow around a pier is determined by the size and form of the pier.

(4) A layer of uniform cohesion less bed material of thickness h is described by the particle size distribution of sediment, values of its standard deviation σ_g, specific gravity S_s, particle size, d particle shape K_f and angle of repose of sediment ϕ.

(5) Scour is a dynamic process which seeks to establish a new equilibrium between the flow of the fluid and the resistance to motion of the bed particles, by the erosion of the flow boundary, the local scour deepens progressively with time t.

(6) Local scour around a pier is influenced by the presence of another pier in its vicinity due to mutual interference of piers and thus the scour depth varies with pier spacing between the piers along direction of flow 'x' and across direction of flow, Z_c.

(7) Local scour is highly sensitive to orientation of piers in a pier group with respect to the direction of flow (*i.e.*, the angle of attack to the flow, α).

Local scour of cohesion less sediment at a bridge pier is thus described by the following collection of parameters.

Fluid	(ρ, ν, T)
Flow	(g, y_0, U, U_*)
Pier	(b, η_1, η_4)
Sediment	$(d, S_s, \sigma_g, h_{sed}, K_f, \phi)$
Time	(t)

For local scour around group of piers, following parameters are also considered.

(Pattern of piers arrangement in plan) Tandem, lateral, staggered etc.

Orientation of piers with reference to flow direction α

Radial pier spacing along angle of attack (R_b)

Pier spacing along direction of flow (x) or (X_c)

Pier spacing across direction of flow (Z_c)

Angle of attack (α)

For group of piers with collar, following parameter are also considered.

Collar width (W_c)

Collar elevation (H_c)

Orientation of collar (α)

The large number of interacting parameters make the analysis of the local scour of bed sediment around a bridge pier very difficult. This has forced the researchers to the use of dimensional analysis. However, the dimensional analysis is only a technique for the grouping of variables, and yields in itself no information. The functional relationship between the dimensionless parameters have to be obtained from experiments, but when the number of dimensionless parameters is large, severe experimental problems arise. Frequently, in experimental studies of local scour around a bridge pier, the influence of a particular parameter is obscured or modified by the effects of other parameters. This has resulted in some quite diverse interpretations of the influence of certain parameters on the development of local scour around a pier. With this view point, it is imperative in experimental studies to hold all variables constant except one the effect of which is to be studied.

6.3 Equilibrium Scour Depth around a Group of Bridge Piers Founded in Cohesion less sediment

Due to the complex nature of the interaction among the flow, pier and sediment, the process of local scour is generally studied with the help of experiments. It is clear from the literature in Chapter II that the depth of scour '*ds*' around the pier can be expressed as a function of the independent variables:

$$d_s = f\left(U, g, U_*, l, b, \alpha, K_s\, y_0, d_{50}, \rho_s, \sigma_g, h_{sed}, B_c, S_0, K_f, C, \rho, \nu, t, b_r, K_g, x, Z_c, R_b\right) \qquad (6.0)$$

Where,

ds = maximum depth of scour around a bridge pier; U = mean velocity of approach flow; g = gravitational acceleration, U_* = shear velocity; b = characteristic size of pier; l = pier

length parallel to the approach flow; α = angle of approach flow with respect to the pier axis; K_s = factor indicating the effect of pier shape; y_0 = depth of approach flow; d_{50} = median sediment size; ρ_s = relative density of sediment, σ_g = geometric standard deviation of particle size distribution; h_{sed} = thickness of sediment layer, B_c = channel width; S_0 = channel bed slope; K_f = factor indicating the effect of grain shape; C = cohesion of bed material; ρ = density of water; ν = Kinematic viscosity of water, t = duration of flow, $b_r = b_{us} / b_{ds}$ = pier size ratio for tandem arrangement of piers, K_g = factor indicating the group effect of piers; x = clear longitudinal spacing between the piers; Z_c = center to center lateral spacing between the piers and R_b = radial spacing between two piers aligned in staggered arrangement.

When the pier is protected by using a collar plate, width of the collar plate W_c and its elevation above the initial bed level H_c are the additional variables to be considered for the estimation of scour depth around the piers group. The relationship (6.0) then modifies to:

$$d_s = f\left(U, g, U_*, L, b, \alpha, K_s\, y_0, d_{50}, \rho_s, \sigma_g, h, B_c, S_0, K_f, C, \rho, \nu, t, b_r, K_g, x, Z_c, R_b, W_c, H_c\right) \quad (6.1)$$

The parameters influencing the local scour around a smooth cylindrical pier in cohesion less uniform spherical sediment under uniform flow condition can be assembled in a number of dimensionless terms. Dimensionless terms can be determined by using Buckingham's л theorem (Shames, 1992).

It can be argued that ρ_s in itself is not as significant as is its submerged weight, $\gamma' = g(\rho_s - \rho)$, which gives a measure of the buoyancy forces acting on a particle. Substituting, γ' for ρ_s and rearranging the dimensionless terms, the following expression is obtained under the assumption of a smooth, vertically mounted pier over a uniform non-cohesive bed material having a constant shape factor and density in a wide, prismatic, straight and smooth channel with no significant bed factor:

$$y_s = f_1\left(y, F, F_d, F_b, \mathrm{Re}_f, \mathrm{Re}_b, P_r, \eta, \eta_1, \eta_2, t_r, \beta, \sigma_g, L_r, Z_r, \alpha, b_r, \phi, S_0, R_{b(r)} W_r, H_r\right) \quad (6.2)$$

Where, $y_s = d_s / b$ (relative scour depth); $y = y_0 / b$ (relative approach flow depth); $F = U / \sqrt{g y_0}$ is the Froude number of the approach flow; $F_d = (\rho U^2 / \gamma' d_{50})$ is the particle Froude number; $F_b = U / \sqrt{gb}$ is the pier Froude number; $\mathrm{Re}_f = U y_0 / \nu$ is the flow Reynolds number; $\mathrm{Re}_b = Ub / \nu$ is the pier Reynolds number; $P_r = L / b$ is pier length to pier width ratio; $\eta = U_* / U$ *or* U / U_c is the flow intensity; η_1 is the pier shape factor; $\eta_2 = B / b$ is the aspect ratio of pier to channel width; $t_r = Ut / b$ is the time parameter; $\beta = b / d_{50}$ is pier size to sediment size ratio, σ_g is the geometric standard deviation of particle size distribution; $L_r = x / b$ is the relative longitudinal pier spacing; $Z_r = Zc / b$ is the center to center lateral relative pier spacing; α is the angle of attack of flow and $b_r = b_{up} / b_{dn}$ is the pier size ratio for tandem arrangement of piers, ϕ is angle of repose of grains, $S_0 =$ channel bed slope, $R_{b(r)} = R_b / b$ is the relative radial spacing between two piers in staggered arrangement, $W_r = W_c / b$ is the relative collar width and $H_r = H_c / y_0$ is the relative elevation of collar plate above the original bed level.

Experimental studies have been conducted by considering only certain aspects of the problem and accepting the other parameters to be constants (Yanmaz and Altinbilek, 1991). Therefore, the number of dimensionless terms can then be reduced by considering the relative importance of the terms.

For a case with a constant bed slope, the term $\eta = U_* / U$ is a function of y_0 only. So, its variation is treated in the term $y = y_0 / b$. Further, it can be argued that U_* / U in present study is practically constant at 0.95, therefore, the term $\eta = U_* / U$ can be dropped. Because the condition $b / d_{50} < 25$ is unlikely to occur in practice (Melville, 1997), the effect of $\beta = b / d_{50}$ term is neglected. The effect of viscosity is considered negligible for the highly turbulent flow in the scour process so that the term $\mathrm{Re}_b = Ub / \nu$ can be dropped. Since the present study is related to sand in water, the term $(\rho U^2 / \gamma' d_{50})$ is in effect a particle Froude number $F_d = U / \sqrt{g d_{50}}$. For given velocity, flow depth and sediment size, flow Froude number F and particle Froude number F_d differ only by a constant, indicating

that one of the term is redundant. The terms R_{ef}, F, F_d and ϕ can be dropped as these are constants for constant flow depth, flow velocity and same sediment conditions used in present study. The aspect ratio of channel width to pier width, η_2 in present study is greater than 8.0 (Shen et. al., 1966), the influence of η_2, therefore, can be neglected. Since circular piers are used in present study, the terms P_r and η_1 can also be neglected.

Since all the experiments were run at $y_0 / b > 2.6$, the term y can be dropped. As two sizes of piers in tandem arrangement are used, the term b_r is constant and thus can be dropped. As all the experiments were run at same flow condition, F_b can be neglected. Since the experiments at piers group were run with single size collar placed at original bed level, the terms W_r and H_r can be dropped. Furthermore, as the relationships for the estimation of scour depth for piers group are developed in terms of the scour depth at an isolated pier, the term F_b can be dropped.

Thus the relationship (6.2) modifies to

$$y_s = f_2 (L_r, Z_r, \alpha, b, R_{b(r)}, t_r) \tag{6.3}$$

The equations (6.3), (6.2) and (6.1) represent a general functional relationship for all phases of present study. The functional relationships for each of these phases are then obtained separately for the same sediment and flow conditions.

6.4 Scour Depth Estimation Using Artificial Neural Network (*ANN*) Based Modeling Approach

The depth of scour is an important parameter in determining the minimum depth of foundations as it reduces the lateral capacity of the foundation. It is for this reason that extensive experimental investigation has been carried out to understand the complex process of scour around group of piers and to determine the method of estimating the scour depth for various piers group arrangements.

It is extremely difficult to formulate mathematical models that accurately represent the scour process and geometry of scour hole, which develops under the influence of three dimensional flow around a bridge pier. Thus it is a common practice to apply empirical

relationships based on laboratory data for estimation of the scour around piers. Since there are numerous effective parameters, and the interaction of these parameters is highly complicated, the accuracy of the empirical relationships is very subjective and highly depends on the user's ability and knowledge. An artificial neural network, on the other hand, is an applicable and powerful tool to solve this problem. In addition, it has ability to learn from examples and to generalize its learning which makes it well suited to situations where the problem complexity precludes the development of empirical relationships.

A number of empirical relationships have been developed to estimate equilibrium scour depth at a single bridge pier namely; Laursen and Toch (1956), Shen *et. al.* (1969), Hancu (1971), Melville (1975), Hjorth (1975), Breausers *et. al.* (1977), Ettema (1980), baker (1981), Melville and Sutherland (1988), Dey (1997), CSU (2001), Melville and Chew (1999) and Sheppard (2004). Each of these relationships varies significantly, highlighting the fact that there is a lack of knowledge in predicting scour depth and that a more universal solution would be beneficial.

Since conventional scour depth predictive empirical formulae are not able to provide sufficiently accurate results, an alternative approach namely; *ANN* based scour depth estimation has been implemented in the present study. The *ANN* based scour depth modelling approach is utilised to examine the usefulness of the approach for accurately estimating the scour depth from the experimental data. As all the factors affecting scouring at a circular pier (namely, pier shape, pier size, sediment size depth of flow, velocity of flow, discharge, flume), except pier spacing $\left(\frac{x}{b}\right)$ or $\left(\frac{X_c}{b}\right)$ or $\left(\frac{Z_c}{b}\right)$ or $\left(\frac{R_b}{b}\right)$ or angle of attack 'α' are same for the mutually interacting piers, pier spacing or the angle of attack is only the dependent variable used in modeling for evaluating the effect of mutual interference of piers on local scour. Therefore, in this approach, scour depth is estimated by keeping all other scour affecting parameters constant, and taking into account only the effect of pier spacing for different pier arrangements (*i.e.*, tandem, lateral, and staggered pier arrangement) and taking into account only the effect of angle for piers group aligned at an angle of attack to the flow direction. Emphasis has been laid on derivation of optimal neural network architecture capable of producing scour depth estimates with

desired accuracy through the use of only one input variable *i.e.*, the pier spacing, $\left(\frac{x}{b}\right)$ or $\left(\frac{X_c}{b}\right)$ or $\left(\frac{Z_c}{b}\right)$ or $\left(\frac{R_b}{b}\right)$ or angle of attack (α).

A general framework of the methodology adopted for the development of *ANN* based scour depth estimation approach is described and the steps involved are:

(i) Selection of input and output variables

(ii) Data normalisation

(iii) Design of *ANN* architecture

(iv) Training of *ANN*

(v) Processing of unseen data

(i) Selection of input and output variables

Only a single input variable *i.e.*, the pier spacing, $\left(\frac{x}{b}\right)$ or $\left(\frac{X_c}{b}\right)$ or $\left(\frac{Zc}{b}\right)$ or $\left(\frac{R_b}{b}\right)$ or angle of attack (α) that may have an effect on the scour depth around a group of piers placed in different pier arrangements, has been selected. Several neural networks architectures each for different pier arrangement have been designed in such a way that these have pier spacing, $\left(\frac{x}{b}\right)$ or $\left(\frac{X_c}{b}\right)$ or $\left(\frac{Z_c}{b}\right)$ or $\left(\frac{R_b}{b}\right)$ as input variable and scour depth '*ds*' as an output/target variable.

(ii) Data normalisation

The data corresponding to input variables acquired from laboratory experiments have been scaled from 0.1 to 0.9 before being input to *ANN*, using the following equation:

$$X_{nd} = 0.1 + 0.8 \times \left(\frac{X_i}{X_{\max}}\right) \tag{6.4}$$

Where, X_{nd} is the normalised dimensionless variable, X_i is the observed value of the variable and $X_{\max}$ is the maximum value in the data set. The significance of normalisation is to restrict the weighted sum at any computational neuron within limits so as to avoid large numerical error in the computation of logistic nonlinear output function.

(iii) Design of *ANN* architecture

In order to design an optimal *ANN* architecture, the number of units in the input and output layer are defined according to input *i.e.*, the pier spacing, $\left(\frac{x}{b}\right)$ or $\left(\frac{X_c}{b}\right)$ or $\left(\frac{Z_c}{b}\right)$ or $\left(\frac{R_b}{b}\right)$ or angle of attack (α) and an output variable (*i.e.*, scour depth '*ds*') respectively. So as to keep the architecture simple, a single hidden layer has been considered. The optimum number of neurons of the hidden layer has been determined by trial and error. Altogether, 26 neural network architectures for the data corresponding to each of the pier arrangement are designed.

The data have been partitioned into two sets, one each for training and validation of neural networks. Care has been taken that each subset contained a complete and equal representation of the input and output variables that were used to develop and test the approach. Therefore, about 70% of the entire data set has been used for training whereas remaining 30% has been kept for testing.

(iv) Training of *ANN*

The neural networks have been trained using the well known feed forward back propagation learning algorithm available in the MATLAB neural network toolbox. The logistic sigmoid function has been used as the transfer function. Both training and testing data are put through the training process. The connection weights, bias and the number of neurons in the hidden layer (can be interpreted as the *ANN* model parameters) are adjusted during the training process through minimisation of root mean square error (*rmse*) using the *Trainlm* function based on the Levenberg-Marquardt method. For each *ANN* architecture, the training process is repeated starting from independent initial condition ensuring selection of the best performing network. The trend of decrease in *rmse* over training and testing data sets has been used to decide the optimal training. Initially, errors on both the training and the testing data decrease over a number of iterations until they reach a constant minimum value for all the trained neural networks. The training is stopped at a point when the least difference between the training and testing data error has been observed. This has been done to avoid overtraining of the

network. The number of hidden neurons has been varied from 1 to a maximum of 15 with an increment of 1. Similarly, the learning rate has also been changed in a defined range from 0.001 to 0.5 at an increment of 0.001. These trials have led to the identification of the best neural network architectures for a given data set. After training of each ANN, the final values of learning rate, number of iterations needed for training and number of neurons in the hidden layer were attained and are tested in Table 6.1.

(v) Processing of unseen data

The trained networks have been used to process the unseen data in the form of validation data. The neural network results are thus analysed to examine the usefulness of *ANN* based modelling approach to estimate scour depth at varying pier spacing and pier arrangement.

6.5 Analysis of Results Obtained from ANN Based Modeling

The *ANN* based modelling approach was implemented with the objective of exploring an alternative method of estimating scour depth without involving complicated equations and theories. Only single input variable *viz.* pier spacing, $\left(\frac{x}{b}\right)$ or $\left(\frac{X_c}{b}\right)$ or $\left(\frac{Z_c}{b}\right)$or $\left(\frac{R_b}{b}\right)$ for pier groups aligned with the flow or angle of attack 'α' for pier groups misaligned with the flow, was selected to train the several created neural network architectures for different pier arrangements while, the rest (*e.g.*, hydraulic and sediment parameters) were kept constant. Thus, in all, a total of 26 *ANN* architectures were trained and tested. These architectures are shown in Figs.6.1 to 6.10. The final adjusted weight values of trained networks are also shown in Figs. 6.1 to 6.26. Table 6.1 shows the details of ANN architectures (*e.g.*, input, output and hidden layer, number of iterations and learning rates) for different pier arrangements.

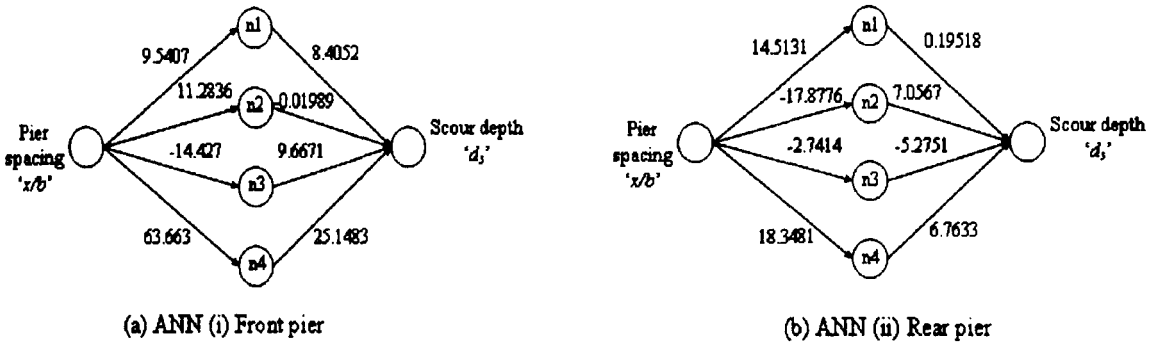

(a) ANN (i) Front pier

(b) ANN (ii) Rear pier

Fig. 6.1 ANN architectures for two piers in tandem arrangement

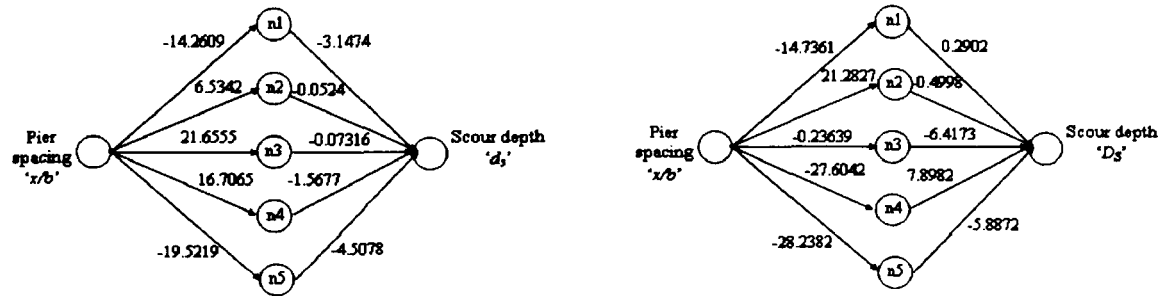

(a) ANN (i) Front pier

(b) ANN (ii) Middle pier

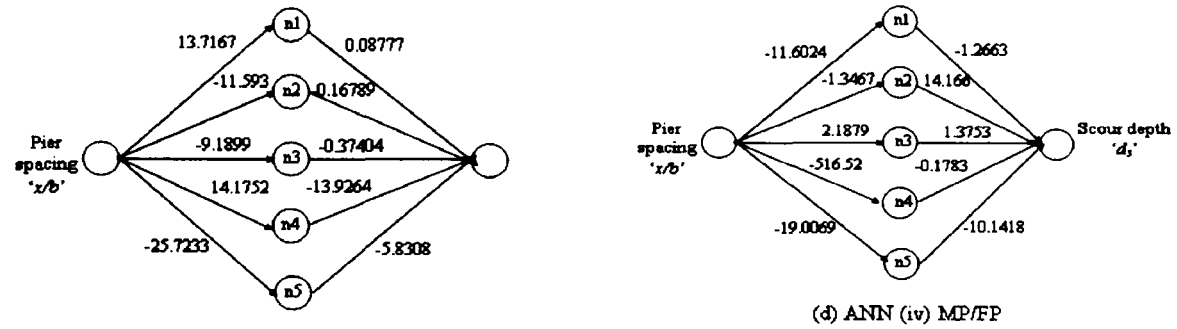

(c) ANN iii) Rear pier

(d) ANN (iv) MP/FP

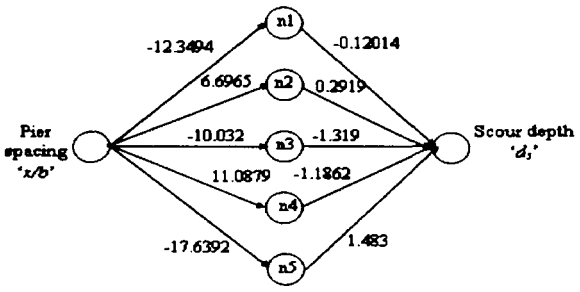

(e) ANN (v) RP/FP

Fig. 6.2 ANN architectures for three piers in tandem arrangement

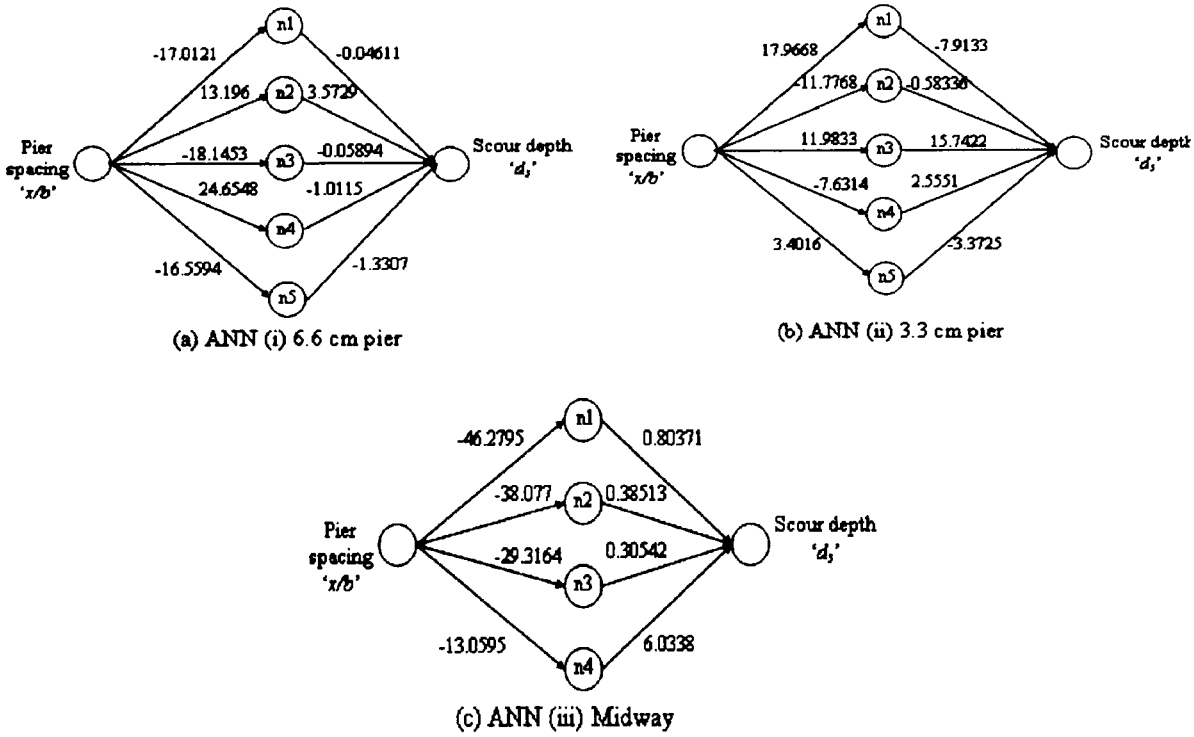

(a) ANN (i) 6.6 cm pier

(b) ANN (ii) 3.3 cm pier

(c) ANN (iii) Midway

Fig.6.3 ANN architectures for two piers of different size in tandem arrangement (6.6 cm at front and 3.3 cm at rear)

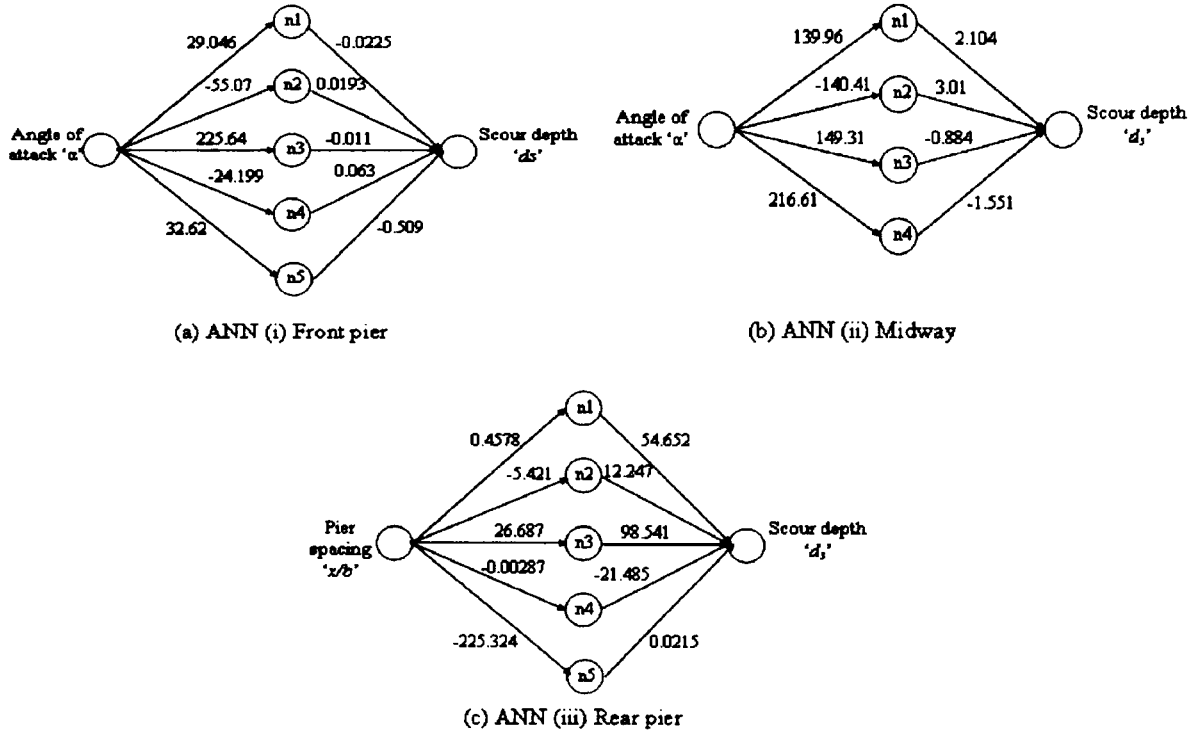

(a) ANN (i) Front pier

(b) ANN (ii) Midway

(c) ANN (iii) Rear pier

Fig.6.4 ANN architectures for two piers of different size in tandem arrangement (3.3 cm at front and 6.6 cm at rear)

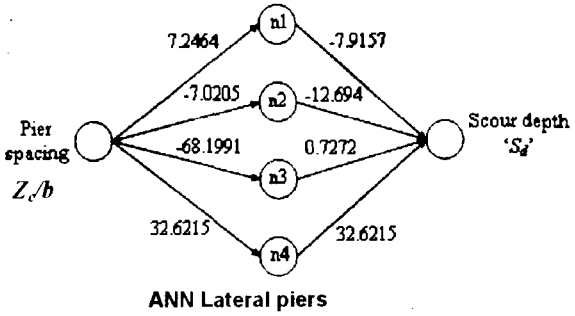

Fig. 6.5 ANN architectures for Two piers in lateral arrangement

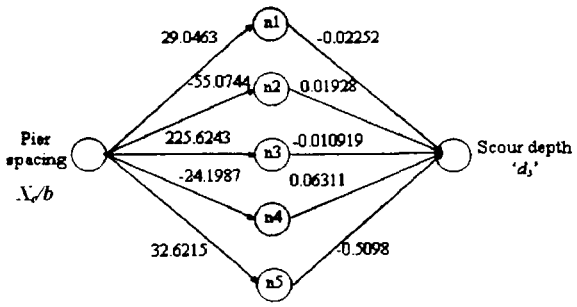

(a) ANN (i) Upstream piers

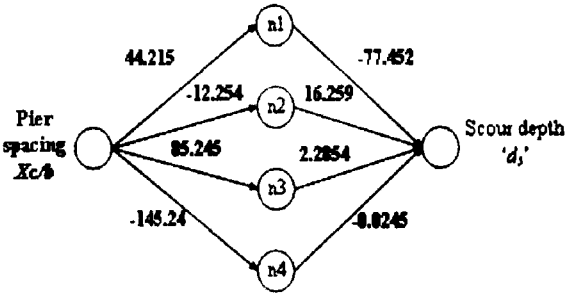

(b) ANN (ii) Downstream pier

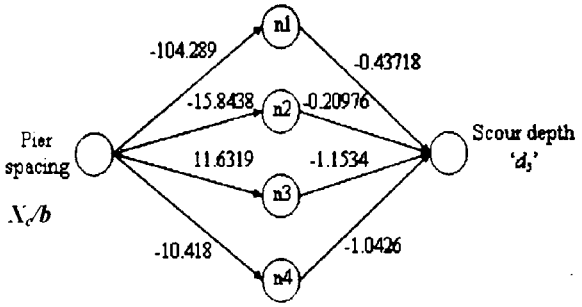

(c) ANN (iii) Downstream piers/Upstream piers

Fig.6.6 ANN architectures for three piers in staggered arrangement

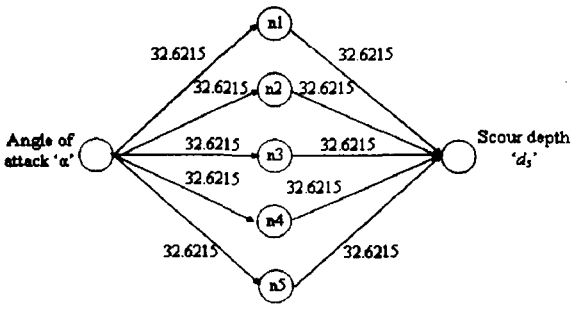

(a) ANN (i) Front pier

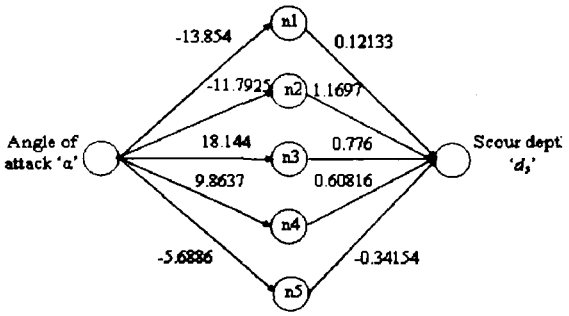

(b) ANN (ii) Rear pier

Fig. 6.7 ANN architectures for two piers at constant radial distance and varying angles of attack

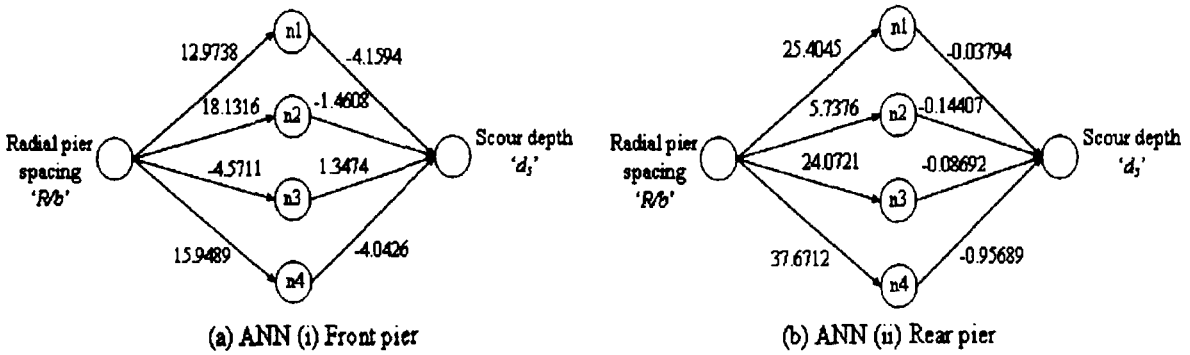

(a) ANN (i) Front pier (b) ANN (ii) Rear pier

Fig.6.8 ANN architectures for two piers at constant angle of attack and varying radial pier spacings R/b

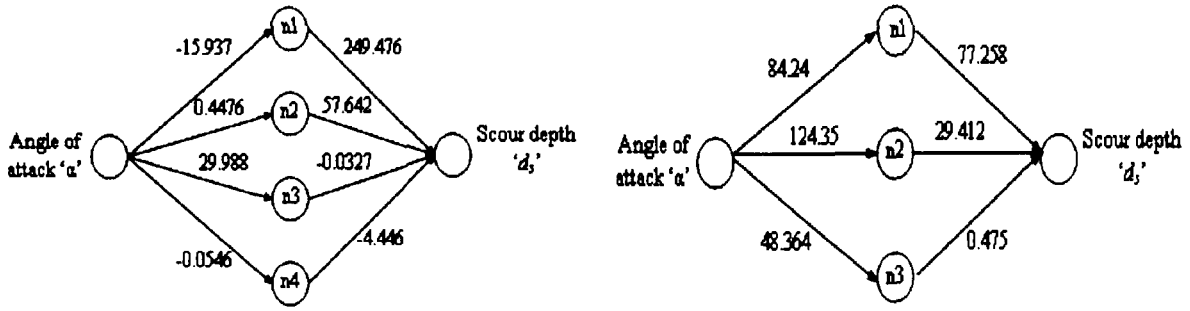

(a) ANN (i); without collar (b) ANN (ii) with collar

Fig. 6.9 ANN architectures for a group of piers comprising of cylinders of different sizes with and without collar

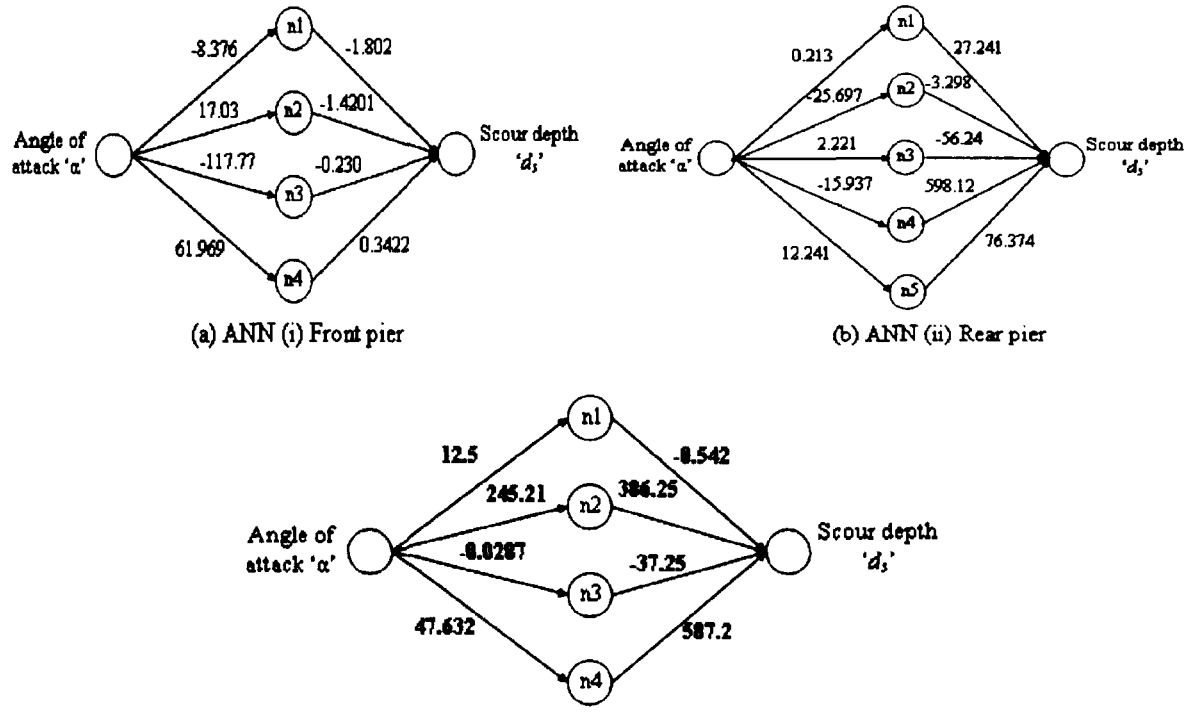

(a) ANN (i) Front pier (b) ANN (ii) Rear pier

(c) ANN (iii) With collar

Fig.6.10 ANN architectures for a group of two piers with and without collar

Table 6.1 Details of ANN Architectures

S No.	Pier arrangement for creating *ANN* architecture	Cases for training *ANN*	Input variable	*ANN* architectures *I - H - O**	No. of iterations	Learning rate μ	*Output variables*
1	Two piers in tandem	i) FP ii) RP	Pier spacing '*x/b*'	1 - 4 - 1 1 - 4 - 1	245 265	0.00085 0.00095	Scour depth '*d_s*'
2	Three piers in tandem	i) FP ii) MP iii) RP iv) MP/FP v) RP/FP		1- 5 - 1 1- 5 - 1 1- 5 -1 1- 5 - 1 1- 5 - 1	195 230 180 175 350	0.00115 0.00090 0.00085 0.00088 0.00055	
3	6.6 cm pier at front and 3.3 cm at rear in tandem	i) 6.6 cm pier ii) 3.3 cm pier iii) Midway		1- 5 - 1 1- 5 - 1 1 - 4 -1	485 365 280	0.00070 0.00095 0.00015	
4	3.3 cm pier at front and 6.6 cm at rear in tandem	i) FP ii) RP		1- 5 - 1 1- 5 - 1	495 650	0.00065 0.00095	
5	Staggered piers	i) UP ii) DP iii) DP/UP		1 - 4 - 1 1 - 4 - 1 1 - 4 - 1	335 750 380	0.00095 0.00026 0.00250	
6	Transverse piers	FP or RP		1 - 4 - 1	180	0.00110	
7	Constant angle with varying radius	i) FP ii) RP	Radial pier spacing '*R/b*'	1 - 4 - 1 1 - 4 - 1	375 350	0.00085 0.00095	
8	Constant radius with varying angle	i) FP ii) RP	Angle of attack 'α'	1 - 5 - 1 1 - 5 - 1	165 320	0.00112 0.00120	
9	Group of piers of varying sizes	i) Without collar ii) With collar		1 - 4 - 1	460	0.000095	
10	Group of two piers of 4.15 cm diameter without collar	i) FP ii) RP		1 - 4 – 1 1 - 5 - 1	585 675	0.000770 0.000850	
11	Group of two piers of 4.15 cm diameter with collar	Pier group with collar		1 - 4 - 1	760	0.000550	

I - H - O : Input –Hidden –output; FP: Front pier; RP: Rear pier; UP: Upstream pier; DP: Downstream pier; MP: Middle pier; Midway: in between the piers*

Table 6.2 Results obtained from ANN based modeling approach

Sl. No.	Pier arrangement for creating *ANN* architecture	Cases for training *ANN*	Input variable	Output variable	Coefficient of determination R^2		Root mean square error *rmse*	
					Training data	Testing data	Training data	Testing data
1	Two piers in tandem	i) FP ii) RP	Pier spacing 'x/b'	Scour depth 'd_s'	0.9964 0.9979	0.9987 0.9712	7.69×10^{-4} 5.7×10^{-4}	1.39×10^{-3} 2.87×10^{-3}
2	Three piers in tandem	i) FP ii) MP iii) RP iv) MP/FP v) RP/FP			0.9999 0.9963 0.9987 0.9725 0.9998	0.9813 0.9897 0.9938 0.9816 0.8905	5.47×10^{-5} 4.0×10^{-4} 4.31×10^{-4} 1.25×10^{-3} 2.01×10^{-4}	9.64×10^{-4} 7.77×10^{-4} 6.94×10^{-4} 3.1×10^{-3} 4.37×10^{-3}
3	6.6 cm pier at front and 3.3 cm at rear in tandem	i) 6.6 cm pier ii) 3.3 cm pier iii) Midway			0.9823 0.9988 0.9999	0.9547 0.9750 0.9995	5.86×10^{-4} 9.75×10^{-4} 4.31×10^{-4}	1.14×10^{-3} 6.85×10^{-3} 2.03×10^{-3}
4	3.3 cm pier at front and 6.6 cm at rear in tandem	i) FP ii) RP			0.9865 0.9999	0.9662 0.9941	3.39×10^{-5} 4.31×10^{-5}	3.21×10^{-3} 2.25×10^{-3}
5	Staggered piers	i) UP ii) DP iii) DP/UP			0.8865 0.9936 0.9971	0.8651 0.9987 0.9761	3.51×10^{-3} 1.066×10^{-3} 6.77×10^{-4}	4.62×10^{-4} 3.276×10^{-3} 2.95×10^{-3}
6	Transverse piers	FP or RP			0.998	0.9890	2.1×10^{-4}	3.0×10^{-3}
7	Constant angle with varying radius	i) FP ii) RP	Radial pier spacing 'R/b'		0.9996 0.9999	0.9992 0.9964	3.78×10^{-4} 2.45×10^{-4}	4.62×10^{-3} 1.28×10^{-3}
8	Constant radius with varying angle	i) FP ii) RP	Angle of attack 'α'		0.964 0.998	0.9830 0.9550	8.48×10^{-4} 4.44×10^{-4}	1.1×10^{-3} 3.9×10^{-3}
9	Group of piers of varying sizes	i) Without collar ii) With collar			0.999 0.999	0.9990 0.9990	1.08×10^{-6} 4.09×10^{-2}	0.05×10^{-4} 6.21×10^{-3}
10	Group of two piers of 4.15 cm diameter without collar	i) FP ii) RP			0.978 0.974	0.9870 0.9660	3.85×10^{-5} 2.42×10^{-5}	1.21×10^{-4} 0.68×10^{-4}
11	Group of two piers of 4.15 cm diameter with collar	Pier group with collar			0.9935	0.0.9873	1.808×10^{-2}	1.9345×10^{-2}

I - H - O : Input –Hidden –output; FP: Front pier; RP: Rear pier; UP: Upstream pier; DP: Downstream pier; MP: Middle pier; Midway: in between the piers*

The analysis of results obtained from *ANN* based modeling approach was also carried out in terms of the R^2 and *rmse* values between the estimated and observed scour depth values and are given in Table 6.2.

These results reveal that for training, testing and validation sets, all the neural networks trained with the data having pier spacing or angle of attack as the input produced higher R^2 and lower *rmse* values of the order ~ 0.99. Also, almost all the neural networks trained required relatively equal number of iterations to reach the global minima.

Scatter plots between observed and estimated scour depths; for ANN trained with pier spacing and angle of attack were drawn for the data obtained from present experiments. These scatter plots are shown in Figs. (6.11 to 6.20). A symmetric distribution of the data around the line of best agreement in training, testing and validation for all the architectures may be noted in Figs. (6.11 to 6.20).

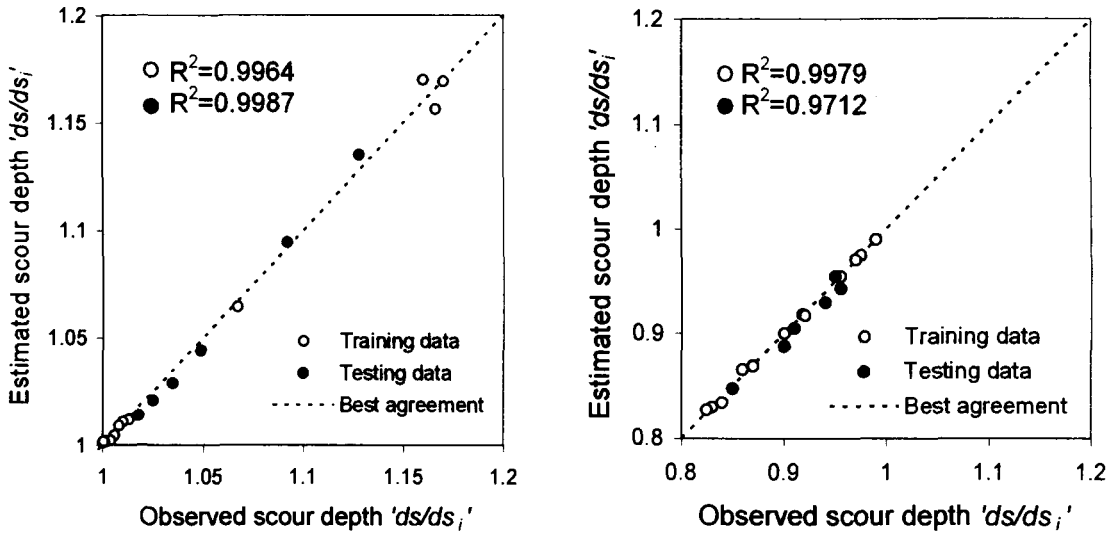

Fig.6.11 Scatter plots between neural network estimated and observed scour depth for training and testing data set for two piers in tandem arrangement (a) Front pier (b) Rear pier.

Fig. 6.11 to 6.20 Scatter plots between neural network estimates and observed scour depths for training and testing data set of two same size piers placed in tandem arrangement.

Thus, scour depth estimated from *ANN* based modelling approach would be immensely useful in the design of pier foundation as well as other hydrological studies.

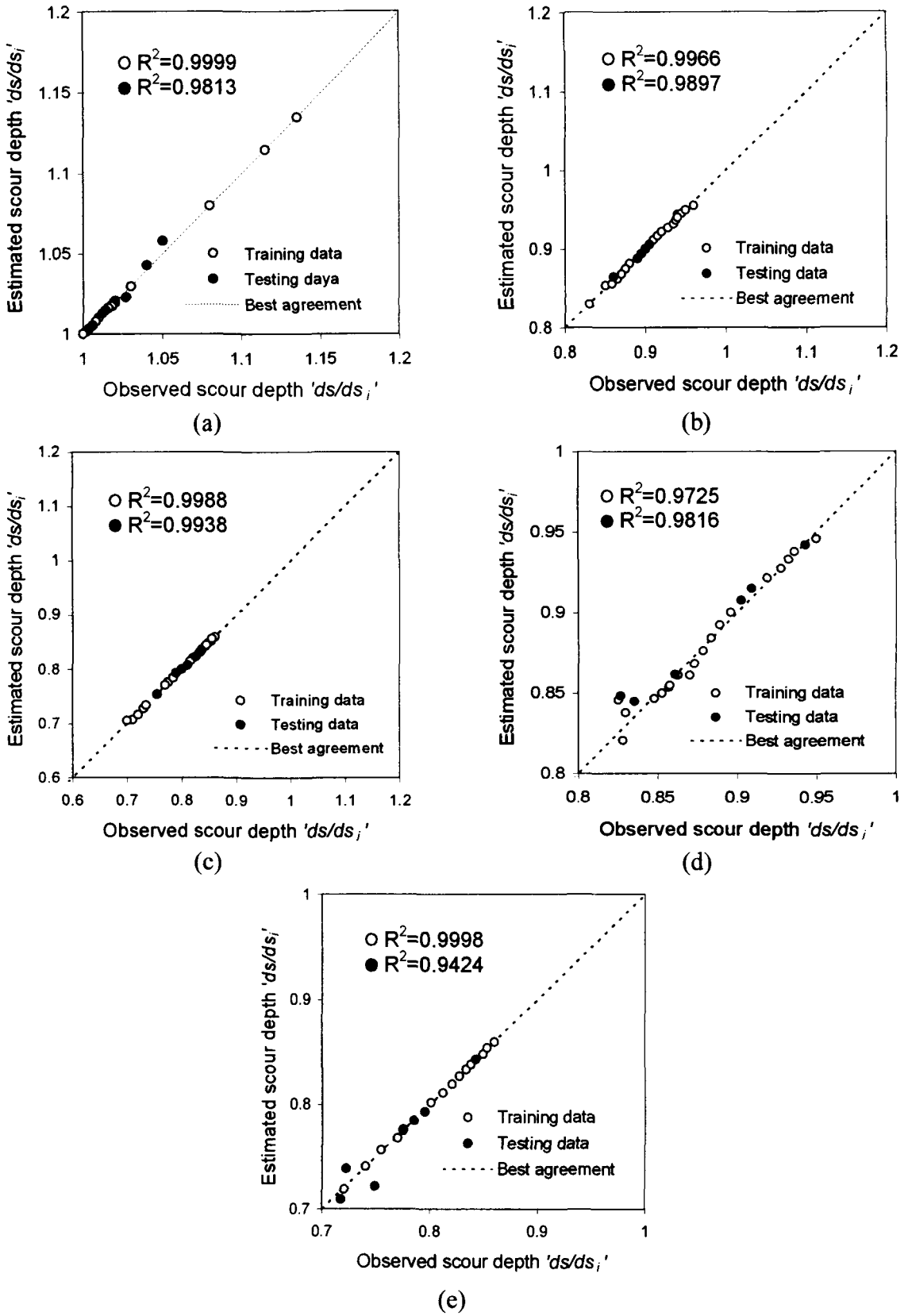

Fig. 6.12 Scatter plots between neural network estimated and observed scour depth for training and testing dataset for three piers tandem arrangement (a) Front pier (b) Middle pier (c) Rear pier (d) Middle pier/Front pier (e) Rear pier/Front pier.

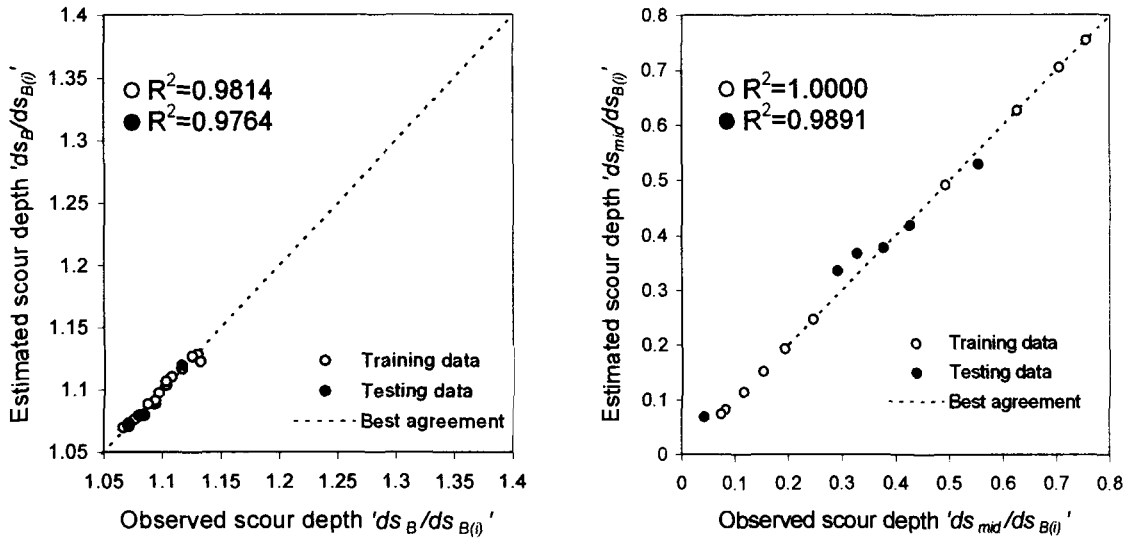

(a)

(b)

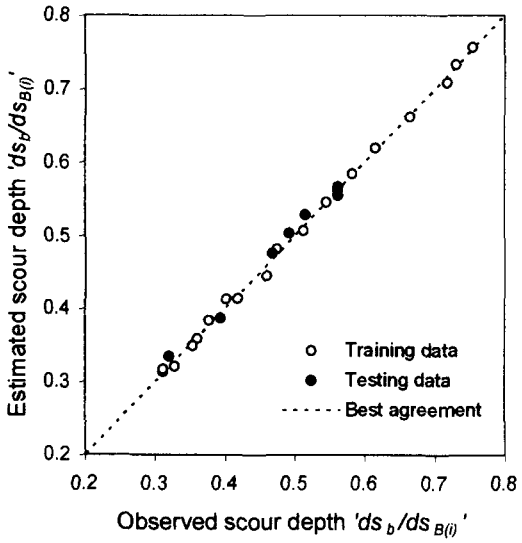

(c)

Fig.6.13 Scatter plots between neural network estimated and observed scour depth for training and testing data set for [6.6 cm pier (Big pier) at front and 3.3 cm pier (small pier) at rear] in tandem arrangement (a) Front pier (b) Midway (c) Rear pier.

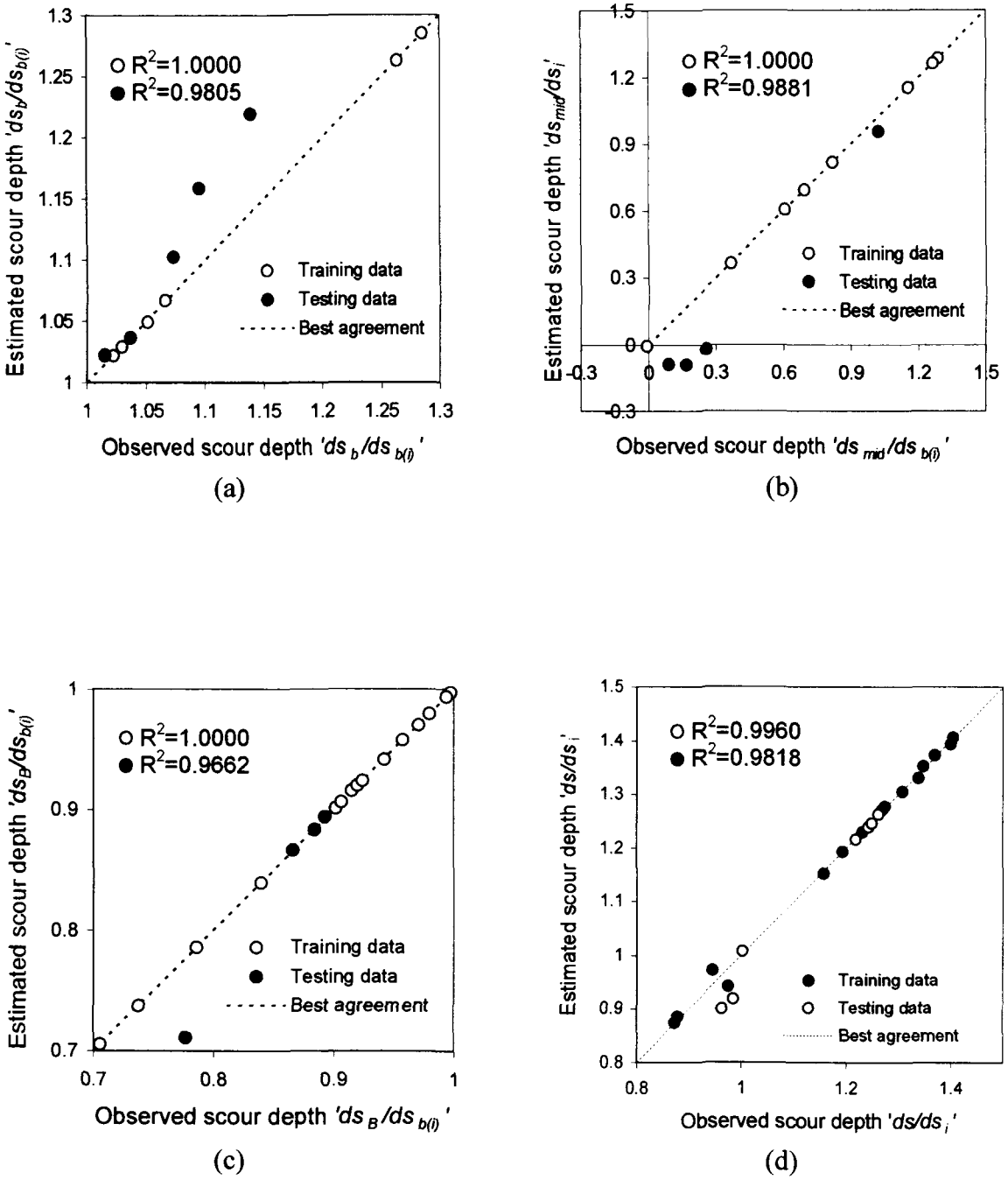

Fig. 6.14 Scatter plots between neural network estimated and observed scour depth for training and testing data set for [3.3 cm pier (small pier) at front and 6.6 cm pier (big pier) at rear] in tandem arrangement (a) Front pier (b) Midway (c) Rear pier (d) Rear pier/Front pier.

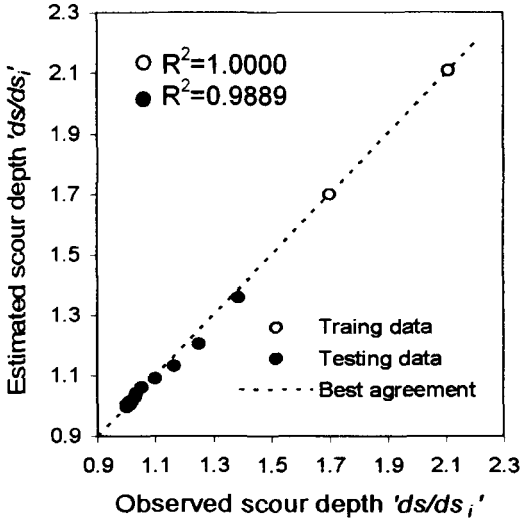

Fig.6.15 Scatter plots between neural network estimated and observed scour depth for training and testing dataset for two piers in lateral arrangement.

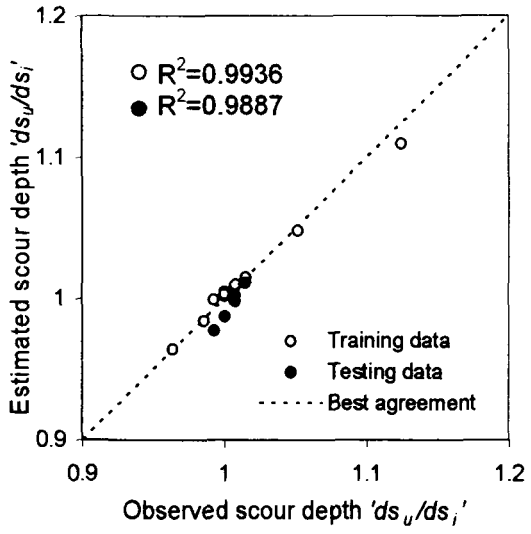

(a)

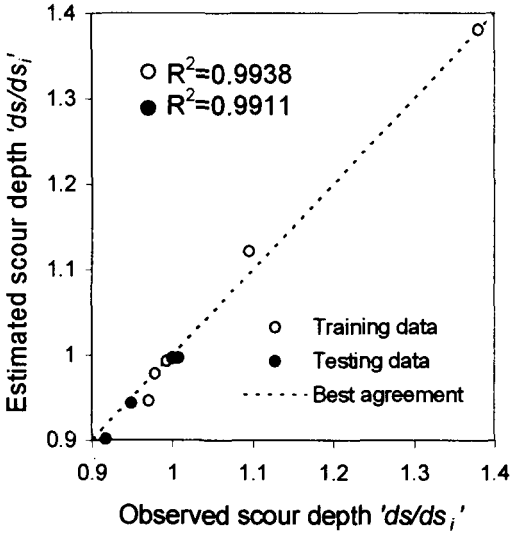

(b)

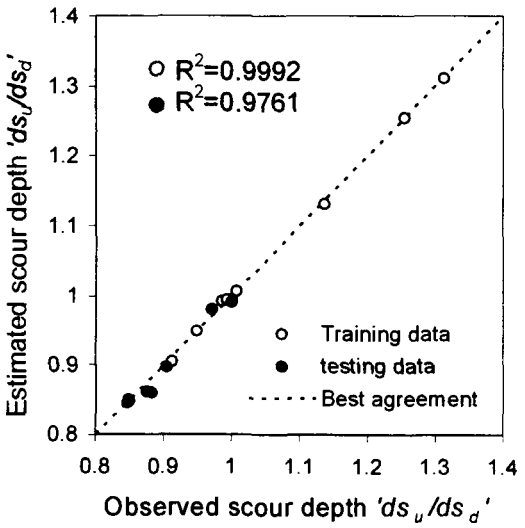

(c)

Fig.6.16 Scatter plots between neural network estimated and observed scour depth for training and testing dataset for three piers in staggered arrangement (a) Upstream piers (b) Downstream pier (c) Downstream pier/upstream piers.

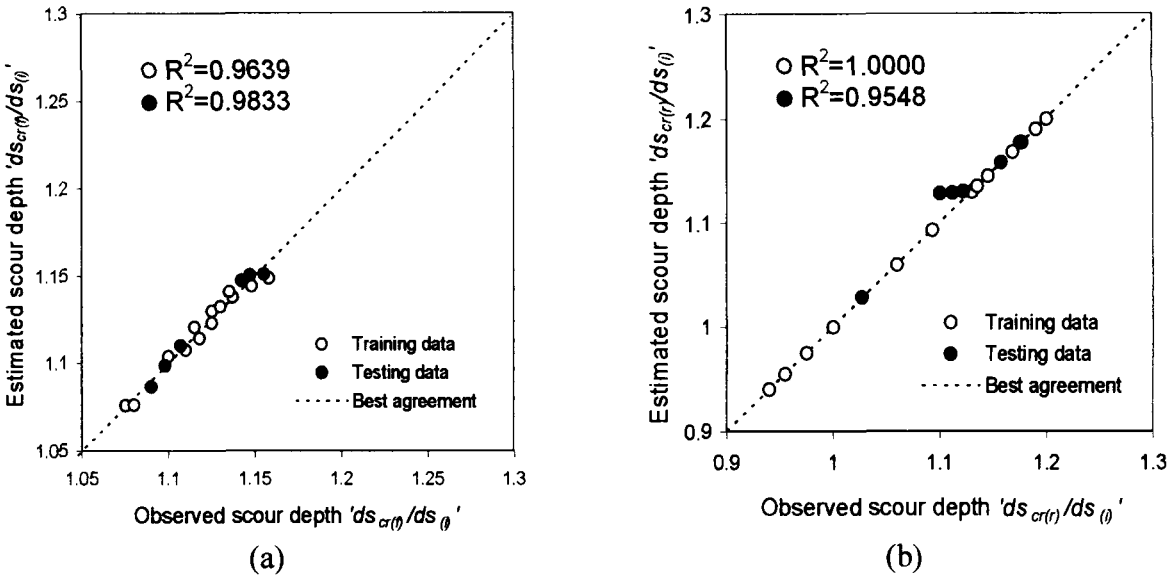

Fig.6.17 Scatter plots between neural network estimated and observed scour depth for training and testing dataset for two piers aligned at constant radial spacing *R/b* and varying angles of attack (a) Front piers (b) Rear pier.

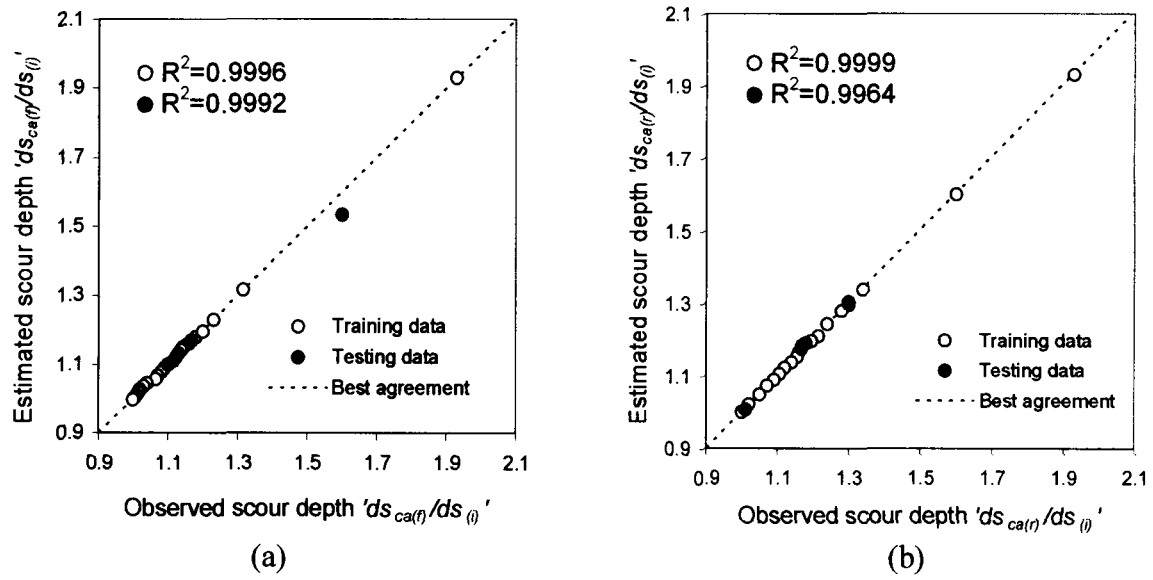

Fig. 6.18 Scatter plots between neural network estimated and observed scour depth for training and testing dataset for two piers aligned at constant angle of attack and varying radial spacing R/b (a) Front piers (b) Rear pier.

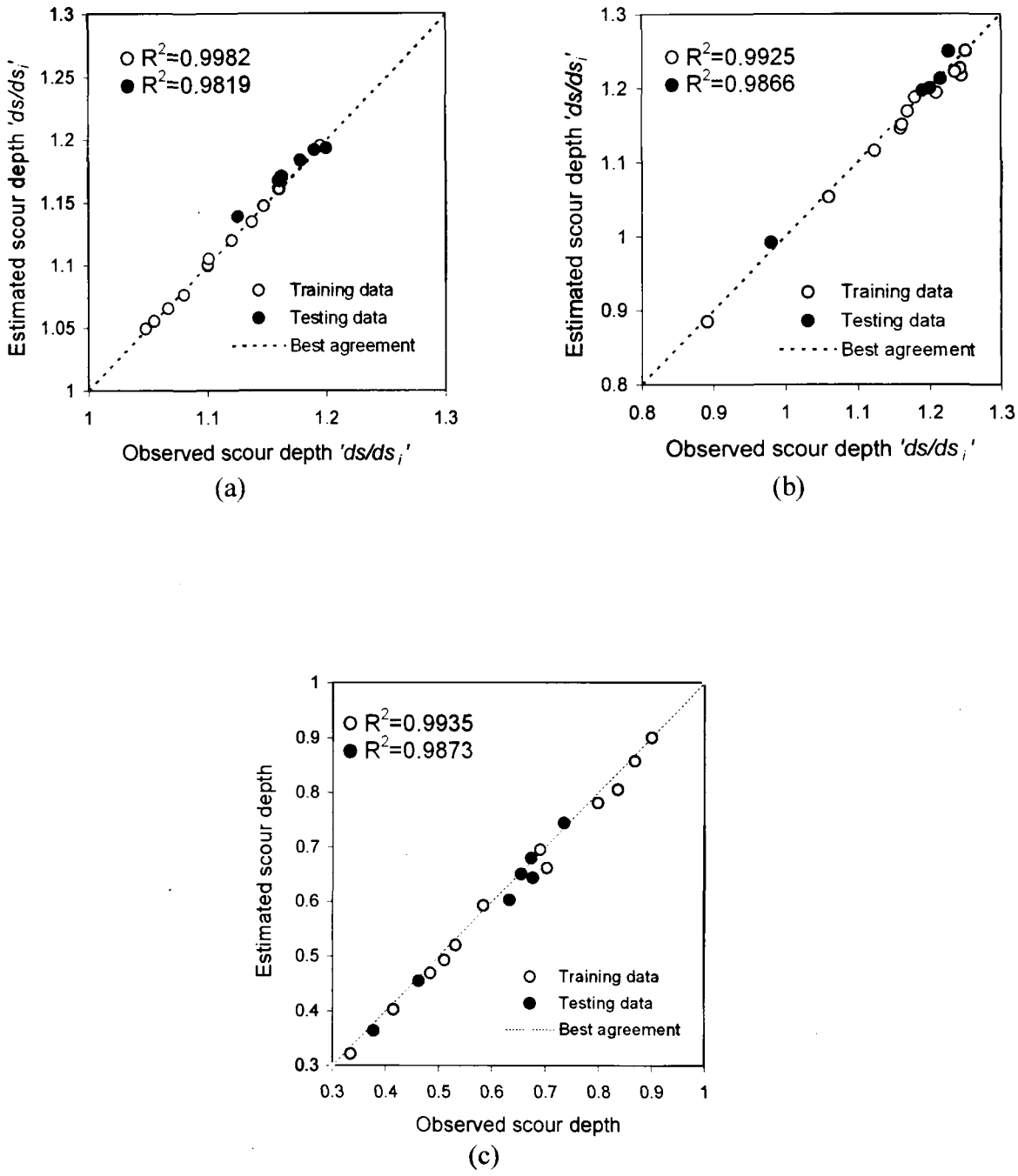

Fig. 6.19 Scatter plots between neural network estimated and observed scour depth for training and testing dataset for a group of two piers aligned at various angles of attack with and without collar (a) Front piers (without collar) (b) Rear pier (without collar) (c) With collar.

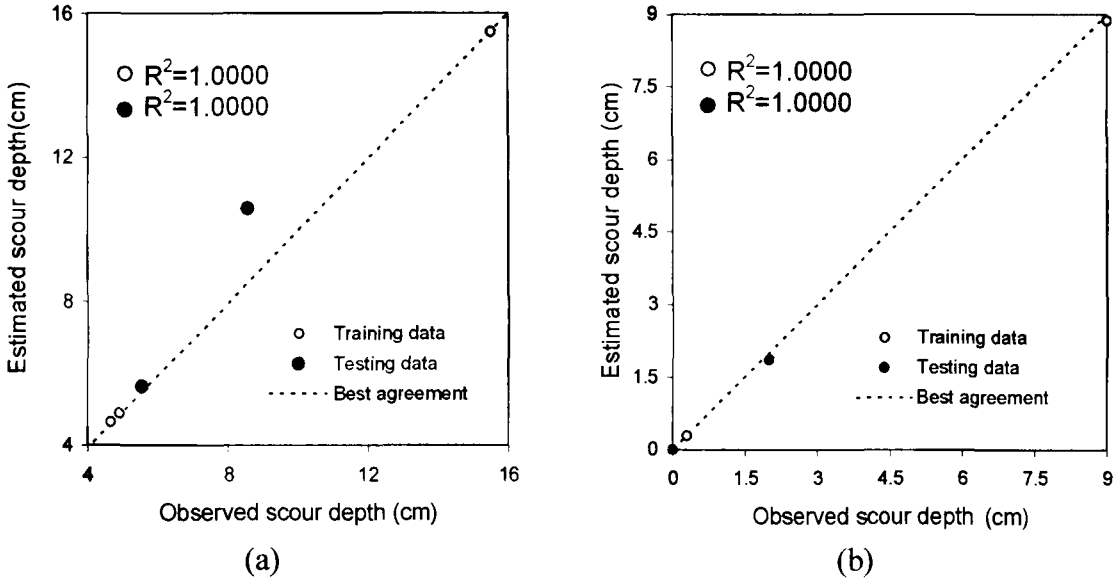

Fig. 6.20 Scatter plots between neural network estimated and observed scour depth for training and testing dataset for a group of varying sized cylinders aligned at various angles of attack (a) Without collar (b) With collar.

CHAPTER – VII

CONCLUSIONS AND FUTURE SCOPE

7.0 General

Rapid urbanization and increased traffic volume is identified as a major problem which results in frequent traffic jams due to which traffic movement is halted which causes enormous economical losses and consequently affects adversely the development of the country. In such eventuality construction of new bridges in the proximity of existing ones is found to be imminent to facilitate efficient and smooth traffic movement.

There are limitations of spacing between existing and new bridges due to the problem of land acquisition. In that context, the scour depth and bed configuration pattern around the existing and new bridges need to be examined. Furthermore, for geo-technical and economical reasons, pier groups have been more and more popular in bridge design. Thus, there are many conditions in the field in which multiple piers are to be provided in bridges at short spacings.

The main objective of the present experimental investigation was to study the effect of mutual interference of bridge piers on local scour. The mutual interference is dependent on the pattern of placement of piers in the riverbed, and it was, therefore, decided first to study the local scour at a single pier so as to form a base against which the effect of mutual interference of bridge piers could be evaluated. This task was accomplished by collecting relevant local scour data through carefully controlled experiments conducted on piers placed in various arrangements. On the basis of these scour data, the scour depth at piers placed in different patterns of arrangement was then modeled. In addition, models were developed for the prediction of scour depth at pier groups with and without collar installed around them; to investigate the means for scour depth mitigation.

The conclusions arrived at in the study are summarized below

From exhaustive literature survey on pier scour it is found that the problem of local scour around bridge piers received a lot of attention in the past from theoretical and constructive point of view in an attempt to quantify the equilibrium depth of scour, however, almost all the equations have been derived for the case of a single pier.

In the light of above discussion it can be concluded that if a bridge pier is merely designed based on the method of design for single pier, it may lead to the bridge failure because mutual interference of several piers can enhance the scour depth at the piers. Considerable engineering judgment must therefore, be used when estimating the depth of scour around group of piers in order to achieve a satisfactory and also a cost-effective design.

Extensive data on local scour like, scour depth, areal extents of scour, scour depth profiles along and across flow direction, lengths and slopes of scour holes at upstream and downstream faces of piers, width of scour holes, length of sediment deposition at downstream face of piers and temporal scour depth variation, were collected through experiments for different pier arrangements.

Two modeling approaches namely graphical relationships based approach and ANN based approach, have been developed and implemented for the evaluation of effect of mutual interference of bridge piers on local scour. The results from both, the experimental based approach as well as ANN based approach, were found to be in close agreement with each other (R^2~0.96-0.99).

The results reveal that for training and testing data sets, all the neural networks trained, produced higher R^2 and lower RMSE values of the order ~0.99. Also, almost all the neural networks trained required relatively equal number of iterations to reach the global minima.

Application of ANN on author's experimental data produces good estimate of scour depth at pier groups arranged in different patterns and these results are well comparable with existing published data of Hannah (1978), Chabert and Engeldinger (1956), Richardson *et.. al.* (1993) and Zarrati *et. al.*(2006). The correlation coefficient R^2 between observed and ANN estimated scour depths represents the predictive ability of ANN models.

In the case of two piers in tandem arrangement, the scour depth at front pier gets enhanced by 17% at pier spacing x/b=1.5 and scour depth at rear pier gets reduces by 33 % at pier spacing x/b=12.5.as compared to the scour depth at single pier. **Based on these findings it is suggested that the rear pier in tandem arrangement should be placed at *x/b*=12.5 to achieve economy in pier design.**

In the case of three identical circular piers placed in tandem arrangement, the scour depth at front and middle piers increases by 11% and 15.5% respectively whereas at rear pier gets reduced by about 33.5%, as compared to that of a single pier. **These findings suggest that the middle pier be placed at clear pier spacing of *x/b*=15 from front and rear piers to for economical design of pier.**

In the case of big pier at front and small pier at rear placed in tandem arrangement, the maximum scour depth at big pier at pier spacing *x/b*=0, is slightly less than that at single big pier, while the scour depth at big pier gets enhanced by 7.15 % as compared to that of a single big pier at pier spacing *x/b*=10. The scour depth at small pier relative to that of single small pier becomes 1.35 times deeper at *x/b*=0 and 0.57 times shallower at x/b=35 **Based on these findings, it is suggested that small pier at rear of big pier be placed at *x/b*=35 for economical design of pier.**

In the case of small pier at front and big pier at rear placed in tandem arrangement, the maximum scour depth at small pier at *x/b*=0 gets enhanced by 28.5 % as compared to that at an isolated small pier, however, the scour depth at big pier gets reduced by 23% at the same pier spacing. As compared to an isolated pier, the scour depth at big pier at *x/b*= 5 gets reduced by 37%. **These findings suggest that big pier at rear be placed at *x/b*=5 from small front pier to economy in pier design.**

At zero lateral pier spacing, the scour depth is 1.95 times of that occurring at an isolated pier. At lateral pier spacing of one pier diameter, though the scour depth at two piers quickly decreases, nevertheless, it remains 21 % higher than that of an isolated pier. At lateral pier spacing of 8 times the pier diameter, although, the scour depth at two piers becomes same as that of an isolated pier, but the size of the scour holes are not identical to that for an isolated pier. **These findings suggest that the two piers should be placed at lateral pier spacing *Zc/b*>8.**

When two piers on upstream normal to the flow and one pier in the middle on downstream are placed in staggered pattern at X_c/b=10, scour depth at upstream and downstream piers gets enhanced by 12.5% and 40.5% as compared to that at an isolated pier respectively. However, at X_c/b=40, the scour depth at downstream pier gets reduced by 17.1% as compared to that at an isolated pier. **It can, therefore, be concluded that the pier at downstream of upstream piers should be placed at 40 pier diameter spacing.**

In the case of two piers placed at constant angle of attack of α=45° and radial pier spacings *R/b*=0, the scour depth at this piers group gets enhanced by 12% as compared to that occurs at the same piers group aligned normal to the flow at *Zc/b*=0. However, when *R/b* =1, the scour depths at upstream and downstream piers get enhanced by 35% and 38% as compared to that occur at an isolated pier respectively. **These findings suggest that the downstream pier should be placed at 6<*R/b*<12 for economical piers design.**

In the case of two piers placed at constant radial pier spacing *R/b*=5 and angle of attack α=0°, scour depth at upstream and downstream piers equals to 1.1 and 0.96 times of that occur at an isolated pier respectively. When α becomes 45°, scour depths at upstream and downstream piers get enhanced by 17.4% and 24.1% as compared to the scour depth of an isolated pier respectively. At α=90°, the scour depths of two piers become equal but are 4.5% higher than that at an isolated pier. **These findings suggest that the downstream pier be placed at $\alpha \leq 15°$ as various hydraulic effects interplaying between the two piers have little impact on scour depth at downstream pier, however, the scour depth at upstream pier gets affected and increases about 10 % higher than that at an isolated pier. Placement of rear pier at α=45° in any case, should be avoided as the scour depths at front and rear piers are found to be maximum at α=45°.**

In the case of piers group comprising of varied sizes of piers without collar at α=0°, a reduction of 44% in the scour depth as compared to single pier of diameter equal to the diameter of the largest cylinder used in this pier group, is achieved. The use of this pier group without collar upto α=10° is found to be very effective as its use reduces the scour depth by 33% as compared to single pier of diameter equal to the diameter of largest cylinder used in this pier group. It is worthwhile to mention that the use of this pier group without collar as compared to an equivalent round nose rectangular pier of same length to width ratio as that of piers group, produces 43 % reduction in scour depth upto 7.5°angle while 30% and 4.5 % at α=15° and α=30° respectively. Application of collar to this pier group produces 100% reduction in the scour depth upto 7.5° angle of attack. However, at α=30° reduction in scour depth decreases to 42%. **These results suggest that the group of varied size piers with collar should not be aligned at an angle of**

attack more than 15° to achieve economy in pier design as the scour depth upto α =15° is substantially low.

In the case of a group of two circular piers of 41.5 mm diameter without collar at α =0° the scour depth of front pier enhances by 10% as compared to that of single 41.5 mm pier while at α =45°, scour depth of front pier increases by 17.7%. At α =90°, the scour depth at the two piers is found about 16% higher than that of single 41.5 mm pier. Application of a collar to this pier group yields excellent results for smaller angles of attack. The maximum reduction in scour depth with collar relative to that without collar at 0° angle is found to be 78.57%. However, an increase in angle of attack reduces the scour depth reduction efficiency of collar. At α =90°, the percent reduction leftovers only 23.07%. Use of this pier group as an alternative to an equivalent round nose rectangular pier without collar at α =0° produces a scour depth about 0.89 times of that occur at an isolated round-nosed rectangular pier of the same length to width ratio as that of the pier group. These results are well comparable with the findings of Zarrati *et. al.* (2006). **These results suggest that the group of two piers with collar should be used instead of a rectangular pier to reduce the scour depth and achieve economy in pier design.**

These findings acquired in present investigation suggest that the group effect of piers on local scour is highly significant and should be properly incorporated in the pier design. The results of this study constitute a methodology for realistic estimation of scour depth at group of bridge piers and impact of mutual interference of bridge piers on local scour. The study is expected to provide a valuable record and practical guidance for tackling the problems of pier group local scour.

7.1 Scope for future studies

It will be interesting to extend the study on piers arranged in various patterns for live-bed scour under varied flow, sediment and pier conditions.

In the present study on bridge pier protection against scouring, although, good results are achieved by applying a collar to groups of pier; nevertheless, the study can be extended for varied size collars.

Additional data on local scour around group of piers placed in various arrangements by conducting longer duration tests are needed to further fortify/strengthen the results.

REFERENCES

A.S.C.E. Committee on Sedimentation (1975). Manual No.154, Sedimentation Engineering.

Abbott, J.E. (1964).The dynamics of a single grain in a stream, Ph.D. Thesis, Imperial College of Science and Technology, (University of London).

Ahmad, M.(1962). Discussion of scour at bridge crossings by E.M. Laursen, Transactions, ASCE, Vol. 127, Part 1, pp. 198-206.

Ahmad. F. and Rajaratnam N.(2000).Observation on flow around bridge abutment, J. of Hyd. Engrg., ASCE, 126(1), pp. 51-59.

Ahmed, F. and Rajaratnam, N.(1998). Flow around bridge piers. J. Hyd. Engrg., A.S.C.E., Vol. 124, No. 3, pp. 288-299.

Akbulbut S, Samet Hsiloglu A, Pamuken S. (2004).Data generation for shear modulus and damping ration in reinforced sands using adaptive neuro-fuzzy inference system, Soil Dynam. Earthquake Engrg, 24, pp. 805–14.

American Society of Civil Engineers (1977). Sedimentation Engineering, Manual 54, Vito A. Vanoni, Editor.

Anderson, A.G. (1974). Scour at bridge waterways-a review, Washington, D.C., U.S. Federal Highway Administration, RD-75-89, 29 p.

Arunachalam, K. (1965). Scour around bridge piers, Journal of Indian Road Congress, No. 2, August, pp. 189-210.

Arunachalam, K. (1967). Discussion: Measurement of bridge scour and bed changes in flooding river, Thomas Telford Journals, 36, Issue: 2, pp. 397-421.

ASCE Task committee on Application of Neural Networks in Hydrology (2000-a), Artificial neural networks in hydrology I: Preliminary Concepts, J. of Hydrologic. Engrg., ASCE, Vol. 5, No. 2, pp. 115-123.

ASCE Task committee on Application of Neural Networks in Hydrology (2000-b), artificial neural networks in hydrology II: Hydrologic applications, J. of Hydrologic. Engrg., ASCE, Vol. 5, No. 2, pp. 124-127.

Azamathulla H.Md. (2005). Neural networks to estimate scour downstream of ski-jump bucket spillway, PhD thesis, Indian Institute of Technology, Bombay.

Azamathulla, H. Md., Deo, M. C. and Deolalikar, P. B. (2006). Estimation of scour below spillways using neural networks, IAHR, Journal of Hydraulic Research, 44(1), 61-69.

Azamathulla, H. Md., Deo, M.C. and Deolalikar P.B.(2008). Alternative neural networks to estimate the scour below spillways, Advances in Engineering Software, 39, pp. 689–698.

Azamathulla, H.Md, Deo, M.C., and Deolalikar, P.B. (2005). Alternative neuro-nets to estimate spillway scour. In: Topping BHV, editor. Proceedings of the eighth international conference on the application of artificial intelligence to civil structural and environmental engineering, Stirling, United Kingdom: Civil-Comp Press; Paper 47.

Azinfar, H, Kells, J.A., Elshorbagy, A. (2004) Use of artificial neural networks in the prediction of local scour, In: Proceedings of 32nd annual general conference of the Canadian society for civil engineering, pp., GC-350, pp. 1–10.

Azmathullau, H. Md., Deo, M.C. and Deolalikar, P.B. (2005). Neural networks for estimation of scour downstream of a ski-jump bucket, Journal of Hydraulic Engineering, ASCE 131 (10), pp. 898–908.

Babaeyan-Koopaei, K. and Valentine, E. M. (1999). Bridge pier scour in self-formed laboratory channels, The XXVIII IAHR congress, pp. 22-27.

Baker, C.J. (1979). Laminar horseshoe vortex, Journal of Fluid Mechanics, Vol. 95, Part 2, pp. 347-367.

Baker, C.J. (1980 a). Theoretical approach to the prediction of scour around bridge piers, Journal of Hydraulic Research, Vol. 18, No. 1,pp.1-12.

Baker, C.J. (1980 b). The turbulent horseshoe vortex, Journal of Wind Engineering and Industrial Aerodynamics, 6, pp. 9-23.

Baker, C.J. (1981). New design equation for scour around bridge piers, J. of Hydraulic Division, A.S.C.E., Vol. 107, HY-4.

Baker, C.J. (1985). The position of points of maximum and minimum shear stress upstream of cylinders mounted normal to flat plates, Journal of Wind Engineering and Industrial Aerodynamics, 18, pp. 263-274.

Basak, V., Baslamish, Y. and Ergun, O. (1975). Maximum equilibrium scour depth around linear-axis square cross–section pier groups, Report No. 583, State Hydraulic Works, Ankara, Turkey, (in Turkish).

Basak, V., Baslamish, Y. and Ergun, O. (1977). Local scour depths around circular pier groups aligned with the flow, Report No. 641, State Hydraulic Works, Ankara, Turkey, (in Turkish).

Bata, C. (1960). Scour around bridge piers, Inst. Za Vodoprivedu, Jaroslav Cerni Belgrad, Yugoslavia.

Bateni *et al.*(2007). Neural network and neuro-fuzzy assessments for scour depth around bridge piers, Journal of Engineering Applications of Artificial Intelligence, Vol. 20, pp. 401–414.

Bateni, S. M., Jeng, D.S. and Melville, B. W.(2007). Bayesian neural networks for prediction of equilibrium and time-dependent scour depth around bridge piers, J. of Advances in Engineering Software 38, 102–111.

Bateni, S.M. & Jeng, D.S. (2007): Estimation of pile group scour using adaptive neuro-fuzzy approach, Ocean Engineering 34(8–9), pp. 1344-1354.

Belik, L. (1973). Secondary flow about circular cylinders mounted normal to a flat plate, Aeronautical Quarterly, Vol. 24, Part 1, pp. 211-252.

Birikundavyi, S., Labib, R., Trung, H. and Rousselle J. (2002). Performance of neural networks in daily stream flow forecasting, Journal of Hydrological Engineering, Vol. 7, No. 5, pp. 392-398.

Bishop, C. M.(1995). Neural networks for pattern recognition, Oxford: Oxford University Press.

Blamire, P. A. (1994) An investigation into the identification and classification of urban areas from remotely sensed satellite data using neural networks, MSc Dissertation, University of Edinburgh, Edinburgh, UK.

Blench, T. (1962). Discussion on Scour. Transactions, ASCE, Vol. 127, Part 1, p. 180.

Blench, T. (1965). Mobile Bed Fluviology, University of Alberta Press.

Blench, T. (1969). Mobile Bed Fluviology, University of Alberta Press, Edmonton, Alberta, Canada.

Bonasoundas, Dr. Ing. (1973). Flow structure and scour problem at circular bridge piers, Report No; 28, Oskar Von, Miller Institute, Munich Technical University.

Breusers, H.N.C. (1967). Time scale of two-dimensional local scour, Proc. 12th Congress, I.A.H.R., Vol. 3, pp. 275-282.

Breusers, H.N.C. (1972). Local scour near offshore structures, Delft Hydraulics Laboratory, Publication No. 105.

Breusers, H.N.C. and Raudkivi, A.J.(1991). Scouring, hydraulic structure manual, I.A.H.R., Balkema, Rotterdam, Netherlands.

Breusers, H.N.C., Nicollet, G. and Shen, H.W.(1977). Local scour around cylindrical piers, J. Hydr. Res., Delft, The Netherlands, 15(3), pp. 211-252.

Breusers, H.N.C., Nicollet, G. and Shen, H.W.(1997). Local scour around cylindrical piers, Journal of Hydraulic Research, Vol. 15, No. 3, pp. 211-252.

Brice, J.C. and Blodgett, J.C. (1978). Countermeasures for Hydraulic Problems at Bridges, Vol. 1 & 2, Federal Highway Administration, U.S. Department of Transportation, pp. 10-23.

Bureau of Indian Standards (1985). Criteria of hydraulic design of bucket type energy dissipaters, BIS: 7365. New Delhi, India.

Campolo, M., Andreussi P. and Soldati, A. (1997). River flood forecasting with a neural network model, J. of Water Resources Res., 35 (4), pp. 1191-1197.

Carsten, T. and Sharma, H.R. (1975) Local scour around large obstructions, Proc. 16th Congress I.A.H.R., Sao Paulo, Brazil, Vol. 2 B32, pp. 251-262.

Carstens, M.R. (1966). Similarity laws for localized Scour, J. of Hydraulic Div., ASCE, Vol. 92, No. HY3, pp. 13-36.

Cecin, K. and Bayazit, K.(1973). Critical shear stress of armored beds, Proc. 15th Congress, I.A.H.R., Istanbul, Vol. 1, A60, pp. 493-500.

Chabert, J. and Engeldinger, P.(1956). Etude des Affouillement autour des Piles des ponts (Study on Scour around Bridge Piers), Laboratoire National d'Hydraulique, Chatou, France.

Chang, H.H. (1998). Fluvial processes in river engineering, John Wiley & Sons, 432p.

Chee, R.K.W. (1982). Live-bed scour at bridge piers, Rep. No. 290, School of Engrg. University of Auckland, Auckland, New Zealand.

Chepil, W.S. (1958). The use of evenly spaced hemispheres to evaluate aerodynamic *forces on a soil Surface, Trans. American Geophys. Union*, Vol. 39, No. 3.

Cheremisinoff, P.N., Cheremisinoff, N.P. and Chang, S.L. (1987). Hydraulic mechanics-2, Civil Engineering Practice, Technomic Publishing Company, Inc. Lancaster, Pennsylvania, U.S.A. 780 p.

Chiew, Y.M. (1984). Local scour at bridge piers, Rep. No. 355, Dept. of Civ. Engg., University of Auckland, Auckland, New Zealand.

Chiew, Y.M. (1992). Scour Protection at Bridge Piers, J. of Hydr. Engrg. ASCE, 118(9), pp.1260-1269.

Chiew, Y.M. (1995). Mechanics of riprap failure at bridge piers, J. of Hydr. Engrg. ASCE, 121(9), pp. 635-643.

Chiew, Y.M. (2004). Local scour and riprap stability at bridge piers in a degrading channel, Journal of Hydraulic Engineering, ASCE, 130(3), pp. 218-226.

Chiew, Y.M. and Lim, F.H. (2000). Failure behavior of riprap layers at bridge piers under live-bed conditions, Journal of Hydraulic Engineering, ASCE, 126(1), pp. 43-55.

Chiew, Y.M. and Melville, B.M. (1987). Local scour around bridge piers, J. of Hydraulic Research, I.A.H.R., Vol. 25, No. 1.

Chitale, S.V. (1960). Discussion of scour at bridge crossings, by E.M. Laursen, Transactions, ASCE, Vol. 1217, Part 1, 1962, pp. 191-196.

Choi Sung and Cheong (2006). Prediction of local scour around bridge piers using artificial neural net works, Journal of the American Water Resources Association.

Christiansen, B.A. (1969). Effective grain-size in sediment transport, Proc., I.A.H.R.,13th Congress, Vol. 3, Kyoto, p. 223.

Christiansen, B.A. (1975). On the stochastic nature of scour initiation, Proc. 16th Congress, I.A.H.R., Sao Paulo, Vol. 2, pp. 65-72.

Coleman, N.L. (1967). A theoretical and experimental study of drag and lift forces acting on a sphere resting on a hypothetical streambed, Proc. I.A.H.R., 12th Congress, Ft. Collins, Vol. 3, pp. 185-192.

Coleman, N.L. (1971). Analyzing laboratory measurements of scour at cylindrical piers in sand beds, Proc. 14th IAHR Congress, Paris, 3, pp. 307-313.

Coleman, S.E., and B.W. Melville (2001). Case study: New Zealand bridge scour experiences, J. Hydraulic Engrg., ASCE, 127, pp. 535-546.

Coppola, Jr. E., Szidarovszky, F., Poulton, M. and Charles, E. (2003) Artificial neural network approach for predicting transient water level in a multilayered ground water system under variable state, pumping and climate conditions, J. of Hydrol. Engrg., ASCE, 8(6), pp. 348-360.

Croad, R.N. (1993). Bridge pier scour protection using riprap, Central Laboratories Report No. PR3-0071, Works Consultancy Services, N.Z.

Cunha, L., Veiga, Da. (1975). Discussion on local scour around bridge Piers, by Shen, Schneider and Karaki, Proc. A.S.C.E., Journal Hydraulics Division, Vol. 96, HY8.

Cunha, L., Veigo, Da. (1975). Time evolution of scour, Proc. 16th Congress I.A.H.R., Sao Paulo, Brazil, Vol. 2, pp. 285-299.

Dargahi, B. (1987). Flow field and local scouring around a cylinder, Bulletin No. 137, R. Inst. Tech. Hydr. Lab., Stockholm, Sweden.

Dargahi, B. (1989). The turbulent flow field around a circular cylinder, Experiments in Fluids, 8, pp. 1-12.

Dargahi, B. (1990). Controlling mechanism of local scouring, J. Hydr. Engrg., ASCE, Vol. 116, No. 10, pp. 1197-1214.

Davoren, A. (1985). Local scour around a cylindrical bridge pier, Publication No. 3, Hydrology Centre, Ministry of Works and Development, Christchurch, New Zealand.

Dawson, C.W. and Wilby, R.L. (2001). Hydrological modeling using artificial neural networks, Prog. Phys Geog; 25 (1), pp. 80–108.

Dey, S. (1997). Local scour at bridge piers, Part I, A Review of development of research, International Journal of Sediment Research, IJSH, 12(2), pp.23-46.

Dey, S. (1999). Time variation of scour in the vicinity of circular Piers, Water and Marine Engineering Journal, Proceedings of Institution of Civil Engineers, Thomas Telford Journals, London, 136(2):pp.67-75, Paper 11426.

Dey, S. and Barbhuiya, A.K. (2004). Clear water scour at abutments in thinly armored beds, Journal of Hydraulic Engineering, ASCE, 130(7), pp.622-634.

Dey, S. and Raikar, R. V. (2007). Characteristics of horseshoe vortex in developing scour holes at piers, Journal of Hydraulic Engineering, ASCE, Vol.133, pp. 399-413

Dey, S., Bose, S.K. and Sastry, G. L.N., (1995). Clear-water scour at circular piers: A model., Am. Soc. Civ. Eng., J. Hydr. Engrg., 121(12), pp.869-876.

Dietz, J.W. (1969). Local scour in fine and light bed materials by two-dimensional flow, Report No. 155; Theodor-Rehbock-Laboratory for River Improvement, University of Karsruhe.

Dietz, J.W. (1972). Construction of long piers at oblique currents illustrated by the BAB-Main bridge eddershelm and systematic model tests on scour formation at piers, Mitteilungsblatt der Bundersanstalt fur Wasserbau, No. 31, Karlsruhe, pp. 79-109.

Dietz, J.W. (1973). Kalkbildung an einem Kreiszylindrischen Pfeilerpaar, Die Bautechnic, 50, pp. 203-208.

Doeglas, D.J. (1946). Interpretation of the results of mechanical analysis, Journal of Sediment Petrology, 16, pp. 19-40.

DOT, U. S. (1993). Evaluating scour at bridges, Hydraulic Engineering Circular 18, J. of Federal highway administration, 2, pp. 1-4.

Dou, X. (1997). Numerical simulation of three-dimensional flow field and local scour at bridge crossings, Ph. D. Thesis Oxford, MS USA: University of Mississippi.

Elliot, K.R. and Baker, C.J. (1985). Effect of pier spacing on scour around bridge piers, Journal of Hydraulics Divn., Proc. ASCE, Vol. 111, No. 7, pp. 1105-1109.

El-Taher, R.M. (1982). A numerical study of the interference effects in uniform shear flow over two circular cylinders, J. Eng. Sci., 81, pp. 86-92.

El-Taher, R.M. (1984). Experimental study on the interaction between a pair of circular cylinders normal to a uniform shear flow, J. Wind Eng. Ind. Aerodyn., 17, pp. 117-132.

El-Taher, R.M. (1985). Flow around two parallel circular cylinders in a linear shear flow, J. Wind Engg. Ind. Aerodyn, Vol. 21, pp. 251-272.

Ettema, R. (1976). Influence of bed material gradation on local scour, Report No 124, School of Engineering, University of Auckland, New Zealand.

Ettema, R. (1980). Scour at bridge piers, Rep. No. 216, School of Engrg. University of Auckland, Auckland, New Zealand.

Ettema, R. E., Melville B.W. and Barkdoll B. (1999). Closure: A scale effect in pier-scour experiments Journal of Hydraulic Engineering, ASCE, 125 (8), pp. 895-896.

Ettema, R. Mostafa, E.A., Melville, B.W. and Yassin, A.A. (1998). Local scour at skewed piers, J. Hydr. Engrg. ASCE, 124(7), pp. 756-759.

Ettema, R., Fujita, I., Muste, M. and Kruger, A., (1997b). Particle-image velocimetry for whole-field measurement of ice velocities, Cold Regions Science and Technology v 26 n 2 Oct 1997 p 97

Ettema, R., Fujita, I., Muste, M., and Kruger, A., (1997a). Particle-image velocimetry for ice-field velocities, Proc. 1997 27th Congr. Int. Assoc. Hydr. Resrch, IAHR. Part B-1 vB pt 1 ASCE p 137

Fausett, L. (1994). Fundamentals of neural networks, architectures, algorithms and applications, upper saddle river, New Jersey, USA: Prentice-Hall, 462.

Fenton, J.R. and Abbott, J.E., (1977). Initial movement of grains on a stream bed: the effect of relative protrusion, Proc. Roy. Soc. Lond. A, 352, pp. 523-537.

Folk, R.L. (1968). Petrology of sedimentary rocks, University of Texas, Geology, 370K, 383L, 383M.

Foody, G. M. (1995). Using prior knowledge in artificial neural network classification with a minimal training set, International Journal of Remote Sensing, 16, 301-312.

French, M. N., Krajewski, W. F. and Cuykendall, R. R. (1992). Rainfall forecasting in space and time using a neural network , J. of Hydrology, pp. 137: 1-31.

Froehlich, D.C. (1988). Analysis of onsite measurements of scour at piers, Proc., ASCE Nat. Hydr. Engrg. Conf., ASCE, Reston, Va.

Gao, D., Posada, L. and Nordin, C.F. (1994). Pier scour equations used in the People's Republic of China, Rep. No FHWA-SA-93-076. Fed. Hwy. Admin. U.S. Dept. of Transp., McLean, Va.

Garde, R. J., Ranga Raju, K.G. and Kothyari, U. C. (1987). Effect of unsteadiness and stratification on local scour, Reasearch report, Civil Engineering Department, University of Roorkee, India.

Garde, R.J. (1961). Local bed variation at bridge piers in alluvial channels, University of Roorkee Research Journal, Vol. 4, No. 1.

Garde, R.J. and Hasan, S.M. (1967). An experimental investigation of degradation in alluvial channels, Proc. 12th Congress I.A.H.R. Pt. Collins, Colorado, Vol. 3, pp. 38-45.

Garde, R.J. and Kothyari, U.C. (1995). State of art report on scour around bridge piers, Pune, India.

Garde, R.J., Ranga Raju, K.G. and Kothyari, U.C. (1989). Effect of unsteadiness and stratification on local scour. Research Report, Civil Engineering Department, University of Roorkee, Roorkee (U.P.).

Gessler, J. (1971). Beginning and ceasing of sediment motion, river mechanics, Volume 1, Chap. 7, edited and published by Hsieh Wen Shen, Colorado State University, Fort Collins, Colo., pp. 7-1 through 7-22.

Gessler, J. (1971).Critical shear stress of sediment mixtures, Proceedings, 14th Congress of the I.A.H.R., Vol. 3, C1, Paris, France.

Graf, W.H. (1995). Local scour around piers, Annu. Rep., Laboratoire de Recherches Hydrauliques, Ecole Polytechnique Federale de Lausanne, Lausanne, Switzerland, B.33.1 – B.33.8.

Graf, W.H. and Istiarto, I. (2002), Flow Pattern in the Scour Hole Around a Cylinder, J. of Hydr. Res., IAHR, Vol. 40, No. 1, pp. 13-20.

Graf, W.H. and Yulistiyanto (1988). Experiments on flow around a cylinder; the velocity and vorticity fields, J. Hydraulic Research, I.A.H.R., Vol. 36, No. 4, pp. 637-653.

Grubert, JP. (1995) Application of neural networks in stratified flow stability analysis, J. of Hydrol. Engrg., 121(7), pp. 523-532.

Grubert, JP. (1995). Prediction of estuarine instabilities with artificial neural networks, J of Comput Civil Eng; 9 (4), pp. 266–74.

Gupta, A.K. and Gangadharaiah, T. (1992). Local scour reduction by a delta wing-lick passive device, Proc., 8th Congr. of Asia and Pacific Reg. Div., 2, CWPRS, Pune, India, pp. B471-B481.

Hadfield, A.C. (1997). Sacrificial piles as a bridge pier scour counter-measure, ME thesis, Civ. and Resour. Engrg. Dept., University of Auckland, Auckland, New Zealand.

Hager, W. H. and Oliveto, G. (2002). Shields' entrainment criterion in bridge hydraulics, journal of hydraulic engineering, ASCE, 128 (5), pp. 538-542.

Hager, W. H., Unger, J., and Oliveto, G. (2002). Entrainment criterion for bridge piers and abutments, River flow 2002, Vol. 2, D. Bousmar and Y. Zech, eds., Swets & Zeitlinger, Lisse, pp. 1053–1058.

Haghighat, M.(1993). Scour around bridge pier group, ME thesis, University of Roorkee, Roorkee, India.

Hancu, S. (1971). Sur le calcul des affouillements locaux dams la zone des piles des ponts, Proc., 14th IAHR Congress, Vol. 3, International Association for Hydraulic Research, Delft, The Netherlands, pp. 299-313.

Hannah, C.R. (1978). Scour at pile groups, University of Canterbury, N.Z., Civil Engineering Research Rep. No. 78-3, 92.

Harwood, N.J. (1977), Local scour at a bridge pier caused by flood waves, M.E. Thesis, University of Canterbury, Christchurch.

HEC-18(1991). Evaluating scour at bridges, Hydraulic Engineering Circular No. 18, Federal Highway Administration (FHWA), USDOT, Washington, D.C.

HEC-6 (1976). Scour and deposition in rivers and reservoirs, computer program, Hydrologic Engineering Center, United States Army Corps of Engineers, Davis, Calif.,

Hepner, G. F., Logan, T., Ritter, N. and Bryant, N. (1990) Artificial neural network classification using a minimal training set: comparison to conventional supervised classification, Photogrammetric Engineering and Remote Sensing, 56, pp. 469-473.

Herbertson, J.G. and Ibrahim, A.A.(1992). Interaction between bridge piers and scour protection devices, Proc. Int. Conf. on Protection of the Nile and Other Major Rivers, Cairo, Egypt.

Hidalgo, C. (1994). Hydraulic test on local scour around bridge pier founded on piling, MS thesis, Civ. Engrg. School, Barcelona, Spain (in Spanish).

Hinze, J.O. (1959) Turbulence, McGraw-Hill Publishing Co., Inc., New York, N.Y.

Hjorth, P. (1975). Studies on the nature of local scour, Bulletin Series A, No. 46, Department of Water Resources Engrg., Lund Institute of Technology, Lund, Sweden.

Hjorth, P. (1977), A stochastic model for progressive scour, Proc. Int. Symposium on Stochastic Hydraulics 2d., University of Lund, Sweden, Water Resources Publn.

Hoffmans CJCM, Booij R., (1993). Two dimensional mathematical modeling of local scour holes, J of Hydraul Res Int. Assoc Hydraul. Res., 31(5), pp. 615–34.

Hoffmans, GJCM. and Verheij H.J. (1997). Scour manual, Rotterdam/Brookfield: A.A. Balkema.

Holmes, P.S. (1974), Analysis and prediction of scour at railway bridges in New Zealand, Report presented to N.Z. Railways.

Hopkins, G.R., Vance, R.W. and Kasraie, B.(1975). Scour around bridge piers, Interim Report prepared for Federal Highway Admin., Report No. F.H.W.A.-RD-75-76.

Incyth, Lha. (1982). Estudio sobre modelo del aliviadero de la Presa Casa de Piedra, Informe Final. DOH-044-03-82, Ezeiza, Argentina.

Indian Railway Standards (1985), Code of practice for the design of substructures and foundations of bridges (revised).

Inglis, C.C. (1949). The Behaviour and Control of Rivers and Canals, Chapter 8, Part I and II, C.W.P.I.N.R.S. Research Publication 13, Poona, India, pp. pp. 35-38.

Inglis, C.C. Thomas, A.R. and Joglekar, D.V.(1939). The protection of bridge piers against scour, Annual Report of work done during 1938-1939, Central Irrigation and Hydrodynamics Research Station, Poona, Research Publication No.2.

Irvine, H.M. and Sutherland, A.J. (1973), A probabilistic approach to the initiation of movement of non-cohesive sediments, Proc. Int. Symposium on River Mechanics, Bangkok, I.A.H.R., Vol. I, pp. 383-394.

Ishihara, T.(1942). Experimental study on scour at bridge piers, Trans. of Japanese Soc. of Civil Eng., Vol. 24, No. 1, pp. 28-55.

Islam, M.N., Garde, R.J. and Ranga Raju, K.G.(1986). Temporal variation of Local scour, Proc, I.A.H.R. Symposium on Scale Effects in Modelling Sediment Transport Phenomenon, Toronto, Canada, pp. 252-262.

Ismail, Z. and Sidek, F. J. (2002). Scour Investigation around a Group of Two Piers, Procs 13th Congress of the Asia Pacific Division of the International Association for Hydraulic Engineering and Research (APD - IAHR), Singapore, 6 - 8 August.

Jain A, Srinivasulu Sudheer, K.P.S. (2004). Identification of physical processes inherent in artificial neural network rainfall runoff models, Hydrol. Process; 18 (3), 571–81.

Jain, B.P. and Modi, P.N.(1986). Comparative study of various formulate on scour around bridge piers, Journal of the Institution of Engineers, India, Vol. 67, Part 3, pp. 149-159.

Jain, S.C. (1981). Maximum clear-water scour around cylindrical piers, J. of Hydraulic Div., A.S.C.E., Vol. 107, HY-5, pp. 611-626.

Jain, S.C. and Fischer, E.E.(1979). Scour around bridge piers at high Froude numbers, Report No. FH-WA-RD-79-104, Federal Highway Administration, Washington D.C.

Jain, S.C. and Fischer, E.E.(1980). Scour around bridge piers at high flow velocities, J. Hydr. Div., ASCE, 106(11), 1827-1842.

Jang J.S.R, Sun, C.T. (1995). Neuro-fuzzy modelling and control, Proc IEEE, 83 (3), pp. 378–406.

Jarocki, W.(1961). Effect of piers on water streams and bed forms, Proc. 9th Congress I.A.H.R., Dubrovink, Yugoslavia, pp. 1147-1153.

Jeng *et al.*(2005). Neural Network assessment for scour depth around bridge piers, Research Report No R855, Department of Civil Engineering, The University of Sydney, Australia.

Jens, Unger and Willi, H. Hager (2006) Riprap Failure at Circular Bridge Piers, journal of hydraulic engineering, ASCE, 132: (4), pp. 354-362

Johnson, P.A. (1995). Comparison of pier-scour equations using field data, J. Hydr. Engrg., ASCE, Vol. 121, No. 8, pp 626- 629.

Johnson, P.A. and Dock, D.A. (1996). Probabilistic bridge scour estimates, J. Hydr. Engrg. ASCE, 124 (7), 750-754.

Johnson, P.A., and Ayyub, B.M. (1992). Assessment of time-variant bridge reliability due to pier scour, J. Hydr. Engrg., ASCE, 118(6).

Johnson, P.A., and McCuen, R.H.(1991). A temporal spatial pier scour model, Transp. Res. Rec. 1319, Transportation Research Board, Washington, D.C. pp. 143-149.

Johnson, Peggy A. (1999). Scour at wide piers relative to flow depth, Stream Stability and Scour at Highway Bridges, Compendium of ASCE conference papers edited by E.V. Richardson and P.F. Lagasse, pp. 280-287.

Jones, S.T., Kilgore, R.T., and Mistichelli, M.P. (1992). Effects of footing location on bridge pier scour, J. Hydr. Engrg., ASCE, 118(2), pp. 280-290.

Kambekar, A.R., Deo, M.C. (2003). Estimation of pile group scour using neural networks, Appl Ocean Res, 25 (4), pp. 225–34.

Kamil, H.M. Ali, and Othman Karim (2002). Simulation of flow around piers, J. of Hydraulic Research Vol. 40, No. 2, pp. 161-174.

Karim OA, Ali KHM (2000). Prediction of flow patterns in local scour holes caused by turbulent water jets, IAHR J. of Hydraul. Res., 38 (4), pp. 279–88.

Kazeminezhad, M.H., Etemad-Shahidi, A. and Mousavi, S.J. (2005). Application of fuzzy inference system in the prediction of wave parameters, Ocean Engineering, 32, pp. 1709–1725.

Keutner, C. (1932). Stream flow patterns around the river piers of different horizontal cross-sectional forms and their effect on the stream bed, Die Bautechnik, Vol.10, No. 12, pp. 161-170.

Khosronejad, G. A. Montazer and M. Ghodsian (2004). Estimation of Sour hole properties around vertical pile using ANNs, International Journal of Sediment Research, Vol. 18, No. 4, 2003, pp. 290-300

Kikkawa, H., Fukuoda, S., Sogawa, H. (1973), Study on localized scour around a bridge pier and its prevention, Proc. Symposium on River Mechanics, I.A.H.R., Bangkok, Vol. 1, pp. 105-116.

Klingeman, P.C. (1973), Hydrological evaluations in bridge pier scour design, Proc. A.S.C.E., Journal Hydraulics Div., Vol. 99, HY12.

Knezevic, B., (1960), Prilog proucavanju erozijc oko mostovskih stubova, (Serbian), (Contributions to Research Work of Erosion around Bridge Piers), Institut za

Knight, D.W. (1975), A laboratory study of local scour at bridge piers, Proc. 16th Congress I.A.H.R., Sao Paulo, Brazil, Vol. 2, pp. 243-250.

Komura, S. (1966). Equilibrium depth of scour in long contractions, Journal of Hydraulics Divn., Proc. ASCE, Vol. 92, HY-5.

Kosko B. (1992). Neural networks and fuzzy systems, Englewood Cliffs, NJ: Prentice Hall.

Kothyari, U.C., (1989). Scour around bridge piers, Ph.D. Thesis, Univ. of Roorkee, Roorkee, India.

Kothyari, U.C., Garde, R.J. and Ranga Raju, K.G. (1992 a). Temporal variation of scour around circular bridge piers, J. of Hydraulic Engg., A.S.C.E., Vol. 118, No. 8, Aug., pp. 1091-1105.

Kothyari, U.C., Garde, R.J. and Ranga Raju, K.G. (1992 b). Live-bed scour around cylindrical bridge piers, J. of Hydraulic Research, I.A.H.R., Vol. 30, No. 5, pp. 701-715.

Krumbein, W.C. (1937). Sediments and experimental curves, Journal of Geology, Vol. 45, pp. 571-601

Krumbein, W.C. (1938), Size frequency distributions and the normal phi curve, Journal of Sedimentary Petrology, Vol. 8, pp. 84-90.

Kumar, V., (1996). Reduction of scour around bridge pier using protective devices, PhD thesis, University of Roorkee, Roorkee, India.

Kumar, V., Ranga Raju, K.G. and Vittal, N. (1995). Jet-flow model for equilibrium scour depth around cylindrical piers, 6th International Symposium on River Sedimentation, New Delhi, pp. 955-965.

Kumar, V., Ranga Raju, K.G. and Vittal, N. (1999). Reduction of local scour around bridge piers using slot and collar, Technical Note, J. Hydr. Engrg. ASCE, 125(12), pp. 1302-1305.

Kwan, T.F. and Melville, B.W. (1994). Local scour and flow measurements at bridge piers, J. of Hydr. Res. IAHR 32(5), pp. 661-674.

Lacey, G. (1929). Stable channels in alluvium, Proc. Inst. Civil Engineers, Paper No. 4736, Vol. 229, pp. 259-384.

Lacey, G. (1930). Stable channels in alluvium, Minutes of Proceedings, Institution of Civil Engineers.

Lagasse, P.E., Richardson, E.V., Shall, J.D., and Price, G.R. (1997). Instrumentation: measuring scour at bridge piers and abutments, NCHRP Rep. 396, National Cooperative Highway Research Program, Washington, D.C.

Lagasse, PP, Thompson, PL, and Sabol, SA. (1995). Guarding Against Scour, Civil Engineering, American Society of Civil Engineers, June, pp. 56-59.

Landers, M.N., and Mueller, D.S. (1996). Channel scour at bridges in the United States, Rep. No. FHWA-RD-95-184, Fed. Hwy. Admin., U.S. Dept. of Transp., McLean, Va.

Larras, J. (1963). Profondeurs Maximales d'Erosion des Fonds Mobiles autour des Piles en Riviero, Annales des Ponts et Chausses, Vol. 133, No. 4, pp. 441-424.

Larronne, J.B. (1973). A geomorphological approach to coarse bed-material movement in alluvial channels, with special reference to a small appalachian stream, M.Sc. Thesis, McGill University.

Larronne, J.B. and Carson, M.A. (1976), Interrelationships between bed morphology and bed material transport for a small gravel bed channel, Sedimentology, Vol. 23, pp. 67-85.

Laursen and Toch. (1953). Generalized model study of scour around bridge piers and abutments, Reprinted from Proceedings, Minnesota International Hydraulics' Convention, September 1-4, Reprint No. 120, Minncnpolis, Minnesota, state university of Iowa, U.S.

Laursen, E.M. (1958). Scour at bridge crossings, Bulletin No. 8, Iowa Highway Research Board.

Laursen, E.M. (1962). Scour at bridge crossings, Trans. ASCE, Vol. 127, Part 1, pp. 166-179.

Laursen, E.M. (1963). Analysis of relief bridge scour, J. Hydr. Div., ASCE, 89(3), pp. 93-118.

Laursen, E.M. (1970, a). Discussion on local scour around bridge piers by Shen *et. al.*, Proc. A.S.C.E. Journal Hydraulics Div., Vol. 96, HY9.

Laursen, E.M. (1970, b). Bridge design considering scour and risk, Proc. A.S.C.E., Journal Transportation Eng., Vol. 96, TE2, pp. 149-164.

Laursen, E.M. and Toch, A. (1951). Model studies of scour around bridge piers and abutments, Second Progress Report, Proc. 31st Annual Meeting, HRB.

Laursen, E.M. and Toch, A. (1956). Scour around bridge piers and abutments, Iowa Highway Research Board, Bulletin No. 4, Ames, Iowa, USA.

Laursen, E.M., and Toch, A. (1956). Scour around bridge piers and abutments, Bull. No. 4, lowa Highways Research Board, Ames, Iowa.

Lee *et al.* (2007). Neural network modeling for estimation of scour depth around bridge piers, j. of hydrodynamics, Ser.B, 2007,19(3), pp. 378-386

Lee, T. L. (2004). Back-propagation neural network for the long-term tidal predictions, J. of Ocean Eng., 31(2), pp. 225-238.

Lee, T. L. (2006). Neural network prediction of a storm surge, J. of Ocean Engineering, 33 (3-4), pp. 483-494.

Lee, T. L., Jeng D. S. (2002). Application of artificial neural networks in tide forecasting, J. of Ocean Eng., 29 (9), pp. 1003-1022.

Lee, T. L., Jeng D. S., Lin C. *et al.* (2002). Assessment of earthquake-induced liquefaction by artificial neural networks, The 9th International Conference for Computing in Civil and Building Engineering. Taipei, China, pp. 55-60.

Leopold, L.B., Wolman, M.A. and Miller, J.P. (1964). Fluvial processes in geomorphology, Published by Freeman, London, San Francisco.

Lim, F.H. (1998). Riprap protection and its failure mechanisms, A thesis submitted to the School of civil and structural engineering, Nanyang Technological University, Singapore in fulfillment of the requirements for the degree of doctor of philosophy.

Lim, F.H. and Chiew, Y.M. (1996). Stability of riprap layer under live-bed conditions, Proc., Ist Inter. Conf. On new/emerging concepts for rivers, RiverTech'96, Vol.2, pp. 830-837.

Lim, F.H. and Chiew, Y.M. (2001). Parametric study of riprap failure around bridge piers, J of Hyd Research, Vol. 30, No. 1, pp. 61-72.

Lim, S.Y. (1997). Equilibrium clear-water scour around and abutments, J. of Hydr. Engrg., ASCE, 123(3): 237-243.

Lim, S.Y. and Cheng, N.S. (1998). Scouring in long contractions, J. Irrig. And Drain. Engrg., ASCE, 124(5), 258-261.

Link O and Zanke U. (2004). On the time-dependent scour-hole volume evolution around a circular pier in uniform coarse sand. In: Second international conference on scour and erosion, Nanyang University, Nanyang, Singapore.

Liriano, S.L. and Day, R.A., Prediction of scour depth at culvert outlets using neural networks. J. of Hydroinform, Vol. 3 i4. 231-238.

Liu, H.K., Chang, F.M. and Skinner, M.M. (1961). Effect of bridge construction on scour and backwater, Res. No. CER-60-HKL-22, Dept. of Civil Engg, Colorado State University, U.S.A.

Londhe, S.N. and Deo MC. (2003). Wave tranquility studies using neural networks. Marine Struct., 16 (6), pp. 419–36.

Maier, H.R., Dandy, G.C. (2000). Neural networks for prediction and forecasting of water resources variables; a review of modeling issues and applications, Environ Model Software, 15, pp. 101–24.

Makarynskyy, O., Makarynska, D. and Kuhn, M. (2004). Predicting sea level variations with artificial neural networks at Hillarys boat harbour, J. of Coastal and Shelf Science, 61(2), pp. 351-360.

Makarynskyy, O., Pires-silva, A. A. and Makarynska, D. (2005). Artificial neural networks in wave predictions at the west coast of Portugal, J. of Computers and Geosciences, 31 (4), pp. 415-424.

Martins, R..B.F. (1975). Scouring of rocky river beds by free jet spillways, Int. Water Power Dam Constr; 27(4), pp. 152–3.

Martin-Vide, J.P. (1995). Bridge scour and rip-rap in complex geometry–a case study, 6th Int. Symp., River Sedimentation, New Delhi, India, pp. 995-1004.

Martin-Vide, J.P. and Dolz Ripolles, J. (1994). Scour protection at bridge piers: a case study of the Mora bridge on a scale model, Revista de Obras Publicas, 141(3328), pp. 31-40 (in Spanish).

Mase, H. (1995). Evaluation of artificial armour layer stability by neural network method, Proc. 26th Congress of IAHR, London, UK, pp. 341-346.

Mason, P.J. and Arumugam K. (1985). Free jet scour below dams and flip buckets, J. of Hydraul Eng ASCE; 111(2), pp. 220–35.

Mason, R.R., and Shepard, D.M. (1994). Field performance of an acoustic scour-depth monitoring system, Proc. Fundamentals and Advancements in Hydr. Measurements and Experimentation, ASCE, New York, pp. 366-375.

Maza Alvarez, J.A. and Sanchez Bribiesca, J.L. (1964). Contribution al Estudio de la Socovacion Local en Pilas de Puente, Universidae Federal do Reo Grande do Sul, Mexico.

Maza, J.A. (1968). Socavacion en cauces naturals, A. J. Miguel-Rodriguez, translator, Rep. No. 114, School of Engineering, University of Auckland, Auckland, New Zealand.

Melville, B. W. and Coleman, S. E. (2002). Bridge scour, Water Resources Publications, LLC, Colorado, U.S.A.

Melville, B.W. (1975). Local scour at bridge sites, Report No. 117, University of Auckland, School of Engineering, Auckland, and New Zealand.

Melville, B.W. (1988). Scour at bridge sites, chapter 15, Civil Engineering Practice, Hydraulics/Mechanics, and Edited by Cheremisinoff *et al.*, Technomic Publishing Company, and U.S.A.

Melville, B.W. (1997). Pier and abutment scour–integrated approach, J. Hydr. Engrg, ASCE, 123(2), pp. 125-136.

Melville, B.W. and Chiew, Y.M. (1999). Time scale for local scour at bridge piers, J. of Hydr. Engrg., ASCE, 125(1), pp. 59-65.

Melville, B.W. and Coleman, S.E. (2000), Bridge scour: Water Resources Publications, LLC, Colorado, U.S.A., 550p.

Melville, B.W. and Hadfield, A.C. (1999). Use of sacrificial piles as pier scour countermeasures, Journal of Hydraulic Engineering, ASCE, 125(11), pp.1221-1224.

Melville, B.W. and Raudkivi, A.J. (1977). Flow characteristics in local scour at bridge piers, J. Hydr. Res. IAHR, 15, pp. 373-380.

Melville, B.W. and Sutherland, A.J. (1988). Design method for local scour at bridge piers, J. of Hydraulic Division, A.S.C.E., Vol. 114, No. 10, pp. 1210-1226.

Melville, B.W., and Dongol, D.M. (1992). Bridge pier scour with debris accumulation, J. Hydr. Engrg., ASCE, 118(9), pp. 1306-1310.

Melville, B.W., and Sutherland A.J. (1989). Design method for local scour at bridge piers, J. Hydr. Engrg., ASCE, 114(10), pp. 1210-1226.

Melville, B.W., Van Ballegooy, S., Coleman, S.E. and Barkdoll, B. (2006) Scour countermeasures for wing-wall abutments, Journal of Hydraulic Engineering, ASCE, 132(6), pp. 563-574.

Mia, M.F., Nago, H. (2003) Design methods of time-dependent local scour at circular bridge piers, J. of Hydraulic Engrg., 129(6), pp. 420-427.

Miller, J.P.,and Leopold, L.B. (1963). Simple measurements of morphological changes in river channels and hill slopes, changes of climate, Proceedings of the Rome Symposium organized by United Nation Educational, Scientific; and Cultural Organization.

Mostafa, E.A. (19494). Scour around skewed bridge piers, Ph.D. thesis, Dept. of Irrigation and Hydraulics, Alexzandria University, Alexzandria, Egypt.

Muzzammil, M., Gangadhariah, T. (2003). The mean characteristics of horseshoe vortex at a cylindrical pier, J. of Hydraulic Research, Vol. 41, No. 3, pp. 285-297.

Muzzammil, M., Gangadhariah, T. and Gupta A.K. (2004). An experimental investigation of a horseshoe vortex induced by a bridge pier, Water Management Journal, Proceedings of the Institution of Civil Engineers, Thomas Telford Journals, London, 157(2): 109-119, paper 13904.

Nagy, H.M., Watanabe, K. and Hirano, M. (2002) Prediction of sediment load concentration in river using artificial neural network model. J. of Hydraulic Engrg., ASCE, 128(6), pp. 588-595.

Nakagawa, H. and Suzuki, K. (1975). An application of stochastic model of sediment motion to local scour around a bridge pier, Proc. 16th Congress I.A.H.R., Sao Paulo, Brazil, Vol. 2, pp. 228-235.

Nayak, P.C., Sudheer, K.P., Rangan, D.M. and Ramasastri, K.S. (2004). A neuro-fuzzy computing technique for modeling hydrological time series, J. of Hydrol, 291, Elsevier, pp. 52–66.

Nazariha, M. (1996), Design relationships for maximum local scour depth for bridge pier groups, Thesis, Univ. of Ottawa, Ottawa.

Neill, C.R. (1964 b), River bed scour-a review for engineers, Canadian Good Roads Assn., Tech. Pub. No. 23, Ottawa, Canada.

Neill, C.R. (1964). Local scour around bridge piers, Highway and River Engineering Division, Research Council of Alberta, Alberta, Canada.

Neill, C.R. (1968). Note on initial movement of coarse uniform bed-material, Journal of Hyd. Research, I.A.H.R. (Mar.), 6(2).

Neill, C.R. (1970). Discussion on local scour around bridge piers, by Shen, H.W. Schneider, V.R., and Karak, S., Journal of the Hydraulics Division, ASCE, Vol. 96, No. HY5, Proc. Paper 6891, pp. 1224-1227.

Neill, C.R. (1973). Guide to bridge hydraulics, Edited by C.R. Neill, published for Roads and Transportation Assn. of Canada by University of Toronto Press.

Nicollet, G. (1971). Deformation des Lits Alluvionaires Affouillements Autour des Piles de Ponts Cyindriques, Report No. HC 043 684, Laboratoire National d'Hydraulique, Chatou, France.

Nicollet, G. and Ramette, M. (1971). Affouillements an voisinage de Piles des Pont cylindriques circularizes, Proc. 14th Congress, IAHR, Paris, Vol. 3, pp. 315-322.

Odgaard, A.J. and Wang, Y. (1987). Scour prevention at bridge piers, Hydr. Engrg. 87, R.M. Ragan, ed., National Conference, Virginia, 523-527.

Oliveto,G. and Hager, W.H. (2002). Temporal evolution of clear-water pier and abutment scour, J. Hydraulic Engrg., 128(9), 811-820.

Oliveto,G. and Hager, W.H. (2005). Further results to time-dependent local scour at bridge elements, J. Hydraulic Engrg., ASCE 131(2), pp 97-105.

Olsen, N.R.B. and Kjellesvig, H.M. (1998). Three dimensional numerical flow modeling for estimation of local scour depth, J of Hydrol. Res., 36 (4), pp. 579–90.

Olsen, N.R.B. and Melaaen, M.C. (1993). Three dimensional calculations of scour around cylinders, J. of Hydraulic Engrg., Vol. 119, No. 9, pp. 1048-1054.

Onishi, Y., Jain, S.C., and Kennedy, J.F. (1976). Effects of meandering in alluvial streams, Journal of Hydraulics Division, ASCE, Vol. 102, No. HY7, Proc. Paper 12248, July, pp. 899-917.

Paice,C. and Hey, R. (1993). The control and monitoring of local scour at bridge piers, Proc, Hydr. Engrg. Conf., ASCE, New York, 1061-1066.

Paintal, A.S. (1971 a). Concept of critical shear stress in loose boundary open channels, Journal Hydraulic Research, I.A.H.R., Vol. 9, No 1, pp. 91-109.

Pao, Y. (1989). Adaptive pattern recognition and neural networks, (New York: Addison-Wesley).

Paola, J. D. and Schowengerdt, R. A. (1994). Comparisons of neural networks to standard techniques for image classification and correlation. Proceedings of the International Geosciences and Remote Sensing Symposium (IGARSS'94), Pasadena, USA, 1404-1406.

Parker. *et al* (1998). Countermeasures to protect bridge piers from scour, Vol. 2, Final Report, NCHRP project 24-07, Transportation Research Board, National Academy of Science, Washington D.C.

Parola, A.C. (1993). Stability of riprap at bridge piers, J. of Hydr. Engrg. ASCE, 119, 1080-1093.

Parola, A.C., Jr. and Jones, J.S. (1991), Sizing riprap to protect bridge piers from scour, Transport. Res. Rec. (1290), 276-280.

Patrick Dare Alabi (2006). Time Development of local scour at a bridge pier fitted with a collar, A thesis submitted to the college of graduate studies and research in partial fulfillment of the requirements for the degree of master of science in the department of civil and geotechnical engineering, University of Saskatchewan, Saskatoon, Saskatchewan, Canada.

Peirce, T.J., Jarman, R.T. and Turbille, C.M. (1970). An experimental study of silt scouring, Proc. Inst. Civil Engrs., Vol. 45, pp. 231-243.

Pettijohn, F.J. (1949). Sedimentary rocks, Harper, New York, pp. 526.

Posey, C.J. (1949). Why bridges fail in floods, Civil Engineering, Vol. 19, pp. 42-90.

Posey, C.J. (1949). Why bridges fail in floods, Civil Engineering, Vol. 19, pp. 42-90.

Posey, C.J. (1963). Scour at bridge piers: Protection of threatened piers, Civil Engineering, N.Y., pp. 48-49.

Posey, C.J. (1974). Tests of scour protection for bridge piers, Proc. A.S.C.E., Journal Hydraulics Div., Vol. 100, HY12, pp. 1773-1783.

Posey, C.J., Appel, D.W. and Chamnas, E. Jr. (1957). Investigation of flexible mats to reduce scour around bridge piers, Highway Research Board, Research Report No. 13-B, Washington, D.C.

Qadar, A. (1981). The vortex scour mechanism at bridge piers, Proceedings of Institution of Civil Engineers, Vol. 71, Pt. 2, pp. 739-75

Raikar, R. V., Nagesh Kumar, D and Dey, S (2004). End depth computation in inverted semicircular channels using ANNs, Flow Measurement and Instrumentation, 15.

Raudkivi, A.J. (1976). Loose boundary hydraulics, Pergamon Press, Elmsford, N.Y.

Raudkivi, A.J. (1978). Scour at bridge piers: effects of grading and layering, Seminar on Bridge Design and Research, University of Auckland, Vol. 4, pp. 129-136.

Raudkivi, A.J. (1982). Grundlagen des sediment transports, Report SEB79, Universitat Hannover, 1981 (published by Springer.

Raudkivi, A.J. (1986). Functional trends of scour at bridge piers, J. of Hydr. Engrg, ASCE, Vol 109, No 3, pp 338 -350.

Raudkivi, A.J. (1988). Functional trends of scour at bridge piers, J. of Hydraulic Engg, A.S.C.E., Vol. 112, No. 1, pp. 1-13.

Raudkivi, A.J. (1990). Loose boundary hydraulics, 3rd Edition, Pergamon Press, Chap. 9, New York, U.S.A.

Raudkivi, A.J. (1998). Loose boundary hydraulics, 4th Edition Rotterdam; Brookfield, VT: Balkema, 496p.

Raudkivi, A.J. and Ettema, R. (1977). Effect of sediment gradation on clear water scour, Journal of the Hydraulics Division, ASCE, Vol. 103, No. HY10, Oct., pp. 1209-1213.

Raudkivi, A.J. and Ettema, R. (1983). Clear-water scour at cylindrical piers, J. of Hydraulic Engrg., A.S.C.E., Vol. 109, No. 10, pp. 338-350.

Raudkivi, A.J. and Sutherland, A.J. (1981). Scour at bridge crossings, Report No. 51, Road Research Unit, National Roads Board, and Wellington, New Zealand.

Reineck, H.E. and Singh, I.B. (1973). Local scour around bridge Piers, Proc. A.S.C.E., Journal Hydraulics Div., Vol. 96, HY7, pp. 1636-1637.

Richardson, E.V. and Abed, L. (1993). Top width of pier scour holes in free and pressure flow. Proc., Nat. Conf. Hydraulic Engrg. Part 1 (of 2) Jul 25-30, pt 1 1993 ASCE p 911.

Richardson, E.V. and Davis, S.R. (1995). Evaluating scour at bridges, Rep. No. FHWA-IP-90-017 (HEC-18), Federal Administration, U.S. Department of Transportation, Washington D.C.

Richardson, E.V., and Davis, S.R. (2001).Evaluating scour at bridges (4th ed.): Washington, DC, Federal Highway Administration Hydraulic Engineering Circular No. 18, FHWA NHI 01-001, 378 p.

Richardson, E.V., Simons, D.B., Karaki, S., Mahmood, K. and Stevens, M.A. (1975). Highways in the River Environment Design Considerations, Training and Design Manual Prepared for the Federal Highway Administration.

Richardson, J. E. and Panchang, V. G. (1998). Three-dimensional simulation of scour-inducing flow at bridge piers, Journal of Hydraulic Engineering, ASCE., 124, pp. 530-540.

Richardson, J.E. and Pancheng, V.G. (1998). Three dimensional Simulation of Scour Inducing Flow at Bridge Piers, J. Hydr. Engrg. ASCE, 124(5).

Ripley, B. D. (1996). Pattern Recognition and Neural Networks. (Cambridge: Cambridge University Press).

Roper, A.T. (1967). A cylinder in a shear layer flow, Thesis presented to Colorado State University, at Fort Collins, Colo., in partial fulfillment of the requirements for the degree of Doctor of Philosophy.

Roper, A.T., Schneider, V.R. and Shen, H.W. (1967). Analytical approach to local scour, Proc. 12th Congress I.A.H.R. Ft. Collins, Vol. 3, pp. 151-161.

Roulund, A., Sumer B. M. and Fredsoe, J. (1999). 3D mathematical modeling of scour around a circular pile in current, Proc. 7th Int'l Symposium on River Sedimentation and 2nd Int'l Symposium on Environmental Hydraulics '98. Hong Kong, China, pp. 131-138.

Rouse, H. (1939). Laws of transportation of sediment by streams; suspended load, Reprint No. 21, Univ. of Iowa, Iowa City, Iowa, Reprints in Engineering.

Rumelhart, D.E., McClelland, J. L. and PDP Group (1986). Parallel distributed processing: Explorations in the Microstructure of Cognition: Vol.1 Foundations. (London: The MIT Press).

Salehi Neyshabouri Ali, A., Barron, R.M. and Ferreira da, Silva, A. M. (2001). Numerical prediction of scour caused by a free falling jet, In: 9th annual conference of the CFD society of Canada, CFD 2001, May 27–29, Waterloo, Canada, pp. 284–8.

Sarma, K.V.N. and Krishnamurthy, M. (1969). Design formula for scour depth around bridge piers, Annual Report, Publication No. 33, Civil and Hydraulics Dept., Indian Inst. of Science, Bangalore, India.

Sayed, T., Tavakolie, A. and Razavi, A. (2003). Comparison of adaptive network based fuzzy inference systems and B-spline neuro-fuzzy mode choice models, ASCE J. of Comput Civil Eng; 17 (2), pp. 123–30.

Schneible, D.E. (1951). An investigation of the effect of bridge pier shape on the relative depth of scour, M.Sc. Thesis, Graduate College of the State, University of Iowa, Iowa City, Iowa.

Shah, B.P. (1988). Interference effects on scour depth around bridge piers, M.Tech. Thesis, Department of Civil Engineering, Indian Institute of Technology, Kanpur, India.

Shames, I. H. (1992). Mechanics of fluids. McGraw Hill, Singapore.

Shen, H. W., Schneider, V. R. and Karaki, S. S. (1966). Mechanics of local scour, data supplement, prepared for bureau of public roads, Office of Research and Development, Civil Engineering Department, Colorado State University, Fort Collins, CO, Report CER66-67HWS27

Shen, H.W. (1971). Scour near piers, river mechanics, Vol. II, Chap. 23, Ft. Collins, Colo.

Shen, H.W., Ogawa, Y., Karaki, S.S. (1963). Time variation of bed deformation near bridge piers, Proc.10th Congress I.A.H.R., Leningrad, Paper No. 3.14.

Shen, H.W., Schneider, V.R. and Karaki, S. (1969). Local scour around bridge piers, J. of Hydraulic Div., A.S.C.E., Vo. 95, No. 6, pp. 1919-1940.

Shen, H.W., Schneider, V.R., and Karaki, S.S. (1966). Mechanics of local scour, U.S. Department of Commerce, National Bureau of Standards, Institute for Applied Technology, Washington, D.C.

Shen, H.W., Schneider, V.R., Karaki, S.S. (1971). Closure to local scour around bridge piers, Proc. A.S.C.E., Journal Hydraulics Div., Vol. 97, HY9.

Sheppard, *et al.* (2004). Large scale clear-water local pier scour experiments, J. Hydr. Engrg., Volume 130, Issue 10, pp. 657-963.

Shields, A. (1936). Anwendung der Ahnlichkeitsmechanik und der turbulenz Forschung auf die Geschiebebe-wegung Mitteilungen de Preuss, Versuchsanst. F. Wasserbau U. Schiffbau, Berlin, Heft. 26. See also translation by W.P. Ott and J.C. Van Uchelen, U.S. Dept. of Agriculture, Soil Conservation Ser. Coop. Lab. C.I.T.

Singh, K.K., Verma, D.V.S. and Tiwari, N.K. (1995). Scour protection at circular bridge piers, 6th Int. Symp. on River Sedimentation, New Delhi.

Small, A.F. (1969). Hydrodynamic excitation of bridge piers, M.E. Thesis, University of Auckland, Auckland.

Smith, C.D. (1984). Scour control at outlook bridge – A case study, Canadian. J. Civ. Engrg., Ottawa, 101, 709-716.

Smith, D.W. (1976). Bridge failures, Proc. I.C.E. Vol. 60, Pt. 1, pp. 367-383.

Sumer, B. M., Fredsoe, J. and Jensen, K. (1994) A note on span wise correlation on a freely vibrating cylinder in oscillatory flow. Journal of Fluids and Structures, 8(3): 231-238.

Sumer, B.M. and Fredsoe, J. (1997). Hydrodynamics around Cylindrical Structures, Singapore: World Scientific.

Sumer, B.M., Fredsoe, J. and Christiansen, N. (1992). Scour around vertical piles in waves, Journal of Waterway, Port, Coastal and Ocean Engineering, ASCE, 118 (1), pp. 15–31.

Sumer, B.M., Fredsoe, J. and Christiansen, N. (1992). Time scale of scour around a vertical pile, in Proc. 2nd Int. Offshore and Polar Engineering Conf., vol. 3, San Francisco, C. A., pp. 308-315.

Sumer, B.M., Fredsoe, J. and Christiansen, N. (1993). Influence of cross-section on wave scour around piles, ASCE, J. Waterway Port Coastal Ocean Eng., Vol. 119, No. 5, pp. 477-495.

Tanaka, S. and Yano, M.(1967). Local scour around a circular cylinder, Proc. 12th Congress I.A.H.R., Ft. Collins, Colorado, Vol. 3, pp. 193-201.

Tarapore, Z.S. (1967). Determination of depth of scour around an obstruction in an alluvial channel, Proc. 12th Congress I.A.H.R., Ft. Collins, Colorado, Vol. 3, pp. 17-25.

Task Committee (1966). Sediment transportation mechanics: E. Initiation of Motion, Proc. A.S.C.E. Journal of Hydraulics Div., Vol. 92, HY2.

Tay, J.H., Zhang, X. (1999). Neural fuzzy modelling of anaerobic biological waste water treatment systems, ASCE J. of Environ Eng; 125 (12), pp. 1149–59.

The ASCE Task Committee (2000). The ASCE Task Committee on Application of artificial neural networks in hydrology. J of Hydrol. Engrg. ASCE; 5(2):115–37.

Thirumalaiah, K., Deo, M. C. (2000). Hydrological forecasting using neural networks, ASCE J. of Hydrol Eng., 5 (2), pp. 180–9.

Thirumalaiah, K., Deo, M.C. (1998). River stage forecasting using artificial neural networks, ASCE J. of Hydrol Eng., 3 (1), pp. 26–32.

Thomas, A.R. (1962). Discussion on scour at bridge crossings, Trans. A.S.C.E., Vol. 127, pt. 1.

Thomas, A.R. (1970). Discussion on local scour around bridge piers by Shen *et. al.*, (1969). Proc. A.S.C.E. Journal Hydraulics Div., Vol. 96, HY9.

Thomas, Z. (1967). An Interesting hydraulic effect occurring at local scour, Proc. 12th Congress, I.A.H.R., Ft. Collins, Colorado, Vol. 3, pp. 125-134.

Thomas, Z. (1971). Time development of the deformation of an alluvial bottom, Proc. 14th Congress, I.A.H.R., Vol. 3, pp. 331-338.

Thomas, Z. (1975). Scour of water structures and erosion of loose media by flowing fluids, Report No. 140, Hydraulic Research Institute, Prague-Podbaba, Czechoslovakia.

Timonoff, V.E. (1929). Experiments on the spacing of bridge piers in the case of parallel bridges, Hydraulic Laboratory Practice, edited by J.R. Freeman, Am. Soc. of Mech. Engrs., New York.

Tison, L.J. (1940). Scour around bridge piers in rivers, Annales des Travaux Publics de Beligique, 41, No. 6, pp. 813-871.

Tison, L.J. (1961). Local scour in rivers, J. of Geographical Research, Vol. 66, No. 12, pp. 4227-4232.

Trent R, Gagarin N, Rhodes J. (1993). Estimating pier scour with artificial neural networks, In: Proceedings of the ASCE conference on hydrological engineering, San Francisco, California, pp. 1043–1048.

Trent, R., Albert, M. and Gagarin N. (1993). An artificial neural networks for computing sediment transport, In: Proceedings of the ASCE conference on hydrological engineering, San Francisco, pp. 1049–54.

Tsai C. P. and Lee T. L. (1999). Back-propagation neural network in tidal-level forecasting J. of Water w Port Coastal and Ocean Eng., 12 (4), pp. 195-202.

Tseng M. H., Yen C. L. and Song C. S. (2000). Computation of three dimensional flows around square and circular piers. J. of International Journal for Numerical Methods in Fluids, 33: 695-710.

Tsujimoto, T. and Mizukami, T. (1985). Physical modelling of local scour at a front foot of a circular cylindrical pier, (Japanese). Proc. 29th Japanese Conference on Hydraulics, J.S.C.E.

U.S. DOT. (1993). Evaluation scour at bridges, Hydr. Engrg. Circular No. 18, FHWA-IP-90-017. Fed. Hwy. Admin., U.S. Dept. of Trans. McLean, Va.

Unger, J. and Hager, W. (2005). Discussion of the mean characteristics of horseshoe vortex at a cylindrical pier, J. of Hydraulic Research. Vol. 43, No. 5, pp. 584-587.

Utami, T. (1974). Local flow at the upstream side of bridge piers in laminar condition, Trans. Japanese Soc. Civil Engrs., Vol. 6, pp. 74-75.

Utami, T. (1976). Local flow just upstream side of bridge piers, Trans. Japanese Soc. Civil Engrs, Hydraulic and Sanitary Div., Vol. 8, pp. 133-134.

Vanoni, V.A. and N.H. Brooks (1957). Laboratory studies of Roughness and Suspended Load of Alluvial Streams, Caltec Report, No. E-68.

Vanoni, V.A. *et. al.* (1961). Lecture notes on sediment transportation and channel stability, Report No. KH-RI, W.M. Keck Laboratory of Hydraulics and Water Resources, California Institute of Technology, Pasadena, Calif.

Vanoni, V.A. *et. al.* (1975). Sediment transportation mechanics; initiation of motion, In Sedimentation Engineering, A.S.C.E. – Manuals and Reports on Engineering Practice,No. 54, 51-114.

Vanoni, V.A. *et. al.* (1975). Sedimentation Engineering, Manuals and Reports on Engineering Practice, No. 54, ASCE.